UNIVERSITÉ LAVAL

PARP-1 activation regulates the DNA damage response to DNA double-strand breaks

Thèse

Jana Krietsch

Doctorat en Biologie cellulaire et moléculaire
Philosophiæ Doctor (Ph.D.)

Québec, Canada

RÉSUMÉ

Les cassures double-brin de l'ADN, lorsque incorrectement réparées, peuvent avoir des conséquences fatales telles que des délétions et des réarrangements chromosomiques, favorisant la carcinogenèse. La poly(ADP-ribosyl)ation réalisée par la protéine poly(ADP-ribose) polymérase-1 (PARP-1) est l'une des premières modifications post-traductionnelles qui se produisent en réponse aux dommages à l'ADN. La PARP-1 utilise la nicotinamide pour générer un polymère chargé négativement, nommé poly(ADP-ribose) polymère (PAR), lequel est attaché en majorité à la PARP-1 elle-même ainsi qu'à d'autres protéines cibles. Le PAR a récemment été reconnu comme un signal de recrutement pour certaines protéines de réparation aux sites de dommages à l'ADN, mais un débat est en cours quant au rôle précis de la PARP-1 et du PAR dans la réponse aux dommages de l'ADN.

Au cours de mon projet de doctorat, nous avons pu confirmer que les protéines qui se retrouvent en complexe avec le PAR immédiatement après les dommages à l'ADN sont principalement des facteurs de réparation. Étonnamment, les complexes protéiques associés au PAR pendant la période de récupération suite aux dommages sont enrichis en facteurs de liaison à l'ARN. Toutefois, la protéine liant l'ARN la plus abondante que nous avons détectée dans l'interactome du PAR, soit NONO, ne suit pas cette dernière cinétique puisqu'elle est fortement enrichie immédiatement après les dommages à l'ADN.

Notre étude subséquente de NONO dans la réponse aux cassures double-brin de l'ADN a étonnamment révélé une implication directe de celle-ci par le mécanismede réparation de jonction des extrémités non-homologues. En plus, nous avons constaté que NONO se lie fortement et spécifiquement au PAR via son motif 1 de la reconnaissance de l'ARN, soulignant la compétition entre les PAR et l'ARN pour le même site de liaison. Fait intéressant, le recrutement *in vivo* de NONO aux sites de dommages de l'ADN dépend entièrement du PAR et nécessite le motif 1 de la reconnaissance de l'ARN.

En conclusion, nos résultats établissent NONO comme une nouvelle protéine impliquée dans la réponse aux cassures double-brin de l'ADN et plus généralement démontrent un autre niveau de complexité supplémentaire dans l'interdépendance de la biologie de l'ARN et la réparation de l'ADN.

ABSTRACT

DNA double-strand breaks are potentially lethal lesions, which if not repaired correctly, can have harmful consequences such as carcinogenesis promoted by chromosome deletions and rearrangements. Poly(ADP-ribosyl)ation carried out by poly(ADP-ribose) polymerase 1 (PARP-1) is one of the first posttranslational modifications occurring in response to DNA damage. In brief, PARP-1 uses nicotinamide to generate a negatively charged polymer called poly(ADP-ribose) polymer (PAR), that can be attached to acceptor proteins, which is to a large extent PARP-1 itself. PAR has recently been recognized as a recruitment signal for key DNA repair proteins to sites of DNA damage but the precise role of PARP-1 and its catalytic product PAR in the DNA damage response are still a matter of ongoing debate.

Throughout my doctoral work, we confirmed that the proteins in complex with PAR promptly after DNA damage are mostly DNA repair proteins, whereas during the period of recovery from DNA damage, the PAR interactome is highly enriched with RNA processing factors. Interestingly, one of the most abundant RNA-binding proteins detected in the PAR interactome, namely NONO, did not follow these kinetics as it was highly enriched immediately after DNA damage in the DNA repair protein complexes centered on PAR.

Our subsequent investigation of NONO in the DNA damage response to double-strand breaks strikingly revealed a direct implication for NONO in repair by nonhomologous end joining (NHEJ). Moreover, we found that NONO strongly and specifically binds to PAR through its RNA-recognition motif 1 (RRM1), highlighting competition between PAR and RNA for the same binding site. Remarkably, the *in vivo* recruitment of NONO to DNA damage sites completely depends on PAR and requires the RRM1 motif.

In conclusion, our results establish NONO as a new protein implicated in the DNA damage response to double-strand break and in broader terms add another layer of complexity to the cross-talk between RNA-biology and DNA repair.

TABLE OF CONTENTS

LIST OF TABLES

LIST OF FIGURES

CHAPTER 1

CHAPTER 2

CHAPTER 3

CHAPTER 4

CHAPTER 5

ANNEX

ABBREVIATIONS

53BP1: p53 binding protein 1

AA: Amino acid

AC: Alternating current

AIF: Apoptosis inducing factor

Alt-NHEJ: Alternative NHEJ

AMP: Adenosine monophosphate

Asp: Aspartic acid

ATM: Ataxia telangiectasia mutated

ATP: Adenosine triphosphate

ATR: Ataxia telangiectasia and Rad3-related protein

BER: Base excision repair

BLM: Bloom

BRCA1: Breast cancer type 1 subsceptibility protein

BRCA2: Breast cancer type 2 subsceptibility protein

BRCT: BRCA1 carboxy-terminal

Cas9: Caspase 9

CDK: Cycline-dependent kinase

CHK1: Checkpoint kinase-1

CHK2: Checkpoint kinase-2

CRISPR: Clustered, regularly interspaced short palindromic repeats

CYP17: Cytochrome P450, family 17 gene

DBHS: Drosophila behavior human splicing family

DDR: DNA damage response

DNA: Deoxyribonucleic acid

DNA-PKcs: DNA-dependent protein kinase catalytic subunit

DSB: Double-strand break

DSBR: Double-strand break repair

EMSA: Electrophoretic mobility shift assay

FA: Fanconi Anemia

FUS: Fused in Sarcoma

Glu: Glutamic acid

HDAC: Histone deacetylase

HnRNP: Heterogenous ribonucleoprotein

HPLC: High-performance liquid chromatography

HR: Homologous recombination

HU: Hydroxyurea

ICL: Interstrand crosslink

IR: Ionizing radiation

IRIF: Ionizing radiation induced foci

iTRAQ: Isobaric tag for relative and absolute quantitation

kDa: Kilo Dalton

Lys: Lysine

MALDI: Matrix-assisted laser desorption/ionization

MAR: Mono (ADP-ribose)

MDC1: Mediator of DNA damage checkpoint protein 1

MEF: Mouse embryonic fibroblast

MMR: Mismatch repair

MMS: Methyl methanesulfonate

MNNG: N-Methyl-N′-nitro-N-nitrosoguanidine

MS: Mass spectrometry

M/z-ratio: Mass-to-charge-ratio

Nam: Nicotinamide

NCS: Neocarzinostatin

NEAT1: Nuclear enriched abundant transcript 1

NER: Nucleotide excision repair

NHEJ: Nonhomologous end joining

NLS: Nuclear localization signal

NONO: Non-POU domain-containing octamer-binding protein

NOPS: NONA/ paraspeckle

p53: Protein 53

PALB2: Partner and localizer of BRCA2

PAR: Poly(ADP-ribose) polymer

PARP: Poly(ADP-ribose) polymerase

PARG: Poly(ADP-ribose) glycohydrolase

PBM: Polymer-binding motif

PBZ: Polymer-binding zinc finger

PIKKs: Phosphatidyl inositol 3' kinase-related kinases

PSPC1: Paraspeckle component 1

PTM: Posttranslational modification

RBP: RNA binding protein

RNA: Ribonucleic acid

RNP: Ribonucleoprotein

ROS: Reactive oxygen species

RPA: Replication protein A

RRM: RNA recognition motif

SCE: Sister chromatid exchange

SF-1: Steroidogenic factor 1

SFPQ: Splicing factor proline/ glutamine-rich

ShRNA: Short hairpin RNA

SILAC: Stable isotope labeling by amino acids in cell culture

SiRNA: Small interfering RNA

SSA: Single-strand annealing

SSB: Single-strand break

ssDNA: single-stranded DNA

TOF: Time-of-flight

UniProt: Universal Protein Resource

UTR: Untranslated region

UV: Ultra violet

XRCC1: X-ray repair cross-complementing protein 3

XRCC3: X-ray repair cross-complementing protein 1

Znf: Zinc finger

ACKNOWLEDGEMENTS

One of the joys of completing this thesis is to look over the challenging journey past with colleagues, friends and family that have been supporting me. First and foremost I would like to thank my PhD supervisor Dr Jean-Yves Masson, whose joy and enthusiasm for science have been contagious and motivating at all times. I could not have asked for a better mentor, someone who is inspirational, patient and supportive. With his high standards, creative mind and sense of humor (even in times when I had lost mine), he has been a role-model I feel privileged to have worked for. I had the chance to have a supervisor that is involved in a student's project, never getting tired of discussing results and giving feedback even regarding career projects after the PhD.

Secondly, I am deeply grateful to my co-supervisor Dr Guy G. Poirier, who I see as the driving force behind my PhD. It was Guy who had invited me to come to Québec (and picked me up at the airport in person) in order to build the bridge between PARPs and DNA repair. Already within the first year of my PhD he did not hesitate in sending me to present and discuss my work at the reputable Keystone meeting on DNA repair and permitted me to write a book chapter on the fundamental subject of my PhD. Thank you Guy for supporting me and always being open for inspiring discussions. I truly admire the career you have accomplished due to hard work and creative thinking and the milestones you have set.

I am truly thankful to both of my bosses for having given me several opportunities to present my work at national and international congresses and to exchange ideas with and learn first hand from some of the leading researchers in the field. I will not forget my 10-hour-lab meeting with Jean-Yves, Joris and Ranjan in the car on the way to London, Ontario (which, as we know now, is even further away from Québec than Toronto…). Nor will I forget my trip to Montréal with Guy where I learned about the history of his research on PARPs since the year I was born. I even had the privilege to learn about the current view on PARP inhibitors first hand from Dr Scott Kauffmann, who graciously took the time to show Michèle Rouleau and myself around the Mayo Clinics in Rochester.

I want to direct special thanks to Michèle, who has been an exceptional mentor and a friend. I have learned immensely from fruitful and critical discussions with you, one good example being drawing PARP-inhibitor models on the plane to Rochester with you. You were at any time open for helping, discussing, reading drafts over and over again, which has been extremely precious to me. I will not forget how you selflessly stood up for me Michèle!

I would also like to thank the organizations FQRNT and ACCEM, who with their scholarships, have contributed to the accomplishment of my PhD project. Thanks to the Jury of this thesis, composed of Martin Simard, Girish Shah, El Bashir Affar, Michèle Rouleau and Jean-Yves Masson, for having accepted to read and evaluate my work.

The past and present members of the Masson and Poirier lab have contributed immensely to my professional and personal time in Québec. I have gratefully appreciated everyday discussions ranging from creative problem solving, over fundamental philosophical science questions, to rather less scientific coffee breaks and our 5 à 7s. I would like to thank Joris Pauty for being such a good friend and critical colleague.

Lastly I would like to thank my parents, Torsten and Gabriele as well as my brother Hannes for encouraging and supporting me all along the way even from across the Atlantic Ocean. You made me understand that one can achieve anything as long as one works hard for it. Thank you Pierre-Michel for putting my feet back on the ground and showing me what is important in life! You made me go to the lab each day with a smile and the desire to finish my day on time. Special thanks to Boulette who made me laugh at least once a day.

May this thesis be a pleasure to read for all of you!

PREFACE

The scientific work presented in this thesis is the product of nearly four years of work as a doctorate student in the laboratories of the Drs Guy G. Poirier and Jean-Yves Masson. Throughout this time I have contributed as first author to three manuscripts.

"Poly(ADP-Ribose) Polymerase at the Interface of DNA Damage Signaling and DNA Repair." (Krietsch J, Rouleau M, Lebel M, Poirier GG, Masson JY) is a book chapter published in "Advances in DNA repair in Cancer Research" (Panasci L, Aloyz R, Alaoui-Jamali M; (Eds.) in 2013). I wrote the manuscript and generated the Figures but would not have succeeded without critical discussion with the co-authors mentioned on the manuscript. (**Chapter 2**)

I had the privilege of contributing to the manuscript: "Quantitative proteomics profiling of the poly(ADP-ribose)-related response to genotoxic stress." (Gagné JP, Pic E, Isabelle M, Krietsch J, Éthier C, Paquet É, Kelly I, Boutin M, Moon KM, Foster LJ, Poirier GG). The manuscript was published as a highlight article in Nucleic Acids Research in May 2012. My contributions are minor and lie in control experiments and reviewing of the manuscript. However, as the publication is fundamental for the comprehension of my thesis, I have added it as **Chapter 3**.

Thirdly, my scientific results on NONO have been published in Nucleic Acids Research: "PARP activation regulates the RNA-binding protein NONO in the DNA damage response to DNA double-strand breaks." (Krietsch J, Caron MC, Gagné JP, Ethier C, Vignard J, Vincent M, Rouleau M, Hendzel MJ, Poirier GG, Masson JY; Nucleic Acids Research in November 2012). I have performed all of the experiments and done the writing and yet had precious help from the co-authors mentioned. (**Chapter 4**)

The fourth publication is a review of the current knowledge on PAR-binding domains, proteins possessing them and their implication in cellular processes: "Reprogramming cellular events by poly(ADP-ribose)-binding proteins." (Krietsch J, Rouleau M, Pic E,

Ethier C, Dawson TM, Dawson VL, Masson JY, Poirier GG, Gagné JP; Mol Aspects Med in December 2012). This manuscript is the fruit of an excellent teamwork, with major contributions of Michèle Rouleau and Jean-Philippe Gagné. I have completed the majority of the writing and generated all the Figures (**Annex**).

Lastly, as a co-first author I have contributed to a video-publication in the Journal of Visualized Experiments, which I have added to the **Annex** of this thesis. "GST-His purification: A Two-step Affinity Purification Protocol Yielding Full-length Purified Proteins. " (Maity R*, Pauty J*, Krietsch J*, Buisson R, Genois MM, Masson JY, J Vis Exp in October 2013). *equally contributed

Other side-projects with various collaborators of Dr Jean-Yves Masson and Dr Guy G. Poirier, such as Dr Dan Durocher, are beyond the subject of my thesis and hence not included in the document.

Für meine Eltern

Learn from yesterday, live for today, hope for tomorrow.
The important thing is to not stop questioning.

ALBERT EINSTEIN

CHAPTER 1
INTRODUCTION

Genomic instability caused by DNA damage can promote carcinogenesis or accelerate aging. Hence, the proper repair of damage to the DNA is crucial for restoring genomic integrity. The enzyme poly (ADP-ribose) polymerase-1 (PARP-1) is an important player in the DNA damage response and compounds that block its enzymatic activity are able to specifically kill certain types of cancer cells with a repair-deficient background. However, the specific roles of PARP-1 and its interactome in the DNA damage response to double-strand breaks remain to be defined in greater detail. *This is hence the central subject of my thesis and will be introduced in the following.*

1.1 The DNA damage response to DSBs is a multilayered process

Each day the integrity of our genetic material is continuously challenged by a variety of damaging chemical reactions. The estimated number of damaging events on the DNA of a single cell ranges from 10^4 to 10^6 per day (Hoeijmakers, 2009).

1.1.1 Sources for and types of DNA damage

The high number of damaging events mentioned before implies that DNA is inherently unstable as some of its bonds are prone to hydrolysis under physiological conditions. Moreover the DNA sequence can be altered spontaneously as through misincorporation of nucleotides during DNA replication, interconversion of bases caused by their deamination, loss of bases caused by depurination, modification of bases by alkylation and others. Reactive oxygen species (ROS) such as hydroxyl radicals and superoxides are produced by moving electrons along the electron-transport chain in mitochondria, which can cause mutations. ROS and nitrogen compounds are also produced by neutrophils and macrophages at sites of inflammation (Kawanishi et al., 2006; Krejci et al., 2012).

Various environmental factors (Figure 1A) are sources for accidental DNA damage: Natural UV radiation can cause aberrations such as pyrimidine-dimers and 4-6-photoproducts in the DNA helix that interfere with its proper replication and transcription. Dramatic consequences for the DNA can also result from radiation or ionizing radiation

(IR) (as e.g. cosmic radiation and clinical treatments employing x-rays and gamma rays) which cause DNA single-strand breaks (SSBs) and double-strand breaks (DSBs). DNA DSBs are some of the most toxic lesions, as they do not leave an intact template strand to be used for repair.

Interestingly, differing from non-cancerous cells, cancerous cells proliferate very rapidly despite the presence of DNA damage due in part to defects in cell-cycle checkpoints. This is why cancer radio- and chemotherapy is often based on IR or a variety of drugs that voluntarily introduce DNA DSBs to provoke apoptosis. Radiomimetic drugs such as neocarzinostatin (NCS) mimic the effect of ionizing radiation. Alkylating agents, such as methyl methanesulfonate (MMS) or N-methyl-N'-nitro-N-nitrosoguanidine (MNNG) attach alkyl groups to bases, whereas cross-linking agents such as mitomycin C (MMC), cisplatin or nitrogen mustard crosslink either bases on the same strand (intrastrand crosslinks) or between different strands (interstrand crosslinks). Differently, chemical compounds such as camptothecin and etoposide inhibit the enzyme topoisomerase I or II, respectively, by trapping the enzyme on the DNA and hence interfere with DNA replication, which induces either SSBs or DSBs.

In mitotic cells, DSBs can occur naturally to ensure antibody diversity for our immune system. These DSBs are willingly introduced in early stages of T-cell receptor or immunoglobulin production in a mechanism called somatic recombination or V(D)J recombination. Moreover, in meiotic cells, genetic diversity between individuals is guaranteed by a recombination mechanism, which is initiated by a DSB catalyzed by the enzyme named Spo11.

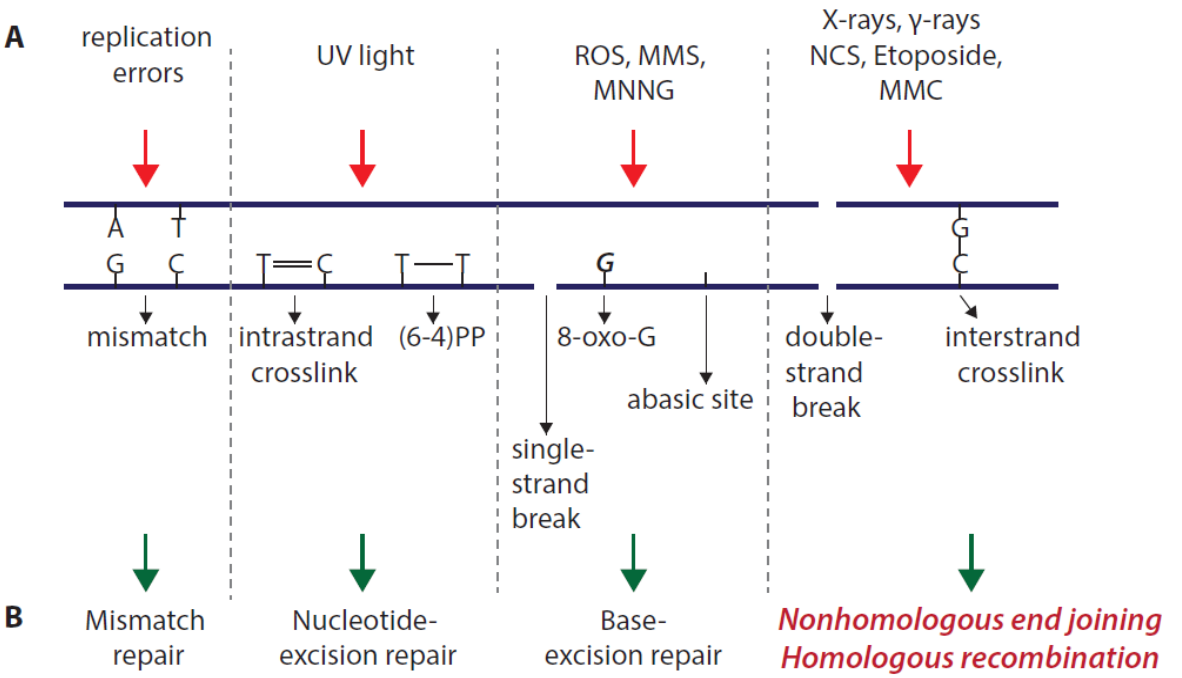

Figure 1: DNA damage types and repair pathways
(A) A variety of DNA damaging factors (e.g. UV light) and agents (e.g. NCS, MNNG, etoposide) are continuously challenging the integrity of DNA sequences by introducing different types of DNA damage. (UV: ultra violet; ROS: reactive oxygen species; MMS: methyl methanesulfonate; PP: photo product; MNNG: N-methyl-N'-nitro-N-nitrosoguanidine; NCS: neocarzinostatin; MMC: mitomycin C) **(B)** Specialized repair mechanisms have evolved for the different DNA damage types to restore genomic DNA sequences. *(Inspired by:(Hoeijmakers, 2001))*

1.1.2 DNA repair mechanisms

Specific repair mechanisms to counteract most types of damage have evolved (Figure 1B): Mispaired bases are replaced by the correct bases through the mismatch repair (MMR) mechanism, whereas chemical alterations of bases lead to their replacement by a process called base excision repair (BER). Nucleotide excision repair (NER) corrects rather complex lesions such as intrastrand crosslinks and pyrimidine dimers. Interstrand crosslinks (ICLs) on the other hand are repaired by proteins of the Fanconi Anemia (FA) pathway and homologous recombination (HR) repair.

Single-strand breaks (SSBs) are eliminated by SSB repair. The most hazardous lesions, DSBs, can be repaired by four different pathways (Figure 2A-D): nonhomologous end

joining (NHEJ), alternative nonhomologous end joining (alt-NHEJ), homologous recombination (HR) and single-strand annealing (SSA).

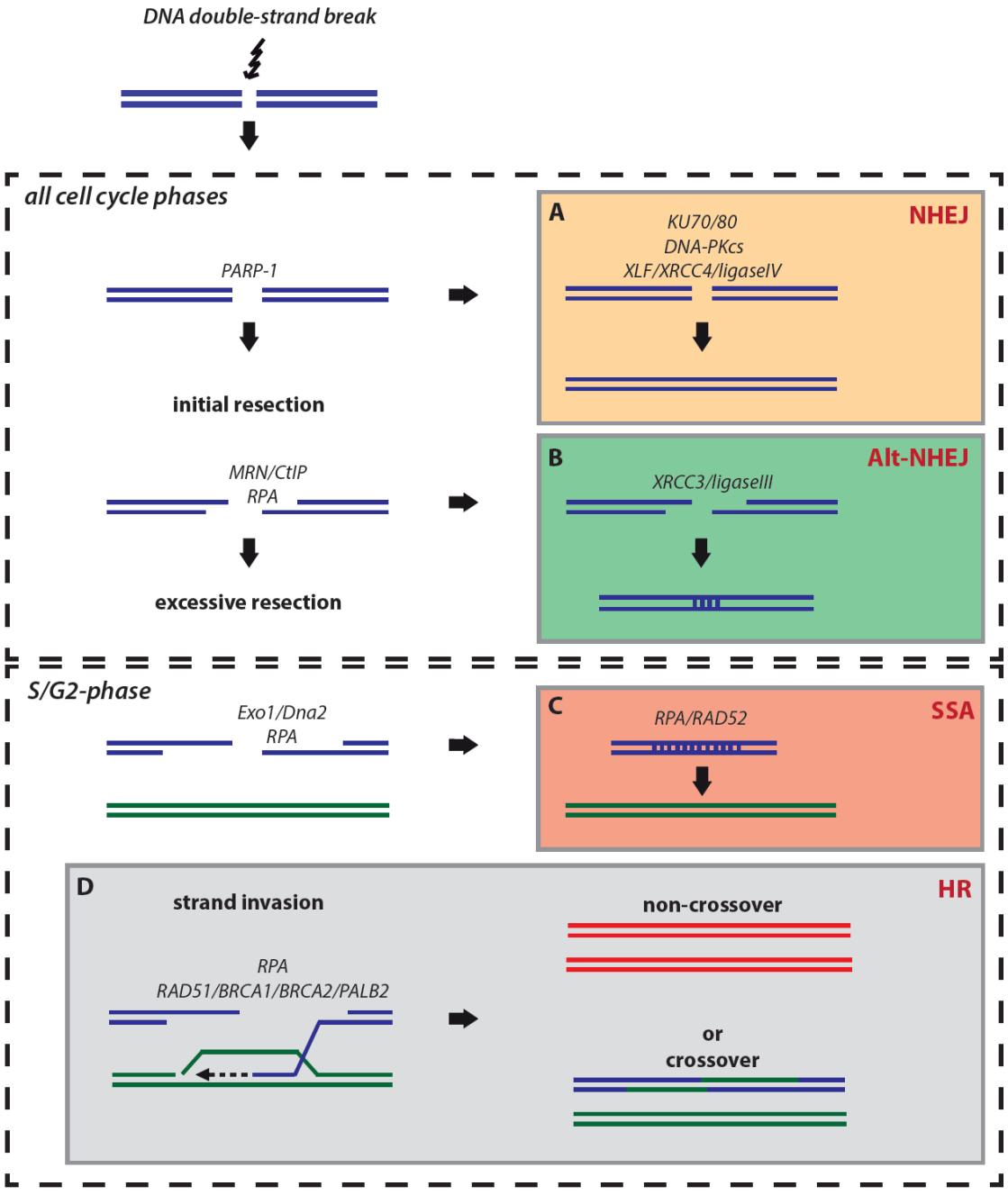

(*See Figure legend on the next page.*)

Figure 2: Simplified overview of the four pathways repairing DSBs in higher eukaryotes
After the generation of a DSB, PARP-1 is one of the first molecules to arrive at the free DNA ends. This may lead to the recruitment of the MRN-complex, which carries out initial end resection in all cell-cycle phases. **(A)** In the case of NHEJ, DNA ends are left unresected. The end joining reaction is catalyzed by Ku70/Ku80, DNA-PKcs and finalized by the XLF/XRCC4/ligase IV complex. **(B)** An alternative-NHEJ reaction based on XRCC3/ligase III has been described in the absence of key NHEJ proteins, such as ligase IV. This mechanism has been suggested to require short-range end resection as carried out by MRN. In S-/G2-phase of the cell cycle, the initial end resection by MRN can be followed by excessive end resection, possibly carried out by Exo1/Dna2 setting the stage for two possible repair mechanisms **(C)** SSA, which is mediated by RPA/RAD52, or **(D)** HR. In the latter case, the free single-strand DNA branches are protected by RPA, which is then replaced by RAD51, leading to strand invasion of the sister chromatid, D-loop formation, and its resolution with possible crossover or non-crossover outcomes. *(Inspired by:(Krejci et al., 2012))*

The understanding of the individual DSB repair pathways is crucial for my thesis. I have reviewed the current literature on NHEJ and HR with a focus drawn to PARP-1 in a manuscript, which has been published as a book chapter in 2013 in "Advances in DNA repair and Cancer Therapy." The reader is kindly referred to Chapter 2 of this thesis.

1.1.3 DSB sensing, signaling and checkpoint control

The cellular response to DNA double-strand breaks consists not only of its respective repair mechanism, but is rather a multilayered signal-transduction pathway, composed of DNA damage sensors, signaling factors and actual repair proteins. The misuse of any of these factors can have disastrous consequences for genomic integrity. Hence, mechanisms have evolved to recruit the appropriate enzyme at the right time to a specific place of action.

In a first step after the introduction of DNA DSBs, a signal has to be transmitted to stop the cell from proliferating and therewith replicating the error, allowing time for the restoration of the original DNA sequence. Sensor proteins are immediately detecting DNA DSBs and rapidly being recruited to the break sites to activate the coordinated choreography of DNA DSB repair. The recruitment events of DNA sensor and repair proteins lead to an enrichment of up to 10^3 of individual repair proteins (Lisby et al., 2004) at the DSB and can hence conveniently be visualized by fluorescence imaging of so called DNA repair foci,

often named ionizing radiation induced foci (IRIF) (Bekker-Jensen and Mailand, 2010). Interestingly, it has been elegantly demonstrated in experiments with yeast and mammalian cells, that a forced coupling of certain proteins such as NBS1 to chromatin can initiate a DNA damage response, even in the absence of DNA damage (Soutoglou and Misteli, 2008), (Bonilla et al., 2008), (Yeung and Durocher, 2008).

Within a broad spectrum of roles for posttranslational modifications (PTMs) is remodeling the local chromatin architecture and determining the precise timing and order of protein recruitment to the DNA damage site. One of the fastest sensor proteins to arrive within milliseconds at a newly generated DSB is PARP-1. Once bound to the free DNA ends, the enzyme catalyzes a reaction generating a polymer named poly(ADP-ribose) (PAR). This PTM serves as a platform to recruit a variety of DDR factors, such as the MRN/ATM complexes (see Figure 3A and B). *PARP-1, with its catalytic product PAR, is the major subject of my thesis and is hence discussed in detail below and in the following chapters.*

One of the hallmark PTMs after the generation of a DSB is the phosphorylation of serine 139 on the histone variant H2AX, which is flanking the break-site (leading to a product called γ-H2AX), by Ataxia telangiectasia mutated (ATM**)** (see Figure 3A). ATM, under normal conditions, exists as an unphosphorylated dimer. However, once the enzyme has recognized DSBs, it becomes monomeric and autophosphorylated, leading to its activation (Bakkenist and Kastan, 2003). γ-H2AX is quickly bound by the C-terminal of the mediator of DNA damage checkpoint protein 1 (MDC1) (Stucki, 2009) which, in concerted action with ATM and NBS1, spreads this event further from the break site in a positive feed-back loop mechanism (see Figure 3C). This phosphorylation event spreads in a distance up to one or two megabases from the DSB and initiates subsequent repair cascades (Harper and Elledge, 2007), (Lou et al., 2006). MDC1 itself also gets phosphorylated by ATM, which in consequence recruits RNF8 (Figure 3D) to the break-site, an enzyme that ubiquitinates H2A and H2AX on K63 (Huen et al., 2007), (Kolas et al., 2007), (Mailand et al., 2007). The ubiquitin chains generated by RNF8 are then quickly recognized by RNF168 (Doil et al., 2009), (Stewart et al., 2009) which further stimulates H2AK13/K15 monoubiquitinylation. The events described above are followed by sumoylation and

methylation cascades that lead to the recruitment of 53BP1 (Figure 3E) (Fradet-Turcotte et al., 2013) and BRCA1 (Watanabe et al., 2013), constituting the ying and yang for DSB repair pathway choice through the regulation of DNA end resection (Escribano-Diaz et al., 2013), (Chapman et al., 2013b), (Zimmermann et al., 2013), (Zimmermann and de Lange, 2013), (Kakarougkas et al., 2013).

Meanwhile, following the binding of sensor and signaling proteins to DNA lesions, the protein family of phosphatidylinositol 3-kinase-like protein kinases (PIKKs), composed of ATM, Ataxia telangiectasia and Rad 3-related **(**ATR**)** and DNA-dependent protein kinase (DNA-PK), activates the DDR by phosphorylating mediator and repair proteins, which in some cases leads to their recruitment to the damage site. In the case of excessive and irreparable damage, the above mentioned protein family can initiate cell death instead of repair. The homology between the three PIKK-family members may suggest a common *modus operandi* and indeed, all three proteins recognize a common motif in their substrates (Ser/Thr-Gln-Glu) (Kim et al., 1999), (Rathbun et al., 1999), (Anderson and Lees-Miller, 1992), (Bannister et al., 1993). However, whereas DNA-PK phosphorylates itself and a small group of proteins involved in NHEJ, ATM has hundreds of targets involved in different cellular processes. ATR, together with its partner protein called ATR-interacting protein (ATRIP), is activated subsequently to its binding of replication protein A (RPA) coated ssDNA, which can be generated at stalled replication forks for instance. Besides their various targets that act in the DNA damage response, the two best studied ATM/ATR targets are the kinases CHK1 and CHK2, which in concert with ATM/ATR, act to reduce cyclin-dependent kinase (CDK) activity by various mechanisms, some of which are regulated by p53 (Figure 3F) (Bartek and Lukas, 2007). Given the fact that the down-regulation of CDKs arrests G1-S, intra-S and G2-M cell-cycle progression, time is given to accurately repair the DNA damage. Hence, generally, PIKKs fine-tune the balance between cell-cycle arrest, actual repair and apoptosis in case of excessive DNA damage.

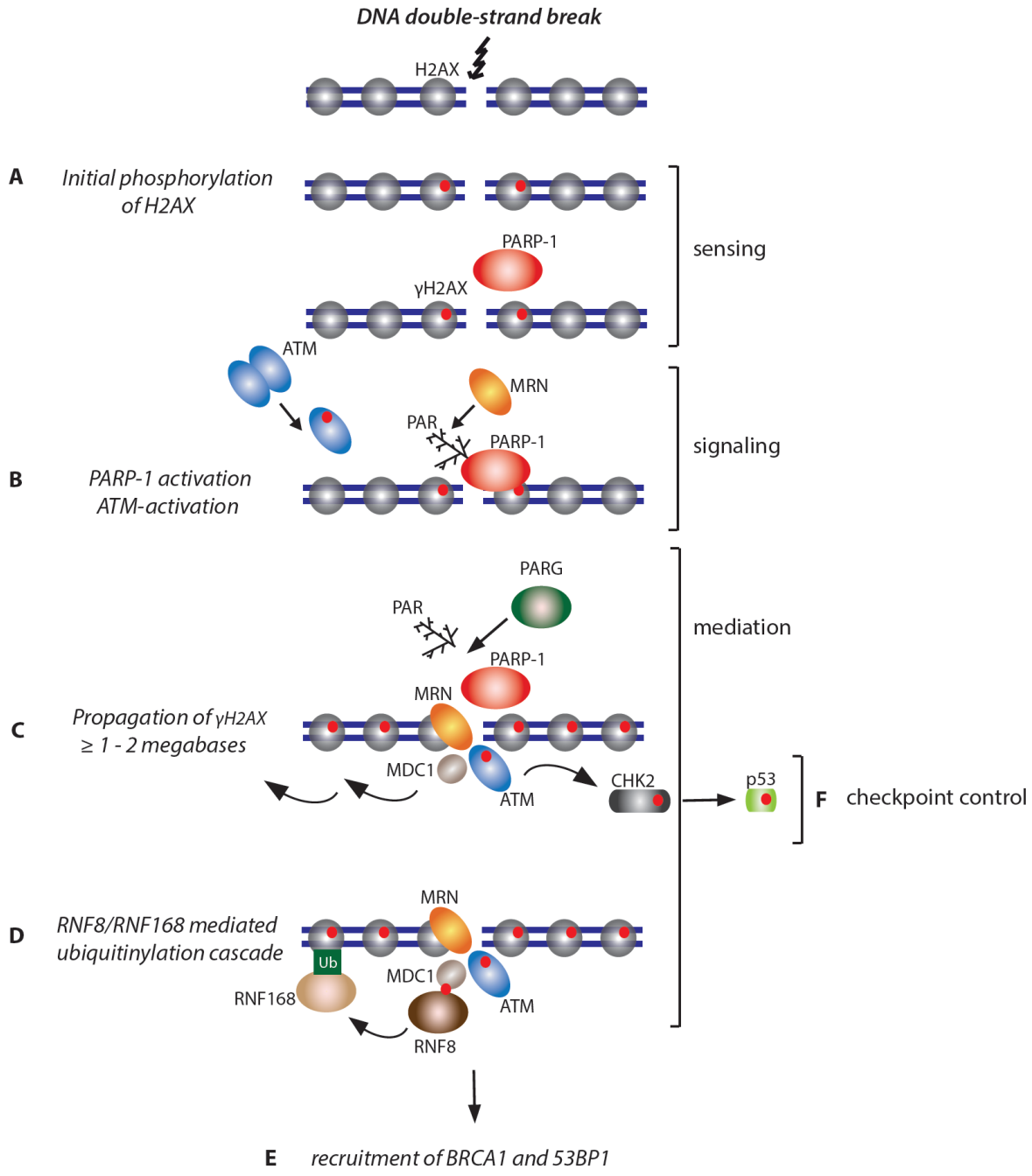

(*See Figure legend on the next page.*)

Figure 3: The DNA damage response to DSBs is a multilayered process
(A) Newly generated DSBs are rapidly marked by ATM, phosphorylating H2AX which is proximal to the break side. PARP-1 is one of the fastest DNA DSB sensors and rapidly recruited to the damage site. **(B)** Once bound to the DNA, PARP-1 is catalytically activated, generating the polymer (PAR), which leads to the recruitment of MRN and additional ATM. **(C)** Signal propagation is promoted by the subsequent phosphorylation of H2AX up to two megabases from the DSB. Moreover, PARG hydrolyses PAR, hence enabling another round of PARylation. (**D**) MDC1 is phosphorylated by ATM which initiates the RNF8/RNF168 ubiquitinylation cascade (details are given in the main text). **(E)** The latter event is followed by the recruitment of BRCA1 and 53BP1, two proteins that regulate the decision for the appropriate DSB repair pathway. **(F)** ATM in concerted action with ATR acts to reduce CDKs by a p53 regulated mechanism, which leads to a cell-cycle arrest.

1.2. Poly(ADP-ribose) polymerase

About 50 years ago, Pierre Chambon uncovered a poly-adenine-nucleic acid-like structure, which we nowadays know well as poly(ADP-ribose) polymer (PAR) and sometimes refer to as the "third type of nucleic acid"(D'Amours et al., 1999), (Kim et al., 2005). This ADP-ribose polymer is the catalytic product of the enzymes of the Poly(ADP-ribose) polymerase (PARP) family of proteins.

1.2.1 The PARP family of proteins

Until now, PAR reactions and PARP-like genes have been identified throughout evolution in eubacteria, archaebacteria, from fungi to mammals and even in double-stranded DNA viruses. Surprisingly, however, they are absent in *Saccharomyces cerevisiae* and *Schizosaccharomyces pombe*. Although PARP-1 is the most abundant and best-studied member, at least 16 other PARP orthologues carry the PARP signature, consisting of β-α-loop-β-α-NAD^+-fold (Figure 4). Interestingly, the catalytic PARP residue Glu988 is not conserved in all of these proteins. In some cases, a non-conserved residue replaces it, such as in PARP-7, PARP-9, PARP-10, PARP-13 and PARP-16. Even though 11 PARP family members carry the catalytic residue, when tested for their catalytic activity, only PARP-1, PARP-2, PARP-3 and tankyrase 1 (which are named after an affinity to telomere-associated

(TRF1) proteins and ankyrin repeats) showed significant PARylation activity. Amongst these, PARP-1, PARP-2 and PARP-3 are activated by DSBs and hence grouped as DNA-dependent PARPs, whereas tankyrase activation is DNA-independent but rather depending on interaction with its target proteins. The other enzymes, PARP 6-8, 10-12, and 14-16 are putative or confirmed mono-ADPribose transferases, but do not carry out polymerase activity. The group of Dr Hottiger has therefore suggested a new nomenclature using the term "ADPribosyltransferases (ARTs)" rather than naming the actual transferases all "PARPs" (Hottiger et al., 2010). Moreover, PARP-9 and 13 lack both the NAD^+-binding residue and the catalytic glutamate, and are hence most likely catalytically inactive. As one can see in Figure 4, all of the PARP domains lie within the C-terminus of the proteins, with the only exception being PARP-4/vPARP/ARTD4. Adding even more complexity to this protein family, some members have splice variants that exclude functional protein domains. Prominent examples are splice variants of PARP-13 and -14 that are missing the catalytic PARP domain. The question remains to be solved whether these splice variants can function as dominant-negative mutants.

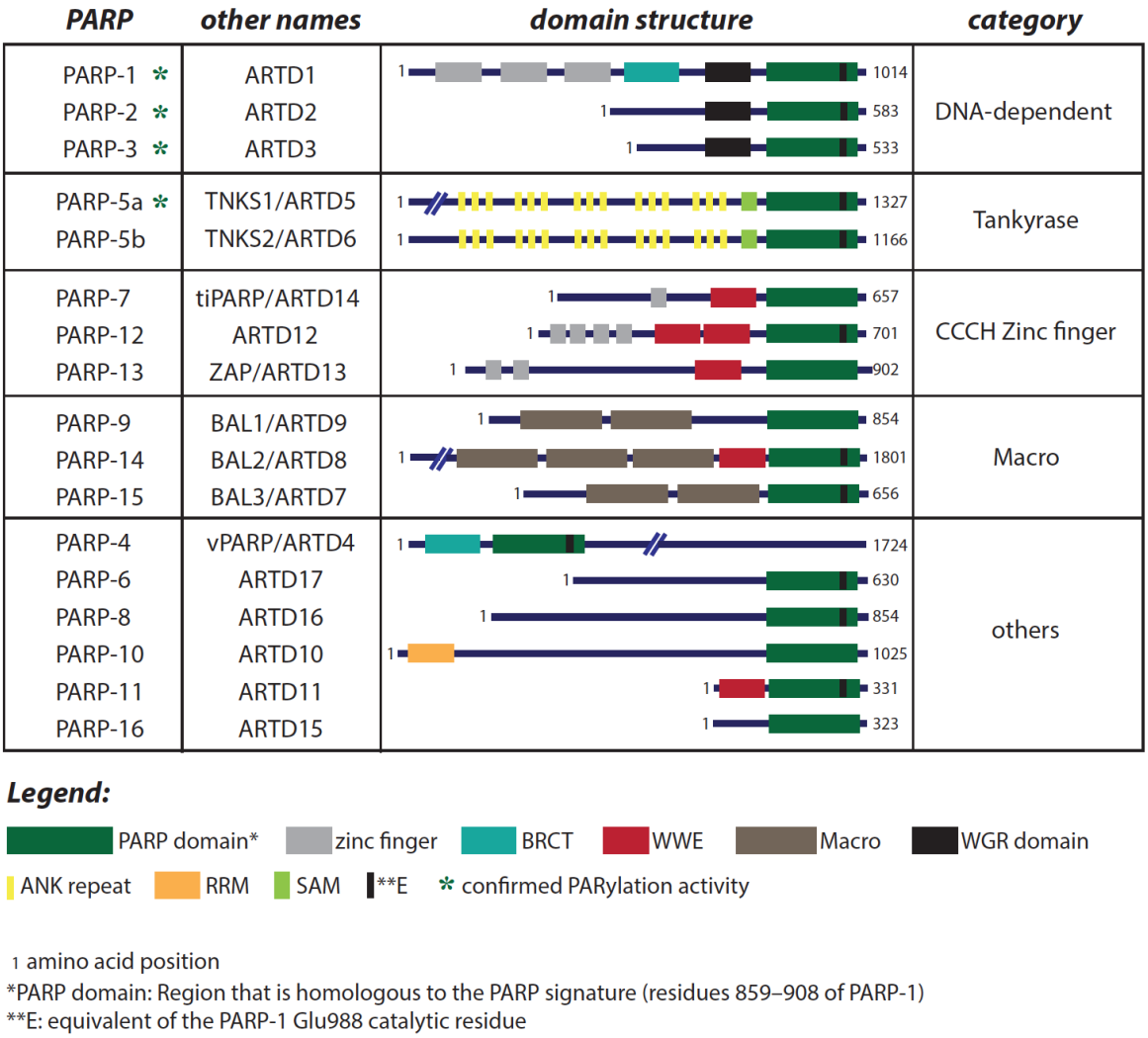

Figure 4: Domain architecture of the PARP family of proteins
Protein domains that are displayed as colored boxes were defined according to Universal Protein Resource (UniProt). Within each predicted PARP-domain, the conserved catalytic residue is darkened. The zinc fingers can either be DNA-binding ($CX_2CX_{28,30}HX_2C$-type in PARP-1) or putatively RNA-binding ($CX_{7\text{-}11}CX_{3\text{-}9}CX_3H$-type in PARP-7, PARP-12, PARP-13). The WGR domain is a tryptophane- (W), glycine- (G), arginine- (R) rich motif. The RRM is an RNA binding motif. Macro domains enable in some cases to bind to ADP, ADP-ribose, and PAR and characterize a subgroup of PARPs. The BRCA1 C-terminus (BRCT) domain enables protein-protein interaction. The WWE-domain is named after three conserved residues W and E (tryptophan and glutamate, respectively) and is a putative *iso*-ADP-ribose-binding domain. SAM is a protein- or RNA-interaction module. *(Inspired by: (Hottiger et al., 2010) and (Schreiber et al., 2006).*

1.2.2 PARylation

PARP-1 can bind to many DNA structures as well as nucleosomes and depends on NAD^+ as a substrate to synthesize the negatively charged polymer on target/ acceptor proteins. Best understood to date is PARP-1 activation in response to DNA damage, such as DNA nicks and DNA DSBs, where the catalytic activity of PARP-1 increases up to 500-fold (Hassler and Ladurner, 2012). PAR is rapidly generated in response to DNA damage and functions as a posttranslational modification on glutamate/ aspartate residues of target proteins (Althaus and Richter, 1987), (Hassa et al., 2006). Recent work of Dr Hottiger's lab has identified lysines as potential PARylation acceptor sites (Altmeyer et al., 2009). PARP-1 mostly modifies itself, a step which is called automodification. The ADP-ribose units are linked via glycosidic bonds between the ribose molecules, resulting in a polymer that can be linear or branched. In the elongation step, the adenine-proximal ribose units from the PAR chain terminus are joined with an α(1→2) O-glycosidic bond, whereas in the branching reaction the ADP-ribose junction occurs between two nicotinamide-proximal ribose (N-ribose) rings. Polymers can grow to lengths of up to 200 units of ADP-ribose and branching may occur every 20 to 50 units (Kiehlbauch et al., 1993). Most PAR in cells is rapidly degraded by the poly(ADP-ribose) glycohydrolase (PARG), who executes exo- and endoglycosidase activities. The rapid degradation of PAR by PARG quickly enables a new round of PARylation (Luo and Kraus, 2012) (Figure 5).

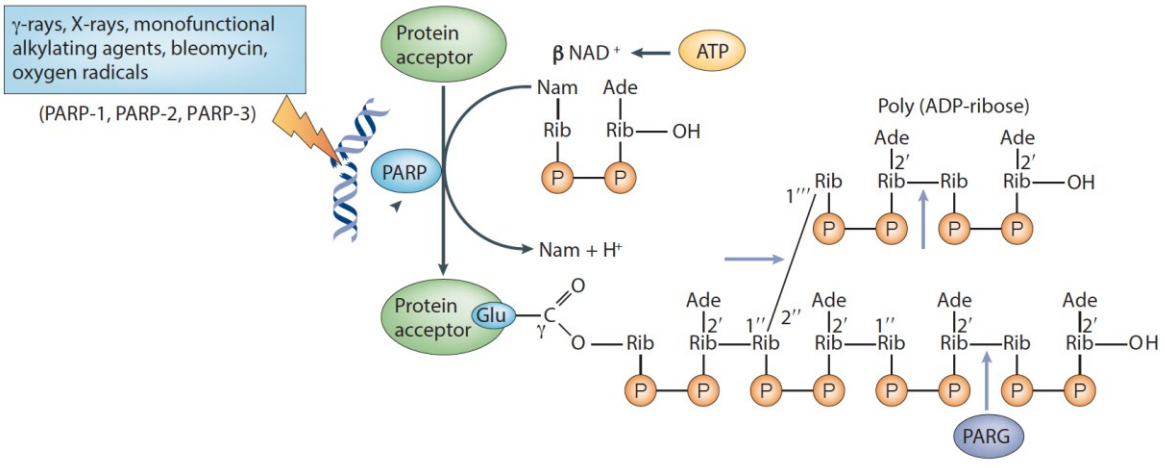

(Figure legend on the next page.)

Figure 5: Life-cycle of PAR in response to DNA-strand breaks
DNA-dependent PARPs (PARP-1, PARP-2 and PARP-3) hydrolyse NAD^+, releasing nicotinamide (Nam) and a proton (H^+) upon encountering DNA ends and successively transfer ADP-ribose moieties to nuclear acceptor/target proteins. By a stepwise addition of subsequent ADP-ribose molecules onto the first one, a linear or branched PAR-chain can be produced. The counterpart of PARP-1, namely PARG carries out endo- and exoglycosidic activities and quickly hydrolyses the generated PAR. *Adapted from: (Schreiber et al., 2006).*

1.2.3 Erasing PARylation by the PAR-degrading enzyme PARG

The reversion of post-translational modifications such as PARylation is crucial in order to guarantee temporarily-controlled repair and to proceed to subsequent stages. The enzyme poly(ADP-ribose)glycohydrolase (PARG), with its exo- and endoglycosidase activities, quickly enables the metabolic turnover of PAR hence enabling a new round of PARylation. Even though the half-life of PAR lies within seconds to minutes, the consequences of PAR metabolism can persist much longer. When PARP-1 is strongly activated such as in the presence of excessive DNA damage, the life-cycle of PAR consumes high amounts of NAD^+ and ATP, which can have disastrous consequences for a cell's fate, such as acidification (Affar el et al., 2002), necrosis (Xu et al., 2006), (Artus et al., 2010) or parthanatos. The latter is a caspase-independent form of cell death that is triggered by the release of apoptosis-inducing factor (AIF) from mitochondria, which is mediated by PAR (Yu et al., 2006; Yu et al., 2002), (Andrabi et al., 2006), (Wang et al., 2011). At the same time, the hydrolysis of PAR generates AMP, which is then recognized by the sensor protein named AMP-activated protein kinase (AMPK) (Hardie, 2007), (Huang et al., 2009), (Ethier et al., 2012).

Recent elegant structural studies of PARG with bacterial, protozoan and mammalian origin revealed the exciting finding that these enzymes consist mainly of a Macro domain-like-PAR interaction module (which resembles those found in PARP-9, -13 and -14 (see Figure 4)) complemented with a PARG-specific catalytic loop, which contains the key catalytic residues (Dunstan et al., 2012; Slade et al., 2011), (Kim et al., 2012).

Interestingly, a single gene for PARG encodes four different isoforms located in different cellular compartments. Besides a highly active nuclear isoform of 110 kDa, a short mitochondrial isoform of 65 kDa, as well as a two cytoplasmic splice variants of 102 kDa (missing exon 1) and 99 kDa (missing exon 1 and 2) (Meyer-Ficca et al., 2004), (Gagne et al., 2006) have been described.

Mice that are homozygous for a deletion of exon 4 in the PARG gene, which resulted in the depletion of all four PARG isoforms, have been shown to be embryonic lethal at an early stage (around day 3.5) due to the excessive accumulation of PAR (Koh et al., 2004). The protective role of PARG in the DNA damage response to DSBs is underpinned by the observation that a gene disruption of its 110 kDa nuclear isoform in mouse embryonic stem cells renders those more sensitive to γ-irradiation and alkylating agents (Cortes et al., 2004), (Gao et al., 2007), (Min et al., 2010). Moreover the gene-disruption of $PARG_{110}$ in mouse embryonic fibroblasts (MEFs) showed increased sister chromatid exanges (SCEs), micronuclei formation and an increased number of RAD51-IRIF after HU-treatment (Min et al., 2010). However, whether the contribution of PARG to the DNA damage response lies solely in counteracting the enzymatic activity of PARP-1 by degrading PAR, or whether PARG has independent enzymatic functions remains to be investigated.

Excitement has been growing in the field due to a recently discovered enzyme capable of degrading PAR which is ADP-ribosyl-acceptor hydrolase 3 (ARH3) (Oka et al., 2006). In a study from the Moss lab it has been recently suggested that ARH3 and PARG act sequentially, with PARG primarily detaching covalent PAR-modifications from acceptor proteins and ARH3 degrading free PAR and hence lowering the nuclear and cytoplasmic PAR-levels in order to prevent from PAR translocation and hence parthanatos. In addition, even though MAR-hydrolase activity has been observed in cells, debates are still ongoing whether or not PARG is capable of detaching the final ADP-ribose moiety which is directly attached to proteins (Oka et al., 1984) (Sharifi et al., 2013) (Slade et al., 2011). Only very recently, the enzymes possessing hydrolase activity have been uncovered, namely MacroD1, MacroD2 and C6orf130/ terminal ADPr-ribose glycohydrolase (TARG) and

interestingly, similar to PARG, they contain a macro domain (Jankevicius et al., 2013), (Rosenthal et al., 2013), (Sharifi et al., 2013), (Steffen and Pascal, 2013).

1.2.4 PARP-1 is activated by DNA damage

The mechanism of how DNA damage detection is coupled to PARylation has been a puzzling question due to the fact that DNA-binding is mediated by the N-terminus, whereas the catalytic domain lies in C-terminal end of the protein. Only recently the analysis of the 6 modular domains of PARP-1 has answered some important questions. The enzyme possesses three zinc finger domains (Znf1, Znf2 and Znf3), of which the two homologous zinc fingers Znf1 and Znf2 are located in close proximity to the N-terminus of the protein and recognize specific DNA-structures regardless of the base pair sequence. Znf3 on the other hand has a distinct structure and function from the other two (Langelier et al., 2008), (Tao et al., 2008). Additionally, PARP-1 contains a nuclear localization sequence (NLS), a leucine-zipper motif mediating homo-or heterodimerization and a central BRCT-binding motif. A C-terminal catalytic motif is composed of two subdomains, ART and HD. Most importantly, the ART domain is conserved among the ART/PARP-family of proteins and bears the NAD^+-binding residues and performs catalysis (D'Amours et al., 1999), (Langelier et al., 2012). In case of PARP-1, the catalytic domain carries out three distinct activities: the attachment of the initial ADP-ribose unit onto acceptor amino acid side chains, the polymerization step in which more ADP-ribose units are attached to the initial unit, and the introduction of branches in the polymer chains. The BRCT-domain was thought to contain the major residues of automodification (Tao et al., 2009). Interestingly, a recent study from our lab not only confirmed these results but identified 10 additional automodification residues within WGR, Znf2 and ART (Chapman et al., 2013a) with potential new, yet undiscovered roles in the regulation of PARP-1.

Only recently it has elegantly been demonstrated by the Drs Langelier, Pascal and others (Langelier et al., 2012), (Ali et al., 2012) how PARP-1 uses its specialized zinc fingers to detect DNA damage in a sequence-independent interaction with exposed nucleotide bases as they are found on many types of damaged DNA. How this protein-DNA interaction is then translated into catalytic activity has been suggested by the crystallization of a near full-

length PARP-1 (containing Znf1, Znf3 and WGR-CAT) loaded onto double-stranded DNA. In this study it has been suggested that the protein collapses on the DNA, with the Znf1, Znf3 and WGR collaboratively binding to DNA residues, resulting in a network of interdomain-contacts (Langelier and Pascal, 2013; Langelier et al., 2012), which leads to the transmission of the detected DNA damage to the catalytic domain (Figure 6). Earlier studies by the same group suggest that Znf2 and BRCT domains are dispensable for PARP-1-DNA-interaction (Langelier et al., 2011), (Langelier et al., 2012), (Altmeyer et al., 2009). However, these results need to be interpreted carefully as others have demonstrated that Znf2 is involved in binding of DNA breaks (Eustermann et al., 2011). Altogether, interdomain communication of PARP-1 seems necessary for its catalytic activation by DNA, but resolving the structure of the full-length PARP protein is crucial to the understanding of the biological role of each domain.

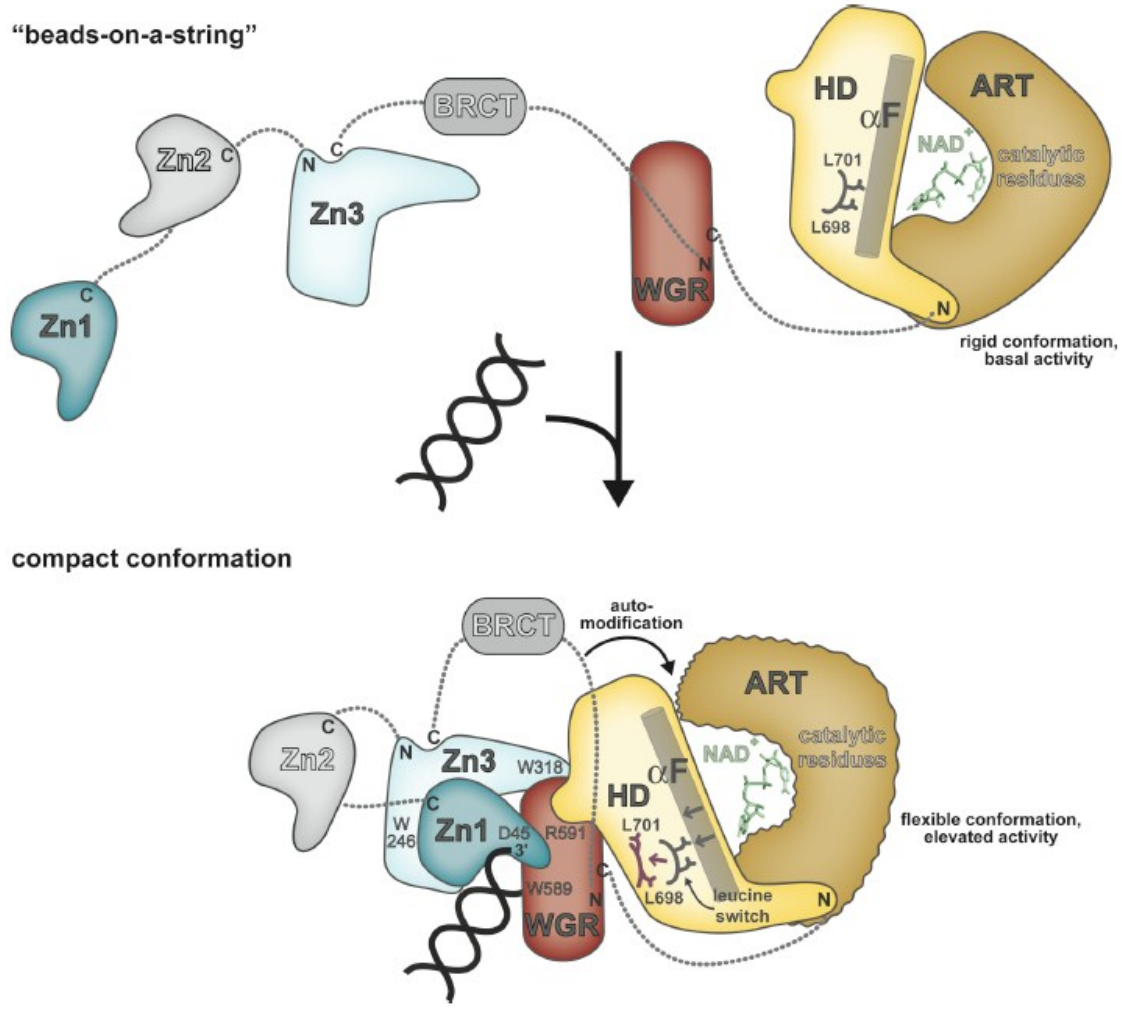

(Figure legend on the next page.)

Figure 6: DNA dependent activation of PARP-1
The Zn1/Znf1 and Zn3/Znf3 together with the WGR-domain have collectively collapsed onto a DNA double-strand break after automodification of PARP-1. The residues crucial for PARP-1-DNA-binding have been indicated (W589 and R591 in the WGR and D45 in the Zn1/Znf1). PARP-1 mainly interacts with the ribose-phosphate backbone of the DNA in a sequence unspecific manner. *Adapted from:(Langelier et al., 2012).*

Interestingly, PARP-1 activity can also be regulated by posttranslational modifications. AutoPARylation of PARP-1 for instance decreases the enzyme's catalytic activity, whereas phosphorylation by ERK1/2 can increase activity, as suggested by (Kauppinen et al., 2006).

1.2.5 PARP-1 influences DNA repair, chromatin structure, transcription

Generally, due to the high negative charge of PAR (twice the charge of DNA or RNA) PARylation of target proteins changes their physico-chemical characteristics dramatically and hence can influence their protein-protein or protein-DNA/RNA-interaction. Given the high affinity of many proteins for newly generated PAR, PAR itself is seen as an interaction scaffold and leads to PAR-mediated protein relocalization in different cellular contexts. PARP-1 has many protein partners in the nucleus ranging from those that (1) repair DNA, (2) regulate transcription, (3) methylate DNA and (4) modulate the chromatin structure (Krishnakumar and Kraus, 2010b). Many of these are also direct targets for PARylation (such as p53 (Mendoza-Alvarez and Alvarez-Gonzalez, 2001), (Kanai et al., 2007)).

Due to its high affinity for and its catalytic activation by DNA nicks and DSBs as mentioned above, PARP-1 has been extensively studied in the context of BER and DSB repair (DSBR). *The potential roles of PARP-1 in DSBR are a central subject of my thesis. We have discussed the current literature on this subject in a book chapter that has been published in "Advances in DNA Repair in Cancer Therapy" in 2013. The manuscript has been added as Chapter 2 to my thesis.*

Additionally, it has been suggested that PARP-1 is activated by DNA lesions introduced by UV light (such as thymidine dimers) and contributes therewith to nucleotide excision repair

(NER) (Vodenicharov et al., 2005). Herein, PARP-1 possibly stabilizes DNA-binding protein 2 and recruits ALC1 (Pines et al., 2012), (Robu et al., 2013), (King et al., 2012).

Since its discovery, studies on PARP-1 had its major focus on DNA damage detection and signaling. However, in the past few years, a body of evidence had been growing for additional roles of PARP-1, as for instance in the regulation of gene expression (Krishnakumar and Kraus, 2010b), (Kraus, 2008). It already became evident in the late 1960s that PARP-1 can be considered as a chromatin modulator as major targets for PARylation are histones, which is due to the negative charge leading to relaxation of the chromatin (Honjo et al., 1968), (Nakazawa et al., 1968), (Otake et al., 1969). Dr G.G. Poirier had elegantly shown in 1982 using native pancreatic chromatin in his electron micrographs, that PARP-1 in the presence of NAD^+ is able to relax chromatin (Poirier et al., 1982). In contradiction to the aforementioned findings, the lab of Dr. Ladurner has recently published mechanistic insights on how the macrodomain-containing histone macroH2A1.1 senses PAR generated at damage sites through its macrodomain, leading to the compactation of local chromatin and a reduced recruitment of Ku70 and Ku80 (Timinszky et al., 2009).

Adding another layer of complexity to the biology of PARP-1, the lab of Dr Lee W. Kraus had demonstrated that the protein can be detected at many promoters of actively transcribed genes (Krishnakumar et al., 2008). This binding correlates with Polymerase II-binding and the presence of H3 lysine 4 trimethylation, a modification of Histone 3, which marks active promoters and indicates gene expression. As mentioned before, in response to genotoxic stress, PARP-1 is recruited to DNA damage sites. However, whether the overall distribution of PARP-1 changes (from active promoters to DNA damage sites) is still not clear. Moreover, in an indirect manner, PARP-1 can modify the chromatin landscape by PARylating KDM5B, which inhibits its chromatin binding ability and hence its ability to demethylate H3 lysine 4 trimethyl (H3K4me3) (Krishnakumar and Kraus, 2010a).

Interestingly, PARP-1 has been suggested to influence transcriptional activity at the sites of DNA damage by recruiting the chromatin-remodeling transcriptional repressor proteins of

the polycomb group (such as RING1 and EZH1) and components of the repressive NuRD nucleosome remodeling and deacetylase complex (e.g. MTA1) (Chou et al., 2010). The previous study suggests that at DNA damage sites, the role of PAR-mediated signaling is important to facilitate the removal of nascent RNA and elongating RNA polymerases to block transcription in favor of DNA repair. However, whether this occurs in a direct manner and what the specific function of PARP-1 may be in RNA biology remains an interesting question to be addressed in future studies.

1.2.6 The readers of PARylation

As mentioned above, the enzymatically active PARPs (predominantly PARP-1) use NAD^+ as a donor of ADP-ribose units for the synthesis of PAR. To date, four different well established PAR-binding motifs have been described (Figure 7): The highly abundant PAR-binding motif (PBM), the PAR-binding zinc-finger (PBZ), the Macro domain and the most recently discovered WWE domain. Some of the these domains are even found in PARP proteins themselves (Figure 4). Additionally, examples for RRM (Krietsch et al., 2012), FHA, BRCT-domains (Li et al., 2013) and GAR-domains (Isabelle et al., 2012) that have an affinity for PAR have been recently uncovered.

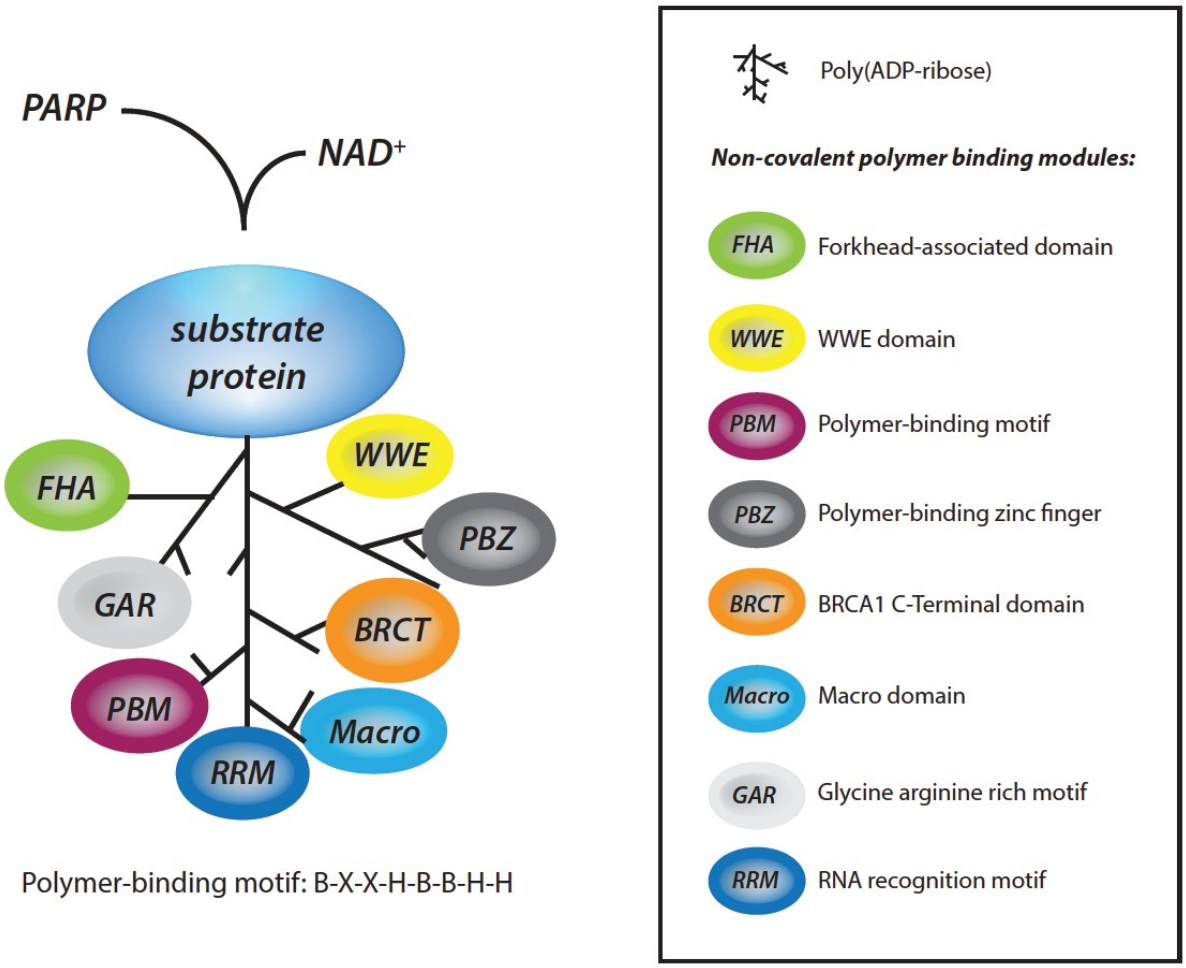

Figure 7: Schematic illustration of covalently attached PAR and non-covalently bound PAR by polymer binding motifs (PBM)
PAR can be covalently attached to the Lys, Glu or Asp residues of substrate proteins. Free or covalently attached PAR functions itself as a signal transducer through non-covalent binding to proteins containing the protein domains displayed as colored circles. *(Modified from (Krietsch et al., 2013).*

Within the last few years, the list of proteins containing PAR-binding motifs, enabling non-covalent binding to PAR, has been rapidly expanding. *We have discussed the current literature on PAR-binding modules, the proteins containing them and their respective role in cellular pathways in a manuscript published in "Molecular Aspects of Medicine". The subject of the review article lies beyond the main topic of this thesis which is why it was added to the Annex.*

1.2.7 Inhibition of PARylation as a therapeutic strategy for cancer treatment

Inhibition of the catalytic activity of PARP-1 has become a promising therapeutic approach for several human diseases, predominantly cancer. Most prominent PARP inhibition has been observed with inhibitors that act as competitors to NAD^+, aiming for the same binding site in the PARP molecule. A fundamental feature of cancer cells as mentioned earlier is a rapid proliferation rate in the presence of high genomic instability when compared to noncancerous cells (Hanahan and Weinberg, 2000). Thus, it is not surprising that exposure to chemicals or physical agents that introduce DNA damage and genomic instability can cause mutations and lead to the development of cancers. In line with that, inherited defects in the DNA damage response often correlate with cancer-predisposition. Paradoxically, if surgery alone is not sufficient, the most prevalent cancer treatments to date are radiotherapy and chemotherapy, both introducing excessive DNA damage. As mentioned previously, PARP-1 and PARP-2 facilitate DNA repair and the PAR produced in response to damage serves as a platform to recruit DNA repair proteins, which is why in the early 1980s, first PARP inhibitors, the rather unspecific benzamides (Purnell and Whish, 1980), were developed in order to inhibit PARP activity. Later on, a new and more specific class of PARP inhibitors has entered clinical trials either as chemopotentiator or as a single-agent therapy (for review see (Rouleau et al., 2010) and (Garber, 2013)).

Numerous clinical trials, many of which focus on a principle entitled “synthetic lethality”, are now in progress or finished, mainly with breast, ovarian and uterine cancers (Rouleau et al., 2010), (Garber, 2013). Synthetic lethality arises when the combination of two dysfunctional proteins leads to cell death whereas only one would have left cell viability unaffected. In the case of PARP inhibitors, PARP inhibition has been coupled with mutations in key DNA repair genes such as BRCA1 or BRCA2 (Bryant et al., 2005), (Farmer et al., 2005). Thereby PARP inhibitors target cells that are already defective in one repair pathway by inhibiting another, leaving DNA repair-proficient cells unaffected.

In addition to the well-studied examples of BRCA1 and -2, phosphatidylinositol 3,4,5-trisphosphate 3-phosphatase and dual-specificity protein phosphatase (PTEN), that regulates the expression level of RAD51, is often mutated in cancer cells, which in some

cases renders them sensitive to PARP inhibitors (Mendes-Pereira et al., 2009). Moreover, breast cancer cells deficient for p53 lose their resistance to doxorubicin (a clinically active antitumor anthracycline antibiotic that promotes apoptosis) when treated with a PARP inhibitor (Munoz-Gamez et al., 2005).

Over six phase III clinical trials are already ongoing or about to be started in the United States (Table 1 as adapted from (Garber, 2013)). However, even though extensive effort has been undertaken to put PARP inhibitors into clinics, the mechanistic action of these drugs as well as their specificity are surprisingly little understood and need further investigation.

Table 1: PARP inhibitors in late-stage clinical trials
Adapted from: (Garber, 2013).

Company	Inhibitor	Phase III indications
Astra Zeneca	Olaparib (AZD-2281)	Ovarian cancer with BRCA mutations
Tesaro (licensed from Merck)	Niraparib (MK4827)	BRCA and non-BRCA-platinum-sensitive serous ovarian cancer
BioMarin Pharmaceuticals	BMN 673	Germline *BRCA*-mutant metastatic breast cancer
Clovis Oncology (licensed from Pfizer)	Rucaparib (CO288)	BRCA and non-BRCA platinum-sensitive serous ovarian cancer, maintenance setting
AbbVie	Veliparib (ABT-888)	Undisclosed to date

Several mechanistic explanations have been given for the synthetic lethal relationship between PARP inhibitors and homologous recombination defects (reviewed in (De Lorenzo et al., 2013). In brief, PARP inhibition (i) disables the BER pathway, leading to the accumulation of DSBs which cannot be repaired by HR, (ii) activates the error-prone NHEJ

pathway and/or (iii) traps the PARP-1 protein at DNA damage sites and hence prevents from the recruitment of important repair factors.

Besides the mechanism, another fundamental question still being debated is concerning the specificity of PARP inhibitors used already in clinics for the individual PARP proteins and for the specific cellular context of PARP (e.g. DNA repair or transcription). Only very recently, it has been demonstrated that compounds that have reached phase III clinical trials can bind to and inhibit several PARP family members (Wahlberg et al., 2012). Moreover, there might be a therapeutic interest in inhibitors that specifically inhibit PARPs role in the DDR but leaving its role in RNA biology unaffected.

Conclusively, fundamental research on the functions of PARPs and their partner proteins in the DNA damage response as presented in this thesis are indispensable to understand and improve current therapeutic strategies which are based on the inhibition of the catalytic activity of PARP-1.

1.3 Mass spectrometry-based proteomics as an approach to analyze the PAR-interactome

The enzymatic activation of PARP-1 resulting in PARylation is one of the earliest events in DNA damage sensing and signaling. Key factors of the DDR are recruited to the sites of damage in a PAR-dependent manner, hence PAR acts as a scaffold molecule, facilitating accurate repair. It is therefore of great interest to understand the PAR-protein interactions in greater detail. An increasingly powerful technology to identify components of protein complexes is mass spectrometry-based proteomics. This technically challenging approach has been used exhaustively in our lab and others to identify PAR-binding proteins in the response to DNA damage (Gagne et al., 2003), (Gagne et al., 2008), (Gagne et al., 2011), (Gagne et al., 2012), (Isabelle et al., 2012). *A very brief description of the principles of*

peptide sequencing which is important for the interpretation of proteomics data as presented in my thesis is given in the following.

1.3.1 The principle of peptide sequencing

In the 1990s mass spectrometry (MS) approaches for peptide sequencing started to evolve. MS is based on biomolecules that are ionized and, following their specific trajectories in a vacuum system, their mass is measured. As an advantage over older techniques such as Edman sequencing, proteins or peptides do not need to be purified prior to sequencing by MS and there is no problem for identifying chemically modified proteins, hence enabling the characterization of protein complexes.

The first necessary step for a protein sample to be analyzed by MS is the purification of a protein or protein complexes from a biological source as by affinity purification or fractionation. These techniques may be followed by SDS-PAGE or 2D-gel electrophoresis which helps to further separate the components of the complex (Figure 8). Subsequently, purified proteins need then to be converted to peptides. Sequence specific proteases such as trypsin are often used to convert proteins to to peptides, therefore cleaving the proteins on the carboxy-terminal side of arginine and lysine residues.

In a subsequent step, peptide samples are injected into ionization source which can be done directly or through a chromatography approach in order to be separated, such as microscale capillary High-Performance Liquid Chromatography (HPLC), gas chromatography or capillary electrophoresis. Once the sample has entered the ionization source, a process named "electrospray ionization" (whose discovery earned a Nobel Prize in Chemistry in 2002) takes place in which the peptide sample is vaporized and peptides are subsequently ionized using a strong electric potential. Another way to ionize peptides is a two-step mechanism that resembles the electrospray method called matrix-assisted laser desorption/ionization (MALDI). In MALDI, desorption is triggered by a UV laser-beam. The laser-light is heavily absorbed by a matrix, leading to its ablation, which is creating a hot plume. Then the analyte molecules are ionized in the hot plume.

Once inside the vacuum system of the mass spectrometer, a mass analyzer acts in order to separate the ions formed by the ionization source described above in electric fields. Many types of mass analyzers exist, differing in their way of how to determine a peptide mass-to-charge (m/z)-ratio, their achievable resolution and their mass accuracy. In a Q-Q-TOF mass spectrometer, ionized peptides are separated in a quadrupole, based on the stability of their trajectories in the oscillating electric fields that are applied to the rods. In the Time of Flight (TOF) mass-spectrometer on the other hand, the m/z-ratio is measured as a means of time. For that, ions are accelerated and their velocity (which is determined by their mass-to-charge ratio) is measured. A Quadrupole Ion Trap refers to an ion trap that uses constant or radio frequency oscillating alternating current (AC) electric fields to trap the ionized peptides.

Mass spectrometry/ mass spectrometry (MS/MS), also called tandem-MS (because it couples two stages of MS), is a high-resolution method to examine individual ions from a complex mixture of ions. It uses two instead of only one analyzer (MS) which are connected with a collision gas cell enabling structural and sequencing studies.

A detector monitors the ion current, amplifies it and provides a read-out of the mass spectrometer in the data system as MS-peaks (total ion intensity over time), which need to be carefully interpreted. There are two general approaches: *De novo* sequencing is derived solely from the amino-acid sequence obtained from the MS-analysis and relies on data of a very high quality. However, in the 1990s, researchers coupled the peptide-sequencing process with a database-matching approach, overlaying the obtained amino acid sequence (maybe insufficient for *de novo* sequencing) with amino acid sequences from a database of known protein sequences.

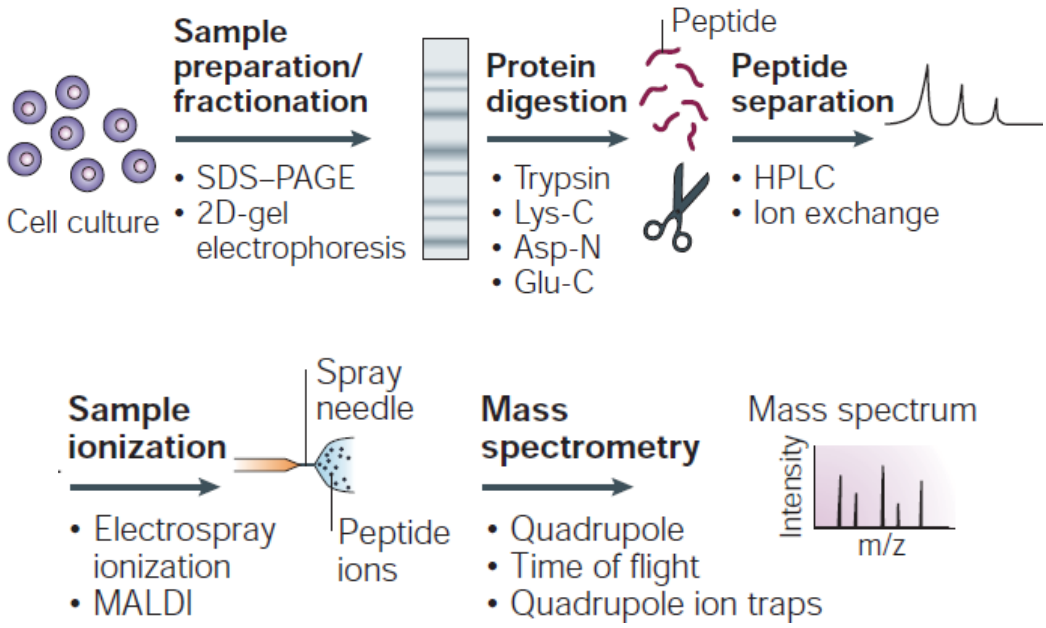

Figure 8: Exemplary mass spectrometry proteomic experiment
A detailed description of the method is given in the text.
Adapted from: (Steen and Mann, 2004).

Generally, protein samples are used in an unlabeled form for MS-analysis. However, for accurate protein quantification (as for instance from two different biological sources) different labeling methods exist. One elegant variant of quantitative proteomics is based on an *in vivo* incorporation of a label into proteins, prior to the MS-analysis. The method is called stable isotope labeling by amino acids in cell culture (SILAC) and relies on metabolic incorporation of a "heavy" or "light" form of the corresponding amino acid (Ong et al., 2002) which enables the distinction between two biological sources (e.g. before and after damage) in the same sample. A second method to study quantitative changes is named isobaric tags for relative and absolute quantitation (iTRAQ) and is based on labeling of the N-terminus of peptides with tags of varying masses. In this approach, differently labeled peptides from different sources can be pooled and identified by MS/MS-approaches.

1.3.2 The PAR interactome as revealed by MS

Over the past few decades, several hundred proteomic studies have been conducted to analyze the diverse physiological contexts in which PARP-1 and its polymer act (reviewed

in (Pic et al., 2011)). Using a MALDI-TOF-MS approach the lab of Dr Guy G. Poirier uncovered as a surprise for the PARP-field in 2003 the heterogenous nuclear ribonucleoproteins (hnRNPs) as a new family of PAR-binding proteins in HeLa cells (Gagne et al., 2003). HnRNPs are generally described as proteins that bind to premature RNA as part of protein complexes that influence mRNA maturation. In the case of the hrp38 and hrp40, their splicing activity has been suggested to be regulated by PARP-1 and PARG (Ji and Tulin, 2009). However, the functions of the individual hnRNPs are not yet well understood and are potentially exceeding the direct subject of RNA biology.

In 2008, a large-scale proteomics approach conducted by the lab of Dr Poirier to identify PAR-interacting proteins not only confirmed the previous study but moreover described proteins from the DNA damage response and chromatin regulation as part of the PAR-interactome (Gagne et al., 2008).

Two years later, in 2010, the lab of Dr Poirier published a LC-MS/MS study, using the two DNA-dependent PARPs PARP-1 and PARP-2 as "bait". Interestingly, in this study, the presence of many RNA-binding proteins were confirmed for the PARP-1-associated proteome. Additionally, key DNA DSBR factors (such as Ku70, Ku80, DNA-PK and others) were identified in complex with either PARP-1, PARP-2 or PARP-3 (Isabelle et al., 2010), (Rouleau et al., 2007).

However, whether the interactions described above are direct and static or rather dynamic assemblies in the response to DNA damage and thus actually biologically relevant, still needs to be carefully examined. *We have hence conducted a proteomic approach that follows protein-dynamics of the whole proteome in the context of PARylation after DNA-damage. The study has been published as a highlight article in Nucleic Acid Research in 2012 and can be found as Chapter 3 of my thesis.*

1.4 RNA-binding proteins in the DNA damage response

As mentioned above, several proteomic studies conducted from our lab and others in the past years uncovered RNA-binding proteins as PAR interactors in response to DNA-damage. Interestingly, an increasing number of studies suggest a mechanistic link between RNA-metabolism and DNA repair (Shanbhag et al., 2010), (Jungmichel et al., 2013). A growing list of RNA-processing proteins seem important for resistance to genotoxic stress in a yet uncharacterized mechanism that relies on catalytic activity of PARP-1, as described in the following.

A prominent example is the heterogenous ribonucleoprotein named RNA-binding motif protein, X chromosome (RBMX) which has been suggested by the group of Dr S.J. Elledge as a positive regulator of the homologous recombination repair pathway (Adamson et al., 2012). A siRNA based screen for proteins that regulate HR revealed that a knockdown of RBMX decreased HR by 7 % (as indicated by the GFP^+-readout of their reporter assay), which can be compared to key HR proteins, such as BRCA2 and RAD51, which decreased the efficiency of HR in the same assay by 5 % and 11 %, respectively. Interestingly, the authors stated that the recruitment of RBMX to DNA-damage sites depends on PARP-1 catalytic activity.

Another protein from the hnRNP family of proteins, namely hnRPUL1, has been shown to be recruited to DNA damage induced in living cells by laser micro-irradiation in a PARP-dependent manner (Hong et al., 2013).

Only very recently, the RNA-binding protein Fused in Sarcoma (FUS) was described as a new PAR-binding protein, which directly interacts with PAR through arginine/ glycine-rich RGG/GAR-domains. The protein recruits to DNA damage sites, which can be blocked by the catalytic inhibition of PARP using the inhibitor PJ-34. Moreover, the authors demonstrated that in *in cellulo* reporter assays FUS promotes NHEJ as well as HR (Mastrocola et al., 2013).

In a refined SILAC LC-MS/MS study using the PAR-binding macro domain as a bait it was only very recently proposed that the above mentioned RBMX and FUS protein as well as other RNA processing factors might also be direct targets of PARP-1, as they were found to be covalently modified in response to four different types of DNA damages (H_2O_2, MMS, UV and IR) (Jungmichel et al., 2013). Moreover, the aforementioned study confirmed the PARylation of proteins that are involved in RNA metabolic processing upon genotoxic stress. The authors had investigated two of their detected PARylated proteins, TAF15 and THRAP3, in a higher resolution and found that PARylation coordinates their subnuclear localization. This interesting finding could explain the intriguing observation made by Dr Choudhary and his group in 2012, where he described that TAF15 migrates towards the damage sites of laser-induced DNA damage whereas THRAP3 was excluded from these sites (Beli et al., 2012). Nevertheless, whether these recruitment behaviors are really PAR-related still needs to be investigated.

Although recent genome-wide proteomics and siRNA screens as described above established a functional intersection of RNA processing with DNA repair, only very few RNA-processing factors have been examined in detail for their specific link to the DDR. Interestingly, our and other proteomic studies identified a protein called "Non-POU-domain-containing-octamer-binding-protein" (NONO) as an abundant potential PAR-binding protein or PARylation target in response to DNA damage (Gagne et al., 2008; Jungmichel et al., 2013), (Isabelle et al., 2012). As described below, first evidence suggested that this protein is important for the cell's response to genotoxic stress. *We have hence chosen to investigate the mechanistic link between the PAR- and RNA-binding-protein NONO with the DNA damage response. A brief introduction on NONO and its paralogues is given in the following and the manuscript containing my scientific findings has been added as Chapter 4 to my thesis.*

1.4.1 Discovery of NONO and its DBHS paralogues

The Drosophila behavior human splicing (DBHS) family of proteins has its name from the no-on-transient-A protein (NONA) protein of *Drosphila melanogaster*, which has been detected on the X-chromosome in a genetic screen in 1993 for visual and courtship

behavioral phenotypes (Stanewsky et al., 1993). In humans, the protein family consists of the Non-POU domain-containing octamer-binding protein (NONO), the splicing factor proline-/ glutamine-rich (SFPQ) and the paraspeckle component 1 (PSPC1). Interestingly, only NONO and SFPQ are highly abundant in cells and ubiquitously expressed. PSPC1 on the other hand is expressed at comparatively low levels. The only cell line described to date that highly expresses all three paralogues is the sertoli cell line TTE3, in which they are thought to enhance androgen-receptor mediated trans-activation (Kuwahara et al., 2006).

Originally searching for a homolog of the *Saccharomyces cerevisiae* splicing factor PRP18 in humans, the group of A.R. Krainer described the nuclear RNA-binding protein, 54 kDa (p54nrb), alias NONO (Dong et al., 1993), as cross-reacting with the PRP18 antibody. Interestingly, NONO has no specific homology with PRP18, but about 70 % sequence similarity with its partner protein SFPQ. For SFPQ, the cDNA sequence and RNA-binding activity was first described by two individual labs in 1991 (Gil et al., 1991), (Patton et al., 1991).

1.4.2 Domain structure of the DBHS proteins

A region of around 300 amino acids (aa) flanked around a tandem RNA-recognition motif (RRM1/RRM2) is conserved between human DBHS proteins (Figure 9). Interestingly, RRMs (also called RNA binding domains (RBD)) or ribonucleoprotein domains (RNPD) are among the most abundant protein domains in eukaryotes and early work had identified these domains in a variety of RNA-binding proteins. Its structure is very well characterized, consisting of an approximate length of 90 amino acids containing two α-helices on a four-stranded β-sheet. However, the mode of RNA/DNA and even protein-protein interaction through these domains has been described only for a few RRM-containing proteins. Around 44 % of all RRM-containing proteins contain more than one of these motifs (from 2 up to 6). In recent years, the spectrum of functions for RRMs has widely broadened: It serves not only as a platform for RNA binding, but also for DNA-protein and protein-protein interactions. Many RRM-containing proteins participate in RNA biogenesis. However, many of them also participate exclusively in processes like transcriptional regulation (Newberry et al., 1999) and most importantly in the DDR (Hamimes et al., 2006). Different

concepts have evolved on how RRM-RRM binding for instance can either increase or compete with RNA binding. Moreover proteins bound to RRMs have been described as competitors for RNA-binding (Clery et al., 2008), (Passon et al., 2012), (Maris et al., 2005), (Birney et al., 1993), (Kenan et al., 1991).

The N-/C- terminal extensions of SFPQ and PSPC1 differ compared to NONO, which is with about ~ 400 amino acids (aa) shorter than the other two paralogues. SFPQ, the longest paralogue, contains an extra ~ 300 aa that are low in complexity (proline/ glutamine-rich), adding up to a total length of ~ 700 aa. At least for NONO and PSPC1, a coiled-coil region of ~ 100 aa putatively responsible for protein-protein interaction has been predicted. NONO and PSPC1 have been predicted to contain a NONA/paraspeckle (NOPS) domain of 52 aa. This domain represents a new form of protein-protein interaction through unique binding to the RRM2 of its DBHS partner protein.

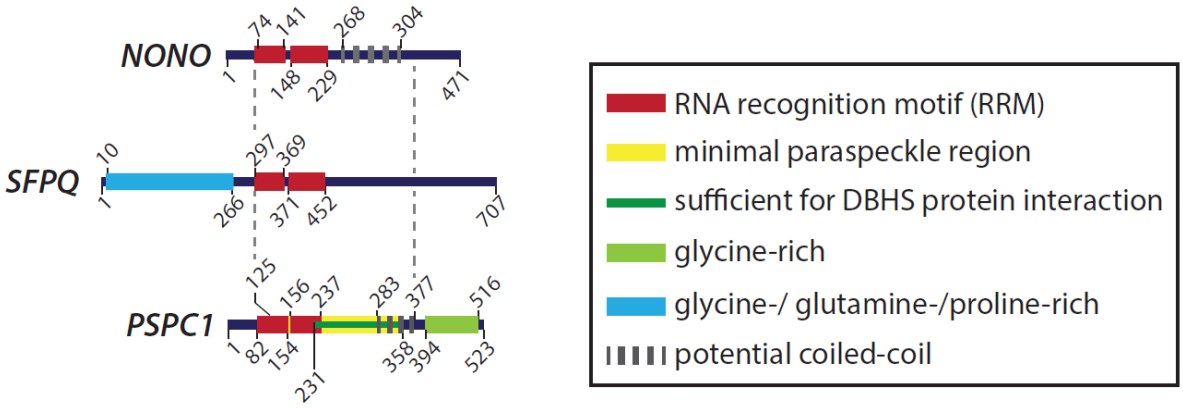

Figure 9: Schematic domain structure of the DBHS protein family members
Protein domains were defined as colored boxes according to Universal Protein Resource (UniProt). The DBHS family of proteins consists of clearly defined structural domains, consisting of two tandem RRMs and in case of NONO and PSPC1 of predicted coiled-coil domain which potentially allows protein-protein-interaction.

1.4.3 DBHS proteins in the context of RNA

Initially after its discovery, NONO was thought to participate in transcriptional co-activation as for example of the androgen receptor (Ishitani et al., 2003), (Dong et al., 2007). However, whether NONO is a transcription factor *per se* and its exact function in RNA maturation is still a matter of ongoing debate.

SFPQ was initially regarded as a pre-mRNA modifying protein due to its affinity for the polypyrimidine tract binding protein (PTB), a characteristic from which the protein got its alternative name "PTB-associated splicing factor" (PSF). SFPQ has been shown to be essential for splicing in *in vitro* experiments (Patton et al., 1993). Another role has been annotated to SFPQ in the context of transcriptional regulation. It has been shown that SFPQ binds the insulin-like response factor element in the porcine *P450scc* gene which normally produces a steroid, however, when SFPQ is bound to the element, transcription is suppressed (Urban et al., 2000), (Urban et al., 2002), (Urban and Bodenburg, 2002).

Both NONO and SFPQ are found in complex with histone deacetylase (HDAC) and a protein named steroidogenic factor-1 (SF-1) and are, in this context, able to repress basal transcription of the human *CYP17* gene, which is involved in steroidogenesis (Sewer et al., 2002), (Sewer and Waterman, 2002).

Also, both NONO and SFPQ have an affinity for defective RNAs. Interestingly, both proteins interact strongly with the ATM target Matrin-3, a protein that is associated with the inner nuclear membrane, but that does not bind to RNA itself. Hence it has been suggested by the group of Dr. Shiloh that Matrin-3 acts like an anchor for NONO/SFPQ to retain edited RNA in the nucleus to prevent from its translation (Salton et al., 2011). The same can also occur in subnuclear bodies termed paraspeckles. Within these paraspeckles, NONO/SFPQ and PSPC1 interact with the long non-coding RNA NEAT1 through binding of adenosine-to-inosine edited inverted-repeat hairpins in its 3'- UTR. At least for NONO, the specific affinity for A-to-I edited RNAs has been confirmed *in vitro* and *in vivo* (Zhang and Carmichael, 2001).

However, despite the proposed roles of NONO and SFPQ in the context of RNA biology, immunofluorescence approaches and proteomic studies have implicated them in a wide range of cellular contexts, as for example in strong association with the chromatin and the nucleolus (Andersen et al., 2002).

1.4.4 DBHS proteins in the context of DNA DSB repair

Interestingly, in addition to their RNA-binding properties, NONO and SFPQ have a strong affinity for DNA, which has led to their investigation in the context of transcription and lately DNA repair. In the case of NONO it was shown more specifically that it binds ssDNA through its N-terminus and dsDNA through its C-terminus (Yang et al., 1993) SFPQ's affinity for DNA has been demonstrated to accelerate the annealing of complementary single-stranded DNA, promoting invasion of a ssDNA-strand into supercoiled DNA (Akhmedov and Lopez, 2000), such as during the D-loop formation step of HR repair.

In a search for protein factors that stimulate end joining reactions in a test tube, a protein complex with a size of around 200 kDa of unknown identity has been described (Bladen et al., 2005). By two-dimensional gel electrophoresis and subsequent mass spectrometry analysis of the bands of interest the authors have been able to identify the two major proteins present in these fractions as NONO and SFPQ. The authors show that the heterodimer NONO/SFPQ potentially stimulates end-ligation of a linearized plasmid. Nevertheless, from these experiments one can neither conclude whether this is intrinsic to the NONO/SFPQ hetero-dimer, nor say whether it resides in a tightly associated protein, nor distinguish between NONO and SFPQ (Bladen et al., 2005).

Subsequent results published from the same group (Li et al., 2009) suggested a role for NONO independent of SFPQ in the cellular survival of low dose ionizing irradiation. From these cellular assays they have proposed that NONO is directly implicated in the DDR response to DSBs. More specifically, the authors have shown that a depletion of the NONO protein by miRNA renders HCT116 cells sensitive to ionizing radiation of two Gray and leads to an accumulation of chromosomal aberrations. Moreover, in IMR-90 cells the

resolution of γH2AX foci induced by ionizing radiation has been delayed by a siRNA directed against NONO in comparison to cells where a control siRNA has been used (Li et al., 2009). However, even though the authors clearly show a role for NONO in radioresistance, they do not provide direct insight on how NONO influences DSB repair.

Surprisingly, different from NONO, SFPQ is essential for human cells even in the absence of DNA damage. Hence, to study SFPQs contribution to cellular sensitivity to ionizing radiation, an elegant genetic rescue assay based on co-transfection of a miRNA directed against SFPQ and a plasmid coding for truncated SFPQ genes had been undertaken. By doing so, the group of Dr William Dynan has clearly demonstrated that a sequence required for radio-resistance lies within the N-terminus. Interestingly, the same sequence that rescues a radio-resistant phenotype in HeLa cells is also of importance for the protein's recruitment to laser-induced DNA damage, independent of its partner protein NONO. In addition, a knock-down of SFPQ increases cellular sensitivity to DNA-crosslinking agents, such as MMC and delays the disappearance of 53BP1 foci (Rajesh et al., 2011).

Moreover, SFPQ directly interacts with RAD51 through its N-terminus and cooperates with it in *in vitro* DNA pairing and strand-displacement assays (Morozumi et al., 2009). SFPQ promotes annealing of complementary ssDNA and invasion of supercoiled DNA by complementary oligos to form a D-loop structure. SFPQ, regardless of its partner protein NONO, has been shown to directly interact with RAD51 with whom it cooperates in strand-displacement assays (Morozumi et al., 2009). Additionally, the group of Douglas L. Pittman suggested that SFPQ directly acts on HR through an interaction with the RAD51 paralogues RAD51D, RAD51C and XRCC2 (Rajesh et al., 2011).

Objectives

As introduced above, catalytic activation of PARP-1 and the generation of PAR are one of the earliest events in the DNA damage response to DSBs. The PAR that is generated upon damage is generally accepted as a scaffold to recruit important factors for the DNA damage response. By mass spectrometry approaches, our lab and others have identified many key DNA repair proteins and as a surprise for the field, RNA-binding proteins in a complex that centers on PAR. However, whether these complexes are based on direct interactions with PAR and if so, whether this interaction is dynamic and actually part of the DDR has been poorly understood. Moreover at the site of DNA damage the role of DNA repair and RNA metabolism is likely to be different. I have hence centered my thesis on the following questions:

1. According to the literature, can PARP-1 be named a DSB repair protein? (Chapter 2)

2. Is the PAR interactome dynamic in response to DNA damage and if so, what is its kinetics? (Chapter 3)

3. Do the DNA damage signaling and repair proteins follow different kinetics than the factors acting on RNA-metabolism? (Chapter 3)

4. The RNA-binding protein NONO is highly abundant in many of the individual MS-analyses of the PAR interactome, but is this protein directly binding to PAR? If so, what is the biological function of its interaction with PAR? (Chapter 4)

5. In the literature, NONO has been suggested to influence the outcome of DSB repair by NHEJ. Can we confirm that NONO is actually involved in repair and if so, is it also affecting the other DSB repair pathway, namely HR? (Chapter 4)

CHAPTER 2

POLY(ADP-)RIBOSE POLYMERASE AT THE INTERFACE OF DNA DAMAGE SIGNALING AND DNA REPAIR

Jana Krietsch[1, 2], Michèle Rouleau[2], Michel Lebel[1], Guy Poirier[2], and Jean-Yves Masson[1,3,4]

[1] Genome Stability Laboratory, Laval University Cancer Research Center, Hôtel-Dieu de Québec, 9 McMahon, Québec city (Qc), G1R 2J6, Canada

[2] Cancer Research Unit, Laval University Medical Research Center, CHUQ-CRCHUL, Québec, QC, Canada, G1V 4G2

[3] Canadian Institutes of Health Research New Investigator.

[4] Corresponding author

Preface

Within the first year of my PhD Dr Guy G. Poirier had been invited by Dr Lawrence Panasci to contribute with a chapter to the book "Advances in DNA repair in Cancer Therapy." I have therefore gratefully taken the opportunity he offered me, which was to review the current literature on the two major expertise of our co-direction: PARP (lab of Dr G.G. Poirier) in the context of DNA repair (lab of Dr J.Y. Masson). This work allowed me to integrate the knowledge in the field and revealed a variety of unanswered questions. For example, PARP-1 has long been considered as a participant in the base excision repair pathway of single-strand breaks. However, its exact role has not been demonstrated and the literature remains controversial. Same has been described for PARP-1 in the context of other repair pathways such as HR and NHEJ. In the present review article I have hence elaborated the longstanding question whether PARP-1 is a DNA repair protein *per se* or rather a DNA damage detection and signaling protein.

I have done all the writing, generated the Figures and have gratefully profited from discussion of the manuscript with all the co-authors mentioned on the manuscript.

Résumé

Les cassures double-brin chromosomiques (CDB) sont extrêmement dangereuses pour la cellule car celle-ci ne dispose plus d'un brin complémentaire intact pour en effectuer la réparation. Si elles ne sont pas réparées avec précision, les chromosomes cassés peuvent subir une grande variété de réarrangements, telles que des translocations, délétions et mutations, pouvant induire la mort cellulaire (Moynahan and Jasin, 2010). L'instabilité génomique peut favoriser le cancer, les anomalies du développement, la neurodégénérescence, l'immunodéficience, le vieillissement, ainsi que l'hypersensibilité aux rayonnements. Chaque jour, une cellule subit environ 50 CDBs générées de façon intrinsèque, comme lors de la synthèse de l'ADN quand la fourche de réplication détecte une base endommagée (Vilenchik and Knudson, 2003). Des CDBs peuvent également être créées au cours de processus métaboliques, tels que le V(D)J et la recombinaison de commutation de classe dans les lymphocytes de vertébrés, la recombinaison méiotique dans des lignées de cellules germinales et la commutation de type sexuel chez la levure. Les sources exogènes, tels que les rayons X, les rayons gamma, les rayons UV, la topoisomérase I + II, peuvent produire des CDBs entre autres types de dommages à l'ADN. La réponse cellulaire aux dommages à l'ADN est constituée de multiples étapes régulatrices, en commençant par la détection des dommages et le recrutement de protéines de réparation au site de dommage jusqu'à l'exécution de la réparation de l'ADN qui réserve différents sorts à la cellule (comme l'apoptose ou l'entrée en différenciation terminale par la sénescence afin d'éviter d'hériter de l'ADN endommagé). Fait intéressant, certains membres de la famille des poly (ADP- ribose) polymérases (PARP) ont été impliqués dans la détection des dommages à l'ADN ainsi que la réparation des cassures simple- et double-brin, leur donnant un rôle unique et universel dans la réponse d'une cellule à l'endommagement de l'ADN. Trois PARPs connues pour être activées par les dommages de l'ADN (PARP- 1 ainsi que PARP- 2 et possiblement PARP- 3) sont discutées dans ce chapitre avec une emphase sur les deux principales voies qui ont évolué pour réparer les CDBs: la jonction des extrémités non-homologues (NHEJ) et la recombinaison homologue (RH).

Abstract

Chromosomal double-strand breaks (DSB) are extremely hazardous to a cell as they do not leave an intact complementary strand to be used for repair. If not repaired accurately, the broken chromosomes undergo a wide variety of rearrangements such as translocations, mutations, and deletions that may lead to cell death (Moynahan and Jasin, 2010). Genomic instability can promote cancer, developmental defects, tissue neurodegeneration, immunodeficiency, aging, as well as hypersensitivity to radiation. Each day a cell encounters approximately up to 50 DSB, generated intrinsically such as during DNA synthesis when the processing replication fork encounters a damaged template (Vilenchik and Knudson, 2003). DSBs can also be created during metabolic processes such as V(D)J recombination and class-switch recombination (CSR) in vertebrate lymphocytes, meiotic recombination in germ cell lines, and mating type switching in yeast. Exogenous sources such as X-rays, gamma rays, UV light, topoisomerase I + II inhibitors can produce DSBs amongst other types of DNA damage. The cellular response to DNA damage consists of multiple regulatory layers starting with sensing the damage, recruitment of repair proteins to the site of damage, and execution of DNA repair with possible outcomes concerning the cells fate (such as apoptosis, entering terminal differentiation through senescence in order to prevent from inheriting damaged DNA). Interestingly, some members of the poly (ADP-ribose) polymerase (PARP) family have been implicated in DNA damage sensing as well as the repair of single-strand breaks (SSB) and DSB, giving them a universal as well as unique role in a cells response to DNA damage. Three PARPs that have been shown to be activated by DNA damage (PARP-1 as well as PARP-2 and possibly PARP-3) are therefore discussed in the following review with a focus on the two major pathways which have evolved to repair DNA DSBs: nonhomologous end joining (NHEJ) and homologous recombination (HR).

2.1 PARPs and their implications in sensing and repairing DNA Damage

The family of poly(ADP-ribose) polymerases (PARPs) also known as ADPribosyltransferases (ARTDs) consists of approximately 17 proteins in humans, estimated by the number of genes encoding proteins that possess an ADP-ribosyl-transferase catalytic domain (Hottiger et al., 2010). PARP-1, PARP-2, PARP-3, and Tankyrases have been well described for their phylogenetically ancient, reversible posttranslational modification mechanism called poly(ADP-ribosyl)ation, which can modulate the function of their target proteins by regulating either enzymatic activities or molecular interactions between proteins, DNA, or RNA (D'Amours et al., 1999). Responding to a large variety of cellular stresses, poly(ADP-ribosyl)ation is implicated in the maintenance of genomic stability, transcriptional regulation (Krishnakumar et al., 2008), energy metabolism, DNA methylation (Caiafa et al., 2009), and cell death (Krishnakumar and Kraus, 2010b), (Heeres and Hergenrother, 2007) . Upon activation, PARPs catalyze a reaction in which NAD^+ molecules are used to generate poly(ADP-ribose) molecules (PAR) of varying length and complexity attached onto a number of acceptor proteins including PARPs themselves (automodification). As the first PARP discovered by Chambon and colleagues in 1963, the PARP-1 enzyme mediates the synthesis of an adenine-containing RNA-like polymer (Chambon et al., 1963). PARP-1 is one of the most abundant nuclear proteins after histones. The first function of PARPs *in vitro* was identified in response to DNA damage: Besides PARP-1, PARP-2, and PARP-3 have been shown to be enzymatically activated by encountering DNA strand breaks *in vitro* (Benjamin and Gill, 1980), (Rulten et al., 2011), (Schreiber et al., 2006) with PARP-1 carrying out ~ 90 % of the overall polymer synthesis and, notably, attaching the bulk of PAR to itself (Krishnakumar and Kraus, 2010b). The generation of knockout mice for PARP-1 further strengthened the hypothesis for a role for PARP-1 in DNA repair. The knockout of PARP-1 or PARP-2 genes in mice is not lethal, suggesting that there is some redundancy between the function of these two PARPs. Importantly, PARP-1 knock-out mice led to the discovery of PARP-2. Notably, the double knockout of PARP-1 and PARP-2 is not viable, indicating that poly(ADP-ribosyl)ation is essential for early embryogenesis (Menissier de Murcia et al., 2003), (de Murcia et al., 1997), (Masutani et al., 1999). The

modular structure of the PARP-1 protein is composed of at least six independent domains, containing two homologous zinc fingers (Zn1 and Zn2) at the extreme N-terminus that form the DNA binding module (Figure 1). Recently, a third zinc binding domain (Zb3) has been identified (Langelier et al., 2008), (Langelier et al., 2010) which can bind DNA and seems not only to be critical for the DNA-dependent catalytic activity of PARP-1, but also involved in modulating chromatin structure. Indeed, Zb3 mutations in the PARP-1 gene revealed a defect in the ability of PARP to compact chromatin. An internal automodification domain contains a BRCA1 C-terminal domain (BRCT) (shared by many DNA damage repair and cell cycle checkpoint proteins—essential for mediating protein–protein interactions) and three lysines that can be targeted for automodification. A catalytic domain is located at the C-terminus of PARP-1 and contains a region named PARP "signature", a highly conserved region in the PARP superfamily responsible for NAD^+ binding. In addition, the C-terminus also bears a WGR domain named after the highly conserved amino acid sequence in the motif (Trp, Gly, Arg) with an unknown function, which is also found in a variety of polyA-polymerases.

PARP-1, PARP-2, and PARP-3 share conserved WGR and catalytic domains. Interestingly, differing from PARP-1, the other two PARPs that can be activated by DNA damage do not contain the same DNA-binding module: Whereas PARP-2 contains a SAF/Acinus/PIAS (SAP) DNA binding domain, the DNA-binding domain of PARP-3 has not been characterized (Hottiger et al., 2010). PARP-1 and PARP-2 are recognized as molecular sensors of SSBs and DSBs in *vivo*. The synthesis of PAR chains is considered one of the earliest events of the DNA damage response as it occurs within seconds (Ciccia and Elledge, 2010). Besides the direct covalent modification on glutamate, aspartate, or lysine residues of various target proteins, some proteins have been elegantly shown to have a high affinity for the free polymer itself. In fact, it has been argued that strong noncovalent binding of PARP or other proteins to PAR rather than covalent modification (Hassa and Hottiger, 2008) affects protein function and/or localization. Consequently, recent progress has been made in defining specific sites for PAR-attachment on target proteins (Altmeyer et al., 2009), (Haenni et al., 2008), (Kanai et al., 2007). Noncovalent binding of proteins to PAR can be through at least four different PAR-binding motifs. One such motif was

identified by our group and is characterized by a sequence of alternating basic and hydrophobic amino acids (Pleschke et al., 2000), (Gagne et al., 2008). Two other PAR-binding motifs have been described - the macrodomain and the PAR-binding zinc finger (PBZ) (Kleine and Luscher, 2009). Only very recently a fourth type of polymer binding domain has been reported: The E3-ubiquitin ligase RNF146 contains a Trp-Trp-Glu (WWE) motif that is binding PAR (Zhang et al., 2011), (Andrabi et al., 2011). Interestingly, this WWE domain has been found in various PARPs (Schreiber et al., 2006).

As mentioned above, PARP-1 is a molecular sensor of DNA strand breaks and the large size and negative charge of the polymer (which exceeds the charge density of DNA about two times) generated upon activation is playing a key role in the spatial and temporal organization of the DNA damage response. The *in vivo* half-life of the polymer generated upon PARP activation is rather short (seconds to minutes) and tightly regulated by the catalytic reactions of poly(ADP-ribose) glycohydrolase (PARG) and possibly ADP-ribose hydrolase (ARH) 3, which are so far the only glycohydrolases known to degrade the polymer (Meyer-Ficca et al., 2004), (Oka et al., 2006). The fact that PARG and ARH3 antagonize PARP activity and thereby detach the polymer from PARP-1 itself re-enables the PARP protein to bind DNA and start a new round of DNA damage signaling. Although the half-life of the polymer is extremely short, its impact on the cellular energy level can be dramatic as PARP hyperactivation following severe DNA damage consumes substantial amounts of the cytosolic and nuclear NAD^+ (and ATP) pool and thereby can result in cell death (David et al., 2009).

Interestingly, the ability of PARP-1 to disrupt and open chromatin structure by PARsylating histones (such as H1 and H2B) and destabilizing nucleosomes has been one of the earliest functions described for the proteins (Poirier et al., 1982), (Mathis and Althaus, 1987), (Huletsky et al., 1989). By disrupting the chromatin structure, DNA repair factors can gain access to a DNA damage site. Recent publications demonstrated that a variety of proteins implicated in DNA repair are recruited in a PAR-dependent manner to DNA single or double strand breaks (Haince et al., 2008). For instance, the Ataxia telangiectasia-

mutated (ATM) protein is recruited to DNA DSBs in a way that is depending on polymer synthesis (Haince et al., 2008).

2.2 Roles of PARP-1 in base excision repair

The role of PARP-1 in the repair of single-strand DNA breaks by base excision repair (BER) became already evident 30 years ago (Durkacz et al., 1980) and has since then been well examined by several investigators (Allinson et al., 2003), (Petermann et al., 2005). Two Nature publications in 2005 from the Helleday and Ashworth groups have revolutionized the understanding of PARP inhibitors in the context of DNA repair (Bryant et al., 2005), (Farmer et al., 2005): The observation of antitumor effects of PARP inhibitors in a HR-deficient background has been explained as resulting from the disability of PARP-1 to respond to endogenous DNA damage through BER (Bryant et al., 2005). However, the question whether SSBs increase after PARP inhibition is still matter of ongoing debates (Strom et al., 2011), (Pachkowski et al., 2009). Moreover, a lack of XRCC1 (another BER protein) in BRCA2 deficient cells (and thus deficient in HR) does not show the same effect as PARP inhibition, questioning the original explanation for increased sensitivity of HR-deficient cells by PARP inhibition. Even though it is well accepted that PARP-1 is implicated in BER, its exact role remains controversial: PAR itself or automodified PARP-1 is said to be necessary for the recruitment of XRCC1, which further leads to the recruitment of polymerase b and DNA ligase III (Leppard et al., 2003), (El-Khamisy et al., 2003), (Prasad et al., 2001). Although PARP-1 seems to attract SSB repair proteins, it seems not to be essential for SSB repair itself as PARP-$1^{-/-}$ knockout mice for example do not show any early onset of tumor formation (Prasad et al., 2001). It has been recently suggested that PARP inhibitors rather trap PARP on the SSB intermediate which is formed during BER, thereby preventing accurate repair (Strom et al., 2011). It is also well accepted that poly(ADP-ribosyl)ation of PARP-1 and histones due to the negative charge of the polymer leads to their dissociation from the DNA which further promotes local chromatin

relaxation (Rouleau et al., 2004). Consequently, one could argue that this alone can facilitate the assembly of repair proteins at the break site emphasizing a passive role for PARP-1 in BER. In association with PARP-1, PARP-2 has been implicated in BER through its ability to interact with XRCC1, DNA polymerase b and DNA ligase III.

Whereas PARP-1 seems to affect early steps of BER, PARP-2 seems to be involved later in the process (Schreiber et al., 2002).

2.3 Double-strand break repair by homologous recombination

Several lines of evidence have accumulated in the past years for a role of PARP-1 in the cellular response to DNA DSB repair. PARP-1 deficient cells are hypersensitive to DSB-inducing agents but most notably to camptothecin (Bowman et al., 2001). This phenotype is also observed in PARP-$1^{-/-}$ chicken DT40 mutants (Hochegger et al., 2006). Camptothecin blocks topoisomerase-I in a state where it is covalently linked to nicked DNA. The resulting protein-DNA crosslinks are DNA replication and transcription blocks. Replication forks stalling at these lesions result in the formation of DNA DSBs that are repaired by HR (Pommier et al., 2003). HR can occur due to an availability of long sequence homologies in the sister chromatid after DNA replication. As the donor sequence used for HR is usually the sister chromatid, one of its key features is the preservation of the genetic material. However, the donor sequence might as well be another homologous region with consequences as deletions, inversions, or loss of heterozygosity (Aguilera and Gomez-Gonzalez, 2008). Whereas NHEJ functions throughout the cell cycle, HR takes mainly place in S/G2 phase due to its necessity for a homolog template, (Takata et al., 1998), (Rodrigue et al., 2006). HR is suggested to be initiated by MRE11-RAD50-NBS1 (MRN), CtIP, Exo1, DNA2, and BLM (Nimonkar et al., 2011) in mammals, with 5‘ to 3‘ end resection to yield a 3‘-single-stranded (ss) DNA overhang which is capable of invading duplex DNA containing a homologous sequence (Sartori et al., 2007), (Nicolette et al.,

2010), (Figure 11). Interestingly, PARP-1 has been put in the context of MRN recruitment as it has been clearly demonstrated that PARP-1 can mediate the initial accumulation of the MRN complex to DSBs independent of γ-H2AX and MDC-1 (Haince et al., 2008). This might have an implication in HR but also on a backup pathway of NHEJ (as discussed later in the text). The replication protein A (RPA) has a high affinity for 3'-ssDNA tails and therefore binds to the newly generated 3'-ssDNA-overhang, a process that normally inhibits RAD51 loading and HR. HR mediators such as BRCA2 (Sung, 2005) and PALB2 (Buisson et al., 2010) are helping to overcome that inhibition and lead to a displacement of RPA by RAD51 (Liu et al., 2010). RAD51 itself, a DNA-dependent ATPase which is homolog to the bacterial RecA protein, is forming nucleoprotein filaments with DNA in a presynaptic step. RAD51 is recruited to DSBs in mammalian cells through BRCA2. Both, BRCA1 and 2 have been elegantly shown to be absolutely necessary for the HR reaction (Moynahan et al., 1999), (Moynahan et al., 2001) and there are several studies putting PALB2 (also known as FANCN) in the center of the BRCA1-BRCA2 complex (Sy et al., 2009), (Zhang et al., 2009a). DSS1, a 70 amino acid protein, has been shown to be crucial for RAD51 foci formation as well and presumably for HR in mammalian cells (Yang et al., 2002). A role for PARP-1 in that step of HR has been suggested to be rather of a regulatory nature than through a direct involvement in the actual mechanism: RAD51 foci are not only still forming in response to hydroxyurea (HU) in PARP-$1^{-/-}$ cells, but their number is also increasing in a PARP-1 deficient background (Schultz et al., 2003). In line with the latter finding it has been shown that in a PARP-1 deficient background (PARP-1 null MEFs) the spontaneous frequency of RAD51 foci is clearly enhanced (Claybon et al., 2010). Interestingly, PAR, the product of catalytically active PARP, has been detected at HU-induced RPA foci raising the possibility that PARP-1 might for example prevent RAD51 from loading (Bryant et al., 2009).

The following synaptic step is characterized by invasion of a homologous sequence to generate a D-loop structure (Figure 11). Therewith the RAD51-ssDNA complex is binding to a complementary ssDNA region within the homologous duplex.

Once formed, the D-loop structure has multiple fates: In the double-strand break repair (DSBR) model, the 3' invading end from the broken chromosome is used to prime DNA synthesis templated by the donor duplex, whereas the other end of the break is presumably captured by the displaced strand from the donor duplex (D-loop) and is used to prime a second round of leading strand DNA synthesis. Therewith a so called double Holliday Junction (dHJ) intermediate is formed that can, after branch migration and fill-in of the ssDNA, be resolved to form cross-over or non-crossover products. In a second model called synthesis dependent strand annealing (SDSA), the invading strand that has been extended by DNA synthesis is displaced and anneals to complementary sequences exposed by 5' to 3' resection of the other side of the break. The remaining gaps can subsequently be filled in by newly synthesized DNA or by ligating the nicks (Mimitou and Symington, 2009). SDSA will result only in non-crossover products.

Collectively, there are several lines of evidence that PARP-1 regulates HR. $PARP1^{-/-}$ DT40 mutants showed more than threefold reduction in gene conversion (Hochegger et al., 2006). Interestingly, the deletion of KU in $PARP1^{-/-}$ DT40 mutants completely reversed this phenotype suggesting that KU has a suppressive effect on HR. On the other hand, PARP-1 has been suggested to rather prevent HR, as the absence of PARP-1 results in an increase of spontaneous somatic HR events *in vivo* (Claybon et al., 2010). PARP-1 also affects replication fork progression on damaged DNA. Indeed, fork progression is not slowed down in $PARP1^{-/-}$ DT40 cells treated with camptothecin.

As fork slowing is correlated with the proficiency of HR, it implicates PARP-1 in the regulation of HR during DNA replication (Sugimura et al., 2008). Additionally, by using the DNA fiber assay, Thomas Helleday and colleagues were able to show that PARP-1 is important for replication fork restart after blocking through HU treatment (Bryant et al., 2009).

2.4 DNA double-strand break repair through nonhomologous end joining

The repair of DSBs by HR has been demonstrated in practically all organisms examined from bacteria, yeast to human and seems to be conserved throughout evolution. Being described as a rather "error free" pathway that is faithfully restoring genetic information it came as a big surprise to the DNA damage field that the major DSB repair pathway in higher eukaryotes is of a kind that does not rely on a homologous template but restores molecular integrity irrespective of the DNA sequence information. In nondividing haploid organisms or in diploid organisms that are not in the S-phase, a homologous template is not available for homology directed repair, setting the stage for a repair mechanism not relying on template homology, called NHEJ. This DSB repair pathway is effective throughout the cell cycle, but of particular importance during G0-, G1 and the early S-phase of cells. DNA DSB ends are often the result of damage to the sugar-phosphate backbone and/or the bases of the terminal nucleotides that have to be removed or processed prior to the religation step, explaining the fact that NHEJ is often mutagenic.

The most striking characteristic of the NHEJ pathway might be its high flexibility in terms of its templates, proteins involved and possible outcomes. The enzymes of the NHEJ pathway exhibit a remarkable tolerance concerning the DNA end substrate configurations they can act on. Different from other more distinct repair pathways, NHEJ enzymes act iteratively. Most of them can function independent of one another. As other repair pathways, NHEJ requires proteins that bring the ends in close proximity, nucleases/ polymerases to process unligatable DNA ends and a ligase to restore integrity of the DNA strands (Lieber, 2010). From studies in which researchers investigated the status of Ku and DNA-PKcs in cell lines that are sensitive to ionizing radiation it became evident by their absence that these two proteins are implicated in NHEJ (Ferguson and Alt, 2001).

The generally accepted model of the "classical" NHEJ pathway is initiated with the heterodimeric complex of Ku70/Ku80 that binds to both ends of a broken DNA molecule (Figure 12). This Ku-DNA complex acts presumably as a scaffold needed for the recruitment of DNA-PKcs, which then functions as a molecular "bridge" between the two

broken ends (Ochi et al., 2010), (Gottlieb and Jackson, 1994). Other than the Ku70/Ku80 complex, the association of Ku70/80 to the DNA-PKcs is transient and most likely stimulated by free DNA ends (Yaneva et al., 1997). In a current model, it has been suggested that upon recruitment, DNA-PK phosphorylates several proteins including Ku70 and itself, which presumably facilitates NHEJ by destabilizing the interaction of the protein itself with DNA, thus providing access for end processing enzymes such as Artemis. Whereas the autophosphorylation of DNA-PKcs on the six-residue ABCDE cluster (T2609 cluster) has been shown to destabilize the protein DNA-binding properties, a phosphorylation on the five-residue PQR cluster (S2056) in return has presumably the opposite effect in protecting the DNA ends from excessive processing (Meek et al., 2008), (Uematsu et al., 2007).

As indicated before, if DNA DSB ends are not 5' phosphorylated and ligatable, they have to be processed prior to the ligation step. Artemis has been revealed to be one of the major processing enzymes, showing a DNA-PK-independent 5'- to 3'-exonuclease activity and a DNA-PK-dependent endonuclease activity (Pawelczak and Turchi, 2010), (Gu et al., 2010).

However Artemis does not seem to be the only nuclease necessary for end-processing in DNA DSB repair, as cells lacking Artemis show higher radiosensitivity but do not have major defects in DNA DSB repair (Wang et al., 2005). For example polynucleotide kinase (PNK), APLF nucleases and terminal deoxynucleotidyl transferase (TdT) have been shown to be able to remove damaged nucleotides in the context of NHEJ (Chappell et al., 2002), (Mahaney et al., 2009). Polymerases being able to insert new DNA at DSBs are polymerase λ and polymerase μ, belonging to the POLX family. These two polymerases have been shown to be able to bind the Ku:DNA complex through their BRCT domains (Capp et al., 2006), (Capp et al., 2007), (Covo et al., 2004).

Major resolution complex for DSB repair through NHEJ has been shown to be the X4-L4 complex (XRCC4, DNA ligase IV and XLF), whereas XRCC4 and XLF do not seem to have an enzymatic function in the process but rather act as cofactors being able to stimulate the ligation activity of ligase IV (Ahnesorg et al., 2006). The aforementioned complex

forms the second physical “bridge” stabilizing the DNA ends and mediating their ultimate rejoining by ligation. The XRCC4-lig IV complex is the most flexible ligase complex known in terms of ligating across gaps and ligates incompatible ends (Deshpande and Wilson, 2007).

From experiments in which at least one of the key NHEJ proteins has been mutated, the observed end-joining activity was still present in such mutant cell lines; this activity has been proposed to be due to a back-up pathway to the “classical” NHEJ pathway. End-joining can for example happen in the absence of DNA ligase IV or Ku70 (Bennardo et al., 2008). As the only remaining DNA ligase activity in vertebrate cells is due to DNA ligase I or III, one or both of the two proteins have to precede end-joining events observed in the absence of ligase IV. Alternative end-joining activity has until now only been demonstrated in the absence of classical factors therewith in the absence of the “classical” NHEJ, indicating an actual backup rather than a coexisting alternative pathway (Simsek and Jasin, 2010). However the possibility that the NHEJ happening in the absence of Ku70 and ligase IV, can act alternatively to the classical pathway has not yet been disproved. From *in vivo* experiments in *S. cerevisiae* and mammals it has been elegantly shown that the variation of the ligation product is diminished as terminal microhomology occurs (Daley et al., 2005).

Besides the key factors described above, there have been other proteins shown to have an impact on the NHEJ reaction. Interestingly, the MRN complex which is known to coordinate DNA DSB repair by HR has recently been shown to promote efficient NHEJ in a $XRCC4^{+/+}$ and $XRCC4^{-/-}$ background in mice embryonic stem cells (Xie et al., 2009). As accessory factors for the ligase reaction through its ability to interact with XRCC4, Polynucleotide kinase (PNK), aprataxin (APTX) and aprataxin- and PNK-like factor (APLF) have been identified (Koch et al., 2004). Interestingly, PARP-3 has been suggested very recently to accelerate DNA ligation during NHEJ in the context of APLF (Rulten et al., 2011). The affinity of PARP-1 for a blunt ended and 3’ single-base overhang DSBs has been shown to be greater than the one of DNA-PK, with a four-fold lower affinity of PARP-1 for SSBs compared to blunt-ended DSBs (D'Silva et al., 1999). Also PARP-1 has been demonstrated to directly interact with Ku proteins *in vitro* and *in vivo*, whereas Ku70,

Ku80 and DNA-PKcs are able to bind PAR (Gagne et al., 2008). PARP-1's PARylation of Ku leads to a decreased binding to DSBs (Li et al., 2004). Moreover, several studies implicated PARP-1 functionally in NHEJ: PARP-1 and Ku80, both being highly abundant in the cell, have been shown to compete for free DNA ends *in vitro* presumably through two distinct NHEJ pathways. Whereas the Ku complex is one of the key factors for the classical NHEJ pathway, PARP-1 seems to also interact with ligase III in the backup pathway (Wang et al., 2006), (Audebert et al., 2004), (Mansour et al., 2010).

2.5 Regulation of the DNA DSB repair pathway choice: Collaboration or competition?

Several factors are channeling the DSB repair pathway choice between NHEJ and HR. It is generally accepted that the cell-cycle phase is one of them. Early studies in vertebrates showed that NHEJ-deficient "scid" cells (carrying a loss-of-function mutation in DNA-PKcs) and $Ku70^{-/-}$ chicken DT40 cells were hypersensitive to IR only in G1 and early S-phase whereas HR-defective $Rad54^{-/-}$ cells were IR sensitive in late S/G2 phase (Lee et al., 1997). The Cdk1 kinase has recently been shown to have control over the key recombination steps giving an elegant explanation for the fluctuating HR efficiency throughout the cell cycle (Ira et al., 2004). Being at the same time one of the main engines for the cell cycle, Cdk1 would be an excellent tool to control the DSB repair pathway choice. Indeed a recent publication suggests that HR and NHEJ are oppositely affected by Cdk1 activity: Whereas HR is activated, NHEJ seems to be repressed (Zhang et al., 2009). Moreover the level of several critical HR proteins (BRCA1, RAD51/52) has been shown to increase from S to G2 phase and that steps of HR are activated by CDKs (Shrivastav et al., 2008) suggesting another potential for regulating the pathway choice through the level of proteins expressed for the corresponding pathway.

A similar observation has been made for the protein level of DNA-PK (Koike et al., 1999). The nature of the DNA lesion plays an additional role to the choice of DSB repair pathway: RAG-mediated DSBs during V(D)J-recombination are certainly repaired through NHEJ (Soulas-Sprauel et al., 2007) whereas Spo11-mediated DSBs generated during meiosis for instance will be repaired by HR (Cole et al., 2010). Besides the key players in HR and NHEJ it has recently been shown that ~ 15–20 % of ionizing irradiation induced foci (IRIF) require additional proteins, such as ATM, Artemis, the MRN-complex, γH2AX, 53BP1, MDC1 and RNF8, RNF168 for repair, some of them being implicated in both DSB repair pathways (Riballo et al., 2004). As an example, 53BP1 has been implicated in NHEJ (Nakamura et al., 2006) whereas 53BP1 deficiency rescues HR in a BRCA1 deficient background by a mechanism dependent on ATM-mediated resection. Interestingly, loss of 53BP1 does not complement the loss of BRCA2, which might be explained by genetic studies that put BRCA2 more downstream in HR in a process following end-resection (Bouwman et al., 2010), (Bunting et al., 2010).

Moreover, the complexity of chromatin may influence repair pathway choice as it has recently been shown that X-ray induced DSBs located in close proximity to heterochromatin predominantly use HR for repair (Beucher et al., 2009). Especially the distance of ionizing radiation-induced foci to heterochromatin and the ATM-dependent phosphorylation of Kap-1 which promotes chromatin relaxation seem to somehow affect repair (Shibata et al., 2011).

An important regulatory step involved in pathway choice is the process of DSB resection, comprising the 5‘- to 3‘- nucleolytic processing of DNA ends by the MRN complex in conjunction with auxiliary factors including CtIP, RECQ helicases, Exo1 and DNA2, being necessary for HR but not for NHEJ. An observation suggesting that competition exists between the two major DSB repair pathways is given by the fact that NHEJ mutants (e.g. Ku70 deficient cells) that have enhanced end resection show increased HR whereas mutants with decreased end resection (e.g. Sae2/CtlP) have increased NHEJ. Possibly, since Ku70 binds DNA ends, it thereby prevents the initial step of HR, the end resection. Surprisingly, Ku depletion in chicken cells actually leads to an overall increased resistance to ionizing

irradiation during late S/G2 phase which can be interpreted as Ku interfering with HR under normal conditions in the mentioned cell cycle phases (Fukushima et al., 2001) Additionally, impairing DNA-PK from binding to a DSB end dramatically promotes the initiation step of HR (Shibata et al., 2011). Interestingly, from double-mutant analysis for NHEJ and HR components it is suggested that the concomitant loss of a protein involved in HR and a protein involved in NHEJ results in a more severe phenotype than one would expect from loss of either single pathway (Mills et al., 2004), promoting rather collaboration of the two pathways. Interestingly, in a study that highlighted rather competition than collaboration between the major DSB repair pathways it has been elegantly shown that PARP-1 is hyperactivated in BRCA2 deficient cells but this hyperactivation cannot be explained by an accumulation of DNA damage, which normally triggers PARP-1 activity (Gottipati et al., 2010).

A new model has been suggested only very recently proposing that in a BRCA2 deficient background PARP-1 might prevent DSB repair through NHEJ, possibly by blocking DNA-PK and Artemis. By adding PARP inhibitors to HR deficient cells, error-prone NHEJ is promoted and the unrestricted NHEJ could then induce genomic instability and eventual lethality (Patel et al., 2011).

Notably, the opposite effect to PARP inhibition has been described for 53BP1 in a BRCA1 negative background: By depletion of 53BP1 ATM-dependent processing of DNA ends is restored which can generate single-stranded DNA which is competent for HR. Thus, the loss of 53BP1 in a BRCA1 negative cell can overcome PARP inhibitor sensitivity (Bunting et al., 2010), (Kass et al., 2010).

2.6 Conclusion

To summarize, more than 40 years of research in the PARP- and PAR fields have uncovered implications in various layers of the DNA damage response to DNA DSBs: The initial processes starting with sensing the DSB and its signaling in order to recruit other repair proteins to the damage site implies PARP-1 and the polymer generated at the damage site. Furthermore, an automodification of the protein leads to its detachment from the DNA which guaranties access for other proteins but also enables another round of damage signaling (Mortusewicz et al., 2007). Interestingly, the polymer generated at the damage site has an important impact on the local chromatin structure due to its largely negative charge. By disrupting the chromatin structure surrounding the damage site, access to the DNA is facilitated (Krishnakumar and Kraus, 2010b).

Besides PARPs implication in sensing and signaling of DNA damage and a role in BER, first lines of evidence have been given that even the choice for the DSB repair pathway is influenced by PARP-1, as the protein seems to block DNA-PKcs and therewith classical NHEJ (Patel et al., 2011). At the same time PARP-1 itself has been shown to be involved in the backup-pathway of NHEJ (Mansour et al., 2010) as well as suppressing HR, indicated by an increase of RAD51 foci in a PARP-1 deficient background (Schultz et al., 2003). PARP-3 on the other hand seems to interact with APLF in NHEJ (Rulten et al., 2011).

Taken together, PARPs are multifunctional regulators of the DNA damage response, expanding the current model of action for PARP inhibition in HR-deficient cancer cells. A mechanism called synthetic lethality explains the original model, meaning that two genetic lesions together lead to cell death whereas a defect in only one of these genes does not. In BRCA1- or BRCA2- deficient cancer cells for example where HR is hampered, the cytotoxic effect of PARP inhibitors has been originally suggested to be due to the cells inability to overcome SSBs by BER, which can further degenerate during replication to form DSBs. These DSBs can in healthy cells but not in HR-deficient cancer cells be repaired by HR (Aly and Ganesan, 2011) (Figure 13a). This view was recently challenged, mostly because it was very difficult to detect increased SSBs after PARP inhibition

(Gottipati et al., 2010). The current view involves the aberrant activation of NHEJ, rather than inhibition of BER by PARP inhibitors in HR-deficient cells, leading to genomic instability and cell death (Patel et al., 2011) (Figure 13b). Hence, even though PARP inhibitors have been put with widespread enthusiasm into clinical trials, the exact molecular effects are still debated and under investigation at the cellular level. How these inhibitors work in the appropriate clinical context still remains elusive. Hence, the PARP field awaits many scientific surprises with fundamental and clinical relevance.

2.7 Figures and legends

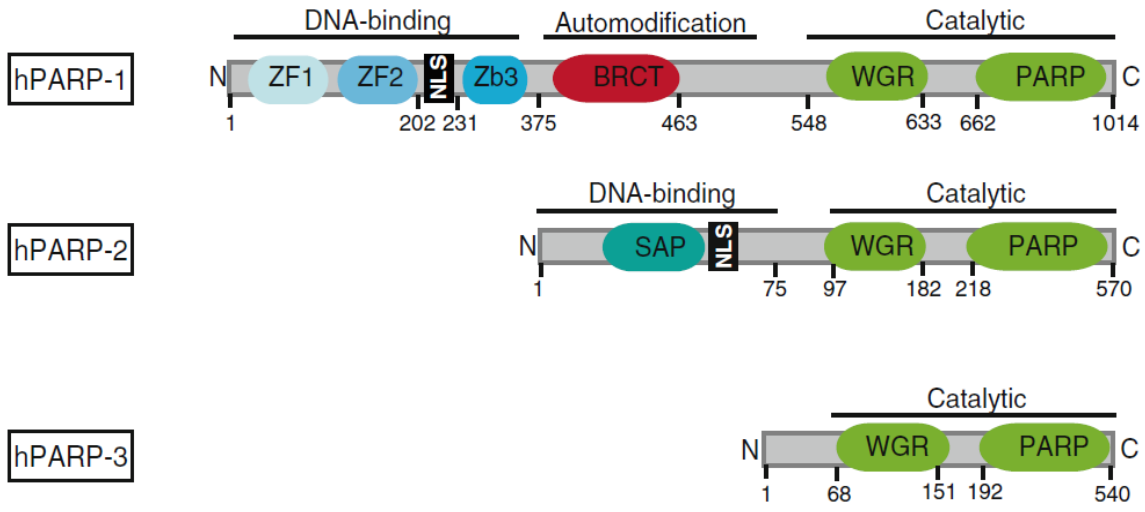

Figure 10: Schematic comparison of the domain architecture of human PARP-1, PARP-2, and PARP-3
The following most significant domains are indicated: zinc finger (ZF/Znf); zinc binding (Zb); carboxyterminal domain (BRCT); the WGR domain, named after a conserved central motif (W-G-R); the PARP signature, representing the catalytic core needed for basal activity; nuclear localization signal (NLS); SAF/Acinus/PIAS-DNA-binding domain (SAP)
Adapted from: (Schreiber et al., 2006).

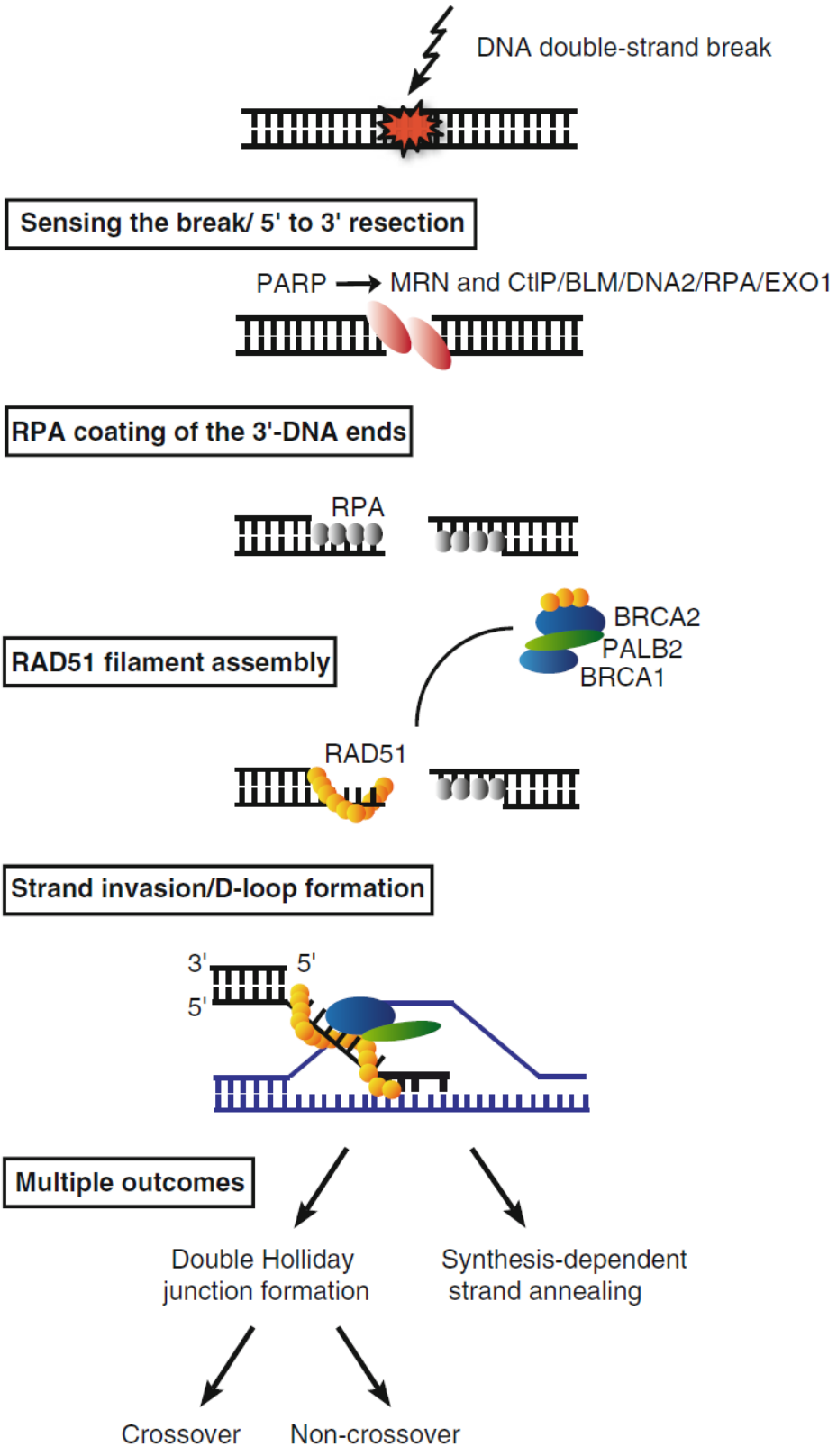

(See legend on the next page.)

Figure 11: Simplified overview of the homologous recombination (HR) repair pathway
Subsequent to DNA damage, the MRN complex (and associated resection machineries) binds and resects free DNA ends to create 3'-overhangs which are then bound by RPA. A complex of BRCA1, PALB2 and BRCA2 mediates the replacement of RPA by RAD51, which leads to the formation of the RAD51 filament coating the 3'-overhang. BRCA1/PALB2/BRCA2 then activates RAD51 to promote the invasion of an undamaged template in a step called strand invasion/ D-loop formation. Resolving of the D-loop structure can occur through synthesis-dependent strand annealing or double Holiday junction formation, generating either crossover or non-crossover products in the latter case.

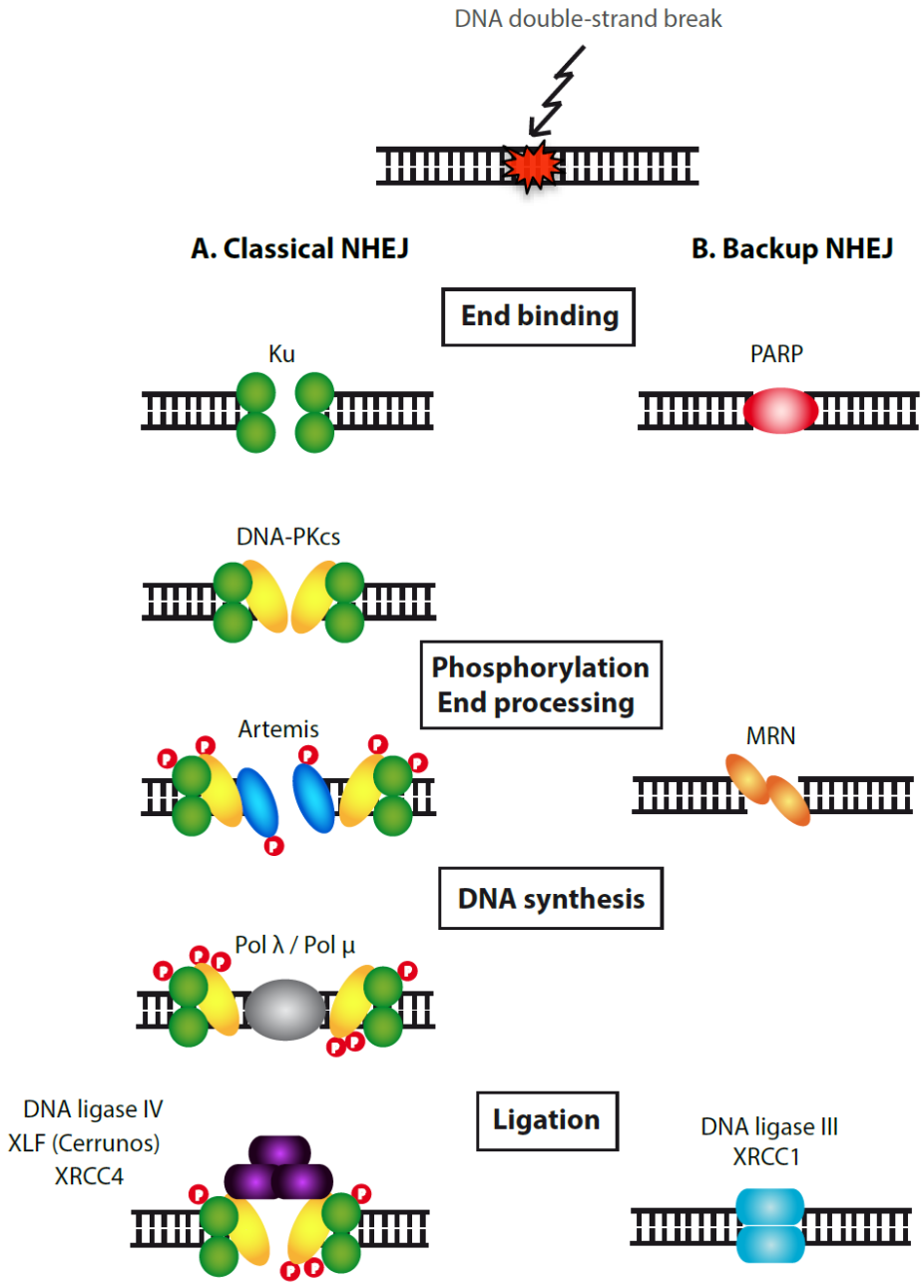

Figure 12: DNA double-strand break repair through nonhomologous end joining (NHEJ)

(A) The classical NHEJ pathway is initiated with Ku70/80 binding to the free DNA ends. The subsequent recruitment of the catalytic subunit of DNA-PK leads to the assembly of the end-bridging DNA-PK complex. DNA-PK then phosphorylates many proteins including Ku70 and itself. This loosens the DNA-PK DNA-binding which gives access to end processing proteins (such as Artemis/ PNK/APLF/ TdT). After a fill-in of missing nucleotides by polymerase l and m the ends are joined by DNA ligase IV in a complex with its accessory factors (XRCC4 and XLF). **(B)** In the absence of or in competition to Ku70 it has been shown that PARP-1 can bind free DNA ends. Ends might further be processed by the MRN complex prior to a ligation by DNA ligase III/XRCC1.

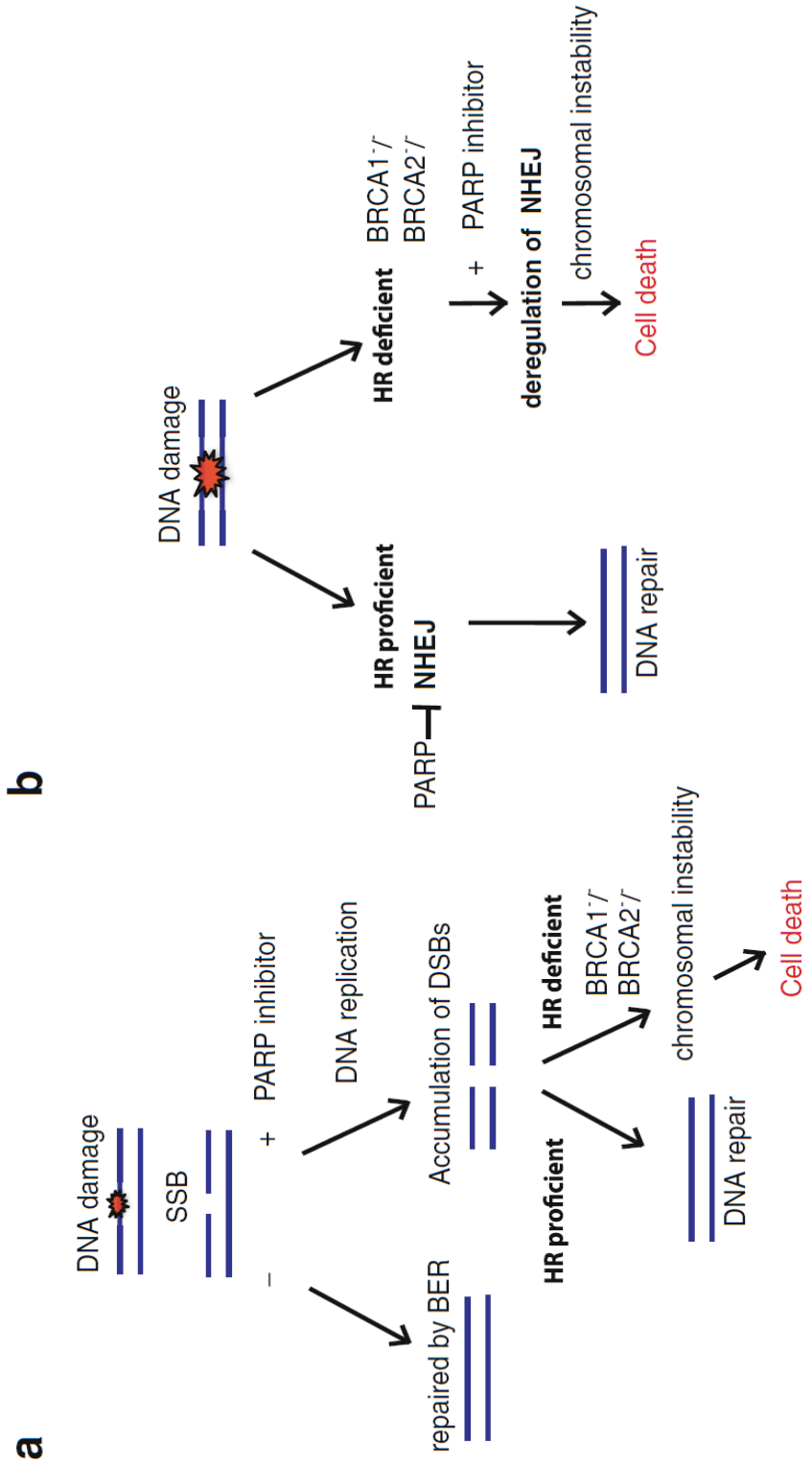

Figure 13: Models explaining the lethality of HR-deficient cells with PARP inhibitors
(A) The synthetic lethality pathway model based on a deficiency in single-strand break repair. **(B)** Model based on error-prone NHEJ. Details are given in the text.

2.8 Acknowledgements

Research from the authors has been supported by the CIHR and the Cancer Research Society. G.P. is a Canada Research Chair in Proteomics and M.L. and J.-Y.M. are FRSQ Senior Investigators JK is a FQRNT scholar.

CHAPTER 3

QUANTITATIVE PROTEOMICS PROFILING OF THE POLY(ADP-RIBOSE)-RELATED RESPONSE TO GENOTOXIC STRESS

Jean-Philippe Gagné [(1)], Émilie Pic [(1)], Maxim Isabelle [(1)], Jana Krietsch [(1,2)], Chantal Éthier [(1)], Éric Paquet [(2)], Isabelle Kelly [(3)], Michel Boutin [(3)], Kyung-Mee Moon [(4)], Leonard J. Foster [(4)] and Guy G. Poirier [(1,5)]

[(1)] Cancer Research Laboratory,

[(2)] Genome Stability Laboratory,

[(3)] Proteomics platform, Québec Genomic Center, Laval University - CHUQ Research Center, Québec, Canada G1V 4G2 and

[(4)] Department of Biochemistry and Molecular Biology, University of British Columbia, Centre for High-Throughput Biology, Vancouver, British Columbia, Canada, V6T 1Z4

[(5)] Corresponding author

Preface

The highly abundant protein PARP-1 is a strong sensor for DNA DSBs. Once bound to the free DNA ends, the protein gets enzymatically activated. Its catalytic product PAR serves then as a platform to recruit proteins of the DNA damage response. The following manuscript is the summary of an extensive study on the protein complexes centered on PAR in response to DNA damage.

The work has been in major parts carried out by Jean-Philippe Gagné who has over the past years developed a high expertise in mass spectrometry. My contribution lies in some of the control experiments for immunofluorescence and western blots and help with the writing of the article. Even though my contribution was rather minor, I chose to add this article as Chapter 3 to my thesis, as the work represents a fundamental aspect for the understanding of my PhD project. The article has been published as a highlight article in Nucleic Acid Research in September 2012.

Résumé

Lors de l'induction de dommages à l'ADN, PARP synthétise un polymère anionique d'ADP- ribose (PAR) auquel plusieurs protéines se lient formant des complexes multiprotéiques. Nous avons utilisé plusieurs approches de protéomique et de purification par affinité pour isoler ces complexes et évaluer la dynamique des protéines en lien au métabolisme du PAR. Comme première approche, nous avons développé une stratégie de piégeage de substrat par laquelle nous démontrons qu'un mutant catalytiquement inactif de la Poly (ADP-ribose)glycohydrolase (PARG) peut agir, grâce à son macrodomaine, comme un appât physiologiquement sélectif pour l'isolation de protéines liant spécifiquement le PAR. En plus des méthodes de purification par affinité avec anticorps, nous avons utilisé une résine d'affinité spécifique au macrodomaine du PAR pour récupérer les protéines de liaison au PAR et leurs complexes. Deuxièmement, nous avons conçu une expérience de cinétique pour explorer les changements dans la composition des complexes multiprotéiques contenant le PAR en réponse à l'activation de la PARP par les dommages alkylants. Le comptage spectral basé sur les analyses par GeLC-MS/MS a été complémenté par des analyses de protéomique quantitative de haute précision par étiquetage isobarique pour la quantification relative et absolue (iTRAQ) - et par marquage isotopique stable des acides aminés en culture cellulaire (SILAC). Ici, nous présentons une ressource précieuse pour l'interprétation de la biologie des systèmes du réseau de la réponse aux dommages de l'ADN dans le contexte de la poly (ADP - ribosyl)ation et nous fournissons une base pour les recherches ultérieures de candidats liant la PAR.

Abstract

Upon DNA damage induction, DNA-dependent Poly(ADP-ribose) polymerases (PARPs) synthesize an anionic Poly(ADP-ribose) (PAR) scaffold to which several proteins bind with the subsequent formation of PAR-associated multiprotein complexes. We have used a combination of affinity purification methods and proteomics approaches to isolate these complexes and assess protein dynamics with respect to PAR metabolism. As a first approach, we developed a substrate trapping strategy by which we demonstrate that a catalytically inactive Poly(ADP-ribose) glycohydrolase (PARG) mutant can act as a physiologically selective bait for the isolation of specific PAR-binding proteins through its macrodomain-like domain. In addition to antibody-mediated affinity-purification methods, we used a PAR macrodomain affinity resin to recover PAR-binding proteins and their complexes. Second, we designed a time course experiment to explore the changes in the composition of PAR-containing multiprotein complexes in response to alkylating DNA damage-mediated PARP activation. Spectral count clustering based on GeLC-MS/MS analysis was complemented with further analyses using high precision quantitative proteomics through isobaric tag for relative and absolute quantitation (iTRAQ)- and Stable isotope labeling by amino acids in cell culture (SILAC)- based proteomics. Here, we present a valuable resource in the interpretation of systems biology of the DNA damage response network in the context of poly(ADP-ribosyl)ation and provide a basis for subsequent investigations of PARbinding protein candidates.

3.1 Introduction

Poly(ADP-ribose) (PAR) turnover is an important process involved in the transient response to DNA damage. The synthesis of PAR that results from the activation of DNA-dependent poly(ADP-ribose) polymerases (PARPs) is one of the earliest steps of DNA damage recognition and signaling in mammalian cells (Tartier et al., 2003). During the response elicited by DNA damage, the addition of PAR to chromatin-related proteins is associated with chromatin decondensation and dynamic nucleosome remodeling that tends to increase the accessibility of repair factors to DNA lesions (Rouleau et al., 2004). Numerous molecules are recruited at DNA damage sites in a PAR-dependent manner. Therefore, PAR itself appears to be a signaling and scaffold molecule involved in the assembly of multi-subunit DNA repair complexes (Malanga and Althaus, 2005). In addition to covalent attachment of PAR to target proteins, specific non-covalent PAR interaction motifs have been characterized. Three major protein interaction modules were identified on the basis of their high affinity for PAR: the macro domain (Till and Ladurner, 2009), the poly(ADP-ribose)- binding zinc finger module (PBZ) (Ahel et al., 2008) and the WWE domain (defined by the conserved residues tryptophan (WW) and glutamic acid (E)) that mediates protein–protein interactions in ubiquitin and ADP-ribose conjugation systems (Aravind, 2001), (Zhang et al., 2011), (Wang et al., 2012). Besides domain-mediated interaction, several proteins are known to interact with PAR through a generally short hydrophobic and basic region (Pleschke et al., 2000), (Althaus et al., 1999), (Gagne et al., 2008). This poly(ADP-ribose)-binding motif is widespread and frequently found in the DNA-binding domains of chromatin regulatory proteins and DNA repair factors. Collectively, PAR-binding proteins generate a DNA repair network of protein factors through physical interactions with PAR. In this view, PAR behaves as a coordinator in the cellular response to genotoxic insults. The macro domain has been the object of the first structural investigations on ADP-ribose recognition (Egloff et al., 2006), (Karras et al., 2005). A macroprotein was also used as a bait to define the ADP-ribosyl proteome, a method that proved to be effective although very limited gains in new protein identifications were achieved (Dani et al., 2009). A recent study from Slade and colleagues revealed that Poly(ADP-ribose) glycohydrolase (PARG) catalytic domain is a distant

member of the ubiquitous ADP-ribose-binding macrodomain family (Slade et al., 2011). PARG is the main enzyme involved in the degradation of PAR. Therefore, we reasoned that a catalytically inactive PARG mutant that forms stable interactions with PAR, would also allow subsequent purification of poly(ADP-ribosyl)ated proteins and PAR-containing protein complexes. A mass spectrometry (MS)-based substrate trapping strategy could further extent the proteome coverage achieved with antibody-mediated affinity-purification procedures. As part of this approach, we also revisited the strategy that couples affinity purification by an ADP-ribose-binding macrodomain (AF1521) with MS. Over the past few years, our work, and that of many other labs exposed the fact that PAR engages in highly specific non-covalent interactions with proteins (Ji, 2011), (Malanga and Althaus, 2011), (Gagne et al., 2011). Strong binding to PAR has the potential to act as a loading platform for a variety of proteins involved in DNA/RNA metabolism (Hassa et al., 2006). Although PAR-binding studies reflect the existence of strong molecular interactions with PAR, it still remains a challenge to identify and quantify transient protein interaction with PAR. The fast and transient dynamics of PAR makes it an extremely challenging task. The use of DNA damaging agents that cause a broad spectrum of DNA lesions are useful tools to assess the modulation of the poly(ADP-ribosyl)ation reaction and the subsequent activation of DNA damage sensing enzymes.

N-methyl-N-nitro-N-nitrosoguanidine (MNNG) has been used for decades as an effective agent to induce massive PAR synthesis through PARP-1 activation. In addition to inducing damage to the DNA bases, MNNG is an alkylating agent known to produce both DNA single-strand breaks (SSBs), as well as double-strand breaks (DSBs) (Banath et al., 2010), (Artus et al., 2010). The exposure of cells to MNNG results in an almost immediate poly(ADPribosyl)ation of target proteins but little is known on their time course profiles, as well as their persistence in PAR-containing protein complexes. As a first approach in this study, we used complementary proteome-mining methods that cover a large part of the accessible PAR proteome. Using antibody-mediated and substrate trapping strategies to isolate PAR-containing protein complexes, we present an overall picture of the PAR proteome. Second, we focused on the highly dynamic composition of PAR-containing protein complexes following an alkylation-induced DNA damage to provide insights into

the functional processes modulated by poly(ADP-ribosyl)ation. The dynamic assembly of PAR-containing protein complexes was revealed by the use of quantitative MS. Strategies for quantitative proteomic profiling included both *in vitro* and *in vivo* labeling approaches, as well as label-free quantitation.

These proteome-wide approaches were coupled to PAR affinity purification and complementary datasets were integrated and modeled for a more thorough insight into PAR-binding protein dynamics. Here, we present the first quantitative proteomics investigation of the PAR-associated proteome modulation in the context of DNA damage and PARP activation.

3.2 Materials and methods

3.2.1 Cell culture, vector construct and transfections

Human embryonic kidney 293 cells (HEK293) and human cervical carcinoma cells (HeLa) were cultured (air/CO_2, 19:1, 37 °C) in Dulbecco's modified Eagle's medium (DMEM) supplemented with 10 % fetal bovine serum (FBS) (Hyclone-Thermo Fisher Scientific, Ottawa, Canada). Penicillin (100 U/ml) and streptomycin (100 mg/ml) (Wisent, St-Bruno, Canada) were added to the culture media. Alkylating DNA damage was introduced using freshly prepared 100 mM MNNG for 5 min. Cells were washed twice with PBS before cell lysis or allowed to recover from the genotoxic insult for 1 or 2 h by replacing the growth medium with supplemented DMEM. A human GFP-PARG-DEAD vector was modified by oligonucleotide-directed mutagenesis of the GFP-hPARG-110 (pEGFP-C1 expression vector, Clontech) previously described in Ref. (Haince et al., 2006). Mutagenic primers were made following the guidelines in the QuikChange® site-directed mutagenesis kit (Stratagene). A mutation was introduced at amino acid position 756 which completely abolishes PARG catalytic activity (E756D) as reported (Patel et al., 2005). Transfections

were carried out with Effectene (Qiagen), as recommended by the manufacturer and cells were harvested 24 h post-transfection.

3.2.2 Immunoprecipitation of PAR-containing protein complexes

HEK293 and HeLa cells were seeded onto 150 mm cell culture dishes and grown up to 80–90 % confluency (~ 15–20 millions cells/dish). Experiments were performed with cell extracts from three dishes per condition. Control cells were pre-incubated for 2 h with 5 mM PARP-1 inhibitor ABT-888 to maintain basal levels of PAR, whereas a fast activation of PARP-1 resulting in a substantial increase in intracellular levels of PAR was performed by incubating the cells with freshly prepared 100 mM MNNG for 5 min. All further steps were performed on ice or at 4 °C. Two PBS washes were carried out prior to protein extraction with 2 ml/plate of lysis buffer [40 mM HEPES pH 7.5, 120 mM NaCl, 0.3 % CHAPS, 1 mM EDTA, 1X Complete^{TM} protease inhibitor cocktail (Roche Applied Science, Indianapolis, IN, USA) and 1 mM PARG inhibitor ADP-HPD (adenosine 50-diphosphate (hydroxymethyl) pyrrolidinediol) (EMD Chemicals, Gibbstown, NJ, USA)]. The whole cell lysates were pooled and placed on ice for 15 min and gently mixed for another 15–20 min on a rotating device for complete lysis. After homogenization, insoluble material was removed from the homogenate by centrifuging at 3000 g for 5 min. Immunoprecipitation (IP) experiments were performed using magnetic Dynabeads^{TM} covalently coupled to Protein G (Invitrogen, Burlington, Canada). The Dynabeads^{TM} (125 ml/condition) were washed twice with 1 ml of 0.1 M sodium acetate buffer, pH 5.0 and coated with 12.5 mg of mouse monoclonal anti-PAR antibody clone 10H (Tulip Biolabs, West Point, PA, USA), anti-GFP (Roche Applied Science, Indianapolis, IN, USA) or equivalent amount of normal mouse IgGs (Calbiochem EMD Biosciences, San Diego, CA, USA). The antibody-coupled Dynabeads^{TM} were incubated for 1 h with 1 ml of PBS containing 1 % (w/v) bovine serum albumin (BSA) (Sigma-Aldrich, Oakville, Canada) to block non-specific antibody-binding sites. The beads were finally washed three times with 1 ml of lysis buffer and added to the precleared PAR-protein extract for 2 h incubation with gentle mixing on a rotating device. Samples were washed five times with 10 ml of lysis buffer for 5 min. Protein complexes were eluted using 250 ml of 3X Laemmli sample buffer containing 5 % β-mercaptoethanol and heated at 65 °C for 5 min in a water bath.

Proteins were resolved using 4–12 % Criterion^{TM} XT Bis–Tris gradient gel (Bio-Rad) and stained with Sypro Ruby (Bio-Rad) according to the manufacturer's instructions. Images were acquired using the Geliance CCD-based bioimaging system (PerkinElmer).

3.2.3 Isolation of PAR-containing complexes using macrodomain PAR affinity resin

PAR-containing protein complexes were isolated with purified GST-Af1521 macrodomain fusion protein construct bound to glutathione beads (Tulip Biolabs, West Point, PA, USA). Macrodomain PAR affinity resin was used essentially as described for IPs except that antibody-coupled magnetic beads are replaced with macrodomain affinity resin suspension (5 ml of the suspension/ ~1 ml of protein extract).

3.2.4 Estimation of PAR levels after exposure to MNNG

The dynamics of PAR was evaluated by a relative quantitation of PAR levels in cells after exposure to MNNG (5 min) and following a recovery period (1 and 2 h). Control and MNNG-treated HEK293 cells were washed with ice-cold PBS and fixed with a 4 % formaldehyde solution in PBS for 15 min. Five PBS washes were performed before membrane permeabilization with a 0.5 % Triton X-100 solution in PBS. Cells were washed three times with PBS and incubated for 90 min at room temperature with anti-PAR monoclonal antibody clone 10H (Tulip BioLabs, West Point, PA, USA) diluted 1:1000 in PBS containing 2 % FBS. PBS washes were performed before incubating cells with an AlexaFluor-488 anti-mouse secondary antibody (Invitrogen). Cells were washed with PBS and counterstained with Hoechst 33342. Fluoromount-G mounting media (Southern Biotechn, Birmingham, AL, USA) was used to prepare microscope slides. Immunofluorescence images were acquired on a Zeiss LSM510 META NLO laser scanning confocal microscope. Zen 2009 software version 5.5 SP1 (Zeiss) was used for image acquisitions and fluorescence intensity measurements. In total, 300 cell nuclei were analyzed from three independent experiments for each experimental condition (100 nuclei/ condition). Relative fluorescence intensity was expressed in arbitrary units (AU) and the data are represented as mean ± standard error of mean (SEM). The recovery of PAR in IP extracts was also determined at the same time-points following MNNG exposure. Aliquots of IP extracts were hand-spotted on Amersham Hybond-N+ positively charged nylon

membrane (GE Healthcare) and probed with antiPAR antibody clone 96-10. Dihydroxyboronyl Bio-Rex (DHBB) purified PAR was used as a reference for the establishment of a standard curve for quantitation (Shah et al., 1995).

3.2.5. Immunoblotting

Whole cell extracts and immunoprecipitates were separated on 4–12 % Criterion XTTM Bis–Tris gradient gel (Bio-Rad) and transferred onto 0.45 mm pore size PVDF membrane (Millipore). After a 1 h incubation with a PBS–MT blocking solution (PBS containing 5 % non-fat dried milk and 0.1 % Tween20), the membrane was probed overnight with primary antibodies (refer to Supplementary Methods for detailed information). Membranes were washed with PBS-MT and species-specific horseradish peroxidase-conjugated secondary antibodies were added for 30 min. Signals were detected with Western Lightning^{TM} Chemiluminescence Reagent Plus kit (Perkin Elmer). Semi-quantitative data was obtained from the scanned films by drawing region of interest (ROIs) around the bands to be quantified. Background signal was subtracted from all images. Signal intensity was expressed as ratios based on density units from control samples using the GeneTool software (PerkinElmer). All data were represented as mean ± standard deviation (SD).

3.2.6 GeLC-MS/MS and label-free spectral counting

SDS–PAGE protein lanes corresponding to immunoprecipitates and negative non-specific IgG control extracts were cut into gel slices using a disposable lane picker (The Gel Company, CA, USA). In-gel protein digest was performed on a MassPrep^{TM} liquid handling station (Waters, Mississauga, Canada) according to the manufacturer's specifications and using sequencing-grade modified trypsin (Promega, Madison, WI, USA). Peptide extracts were dried out using a SpeedVac and separated by online reversed-phase nanoscale capillary liquid chromatography (nanoLC) and analyzed by electrospray MS (ES MS/MS) using a LTQ linear ion trap mass spectrometer (Thermo Electron, San Jose, CA, USA) equipped with a nanoelectrospray ion source (Thermo Electron, San Jose, CA, USA). All MS/MS spectra were analyzed using Mascot (Matrix Science, London, UK; version 2.2.0). Scaffold (version 03_00_02, Proteome Software Inc., Portland, OR, USA) was used to sum the spectral counts, validate MS/MS-based peptide and protein identifications and

group peptides into proteins (refer to Supplementary Methods for detailed information). Semi-quantified proteins by spectral counting analysis were grouped on the basis of their correlated time course profiles following treatment with MNNG. We first normalized every protein spectral counts independently by first subtracting the mean of the spectral counts and then dividing the result by the standard deviation (Z-scores). With this transformation, every protein has a mean of zero and 1 SD. Using the fpc package (Hennig, 2010) in R statistical environment (http://www.r-project.org/) we then identified the optimal number of clusters by running the pamk function (Hennig, 2010). Heatmaps corresponding to 5 min MNNG, 1 and 2 h clusters were generated using MeV software v4.6.1 (http://www.tm4.org/mev/). Functional classification and ID conversion of identified proteins were accomplished by using DAVID (http:/www.david.abcc.ncifcrf.gov).

3.2.7 Isobaric tag for relative and absolute quantitation

For isobaric tag for relative and absolute quantitation (iTRAQ) labeling, proteins were eluted from the Dynabeads with 6 % SDS. Proteins were precipitated overnight with 4 volumes of acetone, centrifuged 15 min at 10000g (4 °C) and pellets were resuspended in 0.5 M triethyl-ammonium bicarbonate (TEAB) containing 0.1 % SDS. Samples were then reduced, alkylated, digested and labeled according to the standard protocol supplied by the manufacturer (Applied Biosystems iTRAQ^{TM} Reagents-Chemistry Reference Guide, P/N4351918A). iTRAQ results were generated from the analysis of four isobaric tags. Control was labeled with iTRAQ reagent 114. The MNNG samples of 5 min, 1 h and 2 h were, respectively, labeled with iTRAQ reagents 115, 116 and 117. Labeled peptides were lyophilized and resuspended in 630 ml of Milli-Q water. An aliquot (315 ml) of this solution containing 0.2 % carrier ampholytes (Bio-Lyte 3/10, Bio-Rad) was used to rehydrate an 18-cm immobilized pH gradient gel strip (pH 3–6), and the other 315 ml containing 0.2 % carrier ampholytes (Ready strip 7–10, Bio-Rad) was used to rehydrate a second 18 cm immobilized pH gradient gel strip (pH 7–10). Rehydratation was set for 10 h at room temperature without any voltage applied. Peptides were focused by applying a voltage of 250 V for 15 min, then 10 000 V for 3 h and finally 10 000 V for a total of 60000 V*h. Immediately after focusing, each strip was cut into 36 segments of 5 mm for a total of 72 fractions. Gel pieces were transferred into a 96-well plate and peptides were

eluted by first incubating the gel pieces for 15 min in 2 % acetonitrile, 1 % formic acid and then for 15 min in 50 % acetonitrile, 1 % formic acid. The extracted peptides were lyophilized using a SpeedVac and resuspended in 25 ml of 0.1 % formic acid in water. An aliquot of 5 ml of this solution was used for LC-MS/MS analysis on an Agilent 1100 nanoLC system coupled to a QSTAR XL equipped with MDS nano ESI source. Raw data (wiff extension file) processing, protein identification, protein quantitation and statistical analyses were undertaken with Protein Pilot software v.3.0 (AB-Sciex) running the Paragon algorithm (Hennig, 2010) (refer to Supplementary Methods for detailed information).

3.2.8 Stable isotope labeling by amino acids in cell culture

Incorporation of stable isotopically labeled amino acids in cell culture (SILAC) was performed essentially as described in (Harsha et al., 2008), (Blagoev and Mann, 2006)). Briefly, HEK293 cells were cultured in DMEM depleted of arginine and lysine. The DMEM was supplemented with 10 % dialyzed FBS (Invitrogen, Carlsbad, CA, USA). Penicillin (100 U/ml) and streptomycin (100 mg/ml) (Wisent, Canada) were added to culture media with Arg and Lys containing naturally-occurring atoms (referred as the light culture) or their stable isotope counterparts [13C6 Lys and 13C6 15N4 Arg (Cambridge Isotope Labs, UK), referred to as the heavy culture]. Cells were grown for at least five divisions to allow full incorporation of labeled amino acids. Cells were tested for complete incorporation of the label. A bicinchoninic acid (BCA) protein assay (Pierce, Canada) was performed on each cell extract before the IP experiment to adjust equivalent amounts of starting material for each condition. The PAR associated protein complexes were immunoprecipitated and eluates were subjected to SDS–PAGE. The fractions were analyzed on a LTQ-Orbitrap Velos coupled to an Agilent 1100 Series nanoflow HPLC instruments using nanospray ionization sources. Protein identification and quantitation were done using Proteome Discoverer (v.1.2, ThermoFisher, Bremen, Germany) and Mascot (v.2.3, Matrix Science) to search against the human IPI database (refer to Supplementary Methods for detailed information).

3.2.9 Data-dependent bioinformatics

3.2.9.1 Gene ontology enrichment analysis

Gene Ontology (GO) term enrichment was performed using DAVID bioinformatics resources (http://david.niaid.nih.gov) (Huang da et al., 2009) to determine whether particular GO terms occur more frequently than expected by chance in a given dataset. Default settings for the Biological Process category were used. The Cytoscape (Shannon et al., 2003) plugin BiNGO (Maere et al., 2005) was also used to assess enrichment of GO terms and to generate diagrams.

3.2.9.2 Network construction and visualization

The Cytoscape plugins Michigan Molecular Interactions (MiMI) plugin (Gao et al., 2009) and BisoGenet (Martin et al., 2010) that both integrates data from multiple well known protein interaction databases were used to retrieve molecular interactions and interaction attributes. Direct protein interactions were displayed using Cytoscape (v2.7.0) using the corresponding official gene symbols. A subnetwork containing the physical interactions between proteins involved in the DNA damage response was extracted from the main network (refer to Supplementary Methods for detailed information).

3.2.10 Recruitment of DNA damage response factors to laser-induced DNA damage sites

The recruitment kinetics of DNA damage response factors was assessed essentially as described (Gagne et al., 2009) with the following modifications. After overnight transfections with Effectene reagent (Qiagen), HEK293 cells expressing GFP-fusion proteins were incubated with fresh medium containing 1 mg/ml of Hoechst 33342 for 30 min at 37 °C. To study the PAR-dependent recruitment of proteins at DNA damage sites, cells were incubated with 5 mM of PARP inhibitor ABT-888 for 2 h prior to micro irradiation and recruitment analysis. A 37 °C pre-heated stage with 5 % CO_2 perfusion was used for the time-lapse on a Zeiss LSM-510 META NLO laser-scanning confocal microscope (40 X objective). Localized DNA damage was generated along a defined region across the nucleus of as single living cell by using a bi-photonic excitation of the Hoechst 33342 dye, generated with a near-infrared 750-nm titanium:sapphire laser line (Chameleon

Ultra, Coherent Inc.) The laser output was set to 3 % with 10 iterations, except for PARP-1 and XRCC1 which were adjusted to 2 % to avoid signal saturation. A Multi-Time macro developed in-house for AIM software v3.2 (Zeiss) was used for image acquisition. Background and photobleaching corrections were applied to each datasets as described (Haince et al., 2008). A minimum of eight recruitments per construct were collected and analyzed. Mean recruitment curves were plotted with Kaleidagraph v4.03.

3.3 Results

3.3.1 Isolation of PAR-containing protein complexes

Before focusing on PAR dynamics, we first conducted a large-scale proteome analysis using nanocapillary liquid chromatography-tandem MS (GeLC-MS/MS) to explore the protein composition of PAR-associated protein complexes at the peak of PAR accumulation in cells following MNNG exposure (MNNG 5 min). To validate and generalize our findings in HEK293 cell extracts, PAR IPs were additionally performed in HeLa whole cell extracts under the same experimental conditions. A schematic workflow of the study is illustrated in Figure 14. High throughput protein–PAR interactions have remained largely inaccessible owing to the transient nature of poly(ADP-ribosyl)ation. In a previous study (Gagne et al., 2008), we reported that mouse monoclonal antibodies against PAR, such as clone 10H, can efficiently pull down PAR in poly(ADP-ribose) glycohydrolase (PARG) knocked-down cells. For the present study, we empirically optimized a low-salt lysis strategy that is both effective in extracting PAR-binding proteins while preserving non-covalent interactions. Using slightly alkaline pH, low ionic strength, a zwitterionic detergent (CHAPS) and a potent PARG inhibitor, we were able to extract and preserve high amounts of PAR over time.

A limitation associated with the use of 10H antibody is the low affinity for short PAR molecules (less than 20 ADP-ribose residues) (Kawamitsu et al., 1984). However, long and

complex (branched) polymers, which are formed following DNA damage induction, are well recognized by 10H antibodies. A complementary tool for the isolation of PAR-containing complexes was also developed based on the use of a catalytically inactive GFP-PARG (PARG-DEAD) isoform. PARG shares structural similarity to the conserved and widespread family of ADPribose-binding macrodomain modules (Slade et al., 2011), (Hassler et al., 2011). In this view, our second approach can be considered as an affinity-purification technique similar to IP, except that catalytically inactive macrodomain-like containing bait was used to pull down proteins trapped into PAR-containing complexes. A macrodomain PAR affinity resin, which consists of purified GST-Af1521 macrodomain (Allen et al., 2003) fusion protein bound to glutathione beads, was also used as a bait to capture PAR-associated protein complexes. Addressing PAR binding requires a systematic approach that can benefit from various alternatives.

Globally, we report the high-confidence identification of 609 proteins (33 621 MS/MS spectra, 2.7 % peptide false discovery rate; a minimum of two unique peptides, (Supplementary Table S1), which several of these are actually associated with the regulation of DNA repair and chromatin remodeling. The 10H and PARG-DEAD datasets share striking similarities but also express differences as PARG-DEAD datasets also include specific PARG-interacting proteins in addition to PAR-associated proteins (Figure 15A). One important difference between the PAR-associated protein datasets coming from antibody (10H) and PARG-DEAD approaches is the bias toward different cellular compartments. When a PARG-DEAD mutant is used as a substrate trapping bait to co-purify PAR-binding proteins, the protein dataset is significantly enriched in nuclear proteins, whereas an antibody-mediated approach targets more mitochondrial proteins (Figure 15B). The vast majority of proteins identified with the Af1521-macroprotein PAR affinity resin were also identified with the PARG-DEAD dataset, an observation consistent with the fact that PARG and Af1521 are both members of the ADP-ribose-binding macrodomain family. The macrodomain PAR affinity resin protein dataset is exclusively composed of nuclear proteins that are coherent with its functions in nucleosome stability and regulation. Globally, a PARG-DEAD ligand binds a wider range of proteins and thus, represents a valuable tool for the isolation of PAR-containing complexes. Furthermore, in

this approach, the bait is expressed *in vivo* in mammalian cells, a feature that more accurately reflects physiological conditions. Figure 15C graphically represents the peptide coverage of all the proteins identified at the peak of PAR accumulation. Proteins are plotted according to the number of unique peptides assigned to each protein (Supplementary Table S1). There is a correlation between protein abundance and the number of unique peptides identified for that protein. Generally, proteins anticipated as being in high abundance, such as PARP-1 in PAR IP extracts, are typically identified by the largest number of unique peptides. Proteins assigned with the fewest number of unique peptides are of low abundance. The fact that several DNA damage response (DDR) regulators scored prominently in either 10H-, PARG-DEAD- and macrodomain-based protein datasets support the biological relevance of both our overall screening strategy and the identification of additional top-scoring hits. Although a peptide count approach is not inherently quantitative, it provides rough estimates of protein abundance that are, in our experience, estimated fairly accurately as most of the PAR-binding proteins known so far are among the proteins with the best peptide coverage. Selected nucleic acids binding proteins are displayed according to their estimated relative abundance (Figure 15C). In addition to PARP-1, the GeLC-MS/MS dataset also contains other PARP family members (PARP-2, PARP-9, PARP-12 and PARP-13) and numerous proteins involved in the maintenance of genome integrity. Most of the PAR-binding proteins previously reported in other studies were identified using our affinity purification procedures, including XRCC1, LIG3, KU70, DNA-PK (Pleschke et al., 2000), CHD4 (Polo et al., 2010), CHD1L (ALC1) (Ahel et al., 2009), (Gottschalk et al., 2009), DEK (Fahrer et al., 2010), NUMA (Chang et al., 2005), MVP (Kickhoefer et al., 1999), BUB3 (Saxena et al., 2002), DNA-PK (Ruscetti et al., 1998), DNMT1 (Reale et al., 2005), SUPT16H (Huang et al., 2006), TOP1 (Malanga and Althaus, 2004), TOP2B (Meyer-Ficca et al., 2011), hnRNPs (Gagne et al., 2003), (Ji and Tulin, 2009) and histones (Panzeter et al., 1993). High-quality spectra were also used to establish a list of proteins identified with unique peptides. Protein identifications were accepted if the corresponding peptide was assigned in at least two independent experiments (Supplementary Table S1). Examples include the chromodomain-helicase-DNA-binding protein 1 (CHD1), DNA repair protein RAD50 and the mitochondrial apoptosis inducing factor (AIF) (Wang et al., 2011). The presence of RAD50, a component of the MRE11-

RAD50-NBS1 (MRN) complex, was validated by western blot analysis in PAR IP extracts (Figure 17A), an indication of the data quality. Being confident that our PAR isolation method is worthy and effective for the analysis of a wide range of PAR-associated protein complexes, we further examined the time-dependent accumulation of DNA repair factors in PAR pull-down extracts up to 2 h following genotoxic insult.

3.3.2 Time-resolved quantitative proteomics analysis of PAR-containing protein complexes

The insights gained by the identification of PAR-associated protein complexes and their DNA damage response pathways can provide valuable clues pointing to target proteins. A major challenge is to understand the dynamic behavior of these targets with respect to PAR. This requires knowledge of the protein dynamics in complex molecular signaling systems tethered together via interactions with heterogeneous PAR. A mean of generating quantitative information on protein networks responsive to DNA damage is to investigate which network components of these are actually accumulating in affinity pull-down experiments targeting PAR.

3.3.2.1 Western blot analysis of DNA damage recognition and repair factors in PAR IP extracts at sequential time-points following PARP activation

To make further analysis on the PAR-associated interactome, we examined the dynamic changes of the PAR-associated protein complexes composition by time course analysis of PAR proteome changes following exposure to MNNG-induced DNA damage. This approach needed to conciliate two opposite requirements. Since the half-life of PAR in cells is estimated to be < 1 minute, PAR hydrolysis must be limited in order to preserve PAR pools with respect to the time required by the pull-down assay. On the other hand, a complete disruption of PAR turnover is not desirable since it would block the dynamics of the targeted protein complexes. To overcome this challenge, the use of a competitive PARG inhibitor (ADP-HPD) (Slama et al., 1995) appeared to be very appropriate. In contrast to an RNAi-based specific knock-down of PARG resulting in sustained cellular PAR levels for a prolonged period of time (Gagne et al., 2008), the use of a PARG inhibitor in cell extracts at the time of lysis enables the normal modulation of cellular PAR levels,

whereas stabilizing PAR in cell extract required for efficient pull-down assays. The turnover of PAR was estimated by polymer-blot analysis and immunofluorescence. Hand-spotted DHBB-purified PAR (Shah et al., 1995) was used as reference to estimate PAR content in IP extracts (Figure 16A). We were able to recover more than 10 pmol of PAR/106 cells, which represent a significant fraction of total PAR formed during alkylation-induced DNA damage (Malanga and Althaus, 1994), (D'Amours et al., 1999). Immunostained PAR quantitation indicate that the recovery of PAR by IP closely match the turnover of PAR in living cells (Figure 16B). Cellular PAR levels reach a maximum (30- to 50-fold increase) after 5 min of MNNG treatment and subsequently decrease to basal levels. After a 2-h recovery period, PAR is nearly undetectable by western blot except for PARP-1, which remains significantly automodified (Figure 17A). In contrast, PAR shows a wide distribution at peak levels from the loading well down to the low molecular weights at the bottom of the blot. This ADP-ribose polymers' size distribution of the products generated by PARPs and PARG interplay are presumably the consequence of the resolution of free and protein-bound PAR from various lengths and branching frequencies. We therefore hypothesized that PAR-containing DNA repair complexes would primarily be isolated in this fraction. As expected, several DNA repair factors are trapped in immunoprecipitates corresponding to MNNG-treated cells, with a predominant enrichment in the 5 min sample that contains the highest levels of PAR (Figure 17A). The presence of PARP-1 and its high confidence interactors indicates that PAR-associated protein complexes are efficiently pulled down. The relatively high level of PARG present in these samples also validates the presence of poly(ADP-ribose) degrading enzymes in these fractions. Semi-quantitative analyses of protein levels were measured by densitometry scanning of western blots shown in Figure 17A. Profiles were generated for every targeted DNA damage response (DDR) factors and their abundance was correlated to PAR dynamics (Figure 17B). The base excision repair (BER) pathway clearly shows a prominent association with PAR, especially as core components of the BER pathway (LIG3 and XRCC1) are hard to detect in control conditions that correspond to the pull down of PAR-containing complexes in the absence of genotoxic insult. This result is consistent with the preferential interaction of the XRCC1/LIG3 complex with the poly(ADP-ribosyl)ated form of PARP-1 (Leppard et al., 2003). In contrast, components of the nonhomologous end

joining (NHEJ) and HR repair pathways are more stably associated with PAR-containing complexes under basal conditions, a characteristic that tends to temper the relative accumulation ratios after DNA damage. As a proof of concept, we identified several DDR targets by western blot analysis of anti-PAR immunoprecipitates with a global accumulation trend that correlates to PAR levels. This observation led us to further explore the dynamics of PAR-associated complexes by quantitative MS.

3.3.2.2 Quantitative proteomics analysis of complex protein mixtures in PAR IP extracts

Quantitative proteomics can reveal changes in protein abundance that can be indicative of a component that has affinity for PAR or likely part of PAR-modulated protein complex, including previously undescribed factors. Several relative and absolute quantitative proteomics techniques have been developed in recent years. Generally, MS-based quantitation methods fall into two categories: label-free or label-based approaches (Schulze and Usadel, 2010), each having specific strengths and limitations (Mallick and Kuster, 2010). Whereas most quantitative proteomics studies rely on either strategy, we undertook a more systematic approach for a thorough analysis of the PAR proteome (Figure 14).

3.3.2.3 Label-free quantitation

The spectral counting method has become an accepted technique to estimate the relative abundance of proteins in highly complex samples. Spectral counting is a large-scale strategy easily applicable to GeLC-MS/MS protein identification. One of the main advantages of the method is that it does not require the use of high resolution mass spectrometers such as those required for quantitative label-based MS approaches. Antibody-mediated affinity purification of PAR-containing protein complexes was performed in HEK293 whole cell extracts after exposure and release from MNNG-induced DNA damage and PARP activation. Untreated cultures were used as a basis for calculating protein ratios derived from peptide spectral counts. A set of 425 proteins was identified (Supplementary Table S2) from which we extracted 275 proteins that follow a kinetics pattern that clusters them into one of the three time-points analyzed after MNNG exposure (Figure 18A). K-means clustering is one of the most popular partitioning methods. We used a robust version of K-means clustering based on medoids by using the pamk function

(partitioning around medoids) (Hennig, 2010) to group proteins identified during our screen based on their time course profiles following exposure to MNNG. The goal of the algorithm is to segregate each protein dynamics into the profiles that they most closely matched. Partitioning around medoids is more robust than K-means in the presence of noise and outliers, an interesting feature since PAR-associated proteins exhibited significant variability over a wide range of ratios. By clustering proteins with similar accumulation trend, we were able to obtain a clear snapshot of protein enrichment in relation with PAR dynamics (Figure 18A). We hypothesized that proteins with a distribution pattern that correlates with PAR levels are presumably proteins with close connection with PAR, whether by being covalently poly(ADP-ribosyl)ated, non-covalent PAR-binders or major components of PAR-associated protein complexes. The top biological processes associated with each clusters of proteins were identified using DAVID bioinformatics resources (Functional gene classification tool based on GO terms) (Huang da et al., 2009). Biological processes were displayed as P-value bar plots (Figure 18B). The P-values represent the probability to see a random enrichment in the displayed biological process. As cells recover from genotoxic stress, we can observe an evolution of the major biological processes associated with PAR turnover. Although there is an overlap among the processes, the first predominant biological process identified at the peak of PAR levels (MNNG 5 min) is related to the DNA damage response which is consistent to the rapid activation of PARPs and PAR synthesis in response to DNA strand breaks. After a 1 h recovery period from MNNG exposure, proteins involved in translational processes are highly over-representative of the PAR-associated proteome, whereas regulatory circuits that control mRNA splicing, stabilization and translation are most prominent after 2 h. Individual protein accumulation trend was displayed in a heatmap for the three time-points analyzed after MNNG exposure (Figure 19). Proteins were grouped according to their kinetics profile. As we could expect, one can observe that PARP-1 is closely related to the kinetics of XRCC1 and LIG3, two stably associated components of the BER pathway. Similarly, KU80 (XRCC5), DNA-PK (PRKDC) and the facilitator of chromatin transcription (FACT) complex subunit SSRP1 are grouped together soon after the induction of DNA damage in the 5 min MNNG cluster. This approach could help to better focus on PAR-responsive

protein complexes involved in biological processes that contain numerous components such as those observed at later time-points following the induction of DNA damage.

3.3.2.4 Label-based quantitation: iTRAQ and SILAC analysis

SILAC (Ong et al., 2002) and iTRAQ (Ross et al., 2004) are two widely used methods to quantify protein abundance in tissue cultures. Whereas SILAC involves metabolic incorporation of isotope mass tags directly into proteins, iTRAQ chemical labeling is performed on peptides after lysis and trypsin digestion. Both SILAC and iTRAQ strategies were coupled to PAR affinity-purification for the quantitation of protein abundance in time-resolved IP extracts following MNNG-induced DNA damage and PARP activation. Ratios of protein abundance were estimated based on datasets from untreated cells that correspond to basal levels of poly(ADP-ribosyl)ation in the absence of genotoxicity. As for any quantitative differential analysis, the most interesting identifications are those that differ by a substantial amount from the rest of the data (outliers). Box plots are particularly useful to display the distribution of a dataset and pinpoint those outliers. Figure 20 shows the box plot diagrams of iTRAQ and SILAC experiments. All the outlier values correspond to important protein accumulation in PAR IP extracts. The intensities of the ratios and the number of outliers decrease as we proceed from 5 min to 1 h and 2 h post-MNNG treatment, an observation consistent with the progressive decrease of PAR levels. Detailed iTRAQ and SILAC datasets are listed in Supplementary Table S3 and S4. Although they are based on different approaches, iTRAQ and SILAC analysis reported a similar set of enriched proteins in PAR IP extracts. The BER (XRCC1, LIG3) and the NHEJ (DNA-PK (PRKDC), XRCC5 (KU80), XRCC6 (KU70) multiprotein repair complexes are consistently found with both methods, as well as the facilitates chromatin transcription (FACT) complex subunits SSRP1 and SUPT16H. Proteins forming the nuclear lamina (LMNA, FLNA, TMPO) are also found with high ratios in consistency with their relative abundance found in GeLC-MS/MS dataset. Of particular interest are other factors that follow the same accumulation trend as did well characterized PAR-binding proteins, suggesting a close link with poly(ADP-ribosyl)ation and chromatin functions. Proteins with high ratios such as barrier to- autointegration factor (BANF1), single-stranded DNA-binding protein (SSBP1) or the thyroid hormone receptor-associated protein 3 (THRAP3)

have not been characterized in the context of PAR metabolism. However, PARP-1 has been found as a chromatin associated partner of BANF1 (Montes de Oca et al., 2009); SSBP1 localizes in H2AX/PARP-1 complexes (Yang et al., 2010) and THRAP3 is a component of the human mediator complex that functionally interacts with PARP-1 (Hassa et al., 2005). Each label-based quantitation method had its own strengths. For example, only SILAC analysis identified APLF (Aprataxin and PNK-like factor) as one of the most enriched protein in 5-min MNNG immunoprecipitates. This is consistent with the fact that APLF contains a PAR-binding PBZ motif (Ahel et al., 2008), (Eustermann et al., 2010), (Li et al., 2010). In addition to APLF, centrin-2 (CETN2) and hexokinase-1 (HK1) were identified with high ratios. However, in such cases, quantitations were based on unique peptides so the measured ratios must be tempered. Finally, one should keep in mind that the proteins displayed in iTRAQ and SILAC box plots (Figure 20) are those with extreme values with respect to the entire dataset. Proteins with more modest enrichment ratios that fall within the upper quartile (75th percentile) still represent interesting PAR-associated candidates. For example, the stress granule-associated PARP-13 was identified in each of the time-points analyzed by SILAC but only after 2 h of MNNG exposure did it stand out from the protein dataset. Another example is NUMA, a poly(ADP-ribosyl)ated protein only found in the 2 h MNNG SILAC dataset with the same modest ratio as DNA-PK (PRKDC), SSBP1 and Mediator of DNA damage checkpoint protein 1 (MDC1) (Refer to Supplementary Tables S3 and S4 for detailed information).

3.3.3 Protein network modeling of PAR-associated proteins

To gain insight into the dynamics of PAR-associated proteins, we mapped a protein interaction network based on datasets derived from MS analysis. The global PAR-responsive proteome modeled on the basis of all the proteins identified in this study resulted in a network of 959 proteins (nodes) and 8931 interactions (edges). The entire network is provided for interactive visualization of protein interactions in the Cytoscape session file (Supplementary Material). The network can be easily loaded and visualized using Cytoscape, which if freely available for download as a open source bioinformatics software (www.cytoscape.org). The ClusterOne algorithm was used to detect clusters of highly connected multiprotein complexes in the global network with associated confidence

values. A group of 6 clusters with $P<0.05$ were detected and extracted from the global PAR proteome. These clusters includes (i) ribosomal proteins (93 proteins), (ii) polyubiquitin-C substrates (200 proteins), (iii) mitochondrial proteins (53 proteins), (iv) mRNA splicing and maturation factors (68 proteins), (v) components of the nuclear pore complex (24 proteins) and (vi) a small group of proteins involved in mitotic cell cycle (7 proteins) (Supplementary Cytoscape session file). To provide context and a more targeted view of our quantitative analysis of the PAR-responsive proteome, we isolated a subnetwork of proteins that reflects significant molecular events linked to DNA damage response and PAR metabolism. We extracted the first neighbors (direct protein–protein interactions) linked to protein components of the main DDR pathways found in our proteomics datasets. All the PARPs identified in this study were extracted in addition to components of the BER (XRCC1, LIG3), NHEJ (DNA-PK, XRCC5, XRCC6) and the FACT complex (SUPT16H, SSRP1). This subnetwork, composed of 164 nodes and 899 edges highlights the emerging importance of PAR in the regulation of DDR (Figure 20). The most enriched proteins in PAR IPs from GeLC-MS/MS, spectral counting, iTRAQ and SILAC datasets (top-scoring proteins) were flagged to underscore their relative abundance. The third quartile value was selected as the cut-off criteria (cut-off point for the highest 25 % of the observed ratios; Supplementary Table S5). This complex network structure represents a part of the DNA damage and repair response protein interaction map closely related to PARP-1 and highlights the value of integrating protein interaction information as it reveals potential PAR-binding candidates to prioritize for functional follow-up. Interestingly, almost all the PARP-1 subnetwork (160 out of 164 proteins) connects to polyubiquitin-C (UBC) according to the interaction databases (Supplementary Cytoscape session file).

3.3.4 Dynamic recruitment of DNA damage response factors to sites of DNA damage

Whichever method was used to explore the PAR interactome during alkylation-induced genotoxic stress, components of the BER and NHEJ repair pathways scored prominently in the quantitative protein profiles. The consistency of this observation strongly suggests that PAR could be an important effector involved in the regulation of these repair processes. It had already been recognized that localized PAR formation facilitates the accumulation of DNA repair factors at sites of broken DNA (Malanga and Althaus, 2005). This is

particularly critical for the scaffolding protein XRCC1 for which recruitment at DNA damage sites depends on the presence of PAR (El-Khamisy et al., 2003), (Masson et al., 1998), (Mortusewicz et al., 2007). In order to study the dynamic recruitment of DNA repair factors, we used a combination of Hoechst 33342 incorporation and near-infrared 750-nm two-photon laser micro-irradiation to induce DNA damage in subnuclear regions of single cells (Figure 22B). As expected, most of the DDR factors targeted in this study are recruited at laser-induced DNA damage sites (Figure 21B). The contribution of PAR to the recruitment process of DNA repair factors was evaluated by treating the cells with the potent PARP inhibitor ABT-888 [reviewed in Ref. (Rouleau et al., 2010)]. We first focused on XRCC1 to validate our approach since its PAR-dependent accumulation at DNA damage sites was clearly demonstrated. Indeed, XRCC1 recruitment at DNA damage sites is severely decreased when PARP-1 is inhibited (Figure 21C). Because XRCC1 acts as a coordinator of BER, we anticipated that PARP-1 inhibition would lead to a reduced accumulation of LIG3 and other BER-associated factors. Although recruited at DNA damages sites with less intensity than XRCC1, we observed a decreased relocation of LIG3 when PARP activity is inhibited. A similar dynamics was observed for the Flap endonuclease 1 (FEN1) which also possesses functions in the BER system. These results underscore the role of PAR in facilitating the recruitment of BER factors and are consistent with the identification of these factors as some of the most enriched proteins in PAR IP extracts. Following the same idea, we anticipated that the recruitment of major components of the NHEJ repair pathway at DNA damage sites would also be influenced by a decrease in the accumulation of PAR. We did see a modest recruitment of each of the targeted NHEJ factors in the path of the laser track (KU70, KU80, XRCC4, LIG4, XLF and ARTEMIS) but none of these showed a significant dependence on PAR to localize at DNA damage sites (Figure 22B). In addition to DNA repair events, extensive chromatin remodeling and histone modifications occur at sites of DNA damage. Following this idea, our attention was directed toward a chromatin remodeling complex consistently trapped in PAR IP extracts, namely the FACT complex SUPT16H/SSRP1 that acts to reorganize nucleosomes.

As a control, we used CHFR, a chromatin remodeling protein that regulates histone modifications and the ATM-dependent DNA damage response pathway after DSBs (Wu et

al., 2011). CHFR possesses a PBZ domain known for its non-covalent interaction with PAR. As expected, CHFR recruitment and retention at DNA damage sites is strongly decreased in presence of ABT-888, whereas SSRP1 recruitment is unaffected (Figure 22C). In our protein clustering experiment, we found that SSRP1 accumulation profile with respect to PAR closely match those found for KU80 and DNA-PK (Figure 19, 5 min MNNG cluster). SSRP1 was also found with high ratio in iTRAQ and SILAC experiments (Figure 19) along with its stable partner SUPT16H. The modest intensity of SSRP1 accumulation at DNA damage sites falls within a similar range as that for the NHEJ factors and this accumulation is also PAR-independent.

3.4 Discussion

This study represents the first reported proteome-wide effort to follow protein dynamics in the context of PAR modulation after DNA damage. In addition to the exploration of the PAR-associated proteome with antibody-mediated affinity purification, MS-based substrate trapping strategies were used as complementary approaches to mine the accessible PAR-associated proteome. These analyses suggest that the presence of PAR in many multiprotein complexes involved in genome surveillance could be functionally relevant. Yet, these complexes are not static, but instead are dynamic assemblies that orchestrate DNA damage signaling and repair. In the present study, the time-correlated relationship between protein entrapment in PAR-containing complexes and PAR dynamics was further investigated using a combination of quantitative proteomics techniques. Despite intrinsic differences between spectral counting, SILAC and iTRAQ methodologies, we identified several proteins whose abundance was consistently correlated to PAR levels. It has been known for a long time that PAR levels are transient and spontaneously resolving after their rapid degradation by PARG. However, there is an apparent gap between our understanding of the initial PAR-associated molecular events underlying DDR and major nuclear reorganization, and the profound impact of PAR on cell fate. In our study of PAR dynamics, we found that several DDR factors are co-eluting with PAR, consistent with the

accumulation of DNA repair factors near the damage site and the current model where PAR is viewed as a loading platform for the repair machinery (Malanga and Althaus, 2005), (Hassa et al., 2006). Recent identification of chromatin associated proteins whose recruitment to DNA damage sites is PAR-dependent [e.g.: CHD4 (Polo et al., 2010), (Chou et al., 2010), MTA1 (Chou et al., 2010), MRE11 (Haince et al., 2008), NBS1 (Haince et al., 2008), ALC1 (Ahel et al., 2009), (Gottschalk et al., 2009), APLF (Harris et al., 2009), (Rulten et al., 2008), XRCC1 (El-Khamisy et al., 2003), BMI-1 (Gieni et al., 2011), MEL-18 (Chou et al., 2010)] also points towards this model. Thus, local poly(ADP-ribosyl)-ation at DNA damage sites may be a common phenomenon for the recruitment of DDR factors that control genome integrity. It is highly likely that more DDR factors and chromatin remodelers found in this study will join this expanding group of proteins. Using laser micro-irradiation and live cell imaging analyses, we have shown that the retention of repair factors at sites of DNA damage can exhibit a wide range of dependency on PAR. Given that PAR formation can be subjected to a 100-fold increase after the induction of DNA damage (Gao et al., 2009), a rapid accumulation at the DNA damage site would logically occur for a non-covalent PAR-binding protein. Indeed, we showed that XRCC1, which possesses a PAR-binding motif (Egloff et al., 2006), and CHFR, a PBZ-containing protein, are both showing a very significant decrease of retention at DNA damage sites when poly(ADP-ribosyl)ation is inhibited. There are a variety of intricate DNA damage response mechanisms that underlie spatial relocation of proteins at DNA breaks. Although poly(ADP-ribosyl)ation appears as the main driving force behind the recruitment of BER factors at DNA damage sites (i.e. XRCC1 and LIG3), this phenomenon is likely to be involved in the regulation of other functions as in the case of NHEJ. The identification of PARP-1, DNA-PK and KU70/80 as predominant PAR-associated protein components suggest that these proteins participate to a same pathway to cope with DNA damage. This finding supports previous studies that established KU70, KU80 and DNA-PK as substrates of PARP-1 (Li et al., 2004), (Galande and Kohwi-Shigematsu, 1999), (Ariumi et al., 1999) and is also consistent with a model where PARP-1/DNA-PK interplay dictates the functional properties of the NHEJ repair complex (Spagnolo et al., 2012). Although the relocation of core NHEJ factors at DNA damage sites is PAR-independent, the presence of PARP-1 and PAR in these complexes appears to play a more downstream role in the DNA

damage response. This can be illustrated by reports indicating that poly(ADP-ribosyl)ation of the KU70/KU80 complex impairs its ability to bind DNA (Li et al., 2004) or the stimulation of DNA-PK activity upon poly(ADP-ribosyl)ation (Ruscetti et al., 1998). A recent study reports that PARP-1 binding to DSBs elicits substantial conformational changes in the DNA-PK dimer assembly (Spagnolo et al., 2012). Following the idea that interactions within a PARP-1/ DNA-PK complex might affect the mechanism of DNA-PK activation, the presence of PAR through automodified PARP-1 could led to structural transitions with functional consequences on NHEJ. This study and most of the current research focus on poly(ADP-ribosyl)ation as an early response to genotoxic stress. However, it is clear that the consequences of poly(ADP-ribosyl)ation are not limited to the early DNA damage response, but also impact on stress response and cytoprotection. Later consequences may include changes in gene expression and global cellular responses of death and survival within hours and days (Schmidt-Ullrich, 2003). This effort represents the most extensive proteomics coverage in the context of PARP activation following DNA damage and contributes to a growing body of evidence that implicates PAR as a coordinator of multiple activities required for maintaining genome integrity.

3.5 Supplementary data

Supplementary Data are available online, containing Supplementary Tables 1–5 and Supplementary Methods. (http://nar.oxfordjournals.org/content/40/16/7788/suppl/DC1)

3.6 Acknowledgements

The authors are grateful to Dr Michèle Rouleau for useful discussions and suggestions for experiments, and Pierre Gagné for his assistance with network modeling and data

processing. The authors also thank the University of British Columbia Proteomics Core Facility for the preparation and analysis of protein samples for SILAC analysis. We are particularly grateful to Dr Sylvie Bourassa who managed most of the samples at the Proteomics Platform of the Quebec Genomics Center and Sandra Breuils-Bonnet for iTRAQ labeling and IEF fractionation.

3.7 Funding

Canadian Institutes for Health Research [CIHR MOP-14052, MOP-74648]. Funding for open access charge: Canadian Institutes of Health Research (CIHR).
Conflict of interest statement. *None declared*.

3.8 Figures and Legends

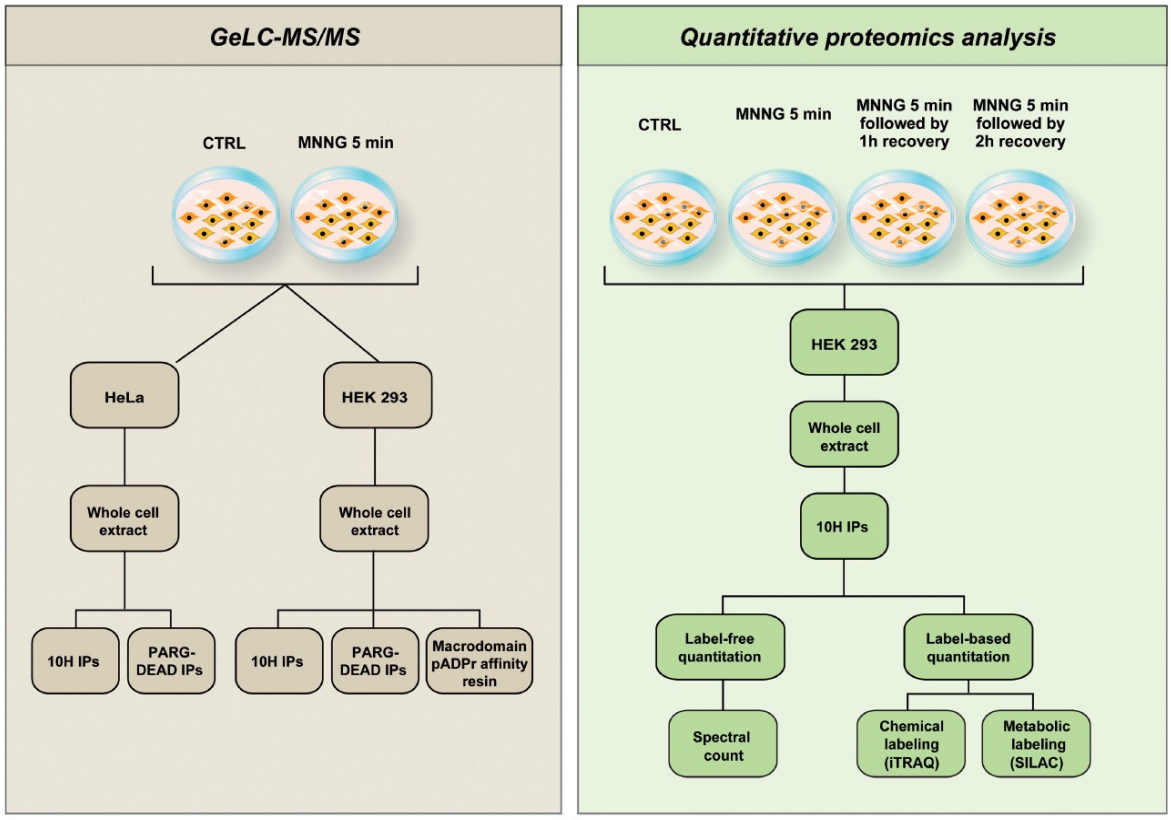

Figure 14: **Schematic representation of the experimental design and proteomics strategies to identify PAR-associated protein complexes**
A combination of affinity-purification procedures coupled with MS was used to generate a global protein profile of PAR-associated protein complexes (GeLC-MS/MS—**left panel**). Proteomics strategies that integrate relative quantitation with affinity-purification MS were used to provide a time-resolved proteome profile of protein networks responsive to PAR turnover (**right panel**). Complementary label-free and label-based quantitative proteomics approaches were used to identify and evaluate protein changes occurring in cells following alkylation-induced DNA damage and PARP activation. 10H IPs: Immunoprecipitations with anti-PAR antibody clone 10H; PARG-DEAD IPs: IP of catalytically inactive PARG, as described in the text.

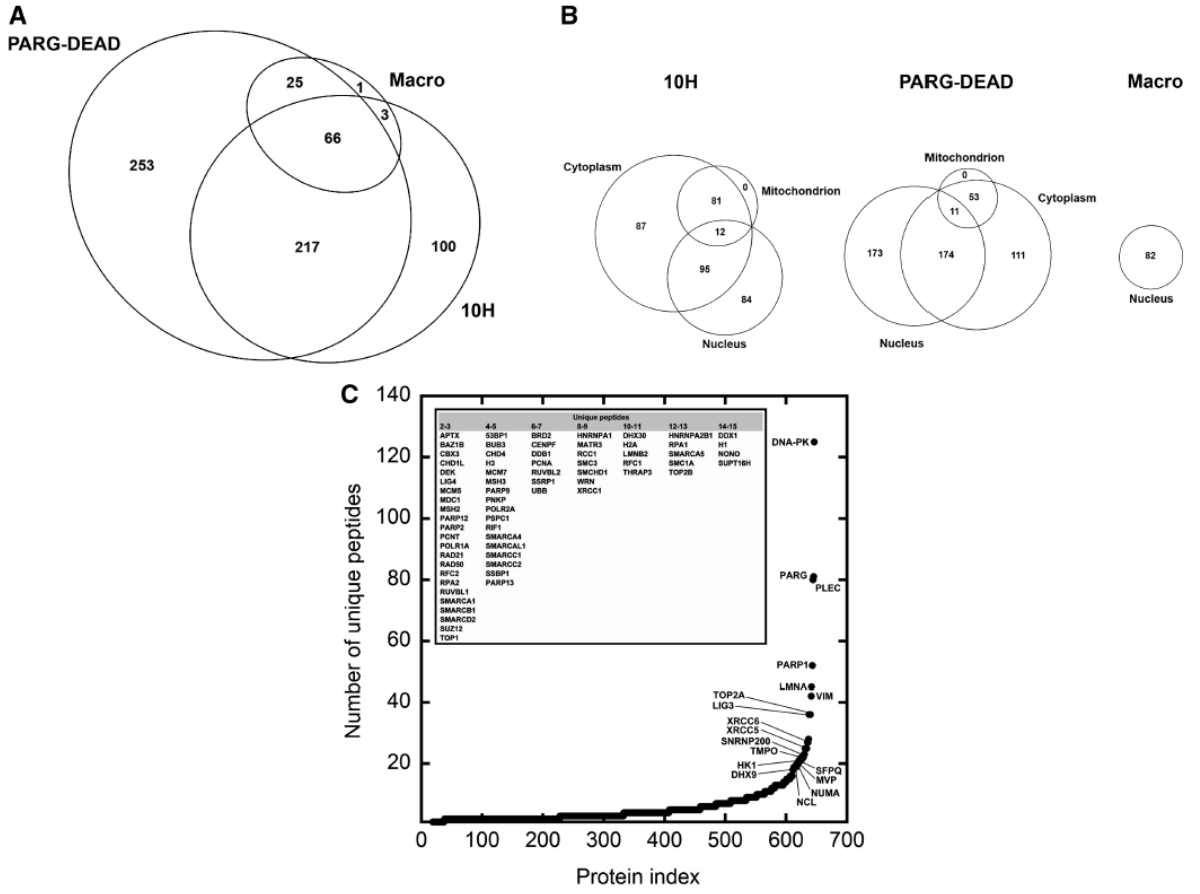

Figure 15: **Diversity of PAR-associated proteins as revealed by gel-based LC-MS/MS analysis**

Complementary proteomic approaches directed towards identification of novel proteins that interact with PAR were integrated to mine the accessible PAR-binding interactome. IPs were performed directly against PAR using a high affinity monoclonal antibody (clone 10H) or indirectly by a novel PAR substrate trapping approach targeting a catalytically inactive PARG mutant and a macrodomain protein (see text for details). **(A)** The area-proportional Venn diagram shows unique and shared protein identifications in PAR-associated protein datasets that originate from each strategies. **(B)** Area-proportional Venn diagrams depicting the distribution of proteins in subcellular compartments for each datasets. Proteins were classified into cytoplasmic, nuclear or mitochondrial compartments according to GO classification. **(C)** Classification of PAR-associated proteins. Proteins are ordered relative to the number of unique peptides assigned. The inner frame lists some DNA damage response factors and chromatin-associated proteins with their corresponding number of unique peptide assignments. Refer to Supplementary Table S1 for detailed protein listing.

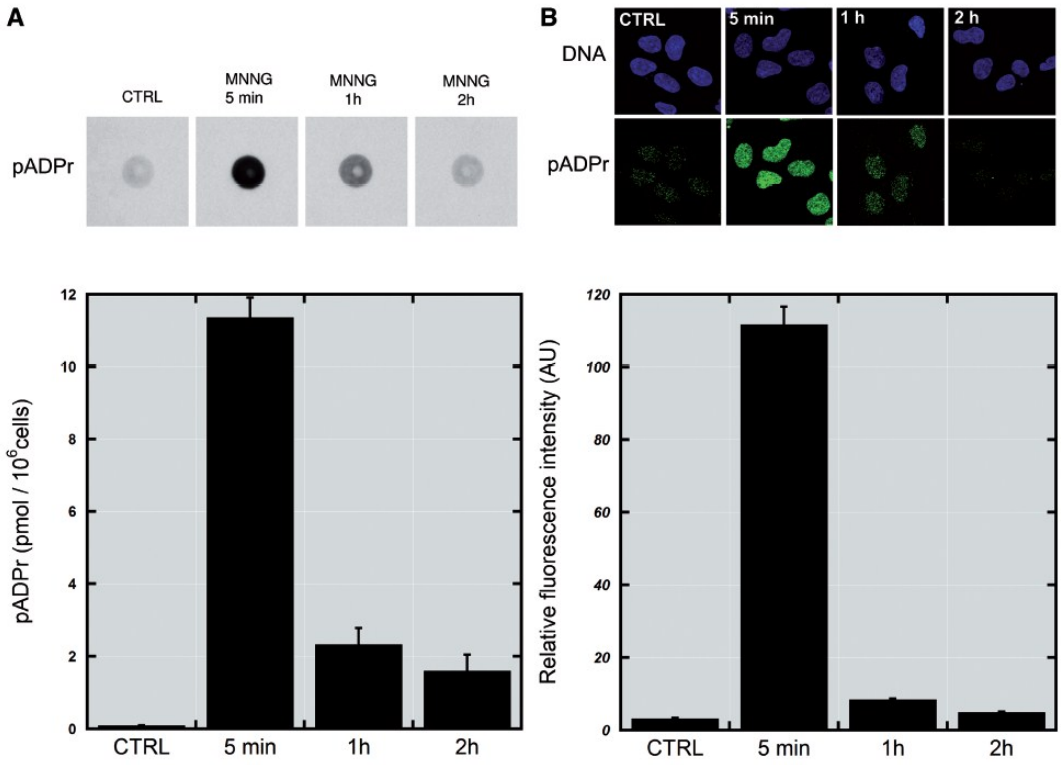

Figure 16: PAR dynamics following MNNG-induced DNA damage and PARP activation

(A) Dot-blot analysis of PAR levels in PAR IP extracts from MNNG-treated HEK293 cells. Cellular material bound to 10H-coupled magnetic beads was eluted and hand-blotted on positively charged nylon membrane. PAR was detected using 96-10 antibody (upper panel). PAR signals in IP extracts were quantified using DHBB-purified PAR as a reference value for quantitation and displayed on a bar graph (lower panel). The data are represented as the mean±SEM (n=4). **(B)** The 10H immunofluorescence labeling of PAR in HEK293 cells exposed to MNNG (upper panel). Confocal fluorescent images were obtained by a Zeiss LSM 510 NLO laser scanning confocal microscope. A region was drawn inside of each nucleus (n=100) to establish the mean fluorescence intensity. Relative PAR levels were plotted on a bar graph (lower panel) and displayed as the mean±SEM (n=3).

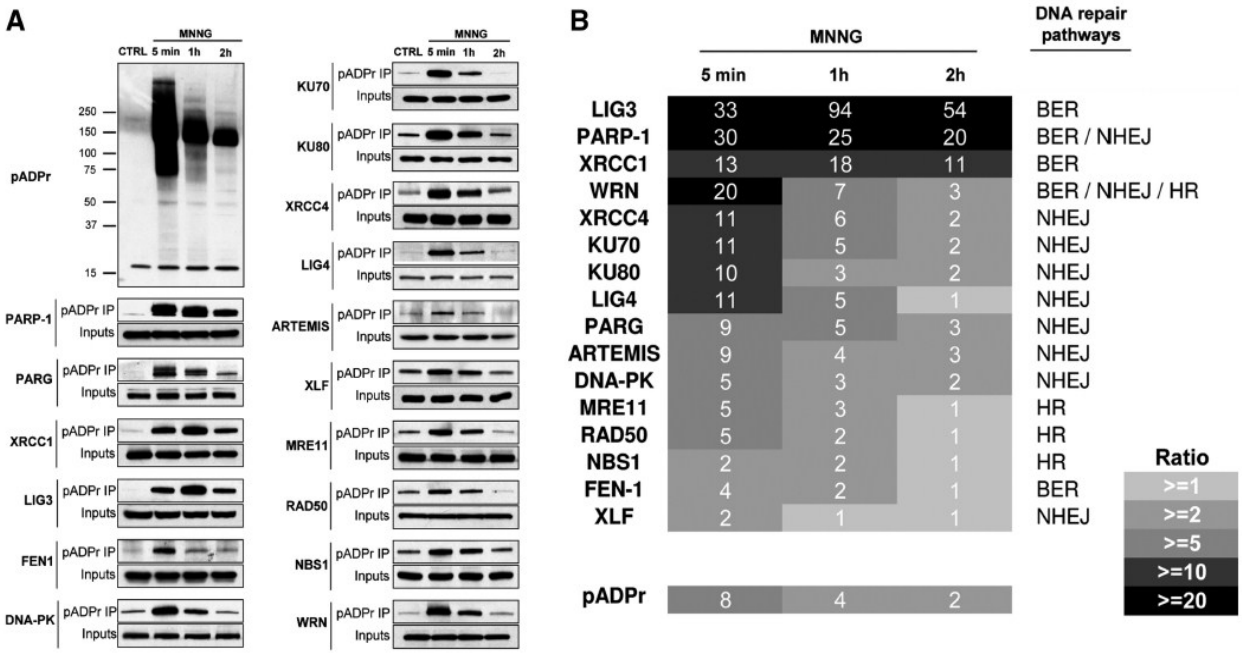

Figure 17: Correlated accumulation of DNA damage response factors with PAR
(A) The 10H-based IPs using HEK293 whole cell extracts were performed to isolate PAR-associated proteins in the context of MNNG-induced DNA damage and PARP activation. Cells were allowed to recover from MNNG by incubation with fresh medium and IPs were performed at the indicated times. Undamaged control cells were pre-incubated 2 h with 5 mM PARP-1 inhibitor ABT-888 before lysis. Several DNA damage response factors were screened for entrapment in anti-PAR IP extracts. Cell lysates (inputs) were also subjected to western blot analysis using the corresponding antibodies. **(B)** PAR levels correlate with the accumulation of several DNA damage response factors involved in major DNA repair pathways. Relative quantitation of western blot signal intensities shown in (A) were measured and expressed relative to control protein levels. A greyscale heatmap ranks each of the protein accumulation ratios.

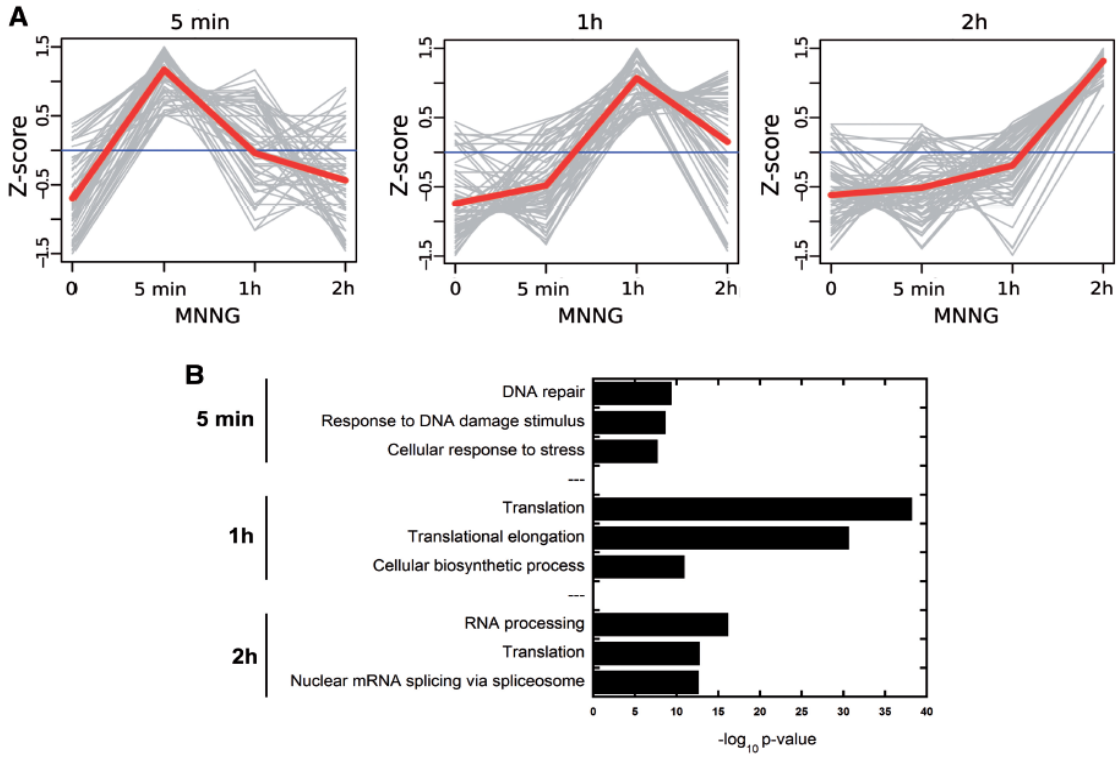

Figure 18: Protein abundance profiles in time-resolved PAR IPs
Spectral counting-based quantitation was combined with Scaffold's protein validation tools to provide a quantitative protein profile. PAR-associated proteins identified by GeLC-MS/MS in IP extracts were grouped by K-means clustering for each treatment, respectively. **(A)** The kinetics of protein accumulation is displayed by trend curves showing the overlay of the proteins grouped by each cluster. The red line represents the mean value at each time-point for all the proteins in the cluster. **(B)** Protein clusters were searched for significant over-representation of proteins belonging to specific pathways according to the GO database using DAVID. Bar plots of the most significant biological processes in each datasets are shown. The significance of the enrichment is expressed as a function of the P-value, which indicates whether a biological process is significantly higher than random expectations. Refer to Supplementary Table S2 for complete protein listing.

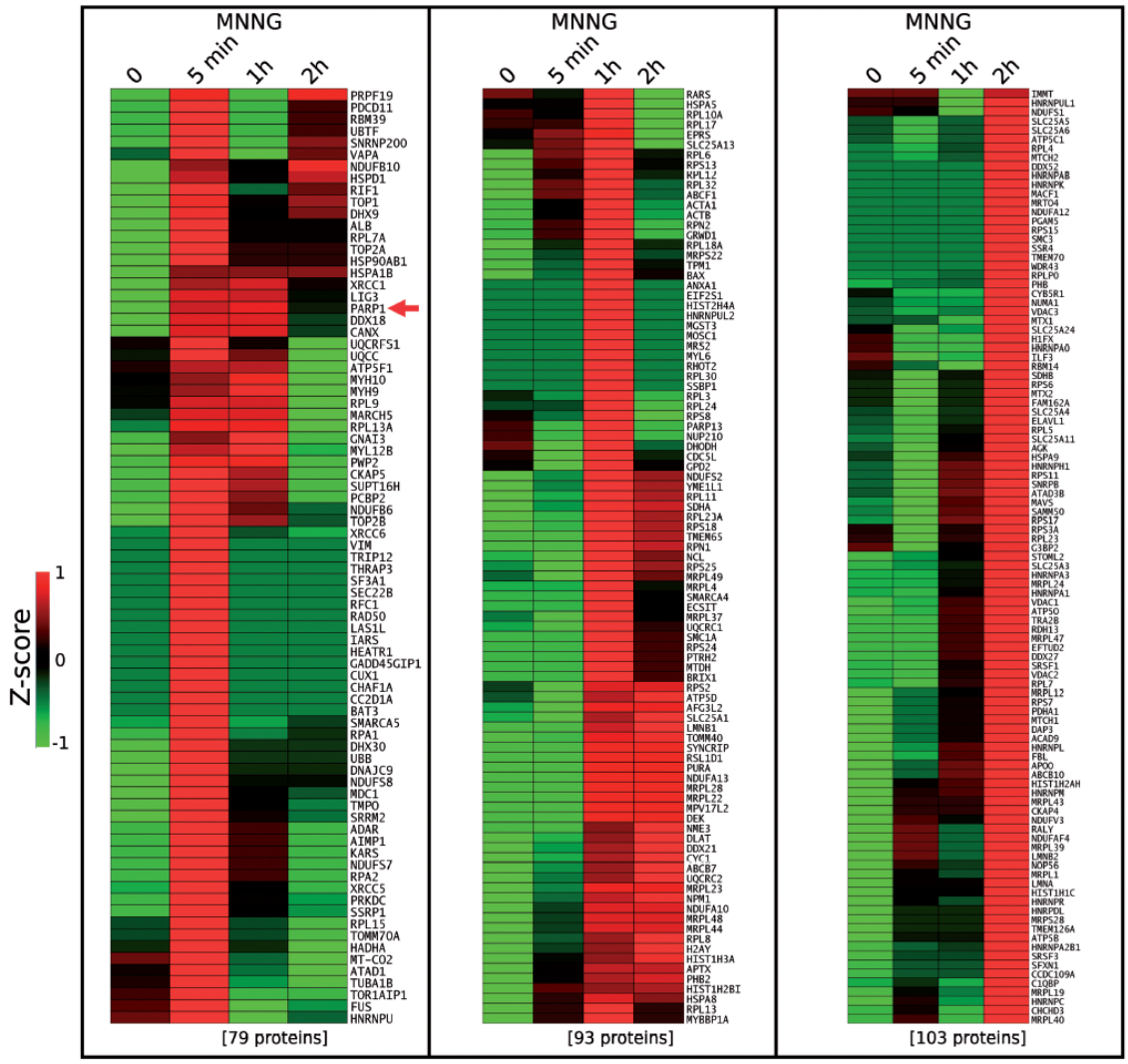

Figure 19: Heatmap analysis with K-means clustering

Temporal profiling of PAR-associated proteins in HEK293 cells upon MNNG exposure was performed based on the GeLC-MS/MS spectral count quantitation. The heatmap displays the three clusters identified by the K-means algorithm that correspond to the time-points analyzed after MNNG exposure. Green indicates the lowest ratio, black indicates an intermediate value and red indicates the highest ratio (protein enrichment). Proteins in each cluster are listed according to their gene symbol. A red arrow indicates the presence of PARP-1.

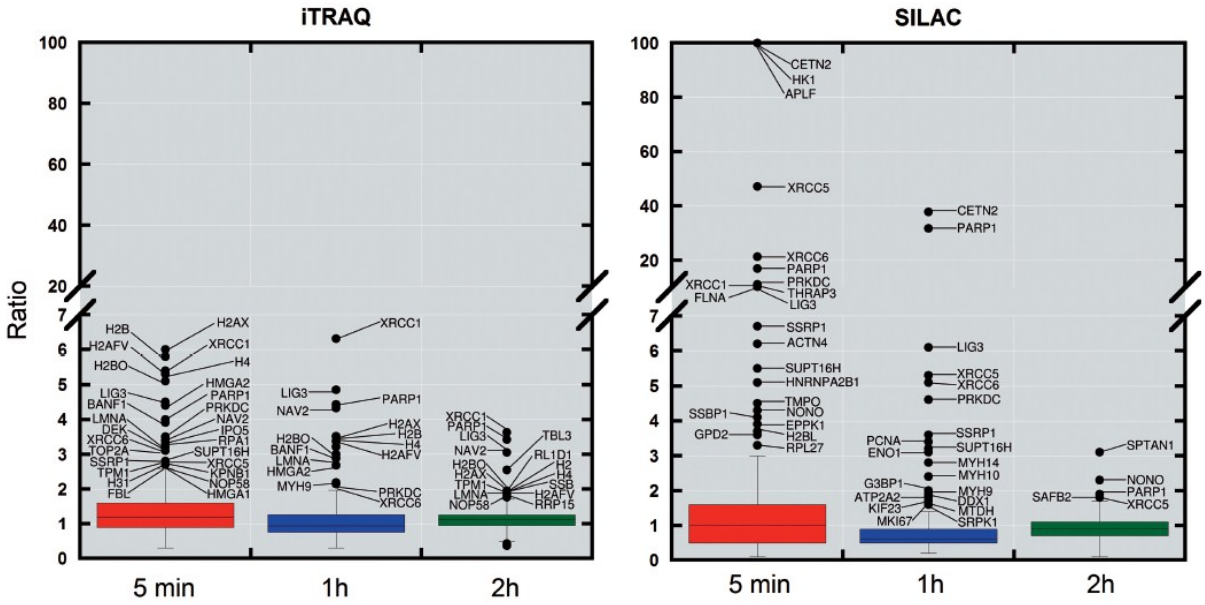

Figure 20: Box plot statistics to define outlier significance for iTRAQ and SILAC analysis

PAR IPs were carried out after each of the three time-points examined following MNNG exposure. Protein isolates were quantified with respect to basal levels of PAR in control IPs. Each box encloses 50% of the data with the median value of the variable displayed as a line. The top and bottom of the box mark the limits of upper and lower quartiles. The vertical lines extending from the top and bottom of each box mark the minimum and maximum values within the data set that fall within an acceptable range (1.5_interquartile distance). Any value outside of this range (outlier) is displayed as an individual point with the corresponding gene symbol. Refer to Supplementary Table S3 (iTRAQ) and Supplementary Table S4 (SILAC) for detailed protein annotations.

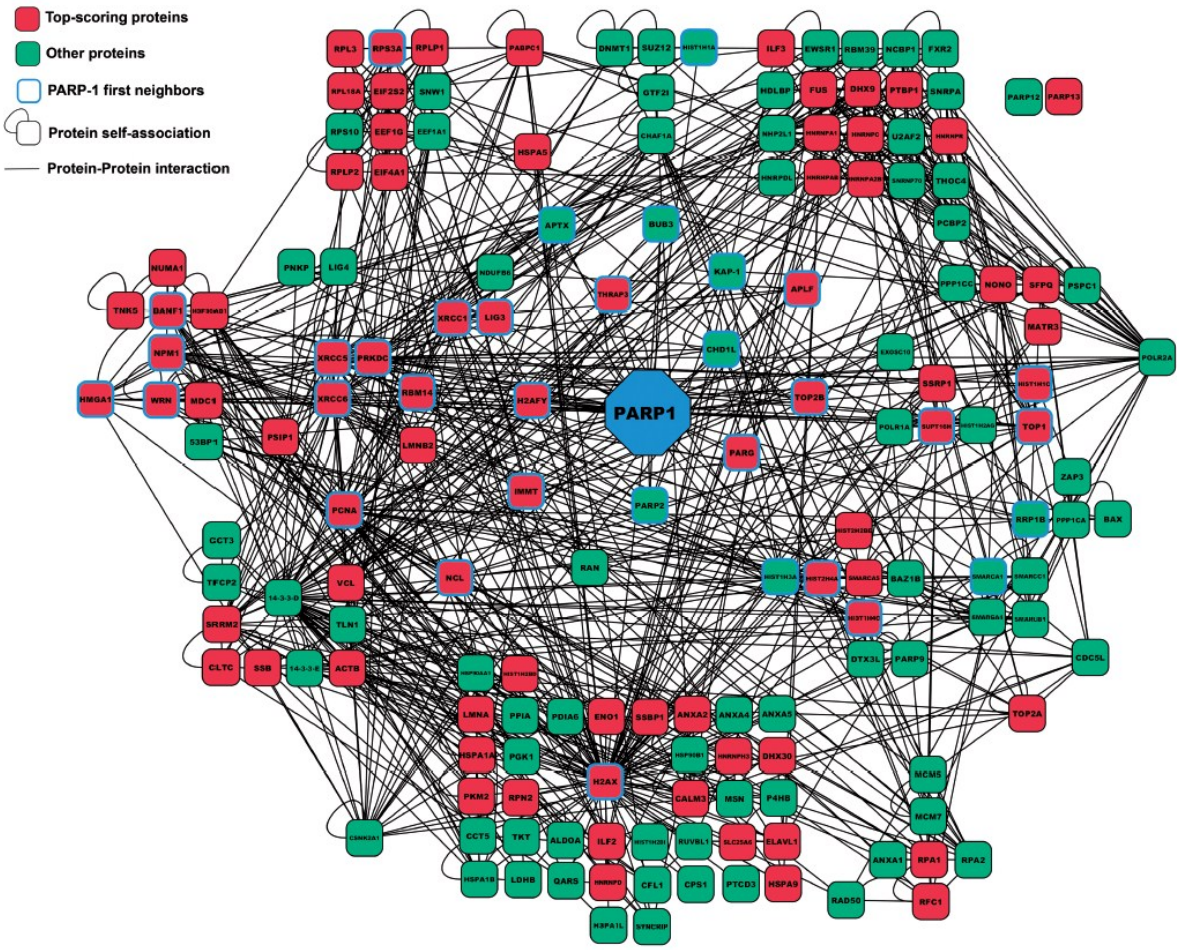

Figure 21: Subnetwork diagram of the PARP-1-centered protein interaction map
Cytoscape was used to construct a global network of the PAR-associated proteome that integrates protein identification from all the proteomics approaches that have been carried out in this study. The diagram shown consists of the nearest-neighbors subnetwork of PARP family members in addition to selected proteins from DNA damage response pathways (See text for details). The subnetwork emphasizes the PAR-associated protein regulatory network centered on PARP-1 in cellular recovery to DNA damage. The red coloring indicates top-scoring proteins and refers to predominant proteins in either of the four datasets (GeLC-MS/MS, Spectral count, iTRAQ, SILAC). Interactions among proteins are reported. The network comprises 164 proteins (nodes) and 899 interactions (edges). Refer to Supplementary Table S5 for complete protein listing.

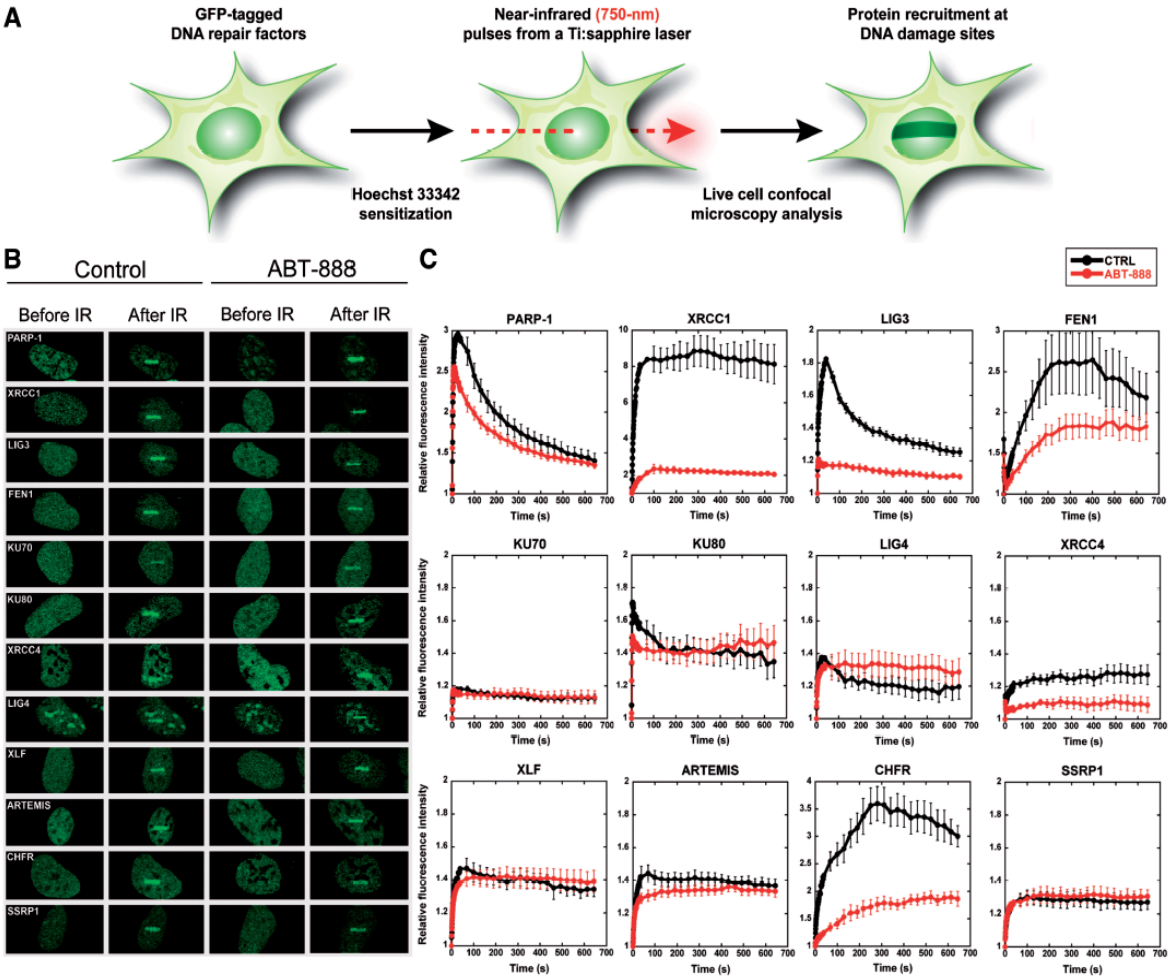

Figure 22: Dynamics of DNA damage response proteins at laser-induced DNA breaks
DNA damage induced by laser micro-irradiation in subnuclear region of single living cells was performed to evaluate the PAR-dependent recruitment of DNA repair factors at DNA damage sites. **(A)** Schematic representation of the micro-irradiation system used to introduce DNA lesions. **(B)** Local accumulation of DNA repair factors at laser-induced DNA damage sites. A 750-nm two-photon laser beam was focused on Hoechst-sensitized cells and the accumulation of GFP-tagged DNA repair factors was monitored on a Zeiss LSM 510 NLO laser scanning confocal microscope. **(C)** Evaluation of the contribution of PAR to the recruitment kinetics of DNA damage response factors at sites of DNA damage. The dynamics of several GFP-tagged proteins involved in DNA repair pathways were analyzed in the context of PARP inhibition (ABT-888). The HEK293 cells transiently expressing the targeted proteins were sensitized with Hoechst 33342 and micro-irradiated with femtosecond near-infrared (750-nm) pulses from a Ti:sapphire laser. The intensity of fluorescence was recorded on a Zeiss LSM 510 NLO laser-scanning confocal microscope. The dynamics of DNA repair factors under normal conditions was compared with the dynamics observed following PARP inhibition with 5 mM ABT-888. Targeted proteins involved in BER (XRCC1, LIG3, FEN1), NHEJ (KU70, KU80, LIG4, XRCC4, XLF, ARTEMIS) and chromatin remodeling (CHFR, SSRP1) are displayed. Because of the rapid

accumulation of DNA repair proteins at DNA damage sites, multiple acquisition rates were used (see ‘Materials and Methods’ section). Background and photobleaching corrections were applied to each dataset. A minimum of eight recruitments per construct were collected and analyzed. The error bars represent the SEM.

CHAPTER 4

PARP ACTIVATION REGULATES THE RNA-BINDING PROTEIN NONO IN THE DNA DAMAGE RESPONSE TO DNA DOUBLE-STRAND BREAKS

Jana Krietsch [1,2], Marie-Christine Caron [2], Jean-Philippe Gagné [1], Chantal Ethier [1], Julien Vignard [2], Michel Vincent [3], Michèle Rouleau [1], Michael J. Hendzel [4], Guy G. Poirier [1, 5] and Jean-Yves Masson [2, 5]

(1) Centre de recherche du CHUQ - Pavillon CHUL - Cancer Axis, Laval University, Québec, G1V 4G2, Canada.
(2) Genome Stability Laboratory, Laval University Cancer Research Center, Hôtel-Dieu de Québec, Québec (Québec), G1R 2J6, Canada
(3) Faculty of Medicine, Laval University, Québec, QC, Canada G1V 0A6 and
(4) Department of Oncology, Faculty of Medicine and Dentistry, University of Alberta, 11560 University Avenue, Edmonton, Alberta, Canada T6G 1Z2
(5) Corresponding author

Preface

As described above, the RNA binding protein NONO has one of the highest enrichment ratios in PAR pulldowns after DNA damage. Interestingly, NONO has been suggested to play a role in the DNA damage response to DNA DSBs. We hence aimed to decipher the potentially PAR-regulated role of NONO in DSB repair.

The following chapter presents my scientific findings which have been published in Nucleic Acid Research. I have done all the experiments and writing but had precious help from the co-authors mentioned on the manuscript. More precisely, Jean-Philippe Gagné has helped me to realize the recruitment experiments and Chantal Éthier has carried out the SPR experiements. Julien Vignard has tought me how to purify proteins by FPLC and Marie-Christine Caron helped me with the generation of cell lines that stably express a repair reporter.

Résumé

Après la génération des cassures double-brin de l'ADN (CDB), la Poly (ADP-ribose) polymérase-1 (PARP-1) est l'une des premières protéines à être recrutées et activés par sa liaison aux extrémités libres de l'ADN. Lors de son activation, la PARP-1 utilise le NAD^+ pour produire de grandes quantités de Poly (ADP-ribose) (PAR), ce qui facilite le recrutement de facteurs de réparation de l'ADN. Ici, nous identifions la protéine de liaison à l'ARN NONO, une protéine partenaire de SFPQ, comme une nouvelle protéine interagissant avec le PAR. Le motif principalement responsable de la liaison de NONO au PAR est le motif 1 de reconnaissance de l'ARN (RRM1), qui est également crucial pour sa fixation aux ARN soulignant la compétition entre les ARN et les PAR. Étonnamment, le recrutement *in vivo* de NONO aux sites de dommages à l'ADN dépend entièrement du PAR, généré par l'activation de PARP-1. En outre, nous montrons que lors du recrutement médié par PAR, NONO stimule la jonction d'extrémités non-homologues (NHEJ) et réprime la recombinaison homologue (RH) *in vivo*. Nos résultats placent donc NONO après l'activation de PARP-1 dans le contexte du choix de la voie de réparation des CDB. Élucider le mécanisme d'action des protéines agissant dans la même voie que PARP-1 est essentiel pour mieux comprendre l'effet de l'interférence sur les voies du PAR par les inhibiteurs de PARP, lesquels ont déjà atteint la phase III des essais cliniques, mais qui sont jusqu'à ce jour très mal compris.

Abstract

After the generation of DNA double-strand breaks (DSBs), poly(ADP-ribose) polymerase-1 (PARP-1) is one of the first proteins to be recruited and activated through its binding to the free DNA ends. Upon activation, PARP-1 uses NAD+ to generate large amounts of poly(ADP-ribose) (PAR), which facilitates the recruitment of DNA repair factors. Here, we identify the RNA-binding protein NONO, a partner protein of SFPQ, as a novel PAR-binding protein. The protein motif being primarily responsible for PAR-binding is the RNA recognition motif 1 (RRM1), which is also crucial for RNA-binding, highlighting a competition between RNA and PAR as they share the same binding site. Strikingly, the *in vivo* recruitment of NONO to DNA damage sites completely depends on PAR, generated by activated PARP-1. Furthermore, we show that upon PAR- dependent recruitment, NONO stimulates nonhomologous end joining (NHEJ) and represses homologous recombination (HR) *in vivo*. Our results therefore place NONO after PARP activation in the context of DNA DSB repair pathway decision. Understanding the mechanism of action of proteins that act in the same pathway as PARP-1 is crucial to shed more light onto the effect of interference on PAR-mediated pathways with PARP inhibitors, which have already reached phase III clinical trials but are until date poorly understood.

4.1 Introduction

Each day, the cells genome is confronted with up to 50 endogenous DNA double-strand breaks (DSBs). These are extremely hazardous for a cell, as they do not leave an intact complementary strand to serve as a template for repair (Vilenchik and Knudson, 2003). If left unrepaired, DSBs can have consequences such as cell death or carcinogenesis. Hence, understanding the mechanisms that lead to successful repair of DSBs will further increase the knowledge of cancer progression and treatments. The DNA damage response (DDR) to DSBs is a multilayered process, initiated with sensing and signaling DNA damage, subsequent recruitment of repair proteins and execution of repair (Ciccia and Elledge, 2010). Poly(ADP-ribose) polymerase-1 (PARP-1) is an abundant and ubiquitous nuclear protein that uses NAD^+ to synthesize a negatively charged polymer, called poly(ADP-ribose) (PAR), onto a variety of target proteins, such as histones, DSB repair factors and PARP-1 itself. This post-translational protein modification has an impact on cellular processes as diverse as transcription (Wacker et al., 2007), cell death (Bouchard et al., 2003) and especially DNA repair (Krishnakumar and Kraus, 2010b). PARP-1 acts as a strong sensor for DNA damage and rapidly produces PAR at newly generated DNA DSBs, provoking therewith local chromatin relaxation due to its negative charge (Wacker et al., 2007) and facilitating the recruitment of repair factors, such as MRE11 (Ciccia and Elledge, 2010), (Haince et al., 2008). The dynamic turnover of PAR within seconds to minutes is executed by poly(ADP-ribose) glycohydrolase (PARG), that possesses endo- and exoglycosidic activities, hence enabling a new round of DNA damage signaling (Slade et al., 2011). For subsequent repair, two major DSB repair pathways have evolved, namely nonhomologous end joining (NHEJ) and homologous recombination (HR). Whereas HR is considered as error-free and restricted to the S/G2-phase (Takata et al., 1998) by its necessity for a homologous template, error-prone NHEJ functions throughout the cell cycle and represents the major pathway for DSB repair in multicellular eukaryotes. Although the NHEJ pathway is highly flexible in terms of substrate ends used for repair, participating repair proteins and possible outcomes, a number of key proteins are indispensable to accomplish classical NHEJ (cNHEJ): Initially, the heterodimeric Ku70/Ku80 complex binds to both ends of the broken DNA molecule (Lieber, 2010). Interestingly, Ku has an

affinity for PAR (Gagne et al., 2008) and is also a direct target for PARylation (Li et al., 2004). The Ku–DNA complex is further bound by the catalytic subunit of DNA–PK (DNA–PKcs) to assemble the end-bridging DNA–PK complex (Meek et al., 2008). If the two ends are not directly ligatable they have to be processed prior to the final ligation step. A variety of proteins (such as Artemis, PNK, APLF nucleases, TdT, polymerases λ and μ) have been implicated in the end-processing step, emphasizing the mechanistic flexibility of the NHEJ reaction (Wang et al., 2005), (Chappell et al., 2002), (Capp et al., 2006), (Capp et al., 2007). The final ligation step is carried out by X4-L4 complex, composed of XRCC4, DNA ligase IV and XLF (Ahnesorg et al., 2006).

Within the last years, growing attention has been drawn to proteins with dual roles in RNA biology and DNA DSB repair. Examples include the Ku protein, which is crucial for the NHEJ pathway but interestingly also for the control of mRNA expression (Giffin et al., 1996), (Woodard et al., 2001), the TFHII complex that acts in nucleotide excision repair as well as in transcriptional initiation mediated by RNA polymerase II (Beck et al., 2008), and recently the RNA-binding protein RBMX and the RNA-splicing factor THRAP3 were implied in the DDR (Adamson et al., 2012), (Beli et al., 2012), (Paulsen et al., 2009). About twenty years ago the group of Harris Busch purified and characterized a heterodimer consisting of a 52 and a 100 kDa subunit, most certainly corresponding to what is nowadays known as the 54 kDa nuclear RNA-binding protein (p54nrb/NONO) and the polypyrimidine tract-binding protein-associated splicing factor (PSF/SFPQ). NONO and SFPQ show 71 % sequence identity and, together with paraspeckle component 1 (PSPC1), belong to a subfamily of RNA recognition motif (RRM) proteins defined by tandem RRM motifs, flanked by an additional region of sequence similarity predicted to promote formation of heteromeric complexes between each of the proteins (Peng et al., 2002). NONO and SFPQ have been implicated in nuclear retention of A- to I-edited RNA as paraspeckle components (Zhang and Carmichael, 2001), pre-mRNA 3'-end formation (Kaneko et al., 2007), cAMP cycling (Amelio et al., 2007) and transcriptional activation (Mathur et al., 2001), (Dong et al., 2007), (Ishitani et al., 2003). Interestingly, apart from their functions in RNA biogenesis, NONO and SFPQ were reported to interact with DNA *in vitro*, which lead to an investigation of their function in the context of DNA repair. Both

proteins are transiently recruited with the same kinetics to DNA damage induced by a laser track in human cells (Salton et al., 2010). Interestingly, a protein complex containing NONO and SFPQ stimulates NHEJ about 10-fold *in vitro* (Bladen et al., 2005). Furthermore, it has been demonstrated that the attenuation of NONO protein expression, independent of its partner protein SFPQ, delays the resolution of γ-H2AX foci after ionizing irradiation and leads to an accumulation of chromosomal aberrations (Li et al., 2009). However, the exact mechanism by which NONO is recruited to DNA damage sites and regulates DSB repair is unclear. Interestingly, a bioinformatics screen from our group for proteins that potentially bind PAR, which is generated within seconds at a new DSB, identified NONO/SFPQ among a variety of NHEJ factors (Gagne et al., 2008), (Gagne et al., 2012), leading to the hypothesis that PARP and its associated polymer regulate NONO.

In this manuscript, we dissect the role of NONO in DSB repair in the context of PARP activation. We suggest here that NONO is directly implicated in NHEJ, and that its recruitment to DNA damage sites is strictly dependent on activated PARP-1. These results highlight the emerging concept of RNA-binding proteins in DSB repair.

4.2 Materials and Methods

4.2.1 Cell lines, cell culture and DNA constructs

HeLa cells and mouse embryonic fibroblasts (MEFs) proficient for PARP-1 and PARP-2 [wild type (WT)], or deficient for either PARP-1 (PARP-$1^{-/-}$) or PARP-2 (PARP-$2^{-/-}$) were cultured in DMEM, while MCF-7 cells were cultured in MEM-alpha (air/CO_2, 19:1, 37°C). Both media were supplemented with 10 % fetal bovine serum and 1 % penicillin/streptomycin. The NHEJ reporter construct 'sGEJ' was kindly provided by Dr. Ralph Scully (Xie et al., 2009) and stably integrated into the genomic DNA of MCF-7 cells by using G418 disulfate salt (400 mg/ml; Sigma) as a selection marker. The HR reporter construct 'DR-GFP' [kindly provided by Dr. Maria Jasin; (Pierce et al., 1999)] was

integrated into the genomic DNA of MCF-7 cells by hygromycin selection (400 mg/ml; Invitrogen). The GFP-NONO construct is a generous gift from Dr. James Patton (Vanderbilt University, Nashville, TN). NONO was cloned for protein purification from the pEGFP vector into a pET-16b (Novagen) vector using the primers shown in Supplementary Table S1. Site-directed mutagenesis on the His-NONO and GFP-NONO constructs was carried out with the QuikChange™ Site-Directed Mutagenesis Kit (Stratagene) using the oligos shown in Supplementary Table S1.

4.2.2 Antibodies and siRNAs

For Western blotting analysis and chromatin-immunoprecipitation (ChIP) experiments, polyclonal antibodies for NONO and SFPQ were obtained from Bethyl laboratories. The monoclonal antibody against GAPDH (6C5) was obtained from Fitzgerald Industries. Polyclonal antibodies for RAD51 and PSPC1 were purchased from Santa Cruz. PARP-1 (C2–10) monoclonal antibody was produced in house as described (37). Gene silencing was performed using siRNA directed against the following target sequences: 5'-GGAAGCCAGCUGCUCGGAAAGCUCU-3' against NONO, 5'-GCCAGCAGCAAG AAAGGCAUUUGAA-3' against SFPQ (Invitrogen). A scrambled siRNA (5'-GACGTCATATACCAAGCTAGTTT-3') from Dharmacon was used as a negative control. Transfection of 5 nM siRNA per condition was performed for 48 h using HiPerfect transfection reagent (Qiagen) according to the manufacturer's protocol. For the siRNA directed against NONO, a second round of transfection (36 h after the first transfection) was performed for another 24 h.

4.2.3 Colony forming assays

Long-term cell viability of HeLa cells transfected with the indicated siRNAs was assessed by colony forming assays. Briefly, a total of 200 cells per condition were plated into 35-mm dishes. Cells were then exposed to ionizing radiation of 0, 0.5 or 2 Gray using a g-irradiator (Gammacell- 40; MDS Nordion). After 7 to 10 days, colonies were fixed with methanol, stained using a 4 g/L solution of methylene blue in methanol, extensively washed with PBS and counted.

4.2.4 Protein purification

Recombinant wild-type human NONO (NONO-WT) and the RRM1-deletion mutant (NONOΔRRM1) proteins were purified from an Escherichia coli BL-21 strain carrying pET16b-10XHis-NONO or pET16b-10XHis- NONOΔRRM1 expression constructs, grown in 4 L of LB media supplemented with 100 mg/ml ampicillin and 25 mg/ml chloramphenicol. Protein expression was induced for 16 hr at 16 °C with 0.1 mM IPTG added to the culture at an OD600 = 0.4. Cells were then harvested by centrifugation and resuspended in 40 ml lysis buffer A (20 mM Tris-HCl pH 8.0, 10 % glycerol, 2 mM β-mercapthoethanol, 500 mM NaCl, 5 mM imidazole, 1 mM PMSF, 1 mg/ml leupeptin, 0.019 TIU/ml aprotinin). Samples were lysed with a Dounce homogenizer (10 strokes with the tight pestle), sonicated using a sonicator (Bioruptor; Diagenode) (10 min at the 'high' setting, 30 s ON and 30 s OFF) and returned to the Dounce for a second round of lysis. Insoluble material was removed by centrifugation at 40 000 rpm for 1 hr at 4 °C and the supernatant subsequently loaded on a 5 ml cobalt-based immobilized metal affinity chromatography resin Talon column (BD Biosciences, Palo Alto, CA). The column was washed and eluted with a linear gradient of imidazole ranging from 5 to 1000 mM prepared in buffer A. Fractions containing His-tagged NONO-WT or NONOΔRRM1 were identified by sodium dodecylsulphate-polyacrylamide gel electrophoresis (SDS-PAGE), carefully selected, pooled and dialyzed for 1 hr against 20 mM Tris-HCl pH 8.0, 375 mM NaCl, 10 % glycerol and 0.0 5 % Tween-20 buffer.

4.2.5 FACS analysis of the cell cycle

Cells were collected by trypsinization, centrifuged and resuspended at 10^6 cells per 300 ml of PBS and fixed with 700 ml of ice-cold ethanol (100 %) while vortexing. Once fixed, cells were washed with PBS and stained with propidium iodide (0.1 % sodium citrate, 0.3 % Nonidet P40, propidium iodide 50 mg/ml and RNAse A 20 mg/ml). Cell cycle analysis was performed on a Beckman Coulter Epics Elite model ESP by using the Expo2 analysis software.

4.2.6 Pulse-field gel electrophoresis

HeLa cells treated with the indicated siRNA were incubated for 2 h at 37 °C in the presence of 500 ng/ml Neocarzinostatin (NCS). After treatment, cells were released for the indicated time points and trypsinized. One percent agarose plugs containing $5*10^6$ cells were prepared with a CHEF disposable plug mold (Bio-Rad). Cells were lysed by incubation of the gel blocks for 72 h at 45 °C in 1 mg/mL proteinase K, 100 mM ethylenediaminetetraacetic acid (EDTA), 0.2 % sodium deoxycholate, 1 % N-laurylsarcosyl. Samples were then washed three times for 1 h each in 20 mM Tris pH 8.0, 50 mM EDTA and embedded into an agarose gel (0.9 % agarose in 0.5 X filtered TBE). DNA separation was performed at 14 °C for 24 h with a two block pulse linear program (block 1: 0.1 s at 30 s, 5.8 V/cm, 14 °C, angle 120_, TBE 0.5X, 12 h; block 2: 0,1 s at 5 s, 3.6 V/cm, 14 °C, angle 110_, TBE 0.5X, 12 h) in a CHEF-DR III Pulsed Field Electrophoresis System (Bio-Rad). The gel was then dried for 30 min at 55 °C and for additional 30 min at room temperature, stained overnight with SYBR green (Molecular Probes) and visualized using a UV lamp. A yeast chromosome PFG marker (NEB 345) served as a ladder for molecular weight.

4.2.7 Nuclear extract preparation

Up to 10^7 HeLa cells per condition were washed three times with PBS, resuspended and incubated for 15 min on ice in 250 ml hypotonic buffer (10 mM Tris pH 7.4, 10 mM $MgCl_2$, 10 mM KCl and 1 mM DTT). The samples were then passed 5 times through a 1 ml syringe with a 27 G needle and centrifuged for 15 min at 3300 g at 4 °C. Pellets were resuspended in 200 ml high salt buffer (hypotonic buffer A with 350 mM NaCl and protease inhibitors) and incubated for 1 h on ice. After centrifugation for 30 min at 13000 rpm at 4 °C, the supernatants were transferred to a clean tube and adjusted to 10 % glycerol (v/v) and 10 mM of β-mercapthoethanol.

4.2.8 Cell fractionation and western blot analysis

Cell fractionation was carried out as described in (Zou et al., 2002) with slight modifications. Briefly, $3*10^6$ HeLa cells per condition were collected and resuspended in 200 mL of buffer A (10 mM HEPES pH 8.0, 10 mM KCl, 1.5 mM $MgCl_2$, 0.34 M sucrose,

10 % glycerol, 1 mM DTT, 1 mM PMSF, 0.1 % Triton-X-100, 10 mM NaF, 1 mM Na_2VO_3, protease inhibitors) and kept for 5 min on ice. The soluble cytoplasmic fraction (S1) was separated from the nuclei (P2) by centrifugation for 4 min at 1300 g at 4 °C. The nuclear fraction P2 was washed twice with 300 mL buffer A then resuspended in 200 mL buffer B (3 mM EDTA, 0.2 mM EGTA, 1 mM DTT, 1 mM PMSF, 10 mM NaF, 1 mM Na_2VO_3, protease inhibitors) and kept for 30 min on ice. The insoluble chromatin fraction (P3) was separated from nuclear soluble proteins (S3) by centrifugation for 4 min at 1700 g at 4 °C. S1 was cleared from insoluble proteins by centrifugation at 14000 rpm for 15 min at 4 °C and the supernatant (S2) was kept for analysis. Cell fractions were subsequently analysed by western blotting as described in (Rodrigue et al., 2006).

4.2.9 ChIP and quantitative polymerase chain reaction

A unique DSB in MCF-7 cells was introduced by electroporating the I-SceI expression vector (pCBASce) into MCF-7 DR-GFP (carrying a chromosomally integrated homology-directed repair site) cells using the Gene Pulser Xcell apparatus (Bio Rad). A total of $2*10^6$ cells per electroporation, resuspended in 650 ml PBS, were mixed with 50 mg of circular plasmid and pulsed at 0.25 kV and 1000 mF in 4-mm cuvettes. Cells were then plated onto 10-cm dishes containing fresh medium and kept at 37 °C for 12 h. To crosslink proteins to DNA, cells were treated for 10 min with a 1 % formaldehyde solution in PBS. Subsequently, glycine to a final concentration of 0.125 M was added to quench the reaction. Cells were collected in ice cold PBS using a cell scraper, washed twice in cold PBS containing 1 mM PMSF, washed for 10 min in solution I (10 mM HEPES, pH 7.5, 10 mM EDTA, 0.5 mM EGTA, 0.75 % Triton X-100) and 10 min in solution II (10 mM HEPES, pH 7.5, 200 mM NaCl, 1 mM EDTA, 0.5 mM EGTA). Cells were resuspended in lysis buffer (25 mM Tris–HCl, pH 7.5, 150 mM NaCl, 1 % Triton X-100, 0.1 % SDS, 0.5 % deoxycholate) and kept for 45 min on ice. To shear chromatin to an average size of 0.5 kb, cells were sonicated with a Bioruptor sonicator (Diagenode) for 10 min (high, 30 s ON, 30 s OFF). Samples were then centrifuged at maximum speed in a benchtop centrifuge until clear and the lysate precleared overnight with Sepharose CL-6B beads. Immunoprecipitation was performed for 2 h in lysis buffer with polyclonal antibodies against NONO. Rabbit anti-human IgG (H+L) antibody (Jackson Immunoresearch

Laboratories) was used as a negative control. Protein–antibody complexes were subsequently incubated with protein A/G beads for 1 h. Complexes were washed twice with RIPA buffer (150 mM NaCl, 50 mM Tris-HCl pH 8.0, 0.1 % SDS, 0.5 % deoxycholate, 1 % NP-40, 1 mM EDTA), once in high salt buffer (50 mM Tris–Cl, pH 8.0, 500 mM NaCl, 0.1 % SDS, 0.5 % deoxycholate, 1 % NP-40, 1 mM EDTA), once in LiCl buffer (50 mM Tris–HCl, pH 8.0, 250 mM LiCl, 1 % NP-40, 0.5 % deoxycholate, 1 mM EDTA) and twice in TE buffer (10 mM Tris–HCl, pH 8.0, 1 mM EDTA, pH 8.0). Beads were resuspended in TE containing 50 mg/ml RNase A and incubated for 30 min at 37 °C. Beads were washed with deionized water and incubated for 15 min in elution buffer (1 % SDS, 0.1 M $NaHCO_3$). Crosslinks were reversed by adding 200 mM NaCl followed by incubation for 6 h at 65 °C. Samples were deproteinized overnight with 300 mg/ml proteinase K and DNA was extracted with phenol–chloroform followed by ethanol precipitation.

Immunoprecipitated DNA was quantified by quantitative polymerase chain reaction (q-PCR) using the Light Cycler Fast Start DNA Master SYBR Green I (Roche Applied Sciences), which is composed of Fast Start Taq DNA polymerase and SYBR Green Dye. Oligonucleotides [Supplementary Table S1; (Ismail et al., 2012)] flanking the break site were designed and optimized for linearity range and efficiency using a light cycler (Roche). Immunoprecipitated DNA samples were amplified in triplicate and values calculated as fold-enrichment compared with the IgG ChIP control and versus GAPDH as a control locus.

4.2.10 PAR-binding assay

PAR-binding properties of purified proteins were analysed as described in (Gagne et al., 2011). Briefly, 500 ng of the indicated protein were either spotted onto a 0.2 -mm pore size nitrocellulose membrane using a slot blot manifold (Bio Rad) or transferred onto a nitrocellulose membrane following separation on an 8 % SDS-PAGE. For both conditions, the membranes were washed three times in TBS-T (10 mM Tris-HCl pH 7.4, 150 mM NaCl, 0.05 % Tween) and incubated for 1 hr at room temperature in TBS-T to allow proper refolding of the protein. Subsequently, the membrane was incubated with 250 nM [32P]-PAR [synthesized as described in (Gagne et al., 2003)] in TBS-T with or without 100-fold

of unlabeled competitor RNA (yeast RNA mix, Ambion). The membrane was then washed extensively in TBS-T, air-dried and subjected to autoradiography.

4.2.11 Surface plasmon resonance spectroscopy

Interaction of 10X-His-tagged NONO with PAR was investigated using surface plasmon resonance (SPR) spectroscopy. The binding experiments were carried out on a ProteOn XPR36 (Bio-Rad) biosensor at 25 °C using the HTE sensor chip (Bio-Rad). The flow cells of the sensor chip were loaded with a nickel solution to saturate the Tris–NTA surface with Ni^{2+}-ions. Purified His-tagged wild-type NONO diluted in 10 mM MOPS [pH 8.0] was injected in one of six channels of the chip at a flow rate of 30 ml/min, until approximately a 5000 resonance unit (RU) level was reached. After a wash with running buffer (PBS [pH 7.4] with 0.005 % (v/v) Tween-20), PAR binding to the immobilized substrates was monitored by injecting a range of concentrations of PAR (500, 250 and 125 nM) along with a blank at a flow rate of 50 ml/min. When the injection of PAR was completed, running buffer was allowed to flow over the immobilized substrates for PAR to dissociate with an association and dissociation phase of 300 and 600 s, respectively. Following dissociation of PAR, the chip surface was regenerated with an injection of 1 M NaCl at a flow rate of 100 ml/ml followed by 100 mM HCl and 300 mM EDTA at a flow rate of 30 ml/min. Interspot channel reference was used for non-specific binding corrections and the blank channel used with each analyte injection served as a double reference to correct for possible baseline drift. Data were analysed using ProteOn Manager Software version 3.1. The Langmuir 1:1 binding model was used to determine the KD values.

4.2.12 Live-cell microscopy and laser micro-irradiation

Recruitment experiments were carried out as described in (Haince et al., 2008). Briefly, cells were grown on glass-bottom dishes (MatTek Corp.) and transfected using Effectene reagent (Invitrogen) with the indicated constructs. Twelve hours post-transfection with GFP-NONO, GFPNONO ΔRRM1 and mCherry-PARG, cells were placed in fresh medium, treated with 10 mM ABT-888 (Enzo Life Sciences; 5 mM stock solution prepared in H_2O) for 2 h and sensitized with 1 mg/ml Hoechst 33342 for 30 min prior to irradiation and live cell analysis of recruitment to DNA damage sites. A 37 °C preheated stage with 5

% CO_2 perfusion was used for the time-lapse on a Zeiss LSM-510 META NLO laser-scanning confocal microscope. Localized DNA damage was generated along a defined region across the nucleus of a single living cell by using a bi-photonic excitation of the Hoechst 33342 dye, generated with a near-infrared 750-nm titanium:sapphire laser line (Chameleon Ultra, Coherent Inc.). The laser output was set to 3 %, and we used 10 iterations to generate localized DSB clearly traceable with a 40X objective. Protein accumulation within the laser path was compared with an undamaged region within the same microirradiated cell. We generally selected cells with low expression levels and normalized the fluorescence intensity in the microirradiated area to the initial fluorescence in the whole nucleus to compensate for photobleaching during acquisition. The average accumulation ± S.E. of fluorescently tagged proteins from at least 10 cells from three independent experiments was plotted.

4.2.13 Immunofluorescence

Laser-irradiated HeLa cells from earlier process were analysed by immunofluorescence (IF) for protein-colocalization with PAR as recently published by our group (Gagne et al., 2012). Briefly, cells were washed three times with ice-cold PBS, fixed for 15 min at room temperature in 4 % formaldehyde diluted in PBS, washed five times with PBS prior to permeabilization with 0.5 % Triton X-100 in PBS for 5 min. After three washes with PBS, cells were incubated with the first antibody diluted in PBS containing 2 % FBS for 90 min at room temperature. Following one wash with 0.1 % Triton-X in PBS and four washes with PBS, cells were incubated with a secondary antibody diluted in PBS containing 2 % FBS for 45 min. Subsequently, cells were washed once with 0.1 % TritonX-100 in PBS, four times with PBS and then mounted in Fluoromount-G mounting media (Southern Biotech, Birmingham, AL). Images were acquired using a Leica 6000 microscope. Volocity software v 5.5 (Perkin-Elmer Improvision) was used for image acquisition.

4.2.14 NHEJ/HR in vivo reporter assays

To analyse I-SceI induced GFP^+-expression in NHEJ or HR reporter MCF-7 cells, cell lines were plated onto cover-slips, treated with the indicated siRNAs for 36 h and subsequently infected with an adenovirus coding for I-SceI. Cells were fixed 24 h post-infection with 4

% paraformaldehyde for 30 min. To enhance the GFP signal-to-noise ratio and therewith enhance the difference in signal intensity between GFP^+ and GFP^- cells, immunofluorescence was conducted as follows. Cells were permeabilized for 5 min with 0.5 % Triton-X/PBS, washed twice with 0.1 % Triton-X/PBS and incubated with 1 % goat serum/PBS for 1 hr to block unspecific antibody binding. Cells were incubated for 1 hr with a polyclonal GFP antibody (Abcam ab290). The percentage of GFP^+ cells per condition was calculated by counting the GFP^+ cells over the total number of cells (2500 cells were counted based on DAPI nuclear staining). The percentage was expressed as fold-change normalized to the control siRNA condition.

4.3 Results

4.3.1 NONO knockdown leads to a decrease in survival of IR-treated cells and deficient NHEJ repair

It has been previously shown that miRNA-mediated knockdown of NONO in HTC 116 cells left cell survival unaffected but sensitized these cells to ionizing irradiation (Li et al., 2009). Here, we verified the necessity of NONO for cell proliferation by measuring the impact of attenuated NONO on the long-term survival of HeLa cells with and without ionizing irradiation. We used siRNA-mediated knockdown to attenuate the NONO protein expression level in HeLa cells. Immunoblotting confirmed that the expression level of NONO was reduced by more than 90 %, whereas the attenuation of NONO did not affect the expression level of its partner protein SFPQ and vice versa (Figure 23A). A knockdown of NONO had no effect on long-term survival (Figure 23B). However, attenuated NONO sensitizes HeLa cells to ionizing irradiation at low (0.5 Gray) and intermediate doses (2.0 Gray), strongly suggesting a defect in DNA DSB repair (Figure 1C). These results suggest that NONO is crucial for survival after ionizing radiation. We therefore analysed the ability of NONO attenuated cells to repair DSBs. Hence, we optimized an assay to assess the sensitivity of these cells to the radiomimetic antibiotic NCS as a means to measure DSB repair kinetics in HeLa cells. NCS consists of an enediyne chromophore, which is tightly

bound to a 113 amino acid single chain protein, the active compound responsible for tandem DNA cleavage and highly potent in the induction of DNA single and especially DSBs (Smith et al., 1994), (Povirk, 1996). Pulse-field gel electrophoresis (PFGE) was accomplished with HeLa cells 48h following transfection with scramble or NONO siRNA and treated for 2 h with 500 ng/ml NCS to introduce DSBs. Cells were then released for 60 or 120 min and DSB repair kinetics indirectly surveyed by analysing the accumulation of DSBs. We observed that NONO protein knockdown by siRNA impairs the recovery from DNA damage as persistent accumulation of DNA DSBs following a 2 h NCS treatment is detected by PFGE (Figure 24A). The slower recovery kinetics observed in the context of NONO depletion provides strong indication for the involvement of NONO in DSB repair. However, this observation could also be explained by an effect on cell cycle checkpoints that occurred in NONO knockdown cells. To rule out the possibility that NONO plays in indirect role in repair by affecting cell cycle progression, we analysed the cell cycle phase distribution of siCTRL and siNONO HeLa cells (Supplementary Figure 1). Neither the knockdown of NONO, nor SFPQ, nor the combined knockdown of both affects cell cycle progression. Similarly, cell cycle phase distribution of MCF-7 cells was unaffected by the knockdown of NONO (data not shown). The observed radiosensitivity and accumulation of DSBs in NONO attenuated cells could be a consequence of diminished NHEJ repair activity. Therefore, we set up a cell-free NHEJ assay that measures the ligation of a ^{32}P-labeled linearized plasmid, after incubation with nuclear extracts derived from siRNA control HeLa cells or knocked down for NONO. The knockdown of NONO in HeLa cells delays NHEJ kinetics *in vitro*, as the end joining reaction with the nuclear extract in which NONO had been knocked-down results in overall less end joining products compared with the control (Figure 24B). In concordance with this observation, less substrate plasmid had been used for the end joining reaction in the absence of NONO. Quantitation of the end joining products at 2 h revealed a 5-fold decrease in end joining products in the NONO knockdown assay, compared with the assay with control cells (Figure 24C).

4.3.2 NONO is strongly associated with the chromatin and localizes near a unique DSB in vivo

The results mentioned earlier confirmed a function for NONO in DNA DSB repair, and suggested that NONO might play a direct role in DNA repair rather than having an indirect effect through RNA biogenesis. One prediction of such a direct role would be to observe physical association of NONO with DNA damage sites. Following this idea, we used ChIP combined with q-PCR using oligonucleotides flanking a unique I-SceI restriction site in MCF-7 cells to monitor the distribution of NONO relative to a DSB. To ensure that the RNA-binding protein NONO is localizing to DNA/chromatin *in vivo* (a prerequisite for ChIP), we fractionated unfixed MCF-7 cells and analysed the chromatin enriched, nuclear soluble and cytoplasmic fractions by western blotting with the indicated antibodies (Figure 25A). Surprisingly, we found that NONO, as its partner proteins SFPQ and PSPC1, is strongly associated with the chromatin and nearly absent in the nuclear soluble and cytoplasmic fractions. PARP-1, RAD51 and GAPDH served as hallmark protein-controls for the nuclear soluble and cytoplasmic fractions, respectively. The results indicate that NONO is associated with the chromatin, even in the absence of exogenous DNA damage and independently of the PARP-1 activation state. Using MCF-7 cells carrying a single I-SceI restriction site, we then combined ChIP with q-PCR to determine the position of NONO relative to a DSB *in vivo*. We con- ducted the ChIP experiment 12hr after transfection with an I-SceI encoding vector, allowing sufficient time for I-SceI expression and generation of the unique DSB. We successfully pulled-down endogenous NONO fixed to the chromatin, as shown in Figure 25B. After purification of the chromatin that has been pulled-down with NONO, we used three sets of primers located at increasing distances from the DSB to evaluate the distribution of NONO (Figure 25C). We were able to detect NONO as close as 464–520 bp from the DSB with a 1.5-fold enrichment compared with the IgG control and after normalization with GAPDH (Figure 25D). This localization resembles that of the NHEJ factor and RNA-processing protein Ku80, as we previously reported (Rodrigue et al., 2006).

4.3.3 NONO is a new PAR-binding protein that binds PAR through its RRM1 motif

The synthesis of PAR that results from the activation of DNA-dependent PARPs is one of the earliest steps of DNA damage recognition and signaling in mammalian cells. PARP-1 has notably been shown to localize to DNA damage sites within milliseconds following laser-induced micro irradiation of sub-nuclear regions (Haince et al., 2008), (Tartier et al., 2003). Our laboratory recently performed a proteome-wide screen for proteins to isolate and identify PAR- containing multiprotein complexes. Interestingly, the RNA-binding protein NONO was consistently identified together with a variety of DNA DSB repair factors (Gagne et al., 2011), (Gagne et al., 2012). A number of DDR factors have been shown to be loaded on DNA damage sites in a PAR-dependent fashion (Haince et al., 2008), (Adamson et al., 2012), (Rulten et al., 2008), (Ahel et al., 2009). To assess PAR-binding properties of NONO *in vitro*, His tagged NONO was expressed in *E. coli* and purified by affinity purification (Figure 26A). Using a PAR-binding assay developed by our group (Gagne et al., 2008), we determined whether NONO binds PAR. As shown in Figure 26B (lane 1), NONO displays a strong affinity for purified ^{32}P-labeled PAR *in vitro*. The unlabeled PAR displaced binding of its cognate ^{32}P-labeled polymer (Figure 26B, lanes 2–4). As NONO is a well-established RNA-binding protein and considering that PAR shares some structural features with nucleic acids, we further examined its affinity for PAR in the presence of increasing amounts of unlabeled competitor RNA (Figure 26C, lanes 1–4). Interestingly, binding of ^{32}P-PAR was slightly reduced when cold RNA was added to the binding reactions, suggesting a competition between PAR and RNA. The RNA-binding protein still exhibits PAR-binding in the presence of 100-fold competitor RNA, underpinning its specificity (Figure 26C). To further characterize the affinity of NONO for PAR with a label-free approach, we used SPR spectroscopy, such as described in (Fahrer et al., 2007). Therefore, purified His-tagged NONO was bound to a HTE sensor chip until a response unit of 5000 RU was reached. Subsequently, purified PAR, produced by PARP-1*in vitro*, was injected at three different concentrations (500, 250 and 125 mnM) to determine the binding affinity to the immobilized NONO protein. Association and dissociation was allowed to proceed for 300 and 600 seconds, respectively. As shown in Figure 26D, the dissociation rate constant (KD) of NONO was determined at $2.32*10^{-8}$ M, hence demonstrates a strong affinity for PAR. As the general model suggests that upon

activation by DNA-binding, PARP-1 generates large amounts of long and branched PAR, we tested whether NONO preferentially binds long and complex PAR over shorter PAR molecules. Hence, we fractionated and purified PAR produced *in vitro* by PARP-1 for our binding analysis. SPR was conducted with two distinct populations of PAR namely complex PAR (60 mer and more average length) and short PAR (less than 30 mers average length). Strikingly, NONO strongly and specifically binds complex PAR, with a KD similar to that observed in Figure 26D but has no affinity for shorter PAR (Supplementary Figure 2A and B). We next sought to locate the PAR-binding-sites within NONO protein. The NONO Drosophila behavior human splicing (DBHS) protein-core consists of clearly defined structural domains (Figure 27A): two tandem RRM domains and a 100-aa segment of predicted coiled-coil structure, putatively responsible for protein-protein interaction with itself and the other two members of the DBHS family (namely PSPC1 and SFPQ). As it had been shown for other RNA-binding proteins that they bind PAR through their RRM1 (Malanga et al., 2008), we used protein fragments containing either the RRM1, RRM2, both RRMs or none of the RRMs for a PAR-binding assay *in vitro* (Figure 27B). Interestingly, we observed that NONO binds PAR with its fragment containing the N-terminal RNA-recognition motif 1 (RRM1) (Figure 27C). These results indicate that the RRM1 has a strong affinity for PAR *in vitro*, and could mediate the interaction between NONO and PAR. We therefore produced and purified a NONO mutant protein, which lacks the RRM1 region (NONOΔRRM1). As the wild-type and mutant NONO proteins were free of contaminants (Figure 27D), we performed an alternative polymer-blot assay without using a detergent-based separation such as SDS-PAGE. By slot-blotting the proteins directly onto a nitrocellulose membrane, we wanted to avoid methods that could disrupt interactions requiring native conformations. Measuring the binding-signal intensity with a phosphorimager revealed that while the full-length protein shows a strong affinity for PAR (as described earlier), the affinity of the NONOΔRRM1 protein for PAR is reduced by 2.5-fold, indicating that we have successfully deleted a principal PAR-binding-motif (Figure 27E).

4.3.4 NONO is PAR-dependently recruited to DNA damage sites

An emerging concept in the DDR is that several proteins, such as MRE11 (Haince et al., 2008), are recruited to DNA damage sites in a PAR-dependent manner to elicit cell cycle arrest or DNA repair. In view of the strong affinity of NONO for PAR *in vitro*, we analysed whether NONO co-localizes with PARP-1 and PAR at DNA damage sites in cells (Figure 28A). We therefore transfected HeLa cells with GFP-NONO and 24 h later induced DNA damage in live-cell conditions by laser micro-irradiation.

Immediately after irradiation, cells were fixed and subjected to immunofluorescence staining. Evidently, GFP-NONO, PARP-1 and PAR are co-localizing at laser-IR-induced DNA damage sites immediately after introducing DNA lesions. To further analyse whether the recruitment of NONO to DNA damage sites is dependent on PAR, we established the recruitment kinetics of GFP-NONO to DNA damage induced by micro-irradiation in HeLa cells in the presence or absence of the specific PARP inhibitor ABT-888. In these live-cell analysis conditions, NONO is transiently recruited with rapid kinetics to DNA damage sites and reaches a maximum within 120 s following local generation of DNA damage sites (Figure 28B and C). Strikingly, we found that the recruitment of NONO to DNA damage sites completely depends on catalytically active PARP, as in none of the cells the protein is recruited in the presence of the specific PARP inhibitor ABT-888. As another mean to assess the PAR-dependency of recruitment of NONO to DNA damage sites, we co-expressed GFP-NONO with mCherry-PARG, the main PAR-degrading enzyme, to prevent PAR accumulation in laser tracks. We have previously shown that overexpression of PARG prevents PAR accumulation after induction of DNA strand breaks (Haince et al., 2006). We indeed found that the recruitment of GFP-NONO to laser tracks is completely abolished by PARG overexpression. This observation is consistent with the finding that PARP inhibition abrogates the recruitment of GFP-NONO and confirms a strict requirement for PAR-binding for its relocation to DNA damage sites. We then sought to define the domain mediating NONO interaction with PAR. Hence, we tested if interaction with PAR occurs through interaction with the RRM1 domain of NONO. As shown in Figure 28A and B, a deletion mutant lacking the RRM1 domain (GFP-NONOΔRRM1) is not recruited to DNA damage sites. This result strongly implicates the RRM1 domain in regulating the interaction

with PAR. Although our results underscore the importance of PAR for NONO dynamics in the DDR, they leave open the question which PARP family member generates the PAR that mediates the recruitment of NONO to DNA damage sites. It is well accepted, that PARP-1 is responsible for 95 % of all PARylation events after DNA damage, whereas PARP-2 carries out almost all of the remaining 5 %. Therefore, we overexpressed GFP-NONO in wild-type and PARP-1$^{-/-}$ MEFs. Recruitment of GFP-NONO was detected in the PARP-1-proficient MEFs with similar kinetics to those in HeLa cells, whereas GFP-NONO was not recruited to the laser track in PARP-1$^{-/-}$cells, highlighting the necessity of PARP-1 to generate PAR at the DNA damage sites (Figure 29). The specificity for PARP-1 is further highlighted by the observation that GFP-NONO is recruited with fast and transient kinetics in PARP-2$^{-/-}$ MEFs similar to that in the WT-MEFs and HeLa cells (Figure 29). Hence, PARP-1 is required to recruit NONO to DNA damage sites, whereas PARP-2 is rather dispensable. Collectively, these results show that the recruitment of NONO is PARP-1 and PAR-dependent, and mediated by the RRM1 region of NONO.

4.3.5 NONO promotes NHEJ and represses HR in vivo in the same pathway as PARP1

As a consequence of the results described above, we hypothesize that NONO plays important regulatory role in the DDR by stimulating DSB repair. Indeed, we showed that NONO promotes cell survival and DSB repair through NHEJ, localizes near a unique DSB site and accumulates to sites of DNA damage in a PAR-dependent fashion. However, a direct implication of NONO in NHEJ has not been shown *in vivo* and the question as whether NONO also influences the other DSB repair pathway, namely HR, has not been answered yet. To address these two key questions, we generated two stable reporter cell lines enabling us to monitor both, NHEJ and HR repair (Figure 30A and B). Each of these cells lines has an integrated cassette comprising an I-SceI-cleavage site that, upon repair by either NHEJ or HR, restores GFP expression, as previously described (Xie et al., 2009), (Pierce et al., 1999). Cells with normal or knocked down expression of NONO were assessed for each repair mechanism as indicated by the percentage of cells that express GFP. In the NHEJ reporter system assay, we found that the knockdown of NONO decreases NHEJ by more than 50 % (Figure 30C). In this same assay, PARP inhibition, with the potent and specific PARP inhibitor ABT-888 also significantly reduced NHEJ

repair. Knowing that NONO is PAR-dependently recruited to DNA DSBs, we combined the siRNA directed against NONO with PARP inhibitor to confirm our findings above. As expected, the siRNA-mediated knockdown of NONO combined with the inhibition of PARP does not have an additive effect in inhibiting NHEJ, indicating that PARP and NONO function in the same pathway and hence supporting the idea of PAR-dependent recruitment. Interestingly, an attenuation of NONO does not only decrease NHEJ but also facilitates repair by HR 40 % (Figure 30D). Again here, when combining siRNA directed against NONO with the PARP-1 inhibitor ABT-888, no additive effect was observed, supporting the same conclusion regarding PAR-dependent recruitment.

4.4 Discussion

Although the RNA binding properties of NONO related to RNA biogenesis and the architecture of paraspeckles have been subject of an abundant literature, [reviewed in (Shav-Tal and Zipori, 2002)], little is known on the functions of NONO in the context of DNA DSB repair. We have conducted a detailed molecular and cellular analysis of NONO in the context of the DDR and our data establish NONO as a PARP1-dependent regulator of DSB repair by facilitating NHEJ and promoting cell survival after irradiation. In the past few years, the list of proteins that possess dual roles in gene regulation and genomic stability through RNA biology and DNA repair, respectively, has largely expanded. Examples include the catalytic subunit of DNA-PK, a core complex of NHEJ that is necessary to arrest RNA-polymerase II transcription after the induction of DSBs (Pankotai et al., 2012) and the Ku protein that has dual roles in transcriptional reinitiation and NHEJ (Woodard et al., 2001). In addition, the heterogeneous nuclear ribonucleoprotein (hnRNP) RBMX acts in alternative splicing and accumulates at DNA damage sites in a PARP-dependent manner (Adamson et al., 2012). Also, the heterogeneous nuclear ribonucleoprotein hnRNPU influences end resection (Polo et al., 2012). Another study highlights the role of the splicing-associated protein THRAP3 in the DNA damage signaling network (Beli et al., 2012). Even PARP-1 itself functions in promoter/enhancer

regulation (Kraus, 2008), single-strand break repair and the alternative NHEJ pathway (Wang et al., 2006), (Mansour et al., 2010). Because of its possible role in RNA biogenesis, it came as a surprise to find that NONO is mostly associated to the chromatin. Moreover, we show here for the first time that NONO is localized with close proximity to a unique DSB *in vivo*. In an earlier study (Rodrigue et al., 2006), we have detected the NHEJ-related protein Ku80 within the same distance to the break-site as NONO (400 bps), suggesting a direct implication for NONO in DNA DSB repair. In line with these findings, the Shiloh group has detected NONO in a protein complex composed of Ku70, Ku80 and Ligase IV (Salton et al., 2010). Here, we are giving further evidence for a direct implication of NONO in DSB repair by showing that down-regulation of NONO protein expression by siRNA sensitizes HeLa cells to ionizing irradiation and decreases NHEJ *in vitro* and *in vivo*. Hence, the data presented complement the recent findings that attenuation of NONO delays the resolution of γ-H2AX foci and results in an increase of chromosomal aberrations following radiation exposure (Li et al., 2009). The fact that cells with attenuated NONO are still viable and capable of NHEJ might be explained by a possible backup through its homologous protein partner PSPC1. The expression level of PSPC1 in the presence of NONO in HeLa cells is very low and increases upon siRNA-mediated knock-down of NONO (data not shown).

PARP-1 is an abundant nuclear chromatin-associated protein, well characterized for its high DNA damage sensing ability. Once encountering free DNA ends, PARP-1 is catalytically activated and generates large amounts of PAR serving as a scaffold for the recruitment of a variety of DNA repair proteins. We performed a large scale analysis of proteins bound to PAR following MNNG exposure. NONO was identified in SILAC experiments with an enrichment ratio (control versus DNA damage), which is one of the strongest in the PAR immunoprecipitates (Gagne et al., 2012). Also after neocarzinostatin treatment, we observed a complex between PAR and NONO as well as PARP-1 and NONO (Supplementary Figure S3). We have previously shown that key DNA repair proteins share a high affinity for PAR, the product of catalytically active PARP-1, with many RNA-binding proteins (Gagne et al., 2003). To date, many proteins have been shown to be recruited in a PAR-dependent manner by cell imaging techniques: MRE11 (Haince et

al., 2008), NBS1 (Haince et al., 2008), APLF (Rulten et al., 2008), XRCC1 (El-Khamisy et al., 2003), CHD4 (Polo et al., 2010), NuRD (Chou et al., 2010) and ALC1(Ahel et al., 2009). However, in none of these studies PAR-dependent recruitment has been directly shown by deleting the PAR-binding module that is necessary for recruitment. We present here for the first time that the RNA-binding protein NONO has a strong and specific affinity for complex PAR *in vitro*, interestingly through its RRM1. We provide several lines of evidence that the recruitment of NONO to DNA lesions is strictly dependent on the presence of PAR. Indeed, we show that NONO relocation to DNA damage sites is suppressed by (I) PARP-1 inhibition with ABT-888; (II) PARG overexpression (the antagonist of PARP-1); (III) loss of PARP-1 expression in PARP-1$^{-/-}$ MEFs and (IV) deleting the PAR-binding motif located within the RRM1. Actually, the characterization of the RRM1 domain of NONO as a PAR-interacting module is consistent with previous studies that also established a similar role for the RRM1 domains of the splicing factor ASF/SF2 (Malanga et al., 2008) and hnRNP A1 (Gagne et al., 2003). It has been suggested that bound PAR competes out RNA-binding properties, therewith modulating the proteins splicing activity. The idea of a direct competition between PAR and RNA for the same site within a protein might also be applicable for RNA-binding proteins in the context of DNA repair. As it is of physiological importance for a cell to stop transcriptional activity (Shanbhag et al., 2010) and initiate repair in response to excessive DNA damage, the PAR, which is largely generated at DNA damage sites, might serve as a molecular switch to direct proteins from RNA biogenesis toward DNA repair. Finally, we show that NONO not only facilitates NHEJ but also represses the other major DSB repair pathway, HR, therewith channeling the DSB repair pathway decision between NHEJ and HR. Interestingly, we find that PARP activity has effects similar to NONO on both pathways and the combination of siRNA-mediated knock-down of NONO with an ABT-888 treatment does not show any additive effect. This suggests that NONO and PARP act in the same pathway, pointing towards the model of PAR-dependent recruitment of NONO. PARP-1 itself has also been shown to play a role in the back-up NHEJ pathway, but exclusively in the absence of classical NHEJ factors such as Ku80 (Mansour et al., 2010). The role of PARP-1 in recruiting NONO in our system can be seen independent of its role in the backup-NHEJ pathway as we and others have observed that a knock-down of NONO

leaves the expression level of protein acting in the classical NHEJ pathway (Ku70/Ku80, DNA-PK, Ligase IV) unaffected suggesting that our system monitors exclusively classical NHEJ (Bladen et al., 2005). Conclusively, our results place NONO in the very early steps of the DDR after PARP activation, promoting the error-prone NHEJ pathway over error-free HR. Underpinning the fact that NONO promotes NHEJ over HR, which is an error-prone repair pathway that facilitates mutagenesis, we found by an Oncomine-based search that NONO is over-expressed in a variety of cancer types, such as colorectal and lung cancer. Within the two aforementioned cancer types, NONO is among the top 1 % over-expressed genes and therefore a promising candidate to investigate in the context of carcinogenesis. Moreover it has been published only very recently that NONO is implicated in the development and progression of malignant melanoma (Schiffner et al., 2011). Further investigation is needed to clarify NONOs possible role as a factor that promotes carcinogenesis.

Collectively, our study strengthens the suggested role for NONO in NHEJ and adds another layer of complexity by showing PAR-dependent recruitment through its principal RNA-binding motif. We have much to learn on NONO, a factor potentially promoting carcinogenesis in the context of PARP-activation as it sheds more light onto the mechanism of action of PARP inhibitors, which have already reached phase III clinical trials but are still poorly understood.

4.6 Acknowledgements

The authors thank members of the Masson and Poirier labs for critical reviewing of the manuscript, Mikael Bédard for providing us with NONO protein fragments and Yan Coulombe for precious help in microscopy-based studies. They also acknowledge Valérie Schreiber (Université de Strasbourg, France) for the kind gift of Parp2-/- cells. Jana Krietsch is a Fonds de Recherche du Québec Nature et technologies scholar and Julien

Vignard is a Canadian Institutes of Health Research postdoctoral fellow. Guy G. Poirier holds a Canada Research Chair in Proteomics and Jean-Yves Masson is a Fonds de Recherche en Santé du Québec senior investigator.

4.7 Funding

Funding for open access charge: Canadian Institutes of Health Research (to J.-Y.M. and G.G.P.). Conflict of interest statement. *None declared.*

4.8 Figures and Legends

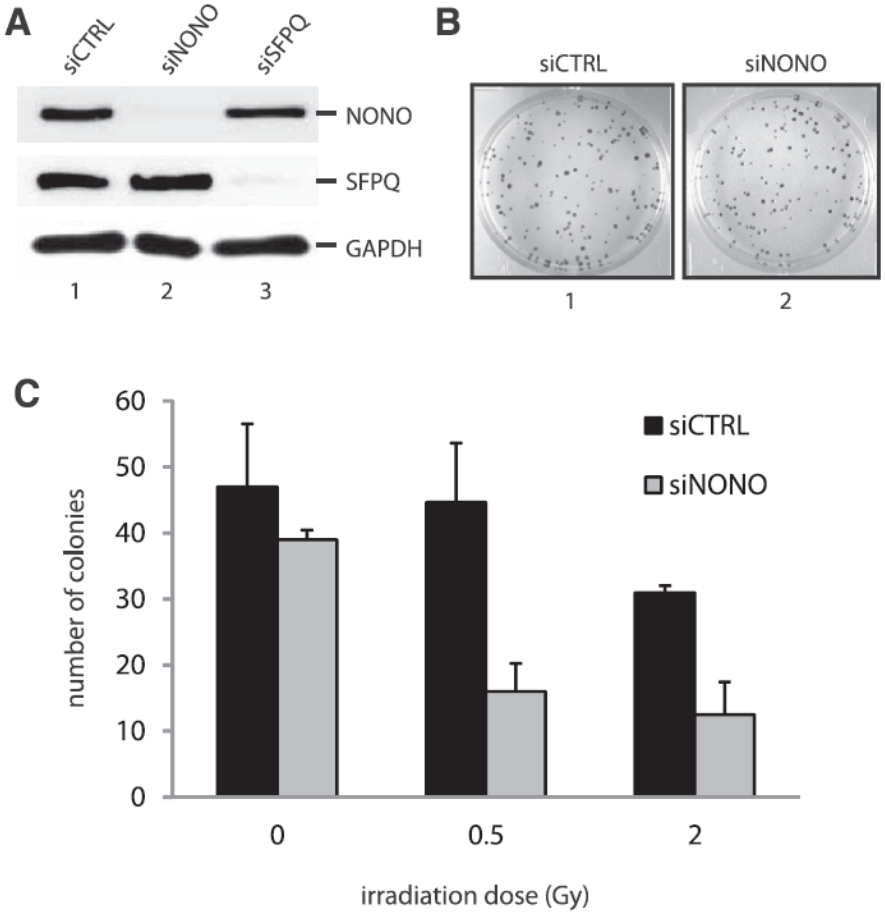

Figure 23: NONO increases cell survival after ionizing irradiation
(A) Western blot analysis demonstrating the efficiency of siRNAs directed against NONO (lane 2) or SFPQ (lane 3) in HeLa cells. **(B)** The clonogenic survival of HeLa cells treated with a scrambled control siRNA (image 1) and a siRNA directed against NONO (image 2) was analysed using a colony forming assay. **(C)** Quantitation of cell survival. HeLa cell colonies were counted 10 days after g-irradiation with 0, 0.5 and 2.0 Gy.

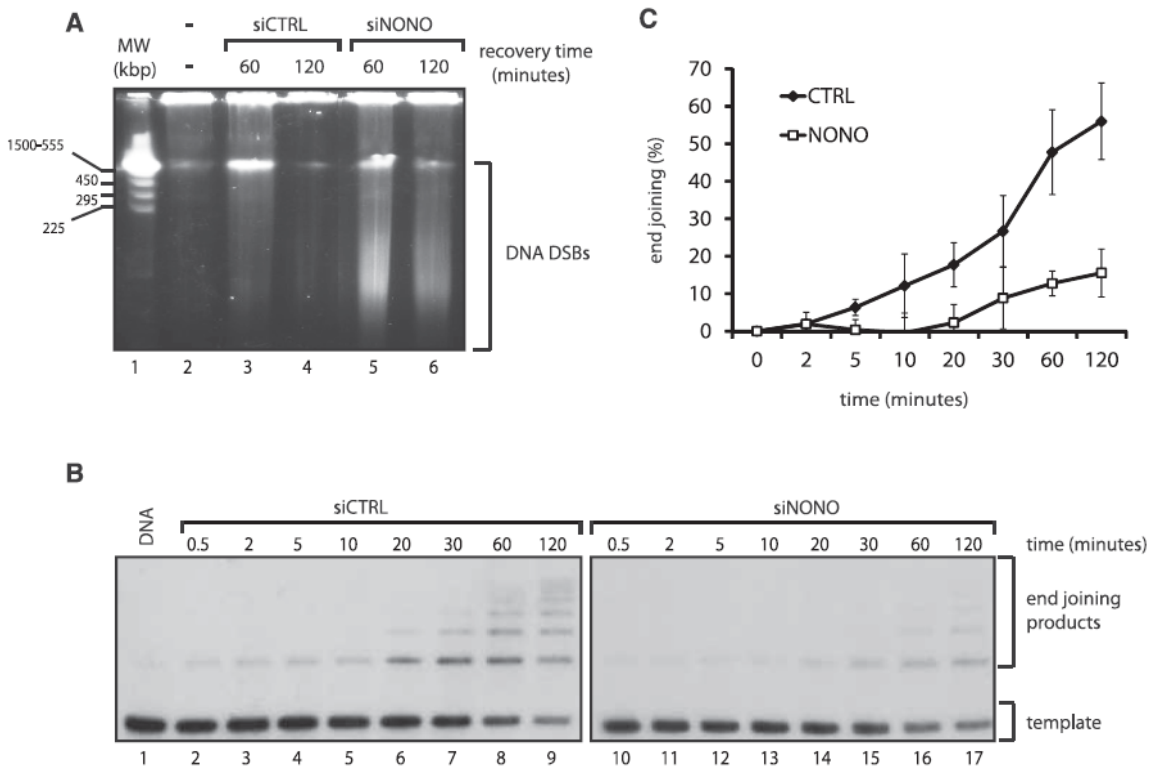

Figure 24: Attenuation of NONO decelerates NHEJ
(A) HeLa cells knocked-down with a scrambled siRNA (lanes 3 and 4) or a siRNA directed against NONO (lanes 5 and 6) were treated for 2 hr with NCS (500 ng/ml) and allowed to recover for either 60 or 120 min. Cells were then collected, embedded and lysed in agarose blocks and used for pulse-field gel electrophoresis. **(B)** A linearized, 32P-end labeled pBluescript was incubated for the indicated times with a nuclear extract derived from HeLa cells treated with a scrambled siRNA (lanes 2–9) or an siRNA directed against NONO (lanes 10–17). **(C)** Quantitation of the end joining events using a phosphorimager: The percent end joining represents the total signal intensity per lane normalized to 100% from which is substracted the % intensity of the remaining template (n=4).

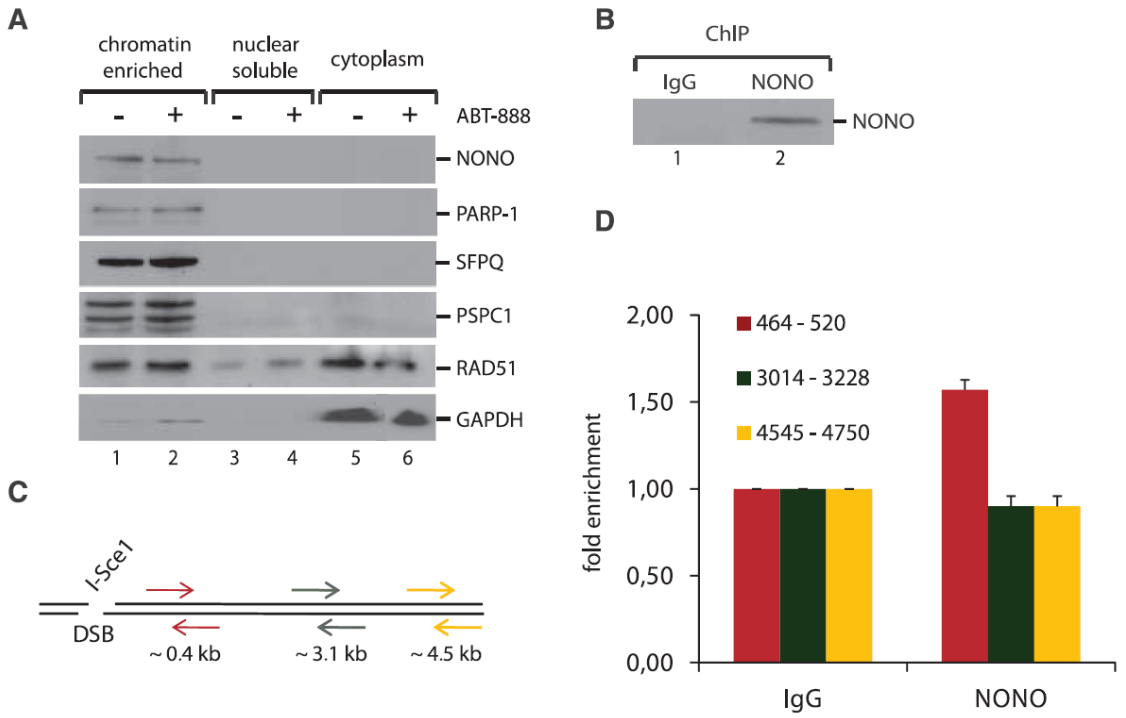

Figure 25: NONO is a chromatin-associated protein and localizes to a unique DSB *in vivo*

(A) Unfixed HeLa cells were treated for 1 hr with 10 mM ABT-888, washed with PBS and fractionated into chromatin-enriched, nuclear soluble and cytoplasmic fractions. Fractions were used for an analysis by western blotting. **(B)** Chromatin immunoprecipitation of NONO from the fixed chromatin of MCF-7 cells, which priorly had been transfected with an I-SceI coding plasmid to generate a unique DSB. An IgG antibody served as a control for the ChIP-experiment. **(C)** Distribution of primer pairs relative to the DSB created by I-SceI. These primers were used in q-PCR analysis of ChIP shown in (D). Primers for GAPDH served as a control for the PCR. **(D)** Quantification of NONO relative to the DSB by PCR (n=3).

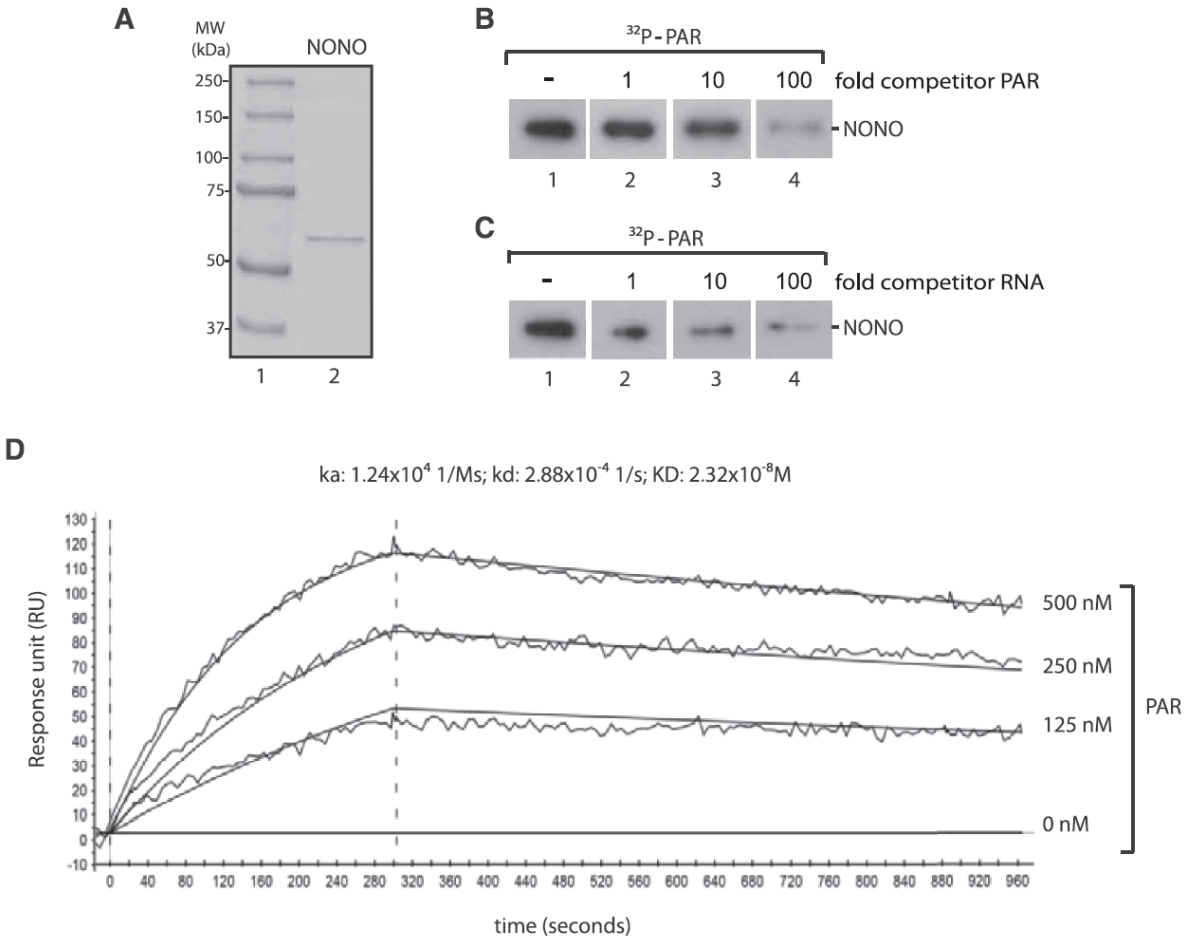

Figure 26: NONO binds PAR *in vitro*

(A) SDS-PAGE of 100 ng purified His-NONO protein stained with Coomassie blue (lane 2). **(B)** *In vitro* PAR-binding assay. 1 mg of purified His-NONO was loaded on an SDS-PAGE, blotted onto a nitrocellulose membrane and incubated in 250 nM 32P-labeled PAR in TBS-T without (lane 1), with 1-fold (lane 2), 10-fold (lane 3) or 100-fold unlabeled competitor PAR (lane 4). **(C)** A PAR-binding assay was conducted as in (B) without (lane 1), with 1-fold (lane 2), 10-fold (lane 3) or 100-fold unlabeled competitor RNA (lane 4). **(D)** Kinetics of PAR binding to purified His-tagged NONO conducted by SPR spectroscopy. To analyse binding kinetics, PAR was injected at three different concentrations (125, 250 and 500 nM). PAR injection was done for 300 s and dissociation data were collected for 600 s. Data were fitted with Langmuir 1:1 interaction plot to calculate rate constants. The sensorgram is representative of three independent experiments.

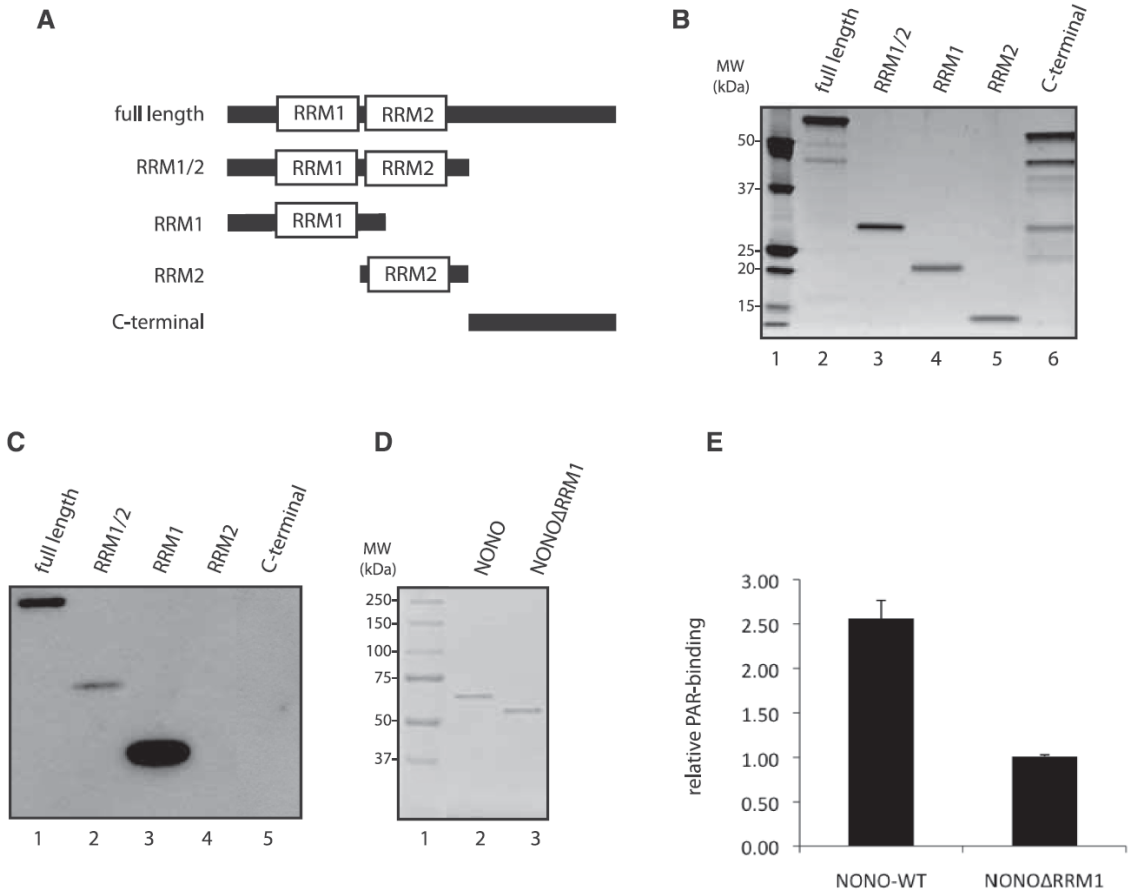

Figure 27: NONO binds PAR through its N-terminal/RNA recognition motif 1 (RRM1)

(A) Protein truncations of NONO flanking the protein domains of interest, namely RRM1 and RRM2. **(B)** SYPRO protein stain of protein fragments loaded on a SDS-PAGE. **(C)** *In vitro* PAR-binding assay using 250 nM 32P-labeled PAR in TBS-T. **(D)** SDS-PAGE of 500 ng His-NONO (lane 2) and His-NONOΔRRM1 (lane 3) each. **(E)** 1 mg of NONO-WT and NONOΔRRM1 purified proteins were slot blotted onto a nitrocellulose membrane and an *in vitro* 32P-labeled PAR-binding assay was conducted in TBS-T. Mean values of the radioactivity signal as quantified by a phosphor-imager from three independent experiments are presented.

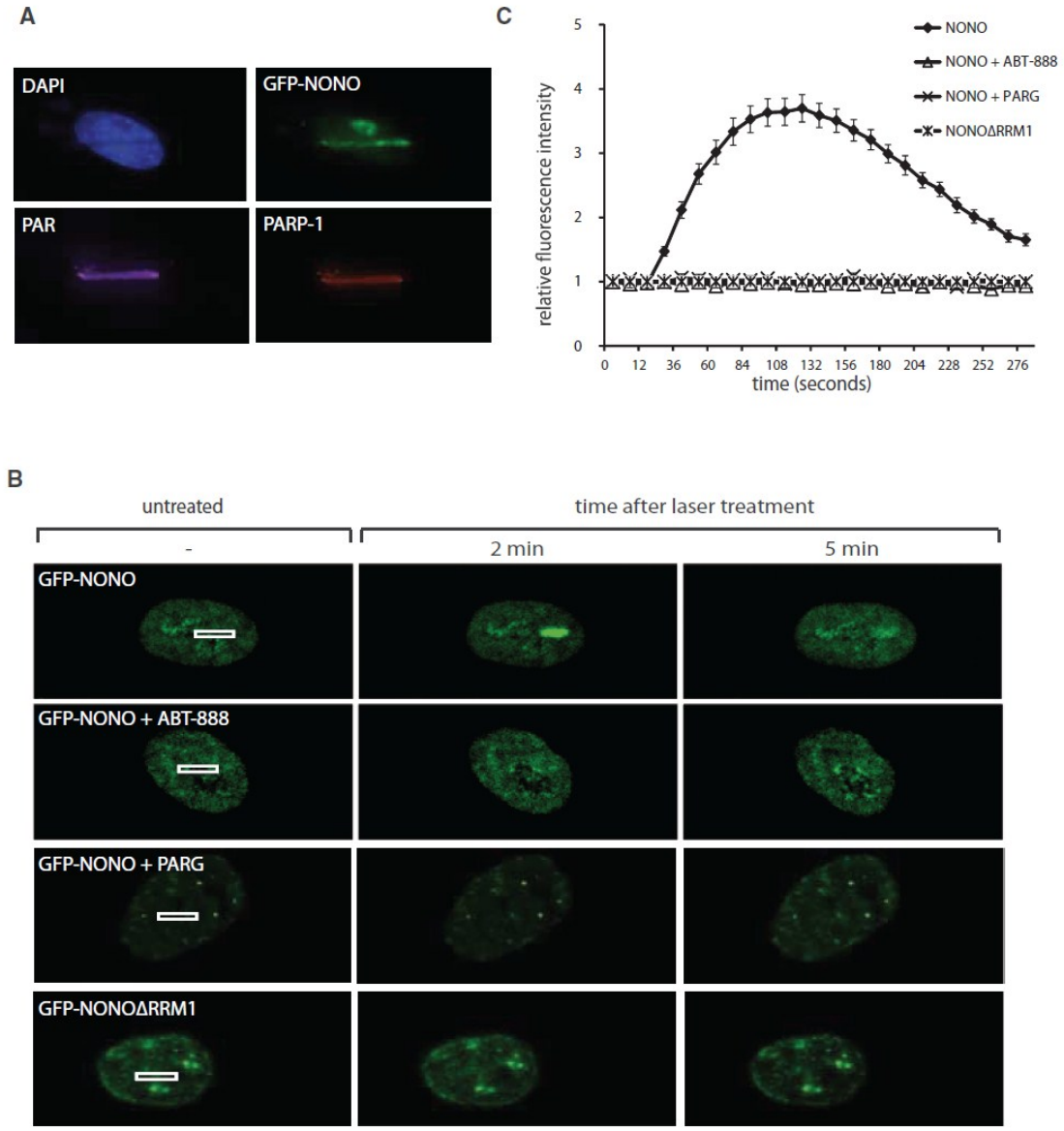

Figure 28: NONO is recruited to DNA damage sites in a PAR-dependent manner
(A) Representative images of laser-irradiated HeLa cells expressing GFP-NONO and subjected to IF for detection of PARP-1 and PAR. **(B)** Representative images of the laser-irradiated cells. HeLa cells were transfected either with the GFP-tagged NONO construct or with a mutant lacking the RRM1. Then cells were either left untreated, treated with 10 mM ABT-888 1 h before irradiation or cotransfected with mCherry-PARG prior to laser microirradiation. **(C)** Statistical analysis of the recruitment kinetics. At least 15 cells per condition in three independent experiments were analysed for their fluorescence intensity above the background.

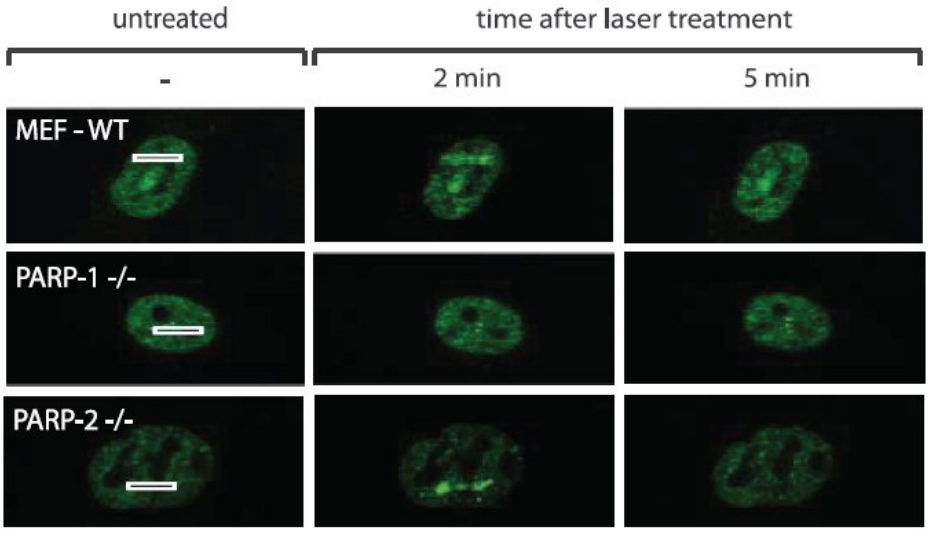

Figure 29: Representative images of laser-irradiated MEFs that were either proficient for PARP-1 and PARP-2 (MEF-WT) or deficient for either PARP-1 (PARP-1$^{-/-}$) or PARP-2 (PARP-2$^{-/-}$)

Mouse embryonic fibroblast (MEF) cells have been transfected with a GFP-NONO construct 24 h before laser microirradiation. At least 20 cells per condition were tested in two independent experiments. Recruitment has been observed in none of the PARP-1$^{-/-}$ MEFs.

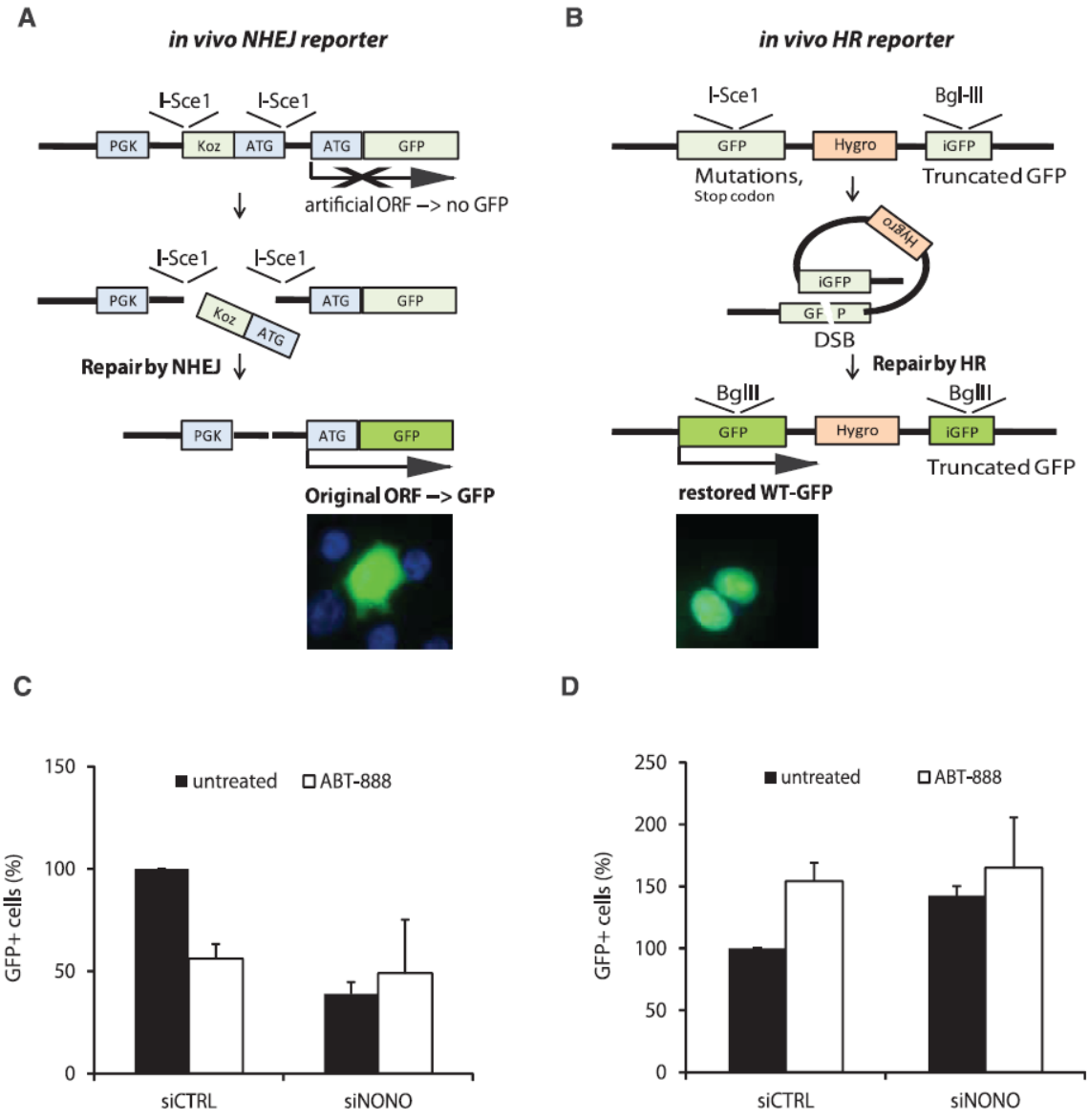

Figure 30: Attenuation of NONO decreases NHEJ and increases HR
(A) Schematic representation of the I-SceI-based NHEJ *in vivo* reporter system. **(B)** Schematic representation of the I-SceI-based HR *in vivo* reporter system. **(C)** NHEJ repair rates in percent with siCTRL or siNONO and with or without 10 mM of the PARP-inhibitor ABT-888. The siCTRL condition was normalized to 100 % (n=3). **(D)** Diagram of the HR repair rates after treatment with siCTRL or siNONO and with or without 10 mM ABT-888. The siCTRL condition was normalized to 100 % (n=3).

4.9 Supplementary Figures

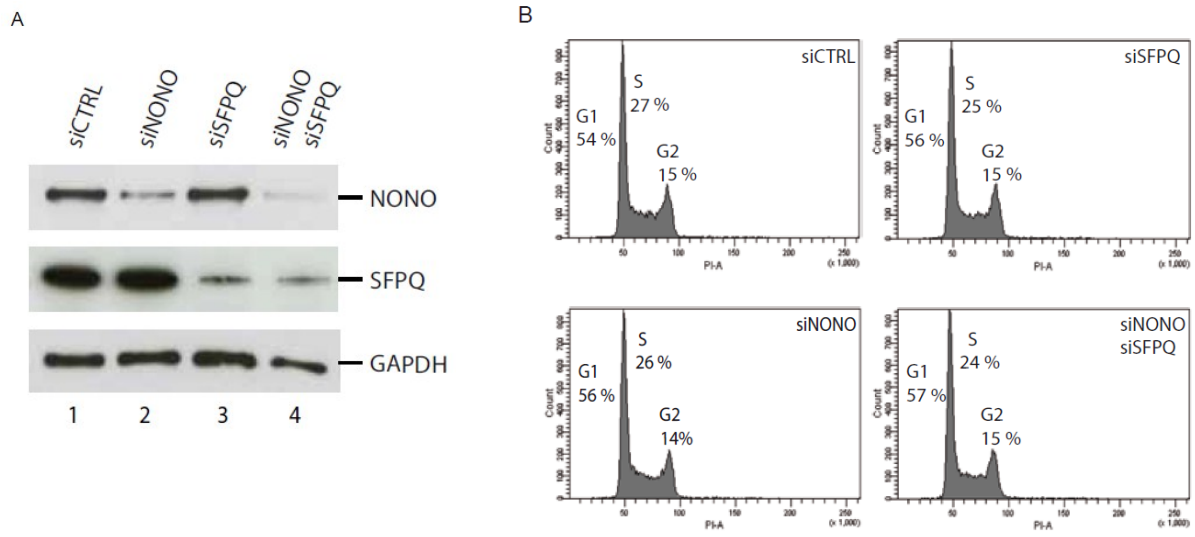

Supplementary Figure 1: Attenuation of neither NONO nor SFPQ effects cell cycle progression.
(A) Representative Western blot analysis of total protein extracts from HeLa cells in which either NONO and/or SFPQ have been knocked-down. **(B)** Cell cycle analysis of HeLa cells pretreated with the indicated siRNAs using propidium iodide (PI). The percentage of cells in each phase of the cell cycle is shown.

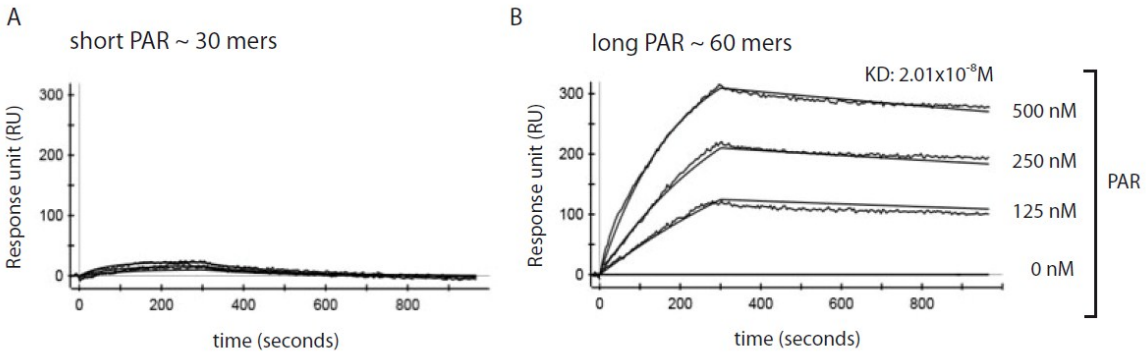

Supplementary Figure 2: SPR binding of different PAR polymer fractions to His-tagged NONO
(A) Sensorgram showing binding of polymer chains with an average of 60 ADP-ribose units to immobilized His-tagged-NONO (KD: 2.01 X 10-8M). **(B)** Sensorgram showing binding of polymer chains with an average of 30 ADP-ribose units to immobilized His-tagged NONO. Results showed no binding of shorter polymer chains.

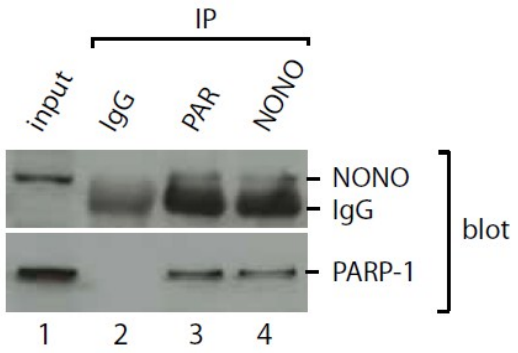

Supplementary Figure 3: NONO co-immunoprecipitates with PAR and PARP-1 in HeLa cells treated with NCS
Prior to immunoprecipitation (IP), HeLa cells were treated for two hours with 100 ng/ml NCS. IPs were performed with antibodies directed against IgG as a control (lane 2), PAR (lane 3) and NONO (lane 4). The input of each protein (lane 1) was immunoblotted against the IPs with antibodies against NONO or PARP-1.

For supplementary material and methods the reader is kindly referred to the online version of this manuscript. (http://nar.oxfordjournals.org/content/40/20/10287/suppl/DC1)

CHAPTER 5
DISCUSSION

The synthesis of poly(ADP-ribose) by the enzyme PARP-1 was discovered by Pierre Chambon about 50 years back (Chambon et al., 1963) and since then this posttranslational modification has been studied in different cellular contexts, most importantly in the response to DNA strand breaks. It is now widely accepted that PAR, which is rapidly generated upon encountering DNA breaks, is serving as a scaffold for DNA repair proteins and, as a surprise for the PARP field, also for RNA processing factors. However, to what extent these interactions with PAR are direct and dynamic and what is the biological role of this interaction for individual proteins remain elusive. *Hence the major objective of my doctoral thesis was to analyze the PAR interactome in response to DNA damage using proteomics approaches, serving as a starting point for the in depth-investigation of one of the predominant proteins in the PAR interactome, namely NONO. In the following, the results obtained will be briefly recapitulated and discussed in the context of the current literature with an opening towards research perspectives.*

5.1 The PAR interactome after DNA damage is a dynamic composition of DNA repair and RNA processing factors

To date most of the proteomic studies published by our lab and others have focused on the early response of PARPs to genotoxic stress (e.g. (Gagne et al., 2003)). As presented in Chapter 3, we have undertaken the first reported proteome-wide effort to follow the dynamics of the PAR-interactome in response to DNA damage. The alkylating agent MNNG has been used for decades to effectively induce PAR synthesis through the induction of both SSBs and DSBs (Banath et al., 2010), (Artus et al., 2010) and has therefore been a useful tool for us to efficiently activate PARP. For our study we chose to investigate the PAR interactome at relatively short-, mid- and long-term time points after recovery from MNNG treatment (5, 60 and 120 minutes, respectively).

5.1.1 Shortly after PARP-activation, PAR is bound by DNA damage recognition, signaling and repair factors

Strikingly we found that, even though there is an overlap among the different processes, the dominant process identified at the time of the peak of PAR synthesis at five minutes is the DNA damage response (see Chapter 3, Figure 18B and 19 left). Consistent with the idea of rapid activation of PARP-1 and hence PAR synthesis upon DNA strand breaks, predominant PAR-associated proteins detected in our pull-downs are chromatin remodeling factors and DNA repair proteins including Ku70, Ku80 and DNA-PK (see Figure 17). Surprisingly however, the three above mentioned proteins are not PAR-dependently recruited to DNA damage in our laser track experiments (Figure 22), suggesting a role for PAR-binding which is rather downstream of or synergistic to initial NHEJ events. Indeed, PARP-1 directly competes for free DNA ends with Ku70 (Wang et al., 2006), (Couto et al., 2011), which itself protects DNA ends from the resection machinery and initiates repair by NHEJ, (Lieber, 2010). This had been originally interpreted as a role for PARP-1 in collaboration with MRE11 in the alternative NHEJ pathway (Audebert et al., 2004). Adding another layer of complexity, Ku70/Ku80 and DNA-PK have been shown to be direct targets of PARP-1, a process which possibly impairs their ability to bind to DNA (Li et al., 2004), (Galande and Kohwi-Shigematsu, 1999), (Ariumi et al., 1999), (Spagnolo et al., 2012) and could thereby regulate the efficiency of NHEJ.

Strikingly, consistent with the remarkably fast kinetics of PARylation upon DNA damage which suggests a role upstream of actual repair, we detected (see Chapter 3, Figure 18) various proteins acting on DNA end resection in the PAR interactome, namely 53BP1, RIF-1 (Zimmermann et al., 2013), (Di Virgilio et al., 2013), (Chapman et al., 2013b), MRE11, Rad50, NBS1 (Yuan and Chen, 2010), RPA1 and RPA2 (Chen et al., 2013). Interestingly, already in 1991 it had been suggested that RPA is a direct target for covalent automodification by PARP-1, a finding that had been interpreted as a function at the DNA replication fork (Eki and Hurwitz, 1991). However, this should be carefully re-analyzed in the context of HR repair as another well established role of RPA independent of DNA replication lies in DNA end resection, where the free ssDNA generated by the MRN complex is rapidly coated by the RPA proteins, which can stimulate resection activity

(Hass et al., 2012), (Haring et al., 2008). Supporting the idea of an interaction between PARP-1 and RPA, we have preliminary results showing that in MEFs, the phosphorylation of RPA at DNA repair centers is abolished in the absence of PARP-1 (Annexes, Figure 32). Moreover, only very recently DNA-PK (mentioned above for its role in NHEJ) was also suggested to influence DNA end resection activity by blocking the recruitment of Exo1 (Zhou and Paull, 2013). Interestingly, also Ku70 has recently been shown to diminish the resection activity of Exo1 *in vitro* (Yang et al., 2013), demonstrating the interplay between the two major DSB repair pathways which could be regulated by PARP-1 catalytic activity.

Other lines of evidence that PARP-1 might influence DNA end resection have emerged within the last years. PAR generated by PARP-1 at DNA damage sites recruits MRE11/NBS1 (Haince et al., 2008), a protein complex that is a key player in HR through the initiation of end resection, but also suggested to be a player in Alt-NHEJ in the context of PARP-1 activation. Moreover, one of the key promoters of DNA end resection is BRCA1. Although it has been shown that γH2AX and MDC1 facilitate its recruitment to DNA damage sites (Harper and Elledge, 2007), BRCA1 is still recruited in the absence of these factors. However, under these conditions, BRCA1 cannot be stably retained at damage sites (Celeste et al., 2003), indicating that BRCA1 recruitment might depend on another DNA-damage signaling factor. Indeed, in May 2013, the group of Dr Xiaochun You published the intriguing discovery that the binding of the BARD BRCT domains to PAR targets BARD and its binding partner BRCA1 to DNA damage sites (Li et al., 2013; Li and Yu, 2013). These results are in line with the emerging concept of a synergistic relationship between PARP-1 activation and γH2AX and ATM phosphorylation (Orsburn et al., 2010) (Celeste et al., 2003). Contradictorily from experiments with PARP-$1^{-/-}$ cells, it has been argued that PARP-1 deficient cells display a hyperrecombinant phenotype (Schultz et al., 2003).

Taken together, the identification of DNA end resection proteins in our datasets in the context of the current literature strongly suggest a role for PARP-1 in balancing DNA end resection. Whether the role of PARP-1 and its polymer is of a stimulatory or inhibitory nature will be an important question to be addressed in the future.

5.1.2 The PAR interactome during recovery from DNA damage is highly enriched in RNA-binding proteins

As described before, the PAR interactome immediately after the induction of DNA damage consists of key proteins involved in the DDR. Interestingly, the composition of the PAR interactome after one and two hours of recovery from the damage is of a strikingly different composition (see Chapter 3, Figure 18 and Figure 19). One hour post-recovery from MNNG exposure, proteins from the transcriptional machinery are predominantly present in the pull-downs, whereas after two hours of recovery, proteins from the RNA splicing, stabilization and translation process are highly correlating with PAR in our pull-downs. Again here, whether these interactions are direct and whether they imply binding to RNA as well will be a subject of future studies. Moreover it would be highly interesting to repeat the kinetics study by replacing the MNNG with NCS, an agent that activates PARP less robustly but introduces DSBs in a direct manner.

One RNA-binding protein caught our special interest as it did not follow the kinetics found for other RNA-processing factors. The RNA-binding protein NONO was already detected in the pull-downs five minutes after DNA damage together with chromatin remodeling and DDR proteins (Chapter 3, Figure 17, SILAC). We were hence tempted to investigate on NONO and its potential role in the DDR through PAR.

5.2 PARP-1 regulates NONO in the DDR to DNA DSBs

As previously mentioned the RNA binding protein NONO displays one of the highest enrichment ratios (control versus DNA damage) in our PAR immunoprecipitates. However, whether this is due to direct binding of NONO to PAR and, if so, what the biological function of these PAR-binding properties is, remained to be examined. Hence, one of the first aims was to test for potential noncovalent PAR-binding properties of NONO in vitro.

5.2.1 NONO is a PAR-binding protein, which binds PAR through its RRM1

We have obtained highly pure His-tagged NONO protein by FPLC purification from *E. coli* and found that NONO binds specifically to PAR with an affinity constant of 2.32 x 10^{-8} as measured by SPR (see Chapter 4, Figure 26D). This strong affinity for complex PAR interestingly resembles those for well-established PAR-binding factors such as XRCC1 or AIF (as reviewed in (Krietsch et al., 2013), see Annexes). Interestingly, the PAR bound to NONO can be competed out by a mixed pool of RNAs (Chapter 4, Figure 26C). Additionally, this PAR-binding is specific for long and branched PAR fractions in our SPR experiments. Strikingly, even though the protein binds RNA molecules, it has a very low affinity for the short and unbranched PAR fraction (which would structurally resemble RNA) in the same experiment (Chapter 4, Supplementary Figure 2). The fact that RNA was able to compete out PAR-binding highly suggests that the RRM1 is the domain responsible PAR-binding motif. Indeed, we found that NONO strongly binds PAR through its N-terminal/RNA-recognition motif 1 (Chapter 4, Figure 27A-C). The deletion of the RRM1 domain from the full-length protein however resulted in diminished but not abolished binding to PAR *in vitro* (see Chapter, Figure 27D-E), indicating that the N-terminal sequence flanking the RRM1 is important for its binding properties or contains yet another undescribed PAR-binding domain.

It has been previously published that the RRM1 of NONO contains four conserved amino acids which are typical for RNA binding (Maris et al., 2005). The RRM2 on the other hand is considered noncanonical, meaning that three of these conserved residues are substituted for other amino acids, indicating that the RRM2 either does not bind RNA or that it binds it in a yet unexpected manner (Passon et al., 2012). Are these *in vitro* binding properties we observed enabling a competition between PAR and RNA in cells? One might speculate that under normal conditions, NONO binds RNA, but in conditions where PAR is generated excessively (as in response to DNA damage) this RNA binding is competed out by PAR. An elegant example for this principle consists in the protein hrp38 (the *Drosophila melanogaster* homologue of human hnRNPA1), which binds PAR noncovalently with the consequence of reduced RNA-binding ability which affects its role in splicing (Ji and

Tulin, 2009). Hence a competition for the same binding site between PAR and RNA could be a molecular switch between RNA processing and DNA repair.

It is also intriguing that the protein contains two heterologous RRM domains whereas only one seems important for RNA-binding (Passon et al., 2012). What is the function of RRM2? From the crystal structure of NONO it had been speculated that its RRM2 is responsible for homo- and heterodimerization with itself and its partner proteins SFPQ and PSPC1 through binding to a respective NOPS domain (Passon et al., 2012). However, RNA binding domains are some of the most flexible protein domains in terms of binding partners (Clery et al., 2008), which makes it tempting to speculate that the RRM2 carries out other yet unknown functions. Another possibility is that the RRM2 increases the binding efficiency of the RRM1 to RNA as it has been proposed for other proteins containing multiple RRM-domains (Clery et al., 2008), (Shamoo et al., 1995).

A concept emerging in the DDR field is that the PAR generated at DNA DSBs serves as a recruitment signal for DNA damage detection and repair proteins (Ciccia and Elledge, 2010). We hence tested whether this applies also for the newly identified PAR-binding protein NONO.

5.2.2 The recruitment of NONO to DNA damage sites is strictly depending on PAR catalyzed by PARP-1

Indeed we found that the recruitment of NONO strictly depends on PAR generated by PARP-1 at DNA damage sites (see Chapter 4, Figure 28). Moreover, the PAR generated by PARP-1 is essential whereas the catalytic activity of PARP-2 is dispensable for NONO's recruitment (Chapter 4, Figure 29). Different from most of the RNA-processing factors found in the PAR pull-downs after one or two hours recovery from DNA damage (Chapter 3, Figure 18), the RNA-binding protein NONO was PAR-dependently recruited to DNA damage sites in an extremely fast and transient manner, with a peak of recruitment kinetics being already at two minutes post DNA damage (Chapter 4, Figure 28C). Moreover, different from other PAR-dependently recruited proteins, such as for instance CHFR or XRCC1 (Chapter 3, Figure 21B), the recruitment of NONO strictly depends on PAR as

shown by three lines of evidence in Chapter 4, Figure 28: The recruitment of GFP-NONO is abolished (i) in the presence of the specific PARP-inhibitor ABT-888, (ii) the overexpression of PARG, (iii) the absence of the PAR-binding motif RRM1 in the NONO full-length protein. Hence, NONO is joining a growing list of RNA-binding proteins that are PAR-dependently recruited to DNA damage sites with similar fast kinetics. Other examples include RNA-binding motif, X-chromosome (RBMX) (Adamson et al., 2012), Thyroid hormone receptor-associated protein 3 (THRAP3) (Jungmichel et al., 2013), (Beli et al., 2012), Serine/arginine-rich splicing factor (ASF/SF2) (Malanga et al., 2008) and fused-in-sarcoma (FUS) translocated-in-sarcoma (TLS) (Mastrocola et al., 2013), (Rulten et al., 2013). Interestingly the recruitment of these RNA processing factors by PAR is upstream of their implication in the DNA damage response, suggesting a cross-talk between RNA-processing and DNA repair. As recently published by Dr Stephen Elledge, the recruitment of RBMX to DNA damage sites is PARP-dependent and the protein indirectly facilitates HR by facilitating proper BRCA2 expression (Adamson et al., 2012). Why RBMX needs to be recruited to DNA damage sites remains to be questioned. Also, for FUS the recruitment to DNA damage sites in laser tracks depends completely on PARP activity (Rulten et al., 2013) where, through a yet unknown mechanism of action, FUS possibly stimulates NHEJ as well as HR (Mastrocola et al., 2013).

A potential cross-talk between RNA-binding proteins and repair as described above did not come as a surprise to the field as for instance local transcription is inhibited at DNA damage sites to allow time for repair (Rockx et al., 2000; Shanbhag et al., 2010). *Due to the evidence given above for other RNA-binding proteins we were tempted to analyze whether NONO is influencing the outcome of DSB repair, which is discussed in the following.*

5.2.3 NONO influences the outcome of NHEJ and HR

Strikingly, we were able to show that NONO is important for cell survival after clinically relevant low doses of ionizing radiation (Chapter 4, Figure 23). This result confirms a similar finding by Dr William Dynan, who has used a miRNA directed against NONO to provoke radiosensitivity in cells (Li et al., 2009). Strikingly, our approach is based on a siRNA and hence diminishing protein expression only transiently, underpinning its

importance to protect from a radiosensitive phenotype. A radiosensitive phenotype has been observed for the ablation of many factors involved in the early response to DNA DSBs (for instance H2AX (Bassing et al., 2003) (Celeste et al., 2002), 53BP1 (Ward et al., 2003) (Morales et al., 2003), ATM (Barlow et al., 1996)), which is hence strongly suggesting an implication for NONO in DSBR. It has to be noted here that its partner protein SFPQ is essential for cell survival whereas NONO seems dispensable for survival in untreated cells (Ha et al., 2011). Is the fact that NONO is dispensable for survival in untreated conditions due to a redundancy between the third DBHS protein PSPC1 and NONO as Dr Dynan had suggested (Li et al., 2009)? One preliminary hint we can provide to support this theory is the fact that upon a siRNA-generated knockdown of NONO, the protein expression of PSPC1 (which is normally relatively low in comparison to NONO and SFPQ, is upregulated (Annexes, Figure 33). It would be extremely interesting in the future to analyze whether a combined knockdown of NONO and PSPC1 impairs cell survival in the absence of DNA damage. Another explanation for why SFPQ (other than NONO) is essential for cell survival, even in the absence of DNA damage, is the possibility raised by (Rajesh et al., 2011) that SFPQ is acting in the displacement loop formation step of the other major DSB repair pathway, namely homologous recombination. The knockout of the key HR factors, such as RAD51, NBS1, Rad50, BRCA1 and BRCA2 in mice is embryonic lethal (Lim and Hasty, 1996), (Tsuzuki et al., 1996), supporting this idea.

It came as a surprise to us that a factor originally discovered in the context of paraspeckles and transcription is predominantly associated with the chromatin in cell fractionation experiments (Chapter 4, Figure 25A) and not in the nuclear soluble fraction as expected. Strikingly, after increasing the resolution on the chromatin to a unique DSB *in vivo* by a chromatin immunoprecipitation approach, we were able to detect NONO at a similar distance as Ku70 (Rodrigue et al., 2006) from the I-SceI-induced break-site (Chapter 4, Figure 25B-D). Since we have detected NONO in close proximity to a DSB we were questioning whether the protein is needed to properly carry out DSB repair. To indirectly measure DNA repair after recovery from NCS treatment, we visualized DNA fragmentation in HeLa cells by pulse-field gel-electrophoresis. We found that, in cells in which NONO has been knocked down, more damaged DNA accumulates when compared to control cells

(Chapter 4, Figure 24A). Even though the key factors carrying out the NHEJ repair pathway have been extensively described (Lieber and Wilson, 2010), it has long been suggested that accessory factors can stimulate the reaction (Baumann and West, 1998), (Bladen et al., 2005). We therefore sought to use a cell-free DSB repair assay that had been developed in the lab of Dr. S. West (Baumann and West, 1998) and found that end-joining activity of a plasmid DNA is strongly diminished in nuclear protein extracts where NONO has been knocked down (Chapter 4, Figure 24B and C). Strikingly, we were able to verify this finding in an *in cellulo* approach for which we stably integrated the NHEJ reporter construct (sGEJ) designed by Dr Ralph Scully (Xie et al., 2009) into the genomic DNA of MCF-7 cells. Therewith we were able to show that a knockdown of NONO by siRNA diminishes NHEJ activity more than 50 % (Chapter 4, Figure 30A and C), which is comparable to the results obtained by Dr Scully for Mre11 in MEFs (Xie et al., 2009).

Taken together, the results described above strongly suggest a role for NONO in the regulation of NHEJ. However, the possibility that the protein also affects the other major DNA DSB repair pathway cannot be excluded. We hence generated a stable MCF-7 cell line carrying the HR reporter construct designed by Dr Maria Jasin in its genomic DNA and indeed found that a knock-down of NONO significantly facilitates HR (Chapter 4, Figure 30B and D).

Proteins like NONO, with dual functions in RNA biology and DNA repair which might link repair and transcription, were rather surprising as so far many classical repair/transcription factors were seen in only one biological process, which was in most cases the process that they have been discovered. Interestingly, this list is rapidly growing. Well established to date is the transcription-coupled repair (TCR) pathway, a subpathway of NER, which preferentially repairs the transcribed DNA strand in expressed genes (Hanawalt and Spivak, 2008), (Mellon et al., 1987). Herein, the Cockayne Syndrome B (CSB), TFHII and Xeroderma pigmentosum G (XPG) proteins are recruited to RNA polymerase II, which has been arrested at DNA damage sites, in order to catalyze repair. Interestingly mutations of NER proteins (namely ERCC6 and ERCC8) can lead to the premature aging syndrome named Cockayne syndrome (CS). The complex multisymptom

phenotype of CS is composed of a congenital disorder characterized by growth-failure, impaired development of the nervous system, abnormal sensitivity to sunlight and premature aging and cannot simply be explained by defects in NER. The problem has been resolved by the discovery that the same set of proteins is as well implied in transcriptional activation (Compe and Egly, 2012), (Kamileri et al., 2012). Whether the transcriptional activity and DNA repair activity are coupled processes or exclude each other will need to be examined.

The list of proteins involved in transcription and repair however is not only restricted to NER. Another prominent example is the protein DNA-PKcs. As described in Chapter 1 and 2, this protein facilitates DNA end processing and resealing at DNA double-strand breaks by NHEJ, but moreover the protein arrests RNA-polymerase II transcription after the induction of DNA DSBs (Pankotai et al., 2012). As described above DNA-PKcs is also a PARylation target and was found in the PAR-interactome post-DNA damage (Chapter 3, Figure 17) and could hence be regulated through PAR-binding. It will hence be highly interesting to investigate whether PARP-1 can regulate DNA-PKcs function in DNA repair and /or transcription.

Most interestingly however is the fact that PARP-1 itself adds another layer of complexity to the cross-talk between RNA biology and repair. As described in detail in Chapter 1 and 2, besides the protein's function in sensing and signaling DNA damage, it is also found at almost all active promoters and able to influence transcription (Krishnakumar and Kraus, 2010b). One might hence speculate that the presence of DNA damage functions as a molecular switch to recruit PARP-1 away from promoters towards the damage sites attracting other proteins like NONO, which are normally involved in RNA biology in order to stop transcription and carry out repair.

In conclusion, although we cannot completely rule out the possibility that NONO protein depletion may also affect DSB responses indirectly (as a result of mRNA transcription or splicing misregulation for instance), the strong phenotype in the repair assays as well as its fast and transient recruitment kinetics and association with DSB repair proteins favors it to

have a direct implication in controlling the cellular response to DSBs. However, what the precise mechanism of action of this protein in DSB repair is and whether or not this implies the presence of RNA will need to be explored in the future.

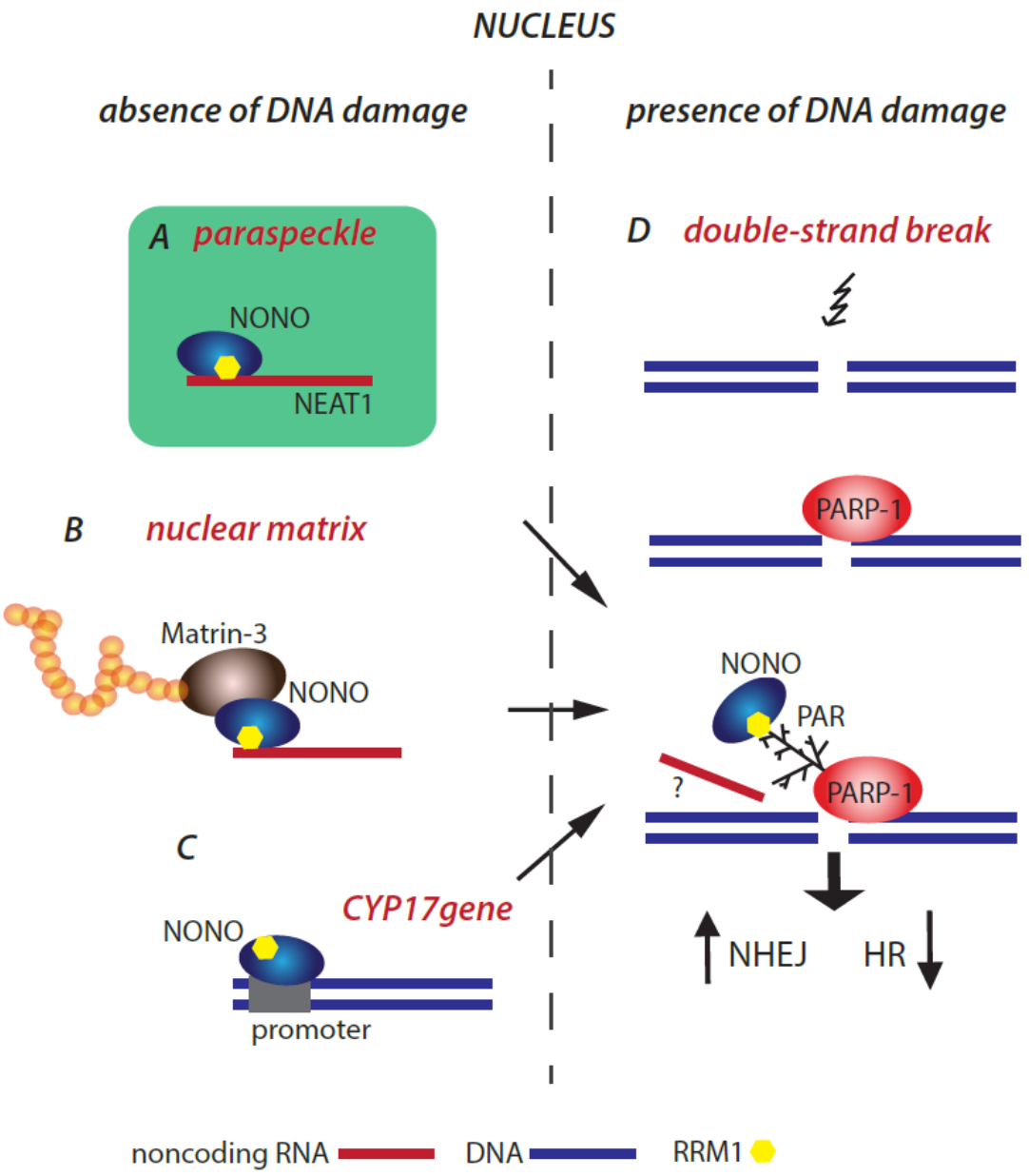

Figure 31: Proposed model for the RNA-binding protein NONO which binds PAR upon DNA damage

(A) NONO is a component of paraspeckles helping the retention of A- to I- edited RNAs such as nuclear enriched abundant transcript 1 (NEAT1) in the nucleus. (**B)** The RNA-binding protein NONO is binding to Matrin-3, which itself binds to the nuclear matrix which may, in the context of paraspeckles, retain long noncoding RNAs in the nucleus. (**C)** NONO is able to repress the basal transcription of the *CYP17* gene. **(D)** After the induction of a DSB, PARP-1 rapidly binds the free DNA ends and automodifies itself which leads to the recruitment of NONO to the damage site, where the protein promotes NHEJ over HR. The potential role of noncoding RNA at the DSB will be an interesting question to be addressed in the future.

5.3 Conclusions

Our work on the interactome of PAR after DNA damage has revealed three interesting observations: (i) Importantly, we learned from our study that the PAR interactome after DNA damage is of a dynamic nature, with a composition of proteins that changes from a short-term towards a long-term DNA damage response, suggesting biological relevance of PAR-protein interactions in many biological processes. (ii) Rapidly upon DNA damage, PAR is interacting with proteins belonging to the DNA damage response and chromatin remodeling factors, amongst them many that channel the DNA repair pathway choice by their role in end resection. (iii) During recovery from DNA damage, PAR attracts RNA processing factors, implying an interplay between RNA biology and DNA repair. This study gives important information on the composition of the PAR interactome post-DNA damage, but leaves the question for direct interaction of individual proteins with PAR unanswered. The study can hence be seen as a starting point for the investigation of individual proteins of the PAR interactome, such as NONO.

Our investigation of NONO in the DNA damage response revealed a direct role in the DNA damage response in a PAR-dependent manner based on the following observations: (i) NONO is binding to PAR generated at DNA damage sites with a very fast kinetics; comparable to other DNA repair factors but different from RNA-processing factors. (ii) NONO is specifically binding long and complex PAR through its RRM1, which is essential for its recruitment to DNA damage sites. (iii) NONO is stimulating NHEJ and repressing HR in the same pathway as PARP-1. Collectively, even though we cannot rule out an indirect mechanism of action for NONO in the DDR, our results strongly suggest a direct implication, possibly in pathway decision between NHEJ and HR.

5.4 Future directions

Despite the progress we have made in understanding the PAR interactome in the DNA damage response and the intriguing finding that the RNA-binding protein NONO is playing a role in the DDR which is regulated by PARP-1, many questions remain unanswered:

5.4.1 Deciphering the potential role of RNA in DNA DSB repair

One may envision several possible mechanisms to explain the role of NONO in the DDR. Firstly, NONO may inhibit nascent transcription at DNA DSBs or remove nascently transcribed RNAs as it has been shown for ATM (Shanbhag et al., 2010). However, it is hard to speculate how this would regulate the HR and NHEJ pathways in opposing ways and not rather generally facilitate DNA repair at the break site.

Only very recently it has been published by the lab of Dr Steve Jackson that hnRNPU-like proteins (described as components of the spliceosome (Jurica et al., 2002)) are able to promote DNA DSB signaling and repair by regulating the DNA end resection step (Polo et al., 2012). As DNA end resection is a means of regulating DNA pathway choice and the NONO protein in our experiments blocks NHEJ and stimulates HR, one may speculate about a possible role for NONO in DNA end resection. The stimulation of NHEJ and repression of HR could be due to an inhibitory effect on exonuclease activities as those carried out by MRE11.

Intriguing is the question whether the mechanisms of action of NONO in DNA DSB repair requires the presence of RNA. As mentioned previously, NONO is found in complex with long noncoding RNAs (lncRNA) in the context of paraspeckles and the nuclear matrix (Chapter 1, section 1.4.3), but it is not clear whether this binding is lost during NONOs recruitment to DNA damage sites. Interestingly lncRNAs could be implied in DNA repair as the expression of many lncRNAs is responsive to DNA damage (Liu and Lu, 2012). But can noncoding RNAs actually be found at DNA damage sites? Indeed, a study in yeast published in 2007 suggests a possible importance for RNAs in DNA repair through a yet

unknown mechanism. The authors have shown that in *Saccharomyces cerevisiae* RNA can serve as a homologous repair template in a way that does not depend on reverse transcriptase activity (Storici et al., 2007). However, it is not clear whether this happens only in the context of local transcription given the high local concentration of the RNA or whether RNA is actually recruited or locally produced for repair. A kinetic assessment of lncRNA biogenesis at unique DSBs in euchromatin versus heterochromatin will be very informative. Five years later, in 2012, the astonishing finding has been made that small noncoding RNAs, named DNA damage response RNAs (DDRNAs) by the authors, which contain the sequence of the DNA damage locus have a direct role in the DNA damage activation. More precisely the authors propose that these small RNAs are generated in response to DNA damage and mediate the accumulation of ATM, MRE11 and 53BP1 but not γH2AX at IRIF (Francia et al., 2012). It would hence be extremely interesting to study the potential role of RNA in our model of PARP-1/NONO at a DNA DSB.

5.4.2 Gene knockout of the human PARP-1 gene as a tool to study human PARP-1 biology

One general problem in the PARP field is that the crucial distinction between PARP-1 protein biology and the mechanism of action of PARP inhibitors has in the past years often been ignored. Even though it had clearly been demonstrated that most of the inhibitors are specific for more than only one PARP protein or some of them do not inhibit PARylation activity at all (Wahlberg et al., 2012), PARP inhibitors have often been used as a control to conclude on biological roles of PARP-1. It should not be surprising that results of recruitment experiments fundamentally differ between assays where an inhibitor of the catalytic activity has been used when compared to a siRNA approach. As described before, PARP-1 is one of the most abundant proteins within cells, which makes attempts to diminish the protein expression by using a siRNA or shRNA quite challenging. Moreover the small levels of residual protein might be sufficient to resemble wild type conditions. We have hence started to establish a gene knockout of the human PARP-1 gene with a system named Clustered Regularly Interspaced Short Palindromic Repeats (CRISPR)/Cas9. This system has originally been descovered as a bacterial immune defense system against intruding viral DNA but has in the past years been adapted for targeted gene knockout in

any desired cell line, requiring only the coexpression of the CRISPR-associated 9 (Cas9) protein and a customizable single guide RNA. We have chosen this approach in order to establish the gene knockout of PARP-1 in human cells. (Annexes, Figure 34). The complete abolishment of the PARP-1 protein in human cell lines will enable the better understanding of the biological roles of PARP as well as its polymer.

REFERENCES

Adamson, B., Smogorzewska, A., Sigoillot, F.D., King, R.W., and Elledge, S.J. (2012). A genome-wide homologous recombination screen identifies the RNA-binding protein RBMX as a component of the DNA-damage response. Nat Cell Biol *14*, 318-328.

Affar el, B., Shah, R.G., Dallaire, A.K., Castonguay, V., and Shah, G.M. (2002). Role of poly(ADP-ribose) polymerase in rapid intracellular acidification induced by alkylating DNA damage. Proc Natl Acad Sci U S A *99*, 245-250.

Aguilera, A., and Gomez-Gonzalez, B. (2008). Genome instability: a mechanistic view of its causes and consequences. Nat Rev Genet *9*, 204-217.

Ahel, D., Horejsi, Z., Wiechens, N., Polo, S.E., Garcia-Wilson, E., Ahel, I., Flynn, H., Skehel, M., West, S.C., Jackson, S.P*., et al.* (2009). Poly(ADP-ribose)-dependent regulation of DNA repair by the chromatin remodeling enzyme ALC1. Science *325*, 1240-1243.

Ahel, I., Ahel, D., Matsusaka, T., Clark, A.J., Pines, J., Boulton, S.J., and West, S.C. (2008). Poly(ADP-ribose)-binding zinc finger motifs in DNA repair/checkpoint proteins. Nature *451*, 81-85.

Ahnesorg, P., Smith, P., and Jackson, S.P. (2006). XLF interacts with the XRCC4-DNA ligase IV complex to promote DNA nonhomologous end-joining. Cell *124*, 301-313.

Akhmedov, A.T., and Lopez, B.S. (2000). Human 100-kDa homologous DNA-pairing protein is the splicing factor PSF and promotes DNA strand invasion. Nucleic Acids Res *28*, 3022-3030.

Ali, A.A., Timinszky, G., Arribas-Bosacoma, R., Kozlowski, M., Hassa, P.O., Hassler, M., Ladurner, A.G., Pearl, L.H., and Oliver, A.W. (2012). The zinc-finger domains of PARP1 cooperate to recognize DNA strand breaks. Nat Struct Mol Biol *19*, 685-692.

Allen, M.D., Buckle, A.M., Cordell, S.C., Lowe, J., and Bycroft, M. (2003). The crystal structure of AF1521 a protein from Archaeoglobus fulgidus with homology to the non-histone domain of macroH2A. J Mol Biol *330*, 503-511.

Allinson, S.L., Dianova, II, and Dianov, G.L. (2003). Poly(ADP-ribose) polymerase in base excision repair: always engaged, but not essential for DNA damage processing. Acta Biochim Pol *50*, 169-179.

Althaus, F.R., Kleczkowska, H.E., Malanga, M., Muntener, C.R., Pleschke, J.M., Ebner, M., and Auer, B. (1999). Poly ADP-ribosylation: a DNA break signal mechanism. Mol Cell Biochem *193*, 5-11.

Althaus, F.R., and Richter, C. (1987). ADP-ribosylation of proteins. Enzymology and biological significance. Mol Biol Biochem Biophys *37*, 1-237.

Altmeyer, M., Messner, S., Hassa, P.O., Fey, M., and Hottiger, M.O. (2009). Molecular mechanism of poly(ADP-ribosyl)ation by PARP1 and identification of lysine residues as ADP-ribose acceptor sites. Nucleic Acids Res *37*, 3723-3738.

Aly, A., and Ganesan, S. (2011). BRCA1, PARP, and 53BP1: conditional synthetic lethality and synthetic viability. J Mol Cell Biol *3*, 66-74.

Amelio, A.L., Miraglia, L.J., Conkright, J.J., Mercer, B.A., Batalov, S., Cavett, V., Orth, A.P., Busby, J., Hogenesch, J.B., and Conkright, M.D. (2007). A coactivator trap identifies NONO (p54nrb) as a component of the cAMP-signaling pathway. Proc Natl Acad Sci U S A *104*, 20314-20319.

Andersen, J.S., Lyon, C.E., Fox, A.H., Leung, A.K., Lam, Y.W., Steen, H., Mann, M., and Lamond, A.I. (2002). Directed proteomic analysis of the human nucleolus. Curr Biol *12*, 1-11.

Anderson, C.W., and Lees-Miller, S.P. (1992). The nuclear serine/threonine protein kinase DNA-PK. Crit Rev Eukaryot Gene Expr *2*, 283-314.

Andrabi, S.A., Kim, N.S., Yu, S.W., Wang, H., Koh, D.W., Sasaki, M., Klaus, J.A., Otsuka, T., Zhang, Z., Koehler, R.C.*, et al.* (2006). Poly(ADP-ribose) (PAR) polymer is a death signal. Proc Natl Acad Sci U S A *103*, 18308-18313.

Aravind, L. (2001). The WWE domain: a common interaction module in protein ubiquitination and ADP ribosylation. Trends Biochem Sci *26*, 273-275.

Ariumi, Y., Masutani, M., Copeland, T.D., Mimori, T., Sugimura, T., Shimotohno, K., Ueda, K., Hatanaka, M., and Noda, M. (1999). Suppression of the poly(ADP-ribose) polymerase activity by DNA-dependent protein kinase in vitro. Oncogene *18*, 4616-4625.

Artus, C., Boujrad, H., Bouharrour, A., Brunelle, M.N., Hoos, S., Yuste, V.J., Lenormand, P., Rousselle, J.C., Namane, A., England, P.*, et al.* (2010). AIF promotes chromatinolysis and caspase-independent programmed necrosis by interacting with histone H2AX. EMBO J *29*, 1585-1599.

Audebert, M., Salles, B., and Calsou, P. (2004). Involvement of poly(ADP-ribose) polymerase-1 and XRCC1/DNA ligase III in an alternative route for DNA double-strand breaks rejoining. J Biol Chem *279*, 55117-55126.

Bakkenist, C.J., and Kastan, M.B. (2003). DNA damage activates ATM through intermolecular autophosphorylation and dimer dissociation. Nature *421*, 499-506.

Banath, J.P., Klokov, D., MacPhail, S.H., Banuelos, C.A., and Olive, P.L. (2010). Residual gammaH2AX foci as an indication of lethal DNA lesions. BMC Cancer *10*, 4.

Bannister, A.J., Gottlieb, T.M., Kouzarides, T., and Jackson, S.P. (1993). c-Jun is phosphorylated by the DNA-dependent protein kinase in vitro; definition of the minimal kinase recognition motif. Nucleic Acids Res *21*, 1289-1295.

Barlow, C., Hirotsune, S., Paylor, R., Liyanage, M., Eckhaus, M., Collins, F., Shiloh, Y., Crawley, J.N., Ried, T., Tagle, D.*, et al.* (1996). Atm-deficient mice: a paradigm of ataxia telangiectasia. Cell *86*, 159-171.

Bartek, J., and Lukas, J. (2007). DNA damage checkpoints: from initiation to recovery or adaptation. Curr Opin Cell Biol *19*, 238-245.

Bassing, C.H., Suh, H., Ferguson, D.O., Chua, K.F., Manis, J., Eckersdorff, M., Gleason, M., Bronson, R., Lee, C., and Alt, F.W. (2003). Histone H2AX: a dosage-dependent suppressor of oncogenic translocations and tumors. Cell *114*, 359-370.

Baumann, P., and West, S.C. (1998). DNA end-joining catalyzed by human cell-free extracts. Proc Natl Acad Sci U S A *95*, 14066-14070.

Beck, B.D., Hah, D.S., and Lee, S.H. (2008). XPB and XPD between transcription and DNA repair. Adv Exp Med Biol *637*, 39-46.

Bekker-Jensen, S., and Mailand, N. (2010). Assembly and function of DNA double-strand break repair foci in mammalian cells. DNA Repair (Amst) *9*, 1219-1228.

Beli, P., Lukashchuk, N., Wagner, S.A., Weinert, B.T., Olsen, J.V., Baskcomb, L., Mann, M., Jackson, S.P., and Choudhary, C. (2012). Proteomic investigations reveal a role for RNA processing factor THRAP3 in the DNA damage response. Mol Cell *46*, 212-225.

Benjamin, R.C., and Gill, D.M. (1980). ADP-ribosylation in mammalian cell ghosts. Dependence of poly(ADP-ribose) synthesis on strand breakage in DNA. J Biol Chem *255*, 10493-10501.

Birney, E., Kumar, S., and Krainer, A.R. (1993). Analysis of the RNA-recognition motif and RS and RGG domains: conservation in metazoan pre-mRNA splicing factors. Nucleic Acids Res *21*, 5803-5816.

Bladen, C.L., Udayakumar, D., Takeda, Y., and Dynan, W.S. (2005). Identification of the polypyrimidine tract binding protein-associated splicing factor.p54(nrb) complex as a candidate DNA double-strand break rejoining factor. J Biol Chem *280*, 5205-5210.

Blagoev, B., and Mann, M. (2006). Quantitative proteomics to study mitogen-activated protein kinases. Methods *40*, 243-250.

Bonilla, C.Y., Melo, J.A., and Toczyski, D.P. (2008). Colocalization of sensors is sufficient to activate the DNA damage checkpoint in the absence of damage. Mol Cell *30*, 267-276.

Bouchard, V.J., Rouleau, M., and Poirier, G.G. (2003). PARP-1, a determinant of cell survival in response to DNA damage. Exp Hematol *31*, 446-454.

Bryant, H.E., Petermann, E., Schultz, N., Jemth, A.S., Loseva, O., Issaeva, N., Johansson, F., Fernandez, S., McGlynn, P., and Helleday, T. (2009). PARP is activated at stalled forks to mediate Mre11-dependent replication restart and recombination. EMBO J *28*, 2601-2615.

Bryant, H.E., Schultz, N., Thomas, H.D., Parker, K.M., Flower, D., Lopez, E., Kyle, S., Meuth, M., Curtin, N.J., and Helleday, T. (2005). Specific killing of BRCA2-deficient tumours with inhibitors of poly(ADP-ribose) polymerase. Nature *434*, 913-917.

Caiafa, P., Guastafierro, T., and Zampieri, M. (2009). Epigenetics: poly(ADP-ribosyl)ation of PARP-1 regulates genomic methylation patterns. FASEB J *23*, 672-678.

Capp, J.P., Boudsocq, F., Bertrand, P., Laroche-Clary, A., Pourquier, P., Lopez, B.S., Cazaux, C., Hoffmann, J.S., and Canitrot, Y. (2006). The DNA polymerase lambda is required for the repair of non-compatible DNA double strand breaks by NHEJ in mammalian cells. Nucleic Acids Res *34*, 2998-3007.

Capp, J.P., Boudsocq, F., Besnard, A.G., Lopez, B.S., Cazaux, C., Hoffmann, J.S., and Canitrot, Y. (2007). Involvement of DNA polymerase mu in the repair of a specific subset of DNA double-strand breaks in mammalian cells. Nucleic Acids Res *35*, 3551-3560.

Celeste, A., Fernandez-Capetillo, O., Kruhlak, M.J., Pilch, D.R., Staudt, D.W., Lee, A., Bonner, R.F., Bonner, W.M., and Nussenzweig, A. (2003). Histone H2AX phosphorylation is dispensable for the initial recognition of DNA breaks. Nat Cell Biol *5*, 675-679.

Celeste, A., Petersen, S., Romanienko, P.J., Fernandez-Capetillo, O., Chen, H.T., Sedelnikova, O.A., Reina-San-Martin, B., Coppola, V., Meffre, E., Difilippantonio, M.J.*, et al.* (2002). Genomic instability in mice lacking histone H2AX. Science *296*, 922-927.

Chambon, P., Weill, J.D., and Mandel, P. (1963). Nicotinamide mononucleotide activation of new DNA-dependent polyadenylic acid synthesizing nuclear enzyme. Biochem Biophys Res Commun *11*, 39-43.

Chang, W., Dynek, J.N., and Smith, S. (2005). NuMA is a major acceptor of poly(ADP-ribosyl)ation by tankyrase 1 in mitosis. Biochem J *391*, 177-184.

Chapman, J.D., Gagne, J.P., Poirier, G.G., and Goodlett, D.R. (2013a). Mapping PARP-1 Auto-ADP-ribosylation Sites by Liquid Chromatography-Tandem Mass Spectrometry. J Proteome Res.

Chapman, J.R., Barral, P., Vannier, J.B., Borel, V., Steger, M., Tomas-Loba, A., Sartori, A.A., Adams, I.R., Batista, F.D., and Boulton, S.J. (2013b). RIF1 is essential for 53BP1-dependent nonhomologous end joining and suppression of DNA double-strand break resection. Mol Cell *49*, 858-871.

Chen, H., Lisby, M., and Symington, L.S. (2013). RPA coordinates DNA end resection and prevents formation of DNA hairpins. Mol Cell *50*, 589-600.

Chou, D.M., Adamson, B., Dephoure, N.E., Tan, X., Nottke, A.C., Hurov, K.E., Gygi, S.P., Colaiacovo, M.P., and Elledge, S.J. (2010). A chromatin localization screen reveals poly (ADP ribose)-regulated recruitment of the repressive polycomb and NuRD complexes to sites of DNA damage. Proc Natl Acad Sci U S A *107*, 18475-18480.

Ciccia, A., and Elledge, S.J. (2010). The DNA damage response: making it safe to play with knives. Mol Cell *40*, 179-204.

Claybon, A., Karia, B., Bruce, C., and Bishop, A.J. (2010). PARP1 suppresses homologous recombination events in mice in vivo. Nucleic Acids Res *38*, 7538-7545.

Clery, A., Blatter, M., and Allain, F.H. (2008). RNA recognition motifs: boring? Not quite. Curr Opin Struct Biol *18*, 290-298.

Cole, F., Keeney, S., and Jasin, M. (2010). Evolutionary conservation of meiotic DSB proteins: more than just Spo11. Genes Dev *24*, 1201-1207.

Compe, E., and Egly, J.M. (2012). TFIIH: when transcription met DNA repair. Nat Rev Mol Cell Biol *13*, 343-354.

Cortes, U., Tong, W.M., Coyle, D.L., Meyer-Ficca, M.L., Meyer, R.G., Petrilli, V., Herceg, Z., Jacobson, E.L., Jacobson, M.K., and Wang, Z.Q. (2004). Depletion of the 110-kilodalton isoform of poly(ADP-ribose) glycohydrolase increases sensitivity to genotoxic and endotoxic stress in mice. Mol Cell Biol *24*, 7163-7178.

Couto, C.A., Wang, H.Y., Green, J.C., Kiely, R., Siddaway, R., Borer, C., Pears, C.J., and Lakin, N.D. (2011). PARP regulates nonhomologous end joining through retention of Ku at double-strand breaks. J Cell Biol *194*, 367-375.

Covo, S., Blanco, L., and Livneh, Z. (2004). Lesion bypass by human DNA polymerase mu reveals a template-dependent, sequence-independent nucleotidyl transferase activity. J Biol Chem *279*, 859-865.

D'Amours, D., Desnoyers, S., D'Silva, I., and Poirier, G.G. (1999). Poly(ADP-ribosyl)ation reactions in the regulation of nuclear functions. Biochem J *342 (Pt 2)*, 249-268.

D'Silva, I., Pelletier, J.D., Lagueux, J., D'Amours, D., Chaudhry, M.A., Weinfeld, M., Lees-Miller, S.P., and Poirier, G.G. (1999). Relative affinities of poly(ADP-ribose) polymerase and DNA-dependent protein kinase for DNA strand interruptions. Biochim Biophys Acta *1430*, 119-126.

Daley, J.M., Palmbos, P.L., Wu, D., and Wilson, T.E. (2005). Nonhomologous end joining in yeast. Annu Rev Genet *39*, 431-451.

Dani, N., Stilla, A., Marchegiani, A., Tamburro, A., Till, S., Ladurner, A.G., Corda, D., and Di Girolamo, M. (2009). Combining affinity purification by ADP-ribose-binding macro domains with

mass spectrometry to define the mammalian ADP-ribosyl proteome. Proc Natl Acad Sci U S A *106*, 4243-4248.

David, K.K., Andrabi, S.A., Dawson, T.M., and Dawson, V.L. (2009). Parthanatos, a messenger of death. Front Biosci *14*, 1116-1128.

De Lorenzo, S.B., Patel, A.G., Hurley, R.M., and Kaufmann, S.H. (2013). The Elephant and the Blind Men: Making Sense of PARP Inhibitors in Homologous Recombination Deficient Tumor Cells. Front Oncol *3*, 228.

de Murcia, J.M., Niedergang, C., Trucco, C., Ricoul, M., Dutrillaux, B., Mark, M., Oliver, F.J., Masson, M., Dierich, A., LeMeur, M.*, et al.* (1997). Requirement of poly(ADP-ribose) polymerase in recovery from DNA damage in mice and in cells. Proc Natl Acad Sci U S A *94*, 7303-7307.

Deshpande, R.A., and Wilson, T.E. (2007). Modes of interaction among yeast Nej1, Lif1 and Dnl4 proteins and comparison to human XLF, XRCC4 and Lig4. DNA Repair (Amst) *6*, 1507-1516.

Di Virgilio, M., Callen, E., Yamane, A., Zhang, W., Jankovic, M., Gitlin, A.D., Feldhahn, N., Resch, W., Oliveira, T.Y., Chait, B.T.*, et al.* (2013). Rif1 prevents resection of DNA breaks and promotes immunoglobulin class switching. Science *339*, 711-715.

Doil, C., Mailand, N., Bekker-Jensen, S., Menard, P., Larsen, D.H., Pepperkok, R., Ellenberg, J., Panier, S., Durocher, D., Bartek, J.*, et al.* (2009). RNF168 binds and amplifies ubiquitin conjugates on damaged chromosomes to allow accumulation of repair proteins. Cell *136*, 435-446.

Dong, B., Horowitz, D.S., Kobayashi, R., and Krainer, A.R. (1993). Purification and cDNA cloning of HeLa cell p54nrb, a nuclear protein with two RNA recognition motifs and extensive homology to human splicing factor PSF and Drosophila NONA/BJ6. Nucleic Acids Res *21*, 4085-4092.

Dong, X., Sweet, J., Challis, J.R., Brown, T., and Lye, S.J. (2007). Transcriptional activity of androgen receptor is modulated by two RNA splicing factors, PSF and p54nrb. Mol Cell Biol *27*, 4863-4875.

Dunstan, M.S., Barkauskaite, E., Lafite, P., Knezevic, C.E., Brassington, A., Ahel, M., Hergenrother, P.J., Leys, D., and Ahel, I. (2012). Structure and mechanism of a canonical poly(ADP-ribose) glycohydrolase. Nat Commun *3*, 878.

Durkacz, B.W., Omidiji, O., Gray, D.A., and Shall, S. (1980). (ADP-ribose)n participates in DNA excision repair. Nature *283*, 593-596.

Egloff, M.P., Malet, H., Putics, A., Heinonen, M., Dutartre, H., Frangeul, A., Gruez, A., Campanacci, V., Cambillau, C., Ziebuhr, J.*, et al.* (2006). Structural and functional basis for ADP-ribose and poly(ADP-ribose) binding by viral macro domains. J Virol *80*, 8493-8502.

Eki, T., and Hurwitz, J. (1991). Influence of poly(ADP-ribose) polymerase on the enzymatic synthesis of SV40 DNA. J Biol Chem *266*, 3087-3100.

El-Khamisy, S.F., Masutani, M., Suzuki, H., and Caldecott, K.W. (2003). A requirement for PARP-1 for the assembly or stability of XRCC1 nuclear foci at sites of oxidative DNA damage. Nucleic Acids Res *31*, 5526-5533.

Escribano-Diaz, C., Orthwein, A., Fradet-Turcotte, A., Xing, M., Young, J.T., Tkac, J., Cook, M.A., Rosebrock, A.P., Munro, M., Canny, M.D.*, et al.* (2013). A cell cycle-dependent regulatory circuit composed of 53BP1-RIF1 and BRCA1-CtIP controls DNA repair pathway choice. Mol Cell *49*, 872-883.

Ethier, C., Tardif, M., Arul, L., and Poirier, G.G. (2012). PARP-1 modulation of mTOR signaling in response to a DNA alkylating agent. PLoS One *7*, e47978.

Eustermann, S., Brockmann, C., Mehrotra, P.V., Yang, J.C., Loakes, D., West, S.C., Ahel, I., and Neuhaus, D. (2010). Solution structures of the two PBZ domains from human APLF and their interaction with poly(ADP-ribose). Nat Struct Mol Biol *17*, 241-243.

Eustermann, S., Videler, H., Yang, J.C., Cole, P.T., Gruszka, D., Veprintsev, D., and Neuhaus, D. (2011). The DNA-binding domain of human PARP-1 interacts with DNA single-strand breaks as a monomer through its second zinc finger. J Mol Biol *407*, 149-170.

Fahrer, J., Kranaster, R., Altmeyer, M., Marx, A., and Burkle, A. (2007). Quantitative analysis of the binding affinity of poly(ADP-ribose) to specific binding proteins as a function of chain length. Nucleic Acids Res *35*, e143.

Fahrer, J., Popp, O., Malanga, M., Beneke, S., Markovitz, D.M., Ferrando-May, E., Burkle, A., and Kappes, F. (2010). High-affinity interaction of poly(ADP-ribose) and the human DEK oncoprotein depends upon chain length. Biochemistry *49*, 7119-7130.

Farmer, H., McCabe, N., Lord, C.J., Tutt, A.N., Johnson, D.A., Richardson, T.B., Santarosa, M., Dillon, K.J., Hickson, I., Knights, C.*, et al.* (2005). Targeting the DNA repair defect in BRCA mutant cells as a therapeutic strategy. Nature *434*, 917-921.

Ferguson, D.O., and Alt, F.W. (2001). DNA double strand break repair and chromosomal translocation: lessons from animal models. Oncogene *20*, 5572-5579.

Fradet-Turcotte, A., Canny, M.D., Escribano-Diaz, C., Orthwein, A., Leung, C.C., Huang, H., Landry, M.C., Kitevski-LeBlanc, J., Noordermeer, S.M., Sicheri, F.*, et al.* (2013). 53BP1 is a reader of the DNA-damage-induced H2A Lys 15 ubiquitin mark. Nature *499*, 50-54.

Francia, S., Michelini, F., Saxena, A., Tang, D., de Hoon, M., Anelli, V., Mione, M., Carninci, P., and d'Adda di Fagagna, F. (2012). Site-specific DICER and DROSHA RNA products control the DNA-damage response. Nature *488*, 231-235.

Gagne, J.P., Haince, J.F., Pic, E., and Poirier, G.G. (2011). Affinity-based assays for the identification and quantitative evaluation of noncovalent poly(ADP-ribose)-binding proteins. Methods Mol Biol *780*, 93-115.

Gagne, J.P., Hendzel, M.J., Droit, A., and Poirier, G.G. (2006). The expanding role of poly(ADP-ribose) metabolism: current challenges and new perspectives. Curr Opin Cell Biol *18*, 145-151.

Gagne, J.P., Hunter, J.M., Labrecque, B., Chabot, B., and Poirier, G.G. (2003). A proteomic approach to the identification of heterogeneous nuclear ribonucleoproteins as a new family of poly(ADP-ribose)-binding proteins. Biochem J *371*, 331-340.

Gagne, J.P., Isabelle, M., Lo, K.S., Bourassa, S., Hendzel, M.J., Dawson, V.L., Dawson, T.M., and Poirier, G.G. (2008). Proteome-wide identification of poly(ADP-ribose) binding proteins and poly(ADP-ribose)-associated protein complexes. Nucleic Acids Res *36*, 6959-6976.

Gagne, J.P., Moreel, X., Gagne, P., Labelle, Y., Droit, A., Chevalier-Pare, M., Bourassa, S., McDonald, D., Hendzel, M.J., Prigent, C.*, et al.* (2009). Proteomic investigation of phosphorylation sites in poly(ADP-ribose) polymerase-1 and poly(ADP-ribose) glycohydrolase. J Proteome Res *8*, 1014-1029.

Gagne, J.P., Pic, E., Isabelle, M., Krietsch, J., Ethier, C., Paquet, E., Kelly, I., Boutin, M., Moon, K.M., Foster, L.J.*, et al.* (2012). Quantitative proteomics profiling of the poly(ADP-ribose)-related response to genotoxic stress. Nucleic Acids Res *40*, 7788-7805.

Galande, S., and Kohwi-Shigematsu, T. (1999). Poly(ADP-ribose) polymerase and Ku autoantigen form a complex and synergistically bind to matrix attachment sequences. J Biol Chem *274*, 20521-20528.

Gao, H., Coyle, D.L., Meyer-Ficca, M.L., Meyer, R.G., Jacobson, E.L., Wang, Z.Q., and Jacobson, M.K. (2007). Altered poly(ADP-ribose) metabolism impairs cellular responses to genotoxic stress in a hypomorphic mutant of poly(ADP-ribose) glycohydrolase. Exp Cell Res *313*, 984-996.

Gao, J., Ade, A.S., Tarcea, V.G., Weymouth, T.E., Mirel, B.R., Jagadish, H.V., and States, D.J. (2009). Integrating and annotating the interactome using the MiMI plugin for cytoscape. Bioinformatics *25*, 137-138.

Garber, K. (2013). PARP inhibitors bounce back. Nat Rev Drug Discov *12*, 725-727.

Gieni, R.S., Ismail, I.H., Campbell, S., and Hendzel, M.J. (2011). Polycomb group proteins in the DNA damage response: a link between radiation resistance and "stemness". Cell Cycle *10*, 883-894.

Giffin, W., Torrance, H., Rodda, D.J., Prefontaine, G.G., Pope, L., and Hache, R.J. (1996). Sequence-specific DNA binding by Ku autoantigen and its effects on transcription. Nature *380*, 265-268.

Gil, A., Sharp, P.A., Jamison, S.F., and Garcia-Blanco, M.A. (1991). Characterization of cDNAs encoding the polypyrimidine tract-binding protein. Genes Dev *5*, 1224-1236.

Gottlieb, T.M., and Jackson, S.P. (1994). Protein kinases and DNA damage. Trends Biochem Sci *19*, 500-503.

Gottschalk, A.J., Timinszky, G., Kong, S.E., Jin, J., Cai, Y., Swanson, S.K., Washburn, M.P., Florens, L., Ladurner, A.G., Conaway, J.W., *et al.* (2009). Poly(ADP-ribosyl)ation directs recruitment and activation of an ATP-dependent chromatin remodeler. Proc Natl Acad Sci U S A *106*, 13770-13774.

Gu, J., Li, S., Zhang, X., Wang, L.C., Niewolik, D., Schwarz, K., Legerski, R.J., Zandi, E., and Lieber, M.R. (2010). DNA-PKcs regulates a single-stranded DNA endonuclease activity of Artemis. DNA Repair (Amst) *9*, 429-437.

Ha, K., Takeda, Y., and Dynan, W.S. (2011). Sequences in PSF/SFPQ mediate radioresistance and recruitment of PSF/SFPQ-containing complexes to DNA damage sites in human cells. DNA Repair (Amst) *10*, 252-259.

Haenni, S.S., Hassa, P.O., Altmeyer, M., Fey, M., Imhof, R., and Hottiger, M.O. (2008). Identification of lysines 36 and 37 of PARP-2 as targets for acetylation and auto-ADP-ribosylation. Int J Biochem Cell Biol *40*, 2274-2283.

Haince, J.F., McDonald, D., Rodrigue, A., Dery, U., Masson, J.Y., Hendzel, M.J., and Poirier, G.G. (2008). PARP1-dependent kinetics of recruitment of MRE11 and NBS1 proteins to multiple DNA damage sites. J Biol Chem *283*, 1197-1208.

Haince, J.F., Ouellet, M.E., McDonald, D., Hendzel, M.J., and Poirier, G.G. (2006). Dynamic relocation of poly(ADP-ribose) glycohydrolase isoforms during radiation-induced DNA damage. Biochim Biophys Acta *1763*, 226-237.

Hamimes, S., Bourgeon, D., Stasiak, A.Z., Stasiak, A., and Van Dyck, E. (2006). Nucleic acid-binding properties of the RRM-containing protein RDM1. Biochem Biophys Res Commun *344*, 87-94.

Hanahan, D., and Weinberg, R.A. (2000). The hallmarks of cancer. Cell *100*, 57-70.

Hanawalt, P.C., and Spivak, G. (2008). Transcription-coupled DNA repair: two decades of progress and surprises. Nat Rev Mol Cell Biol *9*, 958-970.

Hardie, D.G. (2007). AMP-activated/SNF1 protein kinases: conserved guardians of cellular energy. Nat Rev Mol Cell Biol *8*, 774-785.

Haring, S.J., Mason, A.C., Binz, S.K., and Wold, M.S. (2008). Cellular functions of human RPA1. Multiple roles of domains in replication, repair, and checkpoints. J Biol Chem *283*, 19095-19111.

Harper, J.W., and Elledge, S.J. (2007). The DNA damage response: ten years after. Mol Cell *28*, 739-745.

Harris, J.L., Jakob, B., Taucher-Scholz, G., Dianov, G.L., Becherel, O.J., and Lavin, M.F. (2009). Aprataxin, poly-ADP ribose polymerase 1 (PARP-1) and apurinic endonuclease 1 (APE1) function together to protect the genome against oxidative damage. Hum Mol Genet *18*, 4102-4117.

Harsha, H.C., Molina, H., and Pandey, A. (2008). Quantitative proteomics using stable isotope labeling with amino acids in cell culture. Nat Protoc *3*, 505-516.

Hass, C.S., Lam, K., and Wold, M.S. (2012). Repair-specific functions of replication protein A. J Biol Chem *287*, 3908-3918.

Hassa, P.O., Haenni, S.S., Buerki, C., Meier, N.I., Lane, W.S., Owen, H., Gersbach, M., Imhof, R., and Hottiger, M.O. (2005). Acetylation of poly(ADP-ribose) polymerase-1 by p300/CREB-binding protein regulates coactivation of NF-kappaB-dependent transcription. J Biol Chem *280*, 40450-40464.

Hassa, P.O., Haenni, S.S., Elser, M., and Hottiger, M.O. (2006). Nuclear ADP-ribosylation reactions in mammalian cells: where are we today and where are we going? Microbiol Mol Biol Rev *70*, 789-829.

Hassa, P.O., and Hottiger, M.O. (2008). The diverse biological roles of mammalian PARPS, a small but powerful family of poly-ADP-ribose polymerases. Front Biosci *13*, 3046-3082.

Hassler, M., Jankevicius, G., and Ladurner, A.G. (2011). PARG: a macrodomain in disguise. Structure *19*, 1351-1353.

Hassler, M., and Ladurner, A.G. (2012). Towards a structural understanding of PARP1 activation and related signalling ADP-ribosyl-transferases. Curr Opin Struct Biol *22*, 721-729.

Heeres, J.T., and Hergenrother, P.J. (2007). Poly(ADP-ribose) makes a date with death. Curr Opin Chem Biol *11*, 644-653.

Hennig, C. (2010). fpc: Flexible procedures for clustering, Rpackage version 2.0-2. http://CRAN.R-project.org/package=fpc.

Hoeijmakers, J.H. (2001). Genome maintenance mechanisms for preventing cancer. Nature *411*, 366-374.

Hoeijmakers, J.H. (2009). DNA damage, aging, and cancer. N Engl J Med *361*, 1475-1485.

Hong, Z., Jiang, J., Ma, J., Dai, S., Xu, T., Li, H., and Yasui, A. (2013). The role of hnRPUL1 involved in DNA damage response is related to PARP1. PLoS One *8*, e60208.

Honjo, T., Nishizuka, Y., and Hayaishi, O. (1968). Diphtheria toxin-dependent adenosine diphosphate ribosylation of aminoacyl transferase II and inhibition of protein synthesis. J Biol Chem *243*, 3553-3555.

Hottiger, M.O., Hassa, P.O., Luscher, B., Schuler, H., and Koch-Nolte, F. (2010). Toward a unified nomenclature for mammalian ADP-ribosyltransferases. Trends Biochem Sci *35*, 208-219.

Huang da, W., Sherman, B.T., and Lempicki, R.A. (2009). Systematic and integrative analysis of large gene lists using DAVID bioinformatics resources. Nat Protoc *4*, 44-57.

Huang, J.Y., Chen, W.H., Chang, Y.L., Wang, H.T., Chuang, W.T., and Lee, S.C. (2006). Modulation of nucleosome-binding activity of FACT by poly(ADP-ribosyl)ation. Nucleic Acids Res *34*, 2398-2407.

Huang, Q., Wu, Y.T., Tan, H.L., Ong, C.N., and Shen, H.M. (2009). A novel function of poly(ADP-ribose) polymerase-1 in modulation of autophagy and necrosis under oxidative stress. Cell Death Differ *16*, 264-277.

Huen, M.S., Grant, R., Manke, I., Minn, K., Yu, X., Yaffe, M.B., and Chen, J. (2007). RNF8 transduces the DNA-damage signal via histone ubiquitylation and checkpoint protein assembly. Cell *131*, 901-914.

Isabelle, M., Gagne, J.P., Gallouzi, I.E., and Poirier, G.G. (2012). Quantitative proteomics and dynamic imaging reveal that G3BP-mediated stress granule assembly is poly(ADP-ribose)-dependent following exposure to MNNG-induced DNA alkylation. J Cell Sci *125*, 4555-4566.

Isabelle, M., Moreel, X., Gagne, J.P., Rouleau, M., Ethier, C., Gagne, P., Hendzel, M.J., and Poirier, G.G. (2010). Investigation of PARP-1, PARP-2, and PARG interactomes by affinity-purification mass spectrometry. Proteome Sci *8*, 22.

Ishitani, K., Yoshida, T., Kitagawa, H., Ohta, H., Nozawa, S., and Kato, S. (2003). p54nrb acts as a transcriptional coactivator for activation function 1 of the human androgen receptor. Biochem Biophys Res Commun *306*, 660-665.

Ismail, I.H., Gagne, J.P., Caron, M.C., McDonald, D., Xu, Z., Masson, J.Y., Poirier, G.G., and Hendzel, M.J. (2012). CBX4-mediated SUMO modification regulates BMI1 recruitment at sites of DNA damage. Nucleic Acids Res *40*, 5497-5510.

Jankevicius, G., Hassler, M., Golia, B., Rybin, V., Zacharias, M., Timinszky, G., and Ladurner, A.G. (2013). A family of macrodomain proteins reverses cellular mono-ADP-ribosylation. Nat Struct Mol Biol *20*, 508-514.

Ji, Y. (2011). Noncovalent pADPr interaction with proteins and competition with RNA for binding to proteins. Methods Mol Biol *780*, 83-91.

Ji, Y., and Tulin, A.V. (2009). Poly(ADP-ribosyl)ation of heterogeneous nuclear ribonucleoproteins modulates splicing. Nucleic Acids Res *37*, 3501-3513.

Jungmichel, S., Rosenthal, F., Altmeyer, M., Lukas, J., Hottiger, M.O., and Nielsen, M.L. (2013). Proteome-wide Identification of Poly(ADP-Ribosyl)ation Targets in Different Genotoxic Stress Responses. Mol Cell.

Jurica, M.S., Licklider, L.J., Gygi, S.R., Grigorieff, N., and Moore, M.J. (2002). Purification and characterization of native spliceosomes suitable for three-dimensional structural analysis. RNA *8*, 426-439.

Kakarougkas, A., Ismail, A., Katsuki, Y., Freire, R., Shibata, A., and Jeggo, P.A. (2013). Co-operation of BRCA1 and POH1 relieves the barriers posed by 53BP1 and RAP80 to resection. Nucleic Acids Res.

Kamileri, I., Karakasilioti, I., and Garinis, G.A. (2012). Nucleotide excision repair: new tricks with old bricks. Trends Genet *28*, 566-573.

Kanai, M., Hanashiro, K., Kim, S.H., Hanai, S., Boulares, A.H., Miwa, M., and Fukasawa, K. (2007). Inhibition of Crm1-p53 interaction and nuclear export of p53 by poly(ADP-ribosyl)ation. Nat Cell Biol *9*, 1175-1183.

Kaneko, S., Rozenblatt-Rosen, O., Meyerson, M., and Manley, J.L. (2007). The multifunctional protein p54nrb/PSF recruits the exonuclease XRN2 to facilitate pre-mRNA 3' processing and transcription termination. Genes Dev *21*, 1779-1789.

Karras, G.I., Kustatscher, G., Buhecha, H.R., Allen, M.D., Pugieux, C., Sait, F., Bycroft, M., and Ladurner, A.G. (2005). The macro domain is an ADP-ribose binding module. EMBO J *24*, 1911-1920.

Kass, E.M., Moynahan, M.E., and Jasin, M. (2010). Loss of 53BP1 is a gain for BRCA1 mutant cells. Cancer Cell *17*, 423-425.

Kauppinen, T.M., Chan, W.Y., Suh, S.W., Wiggins, A.K., Huang, E.J., and Swanson, R.A. (2006). Direct phosphorylation and regulation of poly(ADP-ribose) polymerase-1 by extracellular signal-regulated kinases 1/2. Proc Natl Acad Sci U S A *103*, 7136-7141.

Kawamitsu, H., Hoshino, H., Okada, H., Miwa, M., Momoi, H., and Sugimura, T. (1984). Monoclonal antibodies to poly(adenosine diphosphate ribose) recognize different structures. Biochemistry *23*, 3771-3777.

Kawanishi, S., Hiraku, Y., Pinlaor, S., and Ma, N. (2006). Oxidative and nitrative DNA damage in animals and patients with inflammatory diseases in relation to inflammation-related carcinogenesis. Biol Chem *387*, 365-372.

Kenan, D.J., Query, C.C., and Keene, J.D. (1991). RNA recognition: towards identifying determinants of specificity. Trends Biochem Sci *16*, 214-220.

Kickhoefer, V.A., Siva, A.C., Kedersha, N.L., Inman, E.M., Ruland, C., Streuli, M., and Rome, L.H. (1999). The 193-kD vault protein, VPARP, is a novel poly(ADP-ribose) polymerase. J Cell Biol *146*, 917-928.

Kiehlbauch, C.C., Aboul-Ela, N., Jacobson, E.L., Ringer, D.P., and Jacobson, M.K. (1993). High resolution fractionation and characterization of ADP-ribose polymers. Anal Biochem *208*, 26-34.

Kim, I.K., Kiefer, J.R., Ho, C.M., Stegeman, R.A., Classen, S., Tainer, J.A., and Ellenberger, T. (2012). Structure of mammalian poly(ADP-ribose) glycohydrolase reveals a flexible tyrosine clasp as a substrate-binding element. Nat Struct Mol Biol *19*, 653-656.

Kim, M.Y., Zhang, T., and Kraus, W.L. (2005). Poly(ADP-ribosyl)ation by PARP-1: 'PAR-laying' NAD+ into a nuclear signal. Genes Dev *19*, 1951-1967.

Kim, S.T., Lim, D.S., Canman, C.E., and Kastan, M.B. (1999). Substrate specificities and identification of putative substrates of ATM kinase family members. J Biol Chem *274*, 37538-37543.

King, B.S., Cooper, K.L., Liu, K.J., and Hudson, L.G. (2012). Poly(ADP-ribose) contributes to an association between poly(ADP-ribose) polymerase-1 and xeroderma pigmentosum complementation group A in nucleotide excision repair. J Biol Chem *287*, 39824-39833.

Kleine, H., and Luscher, B. (2009). Learning how to read ADP-ribosylation. Cell *139*, 17-19.

Koh, D.W., Lawler, A.M., Poitras, M.F., Sasaki, M., Wattler, S., Nehls, M.C., Stoger, T., Poirier, G.G., Dawson, V.L., and Dawson, T.M. (2004). Failure to degrade poly(ADP-ribose) causes increased sensitivity to cytotoxicity and early embryonic lethality. Proc Natl Acad Sci U S A *101*, 17699-17704.

Kolas, N.K., Chapman, J.R., Nakada, S., Ylanko, J., Chahwan, R., Sweeney, F.D., Panier, S., Mendez, M., Wildenhain, J., Thomson, T.M.*, et al.* (2007). Orchestration of the DNA-damage response by the RNF8 ubiquitin ligase. Science *318*, 1637-1640.

Kraus, W.L. (2008). Transcriptional control by PARP-1: chromatin modulation, enhancer-binding, coregulation, and insulation. Curr Opin Cell Biol *20*, 294-302.

Krejci, L., Altmannova, V., Spirek, M., and Zhao, X. (2012). Homologous recombination and its regulation. Nucleic Acids Res *40*, 5795-5818.

Krietsch, J., Caron, M.C., Gagne, J.P., Ethier, C., Vignard, J., Vincent, M., Rouleau, M., Hendzel, M.J., Poirier, G.G., and Masson, J.Y. (2012). PARP activation regulates the RNA-binding protein NONO in the DNA damage response to DNA double-strand breaks. Nucleic Acids Res *40*, 10287-10301.

Krietsch, J., Rouleau, M., Pic, E., Ethier, C., Dawson, T.M., Dawson, V.L., Masson, J.Y., Poirier, G.G., and Gagne, J.P. (2013). Reprogramming cellular events by poly(ADP-ribose)-binding proteins. Mol Aspects Med *34*, 1066-1087.

Krishnakumar, R., Gamble, M.J., Frizzell, K.M., Berrocal, J.G., Kininis, M., and Kraus, W.L. (2008). Reciprocal binding of PARP-1 and histone H1 at promoters specifies transcriptional outcomes. Science *319*, 819-821.

Krishnakumar, R., and Kraus, W.L. (2010a). PARP-1 regulates chromatin structure and transcription through a KDM5B-dependent pathway. Mol Cell *39*, 736-749.

Krishnakumar, R., and Kraus, W.L. (2010b). The PARP side of the nucleus: molecular actions, physiological outcomes, and clinical targets. Mol Cell *39*, 8-24.

Kuwahara, S., Ikei, A., Taguchi, Y., Tabuchi, Y., Fujimoto, N., Obinata, M., Uesugi, S., and Kurihara, Y. (2006). PSPC1, NONO, and SFPQ are expressed in mouse Sertoli cells and may function as coregulators of androgen receptor-mediated transcription. Biol Reprod *75*, 352-359.

Langelier, M.F., and Pascal, J.M. (2013). PARP-1 mechanism for coupling DNA damage detection to poly(ADP-ribose) synthesis. Curr Opin Struct Biol *23*, 134-143.

Langelier, M.F., Planck, J.L., Roy, S., and Pascal, J.M. (2011). Crystal structures of poly(ADP-ribose) polymerase-1 (PARP-1) zinc fingers bound to DNA: structural and functional insights into DNA-dependent PARP-1 activity. J Biol Chem *286*, 10690-10701.

Langelier, M.F., Planck, J.L., Roy, S., and Pascal, J.M. (2012). Structural basis for DNA damage-dependent poly(ADP-ribosyl)ation by human PARP-1. Science *336*, 728-732.

Langelier, M.F., Ruhl, D.D., Planck, J.L., Kraus, W.L., and Pascal, J.M. (2010). The Zn3 domain of human poly(ADP-ribose) polymerase-1 (PARP-1) functions in both DNA-dependent poly(ADP-ribose) synthesis activity and chromatin compaction. J Biol Chem *285*, 18877-18887.

Langelier, M.F., Servent, K.M., Rogers, E.E., and Pascal, J.M. (2008). A third zinc-binding domain of human poly(ADP-ribose) polymerase-1 coordinates DNA-dependent enzyme activation. J Biol Chem *283*, 4105-4114.

Leppard, J.B., Dong, Z., Mackey, Z.B., and Tomkinson, A.E. (2003). Physical and functional interaction between DNA ligase IIIalpha and poly(ADP-Ribose) polymerase 1 in DNA single-strand break repair. Mol Cell Biol *23*, 5919-5927.

Li, B., Navarro, S., Kasahara, N., and Comai, L. (2004). Identification and biochemical characterization of a Werner's syndrome protein complex with Ku70/80 and poly(ADP-ribose) polymerase-1. J Biol Chem *279*, 13659-13667.

Li, G.Y., McCulloch, R.D., Fenton, A.L., Cheung, M., Meng, L., Ikura, M., and Koch, C.A. (2010). Structure and identification of ADP-ribose recognition motifs of APLF and role in the DNA damage response. Proc Natl Acad Sci U S A *107*, 9129-9134.

Li, M., Lu, L.Y., Yang, C.Y., Wang, S., and Yu, X. (2013). The FHA and BRCT domains recognize ADP-ribosylation during DNA damage response. Genes Dev *27*, 1752-1768.

Li, M., and Yu, X. (2013). Function of BRCA1 in the DNA damage response is mediated by ADP-ribosylation. Cancer Cell *23*, 693-704.

Li, S., Kuhne, W.W., Kulharya, A., Hudson, F.Z., Ha, K., Cao, Z., and Dynan, W.S. (2009). Involvement of p54(nrb), a PSF partner protein, in DNA double-strand break repair and radioresistance. Nucleic Acids Res *37*, 6746-6753.

Lieber, M.R. (2010). The mechanism of double-strand DNA break repair by the nonhomologous DNA end-joining pathway. Annu Rev Biochem *79*, 181-211.

Lieber, M.R., and Wilson, T.E. (2010). SnapShot: Nonhomologous DNA end joining (NHEJ). Cell *142*, 496-496 e491.

Lim, D.S., and Hasty, P. (1996). A mutation in mouse rad51 results in an early embryonic lethal that is suppressed by a mutation in p53. Mol Cell Biol *16*, 7133-7143.

Lisby, M., Barlow, J.H., Burgess, R.C., and Rothstein, R. (2004). Choreography of the DNA damage response: spatiotemporal relationships among checkpoint and repair proteins. Cell *118*, 699-713.

Liu, Y., and Lu, X. (2012). Non-coding RNAs in DNA damage response. Am J Cancer Res *2*, 658-675.

Lou, Z., Minter-Dykhouse, K., Franco, S., Gostissa, M., Rivera, M.A., Celeste, A., Manis, J.P., van Deursen, J., Nussenzweig, A., Paull, T.T.*, et al.* (2006). MDC1 maintains genomic stability by participating in the amplification of ATM-dependent DNA damage signals. Mol Cell *21*, 187-200.

Luo, X., and Kraus, W.L. (2012). On PAR with PARP: cellular stress signaling through poly(ADP-ribose) and PARP-1. Genes Dev *26*, 417-432.

Maere, S., Heymans, K., and Kuiper, M. (2005). BiNGO: a Cytoscape plugin to assess overrepresentation of gene ontology categories in biological networks. Bioinformatics *21*, 3448-3449.

Mahaney, B.L., Meek, K., and Lees-Miller, S.P. (2009). Repair of ionizing radiation-induced DNA double-strand breaks by non-homologous end-joining. Biochem J *417*, 639-650.

Mailand, N., Bekker-Jensen, S., Faustrup, H., Melander, F., Bartek, J., Lukas, C., and Lukas, J. (2007). RNF8 ubiquitylates histones at DNA double-strand breaks and promotes assembly of repair proteins. Cell *131*, 887-900.

Malanga, M., and Althaus, F.R. (1994). Poly(ADP-ribose) molecules formed during DNA repair in vivo. J Biol Chem *269*, 17691-17696.

Malanga, M., and Althaus, F.R. (2004). Poly(ADP-ribose) reactivates stalled DNA topoisomerase I and Induces DNA strand break resealing. J Biol Chem *279*, 5244-5248.

Malanga, M., and Althaus, F.R. (2005). The role of poly(ADP-ribose) in the DNA damage signaling network. Biochem Cell Biol *83*, 354-364.

Malanga, M., and Althaus, F.R. (2011). Noncovalent protein interaction with poly(ADP-ribose). Methods Mol Biol *780*, 67-82.

Malanga, M., Czubaty, A., Girstun, A., Staron, K., and Althaus, F.R. (2008). Poly(ADP-ribose) binds to the splicing factor ASF/SF2 and regulates its phosphorylation by DNA topoisomerase I. J Biol Chem *283*, 19991-19998.

Mallick, P., and Kuster, B. (2010). Proteomics: a pragmatic perspective. Nat Biotechnol *28*, 695-709.

Mansour, W.Y., Rhein, T., and Dahm-Daphi, J. (2010). The alternative end-joining pathway for repair of DNA double-strand breaks requires PARP1 but is not dependent upon microhomologies. Nucleic Acids Res *38*, 6065-6077.

Maris, C., Dominguez, C., and Allain, F.H. (2005). The RNA recognition motif, a plastic RNA-binding platform to regulate post-transcriptional gene expression. FEBS J *272*, 2118-2131.

Martin, A., Ochagavia, M.E., Rabasa, L.C., Miranda, J., Fernandez-de-Cossio, J., and Bringas, R. (2010). BisoGenet: a new tool for gene network building, visualization and analysis. BMC Bioinformatics *11*, 91.

Masson, M., Niedergang, C., Schreiber, V., Muller, S., Menissier-de Murcia, J., and de Murcia, G. (1998). XRCC1 is specifically associated with poly(ADP-ribose) polymerase and negatively regulates its activity following DNA damage. Mol Cell Biol *18*, 3563-3571.

Mastrocola, A.S., Kim, S.H., Trinh, A.T., Rodenkirch, L.A., and Tibbetts, R.S. (2013). The RNA-binding protein fused in sarcoma (FUS) functions downstream of poly(ADP-ribose) polymerase (PARP) in response to DNA damage. J Biol Chem *288*, 24731-24741.

Masutani, M., Nozaki, T., Nishiyama, E., Shimokawa, T., Tachi, Y., Suzuki, H., Nakagama, H., Wakabayashi, K., and Sugimura, T. (1999). Function of poly(ADP-ribose) polymerase in response to DNA damage: gene-disruption study in mice. Mol Cell Biochem *193*, 149-152.

Mathis, G., and Althaus, F.R. (1987). Release of core DNA from nucleosomal core particles following (ADP-ribose)n-modification in vitro. Biochem Biophys Res Commun *143*, 1049-1054.

Mathur, M., Tucker, P.W., and Samuels, H.H. (2001). PSF is a novel corepressor that mediates its effect through Sin3A and the DNA binding domain of nuclear hormone receptors. Mol Cell Biol *21*, 2298-2311.

Meek, K., Dang, V., and Lees-Miller, S.P. (2008). DNA-PK: the means to justify the ends? Adv Immunol *99*, 33-58.

Mellon, I., Spivak, G., and Hanawalt, P.C. (1987). Selective removal of transcription-blocking DNA damage from the transcribed strand of the mammalian DHFR gene. Cell *51*, 241-249.

Mendes-Pereira, A.M., Martin, S.A., Brough, R., McCarthy, A., Taylor, J.R., Kim, J.S., Waldman, T., Lord, C.J., and Ashworth, A. (2009). Synthetic lethal targeting of PTEN mutant cells with PARP inhibitors. EMBO Mol Med *1*, 315-322.

Mendoza-Alvarez, H., and Alvarez-Gonzalez, R. (2001). Regulation of p53 sequence-specific DNA-binding by covalent poly(ADP-ribosyl)ation. J Biol Chem *276*, 36425-36430.

Menissier de Murcia, J., Ricoul, M., Tartier, L., Niedergang, C., Huber, A., Dantzer, F., Schreiber, V., Ame, J.C., Dierich, A., LeMeur, M.*, et al.* (2003). Functional interaction between PARP-1 and PARP-2 in chromosome stability and embryonic development in mouse. EMBO J *22*, 2255-2263.

Meyer-Ficca, M.L., Lonchar, J.D., Ihara, M., Meistrich, M.L., Austin, C.A., and Meyer, R.G. (2011). Poly(ADP-ribose) polymerases PARP1 and PARP2 modulate topoisomerase II beta (TOP2B) function during chromatin condensation in mouse spermiogenesis. Biol Reprod *84*, 900-909.

Meyer-Ficca, M.L., Meyer, R.G., Coyle, D.L., Jacobson, E.L., and Jacobson, M.K. (2004). Human poly(ADP-ribose) glycohydrolase is expressed in alternative splice variants yielding isoforms that localize to different cell compartments. Exp Cell Res *297*, 521-532.

Mimitou, E.P., and Symington, L.S. (2009). Nucleases and helicases take center stage in homologous recombination. Trends Biochem Sci *34*, 264-272.

Min, W., Cortes, U., Herceg, Z., Tong, W.M., and Wang, Z.Q. (2010). Deletion of the nuclear isoform of poly(ADP-ribose) glycohydrolase (PARG) reveals its function in DNA repair, genomic stability and tumorigenesis. Carcinogenesis *31*, 2058-2065.

Montes de Oca, R., Shoemaker, C.J., Gucek, M., Cole, R.N., and Wilson, K.L. (2009). Barrier-to-autointegration factor proteome reveals chromatin-regulatory partners. PLoS One *4*, e7050.

Morales, J.C., Xia, Z., Lu, T., Aldrich, M.B., Wang, B., Rosales, C., Kellems, R.E., Hittelman, W.N., Elledge, S.J., and Carpenter, P.B. (2003). Role for the BRCA1 C-terminal repeats (BRCT) protein 53BP1 in maintaining genomic stability. J Biol Chem *278*, 14971-14977.

Morozumi, Y., Takizawa, Y., Takaku, M., and Kurumizaka, H. (2009). Human PSF binds to RAD51 and modulates its homologous-pairing and strand-exchange activities. Nucleic Acids Res *37*, 4296-4307.

Mortusewicz, O., Ame, J.C., Schreiber, V., and Leonhardt, H. (2007). Feedback-regulated poly(ADP-ribosyl)ation by PARP-1 is required for rapid response to DNA damage in living cells. Nucleic Acids Res *35*, 7665-7675.

Moynahan, M.E., Chiu, J.W., Koller, B.H., and Jasin, M. (1999). Brca1 controls homology-directed DNA repair. Mol Cell *4*, 511-518.

Moynahan, M.E., and Jasin, M. (2010). Mitotic homologous recombination maintains genomic stability and suppresses tumorigenesis. Nat Rev Mol Cell Biol *11*, 196-207.

Munoz-Gamez, J.A., Martin-Oliva, D., Aguilar-Quesada, R., Canuelo, A., Nunez, M.I., Valenzuela, M.T., Ruiz de Almodovar, J.M., De Murcia, G., and Oliver, F.J. (2005). PARP inhibition sensitizes p53-deficient breast cancer cells to doxorubicin-induced apoptosis. Biochem J *386*, 119-125.

Nakazawa, K., Ueda, K., Honjo, T., Yoshihara, K., Nishizuka, Y., and Hayaishi, O. (1968). Nicotinamide adenine dinucleotide glycohydrolases and poly adenosine diphosphate ribose synthesis in rat liver. Biochem Biophys Res Commun *32*, 143-149.

Newberry, E.P., Latifi, T., and Towler, D.A. (1999). The RRM domain of MINT, a novel Msx2 binding protein, recognizes and regulates the rat osteocalcin promoter. Biochemistry *38*, 10678-10690.

Ochi, T., Sibanda, B.L., Wu, Q., Chirgadze, D.Y., Bolanos-Garcia, V.M., and Blundell, T.L. (2010). Structural biology of DNA repair: spatial organisation of the multicomponent complexes of nonhomologous end joining. J Nucleic Acids *2010*.

Oka, J., Ueda, K., Hayaishi, O., Komura, H., and Nakanishi, K. (1984). ADP-ribosyl protein lyase. Purification, properties, and identification of the product. J Biol Chem *259*, 986-995.

Oka, S., Kato, J., and Moss, J. (2006). Identification and characterization of a mammalian 39-kDa poly(ADP-ribose) glycohydrolase. J Biol Chem *281*, 705-713.

Ong, S.E., Blagoev, B., Kratchmarova, I., Kristensen, D.B., Steen, H., Pandey, A., and Mann, M. (2002). Stable isotope labeling by amino acids in cell culture, SILAC, as a simple and accurate approach to expression proteomics. Mol Cell Proteomics *1*, 376-386.

Orsburn, B., Escudero, B., Prakash, M., Gesheva, S., Liu, G., Huso, D.L., and Franco, S. (2010). Differential requirement for H2AX and 53BP1 in organismal development and genome maintenance in the absence of poly(ADP)ribosyl polymerase 1. Mol Cell Biol *30*, 2341-2352.

Otake, H., Miwa, M., Fujimura, S., and Sugimura, T. (1969). Binding of ADP-ribose polymer with histone. J Biochem *65*, 145-146.

Pachkowski, B.F., Tano, K., Afonin, V., Elder, R.H., Takeda, S., Watanabe, M., Swenberg, J.A., and Nakamura, J. (2009). Cells deficient in PARP-1 show an accelerated accumulation of DNA

single strand breaks, but not AP sites, over the PARP-1-proficient cells exposed to MMS. Mutat Res *671*, 93-99.

Pankotai, T., Bonhomme, C., Chen, D., and Soutoglou, E. (2012). DNAPKcs-dependent arrest of RNA polymerase II transcription in the presence of DNA breaks. Nat Struct Mol Biol *19*, 276-282.

Panzeter, P.L., Zweifel, B., Malanga, M., Waser, S.H., Richard, M., and Althaus, F.R. (1993). Targeting of histone tails by poly(ADP-ribose). J Biol Chem *268*, 17662-17664.

Passon, D.M., Lee, M., Rackham, O., Stanley, W.A., Sadowska, A., Filipovska, A., Fox, A.H., and Bond, C.S. (2012). Structure of the heterodimer of human NONO and paraspeckle protein component 1 and analysis of its role in subnuclear body formation. Proc Natl Acad Sci U S A *109*, 4846-4850.

Patel, A.G., Sarkaria, J.N., and Kaufmann, S.H. (2011). Nonhomologous end joining drives poly(ADP-ribose) polymerase (PARP) inhibitor lethality in homologous recombination-deficient cells. Proc Natl Acad Sci U S A *108*, 3406-3411.

Patel, C.N., Koh, D.W., Jacobson, M.K., and Oliveira, M.A. (2005). Identification of three critical acidic residues of poly(ADP-ribose) glycohydrolase involved in catalysis: determining the PARG catalytic domain. Biochem J *388*, 493-500.

Patton, J.G., Mayer, S.A., Tempst, P., and Nadal-Ginard, B. (1991). Characterization and molecular cloning of polypyrimidine tract-binding protein: a component of a complex necessary for pre-mRNA splicing. Genes Dev *5*, 1237-1251.

Patton, J.G., Porro, E.B., Galceran, J., Tempst, P., and Nadal-Ginard, B. (1993). Cloning and characterization of PSF, a novel pre-mRNA splicing factor. Genes Dev *7*, 393-406.

Paulsen, R.D., Soni, D.V., Wollman, R., Hahn, A.T., Yee, M.C., Guan, A., Hesley, J.A., Miller, S.C., Cromwell, E.F., Solow-Cordero, D.E*., et al.* (2009). A genome-wide siRNA screen reveals diverse cellular processes and pathways that mediate genome stability. Mol Cell *35*, 228-239.

Pawelczak, K.S., and Turchi, J.J. (2010). Purification and characterization of exonuclease-free Artemis: Implications for DNA-PK-dependent processing of DNA termini in NHEJ-catalyzed DSB repair. DNA Repair (Amst) *9*, 670-677.

Peng, R., Dye, B.T., Perez, I., Barnard, D.C., Thompson, A.B., and Patton, J.G. (2002). PSF and p54nrb bind a conserved stem in U5 snRNA. RNA *8*, 1334-1347.

Petermann, E., Keil, C., and Oei, S.L. (2005). Importance of poly(ADP-ribose) polymerases in the regulation of DNA-dependent processes. Cell Mol Life Sci *62*, 731-738.

Pic, E., Gagne, J.P., and Poirier, G.G. (2011). Mass spectrometry-based functional proteomics of poly(ADP-ribose) polymerase-1. Expert Rev Proteomics *8*, 759-774.

Pierce, A.J., Johnson, R.D., Thompson, L.H., and Jasin, M. (1999). XRCC3 promotes homology-directed repair of DNA damage in mammalian cells. Genes Dev *13*, 2633-2638.

Pines, A., Vrouwe, M.G., Marteijn, J.A., Typas, D., Luijsterburg, M.S., Cansoy, M., Hensbergen, P., Deelder, A., de Groot, A., Matsumoto, S.*, et al.* (2012). PARP1 promotes nucleotide excision repair through DDB2 stabilization and recruitment of ALC1. J Cell Biol *199*, 235-249.

Pleschke, J.M., Kleczkowska, H.E., Strohm, M., and Althaus, F.R. (2000). Poly(ADP-ribose) binds to specific domains in DNA damage checkpoint proteins. J Biol Chem *275*, 40974-40980.

Poirier, G.G., de Murcia, G., Jongstra-Bilen, J., Niedergang, C., and Mandel, P. (1982). Poly(ADP-ribosyl)ation of polynucleosomes causes relaxation of chromatin structure. Proc Natl Acad Sci U S A *79*, 3423-3427.

Polo, S.E., Blackford, A.N., Chapman, J.R., Baskcomb, L., Gravel, S., Rusch, A., Thomas, A., Blundred, R., Smith, P., Kzhyshkowska, J.*, et al.* (2012). Regulation of DNA-end resection by hnRNPU-like proteins promotes DNA double-strand break signaling and repair. Mol Cell *45*, 505-516.

Polo, S.E., Kaidi, A., Baskcomb, L., Galanty, Y., and Jackson, S.P. (2010). Regulation of DNA-damage responses and cell-cycle progression by the chromatin remodelling factor CHD4. EMBO J *29*, 3130-3139.

Pommier, Y., Redon, C., Rao, V.A., Seiler, J.A., Sordet, O., Takemura, H., Antony, S., Meng, L., Liao, Z., Kohlhagen, G.*, et al.* (2003). Repair of and checkpoint response to topoisomerase I-mediated DNA damage. Mutat Res *532*, 173-203.

Povirk, L.F. (1996). DNA damage and mutagenesis by radiomimetic DNA-cleaving agents: bleomycin, neocarzinostatin and other enediynes. Mutat Res *355*, 71-89.

Purnell, M.R., and Whish, W.J. (1980). Novel inhibitors of poly(ADP-ribose) synthetase. Biochem J *185*, 775-777.

Rajesh, C., Baker, D.K., Pierce, A.J., and Pittman, D.L. (2011). The splicing-factor related protein SFPQ/PSF interacts with RAD51D and is necessary for homology-directed repair and sister chromatid cohesion. Nucleic Acids Res *39*, 132-145.

Rathbun, G.A., Ziv, Y., Lai, J.H., Hill, D., Abraham, R.H., Shiloh, Y., and Cantley, L.C. (1999). ATM and lymphoid malignancies; use of oriented peptide libraries to identify novel substrates of ATM critical in downstream signaling pathways. Curr Top Microbiol Immunol *246*, 267-273; discussion 274.

Reale, A., Matteis, G.D., Galleazzi, G., Zampieri, M., and Caiafa, P. (2005). Modulation of DNMT1 activity by ADP-ribose polymers. Oncogene *24*, 13-19.

Robu, M., Shah, R.G., Petitclerc, N., Brind'Amour, J., Kandan-Kulangara, F., and Shah, G.M. (2013). Role of poly(ADP-ribose) polymerase-1 in the removal of UV-induced DNA lesions by nucleotide excision repair. Proc Natl Acad Sci U S A *110*, 1658-1663.

Rodrigue, A., Lafrance, M., Gauthier, M.C., McDonald, D., Hendzel, M., West, S.C., Jasin, M., and Masson, J.Y. (2006). Interplay between human DNA repair proteins at a unique double-strand break in vivo. EMBO J *25*, 222-231.

Rosenthal, F., Feijs, K.L., Frugier, E., Bonalli, M., Forst, A.H., Imhof, R., Winkler, H.C., Fischer, D., Caflisch, A., Hassa, P.O*., et al.* (2013). Macrodomain-containing proteins are new mono-ADP-ribosylhydrolases. Nat Struct Mol Biol *20*, 502-507.

Ross, P.L., Huang, Y.N., Marchese, J.N., Williamson, B., Parker, K., Hattan, S., Khainovski, N., Pillai, S., Dey, S., Daniels, S*., et al.* (2004). Multiplexed protein quantitation in Saccharomyces cerevisiae using amine-reactive isobaric tagging reagents. Mol Cell Proteomics *3*, 1154-1169.

Rouleau, M., Aubin, R.A., and Poirier, G.G. (2004). Poly(ADP-ribosyl)ated chromatin domains: access granted. J Cell Sci *117*, 815-825.

Rouleau, M., McDonald, D., Gagne, P., Ouellet, M.E., Droit, A., Hunter, J.M., Dutertre, S., Prigent, C., Hendzel, M.J., and Poirier, G.G. (2007). PARP-3 associates with polycomb group bodies and with components of the DNA damage repair machinery. J Cell Biochem *100*, 385-401.

Rouleau, M., Patel, A., Hendzel, M.J., Kaufmann, S.H., and Poirier, G.G. (2010). PARP inhibition: PARP1 and beyond. Nat Rev Cancer *10*, 293-301.

Rulten, S.L., Cortes-Ledesma, F., Guo, L., Iles, N.J., and Caldecott, K.W. (2008). APLF (C2orf13) is a novel component of poly(ADP-ribose) signaling in mammalian cells. Mol Cell Biol *28*, 4620-4628.

Rulten, S.L., Fisher, A.E., Robert, I., Zuma, M.C., Rouleau, M., Ju, L., Poirier, G., Reina-San-Martin, B., and Caldecott, K.W. (2011). PARP-3 and APLF function together to accelerate nonhomologous end-joining. Mol Cell *41*, 33-45.

Rulten, S.L., Rotheray, A., Green, R.L., Grundy, G.J., Moore, D.A., Gomez-Herreros, F., Hafezparast, M., and Caldecott, K.W. (2013). PARP-1 dependent recruitment of the amyotrophic lateral sclerosis-associated protein FUS/TLS to sites of oxidative DNA damage. Nucleic Acids Res.

Ruscetti, T., Lehnert, B.E., Halbrook, J., Le Trong, H., Hoekstra, M.F., Chen, D.J., and Peterson, S.R. (1998). Stimulation of the DNA-dependent protein kinase by poly(ADP-ribose) polymerase. J Biol Chem *273*, 14461-14467.

Salton, M., Elkon, R., Borodina, T., Davydov, A., Yaspo, M.L., Halperin, E., and Shiloh, Y. (2011). Matrin 3 binds and stabilizes mRNA. PLoS One *6*, e23882.

Salton, M., Lerenthal, Y., Wang, S.Y., Chen, D.J., and Shiloh, Y. (2010). Involvement of Matrin 3 and SFPQ/NONO in the DNA damage response. Cell Cycle *9*, 1568-1576.

Saxena, A., Saffery, R., Wong, L.H., Kalitsis, P., and Choo, K.H. (2002). Centromere proteins Cenpa, Cenpb, and Bub3 interact with poly(ADP-ribose) polymerase-1 protein and are poly(ADP-ribosyl)ated. J Biol Chem *277*, 26921-26926.

Schmidt-Ullrich, R.K. (2003). Molecular targets in radiation oncology. Oncogene *22*, 5730-5733.

Schreiber, V., Dantzer, F., Ame, J.C., and de Murcia, G. (2006). Poly(ADP-ribose): novel functions for an old molecule. Nat Rev Mol Cell Biol *7*, 517-528.

Schultz, N., Lopez, E., Saleh-Gohari, N., and Helleday, T. (2003). Poly(ADP-ribose) polymerase (PARP-1) has a controlling role in homologous recombination. Nucleic Acids Res *31*, 4959-4964.

Schulze, W.X., and Usadel, B. (2010). Quantitation in mass-spectrometry-based proteomics. Annu Rev Plant Biol *61*, 491-516.

Sewer, M.B., Nguyen, V.Q., Huang, C.J., Tucker, P.W., Kagawa, N., and Waterman, M.R. (2002). Transcriptional activation of human CYP17 in H295R adrenocortical cells depends on complex formation among p54(nrb)/NonO, protein-associated splicing factor, and SF-1, a complex that also participates in repression of transcription. Endocrinology *143*, 1280-1290.

Sewer, M.B., and Waterman, M.R. (2002). Adrenocorticotropin/cyclic adenosine 3',5'-monophosphate-mediated transcription of the human CYP17 gene in the adrenal cortex is dependent on phosphatase activity. Endocrinology *143*, 1769-1777.

Shah, G.M., Poirier, D., Duchaine, C., Brochu, G., Desnoyers, S., Lagueux, J., Verreault, A., Hoflack, J.C., Kirkland, J.B., and Poirier, G.G. (1995). Methods for biochemical study of poly(ADP-ribose) metabolism in vitro and in vivo. Anal Biochem *227*, 1-13.

Shamoo, Y., Abdul-Manan, N., and Williams, K.R. (1995). Multiple RNA binding domains (RBDs) just don't add up. Nucleic Acids Res *23*, 725-728.

Shanbhag, N.M., Rafalska-Metcalf, I.U., Balane-Bolivar, C., Janicki, S.M., and Greenberg, R.A. (2010). ATM-dependent chromatin changes silence transcription in cis to DNA double-strand breaks. Cell *141*, 970-981.

Shannon, P., Markiel, A., Ozier, O., Baliga, N.S., Wang, J.T., Ramage, D., Amin, N., Schwikowski, B., and Ideker, T. (2003). Cytoscape: a software environment for integrated models of biomolecular interaction networks. Genome Res *13*, 2498-2504.

Sharifi, R., Morra, R., Appel, C.D., Tallis, M., Chioza, B., Jankevicius, G., Simpson, M.A., Matic, I., Ozkan, E., Golia, B.*, et al.* (2013). Deficiency of terminal ADP-ribose protein glycohydrolase TARG1/C6orf130 in neurodegenerative disease. EMBO J *32*, 1225-1237.

Shav-Tal, Y., and Zipori, D. (2002). PSF and p54(nrb)/NonO--multi-functional nuclear proteins. FEBS Lett *531*, 109-114.

Shibata, A., Conrad, S., Birraux, J., Geuting, V., Barton, O., Ismail, A., Kakarougkas, A., Meek, K., Taucher-Scholz, G., Lobrich, M.*, et al.* (2011). Factors determining DNA double-strand break repair pathway choice in G2 phase. EMBO J *30*, 1079-1092.

Simsek, D., and Jasin, M. (2010). Alternative end-joining is suppressed by the canonical NHEJ component Xrcc4-ligase IV during chromosomal translocation formation. Nat Struct Mol Biol *17*, 410-416.

Slade, D., Dunstan, M.S., Barkauskaite, E., Weston, R., Lafite, P., Dixon, N., Ahel, M., Leys, D., and Ahel, I. (2011). The structure and catalytic mechanism of a poly(ADP-ribose) glycohydrolase. Nature *477*, 616-620.

Slama, J.T., Aboul-Ela, N., Goli, D.M., Cheesman, B.V., Simmons, A.M., and Jacobson, M.K. (1995). Specific inhibition of poly(ADP-ribose) glycohydrolase by adenosine diphosphate (hydroxymethyl)pyrrolidinediol. J Med Chem *38*, 389-393.

Smith, B.L., Bauer, G.B., and Povirk, L.F. (1994). DNA damage induced by bleomycin, neocarzinostatin, and melphalan in a precisely positioned nucleosome. Asymmetry in protection at the periphery of nucleosome-bound DNA. J Biol Chem *269*, 30587-30594.

Soulas-Sprauel, P., Rivera-Munoz, P., Malivert, L., Le Guyader, G., Abramowski, V., Revy, P., and de Villartay, J.P. (2007). V(D)J and immunoglobulin class switch recombinations: a paradigm to study the regulation of DNA end-joining. Oncogene *26*, 7780-7791.

Soutoglou, E., and Misteli, T. (2008). Activation of the cellular DNA damage response in the absence of DNA lesions. Science *320*, 1507-1510.

Spagnolo, L., Barbeau, J., Curtin, N.J., Morris, E.P., and Pearl, L.H. (2012). Visualization of a DNA-PK/PARP1 complex. Nucleic Acids Res *40*, 4168-4177.

Stanewsky, R., Rendahl, K.G., Dill, M., and Saumweber, H. (1993). Genetic and molecular analysis of the X chromosomal region 14B17-14C4 in Drosophila melanogaster: loss of function in NONA, a nuclear protein common to many cell types, results in specific physiological and behavioral defects. Genetics *135*, 419-442.

Steen, H., and Mann, M. (2004). The ABC's (and XYZ's) of peptide sequencing. Nat Rev Mol Cell Biol *5*, 699-711.

Steffen, J.D., and Pascal, J.M. (2013). New players to the field of ADP-ribosylation make the final cut. EMBO J *32*, 1205-1207.

Stewart, G.S., Panier, S., Townsend, K., Al-Hakim, A.K., Kolas, N.K., Miller, E.S., Nakada, S., Ylanko, J., Olivarius, S., Mendez, M.*, et al.* (2009). The RIDDLE syndrome protein mediates a ubiquitin-dependent signaling cascade at sites of DNA damage. Cell *136*, 420-434.

Storici, F., Bebenek, K., Kunkel, T.A., Gordenin, D.A., and Resnick, M.A. (2007). RNA-templated DNA repair. Nature *447*, 338-341.

Strom, C.E., Johansson, F., Uhlen, M., Szigyarto, C.A., Erixon, K., and Helleday, T. (2011). Poly (ADP-ribose) polymerase (PARP) is not involved in base excision repair but PARP inhibition traps a single-strand intermediate. Nucleic Acids Res *39*, 3166-3175.

Stucki, M. (2009). Histone H2A.X Tyr142 phosphorylation: a novel sWItCH for apoptosis? DNA Repair (Amst) *8*, 873-876.

Sugimura, K., Takebayashi, S., Taguchi, H., Takeda, S., and Okumura, K. (2008). PARP-1 ensures regulation of replication fork progression by homologous recombination on damaged DNA. J Cell Biol *183*, 1203-1212.

Sung, P. (2005). Mediating repair. Nat Struct Mol Biol *12*, 213-214.

Sy, S.M., Huen, M.S., and Chen, J. (2009). PALB2 is an integral component of the BRCA complex required for homologous recombination repair. Proc Natl Acad Sci U S A *106*, 7155-7160.

Tao, Z., Gao, P., Hoffman, D.W., and Liu, H.W. (2008). Domain C of human poly(ADP-ribose) polymerase-1 is important for enzyme activity and contains a novel zinc-ribbon motif. Biochemistry *47*, 5804-5813.

Tao, Z., Gao, P., and Liu, H.W. (2009). Identification of the ADP-ribosylation sites in the PARP-1 automodification domain: analysis and implications. J Am Chem Soc *131*, 14258-14260.

Tartier, L., Spenlehauer, C., Newman, H.C., Folkard, M., Prise, K.M., Michael, B.D., Menissier-de Murcia, J., and de Murcia, G. (2003). Local DNA damage by proton microbeam irradiation induces poly(ADP-ribose) synthesis in mammalian cells. Mutagenesis *18*, 411-416.

Till, S., and Ladurner, A.G. (2009). Sensing NAD metabolites through macro domains. Front Biosci *14*, 3246-3258.

Timinszky, G., Till, S., Hassa, P.O., Hothorn, M., Kustatscher, G., Nijmeijer, B., Colombelli, J., Altmeyer, M., Stelzer, E.H., Scheffzek, K.*, et al.* (2009). A macrodomain-containing histone rearranges chromatin upon sensing PARP1 activation. Nat Struct Mol Biol *16*, 923-929.

Tsuzuki, T., Fujii, Y., Sakumi, K., Tominaga, Y., Nakao, K., Sekiguchi, M., Matsushiro, A., Yoshimura, Y., and MoritaT (1996). Targeted disruption of the Rad51 gene leads to lethality in embryonic mice. Proc Natl Acad Sci U S A *93*, 6236-6240.

Urban, R.J., and Bodenburg, Y. (2002). PTB-associated splicing factor regulates growth factor-stimulated gene expression in mammalian cells. Am J Physiol Endocrinol Metab *283*, E794-798.

Urban, R.J., Bodenburg, Y., Kurosky, A., Wood, T.G., and Gasic, S. (2000). Polypyrimidine tract-binding protein-associated splicing factor is a negative regulator of transcriptional activity of the porcine p450scc insulin-like growth factor response element. Mol Endocrinol *14*, 774-782.

Urban, R.J., Bodenburg, Y.H., and Wood, T.G. (2002). NH2 terminus of PTB-associated splicing factor binds to the porcine P450scc IGF-I response element. Am J Physiol Endocrinol Metab *283*, E423-427.

Vilenchik, M.M., and Knudson, A.G. (2003). Endogenous DNA double-strand breaks: production, fidelity of repair, and induction of cancer. Proc Natl Acad Sci U S A *100*, 12871-12876.

Vodenicharov, M.D., Ghodgaonkar, M.M., Halappanavar, S.S., Shah, R.G., and Shah, G.M. (2005). Mechanism of early biphasic activation of poly(ADP-ribose) polymerase-1 in response to ultraviolet B radiation. J Cell Sci *118*, 589-599.

Wahlberg, E., Karlberg, T., Kouznetsova, E., Markova, N., Macchiarulo, A., Thorsell, A.G., Pol, E., Frostell, A., Ekblad, T., Oncu, D*., et al.* (2012). Family-wide chemical profiling and structural analysis of PARP and tankyrase inhibitors. Nat Biotechnol *30*, 283-288.

Wang, M., Wu, W., Rosidi, B., Zhang, L., Wang, H., and Iliakis, G. (2006). PARP-1 and Ku compete for repair of DNA double strand breaks by distinct NHEJ pathways. Nucleic Acids Res *34*, 6170-6182.

Wang, Y., Kim, N.S., Haince, J.F., Kang, H.C., David, K.K., Andrabi, S.A., Poirier, G.G., Dawson, V.L., and Dawson, T.M. (2011). Poly(ADP-ribose) (PAR) binding to apoptosis-inducing factor is critical for PAR polymerase-1-dependent cell death (parthanatos). Sci Signal *4*, ra20.

Wang, Z., Michaud, G.A., Cheng, Z., Zhang, Y., Hinds, T.R., Fan, E., Cong, F., and Xu, W. (2012). Recognition of the iso-ADP-ribose moiety in poly(ADP-ribose) by WWE domains suggests a general mechanism for poly(ADP-ribosyl)ation-dependent ubiquitination. Genes Dev *26*, 235-240.

Ward, I.M., Minn, K., van Deursen, J., and Chen, J. (2003). p53 Binding protein 53BP1 is required for DNA damage responses and tumor suppression in mice. Mol Cell Biol *23*, 2556-2563.

Watanabe, S., Watanabe, K., Akimov, V., Bartkova, J., Blagoev, B., Lukas, J., and Bartek, J. (2013). JMJD1C demethylates MDC1 to regulate the RNF8 and BRCA1-mediated chromatin response to DNA breaks. Nat Struct Mol Biol.

Woodard, R.L., Lee, K.J., Huang, J., and Dynan, W.S. (2001). Distinct roles for Ku protein in transcriptional reinitiation and DNA repair. J Biol Chem *276*, 15423-15433.

Wu, J., Chen, Y., Lu, L.Y., Wu, Y., Paulsen, M.T., Ljungman, M., Ferguson, D.O., and Yu, X. (2011). Chfr and RNF8 synergistically regulate ATM activation. Nat Struct Mol Biol *18*, 761-768.

Xie, A., Kwok, A., and Scully, R. (2009). Role of mammalian Mre11 in classical and alternative nonhomologous end joining. Nat Struct Mol Biol *16*, 814-818.

Xu, Y., Huang, S., Liu, Z.G., and Han, J. (2006). Poly(ADP-ribose) polymerase-1 signaling to mitochondria in necrotic cell death requires RIP1/TRAF2-mediated JNK1 activation. J Biol Chem *281*, 8788-8795.

Yang, S.H., Zhou, R., Campbell, J., Chen, J., Ha, T., and Paull, T.T. (2013). The SOSS1 single-stranded DNA binding complex promotes DNA end resection in concert with Exo1. EMBO J *32*, 126-139.

Yang, X., Zou, P., Yao, J., Yun, D., Bao, H., Du, R., Long, J., and Chen, X. (2010). Proteomic dissection of cell type-specific H2AX-interacting protein complex associated with hepatocellular carcinoma. J Proteome Res *9*, 1402-1415.

Yang, Y.S., Hanke, J.H., Carayannopoulos, L., Craft, C.M., Capra, J.D., and Tucker, P.W. (1993). NonO, a non-POU-domain-containing, octamer-binding protein, is the mammalian homolog of Drosophila nonAdiss. Mol Cell Biol *13*, 5593-5603.

Yeung, M., and Durocher, D. (2008). Engineering a DNA damage response without DNA damage. Genome Biol *9*, 227.

Yu, S.W., Andrabi, S.A., Wang, H., Kim, N.S., Poirier, G.G., Dawson, T.M., and Dawson, V.L. (2006). Apoptosis-inducing factor mediates poly(ADP-ribose) (PAR) polymer-induced cell death. Proc Natl Acad Sci U S A *103*, 18314-18319.

Yu, S.W., Wang, H., Poitras, M.F., Coombs, C., Bowers, W.J., Federoff, H.J., Poirier, G.G., Dawson, T.M., and Dawson, V.L. (2002). Mediation of poly(ADP-ribose) polymerase-1-dependent cell death by apoptosis-inducing factor. Science *297*, 259-263.

Yuan, J., and Chen, J. (2010). MRE11-RAD50-NBS1 complex dictates DNA repair independent of H2AX. J Biol Chem *285*, 1097-1104.

Zhang, Y., Liu, S., Mickanin, C., Feng, Y., Charlat, O., Michaud, G.A., Schirle, M., Shi, X., Hild, M., Bauer, A.*, et al.* (2011). RNF146 is a poly(ADP-ribose)-directed E3 ligase that regulates axin degradation and Wnt signalling. Nat Cell Biol *13*, 623-629.

Zhang, Y., Shim, E.Y., Davis, M., and Lee, S.E. (2009). Regulation of repair choice: Cdk1 suppresses recruitment of end joining factors at DNA breaks. DNA Repair (Amst) *8*, 1235-1241.

Zhang, Z., and Carmichael, G.G. (2001). The fate of dsRNA in the nucleus: a p54(nrb)-containing complex mediates the nuclear retention of promiscuously A-to-I edited RNAs. Cell *106*, 465-475.

Zhou, Y., and Paull, T.T. (2013). DNA-dependent Protein Kinase regulates DNA end resection in concert with the Mre11-Rad50-Nbs1 (MRN) complex and Ataxia-Telangiectasia-Mutated (ATM). J Biol Chem.

Zimmermann, M., and de Lange, T. (2013). 53BP1: pro choice in DNA repair. Trends Cell Biol.

Zimmermann, M., Lottersberger, F., Buonomo, S.B., Sfeir, A., and de Lange, T. (2013). 53BP1 regulates DSB repair using Rif1 to control 5' end resection. Science *339*, 700-704.

Zou, L., Cortez, D., and Elledge, S.J. (2002). Regulation of ATR substrate selection by Rad17-dependent loading of Rad9 complexes onto chromatin. Genes Dev *16*, 198-208.

ANNEX

Supplementary Figures Chapter 5

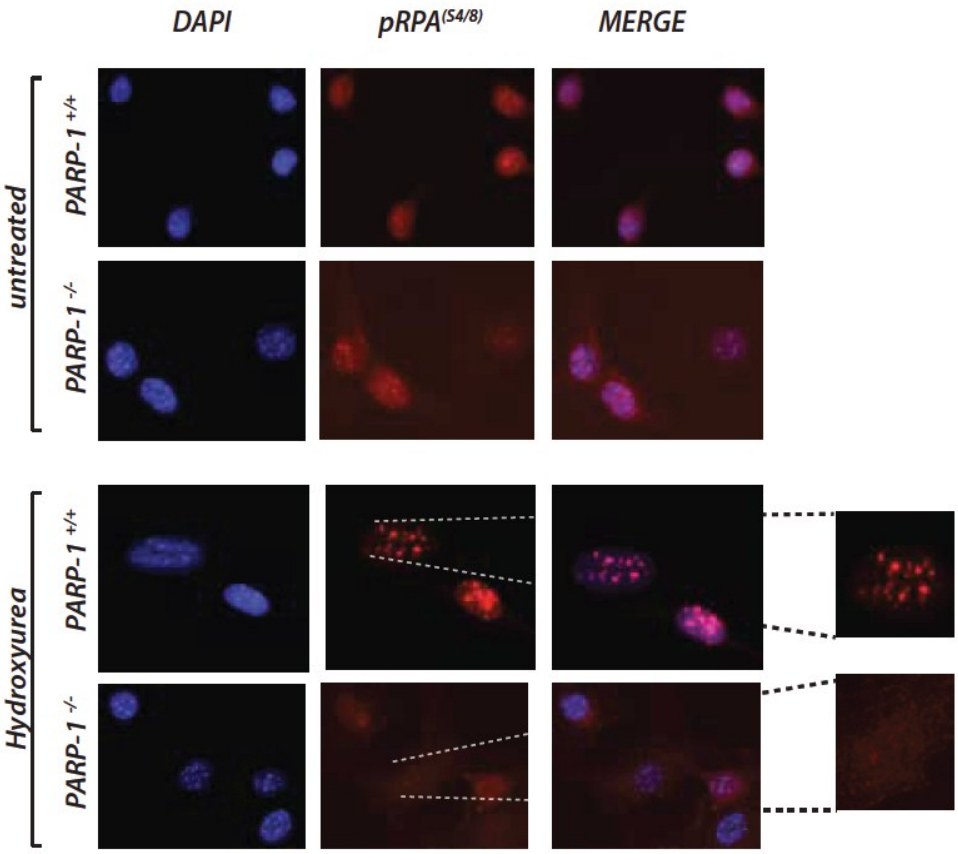

Figure 32: RPA foci formation after HU-treatment is impaired in PARP1$^{-/-}$ MEFs.
Staining for phosphorylated RPA34 (Serine 4/8) was performed in wildtype MEFs or PARP1-deficient MEFs, in the absence or presence of DNA damage induced by Hydroxyurea.

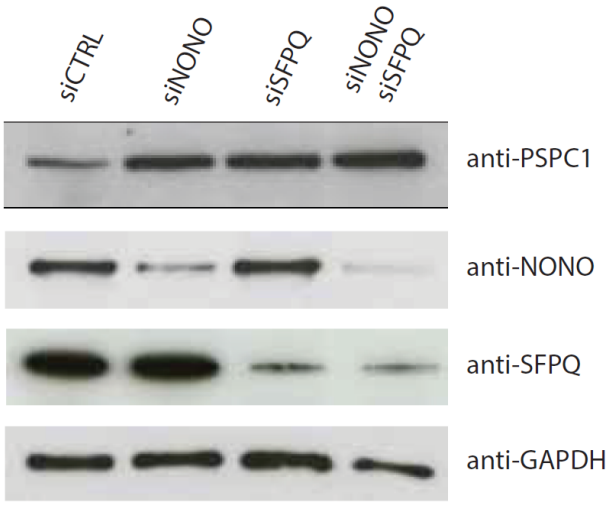

Figure 33: PSPC1 protein expression is upregulated in NONO and SFPQ knockdown cells

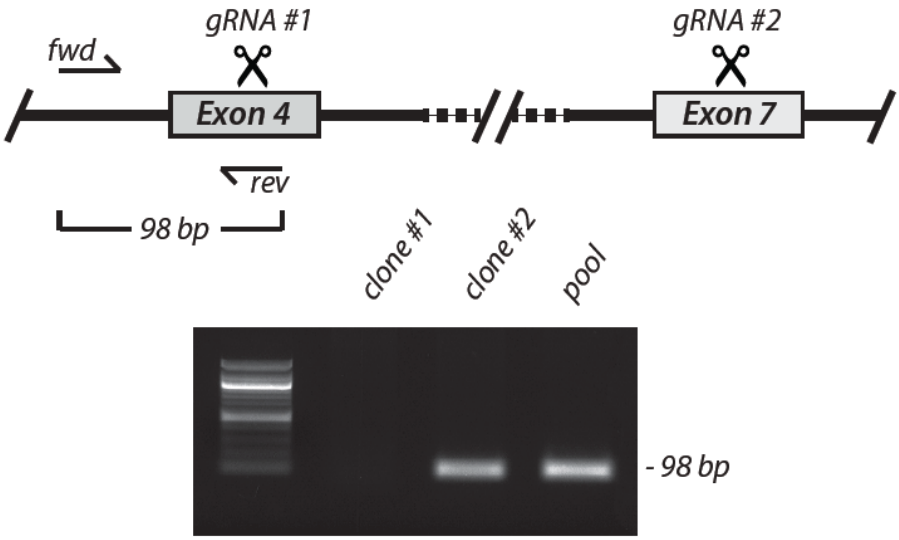

Figure 34: Targeting the PARP-1 gene in human cells using the CRISPR-Cas9 system. Two guideRNAs (gRNA) are used to target Exon 4 and 7, respectively. In clone 1, deletion of Exon 4 can be observed following PCR on genomic DNA. This clone will be tested by Western Blotting for PARP-1 protein expression. This approach will be useful to delete the other two DNA-dependent PARPs (PARP-2 and PARP-3).

Published online 31 August 2012 *Nucleic Acids Research, 2012, Vol. 40, No. 20* ***10287–10301***
doi:10.1093/nar/gks798

PARP activation regulates the RNA-binding protein NONO in the DNA damage response to DNA double-strand breaks

Jana Krietsch[1,2], Marie-Christine Caron[2], Jean-Philippe Gagné[1], Chantal Ethier[1], Julien Vignard[2], Michel Vincent[3], Michèle Rouleau[1], Michael J. Hendzel[4], Guy G. Poirier[1,*] and Jean-Yves Masson[2,*]

[1]Cancer Research Unit, Laval University Medical Research Center, CHUQ-CRCHUL, Québec, QC, Canada G1V 4G2, [2]Genome Stability Laboratory, Laval University Cancer Research Center, Hôtel-Dieu de Québec, QC, Canada G1R 2J6, [3]Faculty of Medicine, Laval University, Québec, QC, Canada G1V 0A6 and [4]Department of Oncology, Faculty of Medicine and Dentistry, University of Alberta, 11560 University Avenue, Edmonton, Alberta, Canada T6G 1Z2

Received May 7, 2012; Revised July 26, 2012; Accepted July 30, 2012

ABSTRACT

After the generation of DNA double-strand breaks (DSBs), poly(ADP-ribose) polymerase-1 (PARP-1) is one of the first proteins to be recruited and activated through its binding to the free DNA ends. Upon activation, PARP-1 uses NAD^+ to generate large amounts of poly(ADP-ribose) (PAR), which facilitates the recruitment of DNA repair factors. Here, we identify the RNA-binding protein NONO, a partner protein of SFPQ, as a novel PAR-binding protein. The protein motif being primarily responsible for PAR-binding is the RNA recognition motif 1 (RRM1), which is also crucial for RNA-binding, highlighting a competition between RNA and PAR as they share the same binding site. Strikingly, the *in vivo* recruitment of NONO to DNA damage sites completely depends on PAR, generated by activated PARP-1. Furthermore, we show that upon PAR-dependent recruitment, NONO stimulates nonhomologous end joining (NHEJ) and represses homologous recombination (HR) *in vivo*. Our results therefore place NONO after PARP activation in the context of DNA DSB repair pathway decision. Understanding the mechanism of action of proteins that act in the same pathway as PARP-1 is crucial to shed more light onto the effect of interference on PAR-mediated pathways with PARP inhibitors, which have already reached phase III clinical trials but are until date poorly understood.

INTRODUCTION

Each day, the cells genome is confronted with up to 50 endogenous DNA double-strand breaks (DSBs). These are extremely hazardous for a cell, as they do not leave an intact complementary strand to serve as a template for repair (1). If left unrepaired, DSBs can have consequences such as cell death or carcinogenesis. Hence, understanding the mechanisms that lead to successful repair of DSBs will further increase the knowledge of cancer progression and treatments. The DNA damage response (DDR) to DSBs is a multilayered process, initiated with sensing and signaling DNA damage, subsequent recruitment of repair proteins and execution of repair (2).

Poly(ADP-ribose) polymerase-1 (PARP-1) is an abundant and ubiquitous nuclear protein that uses NAD^+ to synthesize a negatively charged polymer, called poly(ADP-ribose) (PAR), onto a variety of target proteins, such as histones, DSB repair factors and PARP-1 itself. The latter post-translational protein modification has an impact on cellular processes as diverse as transcription (3), cell death (4) and especially DNA repair (5). PARP-1 acts as a strong sensor for DNA damage and rapidly produces PAR at newly generated DNA DSBs, provoking therewith local chromatin relaxation due to its negative charge (3) and facilitating the recruitment of repair factors, such as MRE11 (2,6). The dynamic turnover of PAR within seconds to minutes is executed by poly(ADP-ribose) glycohydrolase (PARG), that possesses endo- and exoglycosidic activities, hence enabling a new round of DNA damage signaling (7).

For subsequent repair, two major DSB repair pathways have evolved, namely nonhomologous end joining

*To whom correspondence should be addressed. Tel: +1 418 525 4444 (ext 15154); Fax: +1 418 691 5439; Email: jean-yves.masson@crhdq.ulaval.ca
Correspondence may also be addressed to Guy G. Poirier. Tel: +1 418 654 2267; Fax: +1 418 654 2159; Email: guy.poirier@crchul.ulaval.ca

(NHEJ) and homologous recombination (HR). Whereas HR is considered as error-free and restricted to the S/G_2-phase (8) by its necessity for a homologous template, error-prone NHEJ functions throughout the cell cycle and represents the major pathway for DSB repair in multicellular eukaryotes. Although the NHEJ pathway is highly flexible in terms of substrate ends used for repair, participating repair proteins and possible outcomes, a number of key proteins are indispensable to accomplish classical NHEJ (cNHEJ): Initially, the heterodimeric Ku70/Ku80 complex binds to both ends of the broken DNA molecule (9). Interestingly, Ku has an affinity for PAR (10) and is also a direct target for PARylation (11). The Ku–DNA complex is further bound by the catalytic subunit of DNA–PK (DNA–PKcs) to assemble the end-bridging DNA–PK complex (12). If the two ends are not directly ligatable they have to be processed prior to the final ligation step. A variety of proteins (such as Artemis, PNK, APLF nucleases, TdT, polymerases λ and μ) have been implicated in the end-processing step, emphasizing the mechanistic flexibility of the NHEJ reaction (13–16). The final ligation step is carried out by X4-L4 complex, composed of XRCC4, DNA ligase IV and XLF (17).

Within the last years, growing attention has been drawn to proteins with dual roles in RNA biology and DNA DSB repair. Examples include the Ku protein, which is crucial for the NHEJ pathway but interestingly also for the control of mRNA expression (18,19), the TFHII complex that acts in nucleotide excision repair as well as in transcriptional initiation mediated by RNA polymerase II (20), and recently the RNA-binding protein RBMX and the RNA-splicing factor THRAP3 were implied in the DDR (21–23). About twenty years ago the group of Harris Busch purified and characterized a heterodimer consisting of a 52 and a 100 kDa subunit, most certainly corresponding to what is nowadays known as the 54 kDa nuclear RNA-binding protein (p54nrb/NONO) and the polypyrimidine tract-binding protein-associated splicing factor (PSF/SFPQ). NONO and SFPQ show 71% sequence identity and, together with paraspeckle component 1 (PSPC1), belong to a subfamily of RNA recognition motif (RRM) proteins defined by tandem RRM motifs, flanked by an additional region of sequence similarity predicted to promote formation of heteromeric complexes between each of the proteins (24). NONO and SFPQ have been implicated in nuclear retention of A- to I-edited RNA as paraspeckle components (25), pre-mRNA 3′-end formation (26), cAMP cycling (27) and transcriptional activation (28–30). Interestingly, apart from their functions in RNA biogenesis, NONO and SFPQ were reported to interact with DNA *in vitro*, which lead to an investigation of their function in the context of DNA repair. Both proteins are transiently recruited with the same kinetics to DNA damage induced by a laser track in human cells (31). Interestingly, a protein complex containing NONO and SFPQ stimulates NHEJ about 10-fold *in vitro* (32). Furthermore, it has been demonstrated that the attenuation of NONO protein expression, independent of its partner protein SFPQ, delays the resolution of γ-H2AX foci after ionizing irradiation and leads to an accumulation of chromosomal aberrations (33). However, the exact mechanism by which NONO is recruited to DNA damage sites and regulates DSB repair is unclear. Interestingly, a bioinformatics screen from our group for proteins that potentially bind PAR, which is generated within seconds at a new DSB, identified NONO/SFPQ among a variety of NHEJ factors (10,34), leading to the hypothesis that PARP and its associated polymer regulates NONO. In this manuscript, we dissect the role of NONO in DSB repair in the context of PARP activation. We suggest here that NONO is directly implicated in NHEJ, and that its recruitment to DNA damage sites is strictly dependent on activated PARP-1. These results highlight the emerging concept of RNA-binding proteins in DSB repair.

MATERIALS AND METHODS

Cell lines, cell culture, and DNA constructs

HeLa cells and mouse embryonic fibroblasts (MEFs) proficient for PARP-1 and PARP-2 [wild type (WT)], or deficient for either PARP-1 (PARP-$1^{-/-}$) or PARP-2 (PARP-$2^{-/-}$) were cultured in DMEM, while MCF-7 cells were cultured in MEM-alpha (air/CO_2, 19:1, 37°C). Both media were supplemented with 10% fetal bovine serum and 1% penicillin/streptomycin.

The NHEJ reporter construct 'sGEJ' was kindly provided by Dr. Ralph Scully (35) and stably integrated into the genomic DNA of MCF-7 cells by using G418 disulfate salt (400 μg/ml; Sigma) as a selection marker. The HR reporter construct 'DR-GFP' [kindly provided by Dr. Maria Jasin; (36)] was integrated into the genomic DNA of MCF-7 cells by hygromycin selection (400 μg/ml; Invitrogen).

The GFP-NONO construct is a generous gift from Dr. James Patton (Vanderbilt University, Nashville, TN). NONO was cloned for protein purification from the pEGFP vector into a pET-16 b (Novagen) vector using the primers shown in Supplementary Table S1.

Site-directed mutagenesis on the His-NONO and GFP-NONO constructs was carried out with the QuikChange™ Site-Directed Mutagenesis Kit (Stratagene) using the oligos shown in Supplementary Table S1.

Antibodies and siRNAs

For Western blotting analysis and chromatin-immunoprecipitation (ChIP) experiments, polyclonal antibodies for NONO and SFPQ were obtained from Bethyl laboratories. The monoclonal antibody against GAPDH (6C5) was obtained from Fitzgerald Industries. Polyclonal antibodies for RAD51 and PSPC1 were purchased from Santa Cruz. PARP-1 (C2–10) monoclonal antibody was produced in house as described (37).

Gene silencing was performed using siRNA directed against the following target sequences: 5′-GGAAGCCA GCUGCUCGGAAAGCUCU-3′ against NONO, 5′-GC CAGCAGCAAGAAAGGCAUUUGAA-3′ against SFPQ (Invitrogen). A scrambled siRNA (5′-GACGTCA TATACCAAGCTAGTTT-3′) from Dharmacon was used as a negative control. Transfection of 5 nM siRNA per

condition was performed for 48 hr using HiPerfect transfection reagent (Qiagen) according to the manufacturer's protocol. For the siRNA directed against NONO, a second round of transfection (~36 hr after the first transfection) was performed for another 24 hr.

Colony forming assays

Long-term cell viability of HeLa cells transfected with the indicated siRNAs was assessed by colony forming assays. Briefly, a total of 200 cells per condition were plated into 35-mm dishes. Cells were then exposed to ionizing radiation of 0, 0.5 or 2 Gray using a γ-irradiator (Gammacell-40; MDS Nordion). After 7 to 10 days, colonies were fixed with methanol, stained using a 4 g/L solution of methylene blue in methanol, extensively washed with PBS and counted.

Protein purification

Recombinant wild-type human NONO (NONO-WT) and the RRM1-deletion mutant (NONOΔRRM1) proteins were purified from an *Escherichia coli* BL-21 strain carrying pET16b-10XHis-NONO or pET16b-10XHis-NONOΔRRM1 expression constructs, grown in 4 L of LB media supplemented with 100 μg/ml ampicillin and 25 μg/ml chloramphenicol. Protein expression was induced for 16 hr at 16°C with 0.1 mM IPTG added to the culture at an OD_{600} = 0.4. Cells were then harvested by centrifugation and resuspended in 40 ml lysis buffer A (20 mM Tris-HCl pH 8.0, 10% glycerol, 2 mM β-mercapthoethanol, 500 mM NaCl, 5 mM imidazole, 1 mM PMSF, 1 μg/ml leupeptin, 0.019 TIU/ml aprotinin). Samples were lysed with a Dounce homogenizer (10 strokes with the tight pestle), sonicated using a sonicator (Bioruptor; Diagenode) (10 min at the 'high' setting, 30 s ON and 30 s OFF) and returned to the Dounce for a second round of lysis. Insoluble material was removed by centrifugation at 40 000 rpm for 1 hr at 4°C and the supernatant subsequently loaded on a 5 ml cobalt-based immobilized metal affinity chromatography resin Talon column (BD Biosciences, Palo Alto, CA). The column was washed and eluted with a linear gradient of imidazole ranging from 5 to 1000 mM prepared in buffer A. Fractions containing His-tagged NONO-WT or NONOΔRRM1 were identified by sodium dodecyl sulphate-polyacrylamide gel electrophoresis (SDS-PAGE), carefully selected, pooled and dialyzed for 1 hr against 20 mM Tris-HCl pH 8.0, 375 mM NaCl, 10% glycerol and 0.05% Tween-20 buffer.

FACS analysis of the cell cycle

Cells were collected by trypsinization, centrifuged and resuspended at 10^6 cells per 300 μl of PBS and fixed with 700 μl of ice-cold ethanol (100%) while vortexing. Once fixed, cells were washed with PBS and stained with propidium iodide (0.1% sodium citrate, 0.3% Nonidet P40, propidium iodide 50 mg/ml and RNAse A 20 mg/ml). Cell cycle analysis was performed on a Beckman Coulter Epics Elite model ESP by using the Expo2 analysis software.

Pulse-field gel electrophoresis

HeLa cells treated with the indicated siRNA were incubated for 2 hr at 37°C in the presence of 500 ng/ml Neocarzinostatin (NCS). After treatment, cells were released for the indicated time points and trypsinized. One percent agarose plugs containing 5×10^6 cells were prepared with a CHEF-disposable plug mold (Bio-Rad). Cells were lysed by incubation of the gel blocks for 72 hr at 45°C in 1 mg/mL proteinase K, 100 mM ethylenediaminetetraacetic acid (EDTA), 0.2% sodium deoxycholate, 1% *N*-laurylsarcosyl. Samples were then washed three times for 1 hr each in 20 mM Tris pH 8.0, 50 mM EDTA and embedded into an agarose gel (0.9% agarose in 0.5X filtered TBE). DNA separation was performed at 14°C for 24 hr with a two block pulse linear program (block 1: 0.1 s at 30 s, 5.8 V/cm, 14°C, angle 120°, TBE 0.5X, 12 hr; block 2: 0,1 s at 5 s, 3.6 V/cm, 14°C, angle 110°, TBE 0.5X, 12 hr) in a CHEF-DR III Pulsed Field Electrophoresis System (Bio-Rad). The gel was then dried for 30 min at 55°C and for additional 30 min at room temperature, stained overnight with SYBR green (Molecular Probes) and visualized using a UV lamp. A yeast chromosome PFG marker (NEB 345) served as a ladder for molecular weight.

Nuclear extract preparation

Up to 10^7 HeLa cells per condition were washed three times with PBS, resuspended and incubated for 15 min on ice in 250 μl hypotonic buffer (10 mM Tris pH 7.4, 10 mM $MgCl_2$, 10 mM KCl and 1 mM DTT). The samples were then passed 5 times through a 1 ml syringe with a 27G needle and centrifuged for 15 min at $3300 \times g$ at 4°C. Pellets were resuspended in 200 μl high salt buffer (hypotonic buffer A with 350 mM NaCl and protease inhibitors) and incubated for 1 hr on ice. After centrifugation for 30 min at 13 000rpm at 4°C, the supernatants were transferred to a clean tube and adjusted to 10% glycerol (v/v) and 10 μM of β-mercapthoethanol.

Cell fractionation and western blot analysis

Cell fractionation was carried out as described in (38) with slight modifications. Briefly, 3×10^6 HeLa cells per condition were collected and resuspended in 200 μL of buffer A (10 mM HEPES pH 8.0, 10 mM KCl, 1.5 mM $MgCl_2$, 0.34 M sucrose, 10% glycerol, 1 mM DTT, 1 mM PMSF, 0.1% Triton-X-100, 10 mM NaF, 1 mM Na_2VO_3, protease inhibitors) and kept for 5 min on ice. The soluble cytoplasmic fraction (S1) was separated from the nuclei (P2) by centrifugation for 4 min at $1300 \times g$ at 4°C. The nuclear fraction P2 was washed twice with 300 μL buffer A then resuspended in 200 μL buffer B (3 mM EDTA, 0.2 mM EGTA, 1 mM DTT, 1 mM PMSF, 10 mM NaF, 1 mM Na_2VO_3, protease inhibitors) and kept for 30 min on ice. The insoluble chromatin fraction (P3) was separated from nuclear soluble proteins (S3) by centrifugation for 4 min at $1700 \times g$ at 4 °C. S1 was cleared from insoluble proteins by centrifugation at 14 000rpm for 15 min at 4°C and the supernatant (S2) was kept for analysis. Cell fractions

were subsequently analysed by western blotting as described in (39).

ChIP and quantitative polymerase chain reaction

A unique DSB in MCF-7 cells was introduced by electroporating the I-SceI expression vector (pCBASce) into MCF-7 DR-GFP (carrying a chromosomally integrated homology-directed repair site) cells using the Gene Pulser Xcell apparatus (Bio Rad). A total of 2×10^6 cells per electroporation, resuspended in 650 µl PBS, were mixed with 50 µg of circular plasmid and pulsed at 0.25 kV and 1000 µF in 4-mm cuvettes. Cells were then plated onto 10-cm dishes containing fresh medium and kept at 37°C for 12 hr. To crosslink proteins to DNA, cells were treated for 10 min with a 1% formaldehyde solution in PBS. Subsequently, glycine to a final concentration of 0.125 M was added to quench the reaction. Cells were collected in ice cold PBS using a cell scraper, washed twice in cold PBS containing 1 mM PMSF, washed for 10 min in solution I (10 mM HEPES, pH 7.5, 10 mM EDTA, 0.5 mM EGTA, 0.75% Triton X-100) and 10 min in solution II (10 mM HEPES, pH 7.5, 200 mM NaCl, 1 mM EDTA, 0.5 mM EGTA). Cells were resuspended in lysis buffer (25 mM Tris–HCl, pH 7.5, 150 mM NaCl, 1% Triton X-100, 0.1% SDS, 0.5% deoxycholate) and kept for 45 min on ice. To shear chromatin to an average size of 0.5 kb, cells were sonicated with a Bioruptor sonicator (Diagenode) for 10 min (high, 30 s ON, 30 s OFF). Samples were then centrifuged at maximum speed in a benchtop centrifuge until clear and the lysate precleared overnight with Sepharose CL-6B beads. Immunoprecipitation was performed for 2 hr in lysis buffer with polyclonal antibodies against NONO. Rabbit anti-human IgG (H+L) antibody (Jackson Immunoresearch Laboratories) was used as a negative control. Protein–antibody complexes were subsequently incubated with protein A/G beads for 1 hr. Complexes were washed twice with RIPA buffer (150 mM NaCl, 50 mM Tris-HCl pH 8.0, 0.1% SDS, 0.5% deoxycholate, 1% NP-40, 1 mM EDTA), once in high salt buffer (50 mM Tris–Cl, pH 8.0, 500 mM NaCl, 0.1% SDS, 0.5% deoxycholate, 1% NP-40, 1 mM EDTA), once in LiCl buffer (50 mM Tris–HCl, pH 8.0, 250 mM LiCl, 1% NP-40, 0.5% deoxycholate, 1 mM EDTA) and twice in TE buffer (10 mM Tris–HCl, pH 8.0, 1 mM EDTA, pH 8.0). Beads were resuspended in TE containing 50 µg/ml RNase A and incubated for 30 min at 37°C. Beads were washed with deionized water and incubated for 15 min in elution buffer (1% SDS, 0.1 M $NaHCO_3$). Crosslinks were reversed by adding 200 mM NaCl followed by an incubation for 6 hr at 65°C. Samples were deproteinized overnight with 300 µg/ml proteinase K and DNA was extracted with phenol–chloroform followed by ethanol precipitation.

Immunoprecipitated DNA was quantified by quantitative polymerase chain reaction (q-PCR) using the Light Cycler Fast Start DNA Master SYBR Green I (Roche Applied Sciences), which is composed of Fast Start *Taq* DNA polymerase and SYBR Green Dye. Oligonucleotides [Supplementary Table S1; (40)] flanking the break site were designed and optimized for linearity range and efficiency using a light cycler (Roche). Immunoprecipitated DNA samples were amplified in triplicate and values calculated as fold-enrichment compared with the IgG ChIP control and versus GAPDH as a control locus.

PAR-binding assay

PAR-binding properties of purified proteins were analysed as described in (34). Briefly, 500 ng of the indicated protein were either spotted onto a 0.2 -µm pore size nitrocellulose membrane using a slot blot manifold (Bio Rad) or transferred onto a nitrocellulose membrane following separation on an 8% SDS-PAGE. For both conditions, the membranes were washed three times in TBS-T (10 mM Tris-HCl pH 7.4, 150 mM NaCl, 0.05% Tween) and incubated for 1 hr at room temperature in TBS-T to allow proper refolding of the protein. Subsequently, the membrane was incubated with 250 nM [^{32}P]-PAR [synthesized as described in (41)] in TBS-T with or without 100-fold of unlabeled competitor RNA (yeast RNA mix, Ambion). The membrane was then washed extensively in TBS-T, air-dried and subjected to autoradiography.

Surface plasmon resonance spectroscopy

Interaction of 10X-His-tagged NONO with PAR was investigated using surface plasmon resonance (SPR) spectroscopy. The binding experiments were carried out on a ProteOn XPR36 (Bio-Rad) biosensor at 25°C using the HTE sensor chip (Bio-Rad). The flow cells of the sensor chip were loaded with a nickel solution to saturate the Tris–NTA surface with Ni^{2+}-ions. Purified His-tagged wild-type NONO diluted in 10 mM MOPS [pH 8.0] was injected in one of six channels of the chip at a flow rate of 30 µl/min, until approximately a 5000 resonance unit (RU) level was reached. After a wash with running buffer (PBS [pH 7.4] with 0.005% (v/v) Tween-20), PAR binding to the immobilized substrates was monitored by injecting a range of concentrations of PAR (500, 250 and 125 nM) along with a blank at a flow rate of 50 µl/min. When the injection of PAR was completed, running buffer was allowed to flow over the immobilized substrates for PAR to dissociate with an association and dissociation phase of 300 and 600 s, respectively. Following dissociation of PAR, the chip surface was regenerated with an injection of 1 M NaCl at a flow rate of 100 µl/ml followed by 100 mM HCl and 300 mM EDTA at a flow rate of 30 µl/min. Interspot channel reference was used for non-specific binding corrections and the blank channel used with each analyte injection served as a double reference to correct for possible baseline drift. Data were analysed using ProteOn Manager Software version 3.1. The Langmuir 1:1 binding model was used to determine the KD values.

Live-cell microscopy and laser micro-irradiation

Recruitment experiments were carried out as described in (6). Briefly, cells were grown on glass-bottom dishes (MatTek Corp.) and transfected using Effectene reagent (Invitrogen) with the indicated constructs.

Twelve hours post-transfection with GFP-NONO, GFP-NONOΔRRM1 and mCherry-PARG, cells were placed in fresh medium, treated with 10 μM ABT-888 (Enzo Life Sciences; 5 mM stock solution prepared in H_2O) for 2 hr and sensitized with 1 μg/ml Hoechst 33 342 for 30 min prior to irradiation and live cell analysis of recruitment to DNA damage sites. A 37°C preheated stage with 5% CO_2 perfusion was used for the time-lapse on a Zeiss LSM-510 META NLO laser-scanning confocal microscope. Localized DNA damage was generated along a defined region across the nucleus of a single living cell by using a bi-photonic excitation of the Hoechst 33 342 dye, generated with a near-infrared 750-nm titanium:sapphire laser line (Chameleon Ultra, Coherent Inc.). The laser output was set to 3%, and we used 10 iterations to generate localized DSB clearly traceable with a 40× objective. Protein accumulation within the laser path was compared with an undamaged region within the same microirradiated cell. We generally selected cells with low expression levels and normalized the fluorescence intensity in the microirradiated area to the initial fluorescence in the whole nucleus to compensate for photobleaching during acquisition. The average accumulation ± S.E. of fluorescently tagged proteins from at least 10 cells from three independent experiments was plotted.

Immunofluorescence

Laser-irradiated HeLa cells from earlier process were analysed by immunofluorescence (IF) for protein-co-localization with PAR as recently published by our group (42). Briefly, cells were washed three times with ice-cold PBS, fixed for 15 min at room temperature in 4% formaldehyde diluted in PBS, washed five times with PBS prior to permeabilization with 0.5% Triton X-100 in PBS for 5 min. After three washes with PBS, cells were incubated with the first antibody diluted in PBS containing 2% FBS for 90 min at room temperature. Following one wash with 0.1% Triton-X in PBS and four washes with PBS, cells were incubated with a secondary antibody diluted in PBS containing 2% FBS for 45 min. Subsequently, cells were washed once with 0.1% Triton X-100 in PBS, four times with PBS and then mounted in Fluoromount-G mounting media (Southern Biotech, Birmingham, AL). Images were acquired using a Leica 6000 microscope. Volocity software v5.5 (Perkin-Elmer Improvision) was used for image acquisition.

NHEJ/HR *in vivo* reporter assays

To analyse I-SceI induced GFP^+-expression in NHEJ or HR reporter MCF7 cells, cell lines were plated onto cover-slips, treated with the indicated siRNAs for 36 hr and subsequently infected with an adenovirus coding for I-SceI. Cells were fixed 24 hr post-infection with 4% paraformaldehyde for 30 min. To enhance the GFP signal-to-noise ratio and therewith enhance the difference in signal intensity between GFP^+ and GFP^- cells, immunofluorescence was conducted as follows. Cells were permeabilized for 5 min with 0.5% Triton-X/PBS, washed twice with 0.1% Triton-X/PBS and incubated with 1% goat serum/PBS for 1 hr to block unspecific antibody binding. Cells were incubated for 1 hr with a polyclonal GFP antibody (Abcam ab290). The percentage of GFP^+ cells per condition was calculated by counting the GFP^+ cells over the total number of cells (2500 cells were counted based on DAPI nuclear staining). The percentage was expressed as fold-change normalized to the control siRNA condition.

RESULTS

NONO knockdown leads to a decrease in survival of IR-treated cells and deficient NHEJ repair

It has been previously shown that miRNA-mediated knockdown of NONO in HTC 116 cells left cell survival unaffected but sensitized the latter cells to ionizing irradiation (33). Here, we verified the necessity of NONO for cell proliferation by measuring the impact of attenuated NONO on the long-term survival of HeLa cells with and without ionizing irradiation. We used siRNA-mediated knockdown to attenuate the NONO protein expression level in HeLa cells. Immunoblotting confirmed that the expression level of NONO was reduced by more than 90%, whereas the attenuation of NONO did not affect the expression level of its partner protein SFPQ and vice versa (Figure 1A). A knockdown of NONO had no effect on long-term survival (Figure 1B). However, attenuated NONO sensitizes HeLa cells to ionizing irradiation at low (0.5 Gray) and intermediate doses (2.0 Gray), strongly suggesting a defect in DNA DSB repair (Figure 1C).

These results suggest that NONO is crucial for survival after ionizing radiation. We therefore analysed the ability of NONO attenuated cells to repair DSBs. Hence, we optimized an assay to assess the sensitivity of these cells to the radiomimetic antibiotic NCS as a means to measure DSB repair kinetics in HeLa cells. NCS consists of an enediyne chromophore, which is tightly bound to a 113 amino acid single chain protein, the active compound responsible for tandem DNA cleavage and highly potent in the induction of DNA single and especially DSBs (43,44). Pulse-field gel electrophoresis (PFGE) was accomplished with HeLa cells 48 hr following transfection with scramble or NONO siRNA and treated for 2 hr with 500 ng/ml NCS to introduce DSBs. Cells were then released for 60 or 120 min and DSB repair kinetics indirectly surveyed by analysing the accumulation of DSBs. We observed that NONO protein knockdown by siRNA impairs the recovery from DNA damage as persistent accumulation of DNA DSBs following a 2-hr NCS treatment is detected by PFGE (Figure 2A). The slower recovery kinetics observed in the context of NONO depletion provides strong indication for the involvement of NONO in DSB repair. However, this observation could also be explained by an effect on cell cycle checkpoints that occurred in NONO knockdown cells. To rule out the possibility that NONO plays in indirect role in repair by affecting cell cycle progression, we analysed the cell cycle phase distribution of siCTRL and siNONO HeLa cells (Supplementary Figure S1). Neither the knockdown of NONO, nor SFPQ, nor the combined

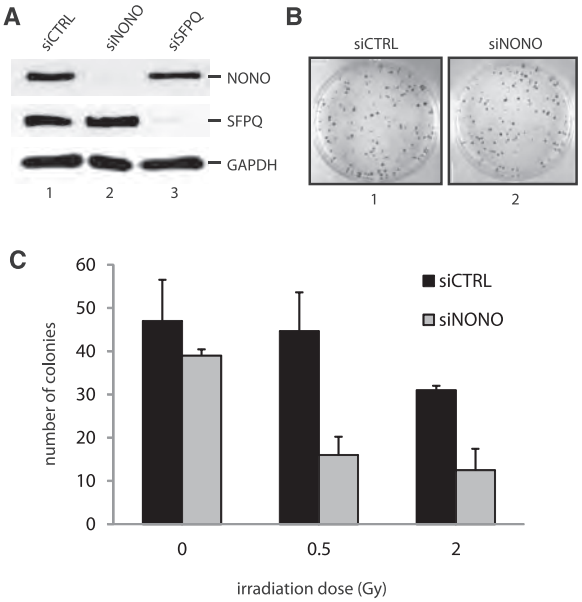

Figure 1. NONO increases cell survival after ionizing irradiation. (**A**) Western blot analysis demonstrating the efficiency of siRNAs directed against NONO (lane 2) or SFPQ (lane 3) in HeLa cells. (**B**) The clonogenic survival of HeLa cells treated with a scrambled control siRNA (image 1) and a siRNA directed against NONO (image 2) was analysed using a colony forming assay. (**C**) Quantitation of cell survival. HeLa cell colonies were counted 10 days after γ-irradiation with 0, 0.5 and 2.0 Gy.

knockdown of both affects cell cycle progression. Similarly, cell cycle phase distribution of MCF-7 cells was unaffected by the knockdown of NONO (data not shown).

The observed radiosensitivity and accumulation of DSBs in NONO attenuated cells could be a consequence of diminished NHEJ repair activity. Therefore, we set up a cell-free NHEJ assay that measures the ligation of a ^{32}P-labeled linearized plasmid, after incubation with nuclear extracts derived from siRNA control HeLa cells or knocked down for NONO. The knockdown of NONO in HeLa cells delays NHEJ kinetics *in vitro*, as the end joining reaction with the nuclear extract in which NONO had been knocked-down results in overall less end joining products compared with the control (Figure 2B). In concordance with this observation, less substrate plasmid had been used for the end joining reaction in the absence of NONO. Quantitation of the end joining products at 2 hr revealed a 5-fold decrease in end joining products in the NONO knockdown assay, compared with the assay with control cells (Figure 2C).

NONO is strongly associated with the chromatin and localizes near a unique DSB *in vivo*

The results mentioned earlier confirmed a function for NONO in DNA DSB repair, and suggested that NONO

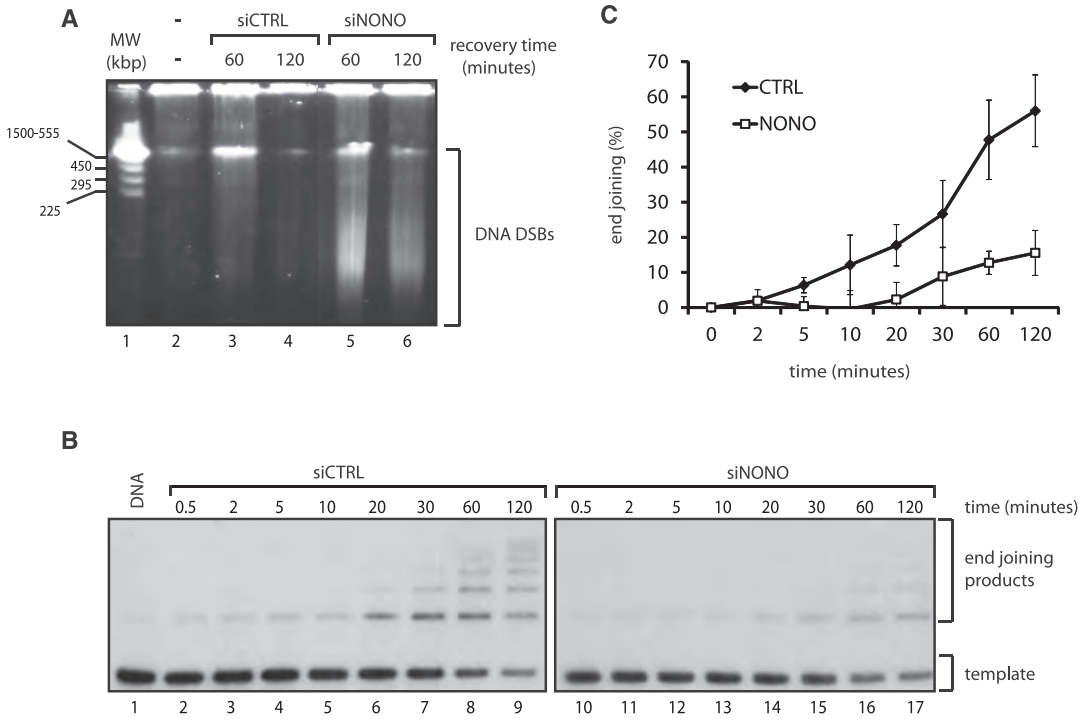

Figure 2. Attenuation of NONO decelerates NHEJ. (**A**) HeLa cells knocked-down with a scrambled siRNA (lanes 3 and 4) or a siRNA directed against NONO (lanes 5 and 6) were treated for 2 hr with NCS (500 ng/ml) and allowed to recover for either 60 or 120 min. Cells were then collected, embedded and lysed in agarose blocks and used for pulse-field gel electrophoresis. (**B**) A linearized, ^{32}P-end-labeled pBluescript was incubated for the indicated times with a nuclear extract derived from HeLa cells treated with a scrambled siRNA (lanes 2–9) or an siRNA directed against NONO (lanes 10–17). (**C**) Quantitation of the end joining events using a phosphorimager: The percent end joining represents the total signal intensity per lane normalized to 100% from which is substracted the % intensity of the remaining template ($n = 4$).

might play a direct role in DNA repair rather than having an indirect effect through RNA biogenesis. One prediction of such a direct role would be to observe physical association of NONO with DNA damage sites. Following this idea, we used ChIP combined with q-PCR using oligonucleotides flanking a unique I-SceI restriction site in MCF-7 cells to monitor the distribution of NONO relative to a DSB.

To ensure that the RNA-binding protein NONO is localizing to DNA/chromatin *in vivo* (a prerequisite for ChIP), we fractionated unfixed MCF-7 cells and analysed the chromatin enriched, nuclear soluble and cytoplasmic fractions by western blotting with the indicated antibodies (Figure 3A). Surprisingly, we found that NONO, as its partner proteins SFPQ and PSPC1, is strongly associated with the chromatin and nearly absent in the nuclear soluble and cytoplasmic fractions. PARP-1, RAD51 and GAPDH served as hallmark protein-controls for the nuclear soluble and cytoplasmic fractions, respectively. The results indicate that NONO is associated with the chromatin, even in the absence of exogenous DNA damage and independently of the PARP-1 activation state.

Using MCF-7 cells carrying a single I-SceI restriction site, we then combined ChIP with q-PCR to determine the position of NONO relative to a DSB *in vivo*. We conducted the ChIP experiment 12 hr after transfection with an I-SceI encoding vector, allowing sufficient time for I-SceI expression and generation of the unique DSB. We successfully pulled-down endogenous NONO fixed to the chromatin, as shown in Figure 3B. After purification of the chromatin that has been pulled-down with NONO, we used three sets of primers located at increasing distances from the DSB to evaluate the distribution of NONO (Figure 3C). We were able to detect NONO as close as 464–520 bp from the DSB with a ~1.5-fold enrichment compared with the IgG control and after normalization with GAPDH (Figure 3D). This localization resembles that of the NHEJ factor and RNA-processing protein Ku80, as we previously reported (39).

NONO is a new PAR-binding protein that binds PAR through its RRM1 motif

The synthesis of PAR that results from the activation of DNA-dependent PARPs is one of the earliest step of DNA damage recognition and signaling in mammalian cells. PARP-1 has notably been shown to localize to DNA damage sites within milliseconds following laser-induced micro irradiation of sub-nuclear regions (6,45).

Our laboratory recently performed a proteome-wide screen for proteins to isolate and identify pADPr-containing multiprotein complexes. Interestingly, the RNA-binding protein NONO was consistently identified together with a variety of DNA DSB repair factors (34,42). A number of DDR factors have been shown to be loaded on DNA damage sites in a PAR-dependent fashion (6,21,46,47). To assess PAR-binding properties of NONO *in vitro*, His-tagged NONO was expressed in *E. coli* and purified by affinity purification (Figure 4A). Using a PAR-binding assay developed by our group (10), we determined whether NONO binds PAR. As shown in

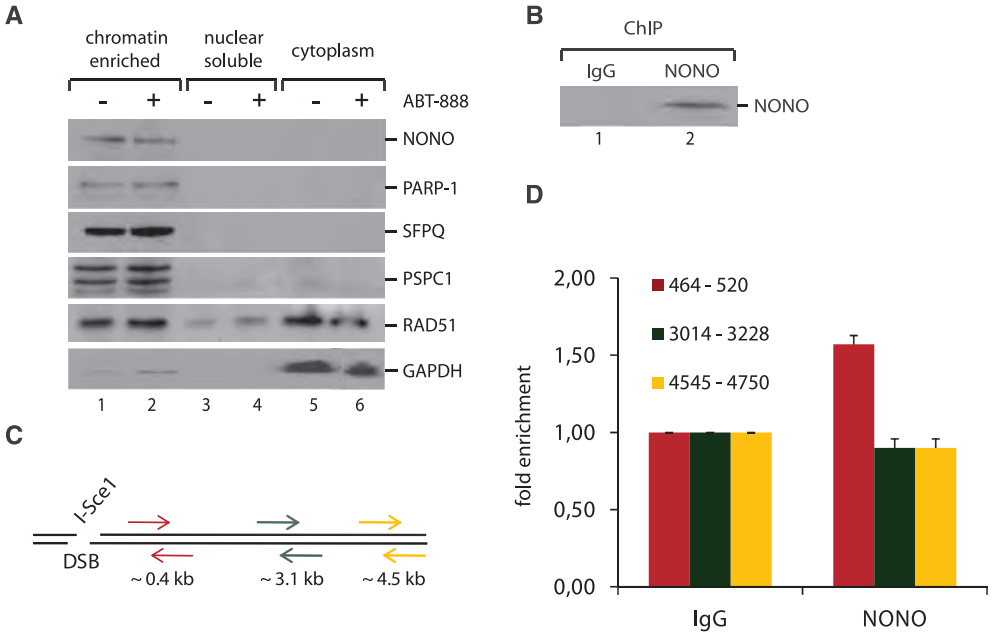

Figure 3. NONO is a chromatin-associated protein and localizes to a unique DSB *in vivo*. (**A**) Unfixed HeLa cells were treated for 1 hr with 10 μM ABT-888, washed with PBS and fractionated into chromatin-enriched, nuclear soluble and cytoplasmic fractions. Fractions were used for an analysis by western blotting. (**B**) Chromatin immunoprecipitation of NONO from the fixed chromatin of MCF-7 cells, which priorly had been transfected with an I-SceI coding plasmid to generate a unique DSB. An IgG antibody served as a control for the ChIP-experiment. (**C**) Distribution of primer pairs relative to the DSB created by I-SceI. These primers were used in q-PCR analysis of ChIP shown in (**D**). Primers for GAPDH served as a control for the PCR. (D) Quantification of NONO relative to the DSB by PCR ($n = 3$).

Figure 4B (lane 1), NONO displays a strong affinity for purified ^{32}P-labeled PAR *in vitro*. The unlabeled PAR displaced binding of its cognate ^{32}P-labeled polymer (Figure 4B, lanes 2–4). As NONO is a well-established RNA-binding protein and considering that PAR shares some structural features with nucleic acids, we further examined its affinity for PAR in the presence of increasing amounts of unlabeled competitor RNA (Figure 4C, lanes 1–4). Interestingly, binding of ^{32}P-PAR was slightly reduced when cold RNA was added to the binding reactions, suggesting a competition between PAR and RNA. The RNA-binding protein still exhibits PAR-binding in the presence of 100-fold competitor RNA, underpinning its specificity (Figure 4B).

To further characterize the affinity of NONO for PAR with a label-free approach, we used SPR spectroscopy, such as described in (48). Therefore, purified His-tagged NONO was bound to a HTE sensor chip until a response unit of 5000 RU was reached. Subsequently, purified PAR, produced by PARP-1 *in vitro*, was injected at three different concentrations (500, 250 and 125 nM) to determine the binding affinity to the immobilized NONO protein. Association and dissociation was allowed to proceed for 300 and 600 seconds, respectively. As shown in Figure 4C, the dissociation rate constant (K_D) of NONO was determined at 2.32×10^{-8} M, hence demonstrates a strong affinity for PAR.

As the general model suggests that upon activation by DNA-binding, PARP-1 generates large amounts of long and branched PAR, we tested whether NONO preferentially binds long and complex PAR over shorter PAR molecules. Hence, we fractionated and purified PAR produced *in vitro* by PARP-1 for our binding analysis. SPR was conducted with two distinct populations of PAR namely complex PAR (60 mer and more average length) and short PAR (less than 30 mers average length). Strikingly, NONO strongly and specifically binds complex PAR, with a K_D similar to that observed in Figure 4C but has no affinity for shorter PAR (Supplementary Figure S2A and B).

We next sought to locate the PAR-binding-sites within NONO protein. The NONO Drosophila behavior human splicing (DBHS) protein-core consists of clearly defined structural domains (Figure 5A): two tandem RRM domains and a 100-aa segment of predicted coiled-coil structure, putatively responsible for protein-protein interaction with itself and the other two members of the DBHS family (namely PSPC1 and SFPQ). As it had been shown

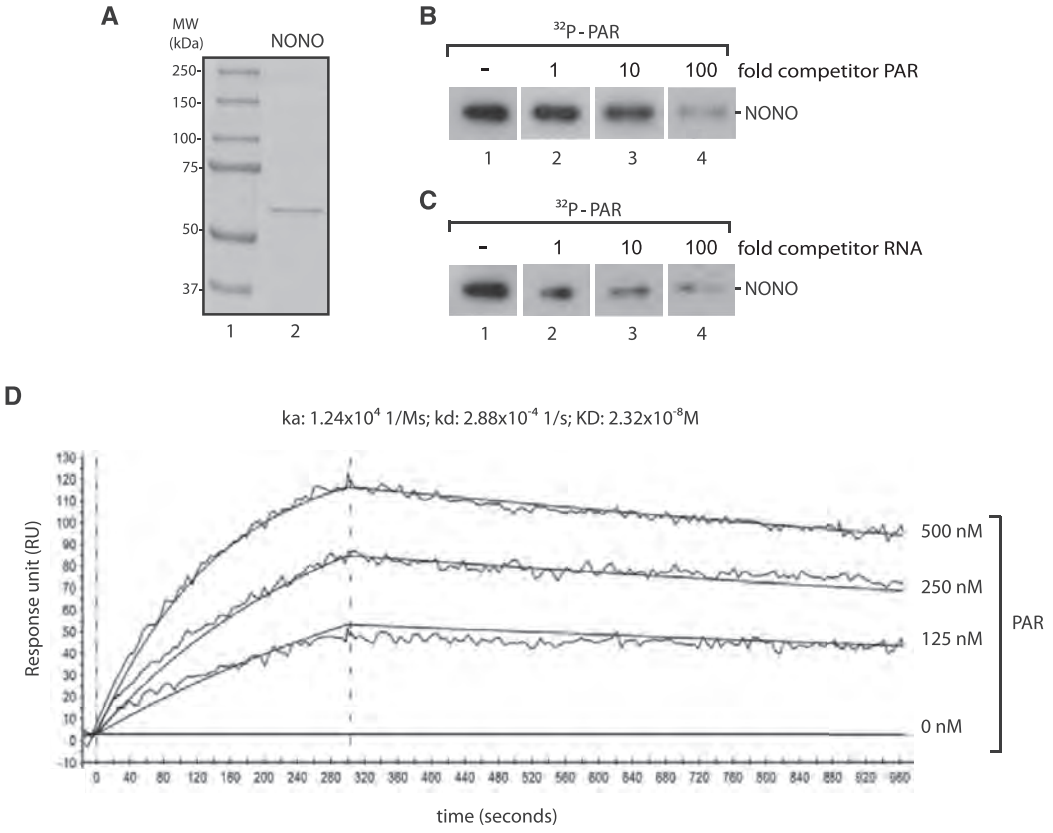

Figure 4. NONO binds PAR *in vitro*. (**A**) SDS-PAGE of 100 ng purified His-NONO protein stained with Coomassie blue (lane 2). (**B**) *In vitro* PAR-binding assay. 1 µg of purified His-NONO was loaded on an SDS-PAGE, blotted onto a nitrocellulose membrane and incubated in 250 nM ^{32}P-labeled PAR in TBS-T without (lane 1), with 1-fold (lane 2), 10-fold (lane 3) or 100-fold unlabeled competitor PAR (lane 4). (**C**) A PAR-binding assay was conducted as in (B) without (lane 1), with 1-fold (lane 2), 10-fold (lane 3) or 100-fold unlabeled competitor RNA (lane 4). (**D**) Kinetics of PAR binding to purified His-tagged NONO conducted by SPR spectroscopy. To analyse binding kinetics, PAR was injected at three different concentrations (125, 250 and 500 nM). PAR injection was done for 300 s and dissociation data were collected for 600 s. Data were fitted with Langmuir 1:1 interaction plot to calculate rate constants. The sensorgram is representative of three independent experiments.

for other RNA-binding proteins that they bind PAR through their RRM1 (49), we used protein fragments containing either the RRM1, RRM2, both RRMs or none of the RRMs for a PAR-binding assay *in vitro* (Figure 5B). Interestingly, we observed that NONO binds PAR with its fragment containing the N-terminal RNA-recognition motif 1 (RRM1) (Figure 5C). These results indicate that the RRM1 has a strong affinity for PAR *in vitro*, and could mediate the interaction between NONO and PAR. We therefore produced and purified a NONO mutant protein, which lacks the RRM1 region (NONOΔRRM1). As the wild-type and mutant NONO proteins were free of contaminants (Figure 5D), we performed an alternative polymer-blot assay without using a detergent-based separation such as SDS-PAGE. By slot-blotting the proteins directly onto a nitrocellulose membrane, we wanted to avoid methods that could disrupt interactions requiring native conformations. Measuring the binding-signal intensity with a phosphorimager revealed that while the full-length protein shows a strong affinity for PAR (as described earlier), the affinity of the NONOΔRRM1 protein for PAR is reduced by 2.5-fold, indicating that we have successfully deleted a principal PAR-binding-motif (Figure 5E).

NONO is PAR-dependently recruited to DNA damage sites

An emerging concept in the DDR is that several proteins, such as MRE11 (6), are recruited to DNA damage sites in a PAR-dependent manner to elicit cell cycle arrest or DNA repair. In view of the strong affinity of NONO for PAR *in vitro*, we analysed whether NONO co-localizes with PARP-1 and PAR at DNA damage sites in cells (Figure 6A). We therefore transfected HeLa cells with GFP-NONO and 24 hr later induced DNA damage in live-cell conditions by laser micro-irradiation. Immediately after irradiation, cells were fixed and subjected to immunofluorescence staining. Evidently, GFP-NONO, PARP-1 and PAR are co-localizing at laser-IR-induced DNA damage sites immediately after introducing DNA lesions.

To further analyse whether the recruitment of NONO to DNA damage sites is dependent on PAR, we established the recruitment kinetics of GFP-NONO to DNA

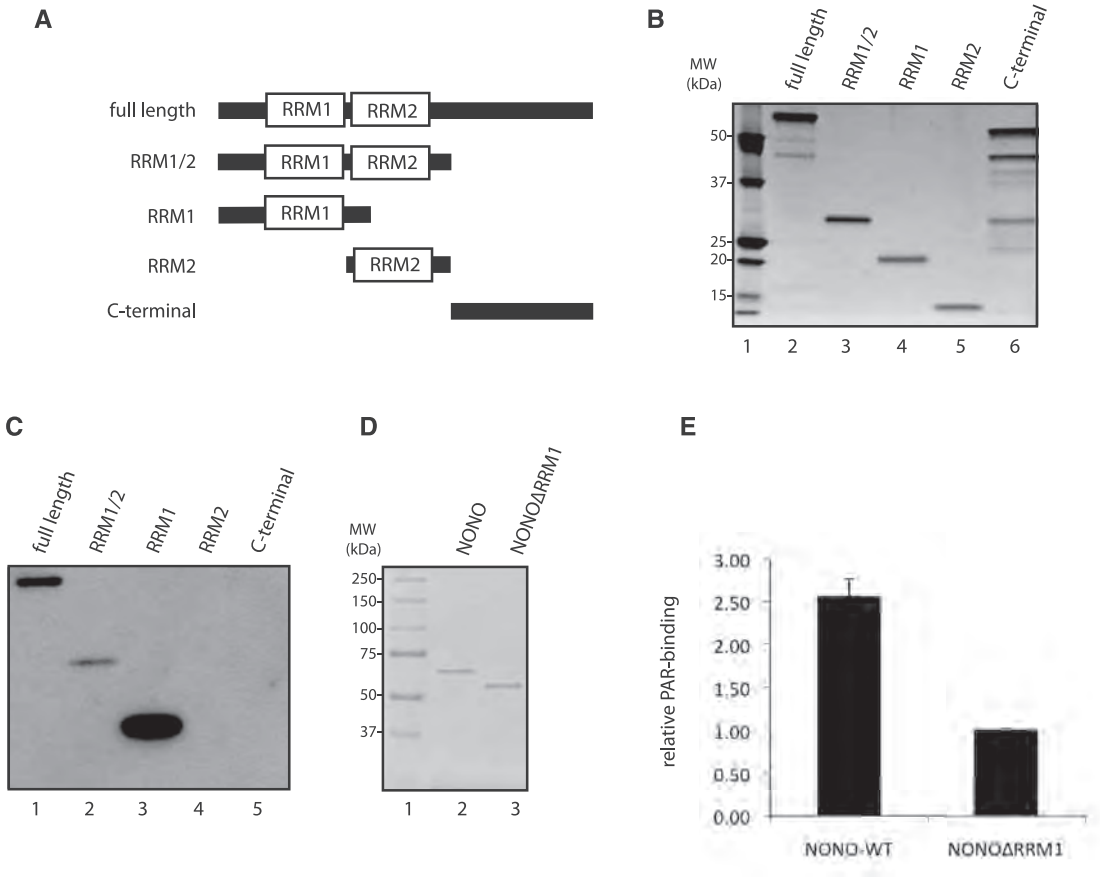

Figure 5. NONO binds PAR through its N-terminal/RNA recognition motif 1 (RRM1). (**A**) Protein truncations of NONO flanking the protein domains of interest, namely RRM1 and RRM2. (**B**) SYPRO protein stain of protein fragments loaded on a SDS-PAGE. (**C**) *In vitro* PAR-binding assay using 250 nM ^{32}P-labeled PAR in TBS-T. (**D**) SDS-PAGE of 500 ng His-NONO (lane 2) and His-NONOΔRRM1 (lane 3) each. (**E**) 1 µg of NONO-WT and NONOΔRRM1 purified proteins were slot blotted onto a nitrocellulose membrane and an *in vitro* ^{32}P-labeled PAR-binding assay was conducted in TBS-T. Mean values of the radioactivity signal as quantified by a phosphorimager from three independent experiments are presented.

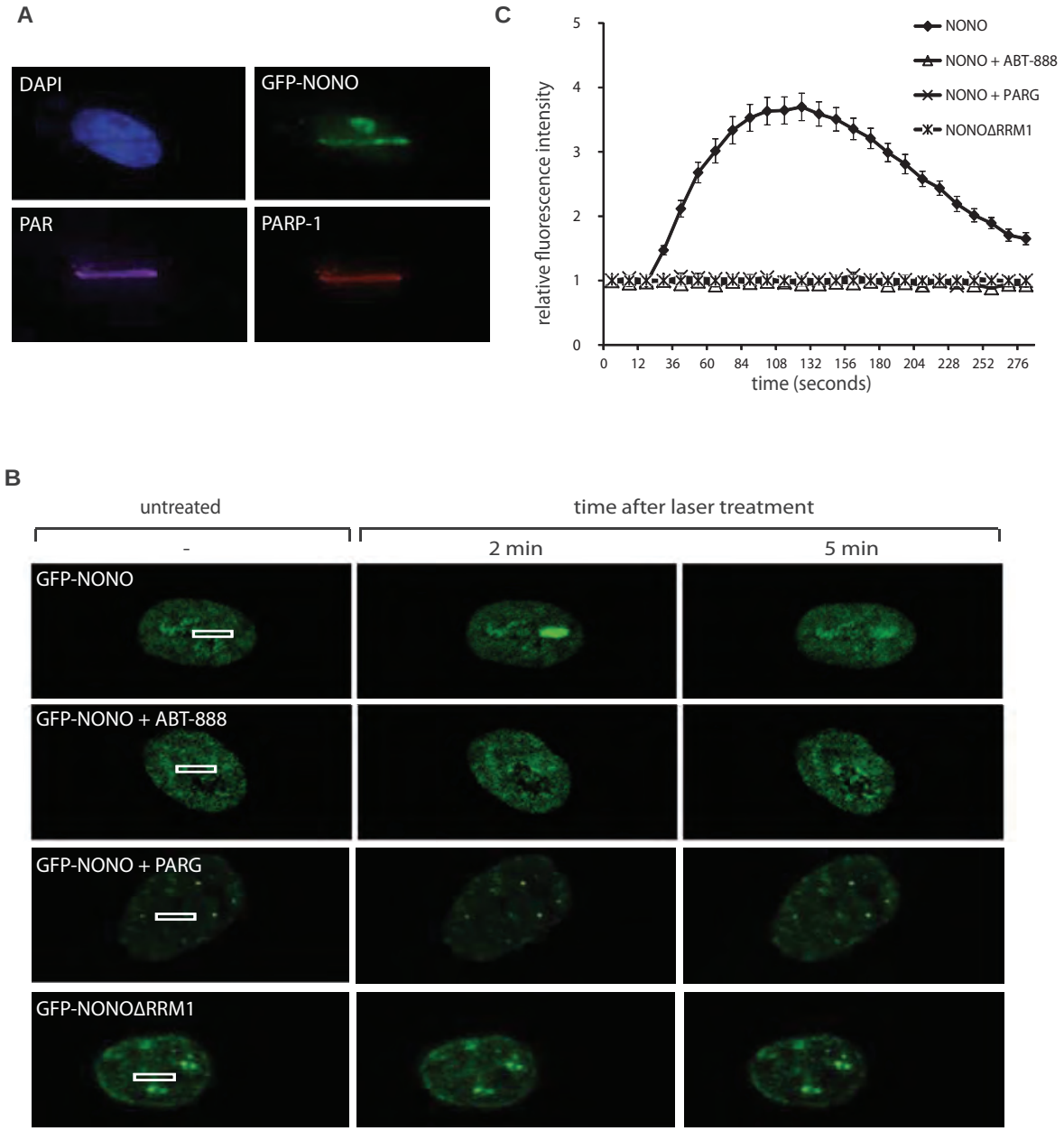

Figure 6. NONO is recruited to DNA damage sites in a PAR-dependent manner. (**A**) Representative images of laser-irradiated HeLa cells expressing GFP-NONO and subjected to IF for detection of PARP-1 and PAR. (**B**) Representative images of the laser-irradiated cells. HeLa cells were transfected either with the GFP-tagged NONO construct or with a mutant lacking the RRM1. Then cells were either left untreated, treated with 10 μM ABT-888 1 hr before irradiation or cotransfected with mCherry-PARG prior to laser microirradiation. (**C**) Statistical analysis of the recruitment kinetics. At least 15 cells per condition in three independent experiments were analysed for their fluorescence intensity above the background.

damage induced by micro-irradiation in HeLa cells in the presence or absence of the specific PARP inhibitor ABT-888. In these live-cell analysis conditions, NONO is transiently recruited with rapid kinetics to DNA damage sites and reaches a maximum within 120 s following local generation of DNA damage sites (Figure 6B and C). Strikingly, we found that the recruitment of NONO to DNA damage sites completely depends on catalytically active PARP, as in none of the cells the protein is recruited in the presence of the specific PARP inhibitor ABT-888. As another mean to assess the PAR-dependency of recruitment of NONO to DNA damage sites, we co-expressed GFP-NONO with mCherry-PARG, the main PAR-degrading enzyme, to prevent PAR accumulation in laser tracks. We have previously shown that overexpression of PARG prevents PAR accumulation after induction of DNA strand breaks (50). We indeed found that the recruitment of GFP-NONO to laser tracks is completely abolished by PARG overexpression.

This observation is consistent with the finding that PARP inhibition abrogates the recruitment of GFP-NONO and confirms a strict requirement for PAR-binding for its relocation to DNA damage sites. We then sought to define the domain mediating NONO interaction with PAR. Hence, we tested if interaction with PAR occurs through interaction with the RRM1 domain of NONO. As shown in Figure 6A and B, a deletion mutant lacking the RRM1 domain (GFP-NONOΔRRM1) is not recruited to DNA damage sites. This result strongly implicates the RRM1 domain in regulating the interaction with PAR.

Although our results underscore the importance of PAR for NONO dynamics in the DDR, they leave open the question which PARP family member generates the PAR that mediates the recruitment of NONO to DNA damage sites. It is well accepted, that PARP-1 is responsible for ~95% of all PARylation events after DNA damage, whereas PARP-2 carries out almost all of the remaining 5%. Therefore, we overexpressed GFP-NONO in wild-type and PARP-$1^{-/-}$ MEFs. Recruitment of GFP-NONO was detected in the PARP-1-proficient MEFs with similar kinetics to those in HeLa cells, whereas GFP-NONO was not recruited to the laser track in PARP-$1^{-/-}$ cells, highlighting the necessity of PARP-1 to generate PAR at the DNA damage sites (Figure 7). The specificity for PARP-1 is further highlighted by the observation that GFP-NONO is recruited with fast and transient kinetics in PARP-$2^{-/-}$ MEFs similar to that in the WT-MEFs and HeLa cells (Figure 7). Hence, PARP-1 is required to recruit NONO to DNA damage sites, whereas PARP-2 is rather dispensable. Collectively, these results show that the recruitment of NONO is PARP-1 and PAR-dependent, and mediated by the RRM1 region of NONO.

NONO promotes NHEJ and represses HR *in vivo* in the same pathway as PARP-1

As a consequence of the results described above, we hypothesize that NONO plays important regulatory role in the DDR by stimulating DSB repair. Indeed, we showed that NONO promotes cell survival and DSB repair through NHEJ, localizes near a unique DSB site and accumulates to sites of DNA damage in a pADPr-dependent fashion. However, a direct implication of NONO in NHEJ has not been shown *in vivo* and the question as whether NONO also influences the other DSB repair pathway, namely HR, has not been answered yet.

To address these two key questions, we generated two stable reporter cell lines enabling us to monitor both, NHEJ and HR repair (Figure 8A and B). Each of these cells lines has an integrated cassette comprising an I-SceI cleavage site that, upon repair by either NHEJ or HR, restores GFP expression, as previously described (35,36). Cells with normal or knocked down expression of NONO were assessed for each repair mechanism as indicated by the percentage of cells that express GFP. In the NHEJ reporter system assay, we found that the knockdown of NONO decreases NHEJ by more than 50% (Figure 8C). In this same assay, PARP inhibition, with the potent and specific PARP inhibitor ABT-888 also significantly reduced NHEJ repair. Knowing that NONO is PAR-dependently recruited to DNA DSBs, we combined the siRNA directed against NONO with PARP inhibitor to confirm our findings above. As expected, the siRNA-mediated knockdown of NONO combined with the inhibition of PARP does not have an additive effect in inhibiting NHEJ, indicating that PARP and NONO function in the same pathway and hence supporting the idea of PAR-dependent recruitment. Interestingly, an attenuation of NONO does not only decrease NHEJ but also facilitates repair by HR ~40% (Figure 8D). Again here, when combining siRNA directed against NONO with the PARP-1 inhibitor ABT-888, no additive effect was observed, supporting the same conclusion regarding PAR-dependent recruitment.

DISCUSSION

Although the RNA binding properties of NONO related to RNA biogenesis and the architecture of paraspeckles have been subject of an abundant literature, [reviewed in (51)], little is known on the functions of NONO in the context of DNA DSB repair. We have conducted a detailed molecular and cellular analysis of NONO in the context of the DDR and our data establish NONO as a PARP-1-dependent regulator of DSB repair by facilitating NHEJ and promoting cell survival after irradiation.

In the past few years, the list of proteins that possess dual roles in gene regulation and genomic stability through RNA biology and DNA repair, respectively, has largely expanded. Examples include the catalytic subunit of DNA-PK, a core complex of NHEJ that is necessary to arrest RNA-polymerase II transcription after the induction of DSBs (52) and the Ku protein that has dual roles in transcriptional reinitiation and NHEJ (19). In addition, the heterogeneous nuclear ribonucleoprotein (hnRNP) RBMX acts in alternative splicing and accumulates at DNA damage sites in a PARP-dependent manner (21). Also, the heterogeneous nuclear ribonucleoprotein hnRNPU influences end resection (53). Another study highlights the role of the splicing-associated protein THRAP3 in the DNA damage signaling network (22). Even PARP-1 itself functions in promoter/enhancer regulation (54), single-strand break repair and the alternative NHEJ pathway (55,56).

Because of its possible role in RNA biogenesis, it came as a surprise to find that NONO is mostly associated to the chromatin. Moreover, we show here for the first time that NONO is localized with close proximity to a unique DSB *in vivo*. In an earlier study (39), we have detected the NHEJ-related protein Ku80 within the same distance to the break-site as NONO (~ 400 bps), suggesting a direct implication for NONO in DNA DSB repair. In line with these findings, the Shiloh group has detected NONO in a protein complex composed of Ku70, Ku80 and Ligase IV (31). Here, we are giving further evidence for a direct implication of NONO in DSB repair by showing that down-regulation of NONO protein expression by siRNA sensitizes HeLa cells to ionizing irradiation and decreases NHEJ *in vitro* and *in vivo*. Hence, the data presented

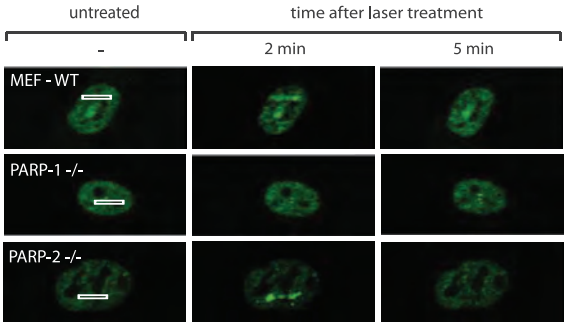

Figure 7. Representative images of laser-irradiated MEFs that were either proficient for PARP-1 and PARP-2 (MEF-WT) or deficient for either PARP-1 (PARP-$1^{-/-}$) or PARP-2 (PARP-$2^{-/-}$). Cells had been transfected with a GFP-NONO construct 24 hr before laser micro-irradiation. At least 20 cells per condition were tested in two independent experiments. Recruitment has been observed in none of the PARP-$1^{-/-}$ MEFs.

complement the recent findings that attenuation of NONO delays the resolution of γ-H2AX foci and results in an increase of chromosomal aberrations following radiation exposure (33). The fact that cells with attenuated NONO are still viable and capable of NHEJ might be explained by a possible backup through its homologous protein partner PSPC1. The expression level of PSPC1 in the presence of NONO in HeLa cells is very low and increases upon siRNA-mediated knock-down of NONO (data not shown).

PARP-1 is an abundant nuclear chromatin-associated protein, well characterized for its high DNA damage sensing ability. Once encountering free DNA ends, PARP-1 is catalytically activated and generates large amounts of PAR serving as a scaffold for the recruitment of a variety of DNA repair proteins. We performed a large scale analysis of proteins bound to PAR following

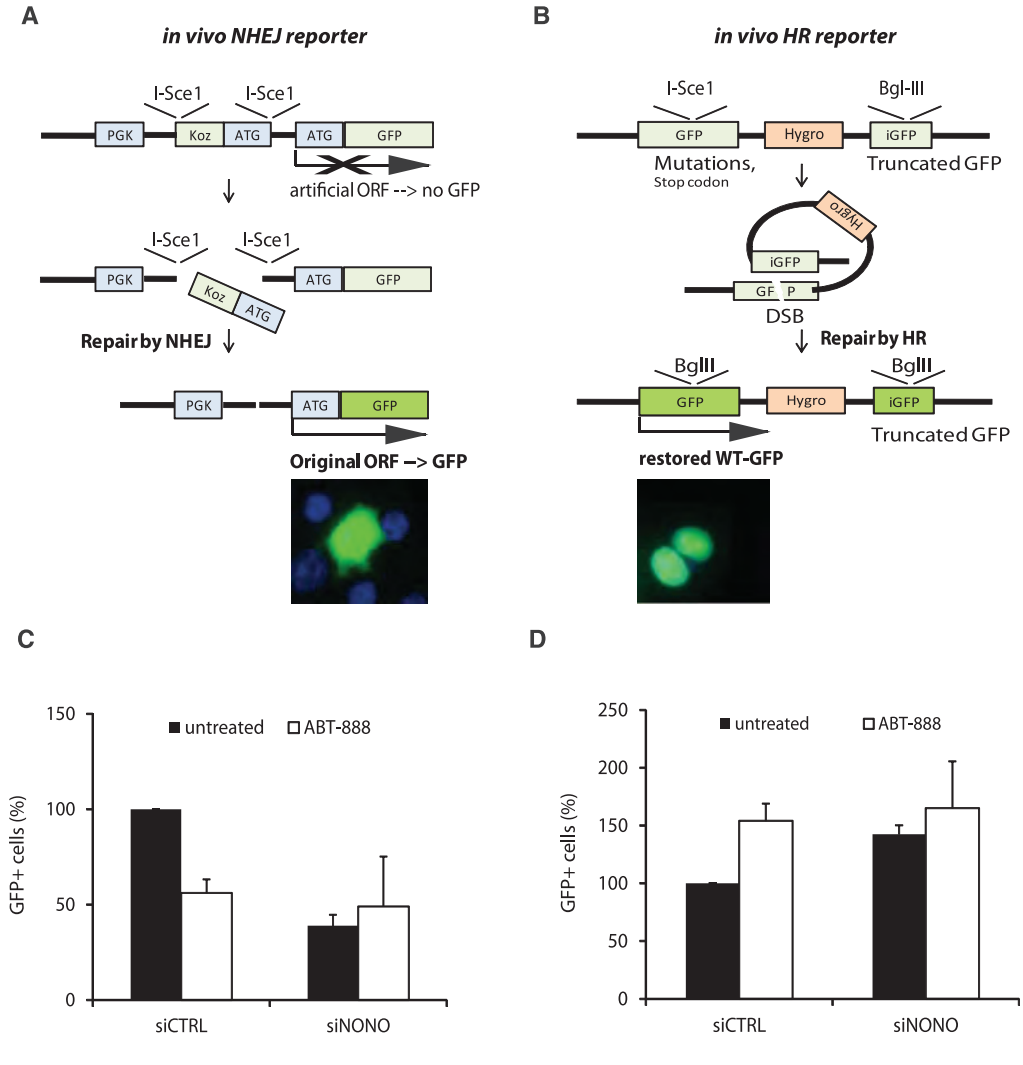

Figure 8. Attenuation of NONO decreases NHEJ and increases HR. (**A**) Schematic representation of the I-SceI-based NHEJ *in vivo* reporter system. (**B**) Schematic representation of the I-SceI-based HR *in vivo* reporter system. (**C**) NHEJ repair rates in percent with siCTRL or siNONO and with or without 10 μM of the PARP-inhibitor ABT-888. The siCTRL condition was normalized to 100% ($n = 3$). (**D**) Diagram of the HR repair rates after treatment with siCTRL or siNONO and with or without 10 μM ABT-888. The siCTRL condition was normalized to 100% ($n = 3$).

MNNG exposure. NONO was identified in SILAC experiments with an enrichment ratio (control versus DNA damage), which is one of the strongest in the pADPr immunoprecipitates (42). Also after neocarzinostatin treatment, we observed a complex between PAR and NONO as well as PARP-1 and NONO (Supplementary Figure S3). We have previously shown that key DNA repair proteins share a high affinity for PAR, the product of catalytically active PARP-1, with many RNA-binding proteins (41). To date, many proteins have been shown to be recruited in a PAR-dependent manner by cell imaging techniques: MRE11 (6), NBS1 (6), APLF (46), XRCC1 (57), CHD4 (58), NuRD (59) and ALC1 (47). However, in none of these studies PAR-dependent recruitment has been directly shown by deleting the PAR-binding module that is necessary for recruitment. We present here for the first time that the RNA-binding protein NONO has a strong and specific affinity for complex PAR *in vitro*, interestingly through its RRM1. We provide several lines of evidence that the recruitment of NONO to DNA lesions is strictly dependent on the presence of PAR. Indeed, we show that NONO relocation to DNA damage sites is suppressed by (I) PARP-1 inhibition with ABT-888; (II) PARG overexpression (the antagonist of PARP-1); (III) loss of PARP-1 expression in PARP-1$^{-/-}$ MEFs and (IV) deleting the PAR-binding motif located within the RRM1. Actually, the characterization of the RRM1 domain of NONO as a PAR-interacting module is consistent with previous studies that also established a similar role for the RRM1 domains of the splicing factor ASF/SF2 (49) and hnRNP A1 (41). It has been suggested that bound PAR competes out RNA-binding properties, therewith modulating the proteins splicing activity. The idea of a direct competition between PAR and RNA for the same site within a protein might also be applicable for RNA-binding proteins in the context of DNA repair. As it is of physiological importance for a cell to stop transcriptional activity (60) and initiate repair in response to excessive DNA damage, the PAR, which is largely generated at DNA damage sites, might serve as a molecular switch to direct proteins from RNA biogenesis toward DNA repair.

Finally, we show that NONO not only facilitates NHEJ but also represses the other major DSB repair pathway, HR, therewith channeling the DSB repair pathway decision between NHEJ and HR. Interestingly, we find that PARP activity has effects similar to NONO on both pathways and the combination of siRNA-mediated knock-down of NONO with an ABT-888 treatment does not show any additive effect. The latter suggests that NONO and PARP act in the same pathway, pointing towards the model of PAR-dependent recruitment of NONO. PARP-1 itself has also been shown to play a role in the back-up NHEJ pathway, but exclusively in the absence of classical NHEJ factors such as Ku80 (56). The role of PARP-1 in recruiting NONO in our system can be seen independent of its role in the backup-NHEJ pathway as we and others have observed that a knock-down of NONO leaves the expression level of proteins acting in the classical NHEJ pathway (Ku70/Ku80, DNA-PK, Ligase IV) unaffected suggesting that our system monitors exclusively classical NHEJ (33). Conclusively, our results place NONO in the very early steps of the DDR after PARP activation, promoting the error-prone NHEJ pathway over error-free HR.

Underpinning the fact that NONO promotes NHEJ over HR, which is an error-prone repair pathway that facilitates mutagenesis, we found by an Oncomine-based search that NONO is over-expressed in a variety of cancer types, such as colorectal and lung cancer. Within the latter two cancer types, NONO is among the top 1% over-expressed genes and therefore a promising candidate to investigate in the context of carcinogenesis. Moreover it has been published only very recently that NONO is implicated in the development and progression of malignant melanoma (61). Further investigation is needed to clarify NONOs possible role as a factor that promotes carcinogenesis.

Collectively, our study strengthens the suggested role for NONO in NHEJ and adds another layer of complexity by showing PAR-dependent recruitment through its principal RNA-binding motif. We have much to learn on NONO, a factor potentially promoting carcinogenesis in the context of PARP-activation as it sheds more light onto the mechanism of action of PARP inhibitors, which have already reached phase III clinical trials but are still poorly understood.

SUPPLEMENTARY DATA

Supplementary Data are available at NAR Online: Supplementary Table 1 and Supplementary Figures 1–3.

ACKNOWLEDGEMENTS

The authors thank members of the Masson and Poirier labs for critical reviewing of the manuscript, Mikaël Bédard for providing us with NONO protein fragments and Yan Coulombe for precious help in microscopy-based studies. They also acknowledge Valérie Schreiber (Université de Strasbourg, France) for the kind gift of Parp2$^{-/-}$ cells. Jana Krietsch is a Fonds de Recherche du Québec Nature et technologies scholar and Julien Vignard is a Canadian Institutes of Health Research postdoctoral fellow. Guy G. Poirier holds a Canada Research Chair in Proteomics and Jean-Yves Masson is a Fonds de Recherche en Santé du Québec senior investigator.

FUNDING

Funding for open access charge: Canadian Institutes of Health Research (to J.-Y.M. and G.G.P.).

Conflict of interest statement. None declared.

REFERENCES

1. Vilenchik,M.M. and Knudson,A.G. (2003) Endogenous DNA double-strand breaks: production, fidelity of repair, and induction of cancer. *Proc. Natl. Acad. Sci. USA*, **100**, 12871–12876.

2. Ciccia,A. and Elledge,S.J. (2010) The DNA damage response: making it safe to play with knives. *Mol. Cell*, **40**, 179–204.
3. Wacker,D.A., Frizzell,K.M., Zhang,T. and Kraus,W.L. (2007) Regulation of chromatin structure and chromatin-dependent transcription by poly(ADP-ribose) polymerase-1: possible targets for drug-based therapies. *Subcell Biochem.*, **41**, 45–69.
4. Bouchard,V.J., Rouleau,M. and Poirier,G.G. (2003) PARP-1, a determinant of cell survival in response to DNA damage. *Exp. Hematol.*, **31**, 446–454.
5. Krishnakumar,R. and Kraus,W.L. (2010) The PARP side of the nucleus: molecular actions, physiological outcomes, and clinical targets. *Mol. Cell.*, **39**, 8–24.
6. Haince,J.F., McDonald,D., Rodrigue,A., Dery,U., Masson,J.Y., Hendzel,M.J. and Poirier,G.G. (2008) PARP1-dependent kinetics of recruitment of MRE11 and NBS1 proteins to multiple DNA damage sites. *J. Biol. Chem.*, **283**, 1197–1208.
7. Slade,D., Dunstan,M.S., Barkauskaite,E., Weston,R., Lafite,P., Dixon,N., Ahel,M., Leys,D. and Ahel,I. (2011) The structure and catalytic mechanism of a poly(ADP-ribose) glycohydrolase. *Nature*, **477**, 616–620.
8. Takata,M., Sasaki,M.S., Sonoda,E., Morrison,C., Hashimoto,M., Utsumi,H., Yamaguchi-Iwai,Y., Shinohara,A. and Takeda,S. (1998) Homologous recombination and non-homologous end-joining pathways of DNA double-strand break repair have overlapping roles in the maintenance of chromosomal integrity in vertebrate cells. *EMBO J.*, **17**, 5497–5508.
9. Lieber,M.R. (2010) The mechanism of double-strand DNA break repair by the nonhomologous DNA end-joining pathway. *Annu Rev. Biochem.*, **79**, 181–211.
10. Gagne,J.P., Isabelle,M., Lo,K.S., Bourassa,S., Hendzel,M.J., Dawson,V.L., Dawson,T.M. and Poirier,G.G. (2008) Proteome-wide identification of poly(ADP-ribose) binding proteins and poly(ADP-ribose)-associated protein complexes. *Nucleic Acids Res.*, **36**, 6959–6976.
11. Li,B., Navarro,S., Kasahara,N. and Comai,L. (2004) Identification and biochemical characterization of a Werner's syndrome protein complex with Ku70/80 and poly(ADP-ribose) polymerase-1. *J. Biol. Chem.*, **279**, 13659–13667.
12. Meek,K., Dang,V. and Lees-Miller,S.P. (2008) DNA-PK: the means to justify the ends? *Adv. Immunol.*, **99**, 33–58.
13. Wang,J., Pluth,J.M., Cooper,P.K., Cowan,M.J., Chen,D.J. and Yannone,S.M. (2005) Artemis deficiency confers a DNA double-strand break repair defect and Artemis phosphorylation status is altered by DNA damage and cell cycle progression. *DNA Repair (Amst)*, **4**, 556–570.
14. Chappell,C., Hanakahi,L.A., Karimi-Busheri,F., Weinfeld,M. and West,S.C. (2002) Involvement of human polynucleotide kinase in double-strand break repair by non-homologous end joining. *EMBO J.*, **21**, 2827–2832.
15. Capp,J.P., Boudsocq,F., Bertrand,P., Laroche-Clary,A., Pourquier,P., Lopez,B.S., Cazaux,C., Hoffmann,J.S. and Canitrot,Y. (2006) The DNA polymerase lambda is required for the repair of non-compatible DNA double strand breaks by NHEJ in mammalian cells. *Nucleic Acids Res.*, **34**, 2998–3007.
16. Capp,J.P., Boudsocq,F., Besnard,A.G., Lopez,B.S., Cazaux,C., Hoffmann,J.S. and Canitrot,Y. (2007) Involvement of DNA polymerase mu in the repair of a specific subset of DNA double-strand breaks in mammalian cells. *Nucleic Acids Res.*, **35**, 3551–3560.
17. Ahnesorg,P., Smith,P. and Jackson,S.P. (2006) XLF interacts with the XRCC4-DNA ligase IV complex to promote DNA nonhomologous end-joining. *Cell*, **124**, 301–313.
18. Giffin,W., Torrance,H., Rodda,D.J., Prefontaine,G.G., Pope,L. and Hache,R.J. (1996) Sequence-specific DNA binding by Ku autoantigen and its effects on transcription. *Nature*, **380**, 265–268.
19. Woodard,R.L., Lee,K.J., Huang,J. and Dynan,W.S. (2001) Distinct roles for Ku protein in transcriptional reinitiation and DNA repair. *J. Biol. Chem.*, **276**, 15423–15433.
20. Beck,B.D., Hah,D.S. and Lee,S.H. (2008) XPB and XPD between transcription and DNA repair. *Adv. Exp. Med. Biol.*, **637**, 39–46.
21. Adamson,B., Smogorzewska,A., Sigoillot,F.D., King,R.W. and Elledge,S.J. (2012) A genome-wide homologous recombination screen identifies the RNA-binding protein RBMX as a component of the DNA-damage response. *Nat. Cell Biol.*, **14**, 318–328.
22. Beli,P., Lukashchuk,N., Wagner,S.A., Weinert,B.T., Olsen,J.V., Baskcomb,L., Mann,M., Jackson,S.P. and Choudhary,C. (2012) Proteomic investigations reveal a role for RNA processing factor THRAP3 in the DNA damage response. *Mol. Cell*, **46**, 212–225.
23. Paulsen,R.D., Soni,D.V., Wollman,R., Hahn,A.T., Yee,M.C., Guan,A., Hesley,J.A., Miller,S.C., Cromwell,E.F., Solow-Cordero,D.E. *et al.* (2009) A genome-wide siRNA screen reveals diverse cellular processes and pathways that mediate genome stability. *Mol. Cell*, **35**, 228–239.
24. Peng,R., Dye,B.T., Perez,I., Barnard,D.C., Thompson,A.B. and Patton,J.G. (2002) PSF and p54nrb bind a conserved stem in U5 snRNA. *RNA*, **8**, 1334–1347.
25. Zhang,Z. and Carmichael,G.G. (2001) The fate of dsRNA in the nucleus: a p54(nrb)-containing complex mediates the nuclear retention of promiscuously A-to-I edited RNAs. *Cell*, **106**, 465–475.
26. Kaneko,S., Rozenblatt-Rosen,O., Meyerson,M. and Manley,J.L. (2007) The multifunctional protein p54nrb/PSF recruits the exonuclease XRN2 to facilitate pre-mRNA 3′ processing and transcription termination. *Genes Dev.*, **21**, 1779–1789.
27. Amelio,A.L., Miraglia,L.J., Conkright,J.J., Mercer,B.A., Batalov,S., Cavett,V., Orth,A.P., Busby,J., Hogenesch,J.B. and Conkright,M.D. (2007) A coactivator trap identifies NONO (p54nrb) as a component of the cAMP-signaling pathway. *Proc. Natl. Acad. Sci. USA*, **104**, 20314–20319.
28. Mathur,M., Tucker,P.W. and Samuels,H.H. (2001) PSF is a novel corepressor that mediates its effect through Sin3A and the DNA binding domain of nuclear hormone receptors. *Mol. Cell Biol.*, **21**, 2298–2311.
29. Dong,X., Sweet,J., Challis,J.R., Brown,T. and Lye,S.J. (2007) Transcriptional activity of androgen receptor is modulated by two RNA splicing factors, PSF and p54nrb. *Mol. Cell Biol.*, **27**, 4863–4875.
30. Ishitani,K., Yoshida,T., Kitagawa,H., Ohta,H., Nozawa,S. and Kato,S. (2003) p54nrb acts as a transcriptional coactivator for activation function 1 of the human androgen receptor. *Biochem. Biophys. Res. Commun.*, **306**, 660–665.
31. Salton,M., Lerenthal,Y., Wang,S.Y., Chen,D.J. and Shiloh,Y. (2010) Involvement of Matrin 3 and SFPQ/NONO in the DNA damage response. *Cell Cycle*, **9**, 1568–1576.
32. Bladen,C.L., Udayakumar,D., Takeda,Y. and Dynan,W.S. (2005) Identification of the polypyrimidine tract binding protein-associated splicing factor.p54(nrb) complex as a candidate DNA double-strand break rejoining factor. *J. Biol. Chem.*, **280**, 5205–5210.
33. Li,S., Kuhne,W.W., Kulharya,A., Hudson,F.Z., Ha,K., Cao,Z. and Dynan,W.S. (2009) Involvement of p54(nrb), a PSF partner protein, in DNA double-strand break repair and radioresistance. *Nucleic Acids Res.*, **37**, 6746–6753.
34. Gagne,J.P., Haince,J.F., Pic,E. and Poirier,G.G. (2011) Affinity-based assays for the identification and quantitative evaluation of noncovalent poly(ADP-ribose)-binding proteins. *Methods Mol. Biol.*, **780**, 93–115.
35. Xie,A., Kwok,A. and Scully,R. (2009) Role of mammalian Mre11 in classical and alternative nonhomologous end joining. *Nat. Struct. Mol. Biol.*, **16**, 814–818.
36. Pierce,A.J., Johnson,R.D., Thompson,L.H. and Jasin,M. (1999) XRCC3 promotes homology-directed repair of DNA damage in mammalian cells. *Genes Dev.*, **13**, 2633–2638.
37. Duriez,P.J., Desnoyers,S., Hoflack,J.C., Shah,G.M., Morelle,B., Bourassa,S., Poirier,G.G. and Talbot,B. (1997) Characterization of anti-peptide antibodies directed towards the automodification domain and apoptotic fragment of poly (ADP-ribose) polymerase. *Biochim. Biophys. Acta*, **1334**, 65–72.
38. Zou,L., Cortez,D. and Elledge,S.J. (2002) Regulation of ATR substrate selection by Rad17-dependent loading of Rad9 complexes onto chromatin. *Genes Dev.*, **16**, 198–208.
39. Rodrigue,A., Lafrance,M., Gauthier,M.C., McDonald,D., Hendzel,M., West,S.C., Jasin,M. and Masson,J.Y. (2006) Interplay between human DNA repair proteins at a unique double-strand break in vivo. *EMBO J.*, **25**, 222–231.
40. Ismail,I.H., Gagne,J.P., Caron,M.C., McDonald,D., Xu,Z., Masson,J.Y., Poirier,G.G. and Hendzel,M.J. (2012)

CBX4-mediated SUMO modification regulates BMI1 recruitment at sites of DNA damage. *Nucleic Acids Res.*, **40**, 5497–5510.
41. Gagne,J.P., Hunter,J.M., Labrecque,B., Chabot,B. and Poirier,G.G. (2003) A proteomic approach to the identification of heterogeneous nuclear ribonucleoproteins as a new family of poly(ADP-ribose)-binding proteins. *Biochem. J.*, **371**, 331–340.
42. Gagne,J.P., Pic,E., Isabelle,M., Krietsch,J., Ethier,C., Paquet,E., Kelly,I., Boutin,M., Moon,K.M., Foster,L.J. *et al.* (2012) Quantitative proteomics profiling of the poly(ADP-ribose)-related response to genotoxic stress. *Nucleic Acids Res*, **40**, 7788–7805.
43. Smith,B.L., Bauer,G.B. and Povirk,L.F. (1994) DNA damage induced by bleomycin, neocarzinostatin, and melphalan in a precisely positioned nucleosome. Asymmetry in protection at the periphery of nucleosome-bound DNA. *J. Biol. Chem.*, **269**, 30587–30594.
44. Povirk,L.F. (1996) DNA damage and mutagenesis by radiomimetic DNA-cleaving agents: bleomycin, neocarzinostatin and other enediynes. *Mutat. Res.*, **355**, 71–89.
45. Tartier,L., Spenlehauer,C., Newman,H.C., Folkard,M., Prise,K.M., Michael,B.D., Menissier-de Murcia,J. and de Murcia,G. (2003) Local DNA damage by proton microbeam irradiation induces poly(ADP-ribose) synthesis in mammalian cells. *Mutagenesis*, **18**, 411–416.
46. Rulten,S.L., Cortes-Ledesma,F., Guo,L., Iles,N.J. and Caldecott,K.W. (2008 Jul) APLF (C2orf13) is a novel component of poly(ADP-ribose) signaling in mammalian cells. *Mol Cell Biol.*, **28**, 4620–4628.
47. Ahel,D., Horejsi,Z., Wiechens,N., Polo,S.E., Garcia-Wilson,E., Ahel,I., Flynn,H., Skehel,M., West,S.C., Jackson,S.P. *et al.* (2009) Poly(ADP-ribose)-dependent regulation of DNA repair by the chromatin remodeling enzyme ALC1. *Science*, **325**, 1240–1243.
48. Fahrer,J., Kranaster,R., Altmeyer,M., Marx,A. and Burkle,A. (2007) Quantitative analysis of the binding affinity of poly(ADP-ribose) to specific binding proteins as a function of chain length. *Nucleic Acids Res.*, **35**, e143.
49. Malanga,M., Czubaty,A., Girstun,A., Staron,K. and Althaus,F.R. (2008) Poly(ADP-ribose) binds to the splicing factor ASF/SF2 and regulates its phosphorylation by DNA topoisomerase I. *J. Biol. Chem.*, **283**, 19991–19998.
50. Haince,J.F., Ouellet,M.E., McDonald,D., Hendzel,M.J. and Poirier,G.G. (2006) Dynamic relocation of poly(ADP-ribose) glycohydrolase isoforms during radiation-induced DNA damage. *Biochim. Biophys. Acta*, **1763**, 226–237.
51. Shav-Tal,Y. and Zipori,D. (2002) PSF and p54(nrb)/NonO—multi-functional nuclear proteins. *FEBS Lett.*, **531**, 109–114.
52. Pankotai,T., Bonhomme,C., Chen,D. and Soutoglou,E. (2012) DNAPKcs-dependent arrest of RNA polymerase II transcription in the presence of DNA breaks. *Nat. Struct. Mol. Biol.*, **19**, 276–282.
53. Polo,S.E., Blackford,A.N., Chapman,J.R., Baskcomb,L., Gravel,S., Rusch,A., Thomas,A., Blundred,R., Smith,P., Kzhyshkowska,J. *et al.* (2012) Regulation of DNA-end resection by hnRNPU-like proteins promotes DNA double-strand break signaling and repair. *Mol. Cell*, **45**, 505–516.
54. Kraus,W.L. (2008) Transcriptional control by PARP-1: chromatin modulation, enhancer-binding, coregulation, and insulation. *Curr. Opin. Cell. Biol.*, **20**, 294–302.
55. Wang,M., Wu,W., Rosidi,B., Zhang,L., Wang,H. and Iliakis,G. (2006) PARP-1 and Ku compete for repair of DNA double strand breaks by distinct NHEJ pathways. *Nucleic Acids Res.*, **34**, 6170–6182.
56. Mansour,W.Y., Rhein,T. and Dahm-Daphi,J. (2010) The alternative end-joining pathway for repair of DNA double-strand breaks requires PARP1 but is not dependent upon microhomologies. *Nucleic Acids Res.*, **38**, 6065–6077.
57. El-Khamisy,S.F., Masutani,M., Suzuki,H. and Caldecott,K.W. (2003) A requirement for PARP-1 for the assembly or stability of XRCC1 nuclear foci at sites of oxidative DNA damage. *Nucleic Acids Res.*, **31**, 5526–5533.
58. Polo,S.E., Kaidi,A., Baskcomb,L., Galanty,Y. and Jackson,S.P. (2010) Regulation of DNA-damage responses and cell-cycle progression by the chromatin remodelling factor CHD4. *EMBO J.*, **29**, 3130–3139.
59. Chou,D.M., Adamson,B., Dephoure,N.E., Tan,X., Nottke,A.C., Hurov,K.E., Gygi,S.P., Colaiacovo,M.P. and Elledge,S.J. (2010) A chromatin localization screen reveals poly(ADP ribose)-regulated recruitment of the repressive polycomb and NuRD complexes to sites of DNA damage. *Proc. Natl. Acad. Sci. USA*, **107**, 18475–18480.
60. Shanbhag,N.M., Rafalska-Metcalf,I.U., Balane-Bolivar,C., Janicki,S.M. and Greenberg,R.A. (2010) ATM-dependent chromatin changes silence transcription in cis to DNA double-strand breaks. *Cell*, **141**, 970–981.
61. Schiffner,S., Zimara,N., Schmid,R. and Bosserhoff,A.K. (2011) p54nrb is a new regulator of progression of malignant melanoma. *Carcinogenesis*, **32**, 1176–1182.

Molecular Aspects of Medicine 34 (2013) 1066–1087

Contents lists available at SciVerse ScienceDirect

Molecular Aspects of Medicine

journal homepage: www.elsevier.com/locate/mam

Review

Reprogramming cellular events by poly(ADP-ribose)-binding proteins

Jana Krietsch [a,b,1], Michèle Rouleau [a,c,1], Émilie Pic [a], Chantal Ethier [a], Ted M. Dawson [d,e,g], Valina L. Dawson [d,e,f,g], Jean-Yves Masson [b,c], Guy G. Poirier [a,c], Jean-Philippe Gagné [a,*]

[a] Centre de recherche du CHUQ – Pavillon CHUL – Cancer Axis, Laval University, Québec, QC, Canada G1V 4G2
[b] Genome Stability Laboratory, Laval University Cancer Research Center, Hôtel-Dieu de Québec, Québec, QC, Canada G1R 2J6
[c] Department of Molecular Biology, Cellular Biochemistry and Pathology, Faculty of Medicine, Laval University, Québec, QC, Canada G1V 0A6
[d] Neuroregeneration and Stem Cell Programs, Institute for Cell Engineering, Johns Hopkins University School of Medicine, Baltimore, MD 21205, USA
[e] Department of Neurology, Johns Hopkins University School of Medicine, Baltimore, MD 21205, USA
[f] Department of Physiology, Johns Hopkins University School of Medicine, Baltimore, MD 21205, USA
[g] Solomon H. Snyder Department of Neuroscience, Johns Hopkins University School of Medicine, Baltimore, MD 21205, USA

ARTICLE INFO

Article history:
Available online 23 December 2012

Keywords:
PARP
PARG
Poly(ADP-ribose)
WWE
PBZ
Macro domain

ABSTRACT

Poly(ADP-ribosyl)ation is a posttranslational modification catalyzed by the poly(ADP-ribose) polymerases (PARPs). These enzymes covalently modify glutamic, aspartic and lysine amino acid side chains of acceptor proteins by the sequential addition of ADP-ribose (ADPr) units. The poly(ADP-ribose) (pADPr) polymers formed alter the physico-chemical characteristics of the substrate with functional consequences on its biological activities. Recently, non-covalent binding to pADPr has emerged as a key mechanism to modulate and coordinate several intracellular pathways including the DNA damage response, protein stability and cell death. In this review, we describe the basis of non-covalent binding to pADPr that has led to the emerging concept of pADPr-responsive signaling pathways. This review emphasizes the structural elements and the modular strategies developed by pADPr-binding proteins to exert a fine-tuned control of a variety of pathways. Poly(ADP-ribosyl)ation reactions are highly regulated processes, both spatially and temporally, for which at least four specialized pADPr-binding modules accommodate different pADPr structures and reprogram protein functions. In this review, we highlight the role of well-characterized and newly discovered pADPr-binding modules in a diverse set of physiological functions.

Contents

* Corresponding author. Address: Centre de Recherche du CHUQ – CHUL, 2705 Boulevard Laurier, Québec, QC, Canada G1V 4G2. Tel.: +1 418 654 2267; fax: +1 418 654 2159.
E-mail address: jean-philippe.gagne@crchul.ulaval.ca (J.-P. Gagné).
[1] These authors contributed equally to this work.

0098-2997/$ - see front matter © 2013 Elsevier Ltd. All rights reserved.
http://dx.doi.org/10.1016/j.mam.2012.12.005

1. Introduction

It was almost 50 years ago that poly(ADP-ribose) (pADPr) was discovered as an adenine-containing RNA-like polymer (Chambon et al., 1963) and early on, there were indications that pADPr turnover is very tightly regulated in mammalian cells (Nishizuka et al., 1967; Reeder et al., 1967; Ueda et al., 1972). Cellular levels of pADPr are governed by the finely tuned balance of the synthetic poly(ADP-ribose) polymerases (PARPs) and degrading poly(ADP-ribose) glycohydrolase (PARG) enzyme activities. In the human genome, 17 proteins share a PARP signature sequence homologous to the catalytic domain of the founding and most described member PARP1. In the context of DNA damage, PARP1 generates within minutes approximately 90% of all pADPr, preferentially on itself (automodification). However, pADPr accumulation is transient, as it is rapidly degraded by PARG (Davidovic et al., 2001). Notably, the polymerase activity has been demonstrated for only six of the PARP family members (PARP1, PARP2, PARP3, PARP4/vPARP, Tankyrases 1 and 2). Based on experimental and structural examinations, it has been proposed that the other PARP family members are either inactive (PARP9/BAL and PARP13/ZAP) or carry a mono-ADP-ribosyl transferase activity (PARP6, TiPARP, PARP8, PARP10, PARP11, PARP12, PARP14/BAL2, PARP15/BAL3, PARP16) (Goenka et al., 2007; Hottiger et al., 2010; Kleine et al., 2008). Their functions are only starting to emerge, but suggest an important role for these poorly studied proteins.

1.1. Poly(ADP-ribosyl)ation

The seminal work by Benjamin and Gill (1980a,b) showed that PARP1 activity is highly stimulated by the presence of DNA containing single- and double-strand breaks, a discovery that has been followed up by a succession of studies that linked pADPr metabolism to maintenance of genome stability (Meyer-Ficca et al., 2005). Mono- and poly-(ADP-ribosyl)ation are reversible and phylogenetically ancient posttranslational protein modifications, for which the list of acceptor/target proteins is still expanding. Poly(ADP-ribosyl)ation can be achieved covalently or non-covalently (Fig. 1A). The covalent posttranslational modification (PTM) occurs on glutamic, aspartic or lysine residues, while non-covalent interactions between proteins and pADPr add another level for modulating proteins biological activity. This PTM has profound physico-chemical implications, as poly(ADP-ribose) bears two negatively charged phosphate groups per ADP-ribose (ADPr) residue, i.e. twice as many charges than DNA or RNA (Fig. 1A). The size and flexibility of pADPr polymers render them capable of mediating multiple contacts with protein surfaces, thus providing a significant enhancement in binding efficiency. Such physico-chemical attributes of the pADPr are capable of contributing to the creation of a scaffold for the assembly of multiprotein complexes. Accumulating evidence indicates that pADPr actually conveys a broad spectrum of cellular signals through direct binding of a variety of protein motifs to pADPr, such as the DNA damage response, replication, chromatin structure, transcription, telomere homeostasis and cell death (Krishnakumar and Kraus, 2010).

Given the structural complexity of the pADPr polymers, it is not surprising to observe that several evolutionary conserved protein domains have emerged to accomplish unique functions through interactions with pADPr. Indeed, the average chain length of pADPr synthesized by the PARP family members can range from very short and linear oligomers to extended molecules of up to 200 units and branched at every 20–50 residues (Fig. 1B) (Alvarez-Gonzalez and Jacobson, 1987; D'Amours et al., 1999; Kiehlbauch et al., 1993; Kleine et al., 2008; Tanaka et al., 1977). There are very limited investigations conducted on the physico-chemical properties of pADPr, such as flexibility and conformation, but the formation of helical pADPr structures was postulated upon protein binding (Minaga and Kun, 1983a,b; Schultheisz et al., 2009).

1.2. The emergence of non-covalent pADPr recognition motifs

The first experimental lines of evidence for proteins that bind pADPr in a non-covalent, yet specific, manner were given in the late 1960s and early 1970s when it was shown that histones possess high affinity for pADPr (Honjo et al., 1968; Nakaz-

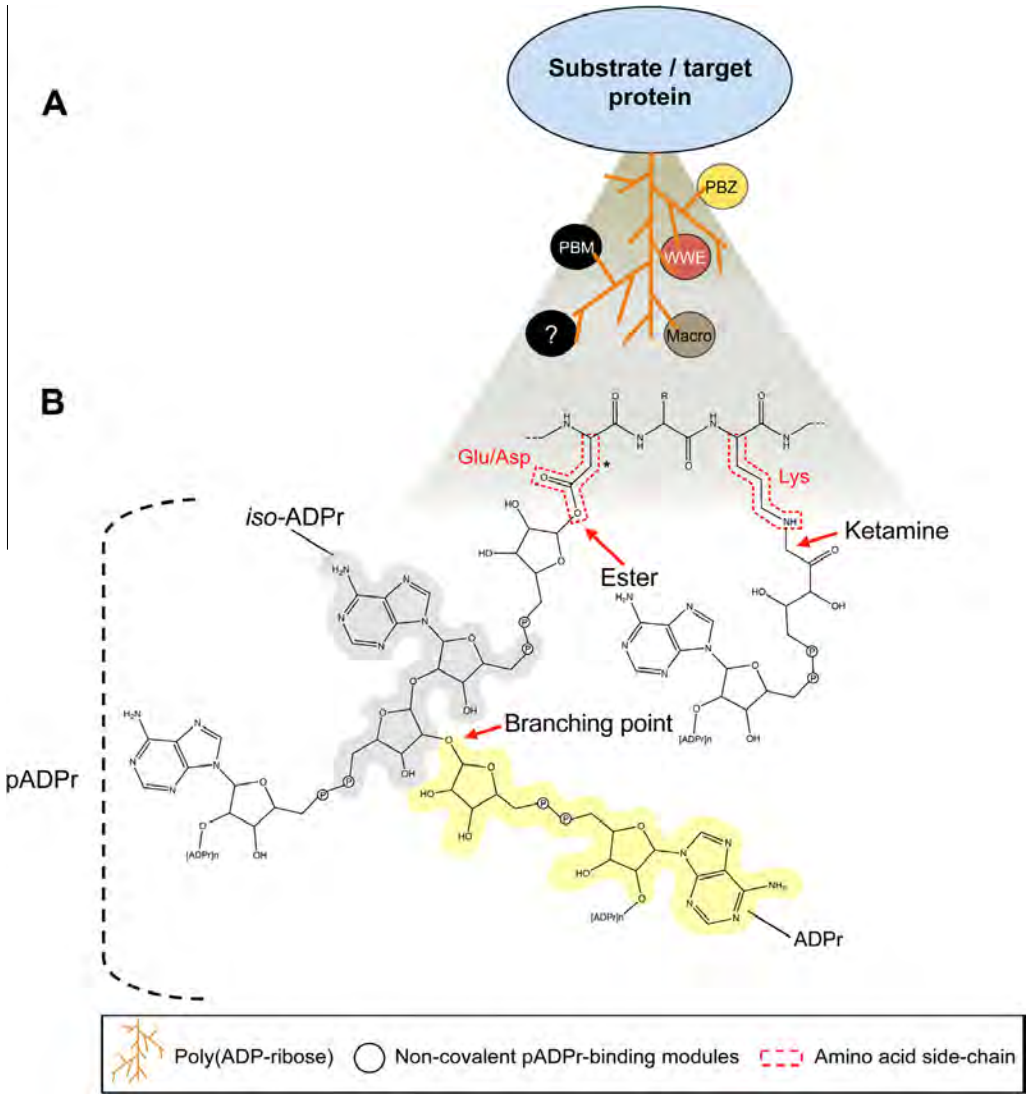

Fig. 1. Covalent and non-covalent mechanisms of protein regulation by poly(ADP-ribosyl)ation. (A) The posttranslational modification of a protein substrate by enzymatic covalent attachment of poly(ADP-ribose) (pADPr) to specific amino acids side chains is represented. On the pADPr structure, a collection of modular protein domains non-covalently binds to pADPr through different recognition mechanisms. There are currently four pADPr-binding protein modules that have been experimentally characterized: the pADPr-binding motif (PBM); pADPr-binding zinc finger motif (PBZ); the macro domain (Macro) and the WWE domain (WWE). Experimental evidence suggests that other protein modules and sequence motifs can read this modification (see Section 3). (B) Detailed view of the covalent poly(ADP-ribosyl)ation. The proximal ADP-ribose (ADPr) is bound by an ester linkage to glutamic (Glu) and aspartic (Asp) amino acid side chains (the asterisk indicates one or two CH_2 units to represent the respective side chains of Asp or Glu) or to lysine (Lys) side chains via a ketamine linkage. The mechanism that determines selective modification of specific residues and the functional significance of this heterogeneity are not known. Additional ADP-ribose units are subsequently attached by O-glycosidic linkages to form linear or branched pADPr. Some components of the pADPr chemical structure recognized by pADPr-binding modules are shown: *iso*-ADPr, grey shadow, ADPr, yellow shadow.

awa et al., 1968; Otake et al., 1969). However, whether the chemical nature of the bond was covalent or non-covalent was a highly debated topic (Adamietz et al., 1975). At that time, the prevailing view was that poly(ADP-ribosyl)ation was a covalent protein posttranslational modification on histones as is phosphorylation or methylation. This concept persisted for years until the 1980s when studies began to report interactions with PARP1-bound pADPr (Ohashi et al., 1983) and free pADPr (Sauermann and Wesierska-Gadek, 1986; Wesierska-Gadek and Sauermann, 1988). In the last decade, rapid progress has been achieved in the identification of pADPr-binding proteins among some of the chromatin-associated non-histone proteins and proteins involved in extranuclear signaling networks. Remarkably, more than four specialized pADPr-binding modules that recognize different structural features of the pADPr are responsible for the functional diversification of the pADPr-responsive cellular pathways. This paper first provides an inventory of the predominant techniques currently used to detect and measure non-covalent protein–pADPr interactions, then turns to an in-depth description of the specialized pADPr-binding modules that recognize different structural features of the pADPr, and finally, presents the functional consequences of this association in pADPr-responsive cellular pathways.

2. Affinity of pADPr-binding domains to ADP-ribose metabolites

Over the years, several different techniques have been developed to characterize the interaction of pADPr with proteins (Gagne et al., 2011). Polymer-blot and electrophoretic mobility shift assays (EMSA) are currently used to determine whether there is binding or not, while isothermal titration calorimetry (ITC), surface plasmon resonance (SPR) and a variation of the EMSA method allow to measure the affinity for pADPr by determining an affinity constant. The polymer-blot assay has also been exploited in saturation binding experiments to determine binding affinity (Wang et al., 2011).

Owing to its simplicity, the polymer-blot assay is the most frequently used method to study pADPr-binding proteins (Gagne et al., 2011). Proteins of interest are either hand-spotted, vacuum-aspirated or separated on a polyacrylamide gel prior to being transferred and renatured onto a nitrocellulose membrane. The interaction with pADPr is subsequently revealed by incubating the membrane with purified label-free pADPr, [^{32}P]-radiolabeled pADPr or biotin-labeled pADPr. Bound pADPr is detected with anti-pADPr antibodies, by autoradiographic exposure or streptavidin conjugates, respectively. This technique is also used with peptide arrays to map the pADPr-binding regions of a protein. In this assay, peptides are chemically synthesized to represent the sequence of putative pADPr-binding sites, such as those predicted *in silico* based on consensus motifs (e.g. PBM, see Section 3.1). EMSA was developed to characterize pADPr–protein non-covalent interactions in solution (Fahrer et al., 2007). Incubations are made in the presence of pADPr and increasing concentrations of a purified protein. Protein-pADPr complexes are subsequently resolved by gel electrophoresis. Free and bound pADPr are detected using a streptavidin conjugate. A shift in the mobility of the protein indicates the formation of a protein–ligand complex. Since all measurements are made at equilibrium, the binding affinities can be calculated using a sigmoidal dose–response curve.

ITC and SPR are elegant label-free biophysical methods specifically designed to study the interaction kinetics between a ligand (such as pADPr) and a target protein. ITC measures the binding affinity and thermodynamics between two biomolecules in solution. In this method, a solution that contains a ligand is titrated into a solution of its binding partner until saturation is reached. A complete thermodynamic profile of the molecular interaction as well as the binding affinity (K_D) are calculated from the heat released or absorbed over time during the interaction. SPR measures in real-time the refractive index changes near a sensor surface. A ligand (such as biotinylated pADPr) is immobilized on the surface of a solid support (chip) and the analyte (protein of interest) is passed over the surface to make contacts with the ligand. Interactions induce a change in the refractive index proportional to the mass on the surface. The data are fitted to a kinetic model to calculate the rate of association (ka), the rate of dissociation (kd) and the binding affinity (K_D = kd/ka).

Each of these methods may also be conducted using fractionated pADPr, allowing further characterization of the binding specificity of a protein for long or short pADPr. In addition, SPR and ITC methods are amenable to determine the critical amino acid residues implicated in the binding of pADPr. Site-specific mutagenesis of critical residues that mediate pADPr-binding typically leads to at least a 10-fold reduction in binding affinity. Collectively, these methods have therefore been critical in characterizing the pADPr binding modules that are described in the following Section 3.

3. Protein modules involved in non-covalent interactions with poly(ADP-ribose)

3.1. PBM: The poly(ADP-ribose)-binding motif

The notion of non-covalent pADPr-binding was originally demonstrated with histones (Sauermann and Wesierska-Gadek, 1986; Wesierska-Gadek and Sauermann, 1988) and later better characterized using pADPr of different lengths and branching frequencies (Panzeter et al., 1992, 1993). This concept was further extended to non-histone proteins such as p53, DNA-PK or KU70/80 and led to the definition of a common polymer-binding domain of 22–26 amino acids that conveyed the specific affinity for pADPr (Table 1) (Althaus et al., 1999; Malanga et al., 1998). Notably, the Althaus group had a strong intuition when they raised the innovative hypothesis that "*PARP-associated polymers may recruit signal proteins to sites of DNA breakage and reprogram their functions*" (Althaus et al., 1999).

The first defined pADPr-binding motif (PBM) was derived from a region of high similarity in a multiple sequence alignment of proteins involved in signaling pathways that control cell cycle progression and DNA damage (Pleschke et al., 2000). This PBM is composed of a property-based sequence motif harboring basic and hydrophobic residues downstream of a lysine- and arginine-rich region (Fig. 2A). Consistent with their previous observation with histones, the authors reported that long and branched pADPr are the preferred ligands of non-chromatin proteins comprising the PBM (Panzeter et al., 1992, 1993; Pleschke et al., 2000).

To better define and address prediction accuracy of the PBM, we adopted a strategy based on a refinement of the consensus PBM motif (Gagne et al., 2008). We showed that restrictions to specific amino acid types exist for positions within the PBM (Fig. 2B). The previously reported preference for hydrophobic residues [ACGVILMFYW] was recovered, but there was a clear tendency for limited residue types to be allowed (mostly aliphatic residues), especially at position −1, +1 and +2 relative to the central K/R doublet (Fig. 2B). Clearly, the PBM refers to the conservation of a physical property pattern rather than a fixed sequence motif. The refined motif offers a more stringent definition of the original motif that decreases the probability of a PBM arising by chance in a protein database search. Computational PBM prediction has proven to be a powerful tool for the identification of protein regions that could mediate interaction with pADPr. They have been shown to convey important functions in animal models. Notably, the PBM discovered in the apoptosis-inducing factor (AIF) is critical for

Table 1
List and functional classification of experimentally demonstrated pADPr-binding proteins.[a]

Description	Motif[b]	pADPr-dependent recruitment at DNA damages[c]	References
DNA damage response and checkpoint			
Aprataxin	n.d	+	Harris et al. (2009)
Aprataxin and PNK-like factor (APLF)	PBZ	+	Eustermann et al. (2010), Li et al. (2010), Rulten et al. (2008) and Rulten et al. (2011)
Cellular tumor antigen p53	PBM		Fahrer et al. (2007) and Pleschke et al. (2000)
Cyclin-dependent kinase inhibitor 1 (p21)	PBM		Pleschke et al. (2000)
DNA excision repair protein ERCC-6	PBM		Gagne et al. (2008)
DNA ligase 3	PBM	+	Gagne et al. (2012), Leppard et al. (2003) and Pleschke et al. (2000)
DNA mismatch repair protein MSH6	PBM		Pleschke et al. (2000)
DNA polymerase epsilon catalytic subunit A (POL ε)	PBM		Pleschke et al. (2000)
DNA repair protein complementing XP-A cells	PBM		Fahrer et al. (2007), Pleschke et al. (2000)
DNA repair protein complementing XP-C cells	n.d	+	Luijsterburg et al. (2012)
DNA repair protein XRCC1	PBM	+	El-Khamisy et al. (2003), Gagne et al. (2012), Mortusewicz and Leonhardt (2007), Pleschke et al. (2000)
DNA topoisomerase 1 (TOP1)	PBM		Malanga and Althaus (2004)
DNA topoisomerase 2-alpha (TOP2A)	PBM		Malanga and Althaus (2005)
DNA-dependent protein kinase catalytic subunit (DNA-PK)	PBM		Pleschke et al. (2000)
Double-strand break repair protein MRE11A	PBM/ GAR	+	Haince et al. (2008)
E3 ubiquitin-protein ligase RNF146 (Iduna)	WWE	+	Andrabi et al. (2011), Callow et al. (2011), Kang et al. (2011), Wang et al. (2012) and Zhou et al. (2011)
Flap endonuclease 1 (FEN1)	n.d	+	Gagne et al. (2012) and Kleppa et al. (2012)
Histone H2A	PBM		Pleschke et al. (2000)
Histone H2B	PBM		Pleschke et al. (2000)
Histone H3	PBM		Pleschke et al. (2000)
Histone H4	PBM		Pleschke et al. (2000)
Nibrin (NBS1)	n.d	+	Haince et al. (2008)
Non-POU domain-containing octamer-binding protein (NONO)	RRM1	+	Krietsch et al. (2012)
RNA-binding motif protein, X chromosome (RBMX)	n.d	+	Adamson et al. (2012)
Serine-protein kinase ATM	PBM		Haince et al. (2007)
X-ray repair cross-complementing protein 6 (XRCC6 / KU70)	PBM		Pleschke et al. (2000)
Werner syndrome ATP-dependent helicase (WRN)	PBM		Popp et al. (2012)
Chromatin regulation and modification			
Core histone macroH2A1.1	Macro	+	Xu et al. (2012)
O-acetyl-ADP-ribose deacetylase MACROD1	Macro		Neuvonen and Ahola (2009)
Chromodomain-helicase-DNA-binding protein 1-like (CHD1L/ALC1)	Macro	+	Ahel et al. (2009), Gottschalk et al. (2009)
Chromodomain-helicase-DNA-binding protein 4 (CHD4)	n.d.	+	Chou et al. (2010), Polo et al. (2010)
Chromodomain-helicase-DNA-binding protein Mi-2 homolog (dMi-2)	K/R-rich		Murawska et al. (2011)
Condensin complex subunit 1 (hCAP-D2)	PBM		Gagne et al. (2008)
DNA methyltransferase 1 (DNMT1)	PBM		Reale et al. (2005) and Zampieri et al. (2012)
E3 SUMO-protein ligase CBX4	n.d	+	Ismail et al. (2012)
Metastasis-associated protein MTA1	n.d	+	Chou et al. (2010)
Polycomb complex protein BMI-1	n.d	+	Gieni et al. (2011)
Protein DEK	PBM		Fahrer et al. (2010)
Apoptosis			
Apoptosis-inducing factor 1, mitochondrial (AIF)	PBM		Wang et al. (2011)
DNA fragmentation factor subunit beta (DFF40/CAD)	PBM		Pleschke et al. (2000), Reh et al. (2005) and West et al. (2005)
E3 ubiquitin-protein ligase RNF146 (Iduna)	WWE	+	Andrabi et al. (2011), Callow et al. (2011), Kang et al. (2011), Wang et al. (2012) and Zhou et al. (2011)
Hexokinase domain-containing protein 1 (HKDC1)	PBM		Gagne et al. (2008)
Transcription, replication and gene expression			
Cellular tumor antigen p53	PBM		Pleschke et al. (2000)
DNA topoisomerase 1 (TOP1)	PBM		Malanga and Althaus, 2004
DNA topoisomerase 2-alpha (TOP2A)	PBM		Malanga and Althaus, 2005
DNA topoisomerase 2-beta (TOP2B)	PBM		Gagne et al. (2008)
E3 SUMO-protein ligase PIAS4 (PIASy)	PBM		Stilmann et al. (2009)
Heterogeneous nuclear ribonucleoprotein A1 (hnRNP A1)	PBM		Gagne et al. (2003,2008), Ji and Tulin (2009, 2012)
NF-kappa-B essential modulator (NEMO/IKKγ)	n.d		Stilmann et al. (2009)
SARS coronavirus non-structural protein nsp3	Macro		Egloff et al. (2006)

Table 1 (*continued*)

Description	Motif[b]	pADPr-dependent recruitment at DNA damages[c]	References
Nuclear factor NF-kappa-B p100 subunit	PBM		Pleschke et al. (2000)
Polycomb group RING finger protein 2 (MEL-18/RNF110)	n.d	+	Chou et al. (2010)
RNA-binding motif protein, X chromosome (RBMX)	n.d	+	Adamson et al. (2012)
Serine/arginine-rich splicing factor 1 (ASF/SF2)	RRM1 / SR		Malanga et al. (2008)
Telomerase reverse transcriptase (TERT)	PBM		Pleschke et al. (2000)
Transcriptional repressor CTCF	PBM		Caiafa et al. (2009)
G3BP1	PBM		Isabelle et al. (2012)
Centromere function and cell cycle checkpoint			
Aurora kinase A-interacting protein	PBM		Gagne et al. (2008)
E3 ubiquitin-protein ligase CHFR	PBZ	+	Gagne et al. (2012), Isogai et al. (2010) and Oberoi et al. (2010)
Histone H3-like centromeric protein A (CENP-A)	PBM		Gagne et al. (2008) and Saxena et al. (2002)
Major centromere autoantigen B (CENP-B)	PBM		Saxena et al. (2002)
Mitotic checkpoint protein BUB3	PBM		Gagne et al. (2008) and Saxena et al. (2002)
Others			
Capsid protein viral protein 1 (VP1)	PBM		Carbone et al. (2006)
Heat shock factor (HSF-1)	PBM		Fossati et al. (2006)
Major vault protein	PBM		Gagne et al. (2008)
Myristoylated alanine-rich C-kinase substrate (MARCKS)	PBM		Pleschke et al. (2000) and Schmitz et al. (1998)
Nicotinamide mononucleotide adenylyltransferase 1 (NMNAT-1)	PBM		Berger et al. (2007)
Nitric oxide synthase, inducible (iNOS)	PBM		Pleschke et al. (2000)

[a] Listed proteins were retrieved from studies that specifically addressed the direct non-covalent binding to pADPr.
[b] n.d. not determined.
[c] Proteins shown to accumulate at DNA-damage sites in a pADPr-dependent fashion.

the ability of AIF to induce cell death by parthanatos (PARP1-dependent cell death) in cells and *in vivo* (Wang et al., 2011). A detailed PBM-pADPr complex has yet to be modeled but a study of the structural features of AIF's PBM showed that it occupies an area on the surface of the protein which could provide stabilizing non-covalent contacts of amino acid side chains with pADPr (Wang et al., 2011). We can only speculate as to whether all PBMs possess common structural features, but a highly exposed solvent-accessible surface must be present to make contacts with pADPr molecules. Based on the helix propensity scale, positively charged amino acids (K/R) have a tendency to form α-helices (Pace and Scholtz, 1998). Since PBMs are located in lysine- and arginine-rich regions, it would be likely to find several of them in a helical conformation.

A summary of pADPr-binding proteins for which binding affinity constants have been determined is given in Table 2. Of particular interest, several reports have shown that pADPr chain length is a crucial determinant for high affinity non-covalent interactions of PBM proteins with pADPr. The binding of the tumor suppressor protein p53, the nucleotide excision repair XPA, and the DEK oncoprotein with long (55-mer) and short (16-mer) pADPr chains were assessed by EMSA and SPR

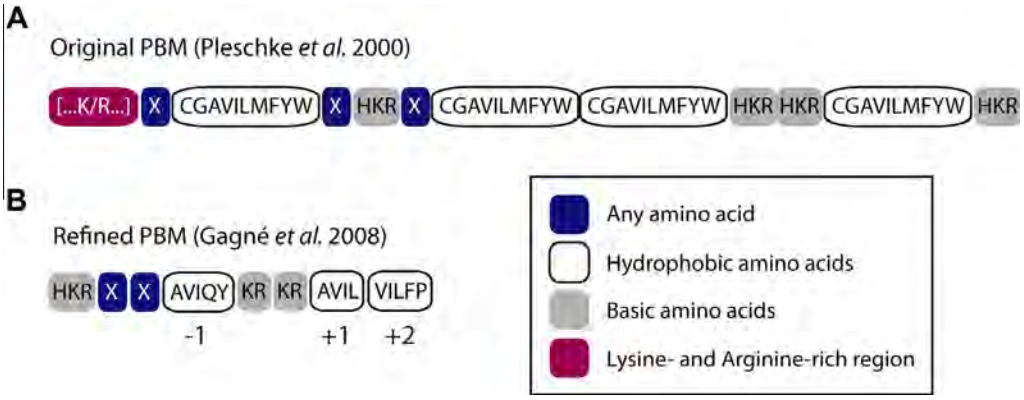

Fig. 2. The non-covalent pADPr-binding motif (PBM). (A) The first PBM has been described by Pleschke and collaborators (2000) in a variety of DNA damage repair and checkpoint proteins. The motif is primarily composed of a hydrophobic and basic amino acid core flanked by a cluster of positively charged residues [. . .K/R. . .]. Each box represents one amino acid position. (B) A refinement of the motif was proposed by Gagne et al. (2008) based on a number of PBM variations found in human proteins. The refined pADPr-binding signature confirmed the overall basic nature of the PBM but represents a minimal stand-alone version of the motif, the K/R-rich N-terminal cluster being dispensable for efficient binding. Outside the dual [KR][KR] site, there are additional preferences for hydrophobic amino acids (positions −1, +1 and +2), mostly those with alkyl side chains. The basic [KR][KR] doublet is an important requirement for the PBM since most substitutions in this region result in a substantially reduced binding affinity for pADPr.

Table 2
List of pADPr-binding proteins with experimentally determined affinity constant (K_D).

	Protein/ peptide/ domain	Method	*O*-acetyl-ADPr K_D [M]	*iso*-ADPr K_D [M]	ADP-ribose K_D [M]	Short pADPr K_D [M]	Long pADPr K_D [M]	NF[d] pADPr K_D [M]	Refs.
PBM	XPA	EMSA				NB[b]	3.2×10^{-7}		Fahrer et al. (2010)
	"	SPR				NB	6.5×10^{-9}		Fahrer et al. (2007)
	p53	EMSA				2.5×10^{-7}	1.3×10^{-7}		Fahrer et al. (2010)
	"	SPR				3.4×10^{-9}	NM[c]		Fahrer et al. (2007)
	DEK	EMSA				NB	6.1×10^{-8}		Fahrer et al. (2010)
	XRCC1	SPR						3.6×10^{-8}	Ahel et al. (2008)
	NONO	SPR				NB	2.01×10^{-8}	2.32×10^{-8}	Krietsch et al. (2012)
	AIF	PBA[a]						6.63×10^{-8}	Wang et al. (2011)
PBZ	CHFR	SPR						5×10^{-10}	Ahel et al. (2008)
	"	SPR						7×10^{-9}	Oberoi et al. (2010)
	APLF	SPR						9×10^{-10}	Ahel et al. (2008)
	APLF/TZF peptide	SPR						9.5×10^{-10}	Li et al. (2010)
	APLF/ZF1 peptide	SPR						5.2×10^{-7}	Li et al. (2010)
	APLF/ZF2 peptide	SPR						8.3×10^{-6}	Li et al. (2010)
Macro	macroH2A1.1	ITC	2.6×10^{-6}						Kustatscher et al., (2005)
	MACROD1	ITC			9×10^{-7}				Neuvonen and Ahola (2009)
	MACROD2	ITC			1.5×10^{-7}				Neuvonen and Ahola (2009)
WWE	Iduna/RNF146	PBA						1.2×10^{-8}	Andrabi et al. (2011)
	Iduna/RNF146 WWE domain	ITC		3.7×10^{-7}	1.7×10^{-3}				He et al., (2012), Wang et al. (2012)
	HUWE1 WWE domain	ITC		1.3×10^{-5}					Wang et al. (2012)
	PARP11 WWE domain	ITC			4.0×10^{-4}				He et al. (2012)

[a] PBA, polymer-blot assay.
[b] NB, no binding.
[c] NM, no model found to describe the binding.
[d] NF, non-fractionated pADPr.

(Fahrer et al., 2007, 2010). These experiments revealed the high affinity (10^{-7} to 10^{-9} M range) of XPA and DEK to long pADPr chains but the lack of binding to short pADPr while p53 bound both short and long chains of pADPr with equivalent affinity.

Remarkably, PBMs are present in a marked number of proteins involved in the response to DNA damage and other chromatin transactions such as chromatin structure, replication and transcription (Table 1). Furthermore, the PBM often overlaps with important regulatory protein domains (Pleschke et al., 2000). This has triggered the idea that upon binding to pADPr, the PBM could shield a regulatory surface by steric hindrance, thus destabilizing several protein–protein or protein–ligand interactions. Alternatively, a highly extended and flexible polymer bound to a protein domain could distort it so that perturbations of the native fold may arise. Globally, molecular crowding by the pADPr provides the basis for the concept of "reprogrammation" of protein functions as suggested (Malanga and Althaus, 2005). Actually, the affinity of several DNA damage response factors for pADPr can modulate (I) the sensing of DNA lesions; (II) the dynamic chromatin remodeling events and (III) the assembly and functionality of DNA repair complexes. We believe that the transient accumulation of pADPr following DNA-dependent PARP activation can result in vast pleiotropic effects on a systems-wide scale that implicates numerous DNA damage response effectors. This is supported by the predominant presence of nucleic acid-interacting proteins in the PBM's prediction datasets (Gagne et al., 2008). Indeed, DNA- and RNA-binding modules are significantly over-represented as putative pADPr-binding modules and thus represent a general class of pADPr-targeted proteins with potential for broad implication in the DNA damage response. However, in some proteins, the PBM is distinct from the nucleic acid binding domains, such as in AIF, providing the ability of pADPr to modulate protein function in the context of nucleic acid binding. Generally, proteins associate in multi-protein complex machineries that execute biological processes that a single protein cannot execute alone. Macromolecules that disrupt or stabilize such complexes drive a wide variety of cellular processes. pADPr possesses the biochemical and structural properties to fulfill such functions through non-covalent interactions.

3.2. Alternative PBMs

Similar to DNA and RNA, the pADPr carries a net negative charge due to its phosphate backbone. Because these three macromolecules tend to bind positively charged protein domains, some competition exists among DNA, RNA or pADPr for the same binding site in specific cellular contexts. Indeed, in addition to the classical PBM, recent studies suggest alternative PBMs located in nucleic acid-interaction domains.

3.2.1. The glycine- and arginine-rich domain (GAR)

The glycine- and arginine-rich domain (GAR) lacks hydrophobic amino acids commonly found in PBMs. This region rather accumulates a very high positive charge owing to the presence of a repetition of arginine residues, thus making it an ideal

binding surface for a polymer with a high negative charge density such as the pADPr. The GAR, also referred to as RGG box and the RG domain, is a protein module typically found in proteins involved in RNA metabolism (Burd and Dreyfuss, 1994) as well as in some chromatin associated proteins (Bernstein and Allis, 2005; Kornblihtt et al., 2009). Selected examples include fibrillarin (FBL), heterogeneous nuclear ribonucleoprotein A1 (hnRNP A1), fragile X mental retardation protein 1 (FMRP), small nuclear ribonucleoprotein Sm D1 (SNRPD1), chromatin target of PRMT1 (Protein arginine *N*-methyltransferase 1) protein (CHTOP), bromodomain and WD repeat-containing protein 3 (BRWD3), cell death and ATM (serine-protein kinase ATM) regulator AVEN, Ras GTPase-activating protein-binding protein 1 (G3BP1), double-strand break repair protein MRE11 and tumor suppressor p53-binding protein 1 (53BP1).

Evidence that the GAR is a pADPr-binding module came from the study of MRE11 (Haince et al., 2008). MRE11, a core component of the MRN complex (MRE11, RAD50 and NBS1), is responsible for the initial recognition of DNA double-strand breaks (DSBs), mediates end-resection by its exonuclease activity and together with 53BP1 and other DNA damage response factors, facilitates repair. The GAR domain of MRE11 is required for its DNA binding activity (Boisvert et al., 2005; Dery et al., 2008) but also mediates its interaction with pADPr as well as its rapid accumulation at DNA strand breaks (Haince et al., 2008). The MRE11 exonuclease activity is inhibited by pADPr *in vitro*, suggesting that pADPr may regulate MRE11-dependent end-resection at DSBs or at stalled replication forks, as recently reported (Ying et al., 2012). Interestingly, several other GAR-containing proteins participate in the DNA damage response and genome surveillance. In view of the high pADPr level that transiently accumulates at sites of damage, it is suspected that the function of some of these GAR-bearing proteins might be regulated by pADPr. 53BP1 regulates repair of DSBs, while the nuclear DNA helicase II (RNA Helicase A) interacts and regulates the DSBs biomarker γ-H2AX (Mischo et al., 2005) and the Werner syndrome helicase (WRN) (Friedemann et al., 2005). The nucleosome remodeling and histone deacetylase (NuRD) complex comprises several core components with affinity for pADPr. Methyl-CpG-binding domain protein 2 (MBD2) has a GAR motif, while CHD4 (chromodomain helicase DNA binding protein 4) and MTA1 (metastasis associated 1) interact with pADPr through a still undefined motif (Chou et al., 2010; Lai and Wade, 2011; Polo et al., 2010). The latter two proteins are involved in the recruitment of the NuRD complex to DNA strand breaks in a pADPr-dependent manner (Lai and Wade, 2011). Our current understanding suggests that the presence of pADPr acts as a recruitment module for the organization of the PARP1-associated DNA repair and chromatin remodeling machinery at DNA lesions. On the other hand, pADPr binding to the GAR domain could be considered as a DNA displacement mechanism required to reconfigure the DNA repair protein complexes and provide access to damaged DNA. It may also interfere with other DNA damage-induced posttranslational modifications, such as PRMT1-dependent arginine methylation in the GAR domain (Bedford and Richard, 2005). This view supports a concept where pADPr is a key orchestrator of the DNA damage response.

Recently, it has been suggested that pADPr regulates post-transcriptional gene regulation in the cytoplasm, notably through the assembly of cytoplasmic stress granules (Leung et al., 2012). In support of this, we showed that the stress granule effector G3BP1 binds pADPr by its GAR domain (Isabelle et al., 2012). Importantly, G3BP1-mediated stress granule assembly is impaired by PARP inhibition during genotoxic insult, suggesting that pADPr is critical for the reprogrammation of messenger ribonucleoparticles in cellular stress responses. This result adds to the experimental evidence that the pADPr-binding protein AIF functions as a negative regulator of stress granules (Cande et al., 2004). These results emphasize the fact that pADPr can perform various functions in several different DNA damage-processing pathways and can enable a crosstalk between the regulation of the early and late steps of the DNA damage response.

3.2.2. The RNA recognition motif (RRM) and Serine/Arginine repeats (SR)

The RNA recognition motif (RRM), also referred to as RNA-binding domain (RBD) or ribonucleoprotein domain (RNP), is the most abundant nucleic acid-binding motif in the human genome (Clery et al., 2008). RRMs are found in a wide variety of RNA and ssDNA-binding proteins. RRMs may be found in conjunction with GAR-containing proteins. One prominent example is hnRNP A1 that possesses two RRMs in addition to its GAR motif. hnRNPs are highly versatile proteins that can participate in various aspects of nucleic acid metabolism: mRNA stability and splicing, DNA replication, chromatin remodeling, telomere maintenance, DNA repair and genome stability (Han et al., 2010). Based on a proteome-wide screen to identify pADPr-binding proteins, our laboratory was the first to identify hnRNPs as a family of proteins with affinity for pADPr (Gagne et al., 2003). More recently, Ji and Tulin (2009) validated this finding by providing evidence that hrp38 (the Drosophila melanogaster homologue of human hnRNP A1) binds pADPr in a non-covalent way *in vivo*, with the consequence of reduced RNA-binding ability. RNA processing factors (such as NONO and RBMX) recently emerged as guardians of genomic stability with widespread involvement in preventing DNA damage (Adamson et al., 2012; Krietsch et al., 2012; Paulsen et al., 2009). Both NONO (Non-POU domain-containing octamer-binding protein) and RBMX (RNA-binding motif protein, X chromosome) comprise RRMs and are recruited in a pADPr-dependent manner to DNA damage (Adamson et al., 2012; Krietsch et al., 2012). We have recently reported the binding of pADPr to the RRM1 domain of NONO. As it was observed for hnRNPA1, pADPr interfered with the interaction of NONO with RNA *in vitro*. Notably, the binding of NONO to pADPr by RRM1 is crucial for the recruitment of NONO to DNA damage sites and influences the outcome of DNA DSB repair. The high binding affinity of pADPr to NONO was assessed by SPR (Table 2). Similar to DEK and XPA described above, NONO showed a strong affinity for non-fractionated and long pADPr chains while no binding was detected for short pADPr chains. These observations therefore provide further support for RRMs as biologically relevant pADPr-binding modules (Krietsch et al., 2012). Given the frequent occurrence of RRM-containing proteins in the human proteome, interactions with pADPr are likely to have a significant impact on cell signaling through a complex network of biochemical pathways.

Another large group of RRM-containing proteins that bind to RNAs are the SR (Serine/Arginine repeats) proteins (Long and Caceres, 2009) that, along with hnRNPs, contribute to the formation of messenger ribonucleoprotein particles (mRNPs). It has been shown that the SR protein ASF/SF2 binds pADPr with high affinity (Malanga et al., 2008). Two domains in ASF/SF2 can mediate the interaction with pADPr: (I) a N-terminal fragment that contains a RRM1 and (II) a C-terminal SR domain (Malanga et al., 2008). Given that the SR domain carries an excess positive charge with the predominance of arginine residues, this pADPr-binding feature resembles that of the GAR which also harbors a basic arginine-rich cluster expected to interact with the phosphate backbone of pADPr. Similarly, strong pADPr-binding was observed in lysine- and arginine-rich (K/R-rich) motifs located in the nucleosome remodeler dMi-2 (Murawska et al., 2011). It remains to be determined whether the presence of a basic electrostatic patch on a protein surface could be considered as a general pADPr-protein interface or if additional structural determinants are required (such as the helical conformation of the SR domain (Sellis et al., 2012)).

3.3. PBZ: a poly(ADP-ribose)-binding zinc finger

Zinc fingers specifically interacting with pADPr rather than DNA or RNA were discovered in a subset of proteins related directly or indirectly with pADPr metabolism (Ahel et al., 2008). This newly identified C2H2-type "pADPr-binding zinc finger" (PBZ) has a consensus sequence defined as [K/R]xxCx[F/Y]GxxCxbbxxxxHxxx[F/Y]xH where b denotes a basic residue and x any residue (Ahel et al., 2008). PBZ domains have been observed only in eukaryotic proteins, excluding yeast. The absence of PBZ motifs in prokaryote and yeast proteins parallels the absence of pADPr metabolism in those, suggesting a co-evolution of the PBZ motif with the presence of PARPs. Only three human proteins appear to carry a PBZ motif: the aprataxin and PNK-like factor (APLF, also called XIP1, PALF), the checkpoint protein with FHA and RING domains (CHFR), and the DNA cross-link repair 1A protein (DCLRE1A/SNM1A) (Fig. 3) (Ahel et al., 2008). Interestingly, the PBZ module was found in some non-human proteins involved in the maintenance of genome integrity or DNA repair: Ku70, Rad17, Parp and Chk2 in *Dictyostelium discoideum* and DNA Ligase in *Caenorhabditis elegans* corresponding to human DNA Ligase III. However, the human orthologues do not contain any PBZ domain (Ahel et al., 2008; Isogai et al., 2010).

Human CHFR and DCLRE1A contain a unique PBZ while APLF has two PBZ placed in tandem (PBZ1 and PBZ2 – Fig. 3). Structural studies of the PBZ domains with small molecules that mimic the features of pADPr have revealed that besides the cysteines and histidines coordinating the Zn ion, critical aromatic residues mediate interactions with the adenine ring of ADPr (Ahel et al., 2008; Eustermann et al., 2010; Isogai et al., 2010; Li et al., 2010; Oberoi et al., 2010). The lack of conservation of most of these critical binding residues in the PBZ sequence of DCLRE1A suggests that it may not bind pADPr, but this has not been experimentally assessed (Oberoi et al., 2010). The affinity of CHFR (5×10^{-10} M) and APLF (9.5×10^{-10} M) for pADPr measured by SPR indicates that this module has the highest affinity for pADPr of all pADPr-binding domains (Table 2). Interestingly, the affinity of APLF for pADPr is in the same range than that of CHFR, despite the fact that it has two PBZ. Each PBZ of APLF binds independently pADPr, but with reduced affinity relative to the tandem PBZ and the full length protein (Table 2) (Ahel et al., 2008; Eustermann et al., 2010; Li et al., 2010; Rulten et al., 2008). Moreover, the affinity of PBZ1 for pADPr is 10-fold higher than that of PBZ2 (Table 2) (Eustermann et al., 2010; Li et al., 2010). These observations are in line with the structural details of CHFR and APLF, which strongly suggested that the CHFR PBZ and the PBZ1 domain of APLF are able to interact with two consecutive ADPr moieties in pADPr while the second PBZ of APLF probably binds only one (Oberoi et al., 2010). These observations are also consistent with the more deleterious effects of mutations in PBZ1 than in PBZ2 for the recruitment of APLF to UV-induced DNA strand breaks (Li et al., 2010; Rulten et al., 2008). PBZ1 may also interact with PARP1 as well, providing further affinity of PBZ1 for automodified PARP1 (Eustermann et al., 2010; Macrae et al., 2008).

The role of APLF in the DNA damage response and repair via the non-homologous end-joining (NHEJ) pathway has been recognized by several research groups (Bekker-Jensen et al., 2007; Iles et al., 2007; Kanno et al., 2007; Li et al., 2010; Macrae et al., 2008; Rulten et al., 2008). APLF comprises a N-terminal FHA domain and displays apurinic-apyrimidinic (AP) endonuclease and 3′-5′ exonuclease activities *in vitro*. APLF is rapidly recruited to DNA strand breaks introduced by UV irradiation via both its FHA and PBZ domains. While the FHA domain mediates interactions with the repair proteins XRCC1 and XRCC4, the tandem PBZ domain directs pADPr-dependent recruitment of APLF to DNA strand breaks, where APLF facilitates NHEJ. Both PARP1 and PARP3-dependent poly(ADP-ribosyl)ation have been shown to promote APLF responses to DNA strand breaks (Rulten et al., 2008, 2011).

Similar to APLF, CHFR comprises a phospho-binding FHA module but also a RING finger domain with E3 ubiquitin ligase activity that plays an essential role in the antephase checkpoint, delaying mitotic entry under certain stress conditions (Chaturvedi et al., 2002; Scolnick and Halazonetis, 2000). This function of CHFR is dependent on its interaction with PARP1 and pADPr, because mutations in the CHFR PBZ that disrupts pADPr-binding as well as PARP inhibitors both abolish the CHFR-dependent mitotic checkpoint (Ahel et al., 2008; Kashima et al., 2012; Oberoi et al., 2010). Recently, a mechanistic interplay behind CHFR and pADPr interactions inducing a mitotic entry delay was uncovered (Kashima et al., 2012). The activation of PARP1 following mitotic stress promotes the pADPr-dependent ubiquitylation of PARP1 by CHFR and its proteasomal degradation (Fig. 4A). This finding further revealed that PARP1 levels must be critically controlled during cell proliferation.

The binding of DCLRE1A to pADPr has not been studied. This protein has an endonuclease function and it is involved in the repair of DNA interstrand cross-links (Hazrati et al., 2008; Yang et al., 2010). However, the putative PBZ does not comprise the aromatic residues needed to contact pADPr, suggesting that its functions are independent of poly(ADP-ribosyl)ation.

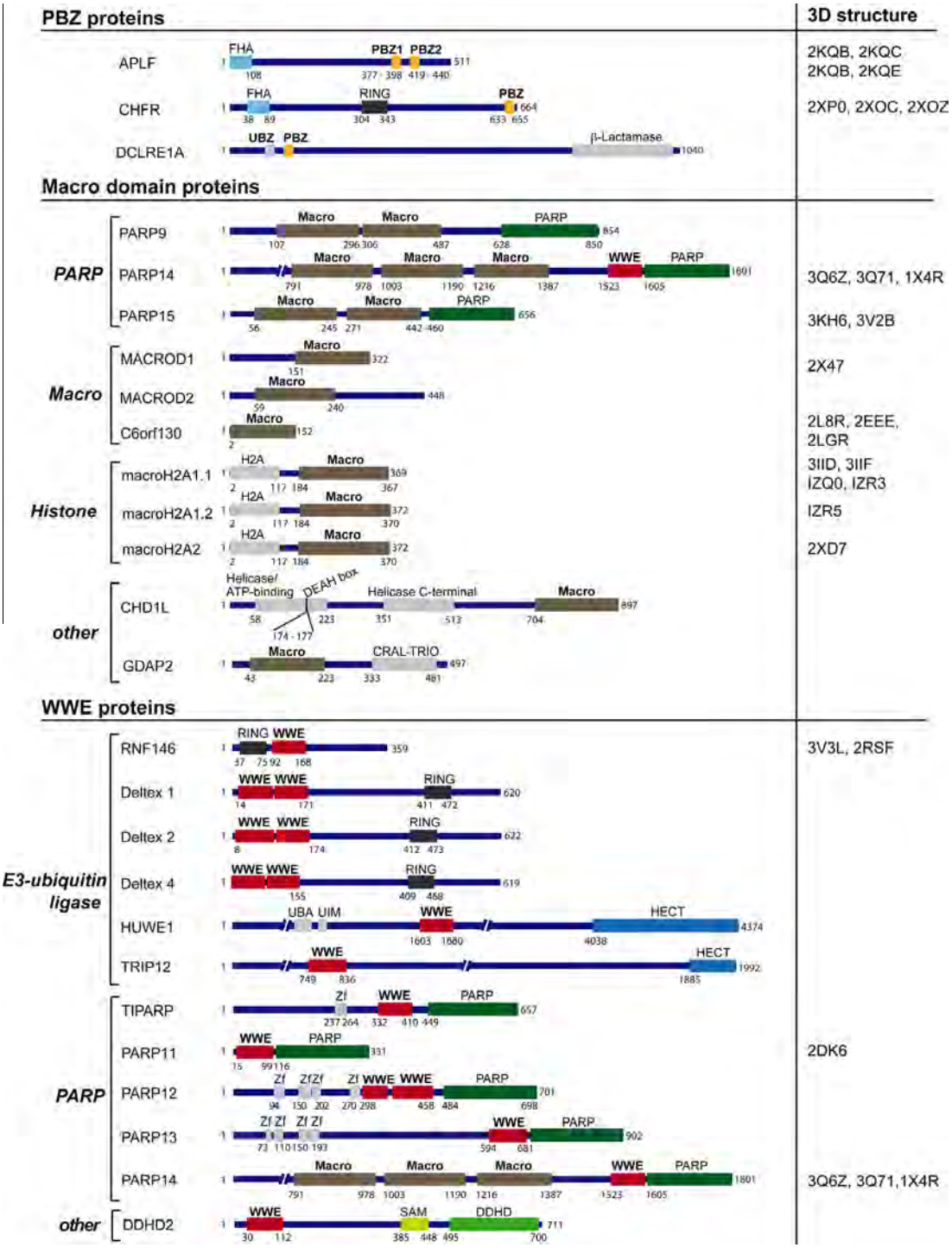

Fig. 3. Schematic representation of human proteins harboring a PBZ, Macro domain or WWE binding module. The three protein folds currently recognized to confer high-affinity to pADPr are listed with their individual protein members. When available, 3D structure accession numbers (Protein Data Bank (PDB)) are given. The domain organization is schematized and drawn to scale according to the Uniprot database. Binding to pADPr remains to be formally demonstrated for some of the listed proteins while binding was undetectable for others. See Sections 3.3–3.5 for more details. FHA, forkhead-associated domain; β-Lactamase, beta-Lactamase domain; RING, RING finger; H2A, domain with similarity to histone H2A; Helicase ATP-binding, helicase superfamily 1/2 ATP-binding domain; DEAH box, DEAH box motif; Helicase C-terminal; Helicase conserved C-terminal domain; CRAL-TRIO, domain named after cellular retinaldehyde-binding protein (CRALBP) and TRIO guanine exchange factor, this domain binds lipophilic molecules; UBA, ubiquitin associated domain; UIM, ubiquitin interaction motif; HECT, homologous to E6-AP carboxyl terminus domain (has E3-ubiquitin ligase activity); Zf, zinc finger; SAM, sterile α motif domain; DDHD, domain named after the conserved residues DDHD.

3.4. The macro domain: an ADP-ribose binding module

The macro domain was first described in a variant of the histone H2A, as a 130–190 amino acid module on the C-terminal side of the histone domain (Pehrson and Fried, 1992). It was soon recognized as an important protein domain, well conserved throughout all living organisms, as well as in a small subset of single-stranded RNA viruses that infect mammalian cells, including coronaviruses, alphaviruses and hepatitis E virus. Determination of the 3D structure of the thermophile *Archaeoglobus fulgidus* macro protein Af1521 provided the first clues to the potential function of this domain. It revealed an organization of helices and sheets reminiscent of the P-loop found in nucleotide hydrolases, suggesting a related enzymatic function for the macro fold (Allen et al., 2003). Additional studies with Af1521 and with the yeast macro domain protein YBR022 W supported this observation as they revealed the ability of these macro domains to hydrolyze ADP-ribose-1''-phosphate into ADPr and inorganic phosphate (Pi) (Karras et al., 2005; Martzen et al., 1999). Subsequent studies indicated that some macro domains could not only interact with ADPr but also with pADPr, making it a novel pADPr-interaction module (Ahel et al., 2009; Gottschalk et al., 2009; Karras et al., 2005; Neuvonen and Ahola, 2009; Timinszky et al., 2009).

Based on primary amino acid sequence comparisons, 11 human proteins comprise a macro domain (Fig. 3). This macro domain may exist on its own (macroD1, also called MDO1 and LRP16, macroD2 also called MDO2 and C6orf130) or in association with the histone fold (macrohistones H2A), the PARP catalytic domain (PARP9, 14 and 15), the SNF2/helicase ATPase domain (ALC1/CHD1L), or the Sec14p/CRAL-TRIO protein–lipid interaction module (GDAP2). Intriguingly, macroPARPs (also called BAL PARPs) have the unique feature of bearing two (PARP9 and PARP15) or even three (PARP14) macro domains in tandem, which, in PARP14, are further associated with two more putative pADPr binding modules, a RRM and a WWE (Fig. 3).

The affinity of most human macro domain proteins for NAD^+-derived metabolites permits the assessment of the importance of this module for pADPr binding and metabolism. It should be stressed that, out of nine macro domain-containing human proteins so far tested for pADPr binding (PARP14 and PARP15 have not been examined), only four bind pADPr (namely macroH2A1.1, CHD1L, macroD1 and PARP9). The others have affinity only for ADPr or *O*-acetyl-ADP-ribose (Fig. 1; Table 2). Furthermore, the detailed structural analysis of macroH2A1.1 revealed that it is able to bind solely the terminal ADPr of the polymer, indicating that its macro domain is in practice an ADPr binding module (Timinszky et al., 2009). Therefore, structural details critically affect the ability of the macro fold binding pocket to accommodate ligands such as ADPr. For instance, the macroH2A1.2 and macroH2A2 variants as well as GDAP2 do not interact with ADPr (Kustatscher et al., 2005; Till and Ladurner, 2009). While the structural characteristics of macroH2A1.2 differ only slightly from those of the macroH2A1.1 variant, three additional amino acid residues in macroH2A1.2 critically fall in the ADPr binding pocket, thereby hindering the interaction (Kustatscher et al., 2005). The structure of some viral macro domains (also called X-domain) has also been investigated as well as their ability to interact with ADPr and pADPr (Egloff et al., 2006; Malet et al., 2009; Neuvonen and Ahola, 2009; Piotrowski et al., 2009). As it is the case for human proteins, some but not all tested present affinity for ADPr or pADPr. The binding of viral macro domains to ADPr is at least 10-fold lower (K_D of the severe acute respiratory syndrome (SARS) coronavirus is 24 μM, that of hepatitis E virus above 50 μM) but interactions with pADPr have been shown by polymer blot assays (Egloff et al., 2006; Neuvonen and Ahola, 2009). It remains to be determined whether this interaction is critical for viral host infections. Collectively, these observations indicate that the presence of a macro fold hints to a possible interaction with ADPr-related metabolites, which however needs to be experimentally addressed.

3.4.1. Hidden macro domains in pADPr-binding proteins

Recent structural analysis of poly(ADP-ribose) glycohydrolase (PARG) revealed the striking finding that its pADPr-interaction module folds in a macro domain-like structure. First identified in the distantly PARG-related bacterial protein DUF2263, this finding was then confirmed with the structural analysis of a protozoan PARG and rat PARG (Dunstan et al., 2012; Kim et al., 2012a; Slade et al., 2011). Therefore, despite minimal sequence similarity between the typical macro domain and PARG, part of the PARG catalytic domain adopts this characteristic macro fold organization in which the PARG sequence signature GGG-X_{6-8}-QEE lines the ADP-ribose binding pocket. However, in the mammalian PARG, additional essential sequences extending beyond the macro domain adopt structural conformations around the macro fold that specify the catalytic pocket and the glycohydrolase activity. Importantly, a unique "tyrosine clasp" near the catalytic pocket offers an explanation for the exoglycosidic and endoglycosidic activities of mammalian PARG towards pADPr (Brochu et al., 1994), the latter endoglycosidic activity lacking in the bacterial PARG (Kim et al., 2012a). These recent findings have thus highlighted that some macro domains may only be revealed once the 3D structure is determined, indicating that there may be other pADPr-binding macro proteins in mammalian cells awaiting identification.

Many of the macro domain-ADPr/pADPr interactions have been examined *in vitro*, using purified macro domains or proteins and purified ADPr/pADPr. Because PARPs catalyze the addition of ADPr onto protein substrates, it will be critical to investigate whether the macro-ADPr interaction can be extended to ADPr covalently attached to acceptor proteins. A recent study using synthetic peptides corresponding to mono-ADP-ribosylated histone H2B tail showed that it could be the case, as macroH2A1.1 did bind such peptides (Moyle and Muir, 2010).

Recent detailed analysis of the enzymatic activity of the macro domain indicates that some deacetylate *O*-acetyl-ADP-ribose. This molecule is produced by the sirtuin deacetylases, which uses NAD^+ as a co-factor to deacetylate proteins. The three stand-alone macro domain proteins, namely macroD1, macroD2, and C6orf130, appear to form a subgroup of macro domain proteins showing this deacetylase activity by cleaving the ester bond between the acetyl group and ADPr. One could envision that some macro domain proteins possessing *O*-acetyl-ADPr deacetylase activity may be able to

hydrolyze the protein-ADPr ester bond (Fig. 1B). Until now, the ability of PARG and ARH3 to fulfill this function has been questioned. The existence of a distinct enzyme (an ADP-ribose lyase) able to hydrolyze the ester bond between the glutamic or aspartic acid residue of the acceptor protein and ADPr has been proposed nearly 30 years ago (Oka et al., 1984), but remains to be characterized. However, the recent indications that lysines could also constitute ADPr acceptor sites on PARP1 and histones, forming a ketamine in this case (Fig. 1B) (Altmeyer et al., 2009; Messner et al., 2010), suggest that there may be more than one "lyase".

Biological functions of macro domain proteins remain to be examined in details. Macrohistones and CHD1L contribute to the structure of chromatin (see Sections 4.4 and 4.5) and regulatory transcriptional functions have been ascribed to PARP9, PARP14, macroD1 and macroH2A variants. The latter macrohistones have been generally linked to transcriptional repression as they induce a more condensed chromatin state and impede access to transcription factors, although in some specific cases they can also promote transcription (reviewed by (Gamble and Kraus, 2010)) (Muthurajan et al., 2011). PARP9 was also shown to repress transcription via its macro domains (Aguiar et al., 2005). In contrast, PARP14, also named CoaSt6 because of its co-activator function for the transcription factor Stat6, promotes interleukin-4 dependent gene activation in a manner dependent on its macrodomains as well on its mono-ADP-ribosyl-transferase activity (Goenka and Boothby, 2006; Goenka et al., 2007). MacroD1, originally named leukemia related protein 16 (LRP16), was identified as a co-activator of androgen and estrogen receptor transcriptional activity as well as of NF-κB (Han et al., 2007; Wu et al., 2011; Yang et al., 2009). This transcriptional co-activation of macroD1 is dependent on its macro domain. Collectively, these examples suggest that pADPr-macro domain interactions contribute to transcriptional regulation.

3.5. The WWE domain

The most recently discovered pADPr-binding motif, the so-called WWE domain, is named after its most conserved amino acids (tryptophan (W) and glutamate (E)), which are flanked by an otherwise rather low degree of sequence conservation (Wang et al., 2012). The 12 human proteins that contain a WWE domain (Fig. 3) belong mostly to two functional classes of proteins, namely those associated with ubiquitylation and those associated with poly(ADP-ribosyl)ation (Wang et al., 2012).

The best studied example is the RING finger protein 146 (RNF146) also called Iduna. pADPr binding of Iduna/RNF146 was first ascribed to a PBM (Kang et al., 2011) which was further defined as part of the WWE domain that mediates the interaction with pADPr (Wang et al., 2012). The structural characteristics of the Iduna/RNF146 WWE domain and its interaction with pADPr were thoroughly investigated by polymer blot assays, NMR and crystallography (Andrabi et al., 2011; Wang et al., 2012). *Iso*-ADPr rather than ADPr is the smallest unit that can be bound by the Iduna/RNF146 domain (Fig. 1B). The lack of interaction between WWE and ADPr was explained by the need for phosphate groups on either side of the adenine-ribose structure to make extensive contacts with the binding pocket. This supported the idea that the WWE domain is a pADPr-binding module because at least two ADPr units are needed to generate the *iso*-ADPr ligand. The proposed structure is compatible with interactions with *iso*-ADPr within longer pADPr chains (Wang et al., 2012), consistent with the co-purification of Iduna/RNF146 with pADPr (Andrabi et al., 2011). Four residues have been identified as crucial for *iso*-ADPr-binding in the Iduna/RNF146 WWE domain. These residues are well conserved throughout most human WWE domains (Wang et al., 2012), including the putative or demonstrated ubiquitin ligases Deltex 1,2,4, HUWE1 and TRIP12, which have been shown by SPR to also bind pADPr (Table 2). The WWE domains of several PARP family members (PARP11, PARP13 and the first WWE of PARP12) also comprise the conserved residues, suggesting that they bind pADPr. Only the binding of PARP11 has been examined, and showed interactions with ADPr and pADPr with rather low affinity (Table 2) (He et al., 2012; Wang et al., 2012). In contrast, two of the residues are not conserved in the second WWE of PARP12, in TiPARP, PARP14 and the putative phospholipase DDHD2, suggesting that these may not bind pADPr, as shown for DDHD2 (DDHD domain containing 2) in *in vitro* binding experiments (Wang et al., 2012).

A common theme among WWE containing proteins is the association with domains of the E3 ligase type, strongly suggesting a functional link between ubiquitylation and poly(ADP-ribosyl)ation. This link was uncovered in the regulation of Wnt/β-catenin signaling pathway by tankyrases and Iduna/RNF146 (Huang et al., 2009; Zhang et al., 2011). This pathway, essential for embryonic development and adult tissue homeostasis, is tightly regulated by the concentration of axin. It turns out that axin is a substrate for tankyrase such that its poly(ADP-ribosyl)ation allows its recognition by Iduna/RNF146. Binding of Iduna/RNF146 to poly(ADP-ribosyl)ated axin triggers axin ubiquitylation and proteasomal degradation (Fig. 4A). Interestingly, we concurrently showed that Iduna/RNF146 plays a prominent role in the context of DNA damage through its pADPr-dependent E3 ligase activity as it also ubiquitylates several DNA repair factors in a way that depends on pADPr. PARP1/2, KU70, XRCC1 and DNA ligase III were identified as Iduna/RNF146 substrates when poly(ADP-ribosyl)ated by PARP1 (see Section 4.2 and Fig. 4B and E) (Kang et al., 2011).

The cross-talk between ubiquitylation and poly(ADP-ribosyl)ation may not be restricted to Iduna/RNF146 but awaits further experimental examination. For instance, the E3 ligases Deltex1, Deltex2 and Deltex3 play a role in notch signaling. The N-terminus of these proteins contains tandem WWE motifs mediating interactions with the ankyrin repeats of Notch intracellular domain. Several studies performed *in vivo* and in cell culture have shown that Notch ubiquitylation is promoted by Deltex expression (Baron, 2012; Hori et al., 2004; Matsuno et al., 2002; Mukherjee et al., 2005; Wilkin et al., 2008).

In the context of DNA damage responses, HUWE1 (also called Mule, ARF-BP1, LASU1 and HectH9) and TRIP12 (also called E3 ubiquitin ligase for Arf (ULF)) both belong to the family of HECT domain (homologous to E6-AP carboxyl terminus) E3 ligases. HUWE1 participates in the DNA damage response by tightly regulating steady state levels of XRCC1, DNA polymerase

β, and DNA ligase III (Khoronenkova and Dianov, 2011; Parsons et al., 2009). Several substrates of HUWE1 for ubiquitylation/proteosomal degradation have been identified: Cdc6, the c-Myc oncogene, histones, as well as p53 (Adhikary et al., 2005; Chen et al., 2005; Hall et al., 2007). TRIP12 is a key regulator of the DNA damage response (Gudjonsson et al., 2012) by acting as a guard against excessive spreading of ubiquitylated chromatin at DNA damage sites as it functionally suppresses RNF168, another E3 ligase, which promotes the concerted accumulation of H2A and H2AX at DNA damage site. The importance of pADPr-binding by the WWE motif of HUWE1 and TRIP12 for their recruitment to DNA strand breaks remains to be addressed.

It is interesting to note that the members of the PARP family that carry WWE domains are most likely mono(ADP-ribosyl)transferases and unable to produce the *iso*-ADPr moiety bound by WWE. Little is known about these proteins and their functions. One aspect that may be of further functional relevance is the presence of classical zinc fingers associated with TiPARP, PARP12, PARP13 (Fig. 3). Of these, PARP13 has been examined as an antiviral protein (also named zinc antiviral protein ZAP). PARP13 inhibits the replication of viruses by recruiting the cellular RNA degradation machineries to degrade the viral mRNAs. It targets RNA viruses such as the retroviridae human immunodeficiency virus type 1 (HIV-1) (Chen et al., 2012; Zhu et al., 2011).

4. Cellular processes influenced by protein-pADPr interactions and its clinical applications

4.1. Regulation of protein stability

The mechanistic link between poly(ADP-ribosyl)ation and the regulation of protein degradation is one of the most surprising aspects of the recent advances on poly(ADP-ribosyl)ation. Three research groups identified independently the E3-ligase Iduna/RNF146 as being a key regulator of protein stability in a pADPr-dependent manner (Andrabi et al., 2011; Callow et al., 2011; Kang et al., 2011; Zhang et al., 2011). Remarkably, this pathway appears to function in several biological contexts, regulated not only by PARP1 but also by the tankyrases 1 and 2 (Fig. 4A). In the context of DNA damage, PARP1 automodification triggers its ubiquitylation by Iduna/RNF146 and subsequent degradation by the proteasome (Kang et al., 2011). In the context of Wnt signaling, it is tankyrase-dependent poly(ADP-ribosyl)ation of axin that induces its Iduna/RNF146-dependent proteasomal degradation and subsequent β-catenin-dependent transcription (Callow et al., 2011; Zhang et al., 2011). Iduna/RNF146 binds to pADPr of varying lengths (Andrabi et al., 2011) and ubiquitylates substrates poly(ADP-ribosyl)ated with short chains as occurs with tankyrases (Zhang et al., 2011) and substrates poly(ADP-ribosyl)ated with long chains that occurs with PARP1 (Kang et al., 2011). Thus Iduna/RNF146's dynamic range of protein quality control in the setting of poly(ADP-ribosyl)ation may be extensive. Because of this, there are likely to be multiple checkpoints that control Iduna/RNF146's activity and biological actions that require further investigation. Interestingly, regulation of protein stability in a pADPr-dependent manner is not restricted to WWE-containing E3-ligases because the PBZ-bearing CHFR E3-ligase has been shown recently to ubiquitylate PARP1 to target it for proteasomal degradation in the context of mitotic stress (see Section 3.3; Fig. 4A) (Kashima et al., 2012).

The clinical importance of the tankyrase-Iduna/RNF146-dependent regulation of protein stability was revealed recently in studies focusing on the cherubism-mutated protein 3BP2 (Guettler et al., 2011; Levaot et al., 2011). Cherubism is a rare autosomal dominant human disorder characterized by inflammatory destructive bone lesions resulting in abnormal fibrous tissue growth in the lower part of the face. Approximately 80% of all cherubism patients carry a mutation in the Sh3bp2 gene, which encodes the Src homology 3 domain-binding protein-2 (3BP2). Interestingly, most of these mutations lie within a six amino acid sequence (RSPPDG) that corresponds to the tankyrase substrate-recognition motif (Levaot et al., 2011). Upon successful binding of tankyrase 2 to the latter motif in 3BP2 of healthy cells, 3BP2 is poly(ADP-ribosyl)ated, which serves as a signal for its Iduna/RNF146-directed ubiquitylation and proteasome-mediated degradation (Fig. 4A) (Guettler et al., 2011; Levaot et al., 2011). The regulated degradation of 3BP2 is profoundly disturbed in cherubism patients because the interaction and hence poly(ADP-ribosyl)ation of mutated 3BP2 by tankyrase 2 is impaired, abolishing 3BP2 ubiquitylation by Iduna/RNF146. The abnormal accumulation of 3BP2 within cells appears to alter the signaling balance of SRC kinase multiprotein complex to which it is associated, causing systematic inflammation, and leading to the cherubism phenotype (Guettler et al., 2011; Levaot et al., 2011). Hence, understanding the concerted action of poly(ADP-ribosyl)ation and ubiquitylation might improve therapeutic approaches targeting cherubism.

It is tempting to speculate that the tankyrase-dependent poly(ADP-ribosyl)ation coupled to Iduna/RNF146 ubiquitylation/degradation pathway is a widespread process to regulate protein steady states. By *in silico* searches for putative tankyrase interacting proteins, Guettler et al. (2011) have identified a very large list of proteins carrying the tankyrase interaction sequence RXX(G/P)DG that could constitute potential targets. For instance, the stability of the centrosomal associated protein (CPAP), important for centriole duplication during mitosis, is regulated by tankyrase-dependent poly(ADP-ribosyl)ation and proteasomal degradation (Kim et al., 2012b).

4.2. Cell death – Parthanatos

Massive activation of PARP1 following a genotoxic stress has been long recognized as a critical event in the induction of cell death. However, it is only in recent years that pADPr has been recognized as a death signaling molecule after the identification of

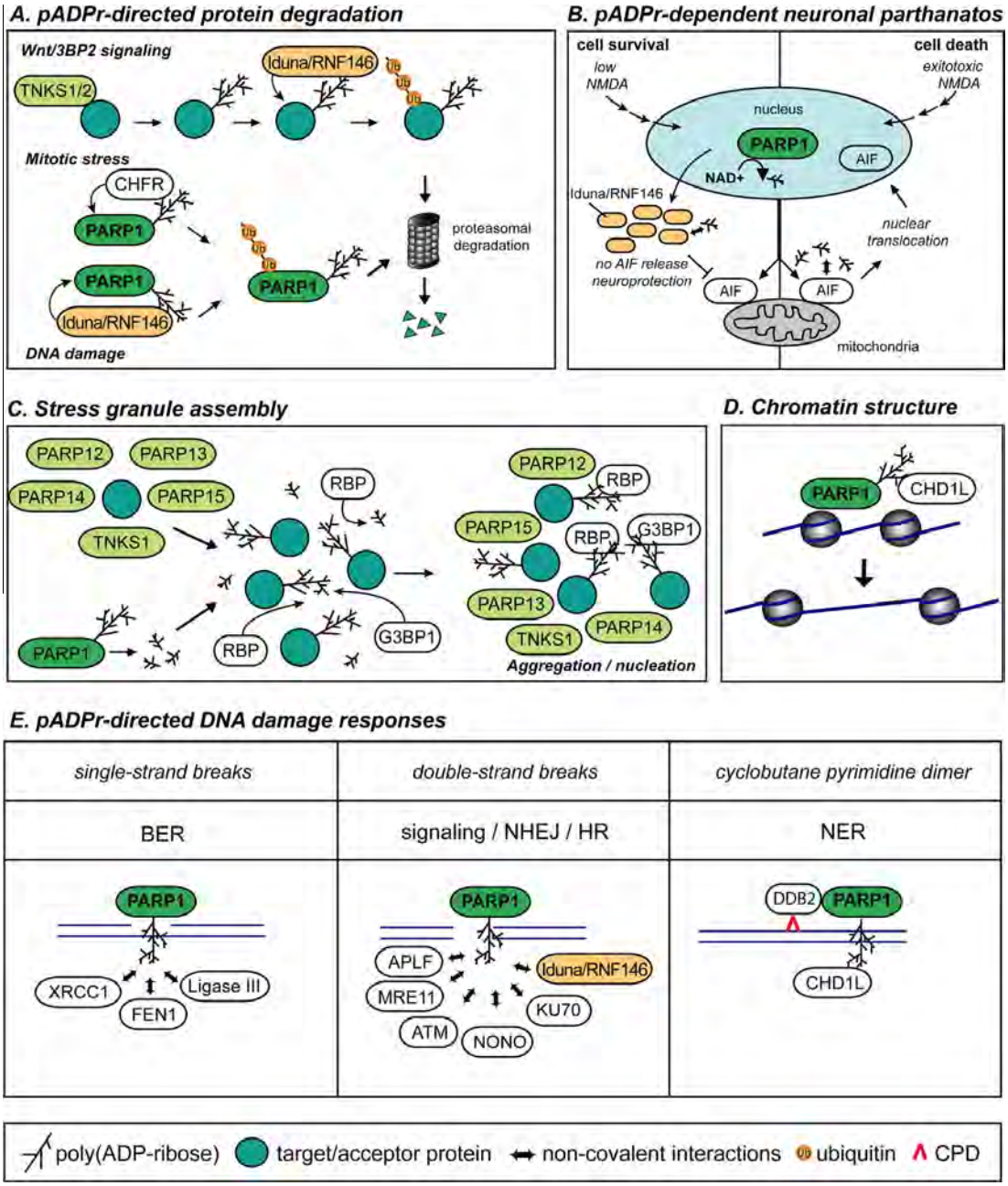

Fig. 4. Schematic models of pADPr regulatory functions. (A) Protein stability can be regulated via pADPr-directed recruitment of ubiquitin-conjugating enzymes. Some protein substrates of tankyrases (TNKS1/2) (3BP2 and axin) or automodified PARP1 undergo proteasomal degradation after ubiquitylation by the WWE-containing E3 ubiquitin ligase Iduna/RNF146 or by the PBZ-containing E3 ubiquitin ligase CHFR (see Sections 3.3 and 4.1 for details). (B) Neuronal cell fate after toxic stress. The excitation of glutamate receptor by *N*-methyl-D-aspartate (NMDA) triggers PARP activation. Non-toxic NMDA activation (left panel) induces the expression of the cell survival factor Iduna/RNF146 and its cytoplasmic accumulation. Interactions of Iduna/RNF146 with pADPr prevent apoptosis inducing factor (AIF) translocation to the nucleus and parthanatos. Excitotoxic activation of glutamate receptors (right panel) fail to induce Iduna/RNF146 expression. The accumulation of cytoplasmic pADPr promotes the release of apoptosis-inducing factor (AIF) from the mitochondria. AIF subsequently translocates to the nucleus and induces parthanatos. See Sections 3.5 and 4.2 for details. (C) pADPr-dependent assembly of stress granules. Two models have been proposed (see Section 4.3 for details). In the first view, cytoplasmic ADPr and pADPr are synthesized by tankyrases and PARP12-15 upon stress exposure. This triggers the aggregation of RNA-binding proteins (RBP) to ADPr/pADPr and stress granule formation. In the second view, the nucleo-cytoplasmic trafficking of pADPr is responsible for its accumulation into the cytoplasm. By virtue of its endoglycosidic activity, PARG releases free and protein-bound pADPr following genotoxic stress and PARP activation. pADPr translocated into the cytoplasm is targeted by G3BP1 and RNA-binding proteins to initiate the aggregation of stress granules. In both views, pADPr in ribonucleoparticles acts as a scaffold for the recruitment of RNA-binding proteins. (D) pADPr plays regulatory roles in the dynamics of chromatin structure. Automodification of PARP1 and poly(ADP-ribosy)ation of histones induce chromatin relaxation. This also involves the chromatin remodeling factor CHD1L, which is recruited to specific sites by pADPr. The ATPase activity of CHD1L is stimulated by pADPr and triggers nucleosome sliding. This possibly facilitates access of the DNA repair machineries. (E) Functions of pADPr in DNA damage responses. DNA strand breaks as well as other types of altered DNA structures and DNA adducts activate PARP1. pADPr triggers the recruitment of proteins and enzymes involved in DNA damage signaling, in base excision repair (BER), non-homologous end joining (NHEJ), homologous recombination (HR) and nucleotide excision repair (NER). See Section 4.5 for details.

pADPr as the trigger of apoptosis inducing factor (AIF)-dependent cell death. This insight came from studies attempting to determine the linkage between PARP1 activation during genotoxic stress and translocation of AIF from the mitochondria to the nucleus (Yu et al., 2002). Experiments to determine the mechanism of how PARP1 activation was intimately coupled to AIF translocation led to the discovery that pADPr translocates from the nucleus to mitochondria where it acts as an AIF releasing factor to cause the mitochondrial-nuclear translocation of AIF, initiating cell death (Fig. 4B) (Andrabi et al., 2006; Yu et al., 2006). This type of cell death, called parthanatos, occurs in neuronal cells following excitotoxicity as well as other cell types in which DNA damage is induced by specific genotoxic agents (Fig. 4B) (Wang et al., 2009). As noted above, the PBM within AIF is required for the release of AIF after PARP1 activation (Wang et al., 2011). It is important to note that the pADPr binding site in AIF is distinct from its DNA binding site. Thus, agents could be designed to block this interaction serving as inhibitors of parthanatos or to enhance the release of AIF for cancer chemotherapeutics. In a screen for cell survival factors, we identified the E3-ligase Iduna/RNF146 as a pADPr-dependent pro-survival factor, triggered by the same pADPr signal, in this case during non-toxic neuronal stress (Fig. 4B) (Andrabi et al., 2011). Iduna/RNF146 protects against parthanatos (pADPr-dependent) cell death mediated by glutamate excitotoxicity both *in vitro* and *in vivo* and against middle cerebral artery occlusion-induced stroke. Iduna/RNF146's protective properties are due to its ability to bind pADPr, consistent with the notion that pADPr can act as a death signal during parthanatos. PARG also inhibits parthanatos via degradation of the pADPr (Koh et al., 2004), whereas Iduna/RNF146 interferes with pADPr death signaling. Together both PARG and Iduna/RNF146 function as inhibitors of parthanatos during genotoxic stress providing endogenous controllers of cell death initiated by activation of PARP1.

Iduna/RNF146 also protects against the *N*-methyl-*N*-nitro-*N*-nitrosoguanidine (MNNG), a DNA damaging agent, and after γ-irradiation rescues cells from G1 arrest and promotes cell survival. Iduna/RNF146 reduces purinic/apyrimidinic (AP) sites after MNNG exposure and it also facilitates DNA repair following γ-irradiation. Iduna/RNF146's protective function not only requires a functional pADPr-binding domain, but its ubiquitin E3 ligase activity as well (Kang et al., 2011). Thus, Iduna/RNF146 links poly(ADP-ribosyl)ation and protein stability in the DNA damage response by controlling the levels of proteins important in this process through modulating the levels of poly(ADP-ribosyl)ated proteins via ubiquitin proteasomal degradation. Identification of Iduna/RNF146's substrates that play roles in parthanatos and DNA repair are the critical next steps.

4.3. Assembly of stress granules

A novel function of pADPr has been recently described in the regulation of stress granules (SG) (Leung et al., 2011, 2012). These structures are composed of cytoplasmic aggregates of stalled pre-initiation mRNA complexes. In addition to a subset of ribosomal proteins and translation initiation factors, the SG contains a variety of RNA-binding proteins that promote its nucleation and participate in the reprogrammation of translation during stress. The localization of several PARPs in SG (PARP12, PARP13, PARP14, PARP15 and tankyrase, called here SG-PARPs) uncovered a connection between poly(ADP-ribosyl)ation reactions and posttranscriptional regulation of gene expression. It has been shown that the overexpression of the SG-PARPs promotes the poly(ADP-ribosyl)ation of mRNA-associated proteins and the assembly of SGs, while PARG overexpression inhibits their appearance supporting a key role for pADPr in the assembly of SG (Fig. 4C). This notion was further supported by the identification of G3BP1, one of the primary nucleator of SGs (Kedersha and Anderson, 2007), as a pADPr-binding protein (Isabelle et al., 2012). In contrast to the cytoplasm-restricted poly(ADP-ribosyl)ation reactions of the SG-PARPs, the G3BP1-associated SG are assembled with a pADPr-dependent mechanism that originates from the nuclear activation of PARP1/2. These two possibilities are schematized in Fig. 4C.

4.4. Chromatin structure

PARP activation results in chromatin relaxation (reviewed in Beneke, 2012; Krishnakumar and Kraus, 2010). The mechanism through which this occurs remains to be characterized. One model stipulates that histones, which are poly(ADP-ribosyl)ated after PARP activation, are less tightly bound to DNA, thereby inducing relaxation (Ball and Yokomori, 2011; Poirier et al., 1982). Another mechanism has arisen from studies of the non-covalent interaction of ALC1/CHD1L with pADPr. PARP1 activation not only recruits this protein to sites of DNA damage, it also stimulates its ATPase activity and induces CHD1L-dependent nucleosome repositioning (Fig. 4D) (Ahel et al., 2009; Gottschalk et al., 2009). This PARP-dependent function of CHD1L may be of importance during DNA damage signaling and repair of DNA strand breaks, as well as of cyclobutane pyrimidine dimers by nucleotide excision repair (Fig. 4E) (Luijsterburg et al., 2012; Pines et al., 2012).

4.5. DNA damage response

Poly(ADP-ribosyl)ation in the context of DNA damage responses has long been recognized, but the concept is emerging that it is not involved in the DNA repair processes *per se*. pADPr synthesis at sites of DNA lesions triggers the recruitment of many DNA damage mediators and repair factors as well as chromatin remodeling and may serve as a scaffold for the assembly of repair complexes (Table 1; Fig. 4E). Regardless of the type of DNA damage, be it single-strand breaks repaired by base excision repair, double-strand breaks repaired by non-homologous end joining or homologous recombination, or cyclobutane pyrimidine dimers repaired by nucleotide excision repair, the recent elucidation of large sets of pADPr-binding proteins and associated complexes supports critical functions for pADPr in the early sensing and signaling of DNA damage (Gagne et al., 2012).

4.6. Clinical implications

A number of cancer cells are crucially dependent on the DNA repair pathways regulated by PARP1. BRCA1 and 2 are the major breast and ovarian susceptibility genes reported. Mutations in the latter genes render cells deficient for DSB repair and exquisitely sensitive to PARP inhibitors. This concept is now being extended to other DNA repair factors, including mutations in ATM, p53 and the MRE11-RAD50-NBS1 complex (Oplustilova et al., 2012; Williamson et al., 2012). Interestingly, the exact mechanism of action of PARP inhibitors is still a matter of ongoing debate (Helleday, 2011; Patel et al., 2011). Large-scale sequencing projects of human genomes, such as the ENCODE project consortium, may help to reveal novel sequence variants or mutations in proteins involved in the maintenance of genomic stability with critical implications in the development of human cancers (Dunham et al., 2012). It is also reasonable to think that a critical mutation in a pADPr-binding motif might have deleterious consequences in signaling pathways that comprise the DNA damage response. Such information might be positively exploited clinically.

While defective DNA damage repair pathways are one type of susceptibility to PARP inhibitors, there appear to be others for which mechanistic basis are failing to be explained at the moment. For instance, the susceptibility of human epidermal growth factor 2 positive (HER2+) breast cancer cells to PARP inhibitors alone was recently shown, independent of defects in HR (Nowsheen et al., 2012). Similarly intriguing is the sensitivity of cancers and cells bearing gene fusions with ETS transcription factors (mainly ERG), including prostate cancer and Ewing's sarcoma, to PARP inhibitors (Brenner et al., 2011, 2012; Garnett et al., 2012). In this case, both the transcriptional and DNA damage signaling functions of PARP1 may be involved to explain the sensitivity (Brenner et al., 2011; Garnett et al., 2012; Schiewer et al., 2012). Based on the latter findings and on the fact that PARP inhibitors have minimal side-effects, they have been in clinical trials for almost a decade, either in combination with chemotherapeutic drugs, as a single-agent or very recently in combination with phosphoinositide 3-kinase (PI3K) inhibitors, that further expand the treatment options for cancer patients (Ibrahim et al., 2012; Javle and Curtin, 2011; Juvekar et al., 2012; Rouleau et al., 2010).

With these examples in mind, and as the list of pADPr-binding proteins and pathways using poly(ADP-ribosyl)ation as signaling mechanisms is still expanding, it becomes crucial to investigate the broad spectrum of biological implications of pADPr-protein interactions. It will undoubtedly lead to a better understanding of more applications of PARP inhibitors as single-agent and combination therapies. For instance, several pADPr-binding proteins have been linked to cancer progression or aggressiveness. PARP9, initially referred to as "BAL PARP", was originally identified as a risk-related gene in diffuse large B-cell aggressive lymphoma, being over-expressed in such cancer cells (Aguiar et al., 2000; Takeyama et al., 2003). Similarly, CHD1L was originally named "amplified in liver cancer 1" (ALC1) because it was discovered as a candidate oncogene in hepatocellular carcinoma (Chen et al., 2009, 2010; Ma et al., 2008).

Further investigation of the mechanistic roles of pADPr in the regulation of cancer-associated protein networks and signaling pathways will be fundamental for the development of innovative treatment strategies, and to overcome resistance to such treatments.

5. Concluding remarks

Our understanding of the role of pADPr has remarkably expanded since the original observation that DNA strand breaks activate PARP1. As described above, in humans, there are at least four pADPr-binding modules (and others perhaps waiting to be discovered), coupled to a discrete number of additional domains linking poly(ADP-ribosyl)ation to ubiquitylation and chromatin structure in several cellular contexts such as protein degradation, DNA damage responses and cell death. Although sufficient to ensure binding to pADPr, these pADPr-binding domains vary widely in their degree of ligand specificity. While some seems to have a general affinity for the polyanionic backbone of biomolecules (i.e. DNA, RNA and pADPr) due to the presence of basic patches of amino acid residues, others evolved to perform specialized functions and exhibit a high degree of target specificity towards pADPr. Currently, the PBZ domain, which forms a divergent C2H2-type zinc finger fold with specialized functions, possesses the highest affinity for pADPr. The C2H2 zinc finger fold is amongst the most prevalent protein motifs in the human proteome and comprises the largest family of regulatory proteins in mammals. With this knowledge, we can speculate that uncharacterized variations in finger-like protrusions might provide the specificity required to recognize different pADPr structures.

Over 60 human proteins have been shown to interact with pADPr (Table 1), but based on *in silico* predictions of the occurrence of the PBM sequence, there may be over 500 of them, and many more if we consider that proteins in complexes with pADPr-binding proteins are (indirectly) affected by pADPr. Because the PBM represents a short contiguous protein segment, examination of other context criteria, such as protein surface accessibility, evolutionary conservation as well as the determination of three-dimensional PBM-bound pADPr complexes will help to establish the local structural environment required for pADPr-binding. Because of this potential that poly(ADP-ribosyl)ation affects a significant portion of the proteome, it is crucial to pursue the extensive examination of the pADPr-protein interactions.

In this regard, it is very intriguing to consider the high number of pADPr-binding proteins working in a single pathway. One may envision that there is a "pADPr code" where the length, complexity, and conformation adopted by pADPr covalently linked to a particular protein target, all contribute to favor some non-covalent interactions relative to others. The remarkably high affinity and processivity of PARG for long pADPr will certainly have a role to play in the regulation of the non-covalent

interactions. Equally intriguing is the presence of several pADPr-binding modules within single proteins (i.e. Deltex, macroPARPs, APLF, etc.). Does it confer higher specificity, stronger interactions, or preference for pADPr in a particular conformation? Or does it organize pADPr in a scaffold as proposed for the formation of stress granules?

The functions of pADPr in pathological conditions (i.e. DNA damage, mitotic stress, etc.) are now better understood. Still, the mechanisms underlying the relocalization of pADPr to the cytoplasm after specific stresses are largely unknown. The physiological aspects of poly(ADP-ribosyl)ation are only starting to emerge as they are more difficult to grasp. pADPr levels often fall below the threshold of detectability using current methods, especially in the cytoplasm. The triggers of pADPr synthesis by the damage-independent PARPs, such as tankyrases and SG-PARPs, are undefined. Nonetheless, in view of their important functional outcomes in regulating protein stability and posttranslational gene expression in the cytoplasm, no doubt that it must be finely regulated. Considering the critical functions of Iduna/RNF146 in directing poly(ADP-ribosyl)ated proteins towards proteasomal degradation, and the high catabolic activity of PARG, it is conceivable that some functional aspects of pADPr-binding proteins may consist in protecting pADPr from degradation, or in shielding the pADPr from Iduna/RNF146/CHFR to protect target proteins from degradation. We can also wonder whether there may be pADPr-dependent deubiquitylases that further regulate this process. It is now important to critically examine the regulation of pADPr degradation by PARG, ARH3 and possibly some macro domain proteins, in cellular contexts where pADPr-binding proteins also operate, to truly understand the extent of signaling afforded by pADPr. Some pathways appear to rely on the generation of free pADPr molecules, requiring an endoglycosidic activity that so far, only PARG is known to display. Our understanding of these fundamental questions now depends on the development of sensitive and quantitative methods for the detection of nuclear and cytoplasmic pADPr structures.

Acknowledgements

We apologize to authors of relevant publications that were not cited in this review due to space limitations. We thank John D. Chapman (Washington University, WA) for help with the drawings of chemical structures. JYM and GGP acknowledge the Canadian Institutes of Health Research for supporting their research. GGP holds a Canadian Research Chair in Proteomics. VLC and TMD acknowledge that their work is supported by grants from the NIH/NINDS NS067525 and NIDA DA000266. TMD is the Leonard and Madlyn Abramson Professor in Neurodegenerative Diseases. JYM is a FRSQ Senior scholar. JK is supported by a scholarship from the FQRNT.

References

Adamietz, P., Oldekop, M., Hilz, H., 1975. Proceedings: is poly(ADP-ribose) covalently bound to nuclear proteins? J. Biochem. 77, 4p.
Adamson, B., Smogorzewska, A., Sigoillot, F.D., King, R.W., Elledge, S.J., 2012. A genome-wide homologous recombination screen identifies the RNA-binding protein RBMX as a component of the DNA-damage response. Nat. Cell Biol. 14, 318–328.
Adhikary, S., Marinoni, F., Hock, A., Hulleman, E., Popov, N., Beier, R., Bernard, S., Quarto, M., Capra, M., Goettig, S., Kogel, U., Scheffner, M., Helin, K., Eilers, M., 2005. The ubiquitin ligase HectH9 regulates transcriptional activation by Myc and is essential for tumor cell proliferation. Cell 123, 409–421.
Aguiar, R.C., Takeyama, K., He, C., Kreinbrink, K., Shipp, M.A., 2005. B-aggressive lymphoma family proteins have unique domains that modulate transcription and exhibit poly(ADP-ribose) polymerase activity. J. Biol. Chem. 280, 33756–33765.
Aguiar, R.C., Yakushijin, Y., Kharbanda, S., Salgia, R., Fletcher, J.A., Shipp, M.A., 2000. BAL is a novel risk-related gene in diffuse large B-cell lymphomas that enhances cellular migration. Blood 96, 4328–4334.
Ahel, D., Horejsi, Z., Wiechens, N., Polo, S.E., Garcia-Wilson, E., Ahel, I., Flynn, H., Skehel, M., West, S.C., Jackson, S.P., Owen-Hughes, T., Boulton, S.J., 2009. Poly(ADP-ribose)-dependent regulation of DNA repair by the chromatin remodeling enzyme ALC1. Science 325, 1240–1243.
Ahel, I., Ahel, D., Matsusaka, T., Clark, A.J., Pines, J., Boulton, S.J., West, S.C., 2008. Poly(ADP-ribose)-binding zinc finger motifs in DNA repair/checkpoint proteins. Nature 451, 81–85.
Allen, M.D., Buckle, A.M., Cordell, S.C., Lowe, J., Bycroft, M., 2003. The crystal structure of AF1521 a protein from *Archaeoglobus fulgidus* with homology to the non-histone domain of macroH2A. J. Mol. Biol. 330, 503–511.
Althaus, F.R., Kleczkowska, H.E., Malanga, M., Muntener, C.R., Pleschke, J.M., Ebner, M., Auer, B., 1999. Poly ADP-ribosylation: a DNA break signal mechanism. Mol. Cell. Biochem. 193, 5–11.
Altmeyer, M., Messner, S., Hassa, P.O., Fey, M., Hottiger, M.O., 2009. Molecular mechanism of poly(ADP-ribosyl)ation by PARP1 and identification of lysine residues as ADP-ribose acceptor sites. Nucleic Acids Res. 37, 3723–3738.
Alvarez-Gonzalez, R., Jacobson, M.K., 1987. Characterization of polymers of adenosine diphosphate ribose generated in vitro and in vivo. Biochemistry 26, 3218–3224.
Andrabi, S.A., Kang, H.C., Haince, J.F., Lee, Y.I., Zhang, J., Chi, Z., West, A.B., Koehler, R.C., Poirier, G.G., Dawson, T.M., Dawson, V.L., 2011. Iduna protects the brain from glutamate excitotoxicity and stroke by interfering with poly(ADP-ribose) polymer-induced cell death. Nat. Med. 17, 692–699.
Andrabi, S.A., Kim, N.S., Yu, S.W., Wang, H., Koh, D.W., Sasaki, M., Klaus, J.A., Otsuka, T., Zhang, Z., Koehler, R.C., Hurn, P.D., Poirier, G.G., Dawson, V.L., Dawson, T.M., 2006. Poly(ADP-ribose) (PAR) polymer is a death signal. Proc. Natl. Acad. Sci. USA 103, 18308–18313.
Ball Jr., A.R., Yokomori, K., 2011. Damage site chromatin: open or closed? Curr. Opin. Cell Biol. 23, 277–283.
Baron, M., 2012. Endocytic routes to Notch activation. Semin. Cell Dev. Biol. 23, 437–442.
Bedford, M.T., Richard, S., 2005. Arginine methylation an emerging regulator of protein function. Mol. Cell 18, 263–272.
Bekker-Jensen, S., Fugger, K., Danielsen, J.R., Gromova, I., Sehested, M., Celis, J., Bartek, J., Lukas, J., Mailand, N., 2007. Human Xip1 (C2orf13) is a novel regulator of cellular responses to DNA strand breaks. J. Biol. Chem. 282, 19638–19643.
Beneke, S., 2012. Regulation of chromatin structure by poly(ADP-ribosyl)ation. Front. Genet. 3, 169.
Benjamin, R.C., Gill, D.M., 1980a. ADP-ribosylation in mammalian cell ghosts. Dependence of poly(ADP-ribose) synthesis on strand breakage in DNA. J. Biol. Chem. 255, 10493–10501.
Benjamin, R.C., Gill, D.M., 1980b. Poly(ADP-ribose) synthesis in vitro programmed by damaged DNA. A comparison of DNA molecules containing different types of strand breaks. J. Biol. Chem. 255, 10502–10508.
Berger, F., Lau, C., Ziegler, M., 2007. Regulation of poly(ADP-ribose) polymerase 1 activity by the phosphorylation state of the nuclear NAD biosynthetic enzyme NMN adenylyl transferase 1. Proc. Natl. Acad. Sci. USA 104, 3765–3770.
Bernstein, E., Allis, C.D., 2005. RNA meets chromatin. Genes Dev. 19, 1635–1655.
Boisvert, F.M., Hendzel, M.J., Masson, J.Y., Richard, S., 2005. Methylation of MRE11 regulates its nuclear compartmentalization. Cell Cycle 4, 981–989.

Brenner, J.C., Ateeq, B., Li, Y., Yocum, A.K., Cao, Q., Asangani, I.A., Patel, S., Wang, X., Liang, H., Yu, J., Palanisamy, N., Siddiqui, J., Yan, W., Cao, X., Mehra, R., Sabolch, A., Basrur, V., Lonigro, R.J., Yang, J., Tomlins, S.A., Maher, C.A., Elenitoba-Johnson, K.S., Hussain, M., Navone, N.M., Pienta, K.J., Varambally, S., Feng, F.Y., Chinnaiyan, A.M., 2011. Mechanistic rationale for inhibition of poly(ADP-ribose) polymerase in ETS gene fusion-positive prostate cancer. Cancer Cell 19, 664–678.

Brenner, J.C., Feng, F.Y., Han, S., Patel, S., Goyal, S.V., Bou-Maroun, L.M., Liu, M., Lonigro, R., Prensner, J.R., Tomlins, S.A., Chinnaiyan, A.M., 2012. PARP-1 inhibition as a targeted strategy to treat Ewing's sarcoma. Cancer Res. 72, 1608–1613.

Brochu, G., Duchaine, C., Thibeault, L., Lagueux, J., Shah, G.M., Poirier, G.G., 1994. Mode of action of poly(ADP-ribose) glycohydrolase. Biochim. Biophys. Acta 1219, 342–350.

Burd, C.G., Dreyfuss, G., 1994. Conserved structures and diversity of functions of RNA-binding proteins. Science 265, 615–621.

Caiafa, P., Guastafierro, T., Zampieri, M., 2009. Epigenetics: poly(ADP-ribosyl)ation of PARP-1 regulates genomic methylation patterns. FASEB J. 23, 672–678.

Callow, M.G., Tran, H., Phu, L., Lau, T., Lee, J., Sandoval, W.N., Liu, P.S., Bheddah, S., Tao, J., Lill, J.R., Hongo, J.A., Davis, D., Kirkpatrick, D.S., Polakis, P., Costa, M., 2011. Ubiquitin ligase RNF146 regulates tankyrase and Axin to promote Wnt signaling. PLoS One 6, e22595.

Cande, C., Vahsen, N., Metivier, D., Tourriere, H., Chebli, K., Garrido, C., Tazi, J., Kroemer, G., 2004. Regulation of cytoplasmic stress granules by apoptosis-inducing factor. J. Cell Sci. 117, 4461–4468.

Carbone, M., Reale, A., Di Sauro, A., Sthandier, O., Garcia, M.I., Maione, R., Caiafa, P., Amati, P., 2006. PARP-1 interaction with VP1 capsid protein regulates polyomavirus early gene expression. J. Mol. Biol. 363, 773–785.

Chambon, P., Weill, J.D., Mandel, P., 1963. Nicotinamide mononucleotide activation of new DNA-dependent polyadenylic acid synthesizing nuclear enzyme. Biochem. Biophys. Res. Commun. 11, 39–43.

Chaturvedi, P., Sudakin, V., Bobiak, M.L., Fisher, P.W., Mattern, M.R., Jablonski, S.A., Hurle, M.R., Zhu, Y., Yen, T.J., Zhou, B.B., 2002. Chfr regulates a mitotic stress pathway through its RING-finger domain with ubiquitin ligase activity. Cancer Res. 62, 1797–1801.

Chen, D., Kon, N., Li, M., Zhang, W., Qin, J., Gu, W., 2005. ARF-BP1/Mule is a critical mediator of the ARF tumor suppressor. Cell 121, 1071–1083.

Chen, L., Chan, T.H., Yuan, Y.F., Hu, L., Huang, J., Ma, S., Wang, J., Dong, S.S., Tang, K.H., Xie, D., Li, Y., Guan, X.Y., 2010. CHD1L promotes hepatocellular carcinoma progression and metastasis in mice and is associated with these processes in human patients. J. Clin. Invest. 120, 1178–1191.

Chen, L., Hu, L., Chan, T.H., Tsao, G.S., Xie, D., Huo, K.K., Fu, L., Ma, S., Zheng, B.J., Guan, X.Y., 2009. Chromodomain helicase/adenosine triphosphatase DNA binding protein 1-like (CHD1l) gene suppresses the nucleus-to-mitochondria translocation of nur77 to sustain hepatocellular carcinoma cell survival. Hepatology 50, 122–129.

Chen, S., Xu, Y., Zhang, K., Wang, X., Sun, J., Gao, G., Liu, Y., 2012. Structure of N-terminal domain of ZAP indicates how a zinc-finger protein recognizes complex RNA. Nat. Struct. Mol. Biol. 19, 430–435.

Chou, D.M., Adamson, B., Dephoure, N.E., Tan, X., Nottke, A.C., Hurov, K.E., Gygi, S.P., Colaiacovo, M.P., Elledge, S.J., 2010. A chromatin localization screen reveals poly (ADP ribose)-regulated recruitment of the repressive polycomb and NuRD complexes to sites of DNA damage. Proc. Natl. Acad. Sci. USA 107, 18475–18480.

Clery, A., Blatter, M., Allain, F.H., 2008. RNA recognition motifs: boring? Not quite. Curr. Opin. Struct. Biol. 18, 290–298.

Davidovic, L., Vodenicharov, M., Affar, E.B., Poirier, G.G., 2001. Importance of poly(ADP-ribose) glycohydrolase in the control of poly(ADP-ribose) metabolism. Exp Cell Res. 268 (1), 7–13.

D'Amours, D., Desnoyers, S., D'Silva, I., Poirier, G.G., 1999. Poly(ADP-ribosyl)ation reactions in the regulation of nuclear functions. Biochem. J. 342, 249–268.

Dery, U., Coulombe, Y., Rodrigue, A., Stasiak, A., Richard, S., Masson, J.Y., 2008. A glycine–arginine domain in control of the human MRE11 DNA repair protein. Mol. Cell Biol 28, 3058–3069.

Dunham, I., Kundaje, A., Aldred, S.F., Collins, P.J., Davis, C.A., Doyle, F., Epstein, C.B., Frietze, S., Harrow, J., Kaul, R., Khatun, J., Lajoie, B.R., Landt, S.G., Lee, B.K., Pauli, F., Rosenbloom, K.R., Sabo, P., Safi, A., Sanyal, A., Shoresh, N., Simon, J.M., Song, L., Trinklein, N.D., Altshuler, R.C., Birney, E., Brown, J.B., Cheng, C., Djebali, S., Dong, X., Ernst, J., Furey, T.S., Gerstein, M., Giardine, B., Greven, M., Hardison, R.C., Harris, R.S., Herrero, J., Hoffman, M.M., Iyer, S., Kelllis, M., Kheradpour, P., Lassman, T., Li, Q., Lin, X., Marinov, G.K., Merkel, A., Mortazavi, A., Parker, S.C., Reddy, T.E., Rozowsky, J., Schlesinger, F., Thurman, R.E., Wang, J., Ward, L.D., Whitfield, T.W., Wilder, S.P., Wu, W., Xi, H.S., Yip, K.Y., Zhuang, J., Bernstein, B.E., Green, E.D., Gunter, C., Snyder, M., Pazin, M.J., Lowdon, R.F., Dillon, L.A., Adams, L.B., Kelly, C.J., Zhang, J., Wexler, J.R., Good, P.J., Feingold, E.A., Crawford, G.E., Dekker, J., Elinitski, L., Farnham, P.J., Giddings, M.C., Gingeras, T.R., Guigo, R., Hubbard, T.J., Kellis, M., Kent, W.J., Lieb, J.D., Margulies, E.H., Myers, R.M., Starnatoyannopoulos, J.A., Tennebaum, S.A., Weng, Z., White, K.P., Wold, B., Yu, Y., Wrobel, J., Risk, B.A., Gunawardena, H.P., Kuiper, H.C., Maier, C.W., Xie, L., Chen, X., Mikkelsen, T.S., Gillespie, S., Goren, A., Ram, O., Zhang, X., Wang, L., Issner, R., Coyne, M.J., Durham, T., Ku, M., Truong, T., Eaton, M.L., Dobin, A., Lassmann, T., Tanzer, A., Lagarde, J., Lin, W., Xue, C., Williams, B.A., Zaleski, C., Roder, M., Kokocinski, F., Abdelhamid, R.F., Alioto, T., Antoshechkin, I., Baer, M.T., Batut, P., Bell, I., Bell, K., Chakrabortty, S., Chrast, J., Curado, J., Derrien, T., Drenkow, J., Dumais, E., Dumais, J., Duttagupta, R., Fastuca, M., Fejes-Toth, K., Ferreira, P., Foissac, S., Fullwood, M.J., Gao, H., Gonzalez, D., Gordon, A., Howald, C., Jha, S., Johnson, R., Kapranov, P., King, B., Kingswood, C., Li, G., Luo, O.J., Park, E., Preall, J.B., Presaud, K., Ribeca, P., Robyr, D., Ruan, X., Sammeth, M., Sandu, K.S., Schaeffer, L., See, L.H., Shahab, A., Skancke, J., Suzuki, A.M., Takahashi, H., Tilgner, H., Trout, D., Walters, N., Wang, H., Hayashizaki, Y., Reymond, A., Antonarakis, S.E., Hannon, G.J., Ruan, Y., Carninci, P., Sloan, C.A., Learned, K., Malladi, V.S., Wong, M.C., Barber, G.P., Cline, M.S., Dreszer, T.R., Heitner, S.G., Karolchik, D., Kirkup, V.M., Meyer, L.R., Long, J.C., Maddren, M., Raney, B.J., Grasfeder, L.L., Giresi, P.G., Battenhouse, A., Sheffield, N.C., Showers, K.A., London, D., Bhinge, A.A., Shestak, C., Schaner, M.R., Kim, S.K., Zhang, Z.Z., Mieczkowski, P.A., Mieczkowska, J.O., Liu, Z., McDaniell, R.M., Ni, Y., Rashid, N.U., Kim, M.J., Adar, S., Zhang, Z., Wang, T., Winter, D., Keefe, D., Iyer, V.R., Sandhu, K.S., Zheng, M., Wang, P., Gertz, J., Vielmetter, J., Partridge, E.C., Varley, K.E., Gasper, C., Bansal, A., Pepke, S., Jain, P., Amrhein, H., Bowling, K.M., Anaya, M., Cross, M.K., Muratet, M.A., Newberry, K.M., McCue, K., Nesmith, A.S., Fisher-Aylor, K.I., Pusey, B., DeSalvo, G., Parker, S.L., Balasubramanian, S., Davis, N.S., Meadows, S.K., Eggleston, T., Newberry, J.S., Levy, S.E., Absher, D.M., Wong, W.H., Blow, M.J., Visel, A., Pennachio, L.A., Elnitski, L., Petrykowska, H.M., Abyzov, A., Aken, B., Barrell, D., Barson, G., Berry, A., Bignell, A., Boychenko, V., Bussotti, G., Davidson, C., Despacio-Reyes, G., Diekhans, M., Ezkurdia, I., Frankish, A., Gilbert, J., Gonzalez, J.M., Griffiths, E., Harte, R., Hendrix, D.A., Hunt, T., Jungreis, I., Kay, M., Khurana, E., Leng, J., Lin, M.F., Loveland, J., Lu, Z., Manthravadi, D., Mariotti, M., Mudge, J., Mukherjee, G., Notredame, C., Pei, B., Rodriguez, J.M., Saunders, G., Sboner, A., Searle, S., Sisu, C., Snow, C., Steward, C., Tapanan, E., Tress, M.L., van Baren, M.J., Washieti, S., Wilming, L., Zadissa, A., Zhengdong, Z., Brent, M., Haussler, D., Valencia, A., Raymond, A., Addleman, N., Alexander, R.P., Auerbach, R.K., Bettinger, K., Bhardwaj, N., Boyle, A.P., Cao, A.R., Cayting, P., Charos, A., Cheng, Y., Eastman, C., Euskirchen, G., Fleming, J.D., Grubert, F., Habegger, L., Hariharan, M., Harmanci, A., Iyenger, S., Jin, V.X., Karczewski, K.J., Kasowski, M., Lacroute, P., Lam, H., Larnarre-Vincent, N., Lian, J., Lindahl-Allen, M., Min, R., Miotto, B., Monahan, H., Moqtaderi, Z., Mu, X.J., O'Geen, H., Ouyang, Z., Patacsil, D., Raha, D., Ramirez, L., Reed, B., Shi, M., Slifer, T., Witt, H., Wu, L., Xu, X., Yan, K.K., Yang, X., Struhl, K., Weissman, S.M., Tenebaum, S.A., Penalva, L.O., Karmakar, S., Bhanvadia, R.R., Choudhury, A., Domanus, M., Ma, L., Moran, J., Victorsen, A., Auer, T., Centarin, L., Eichenlaub, M., Gruhl, F., Heerman, S., Hoeckendorf, B., Inoue, D., Kellner, T., Kirchmaier, S., Mueller, C., Reinhardt, R., Schertel, L., Schneider, S., Sinn, R., Wittbrodt, B., Wittbrodt, J., Jain, G., Balasundaram, G., Bates, D.L., Byron, R., Canfield, T.K., Diegel, M.J., Dunn, D., Ebersol, A.K., Frum, T., Garg, K., Gist, E., Hansen, R.S., Boatman, L., Haugen, E., Humbert, R., Johnson, A.K., Johnson, E.M., Kutyavin, T.M., Lee, K., Lotakis, D., Maurano, M.T., Neph, S.J., Neri, F.V., Nguyen, E.D., Qu, H., Reynolds, A.P., Roach, V., Rynes, E., Sanchez, M.E., Sandstrom, R.S., Shafer, A.O., Stergachis, A.B., Thomas, S., Vernot, B., Vierstra, J., Vong, S., Weaver, M.A., Yan, Y., Zhang, M., Akey, J.A., Bender, M., Dorschner, M.O., Groudine, M., MacCoss, M.J., Navas, P., Stamatoyannopoulos, G., Stamatoyannopoulos, J.A., Beal, K., Brazma, A., Flicek, P., Johnson, N., Lukk, M., Luscombe, N.M., Sobral, D., Vaquerizas, J.M., Batzoglou, S., Sidow, A., Hussami, N., Kyriazopoulou-Panagiotopoulou, S., Libbrecht, M.W., Schaub, M.A., Miller, W., Bickel, P.J., Banfai, B., Boley, N.P., Huang, H., Li, J.J., Noble, W.S., Bilmes, J.A., Buske, O.J., Sahu, A.O., Kharchenko, P.V., Park, P.J., Baker, D., Taylor, J., Lochovsky, L., 2012. An integrated encyclopedia of DNA elements in the human genome. Nature 489, 57–74.

Dunstan, M.S., Barkauskaite, E., Lafite, P., Knezevic, C.E., Brassington, A., Ahel, M., Hergenrother, P.J., Leys, D., Ahel, I., 2012. Structure and mechanism of a canonical poly(ADP-ribose) glycohydrolase. Nat. Commun. 3, 878.

Egloff, M.P., Malet, H., Putics, A., Heinonen, M., Dutartre, H., Frangeul, A., Gruez, A., Campanacci, V., Cambillau, C., Ziebuhr, J., Ahola, T., Canard, B., 2006. Structural and functional basis for ADP-ribose and poly(ADP-ribose) binding by viral macro domains. J. Virol. 80, 8493–8502.

El-Khamisy, S.F., Masutani, M., Suzuki, H., Caldecott, K.W., 2003. A requirement for PARP-1 for the assembly or stability of XRCC1 nuclear foci at sites of oxidative DNA damage. Nucleic Acids Res. 31, 5526–5533.
Eustermann, S., Brockmann, C., Mehrotra, P.V., Yang, J.C., Loakes, D., West, S.C., Ahel, I., Neuhaus, D., 2010. Solution structures of the two PBZ domains from human APLF and their interaction with poly(ADP-ribose). Nat. Struct. Mol. Biol. 17, 241–243.
Fahrer, J., Kranaster, R., Altmeyer, M., Marx, A., Burkle, A., 2007. Quantitative analysis of the binding affinity of poly(ADP-ribose) to specific binding proteins as a function of chain length. Nucleic Acids Res. 35, e143.
Fahrer, J., Popp, O., Malanga, M., Beneke, S., Markovitz, D.M., Ferrando-May, E., Burkle, A., Kappes, F., 2010. High-affinity interaction of poly(ADP-ribose) and the human DEK oncoprotein depends upon chain length. Biochemistry 49, 7119–7130.
Fossati, S., Formentini, L., Wang, Z.Q., Moroni, F., Chiarugi, A., 2006. Poly(ADP-ribosyl)ation regulates heat shock factor-1 activity and the heat shock response in murine fibroblasts. Biochem. Cell Biol. 84, 703–712.
Friedemann, J., Grosse, F., Zhang, S., 2005. Nuclear DNA helicase II (RNA helicase A) interacts with Werner syndrome helicase and stimulates its exonuclease activity. J. Biol. Chem. 280, 31303–31313.
Gagne, J.P., Haince, J.F., Pic, E., Poirier, G.G., 2011. Affinity-based assays for the identification and quantitative evaluation of noncovalent poly(ADP-ribose)-binding proteins. Methods Mol. Biol. 780, 93–115.
Gagne, J.P., Hunter, J.M., Labrecque, B., Chabot, B., Poirier, G.G., 2003. A proteomic approach to the identification of heterogeneous nuclear ribonucleoproteins as a new family of poly(ADP-ribose)-binding proteins. Biochem. J. 371, 331–340.
Gagne, J.P., Isabelle, M., Lo, K.S., Bourassa, S., Hendzel, M.J., Dawson, V.L., Dawson, T.M., Poirier, G.G., 2008. Proteome-wide identification of poly(ADP-ribose) binding proteins and poly(ADP-ribose)-associated protein complexes. Nucleic Acids Res. 36, 6959–6976.
Gagne, J.P., Pic, E., Isabelle, M., Krietsch, J., Ethier, C., Paquet, E., Kelly, I., Boutin, M., Moon, K.M., Foster, L.J., Poirier, G.G., 2012. Quantitative proteomics profiling of the poly(ADP-ribose)-related response to genotoxic stress. Nucleic Acids Res. 40, 7788–7805.
Gamble, M.J., Kraus, W.L., 2010. Multiple facets of the unique histone variant macroH2A: from genomics to cell biology. Cell Cycle 9, 2568–2574.
Garnett, M.J., Edelman, E.J., Heidorn, S.J., Greenman, C.D., Dastur, A., Lau, K.W., Greninger, P., Thompson, I.R., Luo, X., Soares, J., Liu, Q., Iorio, F., Surdez, D., Chen, L., Milano, R.J., Bignell, G.R., Tam, A.T., Davies, H., Stevenson, J.A., Barthorpe, S., Lutz, S.R., Kogera, F., Lawrence, K., McLaren-Douglas, A., Mitropoulos, X., Mironenko, T., Thi, H., Richardson, L., Zhou, W., Jewitt, F., Zhang, T., O'Brien, P., Boisvert, J.L., Price, S., Hur, W., Yang, W., Deng, X., Butler, A., Choi, H.G., Chang, J.W., Baselga, J., Stamenkovic, I., Engelman, J.A., Sharma, S.V., Delattre, O., Saez-Rodriguez, J., Gray, N.S., Settleman, J., Futreal, P.A., Haber, D.A., Stratton, M.R., Ramaswamy, S., McDermott, U., Benes, C.H., 2012. Systematic identification of genomic markers of drug sensitivity in cancer cells. Nature 483, 570–575.
Gieni, R.S., Ismail, I.H., Campbell, S., Hendzel, M.J., 2011. Polycomb group proteins in the DNA damage response: a link between radiation resistance and "stemness". Cell Cycle 10, 883–894.
Goenka, S., Boothby, M., 2006. Selective potentiation of Stat-dependent gene expression by collaborator of Stat6 (CoaSt6), a transcriptional cofactor. Proc. Natl. Acad. Sci. USA 103, 4210–4215.
Goenka, S., Cho, S.H., Boothby, M., 2007. Collaborator of Stat6 (CoaSt6)-associated poly(ADP-ribose) polymerase activity modulates Stat6-dependent gene transcription. J. Biol. Chem. 282, 18732–18739.
Gottschalk, A.J., Timinszky, G., Kong, S.E., Jin, J., Cai, Y., Swanson, S.K., Washburn, M.P., Florens, L., Ladurner, A.G., Conaway, J.W., Conaway, R.C., 2009. Poly(ADP-ribosyl)ation directs recruitment and activation of an ATP-dependent chromatin remodeler. Proc. Natl. Acad. Sci. USA 106, 13770–13774.
Gudjonsson, T., Altmeyer, M., Savic, V., Toledo, L., Dinant, C., Grofte, M., Bartkova, J., Poulsen, M., Oka, Y., Bekker-Jensen, S., Mailand, N., Neumann, B., Heriche, J.K., Shearer, R., Saunders, D., Bartek, J., Lukas, J., Lukas, C., 2012. TRIP12 and UBR5 suppress spreading of chromatin ubiquitylation at damaged chromosomes. Cell 150, 697–709.
Guettler, S., LaRose, J., Petsalaki, E., Gish, G., Scotter, A., Pawson, T., Rottapel, R., Sicheri, F., 2011. Structural basis and sequence rules for substrate recognition by Tankyrase explain the basis for cherubism disease. Cell 147, 1340–1354.
Haince, J.-F., Kozlov, S., Dawson, V.L., Dawson, T.M., Hendzel, M.J., Lavin, M.F., Poirier, G.G., 2007. Ataxia Telangiectasia Mutated (ATM) Signaling Network Is Modulated by a Novel Poly(ADP-ribose)-dependent Pathway in the Early Response to DNA-damaging Agents. J. Biol. Chem. 282, 16441–16453.
Haince, J.F., McDonald, D., Rodrigue, A., Dery, U., Masson, J.Y., Hendzel, M.J., Poirier, G.G., 2008. PARP1-dependent kinetics of recruitment of MRE11 and NBS1 proteins to multiple DNA damage sites. J. Biol. Chem. 283, 1197–1208.
Hall, J.R., Kow, E., Nevis, K.R., Lu, C.K., Luce, K.S., Zhong, Q., Cook, J.G., 2007. Cdc6 stability is regulated by the Huwe1 ubiquitin ligase after DNA damage. Mol. Biol. Cell 18, 3340–3350.
Han, S.P., Tang, Y.H., Smith, R., 2010. Functional diversity of the hnRNPs: past, present and perspectives. Biochem. J. 430, 379–392.
Han, W.D., Zhao, Y.L., Meng, Y.G., Zang, L., Wu, Z.Q., Li, Q., Si, Y.L., Huang, K., Ba, J.M., Morinaga, H., Nomura, M., Mu, Y.M., 2007. Estrogenically regulated LRP16 interacts with estrogen receptor alpha and enhances the receptor's transcriptional activity. Endocr. Relat. Cancer 14, 741–753.
Harris, J.L., Jakob, B., Taucher-Scholz, G., Dianov, G.L., Becherel, O.J., Lavin, M.F., 2009. Aprataxin, poly-ADP ribose polymerase 1 (PARP-1) and apurinic endonuclease 1 (APE1) function together to protect the genome against oxidative damage. Hum. Mol. Genet. 18, 4102–4117.
Hazrati, A., Ramis-Castelltort, M., Sarkar, S., Barber, L.J., Schofield, C.J., Hartley, J.A., McHugh, P.J., 2008. Human SNM1A suppresses the DNA repair defects of yeast pso2 mutants. DNA Repair (Amsterdam) 7, 230–238.
He, F., Tsuda, K., Takahashi, M., Kuwasako, K., Terada, T., Shirouzu, M., Watanabe, S., Kigawa, T., Kobayashi, N., Guntert, P., Yokoyama, S., Muto, Y., 2012. Structural insight into the interaction of ADP-ribose with the PARP WWE domains. FEBS Lett. 586, 3858–3864.
Helleday, T., 2011. The underlying mechanism for the PARP and BRCA synthetic lethality: clearing up the misunderstandings. Mol. Oncol. 5, 387–393.
Honjo, T., Nishizuka, Y., Hayaishi, O., 1968. Diphtheria toxin-dependent adenosine diphosphate ribosylation of aminoacyl transferase II and inhibition of protein synthesis. J. Biol. Chem. 243, 3553–3555.
Hori, K., Fostier, M., Ito, M., Fuwa, T.J., Go, M.J., Okano, H., Baron, M., Matsuno, K., 2004. Drosophila deltex mediates suppressor of Hairless-independent and late-endosomal activation of Notch signaling. Development 131, 5527–5537.
Hottiger, M.O., Hassa, P.O., Luscher, B., Schuler, H., Koch-Nolte, F., 2010. Toward a unified nomenclature for mammalian ADP-ribosyltransferases. Trends Biochem. Sci. 35, 208–219.
Huang, S.M., Mishina, Y.M., Liu, S., Cheung, A., Stegmeier, F., Michaud, G.A., Charlat, O., Wiellette, E., Zhang, Y., Wiessner, S., Hild, M., Shi, X., Wilson, C.J., Mickanin, C., Myer, V., Fazal, A., Tomlinson, R., Serluca, F., Shao, W., Cheng, H., Shultz, M., Rau, C., Schirle, M., Schlegl, J., Ghidelli, S., Fawell, S., Lu, C., Curtis, D., Kirschner, M.W., Lengauer, C., Finan, P.M., Tallarico, J.A., Bouwmeester, T., Porter, J.A., Bauer, A., Cong, F., 2009. Tankyrase inhibition stabilizes axin and antagonizes Wnt signalling. Nature 461, 614–620.
Ibrahim, Y.H., Garcia-Garcia, C., Serra, V., He, L., Torres-Lockhart, K., Prat, A., Anton, P., Cozar, P., Guzman, M., Grueso, J., Rodriguez, O., Calvo, M.T., Aura, C., Diez, O., Rubio, I.T., Perez, J., Rodon, J., Cortes, J., Ellisen, L.W., Scaltriti, M., Baselga, J., 2012. PI3K Inhibition Impairs BRCA1/2 Expression and Sensitizes BRCA-Proficient Triple-Negative Breast Cancer to PARP Inhibition. Cancer Discov.. http://dx.doi.org/10.1158/2159-8290.CD-11-0348.
Iles, N., Rulten, S., El-Khamisy, S.F., Caldecott, K.W., 2007. APLF (C2orf13) is a novel human protein involved in the cellular response to chromosomal DNA strand breaks. Mol. Cell Biol. 27, 3793–3803.
Isabelle, M., Gagne, J.P., Gallouzi, I.E., Poirier, G.G., 2012. Quantitative proteomics and dynamic imaging reveal that G3BP-mediated stress granule assembly is poly(ADP-ribose)-dependent following exposure to MNNG-induced DNA alkylation. J. Cell Sci.. http://dx.doi.org/10.1242/jcs.106963.
Ismail, I.H., Gagne, J.P., Caron, M.C., McDonald, D., Xu, Z., Masson, J.Y., Poirier, G.G., Hendzel, M.J., 2012. CBX4-mediated SUMO modification regulates BMI1 recruitment at sites of DNA damage. Nucleic Acids Res. 40, 5497–5510.
Isogai, S., Kanno, S., Ariyoshi, M., Tochio, H., Ito, Y., Yasui, A., Shirakawa, M., 2010. Solution structure of a zinc-finger domain that binds to poly-ADP-ribose. Genes Cells 15, 101–110.
Javle, M., Curtin, N.J., 2011. The role of PARP in DNA repair and its therapeutic exploitation. Br. J. Cancer 105, 1114–1122.
Ji, Y., Tulin, A.V., 2009. Poly(ADP-ribosyl)ation of heterogeneous nuclear ribonucleoproteins modulates splicing. Nucleic Acids Res. 37, 3501–3513.

Ji, Y., Tulin, A.V., 2012. Poly(ADP-ribose) controls DE-cadherin-dependent stem cell maintenance and oocyte localization. Nat. Commun. 3, 760.
Juvekar, A., Burga, L.N., Hu, H., Lunsford, E.P., Ibrahim, Y.H., Balmana, J., Rajendran, A., Papa, A., Spencer, K., Lyssiotis, C.A., Nardella, C., Pandolfi, P.P., Baselga, J., Scully, R., Asara, J.M., Cantley, L.C., Wulf, G.M., 2012. Combining a PI3K Inhibitor with a PARP Inhibitor Provides an Effective Therapy for BRCA1-Related Breast Cancer. Cancer Discov.. http://dx.doi.org/10.1158/2159-8290.CD-11-0336.
Kang, H.C., Lee, Y.I., Shin, J.H., Andrabi, S.A., Chi, Z., Gagne, J.P., Lee, Y., Ko, H.S., Lee, B.D., Poirier, G.G., Dawson, V.L., Dawson, T.M., 2011. Iduna is a poly(ADP-ribose) (PAR)-dependent E3 ubiquitin ligase that regulates DNA damage. Proc. Natl. Acad. Sci. USA 108, 14103–14108.
Kanno, S., Kuzuoka, H., Sasao, S., Hong, Z., Lan, L., Nakajima, S., Yasui, A., 2007. A novel human AP endonuclease with conserved zinc-finger-like motifs involved in DNA strand break responses. EMBO J. 26, 2094–2103.
Karras, G.I., Kustatscher, G., Buhecha, H.R., Allen, M.D., Pugieux, C., Sait, F., Bycroft, M., Ladurner, A.G., 2005. The macro domain is an ADP-ribose binding module. EMBO J. 24, 1911–1920.
Kashima, L., Idogawa, M., Mita, H., Shitashige, M., Yamada, T., Ogi, K., Suzuki, H., Toyota, M., Ariga, H., Sasaki, Y., Tokino, T., 2012. CHFR protein regulates mitotic checkpoint by targeting PARP-1 protein for ubiquitination and degradation. J. Biol. Chem. 287, 12975–12984.
Kedersha, N., Anderson, P., 2007. Mammalian stress granules and processing bodies. Methods Enzymol. 431, 61–81.
Khoronenkova, S.V., Dianov, G.L., 2011. The emerging role of Mule and ARF in the regulation of base excision repair. FEBS Lett. 585, 2831–2835.
Kiehlbauch, C.C., Aboul-Ela, N., Jacobson, E.L., Ringer, D.P., Jacobson, M.K., 1993. High resolution fractionation and characterization of ADP-ribose polymers. Anal. Biochem. 208, 26–34.
Kim, I.K., Kiefer, J.R., Ho, C.M., Stegeman, R.A., Classen, S., Tainer, J.A., Ellenberger, T., 2012a. Structure of mammalian poly(ADP-ribose) glycohydrolase reveals a flexible tyrosine clasp as a substrate-binding element. Nat. Struct. Mol. Biol. 19, 653–656.
Kim, M.K., Dudognon, C., Smith, S., 2012b. Tankyrase 1 regulates centrosome function by controlling CPAP stability. EMBO Rep. 13, 724–732.
Kleine, H., Poreba, E., Lesniewicz, K., Hassa, P.O., Hottiger, M.O., Litchfield, D.W., Shilton, B.H., Luscher, B., 2008. Substrate-assisted catalysis by PARP10 limits its activity to mono-ADP-ribosylation. Mol. Cell. 32, 57–69.
Kleppa, L., Mari, P.O., Larsen, E., Lien, G.F., Godon, C., Theil, A.F., Nesse, G.J., Wiksen, H., Vermeulen, W., Giglia-Mari, G., Klungland, A., 2012. Kinetics of endogenous mouse FEN1 in base excision repair. Nucleic Acids Res. 40, 9044–9059.
Koh, D.W., Lawler, A.M., Poitras, M.F., Sasaki, M., Wattler, S., Nehls, M.C., Stoger, T., Poirier, G.G., Dawson, V.L., Dawson, T.M., 2004. Failure to degrade poly(ADP-ribose) causes increased sensitivity to cytotoxicity and early embryonic lethality. Proc. Natl. Acad. Sci. USA 101, 17699–17704.
Kornblihtt, A.R., Schor, I.E., Allo, M., Blencowe, B.J., 2009. When chromatin meets splicing. Nat. Struct. Mol. Biol. 16, 902–903.
Krietsch, J., Caron, M.C., Gagne, J.P., Ethier, C., Vignard, J., Vincent, M., Rouleau, M., Hendzel, M.J., Poirier, G.G., Masson, J.Y., 2012. PARP activation regulates the RNA-binding protein NONO in the DNA damage response to DNA double-strand breaks. Nucleic Acids Res.. http://dx.doi.org/10.1093/nar/gks798.
Krishnakumar, R., Kraus, W.L., 2010. The PARP side of the nucleus: molecular actions, physiological outcomes, and clinical targets. Mol. Cell. 39, 8–24.
Kustatscher, G., Hothorn, M., Pugieux, C., Scheffzek, K., Ladurner, A.G., 2005. Splicing regulates NAD metabolite binding to histone macroH2A. Nat. Struct. Mol. Biol. 12, 624–625.
Lai, A.Y., Wade, P.A., 2011. Cancer biology and NuRD: a multifaceted chromatin remodelling complex. Nat. Rev. Cancer 11, 588–596.
Leppard, J.B., Dong, Z., Mackey, Z.B., Tomkinson, A.E., 2003. Physical and functional interaction between DNA ligase IIIalpha and poly(ADP-Ribose) polymerase 1 in DNA single-strand break repair. Mol. Cell Biol. 23, 5919–5927.
Leung, A., Todorova, T., Ando, Y., Chang, P., 2012. Poly(ADP-ribose) regulates post-transcriptional gene regulation in the cytoplasm. RNA Biol. 9, 542–548.
Leung, A.K., Vyas, S., Rood, J.E., Bhutkar, A., Sharp, P.A., Chang, P., 2011. Poly(ADP-ribose) regulates stress responses and microRNA activity in the cytoplasm. Mol. Cell 42, 489–499.
Levaot, N., Voytyuk, O., Dimitriou, I., Sircoulomb, F., Chandrakumar, A., Deckert, M., Krzyzanowski, P.M., Scotter, A., Gu, S., Janmohamed, S., Cong, F., Simoncic, P.D., Ueki, Y., La Rose, J., Rottapel, R., 2011. Loss of Tankyrase-mediated destruction of 3BP2 is the underlying pathogenic mechanism of cherubism. Cell 147, 1324–1339.
Li, G.Y., McCulloch, R.D., Fenton, A.L., Cheung, M., Meng, L., Ikura, M., Koch, C.A., 2010. Structure and identification of ADP-ribose recognition motifs of APLF and role in the DNA damage response. Proc. Natl. Acad. Sci. USA 107, 9129–9134.
Long, J.C., Caceres, J.F., 2009. The SR protein family of splicing factors: master regulators of gene expression. Biochem. J. 417, 15–27.
Luijsterburg, M.S., Lindh, M., Acs, K., Vrouwe, M.G., Pines, A., van Attikum, H., Mullenders, L.H., Dantuma, N.P., 2012. DDB2 promotes chromatin decondensation at UV-induced DNA damage. J. Cell Biol. 197, 267–281.
Ma, N.F., Hu, L., Fung, J.M., Xie, D., Zheng, B.J., Chen, L., Tang, D.J., Fu, L., Wu, Z., Chen, M., Fang, Y., Guan, X.Y., 2008. Isolation and characterization of a novel oncogene, amplified in liver cancer 1, within a commonly amplified region at 1q21 in hepatocellular carcinoma. Hepatology 47, 503–510.
Macrae, C.J., McCulloch, R.D., Ylanko, J., Durocher, D., Koch, C.A., 2008. APLF (C2orf13) facilitates nonhomologous end-joining and undergoes ATM-dependent hyperphosphorylation following ionizing radiation. DNA Repair (Amsterdam) 7, 292–302.
Malanga, M., Althaus, F.R., 2004. Poly(ADP-ribose) reactivates stalled DNA topoisomerase I and Induces DNA strand break resealing. J. Biol. Chem. 279, 5244–5248.
Malanga, M., Althaus, F.R., 2005. The role of poly(ADP-ribose) in the DNA damage signaling network. Biochem. Cell Biol. 83, 354–364.
Malanga, M., Atorino, L., Tramontano, F., Farina, B., Quesada, P., 1998. Poly(ADP-ribose) binding properties of histone H1 variants. Biochim. Biophys. Acta 1399, 154–160.
Malanga, M., Czubaty, A., Girstun, A., Staron, K., Althaus, F.R., 2008. Poly(ADP-ribose) binds to the splicing factor ASF/SF2 and regulates its phosphorylation by DNA topoisomerase I. J. Biol. Chem. 283, 19991–19998.
Malet, H., Coutard, B., Jamal, S., Dutartre, H., Papageorgiou, N., Neuvonen, M., Ahola, T., Forrester, N., Gould, E.A., Lafitte, D., Ferron, F., Lescar, J., Gorbalenya, A.E., de Lamballerie, X., Canard, B., 2009. The crystal structures of Chikungunya and Venezuelan equine encephalitis virus nsP3 macro domains define a conserved adenosine binding pocket. J. Virol. 83, 6534–6545.
Martzen, M.R., McCraith, S.M., Spinelli, S.L., Torres, F.M., Fields, S., Grayhack, E.J., Phizicky, E.M., 1999. A biochemical genomics approach for identifying genes by the activity of their products. Science 286, 1153–1155.
Matsuno, K., Ito, M., Hori, K., Miyashita, F., Suzuki, S., Kishi, N., Artavanis-Tsakonas, S., Okano, H., 2002. Involvement of a proline-rich motif and RING-H2 finger of Deltex in the regulation of Notch signaling. Development 129, 1049–1059.
Messner, S., Altmeyer, M., Zhao, H., Pozivil, A., Roschitzki, B., Gehrig, P., Rutishauser, D., Huang, D., Caflisch, A., Hottiger, M.O., 2010. PARP1 ADP-ribosylates lysine residues of the core histone tails. Nucleic Acids Res. 38, 6350–6362.
Meyer-Ficca, M.L., Meyer, R.G., Jacobson, E.L., Jacobson, M.K., 2005. Poly(ADP-ribose) polymerases: managing genome stability. Int. J. Biochem. Cell Biol. 37, 920–926.
Minaga, T., Kun, E., 1983a. Probable helical conformation of poly(ADP-ribose). The effect of cations on spectral properties. J. Biol. Chem. 258, 5726–5730.
Minaga, T., Kun, E., 1983b. Spectral analysis of the conformation of polyadenosine diphosphoribose. Evidence indicating secondary structure. J. Biol. Chem. 258, 725–730.
Mischo, H.E., Hemmerich, P., Grosse, F., Zhang, S., 2005. Actinomycin D induces histone gamma-H2AX foci and complex formation of gamma-H2AX with Ku70 and nuclear DNA helicase II. J. Biol. Chem. 280, 9586–9594.
Mortusewicz, O., Leonhardt, H., 2007. XRCC1 and PCNA are loading platforms with distinct kinetic properties and different capacities to respond to multiple DNA lesions. BMC Mol. Biol. 8, 81.
Moyle, P.M., Muir, T.W., 2010. Method for the synthesis of mono-ADP-ribose conjugated peptides. J. Am. Chem. Soc. 132, 15878–15880.
Mukherjee, A., Veraksa, A., Bauer, A., Rosse, C., Camonis, J., Artavanis-Tsakonas, S., 2005. Regulation of Notch signalling by non-visual beta-arrestin. Nat. Cell Biol. 7, 1191–1201.
Murawska, M., Hassler, M., Renkawitz-Pohl, R., Ladurner, A., Brehm, A., 2011. Stress-induced PARP activation mediates recruitment of Drosophila Mi-2 to promote heat shock gene expression. PLoS Genet. 7, e1002206.

Muthurajan, U.M., McBryant, S.J., Lu, X., Hansen, J.C., Luger, K., 2011. The linker region of macroH2A promotes self-association of nucleosomal arrays. J. Biol. Chem. 286, 23852–23864.
Nakazawa, K., Ueda, K., Honjo, T., Yoshihara, K., Nishizuka, Y., Hayaishi, O., 1968. Nicotinamide adenine dinucleotide glycohydrolases and poly adenosine diphosphate ribose synthesis in rat liver. Biochem. Biophys. Res. Commun. 32, 143–149.
Neuvonen, M., Ahola, T., 2009. Differential activities of cellular and viral macro domain proteins in binding of ADP-ribose metabolites. J. Mol. Biol. 385, 212–225.
Nishizuka, Y., Ueda, K., Nakazawa, K., Hayaishi, O., 1967. Studies on the polymer of adenosine diphosphate ribose. I. Enzymic formation from nicotinamide adenine dinuclotide in mammalian nuclei. J. Biol. Chem. 242, 3164–3171.
Nowsheen, S., Cooper, T., Bonner, J.A., Lobuglio, A.F., Yang, E.S., 2012. HER2 overexpression renders human breast cancers sensitive to PARP inhibition independently of any defect in homologous recombination DNA repair. Cancer Res. 72, 4796–4806.
Oberoi, J., Richards, M.W., Crumpler, S., Brown, N., Blagg, J., Bayliss, R., 2010. Structural basis of poly(ADP-ribose) recognition by the multizinc binding domain of checkpoint with forkhead-associated and RING domains (CHFR). J. Biol. Chem. 285, 39348–39358.
Ohashi, Y., Ueda, K., Kawaichi, M., Hayaishi, O., 1983. Activation of DNA ligase by poly(ADP-ribose) in chromatin. Proc. Natl. Acad. Sci. USA 80, 3604–3607.
Oka, J., Ueda, K., Hayaishi, O., Komura, H., Nakanishi, K., 1984. ADP-ribosyl protein lyase. Purification, properties, and identification of the product. J. Biol. Chem. 259, 986–995.
Oplustilova, L., Wolanin, K., Mistrik, M., Korinkova, G., Simkova, D., Bouchal, J., Lenobel, R., Bartkova, J., Lau, A., O'Connor, M.J., Lukas, J., Bartek, J., 2012. Evaluation of candidate biomarkers to predict cancer cell sensitivity or resistance to PARP-1 inhibitor treatment. Cell Cycle 11, 3837–3850.
Otake, H., Miwa, M., Fujimura, S., Sugimura, T., 1969. Binding of ADP-ribose polymer with histone. J. Biochem. 65, 145–146.
Pace, C.N., Scholtz, J.M., 1998. A helix propensity scale based on experimental studies of peptides and proteins. Biophys. J. 75, 422–427.
Panzeter, P.L., Realini, C.A., Althaus, F.R., 1992. Noncovalent interactions of poly(adenosine diphosphate ribose) with histones. Biochemistry 31, 1379–1385.
Panzeter, P.L., Zweifel, B., Malanga, M., Waser, S.H., Richard, M., Althaus, F.R., 1993. Targeting of histone tails by poly(ADP-ribose). J. Biol. Chem. 268, 17662–17664.
Parsons, J.L., Tait, P.S., Finch, D., Dianova, I.I., Edelmann, M.J., Khoronenkova, S.V., Kessler, B.M., Sharma, R.A., McKenna, W.G., Dianov, G.L., 2009. Ubiquitin ligase ARF-BP1/Mule modulates base excision repair. EMBO J. 28, 3207–3215.
Patel, A.G., Sarkaria, J.N., Kaufmann, S.H., 2011. Nonhomologous end joining drives poly(ADP-ribose) polymerase (PARP) inhibitor lethality in homologous recombination-deficient cells. Proc. Natl. Acad. Sci. USA 108, 3406–3411.
Paulsen, R.D., Soni, D.V., Wollman, R., Hahn, A.T., Yee, M.C., Guan, A., Hesley, J.A., Miller, S.C., Cromwell, E.F., Solow-Cordero, D.E., Meyer, T., Cimprich, K.A., 2009. A genome-wide siRNA screen reveals diverse cellular processes and pathways that mediate genome stability. Mol. Cell. 35, 228–239.
Pehrson, J.R., Fried, V.A., 1992. MacroH2A, a core histone containing a large nonhistone region. Science 257, 1398–1400.
Pines, A., Vrouwe, M.G., Marteijn, J.A., Typas, D., Luijsterburg, M.S., Cansoy, M., Hensbergen, P., Deelder, A., de Groot, A., Matsumoto, S., Sugasawa, K., Thoma, N., Vermeulen, W., Vrieling, H., Mullenders, L., 2012. PARP1 promotes nucleotide excision repair through DDB2 stabilization and recruitment of ALC1. J. Cell Biol. 199, 235–249.
Piotrowski, Y., Hansen, G., Boomaars-van der Zanden, A.L., Snijder, E.J., Gorbalenya, A.E., Hilgenfeld, R., 2009. Crystal structures of the X-domains of a Group-1 and a Group-3 coronavirus reveal that ADP-ribose-binding may not be a conserved property. Protein Sci. 18, 6–16.
Pleschke, J.M., Kleczkowska, H.E., Strohm, M., Althaus, F.R., 2000. Poly(ADP-ribose) binds to specific domains in DNA damage checkpoint proteins. J. Biol. Chem. 275, 40974–40980.
Poirier, G.G., de Murcia, G., Jongstra-Bilen, J., Niedergang, C., Mandel, P., 1982. Poly(ADP-ribosyl)ation of polynucleosomes causes relaxation of chromatin structure. Proc. Natl. Acad. Sci. USA 79, 3423–3427.
Polo, S.E., Kaidi, A., Baskcomb, L., Galanty, Y., Jackson, S.P., 2010. Regulation of DNA-damage responses and cell-cycle progression by the chromatin remodelling factor CHD4. EMBO J. 29, 3130–3139.
Popp, O., Veith, S., Fahrer, J., Bohr, V.A., Burkle, A., Mangerich, A., 2012. Site-specific non-covalent interaction of the biopolymer poly(ADP-ribose) with the Werner syndrome protein regulates protein functions. ACS Chem. Biol.. http://dx.doi.org/10.1021/cb300363g.
Reale, A., Matteis, G.D., Galleazzi, G., Zampieri, M., Caiafa, P., 2005. Modulation of DNMT1 activity by ADP-ribose polymers. Oncogene 24, 13–19.
Reeder, R.H., Ueda, K., Honjo, T., Nishizuka, Y., Hayaishi, O., 1967. Studies on the polymer of adenosine diphosphate ribose. II. Characterization of the polymer. J. Biol. Chem. 242, 3172–3179.
Reh, S., Korn, C., Gimadutdinow, O., Meiss, G., 2005. Structural basis for stable DNA complex formation by the caspase-activated DNase. J. Biol. Chem. 280, 41707–41715.
Rouleau, M., Patel, A., Hendzel, M.J., Kaufmann, S.H., Poirier, G.G., 2010. PARP inhibition: PARP1 and beyond. Nat. Rev. Cancer 10, 293–301.
Rulten, S.L., Cortes-Ledesma, F., Guo, L., Iles, N.J., Caldecott, K.W., 2008. APLF (C2orf13) is a novel component of poly(ADP-ribose) signaling in mammalian cells. Mol. Cell Biol. 28, 4620–4628.
Rulten, S.L., Fisher, A.E., Robert, I., Zuma, M.C., Rouleau, M., Ju, L., Poirier, G., Reina-San-Martin, B., Caldecott, K.W., 2011. PARP-3 and APLF function together to accelerate nonhomologous end-joining. Mol. Cell 41, 33–45.
Sauermann, G., Wesierska-Gadek, J., 1986. Poly(ADP-ribose) effectively competes with DNA for histone H4 binding. Biochem. Biophys. Res. Commun. 139, 523–529.
Saxena, A., Saffery, R., Wong, L.H., Kalitsis, P., Choo, K.H., 2002. Centromere proteins Cenpa, Cenpb, and Bub3 interact with poly(ADP-ribose) polymerase-1 protein and are poly(ADP-ribosyl)ated. J. Biol. Chem. 277, 26921–26926.
Schiewer, M.J., Goodwin, J.F., Han, S., Brenner, J.C., Augello, M.A., Dean, J.L., Liu, F., Planck, J.L., Ravindranathan, P., Chinnaiyan, A.M., McCue, P., Gomella, L.G., Raj, G.V., Dicker, A.P., Brody, J.R., Pascal, J.M., Centenera, M.M., Butler, L.M., Tilley, W.D., Feng, F.Y., Knudsen, K.E., 2012. Dual roles of PARP-1 promote cancer growth and progression. Cancer Discov.. http://dx.doi.org/10.1158/2159-8290.CD-12-0120.
Schmitz, A.A., Pleschke, J.M., Kleczkowska, H.E., Althaus, F.R., Vergeres, G., 1998. Poly(ADP-ribose) modulates the properties of MARCKS proteins. Biochemistry 37, 9520–9527.
Schultheisz, H.L., Szymczyna, B.R., Williamson, J.R., 2009. Enzymatic synthesis and structural characterization of 13C, 15N-poly(ADP-ribose). J. Am. Chem. Soc. 131, 14571–14578.
Scolnick, D.M., Halazonetis, T.D., 2000. Chfr defines a mitotic stress checkpoint that delays entry into metaphase. Nature 406, 430–435.
Sellis, D., Drosou, V., Vlachakis, D., Voukkalis, N., Giannakouros, T., Vlassi, M., 2012. Phosphorylation of the arginine/serine repeats of lamin B receptor by SRPK1-insights from molecular dynamics simulations. Biochim. Biophys. Acta 1820, 44–55.
Slade, D., Dunstan, M.S., Barkauskaite, E., Weston, R., Lafite, P., Dixon, N., Ahel, M., Leys, D., Ahel, I., 2011. The structure and catalytic mechanism of a poly(ADP-ribose) glycohydrolase. Nature 477, 616–620.
Stilmann, M., Hinz, M., Arslan, S.C., Zimmer, A., Schreiber, V., Scheidereit, C., 2009. A nuclear poly(ADP-ribose)-dependent signalosome confers DNA damage-induced IkappaB kinase activation. Mol. Cell 36, 365–378.
Takeyama, K., Aguiar, R.C., Gu, L., He, C., Freeman, G.J., Kutok, J.L., Aster, J.C., Shipp, M.A., 2003. The BAL-binding protein BBAP and related Deltex family members exhibit ubiquitin-protein isopeptide ligase activity. J. Biol. Chem. 278, 21930–21937.
Tanaka, M., Miwa, M., Hayashi, K., Kubota, K., Matsushima, T., 1977. Separation of oligo(adenosine diphosphate ribose) fractions with various chain lengths and terminal structures. Biochemistry 16, 1485–1489.
Till, S., Ladurner, A.G., 2009. Sensing NAD metabolites through macro domains. Front Biosci. 14, 3246–3258.
Timinszky, G., Till, S., Hassa, P.O., Hothorn, M., Kustatscher, G., Nijmeijer, B., Colombelli, J., Altmeyer, M., Stelzer, E.H., Scheffzek, K., Hottiger, M.O., Ladurner, A.G., 2009. A macrodomain-containing histone rearranges chromatin upon sensing PARP1 activation. Nat. Struct. Mol. Biol. 16, 923–929.
Ueda, K., Oka, J., Naruniya, S., Miyakawa, N., Hayaishi, O., 1972. Poly ADP-ribose glycohydrolase from rat liver nuclei, a novel enzyme degrading the polymer. Biochem. Biophys. Res. Commun. 46, 516–523.

Wang, Y., Dawson, V.L., Dawson, T.M., 2009. Poly(ADP-ribose) signals to mitochondrial AIF: a key event in parthanatos. Exp. Neurol. 218, 193–202.
Wang, Y., Kim, N.S., Haince, J.F., Kang, H.C., David, K.K., Andrabi, S.A., Poirier, G.G., Dawson, V.L., Dawson, T.M., 2011. Poly(ADP-ribose) (PAR) binding to apoptosis-inducing factor is critical for PAR polymerase-1-dependent cell death (parthanatos). Sci. Signal 4, ra20.
Wang, Z., Michaud, G.A., Cheng, Z., Zhang, Y., Hinds, T.R., Fan, E., Cong, F., Xu, W., 2012. Recognition of the iso-ADP-ribose moiety in poly(ADP-ribose) by WWE domains suggests a general mechanism for poly(ADP-ribosyl)ation-dependent ubiquitination. Genes Dev. 26, 235–240.
Wesierska-Gadek, J., Sauermann, G., 1988. The effect of poly(ADP-ribose) on interactions of DNA with histones H1, H3 and H4. Eur. J. Biochem. 173, 675–679.
West, J.D., Ji, C., Marnett, L.J., 2005. Modulation of DNA fragmentation factor 40 nuclease activity by poly(ADP-ribose) polymerase-1. J. Biol. Chem. 280, 15141–15147.
Wilkin, M., Tongngok, P., Gensch, N., Clemence, S., Motoki, M., Yamada, K., Hori, K., Taniguchi-Kanai, M., Franklin, E., Matsuno, K., Baron, M., 2008. Drosophila HOPS and AP-3 complex genes are required for a Deltex-regulated activation of notch in the endosomal trafficking pathway. Dev. Cell 15, 762–772.
Williamson, C.T., Kubota, E., Hamill, J.D., Klimowicz, A., Ye, R., Muzik, H., Dean, M., Tu, L., Gilley, D., Magliocco, A.M., McKay, B.C., Bebb, D.G., Lees-Miller, S.P., 2012. Enhanced cytotoxicity of PARP inhibition in mantle cell lymphoma harbouring mutations in both ATM and p53. EMBO Mol. Med. 4, 515–527.
Wu, Z., Li, Y., Li, X., Ti, D., Zhao, Y., Si, Y., Mei, Q., Zhao, P., Fu, X., Han, W., 2011. LRP16 integrates into NF-kappaB transcriptional complex and is required for its functional activation. PLoS One 6, e18157.
Xu, C., Xu, Y., Gursoy-Yuzugullu, O., Price, B.D., 2012. The histone variant macroH2A1.1 is recruited to DSBs through a mechanism involving PARP1. FEBS Lett. 586, 3920–3925.
Yang, J., Zhao, Y.L., Wu, Z.Q., Si, Y.L., Meng, Y.G., Fu, X.B., Mu, Y.M., Han, W.D., 2009. The single-macro domain protein LRP16 is an essential cofactor of androgen receptor. Endocr. Relat. Cancer 16, 139–153.
Yang, K., Moldovan, G.L., D'Andrea, A.D., 2010. RAD18-dependent recruitment of SNM1A to DNA repair complexes by a ubiquitin-binding zinc finger. J. Biol. Chem. 285, 19085–19091.
Ying, S., Hamdy, F.C., Helleday, T., 2012. Mre11-dependent degradation of stalled DNA replication forks is prevented by BRCA2 and PARP1. Cancer Res. 72, 2814–2821.
Yu, S.W., Andrabi, S.A., Wang, H., Kim, N.S., Poirier, G.G., Dawson, T.M., Dawson, V.L., 2006. Apoptosis-inducing factor mediates poly(ADP-ribose) (PAR) polymer-induced cell death. Proc. Natl. Acad. Sci. USA 103, 18314–18319.
Yu, S.W., Wang, H., Poitras, M.F., Coombs, C., Bowers, W.J., Federoff, H.J., Poirier, G.G., Dawson, T.M., Dawson, V.L., 2002. Mediation of poly(ADP-ribose) polymerase-1-dependent cell death by apoptosis-inducing factor. Science 297, 259–263.
Zampieri, M., Guastafierro, T., Calabrese, R., Ciccarone, F., Bacalini, M.G., Reale, A., Perilli, M., Passananti, C., Caiafa, P., 2012. ADP-ribose polymers localized on Ctcf-Parp1-Dnmt1 complex prevent methylation of Ctcf target sites. Biochem. J. 441, 645–652.
Zhang, Y., Liu, S., Mickanin, C., Feng, Y., Charlat, O., Michaud, G.A., Schirle, M., Shi, X., Hild, M., Bauer, A., Myer, V.E., Finan, P.M., Porter, J.A., Huang, S.M., Cong, F., 2011. RNF146 is a poly(ADP-ribose)-directed E3 ligase that regulates axin degradation and Wnt signalling. Nat. Cell Biol. 13, 623–629.
Zhou, Z.D., Chan, C.H., Xiao, Z.C., Tan, E.K., 2011. Ring finger protein 146/Iduna is a poly(ADP-ribose) polymer binding and PARsylation dependent E3 ubiquitin ligase. Cell Adh. Migr. 5, 463–471.
Zhu, Y., Chen, G., Lv, F., Wang, X., Ji, X., Xu, Y., Sun, J., Wu, L., Zheng, Y.T., Gao, G., 2011. Zinc-finger antiviral protein inhibits HIV-1 infection by selectively targeting multiply spliced viral mRNAs for degradation. Proc. Nat.l Acad. Sci. USA 108, 15834–15839.

7788–7805 Nucleic Acids Research, 2012, Vol. 40, No. 16 Published online 4 June 2012
doi:10.1093/nar/gks486

Quantitative proteomics profiling of the poly(ADP-ribose)-related response to genotoxic stress

Jean-Philippe Gagné[1], Émilie Pic[1], Maxim Isabelle[1], Jana Krietsch[1], Chantal Éthier[1], Éric Paquet[2], Isabelle Kelly[3], Michel Boutin[3], Kyung-Mee Moon[4], Leonard J. Foster[4] and Guy G. Poirier[1,*]

[1]Cancer Research Laboratory, [2]Genome Stability Laboratory, [3]Proteomics platform, Québec Genomic Center, Laval University - CHUQ Research Center, Québec, Canada G1V 4G2 and [4]Department of Biochemistry and Molecular Biology, University of British Columbia, Centre for High-Throughput Biology, Vancouver, British Columbia, Canada, V6T 1Z4

Received May 18, 2011; Revised May 1, 2012; Accepted May 3, 2012

ABSTRACT

Upon DNA damage induction, DNA-dependent poly(ADP-ribose) polymerases (PARPs) synthesize an anionic poly(ADP-ribose) (pADPr) scaffold to which several proteins bind with the subsequent formation of pADPr-associated multiprotein complexes. We have used a combination of affinity-purification methods and proteomics approaches to isolate these complexes and assess protein dynamics with respect to pADPr metabolism. As a first approach, we developed a substrate trapping strategy by which we demonstrate that a catalytically inactive Poly(ADP-ribose) glycohydrolase (PARG) mutant can act as a physiologically selective bait for the isolation of specific pADPr-binding proteins through its macrodomain-like domain. In addition to antibody-mediated affinity-purification methods, we used a pADPr macrodomain affinity resin to recover pADPr-binding proteins and their complexes. Second, we designed a time course experiment to explore the changes in the composition of pADPr-containing multiprotein complexes in response to alkylating DNA damage-mediated PARP activation. Spectral count clustering based on GeLC-MS/MS analysis was complemented with further analyses using high precision quantitative proteomics through isobaric tag for relative and absolute quantitation (iTRAQ)- and Stable isotope labeling by amino acids in cell culture (SILAC)-based proteomics. Here, we present a valuable resource in the interpretation of systems biology of the DNA damage response network in the context of poly(ADP-ribosyl)ation and provide a basis for subsequent investigations of pADPr-binding protein candidates.

INTRODUCTION

Poly(ADP-ribose) (pADPr) turnover is an important process involved in the transient response to DNA damage. The synthesis of pADPr that results from the activation of DNA-dependent poly(ADP-ribose) polymerases (PARPs) is one of the earliest step of DNA damage recognition and signaling in mammalian cells (1). During the response elicited by DNA damage, the addition of pADPr to chromatin-related proteins is associated with chromatin decondensation and dynamic nucleosome remodeling that tends to increase the accessibility of repair factors to DNA lesions (2). Numerous molecules are recruited at DNA- damage sites in a pADPr-dependent manner. Therefore, pADPr itself appears to be a signaling and scaffold molecule involved in the assembly of multi-subunit DNA repair complexes (3). In addition to covalent attachment of pADPr to target proteins, specific non-covalent pADPr interaction motifs have been characterized. Three major protein interaction modules were identified on the basis of their high affinity for pADPr: the macro domain (4), the poly(ADP-ribose)-binding zinc finger module (PBZ) (5) and the WWE domain (defined by the conserved residues tryptophan (WW) and glutamic acid (E)) that mediates protein–protein interactions in ubiquitin and ADP-ribose conjugation systems (6–8).

*To whom correspondence should be addressed. Tel: +1 418 654 2267; Fax: +1 418 654 2159; Email: guy.poirier@crchul.ulaval.ca

The authors wish it to be known that, in their opinion, the first two authors should be regarded as joint First Authors.

Besides domain-mediated interaction, several proteins are known to interact with pADPr through a generally short hydrophobic and basic region (9–11). This poly(ADP-ribose)-binding motif is widespread and frequently found in the DNA-binding domains of chromatin regulatory proteins and DNA repair factors. Collectively, pADPr-binding proteins generate a DNA repair network of protein factors through physical interactions with pADPr. In this view, pADPr behaves as a coordinator in the cellular response to genotoxic insults.

The macro domain has been the object of the first structural investigations on ADP-ribose recognition (12–13). A macroprotein was also used as a bait to define the ADP-ribosyl proteome, a method that proved to be effective although very limited gains in new protein identifications were achieved (14). A recent study from Slade and colleagues revealed that Poly(ADP-ribose) glycohydrolase (PARG) catalytic domain is a distant member of the ubiquitous ADP-ribose-binding macrodomain family (15). PARG is the main enzyme involved in the degradation of pADPr. Therefore, we reasoned that a catalytically inactive PARG mutant that forms stable interactions with pADPr, would also allow subsequent purification of poly(ADP-ribosyl)ated proteins and pADPr-containing protein complexes. A mass spectrometry (MS)-based substrate trapping strategy could further extent the proteome coverage achieved with antibody-mediated affinity-purification procedures. As part of this approach, we also revisited the strategy that couples affinity purification by an ADP-ribose-binding macrodomain (AF1521) with MS.

Over the past few years, our work, and that of many other labs exposed the fact that pADPr engages in highly specific non-covalent interactions with proteins (16–18). Strong binding to pADPr has the potential to act as a loading platform for a variety of proteins involved in DNA/RNA metabolism (19). Although pADPr-binding studies reflect the existence of strong molecular interactions with pADPr, it still remains a challenge to identify and quantify transient protein interaction with pADPr. The fast and transient dynamics of pADPr makes it an extremely challenging task. The use of DNA damaging agents that cause a broad spectrum of DNA lesions are useful tools to assess the modulation of the poly(ADP-ribosyl)ation reaction and the subsequent activation of DNA damage sensing enzymes.

N-methyl-N-nitro-N-nitrosoguanidine (MNNG) has been used for decades as an effective agent to induce massive pADPr synthesis through PARP-1 activation. In addition to inducing damage to the DNA bases, MNNG is an alkylating agent known to produce both DNA single-strand breaks (SSBs), as well as double-strand breaks (DSBs) (20,21). The exposure of cells to MNNG results in an almost immediate poly(ADP-ribosyl)ation of target proteins but little is known on their time course profiles, as well as their persistence in pADPr-containing protein complexes. As a first approach in this study, we used complementary proteome-mining methods that cover a large part of the accessible pADPr proteome. Using antibody-mediated and substrate trapping strategies to isolate pADPr-containing protein complexes, we present an overall picture of the pADPr proteome. Second, we focused on the highly dynamic composition of pADPr-containing protein complexes following an alkylation-induced DNA damage to provide insights into the functional processes modulated by poly(ADP-ribosyl)ation. The dynamic assembly of pADPr-containing protein complexes was revealed by the use of quantitative MS. Strategies for quantitative proteomic profiling included both *in vitro* and *in vivo* labeling approaches, as well as label-free quantitation. These proteome-wide approaches were coupled to pADPr affinity purification and complementary datasets were integrated and modeled for a more thorough insight into pADPr-binding protein dynamics. Here, we present the first quantitative proteomics investigation of the pADPr-associated proteome modulation in the context of DNA damage and PARP activation.

MATERIALS AND METHODS

Cell culture, vector construct and transfections

Human embryonic kidney 293 cells (HEK 293) and human cervical carcinoma cells (HeLa) were cultured (air/CO_2, 19:1, 37°C) in Dulbecco's modified Eagle's medium (DMEM) supplemented with 10% fetal bovine serum (FBS) (Hyclone-ThermoFisher Scientific, Ottawa, Canada). Penicillin (100 U/ml) and streptomycin (100 mg/ml) (Wisent, St-Bruno, Canada) were added to the culture media. Alkylating DNA damage was introduced using freshly prepared 100 µM MNNG for 5 min. Cells were washed twice with PBS before cell lysis or allowed to recover from the genotoxic insult for 1 or 2 h by replacing the growth medium with supplemented DMEM.

A human GFP-PARG-DEAD vector was modified by oligonucleotide-directed mutagenesis of the GFP-hPARG-110 (pEGFP-C1 expression vector, Clontech) previously described in Ref. (22). Mutagenic primers were made following the guidelines in the QuikChange® site-directed mutagenesis kit (Stratagene). A mutation was introduced at amino acid position 756 which completely abolishes PARG catalytic activity (E756D) as reported (23). Transfections were carried out with Effectene (Qiagen), as recommended by the manufacturer and cells were harvested 24 h post-transfection.

Immunoprecipitation of pADPr-containing protein complexes

HEK 293 and HeLa cells were seeded onto 150-mm cell culture dishes and grown up to 80–90% confluency (~15–20 millions cells/dish). Experiments were performed with cell extracts from three dishes per condition. Control cells were pre-incubated for 2 h with 5 µM PARP-1 inhibitor ABT-888 to maintain basal levels of pADPr, whereas a fast activation of PARP-1 resulting in a substantial increase in intracellular levels of pADPr was performed by incubating the cells with freshly prepared 100 µM MNNG for 5 min. All further steps were performed on ice or at 4°C. Two PBS washes were carried out prior to protein extraction with 2 ml/plate of lysis buffer [40 mM HEPES pH 7.5, 120 mM NaCl, 0.3% CHAPS, 1 mM

EDTA, 1X Complete™ protease inhibitor cocktail (Roche Applied Science, Indianapolis, IN, USA) and 1 μM PARG inhibitor ADP-HPD (adenosine 5′-diphosphate (hydroxymethyl) pyrrolidinediol) (EMD Chemicals, Gibbstown, NJ, USA)]. The whole cell lysates were pooled and placed on ice for 15 min and gently mixed for another 15–20 min on a rotating device for complete lysis. After homogenization, insoluble material was removed from the homogenate by centrifuging at 3000*g* for 5 min. Immunoprecipitation (IP) experiments were performed using magnetic Dynabeads™ covalently coupled to Protein G (Invitrogen, Burlington, Canada). The Dynabeads™ (125 μl/condition) were washed twice with 1 ml of 0.1 M sodium acetate buffer, pH 5.0 and coated with 12.5 μg of mouse monoclonal anti-pADPr antibody clone 10H (Tulip Biolabs, West Point, PA, USA), anti-GFP (Roche Applied Science, Indianapolis, IN, USA) or equivalent amount of normal mouse IgGs (Calbiochem-EMD Biosciences, San Diego, CA, USA). The antibody-coupled Dynabeads™ were incubated for 1 h with 1 ml of PBS containing 1% (w/v) bovine serum albumin (BSA) (Sigma-Aldrich, Oakville, Canada) to block non-specific antibody-binding sites. The beads were finally washed three times with 1 ml of lysis buffer and added to the pre-cleared pADPr-protein extract for a 2-h incubation with gentle mixing on a rotating device. Samples were washed five times with 10 ml of lysis buffer for 5 min. Protein complexes were eluted using 250 μl of 3X Laemmli sample buffer containing 5% β-mercaptoethanol and heated at 65°C for 5 min in a water bath. Proteins were resolved using 4–12% Criterion™ XT Bis–Tris gradient gel (Bio-Rad) and stained with Sypro Ruby (Bio-Rad) according to the manufacturer's instructions. Images were acquired using the Geliance CCD-based bioimaging system (PerkinElmer).

Isolation of pADPr-containing complexes using macrodomain pADPr affinity resin

pADPr-containing protein complexes were isolated with purified GST-Af1521 macrodomain fusion protein construct bound to glutathione beads (Tulip Biolabs, West Point, PA, USA). Macrodomain pADPr affinity resin was used essentially as described for IPs except that antibody-coupled magnetic beads are replaced with macrodomain affinity resin suspension (5 μl of the suspension/∼1 ml of protein extract).

Estimation of pADPr levels after exposure to MNNG

The dynamics of pADPr was evaluated by a relative quantitation of pADPr levels in cells after exposure to MNNG (5 min) and following a recovery period (1 and 2 h). Control and MNNG-treated HEK 293 cells were washed with ice-cold PBS and fixed with a 4% formaldehyde solution in PBS for 15 min. Five PBS washes were performed before membrane permeabilization with a 0.5% Triton X-100 solution in PBS. Cells were washed three times with PBS and incubated for 90 min at room temperature with anti-pADPr monoclonal antibody clone 10H (Tulip BioLabs, West Point, PA, USA) diluted 1:1000 in PBS containing 2% FBS. PBS washes were performed before incubating cells with an AlexaFluor-488 anti-mouse secondary antibody (Invitrogen). Cells were washed with PBS and counterstained with Hoechst 33342. Fluoromount-G mounting media (Southern Biotechn, Birmingham, AL, USA) was used to prepare microscope slides. Immunofluorescence images were acquired on a Zeiss LSM510 META NLO laser scanning confocal microscope. Zen 2009 software version 5.5 SP1 (Zeiss) was used for image acquisitions and fluorescence intensity measurements. In total, 300 cell nuclei were analyzed from three independent experiments for each experimental condition (100 nuclei/condition). Relative fluorescence intensity was expressed in arbitrary units (AU) and the data are represented as mean ± standard error of mean (SEM).

The recovery of pADPr in IP extracts was also determined at the same time-points following MNNG exposure. Aliquots of IP extracts were hand-spotted on Amersham Hybond-N+ positively charged nylon membrane (GE Healthcare) and probed with anti-pADPr antibody clone 96-10. Dihydroxyboronyl Bio-Rex (DHBB) purified pADPr was used as a reference for the establishment of a standard curve for quantitation (24).

Immunoblotting

Whole cell extracts and immunoprecipitates were separated on 4–12% Criterion XT™ Bis–Tris gradient gel (Bio-Rad) and transferred onto 0.45 μm pore size PVDF membrane (Millipore). After a 1-h incubation with a PBS–MT blocking solution (PBS containing 5% non-fat dried milk and 0.1% Tween20), the membrane was probed overnight with primary antibodies (refer to Supplementary Methods for detailed information). Membranes were washed with PBS-MT and species-specific horseradish peroxidase-conjugated secondary antibodies were added for 30 min. Signals were detected with Western Lightning™ Chemiluminescence Reagent Plus kit (Perkin Elmer). Semi-quantitative data was obtained from the scanned films by drawing region of interest (ROIs) around the bands to be quantified. Background signal was subtracted from all images. Signal intensity was expressed as ratios based on density units from control samples using the GeneTool software (PerkinElmer). All data were represented as mean ± standard deviation (SD).

GeLC-MS/MS and label-free spectral counting

SDS–PAGE protein lanes corresponding to immunoprecipitates and negative non-specific IgG control extracts were cut into gel slices using a disposable lane picker (The Gel Company, CA, USA). In-gel protein digest was performed on a MassPrep™ liquid handling station (Waters, Mississauga, Canada) according to the manufacturer's specifications and using sequencing-grade modified trypsin (Promega, Madison, WI, USA). Peptide extracts were dried out using a SpeedVac and separated by online reversed-phase nanoscale capillary liquid chromatography (nanoLC) and analyzed by electrospray MS (ES MS/MS)

using a LTQ linear ion trap mass spectrometer (Thermo Electron, San Jose, CA, USA) equipped with a nanoelectrospray ion source (Thermo Electron, San Jose, CA, USA). All MS/MS spectra were analyzed using Mascot (Matrix Science, London, UK; version 2.2.0). Scaffold (version 03_00_02, Proteome Software Inc., Portland, OR, USA) was used to sum the spectral counts, validate MS/MS-based peptide and protein identifications and group peptides into proteins (refer to Supplementary Methods for detailed information).

Semi-quantified proteins by spectral counting analysis were grouped on the basis of their correlated time course profiles following treatment with MNNG. We first normalized every protein spectral counts independently by first subtracting the mean of the spectral counts and then dividing the result by the standard deviation (*Z*-scores). With this transformation, every protein has a mean of zero and 1 SD. Using the *fpc* package (25) in *R* statistical environment (http://www.r-project.org/), we then identified the optimal number of clusters by running the *pamk* function (25). Heatmaps corresponding to 5 min MNNG, 1 and 2 h clusters were generated using MeV software v4.6.1 (http://www.tm4.org/mev/). Functional classification and ID conversion of identified proteins were accomplished by using DAVID (http:/www.david.abcc.ncifcrf.gov).

Isobaric tag for relative and absolute quantitation

For isobaric tag for relative and absolute quantitation (iTRAQ) labeling, proteins were eluted from the Dynabeads with 6% SDS. Proteins were precipitated overnight with 4 volumes of acetone, centrifuged 15 min at 10 000*g* (4°C) and pellets were resuspended in 0.5 M triethyl ammonium bicarbonate (TEAB) containing 0.1% SDS. Samples were then reduced, alkylated, digested and labeled according to the standard protocol supplied by the manufacturer (Applied Biosystems iTRAQ™ Reagents—Chemistry Reference Guide, P/N 4351918A). iTRAQ results were generated from the analysis of four isobaric tags. Control was labeled with iTRAQ reagent 114. The MNNG samples of 5 min, 1 h and 2 h were, respectively, labeled with iTRAQ reagents 115, 116 and 117. Labeled peptides were lyophilized and resuspended in 630 µl of Milli-Q water. An aliquot (315 µl) of this solution containing 0.2% carrier ampholytes (Bio-Lyte 3/10, Bio-Rad) was used to rehydrate an 18-cm immobilized pH gradient gel strip (pH 3–6), and the other 315 µl containing 0.2% carrier ampholytes (Ready strip 7–10, Bio-Rad) was used to rehydrate a second 18-cm immobilized pH gradient gel strip (pH 7–10). Rehydratation was set for 10 h at room temperature without any voltage applied. Peptides were focused by applying a voltage of 250 V for 15 min, then 10 000 V for 3 h and finally 10 000 V for a total of 60 000 V•h. Immediately after focusing, each strip was cut into 36 segments of 5 mm for a total of 72 fractions. Gel pieces were transferred into a 96-well plate and peptides were eluted by first incubating the gel pieces for 15 min in 2% acetonitrile, 1% formic acid and then for 15 min in 50% acetonitrile, 1% formic acid. The extracted peptides were lyophilized using a SpeedVac and resuspended in 25 µl of 0.1% formic acid in water. An aliquot of 5 µl of this solution was used for LC-MS/MS analysis on an Agilent 1100 nanoLC system coupled to a QSTAR XL equipped with MDS nano ESI source. Raw data (wiff extension file) processing, protein identification, protein quantitation and statistical analyses were undertaken with ProteinPilot software v.3.0 (AB-Sciex) running the Paragon algorithm (25) (refer to Supplementary Methods for detailed information).

Stable isotope labeling by amino acids in cell culture

Incorporation of stable isotopically labeled amino acids in cell culture (SILAC) was performed essentially as described in (26,27). Briefly, HEK 293 cells were cultured in DMEM depleted of arginine and lysine. The DMEM was supplemented with 10% dialyzed FBS (Invitrogen, Carlsbad, CA, USA). Penicillin (100 U/ml) and streptomycin (100 mg/ml) (Wisent, Canada) were added to culture media with Arg and Lys containing naturally-occurring atoms (referred as the light culture) or their stable isotope counterparts [$^{13}C_6$ Lys and $^{13}C_6{}^{15}N_4$ Arg (Cambridge Isotope Labs, UK), referred to as the heavy culture]. Cells were grown for at least five divisions to allow full incorporation of labeled amino acids. Cells were tested for complete incorporation of the label. A bicinchoninic acid (BCA) protein assay (Pierce, Canada) was performed on each cell extract before the IP experiment to adjust equivalent amounts of starting material for each condition. The pADPr-associated protein complexes were immunoprecipitated and elulates were subjected to SDS–PAGE. The fractions were analyzed on a LTQ-Orbitrap Velos coupled to an Agilent 1100 Series nanoflow HPLC instruments using nanospray ionization sources. Protein identification and quantitation were done using Proteome Discoverer (v.1.2, ThermoFisher, Bremen, Germany) and Mascot (v.2.3, Matrix Science) to search against the human IPI database (refer to Supplementary Methods for detailed information).

Data-dependent bioinformatics

Gene ontology enrichment analysis

Gene Ontology (GO) term enrichment was performed using DAVID bioinformatics resources (http://david.niaid.nih.gov) (28) to determine whether particular GO terms occur more frequently than expected by chance in a given dataset. Default settings for the Biological Process category were used. The Cytoscape (29) plugin BiNGO (30) was also used to assess enrichment of GO terms and to generate diagrams.

Network construction and visualization

The Cytoscape plugins Michigan Molecular Interactions (MiMI) plugin (31) and BisoGenet (32) that both integrates data from multiple well known protein interaction databases were used to retrieve molecular interactions and interaction attributes. Direct protein interactions were displayed using Cytoscape (v2.7.0) using the corresponding official gene symbols. A subnetwork containing the

physical interactions between proteins involved in the DNA damage response was extracted from the main network (refer to Supplementary Methods for detailed information).

Recruitment of DNA damage response factors to laser-induced DNA damage sites

The recruitment kinetics of DNA damage response factors was assessed essentially as described (33) with the following modifications. After overnight transfections with Effectene reagent (Qiagen), HEK 293 cells expressing GFP fusion proteins were incubated with fresh medium containing 1 μg/ml of Hoechst 33342 for 30 min at 37°C. To study the pADPr-dependent recruitment of proteins at DNA damage sites, cells were incubated with 5 μM of PARP inhibitor ABT-888 for 2 h prior to micro irradiation and recruitment analysis. A 37°C pre-heated stage with 5% CO_2 perfusion was used for the time-lapse on a Zeiss LSM-510 META NLO laser-scanning confocal microscope (40X objective). Localized DNA damage was generated along a defined region across the nucleus of a single living cell by using a bi-photonic excitation of the Hoechst 33342 dye, generated with a near-infrared 750-nm titanium:sapphire laser line (Chameleon Ultra, Coherent Inc.) The laser output was set to 3% with 10 iterations, except for PARP-1 and XRCC1 which were adjusted to 2% to avoid signal saturation. A Multi-Time macro developed in-house for AIM software v3.2 (Zeiss) was used for image acquisition. Background and photobleaching corrections were applied to each datasets as described (34). A minimum of eight recruitments per construct were collected and analyzed. Mean recruitment curves were plotted with Kaleidagraph v4.03.

RESULTS

Isolation of pADPr-containing protein complexes

Before focusing on pADPr dynamics, we first conducted a large-scale proteome analysis using nanocapillary liquid chromatography-tandem MS (GeLC-MS/MS) to explore the protein composition of pADPr-associated protein complexes at the peak of pADPr accumulation in cells following MNNG exposure (MNNG 5 min). To validate and generalize our findings in HEK 293 cell extracts, pADPr IPs were additionally performed in HeLa whole cell extracts under the same experimental conditions. A schematic workflow of the study is illustrated in Figure 1. High-throughput protein–pADPr interactions have remained largely inaccessible owing to the transient nature of poly(ADP-ribosyl)ation. In a previous study (11), we reported that mouse monoclonal antibodies against pADPr, such as clone 10H, can efficiently pull down pADPr in poly(ADP-ribose) glycohydrolase (PARG) knocked-down cells. For the present study, we empirically optimized a low-salt lysis strategy that is both effective in extracting pADPr-binding proteins while preserving non-covalent interactions. Using slightly alkaline pH, low ionic strength, a zwitterionic detergent (CHAPS) and a potent PARG inhibitor, we were able to extract and preserve high amounts of pADPr over time.

A limitation associated with the use of 10H antibody is the low affinity for short pADPr molecules (less than 20 ADP-ribose residues) (35). However, long and complex (branched) polymers, which are formed following DNA damage induction, are well recognized by 10H antibodies. A complementary tool for the isolation of pADPr-containing complexes was also developed based on the use of a catalytically inactive GFP-PARG (PARG-DEAD) isoform. PARG shares structural similarity to the conserved and widespread family of ADP-ribose-binding macrodomain modules (15,36). In this view, our second approach can be considered as an affinity-purification technique similar to IP, except that a catalytically inactive macrodomain-like containing bait was used to pull down proteins trapped into pADPr-containing complexes. A macrodomain pADPr affinity resin, which consists of purified GST-Af1521 macrodomain (37) fusion protein bound to glutathione beads, was also used as a bait to capture pADPr-associated protein complexes. Addressing pADPr binding requires a systematic approach that can benefit from various alternatives.

Globally, we report the high-confidence identification of 609 proteins (33 621 MS/MS spectra, 2.7% peptide false discovery rate; a minimum of two unique peptides, Supplementary Table S1), which several of these are actually associated with the regulation of DNA repair and chromatin remodeling. The 10H and PARG-DEAD datasets share striking similarities but also express differences as PARG-DEAD datasets also include specific PARG-interacting proteins in addition to pADPr-associated proteins (Figure 2A). One important difference between the pADPr-associated protein datasets coming from antibody (10H) and PARG-DEAD approaches is the bias toward different cellular compartments. When a PARG-DEAD mutant is used as a substrate trapping bait to co-purify pADPr-binding proteins, the protein dataset is significantly enriched in nuclear proteins, whereas an antibody-mediated approach targets more mitochondrial proteins (Figure 2B). The vast majority of proteins identified with the Af1521 macroprotein pADPr affinity resin were also identified with the PARG-DEAD dataset, an observation consistent with the fact that PARG and Af1521 are both members of the ADP-ribose-binding macrodomain family. The macrodomain pADPr affinity resin protein dataset is exclusively composed of nuclear proteins that are coherent with its functions in nucleosome stability and regulation. Globally, a PARG-DEAD ligand binds a wider range of proteins and thus, represents a valuable tool for the isolation of pADPr-containing complexes. Furthermore, in this approach, the bait is expressed *in vivo* in mammalian cells, a feature that more accurately reflects physiological conditions.

Figure 2C graphically represents the peptide coverage of all the proteins identified at the peak of pADPr accumulation. Proteins are plotted according to the number of unique peptides assigned to each proteins (Supplementary Table S1). There is a correlation between protein abundance and the number of unique peptides identified for that protein. Generally, proteins anticipated as being in high abundance, such as PARP-1 in pADPr IP extracts,

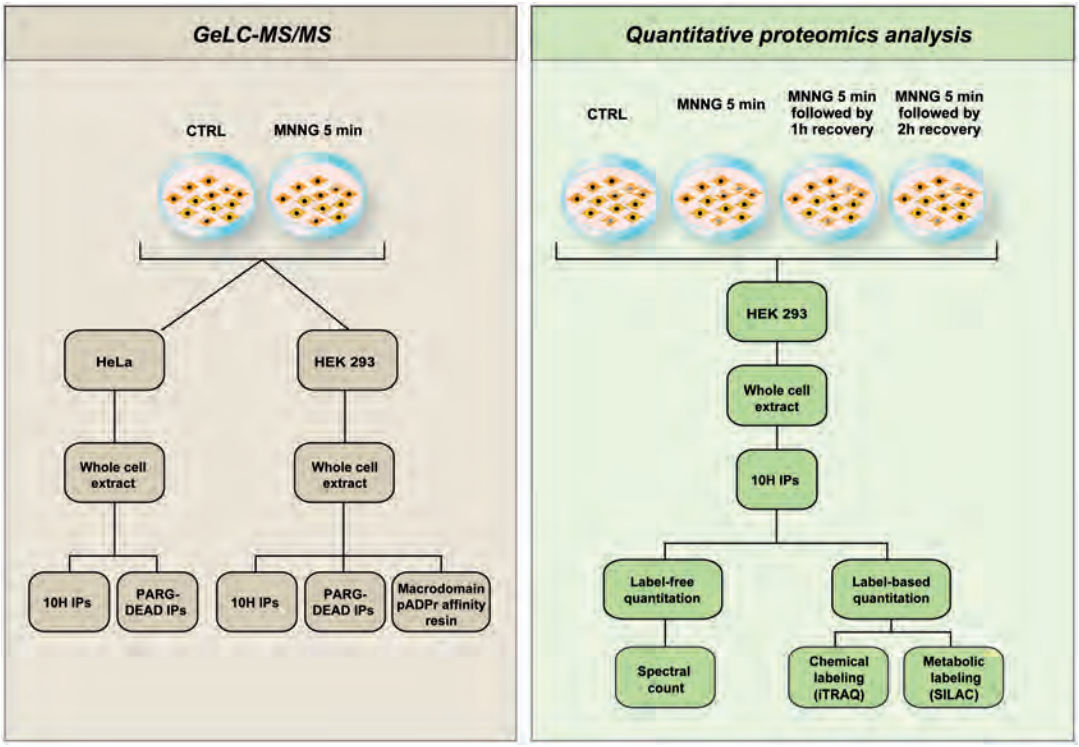

Figure 1. Schematic representation of the experimental design and proteomics strategies to identify pADPr-associated protein complexes. A combination of affinity-purification procedures coupled with MS was used to generate a global protein profile of pADPr-associated protein complexes (GeLC-MS/MS—left panel). Proteomics strategies that integrate relative quantitation with affinity-purification MS were used to provide a time-resolved proteome profile of protein networks responsive to pADPr turnover (right panel). Complementary label-free and label-based quantitative proteomics approaches were used to identify and evaluate protein changes occurring in cells following alkylation-induced DNA damage and PARP activation. 10H IPs: Immunoprecipitations with anti-pADPr antibody clone 10H; PARG-DEAD IPs: IP of catalytically inactive PARG, as described in the text.

are typically identified by the largest number of unique peptides. Proteins assigned with the fewest number of unique peptides are of low abundance. The fact that several DNA damage response (DDR) regulators scored prominently in either 10H-, PARG-DEAD- and macrodomain-based protein datasets support the biological relevance of both our overall screening strategy and the identification of additional top-scoring hits. Although a peptide count approach is not inherently quantitative, it provides rough estimates of protein abundance that are, in our experience, estimated fairly accurately as most of the pADPr-binding proteins known so far are among the proteins with the best peptide coverage. Selected nucleic acids binding proteins are displayed according to their estimated relative abundance (Figure 2C). In addition to PARP-1, the GeLC-MS/MS dataset also contains other PARP family members (PARP-2, PARP-9, PARP-12 and PARP-13) and numerous proteins involved in the maintenance of genome integrity. Most of the pADPr-binding proteins previously reported in other studies were identified using our affinity-purification procedures, including XRCC1 (9), LIG3 (9), KU70 (9), DNA-PK (9), CHD4 (38), CHD1L (ALC1) (39,40), DEK (41), NUMA (42), MVP (43), BUB3 (44), DNA-PK (45), DNMT1 (46), SUPT16H (47), TOP1 (48), TOP2B (49), hnRNPs (50,51) and histones (52).

High-quality spectra were also used to establish a list of proteins identified with unique peptides. Protein identifications were accepted if the corresponding peptide was assigned in at least two independent experiments (Supplementary Table S1). Examples include the chromodomain-helicase-DNA-binding protein 1 (CHD1), DNA repair protein RAD50 and the mitochondrial apoptosis-inducing factor (AIF) (53). The presence of RAD50, a component of the MRE11-RAD50-NBS1 (MRN) complex, was validated by western blot analysis in pADPr IP extracts (Figure 4A), an indication of the data quality.

Being confident that our pADPr isolation method is worthy and effective for the analysis of a wide range of pADPr-associated protein complexes, we further examined the time-dependent accumulation of DNA repair factors in pADPr pull-down extracts up to 2 h following genotoxic insult.

Time-resolved quantitative proteomics analysis of pADPr-containing protein complexes

The insights gained by the identification of pADPr-associated protein complexes and their DNA damage response pathways can provide valuable clues pointing to target proteins. A major challenge is to understand the

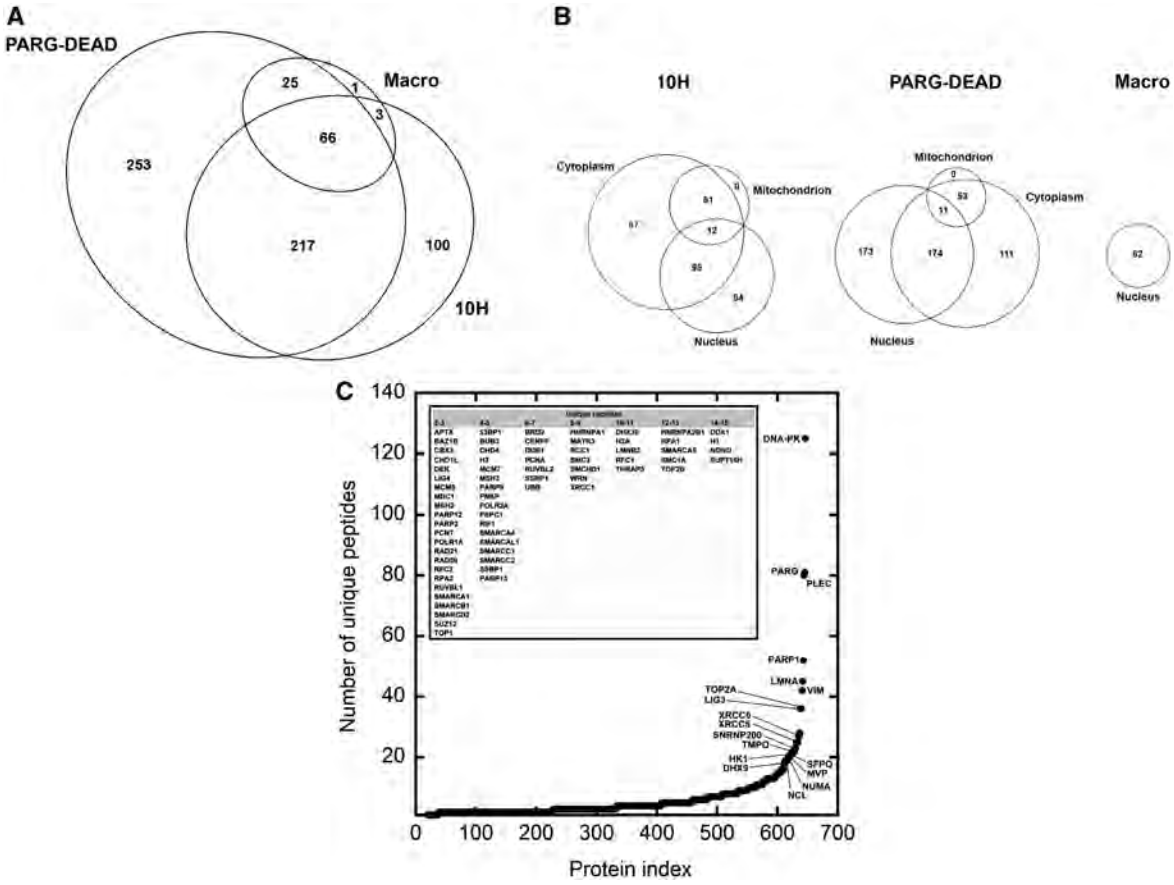

Figure 2. Diversity of pADPr-associated proteins as revealed by gel-based LC-MS/MS analysis. Complementary proteomic approaches directed towards identification of novel proteins that interact with pADPr were integrated to mine the accessible pADPr-binding interactome. IPs were performed directly against pADPr using a high affinity monoclonal antibody (clone 10H) or indirectly by a novel pADPr substrate trapping approach targeting a catalytically inactive PARG mutant and a macrodomain protein (see text for details). (**A**) The area-proportional Venn diagram shows unique and shared protein identifications in pADPr-associated protein datasets that originate from each strategies. (**B**) Area-proportional Venn diagrams depicting the distribution of proteins in subcellular compartments for each datasets. Proteins were classified into cytoplasmic, nuclear or mitochondrial compartments according to GO classification. (**C**) Classification of pADPr-associated proteins. Proteins are ordered relative to the number of unique peptides assigned. The inner frame lists some DNA damage response factors and chromatin-associated proteins with their corresponding number of unique peptide assignments. Refer to Supplementary Table S1 for detailed protein listing.

dynamic behavior of these targets with respect to pADPr. This requires knowledge of the protein dynamics in complex molecular signaling systems tethered together via interactions with heterogeneous pADPr. A mean of generating quantitative information on protein networks responsive to DNA damage is to investigate which network components of these are actually accumulating in affinity pull-down experiments targeting pADPr.

Western blot analysis of DNA damage recognition and repair factors in pADPr IP extracts at sequential time-points following PARP activation

To make further analysis on the pADPr-associated interactome, we examined the dynamic changes of the pADPr-associated protein complexes composition by time course analysis of pADPr proteome changes following exposure to MNNG-induced DNA damage. This approach needed to conciliate two opposite requirements. Since the half-life of pADPr in cells is estimated to be <1 min, pADPr hydrolysis must be limited in order to preserve pADPr pools with respect to the time required by the pull-down assay. On the other hand, a complete disruption of pADPr turnover is not desirable since it would block the dynamics of the targeted protein complexes. To overcome this challenge, the use of a competitive PARG inhibitor (ADP-HPD) (54) appeared to be very appropriate. In contrast to an RNAi-based specific knock-down of PARG resulting in sustained cellular pADPr levels for a prolonged period of time (11), the use of a PARG inhibitor in cell extracts at the time of lysis enables the normal modulation of cellular pADPr levels, whereas stabilizing pADPr in cell extracts required for efficient pull-down assays. The turnover of pADPr was estimated by polymer-blot analysis and immunofluorescence. Hand-spotted DHBB-purified pADPr (24) was used as reference to estimate pADPr content in IP extracts (Figure 3A). We were able to recover more than 10 pmol of pADPr/10^6 cells, which represent a significant fraction of total pADPr formed during alkylation-induced DNA damage (55,56). Immunostained

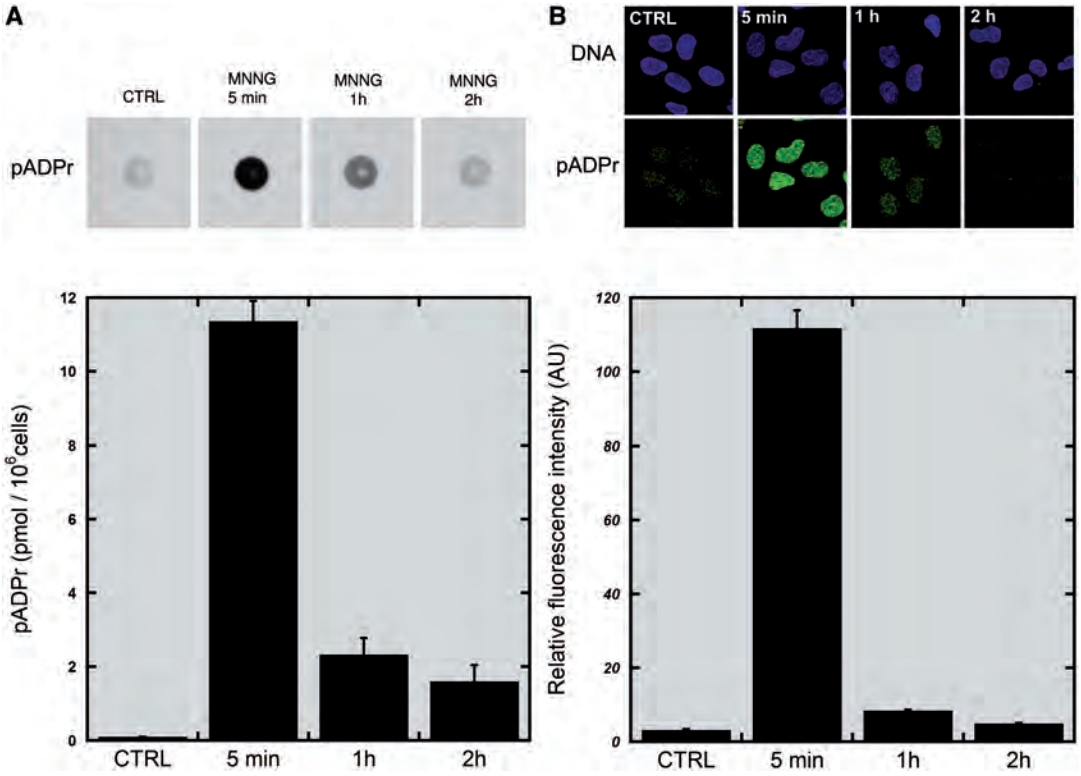

Figure 3. pADPr dynamics following MNNG-induced DNA damage and PARP activation. (**A**) Dot-blot analysis of pADPr levels in pADPr IP extracts from MNNG-treated HEK 293 cells. Cellular material bound to 10H-coupled magnetic beads was eluted and hand-blotted on positively charged nylon membrane. pADPr was detected using 96-10 antibody (upper panel). pADPr signals in IP extracts were quantified using DHBB-purified pADPr as a reference value for quantitation and displayed on a bar graph (lower panel). The data are represented as the mean ± SEM ($n = 4$). (**B**) The 10H immunofluorescence labeling of pADPr in HEK 293 cells exposed to MNNG (upper panel). Confocal fluorescent images were obtained by a Zeiss LSM 510 NLO laser scanning confocal microscope. A region was drawn inside of each nucleus ($n = 100$) to establish the mean fluorescence intensity. Relative pADPr levels were plotted on a bar graph (lower panel) and displayed as the mean ± SEM ($n = 3$).

pADPr quantitation indicate that the recovery of pADPr by IP closely match the turnover of pADPr in living cells (Figure 3B). Cellular pADPr levels reach a maximum (30- to 50-fold increase) after 5 min of MNNG treatment and subsequently decrease to basal levels. After a 2-h recovery period, pADPr is nearly undetectable by western blot except for PARP-1, which remains significantly automodified (Figure 4A). In contrast, pADPr shows a wide distribution at peak levels from the loading well down to the low molecular weights at the bottom of the blot. This ADP-ribose polymers' size distribution of the products generated by PARPs and PARG interplay are presumably the consequence of the resolution of free and protein-bound pADPr from various lengths and branching frequencies. We therefore hypothesized that pADPr-containing DNA repair complexes would primarily be isolated in this fraction. As expected, several DNA repair factors are trapped in immunoprecipitates corresponding to MNNG-treated cells, with a predominant enrichment in the 5 min sample that contains the highest levels of pADPr (Figure 4A). The presence of PARP-1 and its high-confidence interactors indicates that pADPr-associated protein complexes are efficiently pulled down. The relatively high level of PARG present in these samples also validates the presence of poly(ADP-ribose) degrading enzymes in these fractions.

Semi-quantitative analyses of protein levels were measured by densitometry scanning of western blots shown in Figure 4A. Profiles were generated for every targeted DNA damage response (DDR) factors and their abundance was correlated to pADPr dynamics (Figure 4B). The base excision repair (BER) pathway clearly shows a prominent association with pADPr, especially as core components of the BER pathway (LIG3 and XRCC1) are hard to detect in control conditions that correspond to the pull down of pADPr-containing complexes in the absence of genotoxic insult. This result is consistent with the preferential interaction of the XRCC1/LIG3 complex with the poly(ADP-ribosyl)ated form of PARP-1 (57). In contrast, components of the non-homologous end joining (NHEJ) and HR repair pathways are more stably associated with pADPr-containing complexes under basal conditions, a characteristic that tends to temper the relative accumulation ratios after DNA damage.

As a proof of concept, we identified several DDR targets by western blot analysis of anti-pADPr immunoprecipitates with a global accumulation trend that

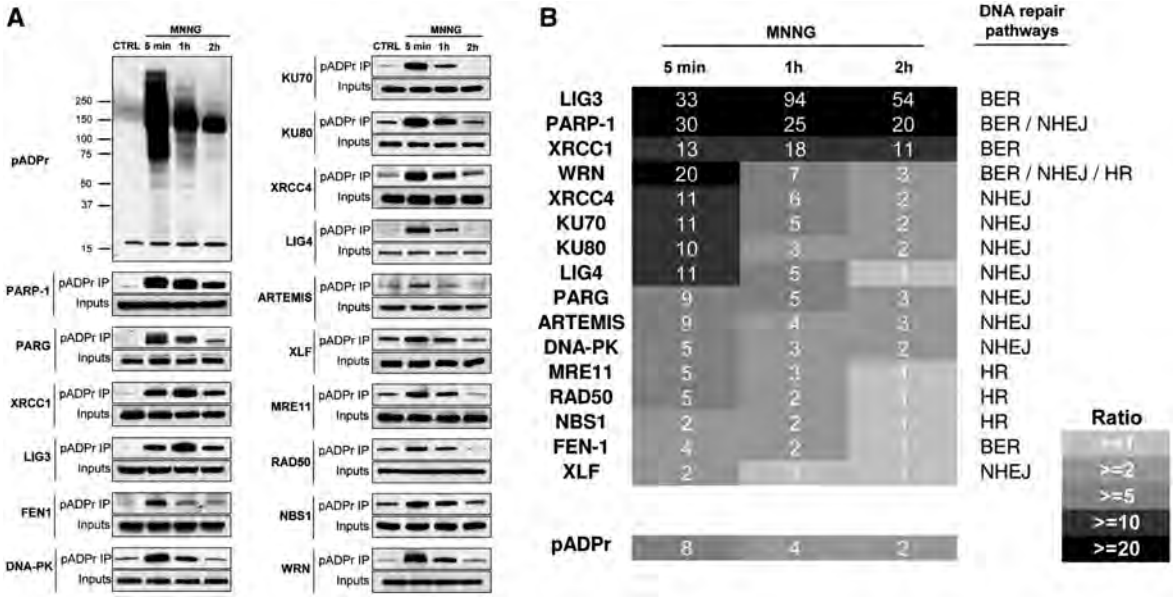

Figure 4. Correlated accumulation of DNA damage response factors with pADPr. (**A**) The 10H-based IPs using HEK 293 whole cell extracts were performed to isolate pADPr-associated proteins in the context of MNNG-induced DNA damage and PARP activation. Cells were allowed to recover from MNNG by incubation with fresh medium and IPs were performed at the indicated times. Undamaged control cells were pre-incubated 2 h with 5-μM PARP-1 inhibitor ABT-888 before lysis. Several DNA damage response factors were screened for entrapment in anti-pADPr IP extracts. Cell lysates (inputs) were also subjected to western blot analysis using the corresponding antibodies. (**B**) pADPr levels correlate with the accumulation of several DNA damage response factors involved in major DNA repair pathways. Relative quantitation of western blot signal intensities shown in (A) were measured and expressed relative to control protein levels. A greyscale heatmap ranks each of the protein accumulation ratios.

correlates to pADPr levels. This observation led us to further explore the dynamics of pADPr-associated complexes by quantitative MS.

Quantitative proteomics analysis of complex protein mixtures in pADPr IP extracts

Quantitative proteomics can reveal changes in protein abundance that can be indicative of a component that has affinity for pADPr or likely part of pADPr-modulated protein complex, including previously undescribed factors. Several relative and absolute quantitative proteomics techniques have been developed in recent years. Generally, MS-based quantitation methods fall into two categories: label-free or label-based approaches (58), each having specific strengths and limitations (59). Whereas most quantitative proteomics studies rely on either strategy, we undertook a more systematic approach for a thorough analysis of the pADPr proteome (Figure 1).

Label-free quantitation

The spectral counting method has become an accepted technique to estimate the relative abundance of proteins in highly complex samples. Spectral counting is a large-scale strategy easily applicable to GeLC-MS/MS protein identification. One of the main advantages of the method is that it does not require the use of high resolution mass spectrometers such as those required for quantitative label-based MS approaches.

Antibody-mediated affinity purification of pADPr-containing protein complexes was performed in HEK 293 whole cell extracts after exposure and release from MNNG-induced DNA damage and PARP activation. Untreated cultures were used as a basis for calculating protein ratios derived from peptide spectral counts. A set of 425 proteins was identified (Supplementary Table S2) from which we extracted 275 proteins that follow a kinetics pattern that clusters them into one of the three time-points analyzed after MNNG exposure (Figure 5A). *K*-means clustering is one of the most popular partitioning method. We used a robust version of *K*-means clustering based on medoids by using the *pamk* function (partitioning around medoids) (25) to group proteins identified during our screen based on their time course profiles following exposure to MNNG. The goal of the algorithm is to segregate each protein dynamics into the profiles that they most closely matched. Partitioning around medoids is more robust than *K*-means in the presence of noise and outliers, an interesting feature since pADPr-associated proteins exhibited significant variability over a wide range of ratios. By clustering proteins with similar accumulation trend, we were able to obtain a clear snapshot of protein enrichment in relation with pADPr dynamics (Figure 5A). We hypothesized that proteins with a distribution pattern that correlates with pADPr levels are presumably proteins with close connection with pADPr, whether by being covalently poly(ADP-ribosyl)ated, non-covalent pADPr-binders or major components of pADPr-associated protein complexes.

The top biological processes associated with each clusters of proteins were identified using DAVID bioinformatics resources (Functional gene classification tool based

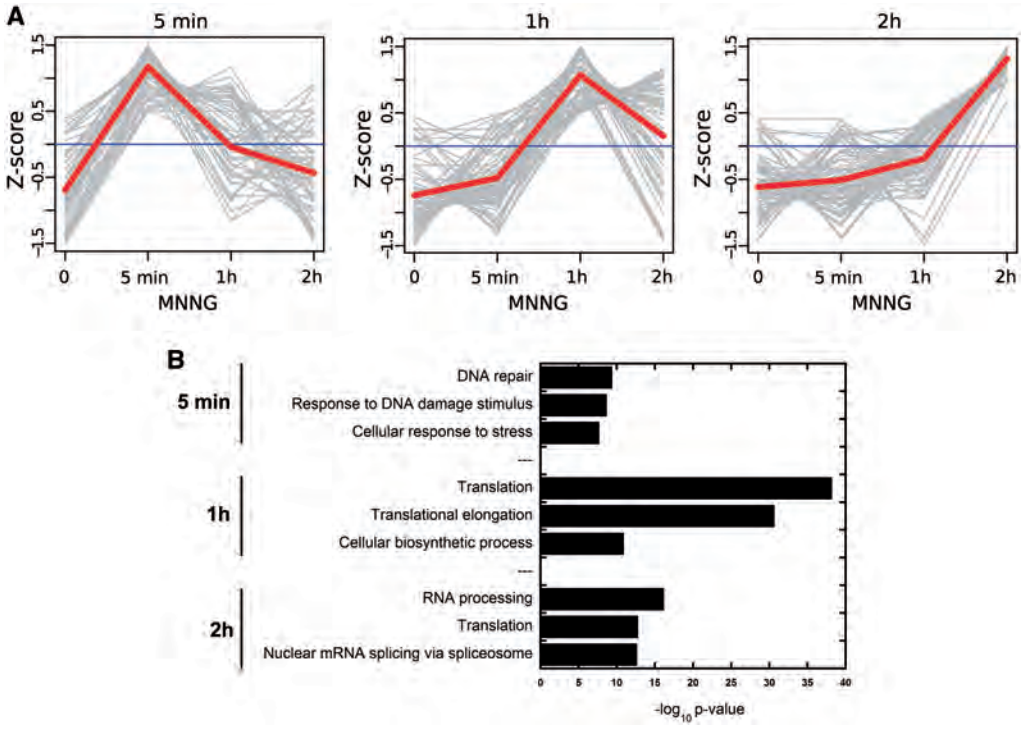

Figure 5. Protein abundance profiles in time-resolved pADPr IPs. Spectral counting-based quantitation was combined with Scaffold's protein validation tools to provide a quantitative protein profile. pADPr-associated proteins identified by GeLC-MS/MS in IP extracts were grouped by *K*-means clustering for each treatment, respectively. (**A**) The kinetics of protein accumulation is displayed by trend curves showing the overlay of the proteins grouped by each cluster. The red line represents the mean value at each time-point for all the proteins in the cluster. (**B**) Protein clusters were searched for significant over-representation of proteins belonging to specific pathways according to the GO database using DAVID. Bar plots of the most significant biological processes in each datasets are shown. The significance of the enrichment is expressed as a function of the *P*-value, which indicates whether a biological process is significantly higher than random expectations. Refer to Supplementary Table S2 for complete protein listing.

on GO terms)(28). Biological processes were displayed as *P*-value bar plots (Figure 5B). The *P*-values represent the probability to see a random enrichment in the displayed biological process. As cells recover from genotoxic stress, we can observe an evolution of the major biological processes associated with pADPr turnover. Although there is an overlap among the processes, the first predominant biological process identified at the peak of pADPr levels (MNNG 5 min) is related to DNA damage response which is consistent to the rapid activation of PARPs and pADPr synthesis in response to DNA strand breaks. After a 1-h recovery period from MNNG exposure, proteins involved in translationnal processes are highly over-representative of the pADPr-associated proteome, whereas regulatory circuits that control mRNA splicing, stabilization and translation are most prominent after 2 h. Individual protein accumulation trend was displayed in a heatmap for the three time-points analyzed after MNNG exposure (Figure 6). Proteins were grouped according to their kinetics profile. As we could expect, one can observe that PARP-1 is closely related to the kinetics of XRCC1 and LIG3, two stably associated components of the BER pathway. Similarly, KU80 (XRCC5), DNA-PK (PRKDC) and the facilitator of chromatin transcription (FACT) complex subunit SSRP1 are grouped together soon after the induction of DNA damage in the 5-min MNNG cluster. This approach could help to better focus on pADPr-responsive protein complexes involved in biological processes that contain numerous components such as those observed at later time-points following the induction of DNA damage.

Label-based quantitation: iTRAQ and SILAC analysis

SILAC (60) and iTRAQ (61) are two widely used methods to quantify protein abundance in tissue cultures. Whereas SILAC involves metabolic incorporation of isotope mass tags directly into proteins, iTRAQ chemical labeling is performed on peptides after lysis and trypsin digestion. Both SILAC and iTRAQ strategies were coupled to pADPr affinity-purification for the quantitation of protein abundance in time-resolved IP extracts following MNNG-induced DNA damage and PARP activation. Ratios of protein abundance were estimated based on datasets from untreated cells that correspond to basal levels of poly(ADP-ribosyl)ation in the absence of genotoxicity. As for any quantitative differential analysis, the most interesting identifications are those that differ by a substantial amount from the rest of the data (outliers). Box plots are particularly useful to display the distribution of a dataset and pinpoint those outliers. Figure 7 shows the box plot diagrams of iTRAQ and SILAC experiments. All the outlier values correspond to important protein accumulation in pADPr IP extracts. The intensities of the ratios and the number of outliers

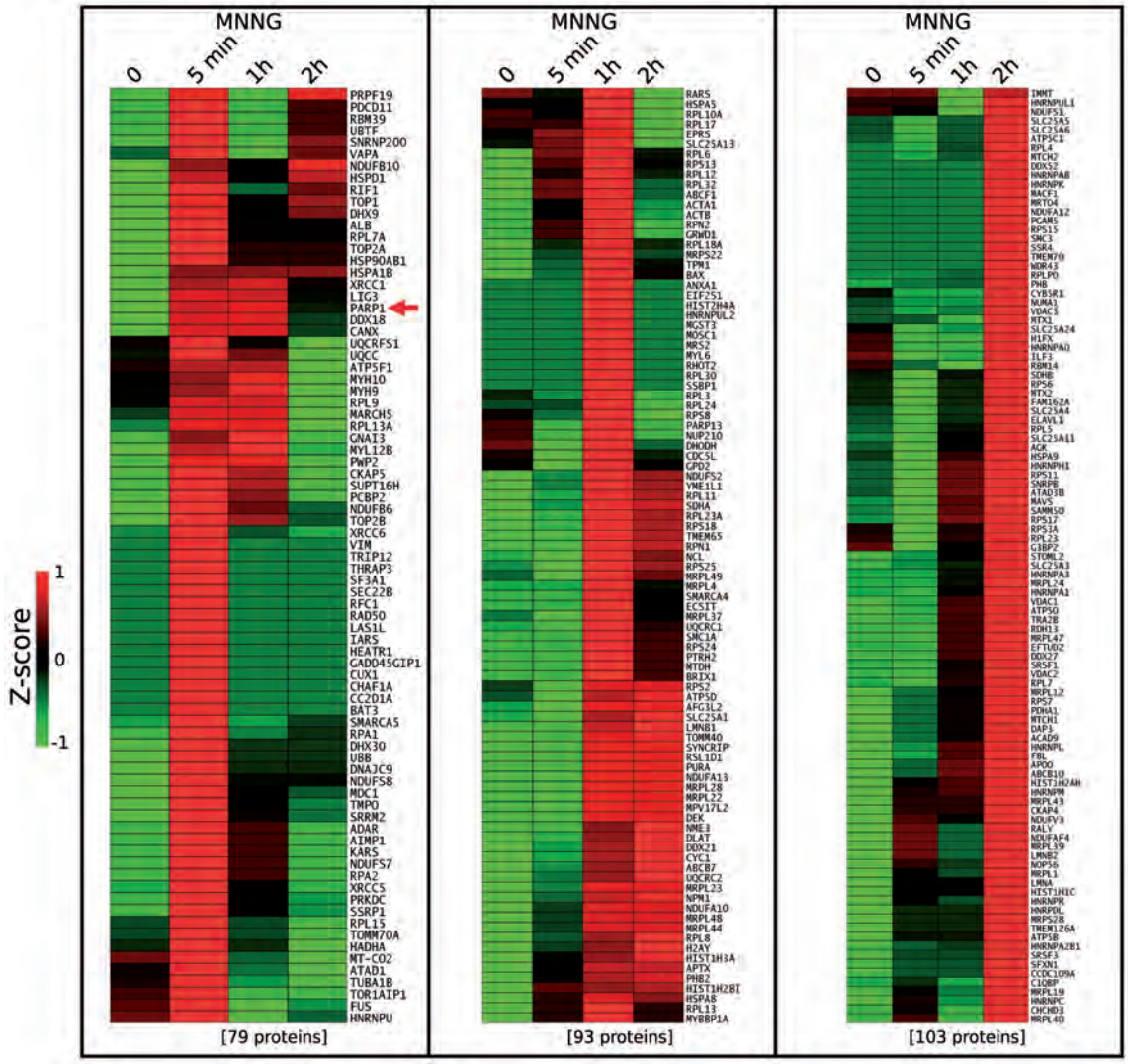

Figure 6. Heatmap analysis with *K*-means clustering. Temporal profiling of pADPr-associated proteins in HEK 293 cells upon MNNG exposure was performed based on the GeLC-MS/MS spectral count quantitation. The heatmap displays the three clusters identified by the *K*-means algorithm that correspond to the time-points analyzed after MNNG exposure. Green indicates the lowest ratio, black indicates an intermediate value and red indicates the highest ratio (protein enrichment). Proteins in each cluster are listed according to their gene symbol. A red arrow indicates the presence of PARP-1.

decrease as we proceed from 5 min to 1 h and 2 h post-MNNG treatment, an observation consistent with the progressive decrease of pADPr levels. Detailed iTRAQ and SILAC datasets are listed in Supplementary Table S3 and S4.

Although they are based on different approaches, iTRAQ and SILAC analysis reported a similar set of enriched proteins in pADPr IP extracts. The BER (XRCC1, LIG3) and the NHEJ (DNA-PK (PRKDC), XRCC5(KU80), XRCC6(KU70) multiprotein repair complexes are consistently found with both methods, as well as the facilitates chromatin transcription (FACT) complex subunits SSRP1 and SUPT16H. Proteins forming the nuclear lamina (LMNA, FLNA, TMPO) are also found with high ratios in consistency with their relative abundance found in GeLC-MS/MS dataset. Of particular interest are other factors that follow the same accumulation trend as did well characterized pADPr-binding proteins, suggesting a close link with poly(ADP-ribosyl)ation and chromatin functions. Proteins with high ratios such as barrier-to-autointegration factor (BANF1), single-stranded DNA-binding protein (SSBP1) or the thyroid hormone receptor-associated protein 3 (THRAP3) have not been characterized in the context of pADPr metabolism. However, PARP-1 has been found as a chromatin-associated partner of BANF1 (62); SSBP1 localizes in H2AX/PARP-1 complexes (63) and THRAP3 is a component of the human mediator complex that functionally interacts with PARP-1 (64).

Each label-based quantitation method had its own strengths. For example, only SILAC analysis identified APLF (Aprataxin and PNK-like factor) as one of the most enriched protein in 5-min MNNG

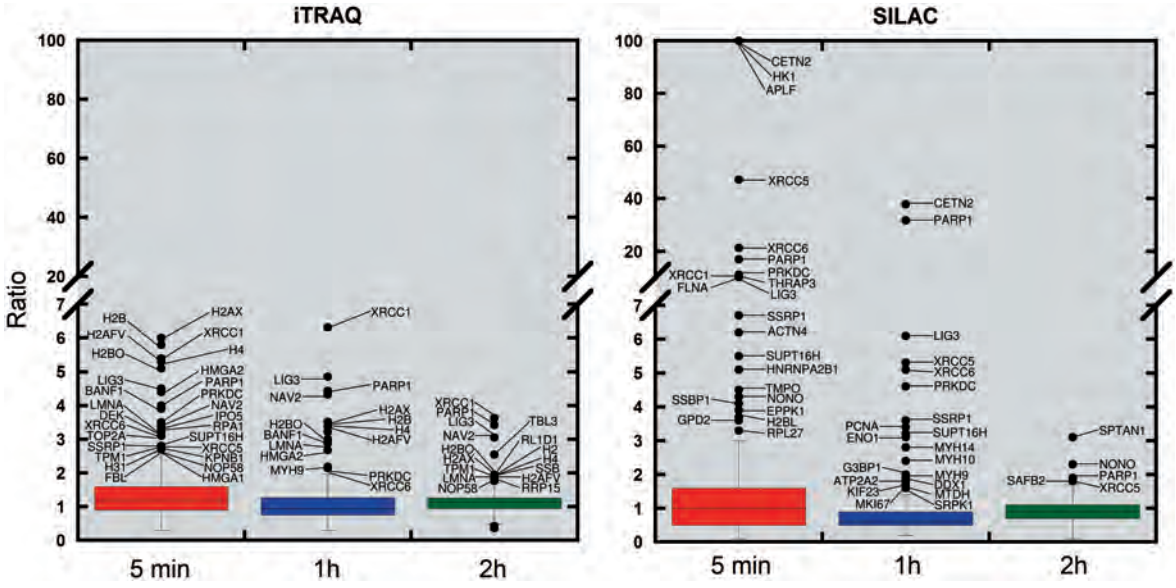

Figure 7. Box plot statistics to define outlier significance for iTRAQ and SILAC analysis. pADPr IPs were carried out after each of the three time-points examined following MNNG exposure. Protein isolates were quantified with respect to basal levels of pADPr in control IPs. Each box encloses 50% of the data with the median value of the variable displayed as a line. The top and bottom of the box mark the limits of upper and lower quartiles. The vertical lines extending from the top and bottom of each box mark the minimum and maximum values within the data set that fall within an acceptable range (1.5 × interquartile distance). Any value outside of this range (outlier) is displayed as an individual point with the corresponding gene symbol. Refer to Supplementary Table S3 (iTRAQ) and Supplementary Table S4 (SILAC) for detailed protein annotations.

immunoprecipitates. This is consistent with the fact that APLF contains a pADPr-binding PBZ motif (5,65,66). In addition to APLF, centrin-2 (CETN2) and hexokinase-1 (HK1) were identified with high ratios. However, in such cases, quantitations were based on unique peptides so the measured ratios must be tempered. Finally, one should keep in mind that the proteins displayed in iTRAQ and SILAC box plots (Figure 7) are those with extreme values with respect to the entire dataset. Proteins with more modest enrichment ratios that fall within the upper quartile (75th percentile) still represent interesting pADPr-associated candidates. For example, the stress granule-associated PARP-13 was identified in each of the time-points analyzed by SILAC but only after 2 h of MNNG exposure did it stand out from the protein dataset. Another example is NUMA, a poly(ADP-ribosyl)ated protein only found in the 2-h MNNG SILAC dataset with the same modest ratio as DNA-PK (PRKDC), SSBP1 and Mediator of DNA damage checkpoint protein 1 (MDC1) (Refer to Supplementary Tables S3 and S4 for detailed information).

Protein network modeling of pADPr-associated proteins

To gain insight into the dynamics of pADPr-associated proteins, we mapped a protein interaction network based on datasets derived from MS analysis. The global pADPr-responsive proteome modeled on the basis of all the proteins identified in this study resulted in a network of 959 proteins (nodes) and 8931 interactions (edges). The entire network is provided for interactive visualization of protein interactions in the Cytoscape session file (Supplementary Material). The network can be easily loaded and visualized using Cytoscape, which if freely available for download as an open source bioinformatics software (www.cytoscape.org). The ClusterOne algorithm was used to detect clusters of highly connected multiprotein complexes in the global network with associated confidence values. A group of 6 clusters with $P < 0.05$ were detected and extracted from the global pADPr proteome. These clusters includes (i) ribosomal proteins (93 proteins), (ii) polyubiquitin-C substrates (200 proteins), (iii) mitochondrial proteins (53 proteins), (iv) mRNA splicing and maturation factors (68 proteins), (v) components of the nuclear pore complex (24 proteins) and (vi) a small group of proteins involved in mitotic cell cycle (7 proteins) (Supplementary Cytoscape session file). To provide context and a more targeted view of our quantitative analysis of the pADPr-responsive proteome, we isolated a subnetwork of proteins that reflects significant molecular events linked to DNA damage response and pADPr metabolism. We extracted the first neighbors (direct protein–protein interactions) linked to protein components of the main DDR pathways found in our proteomics datasets. All the PARPs identified in this study were extracted in addition to components of the BER (XRCC1, LIG3), NHEJ (DNA-PK, XRCC5, XRCC6) and the FACT complex (SUPT16H, SSRP1). This subnetwork, composed of 164 nodes and 899 edges highlights the emerging importance of pADPr in the regulation of DDR (Figure 8). The most enriched proteins in pADPr IPs from GeLC-MS/MS, spectral counting, iTRAQ and SILAC datasets (top-scoring proteins) were flagged to underscore their relative abundance. The third quartile value was selected as the cut-off criteria (cut-off point for the highest 25% of the observed ratios;

Supplementary Table S5). This complex network structure represents a part of the DNA damage and repair response protein interaction map closely related to PARP-1 and highlights the value of integrating protein interaction information as it reveals potential pADPr-binding candidates to prioritize for functional follow-up. Interestingly, almost all the PARP-1 subnetwork (160 out of 164 proteins) connects to polyubiquitin-C (UBC) according to the interaction databases (Supplementary Cytoscape session file).

Dynamic recruitment of DNA damage response factors to sites of DNA damage

Whichever method was used to explore the pADPr interactome during alkylation-induced genotoxic stress, components of the BER and NHEJ repair pathways scored prominently in the quantitative protein profiles. The consistency of this observation strongly suggests that pADPr could be an important effector involved in the regulation of these repair processes. It had already been recognized that localized pADPr formation facilitates the accumulation of DNA repair factors at sites of broken DNA (67). This is particularly critical for the scaffolding protein XRCC1 for which recruitment at DNA damage sites depends on the presence of pADPr (68–70). In order to study the dynamic recruitment of DNA repair factors, we used a combination of Hoechst 33342 incorporation and near-infrared 750-nm two-photon laser micro-irradiation to induce DNA damage in subnuclear regions of single cells (Figure 9A). As expected, most of the DDR factors targeted in this study are recruited at laser-induced DNA damage sites (Figure 9B). The contribution of pADPr to the recruitment process of DNA repair factors was evaluated by treating the cells with

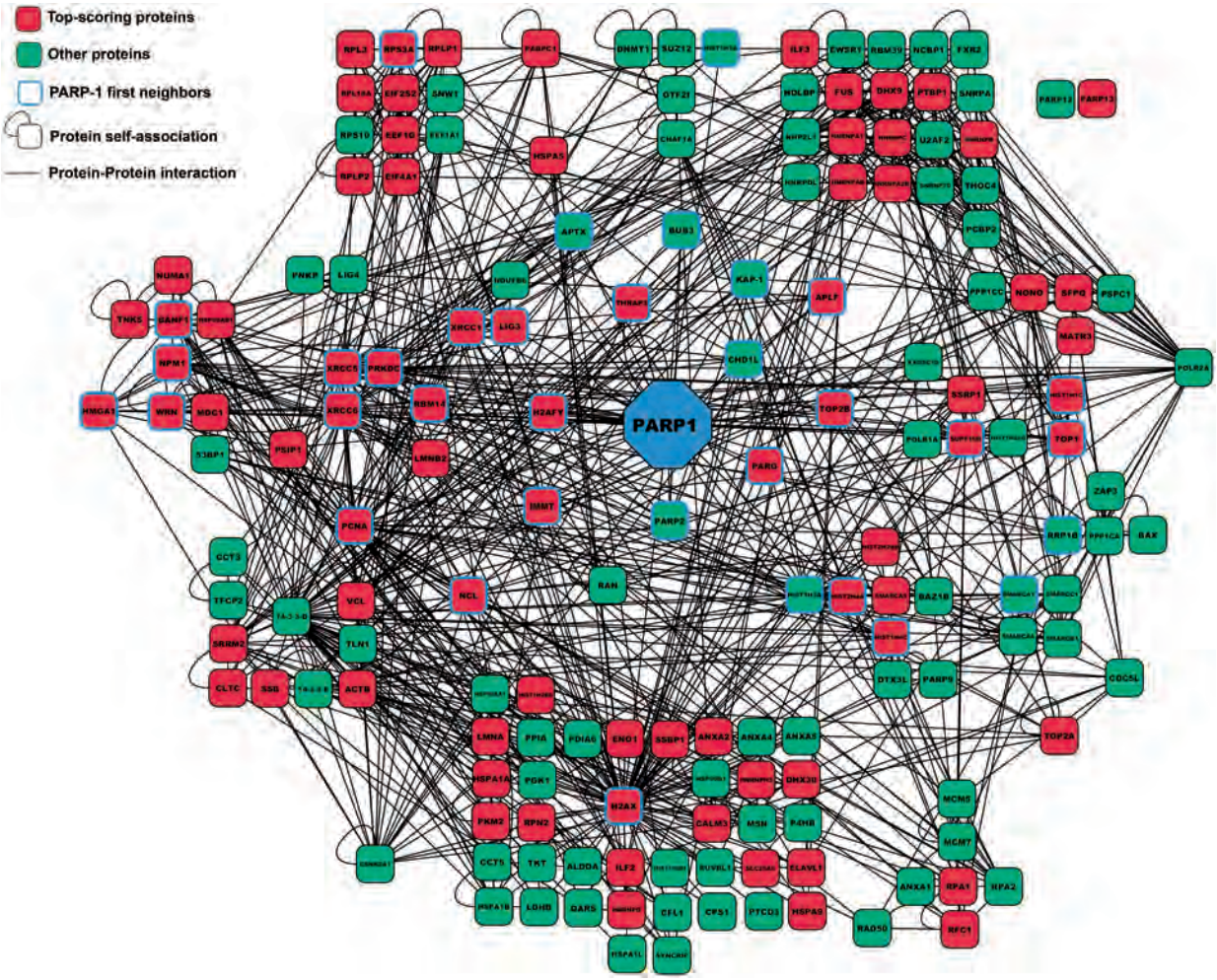

Figure 8. Subnetwork diagram of the PARP-1-centered protein interaction map. Cytoscape was used to construct a global network of the pADPr-associated proteome that integrates protein identification from all the proteomics approaches that have been carried out in this study. The diagram shown consists of the nearest-neighbors subnetwork of PARP family members in addition to selected proteins from DNA damage response pathways (See text for details). The subnetwork emphasizes the pADPr-associated protein regulatory network centered around PARP-1 in cellular recovery to DNA damage. The red coloring indicates top-scoring proteins and refers to predominant proteins in either of the four datasets (GeLC-MS/MS, Spectral count, iTRAQ, SILAC). Interactions among proteins are reported. The network comprises 164 proteins (nodes) and 899 interactions (edges). Refer to Supplementary Table S5 for complete protein listing.

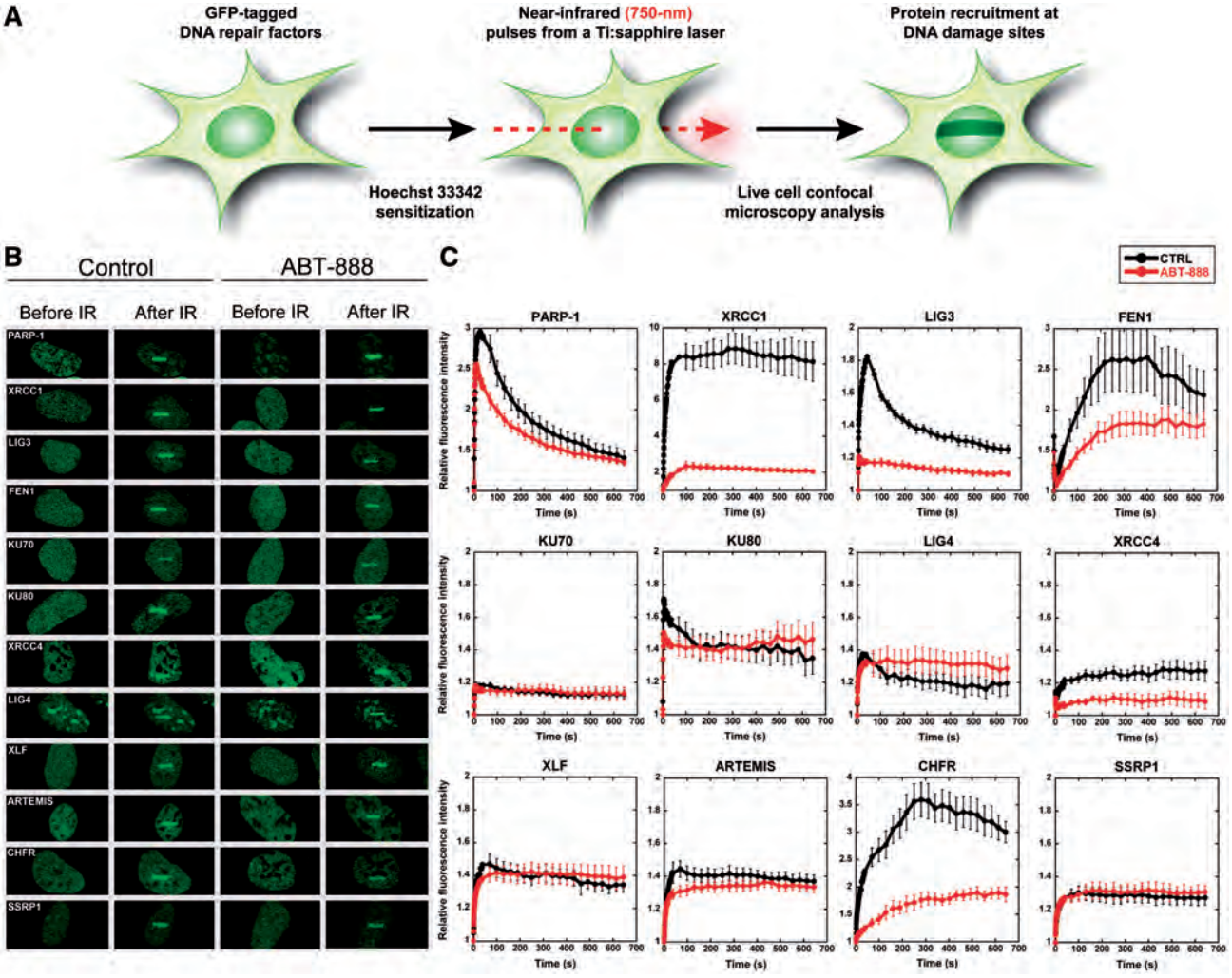

Figure 9. Dynamics of DNA damage response proteins at laser-induced DNA breaks. DNA damage induced by laser micro-irradiation in sub-nuclear region of single living cells was performed to evaluate the pADPr-dependent recruitment of DNA repair factors at DNA damage sites. (**A**) Schematic representation of the micro-irradiation system used to introduce DNA lesions. (**B**) Local accumulation of DNA repair factors at laser-induced DNA damage sites. A 750-nm two-photon laser beam was focused on Hoechst-sensitized cells and the accumulation of GFP-tagged DNA repair factors was monitored on a Zeiss LSM 510 NLO laser scanning confocal microscope. (**C**) Evaluation of the contribution of pADPr to the recruitment kinetics of DNA damage response factors at sites of DNA damage. The dynamics of several GFP-tagged proteins involved in DNA repair pathways were analyzed in the context of PARP inhibition (ABT-888). The HEK 293 cells transiently expressing the targeted proteins were sensitized with Hoechst 33342 and micro-irradiated with femtosecond near-infrared (750-nm) pulses from a Ti:sapphire laser. The intensity of fluorescence was recorded on a Zeiss LSM 510 NLO laser-scanning confocal microscope. The dynamics of DNA repair factors under normal conditions was compared with the dynamics observed following PARP inhibition with 5 μM ABT-888. Targeted proteins involved in BER (XRCC1, LIG3, FEN1), NHEJ (KU70, KU80, LIG4, XRCC4, XLF, ARTEMIS) and chromatin remodeling (CHFR, SSRP1) are displayed. Because of the rapid accumulation of DNA repair proteins at DNA damage sites, multiple acquisition rates were used (see 'Materials and Methods' section). Background and photobleaching corrections were applied to each dataset. A minimum of eight recruitments per construct were collected and analyzed. The error bars represent the SEM.

the potent PARP inhibitor ABT-888 [reviewed in Ref. (71)]. We first focused on XRCC1 to validate our approach since its pADPr-dependent accumulation at DNA damage sites was clearly demonstrated. Indeed, XRCC1 recruitment at DNA damage sites is severely decreased when PARP-1 is inhibited (Figure 9C). Because XRCC1 acts as a coordinator of BER, we anticipated that PARP-1 inhibition would lead to a reduced accumulation of LIG3 and other BER-associated factors. Although recruited at DNA damages sites with less intensity than XRCC1, we observed a decreased relocation of LIG3 when PARP activity is inhibited. A similar dynamics was observed for the Flap endonuclease 1 (FEN1) which also possesses functions in the BER system. These results underscore the role of pADPr in facilitating the recruitment of BER factors and are consistent with the identification of these factors as some of the most enriched proteins in pADPr IP extracts.

Following the same idea, we anticipated that the recruitment of major components of the NHEJ repair pathway

at DNA damage sites would also be influenced by a decrease in the accumulation of pADPr. We did see a modest recruitment of each of the targeted NHEJ factors in the path of the laser track (KU70, KU80, XRCC4, LIG4, XLF and ARTEMIS) but none of these showed a significant dependence on pADPr to localize at DNA damage sites (Figure 9C).

In addition to DNA repair events, extensive chromatin remodeling and histone modifications occur at sites of DNA damage. Following this idea, our attention was directed toward a chromatin remodeling complex consistently trapped in pADPr IP extracts, namely the FACT complex SUPT16H/SSRP1 that acts to reorganize nucleosomes. As a control, we used CHFR, a chromatin remodeling protein that regulates histone modifications and the ATM-dependent DNA damage response pathway after DSBs (72). CHFR possesses a PBZ domain known for its non-covalent interaction with pADPr. As expected, CHFR recruitment and retention at DNA damage sites is strongly decreased in presence of ABT-888, whereas SSRP1 recruitment is unaffected (Figure 9C). In our protein clustering experiment, we found that SSRP1 accumulation profile with respect to pADPr closely match those found for KU80 and DNA-PK (Figure 6, 5-min MNNG cluster). SSRP1 was also found with high ratio in iTRAQ and SILAC experiments (Figure 7) along with its stable partner SUPT16H. The modest intensity of SSRP1 accumulation at DNA damage sites falls within a similar range as that for the NHEJ factors and this accumulation is also pADPr-independent.

DISCUSSION

This study represents the first reported proteome-wide effort to follow protein dynamics in the context of pADPr modulation after DNA damage. In addition to the exploration of the pADPr-associated proteome with antibody-mediated affinity purification, MS-based substrate trapping strategies were used as complementary approaches to mine the accessible pADPr-associated proteome. These analyses suggest that the presence of pADPr in many multiprotein complexes involved in genome surveillance could be functionally relevant. Yet, these complexes are not static, but instead are dynamic assemblies that orchestrate DNA damage signaling and repair. In the present study, the time-correlated relationship between protein entrapment in pADPr-containing complexes and pADPr dynamics was further investigated using a combination of quantitative proteomics techniques. Despite intrinsic differences between spectral counting, SILAC and iTRAQ methodologies, we identified several proteins whose abundance was consistently correlated to pADPr levels.

It has been known for a long time that pADPr levels are transient and spontaneously resolving after their rapid degradation by PARG. However, there is an apparent gap between our understanding of the initial pADPr-associated molecular events underlying DDR and major nuclear reorganization, and the profound impact of pADPr on cell fate. In our study of pADPr dynamics, we found that several DDR factors are co-eluting with pADPr, consistent with the accumulation of DNA repair factors near the damage site and the current model where pADPr is viewed as a loading platform for the repair machinery (3,19). The recent identification of chromatin-associated proteins whose recruitment to DNA damage sites is pADPr-dependent [e.g.: CHD4 (38,73), MTA1(73), MRE11(74), NBS1(74), ALC1(39,40), APLF (75,76), XRCC1 (68), BMI-1 (77), MEL-18 (73)] also points towards this model. Thus, local poly(ADP-ribosyl)ation at DNA damage sites may be a common phenomenon for the recruitment of DDR factors that control genome integrity. It is highly likely that more DDR factors and chromatin remodelers found in this study will join this expanding group of proteins.

Using laser micro-irradiation and live cell imaging analyses, we have shown that the retention of repair factors at sites of DNA damage can exhibit a wide range of dependency on pADPr. Given that pADPr formation can be subjected to a 100-fold increase after the induction of DNA damage (89), a rapid accumulation at the DNA damage site would logically occur for a non-covalent pADPr-binding protein. Indeed, we showed that XRCC1, which possesses a pADPr-binding motif (12), and CHFR, a PBZ-containing protein, are both showing a very significant decrease of retention at DNA damage sites when poly(ADP-ribosyl)ation is inhibited. There are a variety of intricate DNA damage response mechanisms that underlie spatial relocation of proteins at DNA breaks. Although poly(ADP-ribosyl)ation appears as the main driving force behind the recruitment of BER factors at DNA damage sites (i.e. XRCC1 and LIG3), this phenomenon is likely to be involved in the regulation of other functions as in the case of NHEJ. The identification of PARP-1, DNA-PK and KU70/80 as predominant pADPr-associated protein components suggest that these proteins participate to a same pathway to cope with DNA damage. This finding supports previous studies that established KU70, KU80 and DNA-PK as substrates of PARP-1 (78–80) and is also consistent with a model where PARP-1/DNA-PK interplay dictates the functional properties of the NHEJ repair complex (81). Although the relocation of core NHEJ factors at DNA damage sites is pADPr-independent, the presence of PARP-1 and pADPr in these complexes appears to play a more downstream role in the DNA damage response. This can be illustrated by reports indicating that poly(ADP-ribosyl)ation of the KU70/KU80 complex impairs its ability to bind DNA (78) or the stimulation of DNA-PK activity upon poly(ADP-ribosyl)ation (82). A recent study reports that PARP-1 binding to DSBs elicits substantial conformational changes in the DNA-PK dimer assembly (81). Following the idea that interactions within a PARP-1/DNA-PK complex might affect the mechanism of DNA-PK activation, the presence of pADPr through automodified PARP-1 could led to structural transitions with functional consequences on NHEJ.

This study and most of the current research focus on poly(ADP-ribosyl)ation as an early response to genotoxic stress. However, it is clear that the consequences of poly(ADP-ribosyl)ation are not limited to the early

DNA damage response, but also impact on stress response and cytoprotection. Later consequences may include changes in gene expression and global cellular responses of death and survival within hours and days (83).

This effort represents the most extensive proteomics coverage in the context of PARP activation following DNA damage and contributes to a growing body of evidence that implicates pADPr as a coordinator of multiple activities required for maintaining genome integrity.

SUPPLEMENTARY DATA

Supplementary Data are available at NAR Online: Supplementary Tables 1–5, Supplementary Methods and Supplementary References [84–89].

ACKNOWLEDGEMENTS

The authors are grateful to Dr Michèle Rouleau for useful discussions and suggestions for experiments, and Pierre Gagné for his assistance with network modeling and data processing. The authors also thank the University of British Columbia Proteomics Core Facility for the preparation and analysis of protein samples for SILAC analysis. We are particularly grateful to Dr Sylvie Bourassa who managed most of the samples at the Proteomics Platform of the Quebec Genomics Center and Sandra Breuils-Bonnet for iTRAQ labeling and IEF fractionation.

FUNDING

Canadian Institutes for Health Research [CIHR MOP-14052, MOP-74648]. Funding for open access charge: Canadian Institutes of Health Research (CIHR).

Conflict of interest statement. None declared.

REFERENCES

1. Tartier,L., Spenlehauer,C., Newman,H.C., Folkard,M., Prise,K.M., Michael,B.D., Menissier-de Murcia,J. and de Murcia,G. (2003) Local DNA damage by proton microbeam irradiation induces poly(ADP-ribose) synthesis in mammalian cells. *Mutagenesis*, **18**, 411–416.
2. Rouleau,M., Aubin,R.A. and Poirier,G.G. (2004) Poly(ADP-ribosyl)ated chromatin domains: access granted. *J. Cell Sci.*, **117**, 815–825.
3. Malanga,M. and Althaus,F.R. (2005) The role of poly(ADP-ribose) in the DNA damage signaling network. *Biochem. Cell Biol.*, **83**, 354–364.
4. Till,S. and Ladurner,A.G. (2009) Sensing NAD metabolites through macro domains. *Front. Biosci.*, **14**, 3246–3258.
5. Ahel,I., Ahel,D., Matsusaka,T., Clark,A.J., Pines,J., Boulton,S.J. and West,S.C. (2008) Poly(ADP-ribose)-binding zinc finger motifs in DNA repair/checkpoint proteins. *Nature*, **451**, 81–85.
6. Aravind,L. (2001) The WWE domain: a common interaction module in protein ubiquitination and ADP ribosylation. *Trends Biochem. Sci.*, **26**, 273–275.
7. Zhang,Y., Liu,S., Mickanin,C., Feng,Y., Charlat,O., Michaud,G.A., Schirle,M., Shi,X., Hild,M., Bauer,A. *et al.* (2011) RNF146 is a poly(ADP-ribose)-directed E3 ligase that regulates axin degradation and Wnt signalling. *Nat. Cell Biol.*, **13**, 623–629.
8. Wang,Z., Michaud,G.A., Cheng,Z., Zhang,Y., Hinds,T.R., Fan,E., Cong,F. and Xu,W. (2012) Recognition of the iso-ADP-ribose moiety in poly(ADP-ribose) by WWE domains suggests a general mechanism for poly(ADP-ribosyl)ation-dependent ubiquitination. *Genes Dev.*, **26**, 235–240.
9. Pleschke,J.M., Kleczkowska,H.E., Strohm,M. and Althaus,F.R. (2000) Poly(ADP-ribose) binds to specific domains in DNA damage checkpoint proteins. *J. Biol. Chem.*, **275**, 40974–40980.
10. Althaus,F.R., Kleczkowska,H.E., Malanga,M., Muntener,C.R., Pleschke,J.M., Ebner,M. and Auer,B. (1999) Poly ADP-ribosylation: a DNA break signal mechanism. *Mol. Cell Biochem.*, **193**, 5–11.
11. Gagne,J.P., Isabelle,M., Lo,K.S., Bourassa,S., Hendzel,M.J., Dawson,V.L., Dawson,T.M. and Poirier,G.G. (2008) Proteome-wide identification of poly(ADP-ribose) binding proteins and poly(ADP-ribose)-associated protein complexes. *Nucleic Acids Res.*, **36**, 6959–6976.
12. Egloff,M.P., Malet,H., Putics,A., Heinonen,M., Dutartre,H., Frangeul,A., Gruez,A., Campanacci,V., Cambillau,C., Ziebuhr,J. *et al.* (2006) Structural and functional basis for ADP-ribose and poly(ADP-ribose) binding by viral macro domains. *J. Virol.*, **80**, 8493–8502.
13. Karras,G.I., Kustatscher,G., Buhecha,H.R., Allen,M.D., Pugieux,C., Sait,F., Bycroft,M. and Ladurner,A.G. (2005) The macro domain is an ADP-ribose binding module. *EMBO J.*, **24**, 1911–1920.
14. Dani,N., Stilla,A., Marchegiani,A., Tamburro,A., Till,S., Ladurner,A.G., Corda,D. and Di Girolamo,M. (2009) Combining affinity purification by ADP-ribose-binding macro domains with mass spectrometry to define the mammalian ADP-ribosyl proteome. *Proc. Natl Acad. Sci. USA*, **106**, 4243–4248.
15. Slade,D., Dunstan,M.S., Barkauskaite,E., Weston,R., Lafite,P., Dixon,N., Ahel,M., Leys,D. and Ahel,I. (2011) The structure and catalytic mechanism of a poly(ADP-ribose) glycohydrolase. *Nature*, **477**, 616–620.
16. Ji,Y. (2011) Noncovalent pADPr interaction with proteins and competition with RNA for binding to proteins. *Methods Mol. Biol.*, **780**, 83–91.
17. Malanga,M. and Althaus,F.R. (2011) Noncovalent protein interaction with poly(ADP-ribose). *Methods Mol. Biol.*, **780**, 67–82.
18. Gagne,J.P., Haince,J.F., Pic,E. and Poirier,G.G. (2011) Affinity-based assays for the identification and quantitative evaluation of noncovalent poly(ADP-ribose)-binding proteins. *Methods Mol. Biol.*, **780**, 93–115.
19. Hassa,P.O., Haenni,S.S., Elser,M. and Hottiger,M.O. (2006) Nuclear ADP-ribosylation reactions in mammalian cells: where are we today and where are we going? *Microbiol. Mol. Biol. Rev.*, **70**, 789–829.
20. Banath,J.P., Klokov,D., MacPhail,S.H., Banuelos,C.A. and Olive,P.L. (2010) Residual gammaH2AX foci as an indication of lethal DNA lesions. *BMC Cancer*, **10**, 4.
21. Artus,C., Boujrad,H., Bouharrour,A., Brunelle,M.N., Hoos,S., Yuste,V.J., Lenormand,P., Rousselle,J.C., Namane,A., England,P. *et al.* (2010) AIF promotes chromatinolysis and caspase-independent programmed necrosis by interacting with histone H2AX. *EMBO J.*, **29**, 1585–1599.
22. Haince,J.F., Ouellet,M.E., McDonald,D., Hendzel,M.J. and Poirier,G.G. (2006) Dynamic relocation of poly(ADP-ribose) glycohydrolase isoforms during radiation-induced DNA damage. *Biochim. Biophys. Acta*, **1763**, 226–237.
23. Patel,C.N., Koh,D.W., Jacobson,M.K. and Oliveira,M.A. (2005) Identification of three critical acidic residues of poly(ADP-ribose) glycohydrolase involved in catalysis: determining the PARG catalytic domain. *Biochem. J.*, **388**, 493–500.
24. Shah,G.M., Poirier,D., Duchaine,C., Brochu,G., Desnoyers,S., Lagueux,J., Verreault,A., Hoflack,J.C., Kirkland,J.B. and Poirier,G.G. (1995) Methods for biochemical study of poly(ADP-ribose) metabolism in vitro and in vivo. *Anal Biochem.*, **227**, 1–13.
25. Hennig,C. (2010) fpc: Flexible procedures for clustering, Rpackage version 2.0-2. http://CRAN.R-project.org/package=fpc.

26. Harsha,H.C., Molina,H. and Pandey,A. (2008) Quantitative proteomics using stable isotope labeling with amino acids in cell culture. *Nat. Protoc.*, **3**, 505–516.
27. Blagoev,B. and Mann,M. (2006) Quantitative proteomics to study mitogen-activated protein kinases. *Methods*, **40**, 243–250.
28. Huang da,W., Sherman,B.T. and Lempicki,R.A. (2009) Systematic and integrative analysis of large gene lists using DAVID bioinformatics resources. *Nat. Protoc.*, **4**, 44–57.
29. Shannon,P., Markiel,A., Ozier,O., Baliga,N.S., Wang,J.T., Ramage,D., Amin,N., Schwikowski,B. and Ideker,T. (2003) Cytoscape: a software environment for integrated models of biomolecular interaction networks. *Genome Res.*, **13**, 2498–2504.
30. Maere,S., Heymans,K. and Kuiper,M. (2005) BiNGO: a Cytoscape plugin to assess overrepresentation of gene ontology categories in biological networks. *Bioinformatics*, **21**, 3448–3449.
31. Gao,J., Ade,A.S., Tarcea,V.G., Weymouth,T.E., Mirel,B.R., Jagadish,H.V. and States,D.J. (2009) Integrating and annotating the interactome using the MiMI plugin for cytoscape. *Bioinformatics*, **25**, 137–138.
32. Martin,A., Ochagavia,M.E., Rabasa,L.C., Miranda,J., Fernandez-de-Cossio,J. and Bringas,R. (2010) BisoGenet: a new tool for gene network building, visualization and analysis. *BMC Bioinformatics*, **11**, 91.
33. Gagne,J.P., Moreel,X., Gagne,P., Labelle,Y., Droit,A., Chevalier-Pare,M., Bourassa,S., McDonald,D., Hendzel,M.J., Prigent,C. *et al.* (2009) Proteomic investigation of phosphorylation sites in poly(ADP-ribose) polymerase-1 and poly(ADP-ribose) glycohydrolase. *J. Proteome Res.*, **8**, 1014–1029.
34. Haince,J.F., McDonald,D., Rodrigue,A., Dery,U., Masson,J.Y., Hendzel,M.J. and Poirier,G.G. (2008) PARP1-dependent kinetics of recruitment of MRE11 and NBS1 proteins to multiple DNA damage sites. *J. Biol. Chem.*, **283**, 1197–1208.
35. Kawamitsu,H., Hoshino,H., Okada,H., Miwa,M., Momoi,H. and Sugimura,T. (1984) Monoclonal antibodies to poly(adenosine diphosphate ribose) recognize different structures. *Biochemistry*, **23**, 3771–3777.
36. Hassler,M., Jankevicius,G. and Ladurner,A.G. (2011) PARG: a macrodomain in disguise. *Structure*, **19**, 1351–1353.
37. Allen,M.D., Buckle,A.M., Cordell,S.C., Lowe,J. and Bycroft,M. (2003) The crystal structure of AF1521 a protein from *Archaeoglobus fulgidus* with homology to the non-histone domain of macroH2A. *J. Mol. Biol.*, **330**, 503–511.
38. Polo,S.E., Kaidi,A., Baskcomb,L., Galanty,Y. and Jackson,S.P. (2010) Regulation of DNA-damage responses and cell-cycle progression by the chromatin remodelling factor CHD4. *EMBO J.*, **29**, 3130–3139.
39. Ahel,D., Horejsi,Z., Wiechens,N., Polo,S.E., Garcia-Wilson,E., Ahel,I., Flynn,H., Skehel,M., West,S.C., Jackson,S.P. *et al.* (2009) Poly(ADP-ribose)-dependent regulation of DNA repair by the chromatin remodeling enzyme ALC1. *Science*, **325**, 1240–1243.
40. Gottschalk,A.J., Timinszky,G., Kong,S.E., Jin,J., Cai,Y., Swanson,S.K., Washburn,M.P., Florens,L., Ladurner,A.G., Conaway,J.W. *et al.* (2009) Poly(ADP-ribosyl)ation directs recruitment and activation of an ATP-dependent chromatin remodeler. *Proc. Natl Acad. Sci. USA*, **106**, 13770–13774.
41. Fahrer,J., Popp,O., Malanga,M., Beneke,S., Markovitz,D.M., Ferrando-May,E., Burkle,A. and Kappes,F. (2010) High-affinity interaction of poly(ADP-ribose) and the human DEK oncoprotein depends upon chain length. *Biochemistry*, **49**, 7119–7130.
42. Chang,W., Dynek,J.N. and Smith,S. (2005) NuMA is a major acceptor of poly(ADP-ribosyl)ation by tankyrase 1 in mitosis. *Biochem. J.*, **391**, 177–184.
43. Kickhoefer,V.A., Siva,A.C., Kedersha,N.L., Inman,E.M., Ruland,C., Streuli,M. and Rome,L.H. (1999) The 193-kD vault protein, VPARP, is a novel poly(ADP-ribose) polymerase. *J. Cell Biol.*, **146**, 917–928.
44. Saxena,A., Saffery,R., Wong,L.H., Kalitsis,P. and Choo,K.H. (2002) Centromere proteins Cenpa, Cenpb, and Bub3 interact with poly(ADP-ribose) polymerase-1 protein and are poly(ADP-ribosyl)ated. *J. Biol. Chem.*, **277**, 26921–26926.
45. Ruscetti,T., Lehnert,B.E., Halbrook,J., Le Trong,H., Hoekstra,M.F., Chen,D.J. and Peterson,S.R. (1998) Stimulation of the DNA-dependent protein kinase by poly(ADP-ribose) polymerase. *J. Biol. Chem.*, **273**, 14461–14467.
46. Reale,A., Matteis,G.D., Galleazzi,G., Zampieri,M. and Caiafa,P. (2005) Modulation of DNMT1 activity by ADP-ribose polymers. *Oncogene*, **24**, 13–19.
47. Huang,J.Y., Chen,W.H., Chang,Y.L., Wang,H.T., Chuang,W.T. and Lee,S.C. (2006) Modulation of nucleosome-binding activity of FACT by poly(ADP-ribosyl)ation. *Nucleic Acids Res.*, **34**, 2398–2407.
48. Malanga,M. and Althaus,F.R. (2004) Poly(ADP-ribose) reactivates stalled DNA topoisomerase I and induces DNA strand break resealing. *J. Biol. Chem.*, **279**, 5244–5248.
49. Meyer-Ficca,M.L., Lonchar,J.D., Ihara,M., Meistrich,M.L., Austin,C.A. and Meyer,R.G. (2011) Poly(ADP-Ribose) polymerases PARP1 and PARP2 modulate topoisomerase II beta (TOP2B) function during chromatin condensation in mouse spermiogenesis. *Biol. Reprod.*, **84**, 900–909.
50. Gagne,J.P., Hunter,J.M., Labrecque,B., Chabot,B. and Poirier,G.G. (2003) A proteomic approach to the identification of heterogeneous nuclear ribonucleoproteins as a new family of poly(ADP-ribose)-binding proteins. *Biochem. J.*, **371**, 331–340.
51. Ji,Y. and Tulin,A.V. (2009) Poly(ADP-ribosyl)ation of heterogeneous nuclear ribonucleoproteins modulates splicing. *Nucleic Acids Res.*, **37**, 3501–3513.
52. Panzeter,P.L., Zweifel,B., Malanga,M., Waser,S.H., Richard,M. and Althaus,F.R. (1993) Targeting of histone tails by poly(ADP-ribose). *J. Biol. Chem.*, **268**, 17662–17664.
53. Wang,Y., Kim,N.S., Haince,J.F., Kang,H.C., David,K.K., Andrabi,S.A., Poirier,G.G., Dawson,V.L. and Dawson,T.M. (2011) Poly(ADP-ribose) (PAR) binding to apoptosis-inducing factor is critical for PAR polymerase-1-dependent cell death (parthanatos). *Sci. Signal*, **4**, ra20.
54. Slama,J.T., Aboul-Ela,N., Goli,D.M., Cheesman,B.V., Simmons,A.M. and Jacobson,M.K. (1995) Specific inhibition of poly(ADP-ribose) glycohydrolase by adenosine diphosphate (hydroxymethyl)pyrrolidinediol. *J. Med. Chem.*, **38**, 389–393.
55. Malanga,M. and Althaus,F.R. (1994) Poly(ADP-ribose) molecules formed during DNA repair in vivo. *J. Biol. Chem.*, **269**, 17691–17696.
56. D'Amours,D., Desnoyers,S., D'Silva,I. and Poirier,G.G. (1999) Poly(ADP-ribosyl)ation reactions in the regulation of nuclear functions. *Biochem. J.*, **342 (Pt 2)**, 249–268.
57. Leppard,J.B., Dong,Z., Mackey,Z.B. and Tomkinson,A.E. (2003) Physical and functional interaction between DNA ligase IIIalpha and poly(ADP-Ribose) polymerase 1 in DNA single-strand break repair. *Mol. Cell. Biol.*, **23**, 5919–5927.
58. Schulze,W.X. and Usadel,B. (2010) Quantitation in mass-spectrometry-based proteomics. *Annu. Rev. Plant Biol.*, **61**, 491–516.
59. Mallick,P. and Kuster,B. (2010) Proteomics: a pragmatic perspective. *Nat. Biotechnol.*, **28**, 695–709.
60. Ong,S.E., Blagoev,B., Kratchmarova,I., Kristensen,D.B., Steen,H., Pandey,A. and Mann,M. (2002) Stable isotope labeling by amino acids in cell culture, SILAC, as a simple and accurate approach to expression proteomics. *Mol. Cell. Proteomics*, **1**, 376–386.
61. Ross,P.L., Huang,Y.N., Marchese,J.N., Williamson,B., Parker,K., Hattan,S., Khainovski,N., Pillai,S., Dey,S., Daniels,S. *et al.* (2004) Multiplexed protein quantitation in *Saccharomyces cerevisiae* using amine-reactive isobaric tagging reagents. *Mol. Cell. Proteomics.*, **3**, 1154–1169.
62. Montes de Oca,R., Shoemaker,C.J., Gucek,M., Cole,R.N. and Wilson,K.L. (2009) Barrier-to-autointegration factor proteome reveals chromatin-regulatory partners. *PLoS One*, **4**, e7050.
63. Yang,X., Zou,P., Yao,J., Yun,D., Bao,H., Du,R., Long,J. and Chen,X. (2010) Proteomic dissection of cell type-specific H2AX-interacting protein complex associated with hepatocellular carcinoma. *J. Proteome Res.*, **9**, 1402–1415.
64. Hassa,P.O., Haenni,S.S., Buerki,C., Meier,N.I., Lane,W.S., Owen,H., Gersbach,M., Imhof,R. and Hottiger,M.O. (2005) Acetylation of poly(ADP-ribose) polymerase-1 by p300/CREB-binding protein regulates coactivation of NF-kappaB-dependent transcription. *J. Biol. Chem.*, **280**, 40450–40464.
65. Eustermann,S., Brockmann,C., Mehrotra,P.V., Yang,J.C., Loakes,D., West,S.C., Ahel,I. and Neuhaus,D. (2010) Solution structures of the two PBZ domains from human APLF and their interaction with poly(ADP-ribose). *Nat. Struct. Mol. Biol.*, **17**, 241–243.

66. Li,G.Y., McCulloch,R.D., Fenton,A.L., Cheung,M., Meng,L., Ikura,M. and Koch,C.A. (2010) Structure and identification of ADP-ribose recognition motifs of APLF and role in the DNA damage response. *Proc. Natl Acad. Sci. USA*, **107**, 9129–9134.
67. Malanga,M. and Althaus,F.R. (2005) The role of poly(ADP-ribose) in the DNA damage signaling network. *Biochem. Cell Biol.*, **83**, 354–364.
68. El-Khamisy,S.F., Masutani,M., Suzuki,H. and Caldecott,K.W. (2003) A requirement for PARP-1 for the assembly or stability of XRCC1 nuclear foci at sites of oxidative DNA damage. *Nucleic Acids Res.*, **31**, 5526–5533.
69. Masson,M., Niedergang,C., Schreiber,V., Muller,S., Menissier-de Murcia,J. and de Murcia,G. (1998) XRCC1 is specifically associated with poly(ADP-ribose) polymerase and negatively regulates its activity following DNA damage. *Mol. Cell. Biol.*, **18**, 3563–3571.
70. Mortusewicz,O., Ame,J.C., Schreiber,V. and Leonhardt,H. (2007) Feedback-regulated poly(ADP-ribosyl)ation by PARP-1 is required for rapid response to DNA damage in living cells. *Nucleic Acids Res.*, **35**, 7665–7675.
71. Rouleau,M., Patel,A., Hendzel,M.J., Kaufmann,S.H. and Poirier,G.G. (2010) PARP inhibition: PARP1 and beyond. *Nat. Rev. Cancer*, **10**, 293–301.
72. Wu,J., Chen,Y., Lu,L.Y., Wu,Y., Paulsen,M.T., Ljungman,M., Ferguson,D.O. and Yu,X. (2011) Chfr and RNF8 synergistically regulate ATM activation. *Nat. Struct. Mol. Biol.*, **18**, 761–768.
73. Chou,D.M., Adamson,B., Dephoure,N.E., Tan,X., Nottke,A.C., Hurov,K.E., Gygi,S.P., Colaiacovo,M.P. and Elledge,S.J. (2010) A chromatin localization screen reveals poly (ADP ribose)-regulated recruitment of the repressive polycomb and NuRD complexes to sites of DNA damage. *Proc. Natl Acad. Sci. USA*, **107**, 18475–18480.
74. Haince,J.F., McDonald,D., Rodrigue,A., Dery,U., Masson,J.Y., Hendzel,M.J. and Poirier,G.G. (2008) PARP1-dependent kinetics of recruitment of MRE11 and NBS1 proteins to multiple DNA damage sites. *J. Biol. Chem.*, **283**, 1197–1208.
75. Harris,J.L., Jakob,B., Taucher-Scholz,G., Dianov,G.L., Becherel,O.J. and Lavin,M.F. (2009) Aprataxin, poly-ADP ribose polymerase 1 (PARP-1) and apurinic endonuclease 1 (APE1) function together to protect the genome against oxidative damage. *Hum. Mol. Genet.*, **18**, 4102–4117.
76. Rulten,S.L., Cortes-Ledesma,F., Guo,L., Iles,N.J. and Caldecott,K.W. (2008) APLF (C2orf13) is a novel component of poly(ADP-ribose) signaling in mammalian cells. *Mol. Cell Biol.*, **28**, 4620–4628.
77. Gieni,R.S., Ismail,I.H., Campbell,S. and Hendzel,M.J. (2011) Polycomb group proteins in the DNA damage response-A link between radiation resistance and ''stemness''. *Cell Cycle*, **10**, 883–894.
78. Li,B., Navarro,S., Kasahara,N. and Comai,L. (2004) Identification and biochemical characterization of a Werner's syndrome protein complex with Ku70/80 and poly(ADP-ribose) polymerase-1. *J. Biol. Chem.*, **279**, 13659–13667.
79. Galande,S. and Kohwi-Shigematsu,T. (1999) Poly(ADP-ribose) polymerase and Ku autoantigen form a complex and synergistically bind to matrix attachment sequences. *J. Biol. Chem.*, **274**, 20521–20528.
80. Ariumi,Y., Masutani,M., Copeland,T.D., Mimori,T., Sugimura,T., Shimotohno,K., Ueda,K., Hatanaka,M. and Noda,M. (1999) Suppression of the poly(ADP-ribose) polymerase activity by DNA-dependent protein kinase in vitro. *Oncogene*, **18**, 4616–4625.
81. Spagnolo,L., Barbeau,J., Curtin,N.J., Morris,E.P. and Pearl,L.H. (2012) Visualization of a DNA-PK/PARP1 complex. *Nucleic Acids Res.*, **40**, 4168–4177.
82. Ruscetti,T., Lehnert,B.E., Halbrook,J., Le Trong,H., Hoekstra,M.F., Chen,D.J. and Peterson,S.R. (1998) Stimulation of the DNA-dependent protein kinase by poly(ADP-ribose) polymerase. *J. Biol. Chem.*, **273**, 14461–14467.
83. Schmidt-Ullrich,R.K. (2003) Molecular targets in radiation oncology. *Oncogene*, **22**, 5730–5733.
84. Keller,A., Nesvizhskii,A.I., Kolker,E. and Aebersold,R. (2002) Empirical statistical model to estimate the accuracy of peptide identifications made by MS/MS and database search. *Anal Chem.*, **74**, 5383–5392.
85. Nesvizhskii,A.I., Keller,A., Kolker,E. and Aebersold,R. (2003) A statistical model for identifying proteins by tandem mass spectrometry. *Anal Chem.*, **75**, 4646–4658.
86. Shilov,I.V., Seymour,S.L., Patel,A.A., Loboda,A., Tang,W.H., Keating,S.P., Hunter,C.L., Nuwaysir,L.M. and Schaeffer,D.A. (2007) The Paragon Algorithm, a next generation search engine that uses sequence temperature values and feature probabilities to identify peptides from tandem mass spectra. *Mol. Cell. Proteomics*, **6**, 1638–1655.
87. Ishihama,Y., Rappsilber,J. and Mann,M. (2006) Modular stop and go extraction tips with stacked disks for parallel and multidimensional Peptide fractionation in proteomics. *J. Proteome Res.*, **5**, 988–994.
88. Chan,Q.W., Howes,C.G. and Foster,L.J. (2006) Quantitative comparison of caste differences in honeybee hemolymph. *Mol. Cell. Proteomics*, **5**, 2252–2262.
89. Gao,J., Ade,A.S., Tarcea,V.G., Weymouth,T.E., Mirel,B.R., Jagadish,H.V. and States,D.J. (2009) Integrating and annotating the interactome using the MiMI plugin for cytoscape. *Bioinformatics*, **25**, 137–138.

Poly(ADP) Ribose Polymerase at the Interface of DNA Damage Signaling and DNA Repair

Jana Krietsch, Michèle Rouleau, Michel Lebel, Guy Poirier, and Jean-Yves Masson

Chromosomal double-strand breaks (DSBs) are extremely hazardous to a cell as they do not leave an intact complementary strand to be used for repair. If not repaired accurately, the broken chromosomes undergo a wide variety of rearrangements such as translocations, mutations and deletions that may lead to cell death [1]. Genomic instability can promote cancer, developmental defects, tissue neurodegeneration, immunodeficiency, aging, as well as hypersensitivity to radiation. Each day a cell encounters approximately up to 50 DSBs, generated intrinsically such as during DNA synthesis when the processing replication fork encounters a damaged template [2]. DSBs can also be created during metabolic processes such as V(D)J recombination and class-switch recombination in vertebrate lymphocytes, meiotic recombination in germ cell lines, and mating type switching in yeast. Exogenous sources such as X-rays, gamma rays, UV light, topoisomerase I + II inhibitors can produce DSBs amongst other types of DNA damage. The cellular response to DNA

J. Krietsch
Cancer Research Unit, Laval University Medical Research Center, CHUQ-CRCHUL, Québec, QC, Canada G1V 4G2

Genome Stability Laboratory, Laval University Cancer Research Center, Hôtel-Dieu de Québec, Québec, Canada G1R 2J6

M. Rouleau • G. Poirier (✉)
Cancer Research Unit, Laval University Medical Research Center, CHUQ-CRCHUL, Québec, QC, Canada G1V 4G2
e-mail: guy.poirier@crchul.ulaval.ca

M. Lebel
Laval University Cancer Research Center, Hôtel-Dieu de Québec, Québec, Canada G1R 2J6

J.-Y Masson (✉)
Genome Stability Laboratory, Laval University Cancer Research Center, Hôtel-Dieu de Québec, Québec, Canada G1R 2J6
e-mail: Jean-Yves.Masson@crhdq.ulaval.ca

L. Panasci et al. (eds.), *Advances in DNA Repair in Cancer Therapy*,
Cancer Drug Discovery and Development 72, DOI 10.1007/978-1-4614-4741-2_8,

damage consists of multiple regulatory layers starting with sensing the damage, recruitment of repair proteins to the site of damage, and execution of DNA repair with possible outcomes concerning the cell's fate (such as apoptosis, entering terminal differentiation through senescence in order to prevent from inheriting damaged DNA) [3]. Interestingly, some members of the poly (ADP-ribose) polymerase (PARP) family have been implicated in DNA damage sensing as well as the repair of single strand breaks (SSBs) and DSBs, giving them a universal as well as a unique role in a cell's response to DNA damage [4]. Three PARPs that have been shown to be activated by DNA damage (PARP-1 as well as PARP-2 and possibly PARP-3) [5, 27] are therefore discussed in the following review with a focus on the two major pathways which have evolved to repair DNA DSBs: nonhomologous end joining (NHEJ) and homologous recombination (HR).

1 PARPs and Their Implications in Sensing and Repairing DNA Damage

The family of poly(ADP-ribose) polymerases (PARPs) also known as ADP-ribosyltransferases (ARTDs) consists of approximately 17 proteins in humans, estimated by the number of genes encoding proteins that possess an ADP-ribosyl-transferase catalytic domain [6]. PARP-1, PARP-2, PARP-3, and Tankyrases have been well described for their phylogenetically ancient, reversible posttranslational modification mechanism called poly(ADP-ribosyl)ation, which can modulate the function of their target proteins by regulating either enzymatic activities or molecular interactions between proteins, DNA, or RNA [7]. Responding to a large variety of cellular stresses, poly(ADP-ribosyl)ation is implicated in the maintenance of genomic stability, transcriptional regulation [8], energy metabolism, DNA methylation [9], and cell death [4, 10]. Upon activation, PARPs catalyze a reaction in which NAD^+ molecules are used to generate poly(ADP-ribose) molecules (pADPr) of varying length and complexity attached onto a number of acceptor proteins including PARPs themselves (automodification). As the first PARP discovered by Chambon and colleagues in 1963, the PARP-1 enzyme mediates the synthesis of an adenine-containing RNA-like polymer [11]. PARP-1 is one of the most abundant nuclear protein after histones.

The first function of PARPs in vitro was identified in response to DNA damage: Besides PARP-1, PARP-2, and PARP-3 have been shown to be enzymatically activated by encountering DNA strand breaks in vitro [5, 12, 27] with PARP-1 carrying out ~90% of the overall polymer synthesis and, notably, attaching the bulk of pADPr to itself [4]. The generation of knockout mice for PARP-1 further strengthened the hypothesis for a role for PARP-1 in DNA repair. The knock-out of PARP-1 or PARP-2 genes in mice is not lethal, suggesting that there is some redundancy between the function of these two PARPs. Importantly, PARP-1 knock-out mice led to the discovery of PARP-2. Notably, the double knock-out of PARP-1 and PARP-2 is not viable, indicating that poly(ADP-ribosyl)ation is

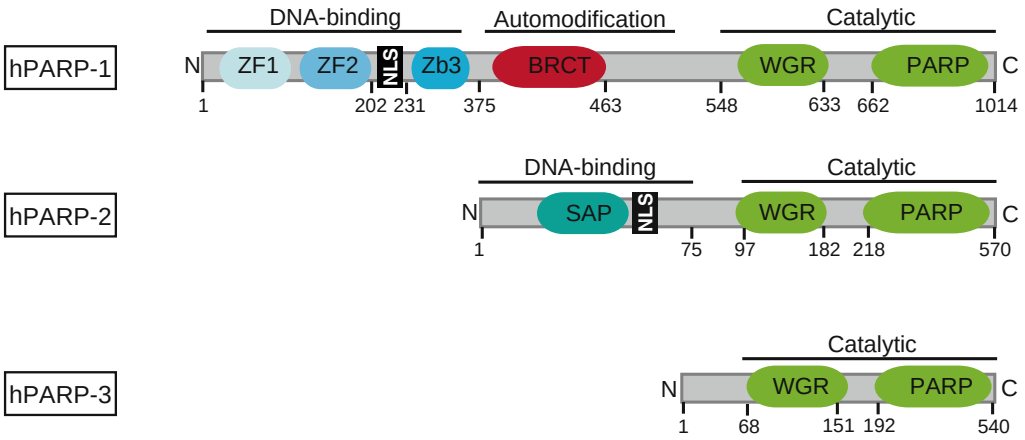

Fig. 1 Schematic comparison of the domain architecture of human PARP-1, PARP-2, and PARP-3. The following most significant domains are indicated: zinc finger (ZF); zinc binding (Zb); carboxyterminal domain (BRCT); the WGR domain, named after a conserved central motif (W-G-R); the PARP signature, representing the catalytic core needed for basal activity; nuclear localization signal (NLS); SAF/Acinus/PIAS-DNA-binding domain (SAP) (adapted from [27])

essential for early embryogenesis [13–15]. The modular structure of the PARP-1 protein is composed of at least six independent domains, containing two homologous zinc fingers (Zn1 and Zn2) at the extreme N-terminus that form the DNA binding module (Fig. 1). Recently, a third zinc binding domain (Zb3) has been identified [16, 17] which can bind DNA and seems not only to be critical for the DNA-dependent catalytic activity of PARP-1, but also involved in modulating chromatin structure. Indeed, Zb3 mutations in PARP-1 gene revealed a defect in the ability of PARP to compact chromatin. An internal automodification domain contains a BRCA1 C-terminal domain (BRCT) (shared by many DNA damage repair and cell cycle checkpoint proteins—essential for mediating protein–protein interactions) and three lysines that can be targeted for automodification. A catalytic domain is located at the C-terminus of PARP-1 and contains a region named PARP "signature," a highly conserved region in the PARP superfamily responsible for NAD^+ binding. In addition, the C-terminus also bears a WGR domain named after the highly conserved amino acid sequence in the motif (Trp, Gly, Arg) with an unknown function, which is also found in a variety of polyA polymerases. PARP-1, PARP-2, and PARP-3 share conserved WGR and catalytic domains. Interestingly, differing from PARP-1, the other two PARPs that can be activated by DNA damage do not contain the same DNA-binding module: Whereas PARP-2 contains a SAF/Acinus/PIAS (SAP) DNA binding domain, the DNA-binding domain of PARP-3 has not been characterized [6].

PARP-1 and PARP-2 are recognized as molecular sensors of SSBs and DSBs in vivo. The synthesis of pADPr chains is considered one of the earliest events of the DNA damage response as it occurs within seconds [3]. Besides the direct covalent modification on glutamate, aspartate, or lysine residues of various target proteins, some proteins have been elegantly shown to have a high affinity for the free

polymer itself. In fact, it has been argued that strong noncovalent binding of PARP or other proteins to pADPr rather than covalent modification [18] affects protein function and/or localization. Consequently, recent progress has been made in defining specific sites for pADPr-attachment on target proteins [19–21]. Noncovalent binding of proteins to pADPr can be through at least four different PAR-binding motifs. One such motif was identified by our group and is characterized by a sequence of alternating basic and hydrophobic amino acids [22, 23]. Two other PAR-binding motifs have been described—the macrodomain and the PAR-binding zinc finger (PBZ) [24]. Only very recently a fourth type of polymer binding domain has been reported: The E3-ubiquitin ligase RNF146 contains a Trp-Trp-Glu (WWE) motif that is binding pADPr [25, 26]. Interestingly, this WWE domain has been found in various PARPs [27].

As mentioned above, PARP-1 is a molecular sensor of DNA strand breaks and the large size and negative charge of the polymer (which exceeds the charge density of DNA about two times) generated upon activation is playing a key role in the spatial and temporal organization of the DNA damage response. The in vivo half-life of the polymer generated upon PARP activation is rather short (seconds to minutes) and tightly regulated by the catalytic reactions of poly(ADP-ribose) glycohydrolase (PARG) and possibly ADP-ribose hydrolase (ARH) 3, which are so far the only glycohydrolases known to degrade the polymer [28, 29]. The fact that PARG and ARH3 antagonize PARP activity and thereby detach the polymer from PARP-1 itself re-enables the latter protein to bind DNA and start a new round of DNA damage signaling. Although the half-life of the polymer is extremely short, its impact on the cellular energy level can be dramatic as PARP hyperactivation following severe DNA damage consumes substantial amounts of the cytosolic and nuclear NAD^+ (and ATP) pool and thereby can result in cell death [30].

Interestingly, the ability of PARP-1 to disrupt and open chromatin structure by PARsylating histones (such as H1 and H2B) and destabilizing nucleosomes has been one of the earliest functions described for the proteins [31–33]. By disrupting the chromatin structure, DNA repair factors can gain access to a DNA damage site. Recent publications demonstrated that a variety of proteins implicated in DNA repair are recruited in a pADPr-dependent manner to DNA single or double strand breaks [34]. For instance, the Ataxia telangiectasia-mutated (ATM) protein is recruited to DNA DSBs in a way that is depending on polymer synthesis [34].

2 Roles of PARP-1 in Base Excision Repair

The role of PARP-1 in the repair of single-strand DNA breaks by base excision repair (BER) became already evident 30 years ago [35] and has since then been well examined by several investigators [36, 37]. Two Nature publications in 2005, from the Helleday and Ashworth groups, have revolutionized the understanding of PARP inhibitors in the context of DNA repair [38, 39]: The observation of antitumor effects of PARP inhibitors in a HR-deficient background has been explained as result from the disability of PARP-1 to respond to endogenous DNA damage through

BER [38]. However, the question whether SSBs increase after PARP inhibition is still matter of ongoing debates [40, 41]. Moreover, a lack of XRCC1 (another BER protein) in BRCA2 deficient cells (and thus deficient in HR) does not show the same effect as PARP inhibition, questioning the original explanation for increased sensitivity of HR-deficient cells by PARP inhibition. Even though it is well accepted that PARP-1 is implicated in BER, its exact role remains controversial: pADPr itself or automodified PARP-1 is said to be necessary for the recruitment of XRCC1, which further leads to the recruitment of polymerase β and DNA ligase III [42–44]. Although PARP-1 seems to attract SSB repair proteins, it seems not to be essential for SSB repair itself as PARP-$1^{-/-}$ knockout mice for example do not show any early onset of tumor formation [14]. It has been recently suggested that PARP inhibitors inhibit rather than trap PARP on the SSB intermediate which is formed during BER, thereby preventing accurate repair [40]. It is also well accepted that poly(ADP-ribosyl)ation of PARP-1 and histones due to the negative charge of the polymer leads to their dissociation from the DNA which further promotes local chromatin relaxation [45]. Consequently, one could argue that this alone can facilitate the assembly of repair proteins at the break site emphasizing a passive role for PARP-1 in BER. In association with PARP-1, PARP-2 has been implicated in BER through its ability to interact with XRCC1, DNA polymerase β and DNA ligase III. Whereas PARP-1 seems to affect early steps of BER, PARP-2 seems to be involved later in the process [46].

3 Double-Strand Break Repair by Homologous Recombination

Several lines of evidence have accumulated in the past years for a role of PARP-1 in the cellular response to DNA DSB repair. PARP-1 deficient cells are hypersensitive to DSB-inducing agents but most notably to camptothecin [47]. This phenotype is also observed in PARP-1(–/–) chicken DT40 mutants [48]. Camptothecin blocks topoisomerase-I in a state where it is covalently linked to nicked DNA. The resulting protein-DNA cross links are DNA replication and transcription blocks. Replication forks stalling at these lesions result in the formation of DNA DSBs that are repaired by HR [49]. HR can occur due to an availability of long sequence homologies in the sister chromatid after DNA replication. As the donor sequence used for HR is usually the sister chromatid, one of its key features is the preservation of the genetic material. However, the donor sequence might as well be another homologous region with consequences as deletions, inversions, or loss of heterozygosity [50]. Whereas NHEJ functions throughout the cell cycle, HR takes mainly place in S/G2 phase due to its necessity for a homolog template [51, 52].

HR is suggested to be initiated by MRE11-RAD50-NBS1 (MRN), CtIP, Exo1, DNA2, and BLM [53] in mammals, with 5′-3′ end resection to yield a 3′ single-stranded (ss) DNA overhang which is capable of invading duplex DNA containing a homologous sequence [54, 55] (Fig. 2). Interestingly, PARP-1 has been put in the context of MRN recruitment as it has been clearly demonstrated that PARP-1 can

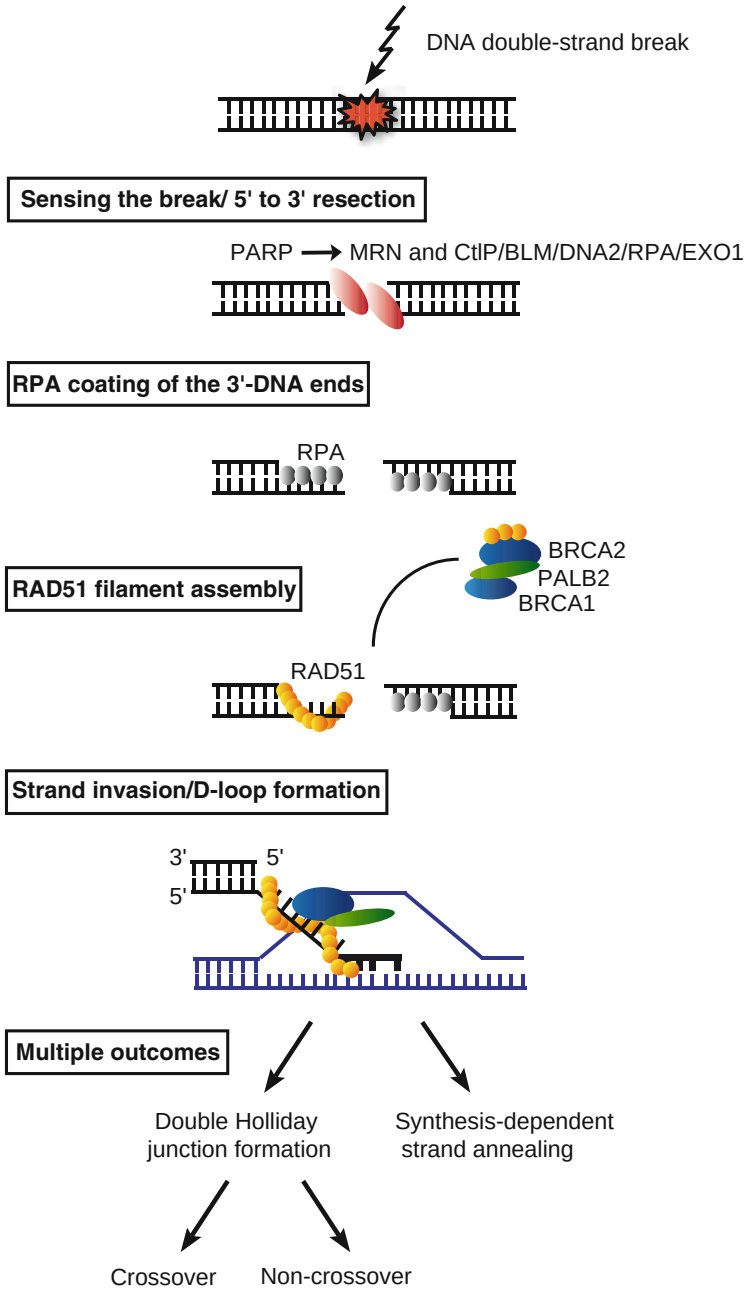

Fig. 2 Simplified overview of the homologous recombination (HR) repair pathway. Subsequent to DNA damage, the MRN complex (and associated resection machineries) binds and resects free DNA ends to create 3′ overhangs which are then bound by RPA. A complex of BRCA1, PALB2 and BRCA2 mediates the replacement of RPA by RAD51, which leads to the formation of the RAD51 filament coating the 3′ overhang. BRCA1/PALB2/BRCA2 then activates RAD51 to promote the invasion of an undamaged template in a step called strand invasion/ D-loop formation. Resolving of the D-loop structure can occur through synthesis-dependent strand annealing or double Holiday junction formation, generating either cross-over or non-cross-over products in the latter case

mediate the initial accumulation of the MRN complex to DSBs independent of γ-H2AX and MDC-1 [34]. This might have an implication in HR but also on a backup pathway of NHEJ (as discussed later in the text).

The replication protein A (RPA) has a high affinity for 3′-ssDNA tails and therefore binds to the newly generated 3′-ssDNA-overhang, a process that normally inhibits RAD51 loading and HR. HR mediators such as BRCA2 [56] and PALB2 [57] are helping to overcome that inhibition and lead to a displacement of RPA by RAD51 [58]. RAD51 itself, a DNA-dependent ATPase which is homolog to the bacterial RecA protein, is forming nucleoprotein filaments with DNA in a presynaptic step. RAD51 is recruited to DSBs in mammalian cells through BRCA2. Both, BRCA1 and 2 have been elegantly shown to be absolutely necessary for the HR reaction [59, 60] and there are several studies putting PALB2 (also known as FANCN) in the center of the BRCA1-BRCA2 complex [61, 62]. DSS1, a 70 amino acid protein, has been shown to be crucial for Rad51 foci formation as well and presumably for HR in mammalian cells [63]. A role for PARP-1 in that step of HR has been suggested to be rather of a regulatory nature than through a direct involvement in the actual mechanism: RAD51 foci are not only still forming in response to hydroxyurea in PARP-1$^{-/-}$ cells, but their number is also increasing in a PARP-1 deficient background [64]. In line with the latter finding it has been shown that in a PARP-1 deficient background (PARP-1 null MEFs) the spontaneous frequency of RAD51 foci is clearly enhanced [65]. Interestingly, pADPr, the product of catalytically active PARP, has been detected at HU-induced RPA foci raising the possibility that PARP-1 might for example prevent RAD51 from loading [66].

The following synaptic step is characterized by invasion of a homologous sequence to generate a D-loop structure (Fig. 2). Therewith the Rad51-ssDNA complex is binding to a complementary ssDNA region within the homologous duplex. Once formed, the D-loop structure has multiple fates: In the double-strand break repair (DSBR) model, the 3′ invading end from the broken chromosome is used to prime DNA synthesis templated by the donor duplex, whereas the other end of the break is presumably captured by the displaced strand from the donor duplex (D-loop) and is used to prime a second round of leading strand DNA synthesis. Therewith a so-called double Holliday Junction (dHJ) intermediate is formed that can, after branch migration and fill-in of the ssDNA, be resolved to form cross-over or non-cross-over products. In a second model called synthesis dependent strand annealing (SDSA), the invading strand that has been extended by DNA synthesis is displaced and anneals to complementary sequences exposed by 5′-3′ resection of the other side of the break. The remaining gaps can subsequently be filled in by newly synthesized DNA or by ligating the nicks [67]. SDSA will result only in non-cross-over products.

Collectively, there are several lines of evidence that PARP-1 regulates HR. PARP1$^{-/-}$ DT40 mutants showed more than threefold reduction in gene conversion [48]. Interestingly, the deletion of KU in PARP1$^{-/-}$ DT40 mutants completely reversed this phenotype suggesting that KU has a suppressive effect on HR. On the other hand, PARP-1 has been suggested to rather prevent HR, as the absence of

PARP-1 results in an increase of spontaneous somatic HR events in vivo [65]. PARP-1 also affects replication fork progression on damaged DNA. Indeed, fork progression is not slowed down in PARP1$^{-/-}$ DT40 cells treated with camptothecin. As fork slowing is correlated with the proficiency of HR, it implicates PARP-1 in the regulation of HR during DNA replication [68]. Additionally, by using the DNA fiber assay, Thomas Helleday and colleagues were able to show that PARP-1 is important for replication fork restart after blocking after HU treatment [66].

4 DNA Double-Strand Break Repair Through Nonhomologous End Joining

The repair of DSBs by HR has been demonstrated in practically all organisms examined from bacteria, yeast to human and seems to be conserved throughout evolution. Being described as a rather "error-free" pathway that is faithfully restoring genetic information it came as a big surprise to the DNA damage field that the major DSB repair pathway in higher eukaryotes is of a kind that does not rely on a homologous template but restores molecular integrity irrespective of the DNA sequence information. In nondividing haploid organisms or in diploid organisms that are not in the S-phase, a homologous template is not available for homology directed repair, setting the stage for a repair mechanism not relying on template homology, called NHEJ. The latter DSB repair pathway is effective throughout the cell cycle, but of particular importance during G0-, G1 and the early S-phase of cells. DNA DSB ends are often the result of damage to the sugar-phosphate backbone and/or the bases of the terminal nucleotides that have to be removed or processed prior to the religation step, explaining the fact that NHEJ is often mutagenic.

The most striking characteristic of the NHEJ pathway might be its high flexibility in terms of its templates, proteins involved and possible outcomes. The enzymes of the NHEJ pathway exhibit a remarkable tolerance concerning the DNA end substrate configurations they can act on. Different from other more distinct repair pathways, NHEJ enzymes act iteratively. Most of them can function independent of one another. As other repair pathways, NHEJ requires proteins that bring the ends in close proximity, nucleases/polymerases to process unligatable DNA ends and a ligase to restore integrity of the DNA strands [69]. From studies in which researchers investigated the status of Ku and DNA-PK$_{cs}$ in cell lines that are sensitive to ionizing radiation it became evident by their absence that these two proteins are implicated in NHEJ [70].

The generally accepted model of the "classical" NHEJ pathway is initiated with the heterodimeric complex of Ku70/Ku80 that binds to both ends of a broken DNA molecule (Fig. 3). This Ku-DNA complex acts presumably as a scaffold needed for the recruitment of DNA-PK$_{cs}$, which then functions as a molecular "bridge" between the two broken ends [71, 72]. Other than the Ku70/Ku80 complex, the association of Ku70/80 to the DNA-PK$_{cs}$ is transient and most likely stimulated by

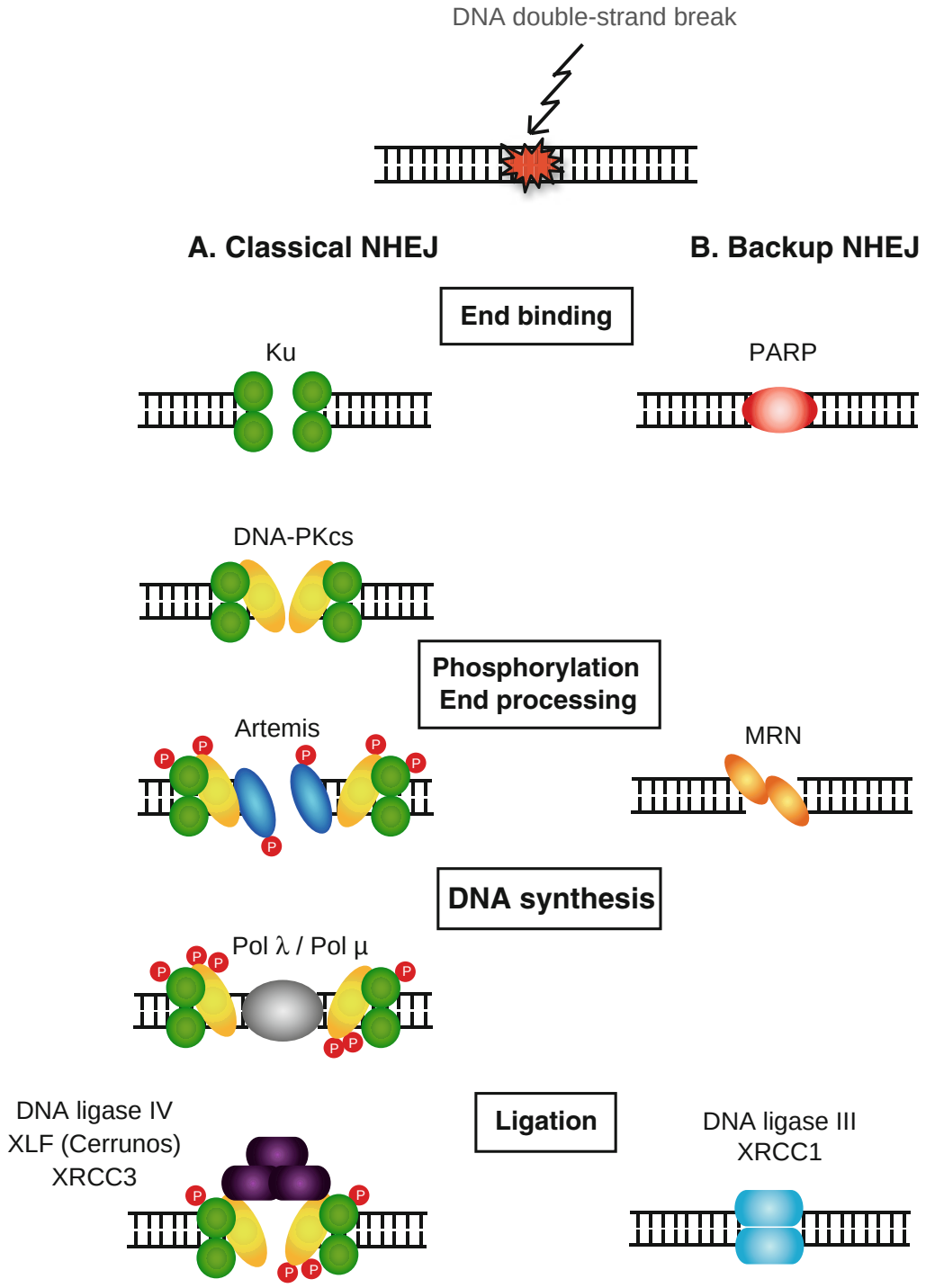

Fig. 3 DNA double-strand break repair through nonhomologous end joining (NHEJ). (**a**). The classical NHEJ pathway is initiated with Ku70/80 binding to the free DNA ends. The subsequent recruitment of the catalytic subunit of DNA-PK leads to the assembly of the end-bridging DNA-PK complex. DNA-PK then phosphorylates many proteins including Ku70 and itself. This loosens the DNA-PK DNA-binding which gives access to end processing proteins (such as Artemis/ PNK/ APLF/ TdT). After a fill-in of missing nucleotides by polymerase λ and μ the ends are joined by DNA ligase IV in a complex with its accessory factors (XRCC4 and XLF). (**b**) In the absence of or in competition to Ku70 it has been shown that PARP-1 can bind free DNA ends. Ends might further be processed by the MRN complex prior to a ligation by DNA ligase III/XRCC1

free DNA ends [73]. In a current model, it has been suggested that upon recruitment in a manner, DNA-PK phosphorylates several proteins including Ku70 and itself, which presumably facilitates NHEJ by destabilizing the interaction of the protein itself with DNA, thus providing access for end processing enzymes such as Artemis. Whereas the autophosphorylation of DNA-PK$_{cs}$ on the six-residue ABCDE cluster (T2609 cluster) has been shown to destabilize the protein DNA-binding properties, a phosphorylation on the five-residue PQR cluster (S2056), in return has presumably the opposite effect in protecting the DNA ends from excessive processing [74, 75].

As indicated before, if DNA DSB ends are not 5′ phosphorylated and ligatable, they have to be processed prior to the ligation step. Artemis has been revealed to be one of the major processing enzymes, showing a DNA-PK-independent 5′- to 3′- exonuclease activity and a DNA-PK-dependent endonuclease activity [76, 77]. However Artemis does not seem to be the only nuclease necessary for end-processing in DNA DSB repair, as cells lacking Artemis show higher radiosensitivity but do not have major defects in DNA DSB repair [78]. For example polynucleotide kinase (PNK), APLF nucleases and terminal deoxynucleotidyl transferase (TdT) have been shown to be able to remove damaged nucleotides in the context of NHEJ [79, 80]. Polymerases being able to insert new DNA at DSBs are polymerase λ and polymerase μ, belonging to the POL X family. The two latter polymerases have been shown to be able to bind the Ku:DNA complex through their BRCT domains [81–83].

Major resolution complex for DSB repair through NHEJ has been shown to be the X4-L4 complex (XRCC4, DNA ligase IV and XLF), whereas XRCC4 and XLF do not seem to have an enzymatic function in the process but rather act as cofactors being able to stimulate the ligation activity of ligase IV [84]. The latter complex forms the second physical “bridge” stabilizing the DNA ends and mediating their ultimate rejoining by ligation. The XRCC4-ligIV complex is the most flexible ligase complex known in terms of ligating across gaps and ligates incompatible ends [85].

From experiments in which at least one of the key NHEJ proteins has been mutated, the observed end-joining activity was still present in such mutant cell lines; this activity has been proposed to be due to a back-up pathway to the “classical” NHEJ pathway. End-joining can for example happen in the absence of DNA ligase IV or Ku70 [86]. As the only remaining DNA ligase activity in vertebrate cells is due to DNA ligase I or III, one or both of the latter two proteins have to proceed end-joining events observed in the absence of ligase IV. Alternative end-joining activity has until now only been demonstrated in the absence of classical factors therewith in the absence of the “classical” NHEJ, indicating an actual backup rather than a coexisting alternative pathway [87]. However the possibility that the NHEJ happening in the absence of Ku70 and ligase IV, can act alternatively to the classical pathway has not yet been disproven. From in vivo experiments in *S. cerevisiae* and mammals it has been elegantly shown that the variation of the ligation product is diminished as terminal microhomology occurs [88].

Besides the key factors described above, there have been other proteins shown to have an impact on the NHEJ reaction. Interestingly, the MRN complex which is known to coordinate DNA DSB repair by HR has recently been shown to promote efficient NHEJ in a XRCC4$^{+/+}$ and XRCC4$^{-/-}$ background in mice embryonic stem cells [89]. As accessory factors for the ligase reaction through its ability to interact with XRCC4, Polynucleotide kinase (PNK), aprataxin (APTX) and aprataxin- and PNK-like factor (APLF) have been identified [90]. Interestingly, PARP-3 has been suggested very recently to accelerate DNA ligation during NHEJ in the context of APLF [12].

The affinity of PARP-1 for a blunt ended and 3′ single-base overhang DSBs has been shown to be greater than the one of DNA-PK, with a fourfold lower affinity of PARP-1 for SSBs compared to blunt-ended DSBs [91]. Also PARP-1 has been demonstrated to directly interact with Ku proteins in vitro and in vivo, whereas Ku70, Ku80 and DNA-PKcs are able to bind pADPr [23]. PARP-1's PARylation of Ku leads to a decreased binding to DSBs [92]. Moreover, several studies implicated PARP-1 functionally in NHEJ: PARP-1 and Ku80, both being highly abundant in the cell, have been shown to compete for free DNA ends in vitro presumably through two distinct NHEJ pathways. Whereas the Ku complex is one of the key factors for the classical NHEJ pathway, PARP-1 seems to also interact with ligase III in the backup pathway [93–95].

5 Regulation of the DNA DSB Repair Pathway Choice (I Suggest to Rephrase this Title): Collaboration or Competition?

Several factors are channeling the DSB repair pathway choice between NHEJ and HR. It is generally accepted that the cell-cycle phase is one of them. Early studies in vertebrates showed that NHEJ-deficient *scid* (carrying a loss-of-function mutation in DNA-PKcs) cells and *Ku70*$^{-/-}$ chicken DT40 cells were hypersensitive to IR only in G1 and early S-phase whereas HR-defective Rad54$^{-/-}$ cells were IR sensitive in late S/G2 phase [96]. The Cdk1 kinase has recently been shown to have control over the key recombination steps giving an elegant explanation for the fluctuating HR efficiency throughout the cell cycle [97]. Being at the same time one of the main engines for the cell cycle, Cdk1 would be an excellent tool to control the DSB repair pathway choice. Indeed a recent publication suggests that HR and NHEJ are oppositely affected by Cdk1 activity: Whereas HR is activated, NHEJ seems to be repressed [98]. Moreover the level of several critical HR proteins (BRCA1, Rad51/52) has been shown to increase from S to G2 phase and that steps of HR are activated by CDKs [99] suggesting another potential for regulating the pathway choice through the level of proteins expressed for the corresponding pathway. A similar observation has been made for the protein level of DNA-PK [100].

The nature of the DNA lesion plays an additional role to the choice of DSB repair pathway: RAG-mediated DSBs during V(D)J-recombination are certainly repaired through NHEJ [101] whereas Spo11-mediated DSBs generated during meiosis for instance will be repaired by HR [102]. Besides the key players in HR and NHEJ it has recently been shown that ~ 15–20% of ionizing irradiation induced foci (IRIF) require additional proteins, such as ATM, Artemis, the MRN-complex, γ-H2AX, 53BP1, MDC1 and RNF8, RNF168 for repair, some of them being implicated in both DSB repair pathways [103]. As an example, 53BP1 has been implicated in NHEJ [104] whereas 53BP1 deficiency rescues HR in a BRCA1 deficient background by a mechanism dependent on ATM-mediated resection. Interestingly, loss of 53BP1 does not complement the loss of BRCA2, which might be explained by genetic studies that put BRCA2 more downstream in HR in a process following end-resection [105, 106].

Moreover, the complexity of chromatin may influence repair pathway choice as it has recently been shown that X-ray induced DSBs located in close proximity to heterochromatin predominantly use HR for repair [107]. Especially the distance of ionizing radiation-induced foci to heterochromatin and the ATM-dependent phosphorylation of Kap-1 which promotes chromatin relaxation seem to somehow affect repair [108].

An important regulatory step involved in pathway choice is the process of DSB resection, comprising the 5′- to-3′ nucleolytic processing of DNA ends by the MRN complex in conjunction with auxiliary factors including CtIP, RECQ helicases, Exo1 and DNA2, being necessary for HR but not for NHEJ. An observation suggesting that competition exists between the two major DSB repair pathways is given by the fact that NHEJ mutants (e.g. Ku70 deficient cells) that have enhanced end resection show increased HR whereas mutants with decreased end resection (e.g., Sae2/CtlP) have increased NHEJ. Possibly, since Ku70 binds DNA ends, it thereby prevents the initial step of HR, the end resection. Surprisingly, Ku depletion in chicken cells actually leads to an overall increased resistance to ionizing irradiation during late S/G2 phase which can be interpreted as Ku interfering with HR under normal conditions in the latter cell cycle phases [109]. Additionally, impairing DNA-PK from binding to a DSB end dramatically promotes the initiation step of HR [108]. Interestingly, from double mutant analysis for NHEJ and HR components it is suggested that the concomitant loss of a protein involved in HR and a protein involved in NHEJ results in a more severe phenotype than one would expect from loss of either single pathway [110], promoting rather collaboration of the two pathways.

Interestingly, in a study that highlighted rather competition than collaboration between the major DSB repair pathways it has been elegantly shown that PARP-1 is hyperactivated in BRCA2 deficient cells but this hyperactivation cannot be explained by an accumulation of DNA damage, which normally triggers PARP activity [111]. A new model has been suggested only very recently proposing that in a BRCA2 deficient background PARP-1 might prevent DSB repair through NHEJ, possibly by blocking DNA-PK and Artemis. By adding PARP inhibitors to HR deficient cells, error-prone NHEJ is promoted and the unrestricted NHEJ could then induce genomic instability and eventual lethality [112].

Notably, the opposite effect to PARP inhibition has been described for 53BP1 in a BRCA1 negative background: By depletion of 53BP1 ATM-dependent processing of DNA ends is restored which can generate single-stranded DNA which is competent for HR. Thus, the loss of 53BP1 in a BRCA1 negative cell can overcome PARP inhibitor sensitivity [106, 113].

6 Conclusions

To summarize, more than 40 years of research in the PARP- and pADPr fields have uncovered implications in various layers of the DNA damage response to DNA DSBs: The initial processes starting with sensing the DSB and signaling of the latter in order to recruit other repair proteins to the damage site implies PARP-1 and the polymer generated at the damage site. Furthermore, an automodification of the protein leads to its detachment from the DNA which guaranties access for other proteins but also enables another round of damage signaling [114]. Interestingly, the polymer generated at the damage site has an important impact on the local chromatin structure due to its largely negative charge. By disrupting the chromatin structure surrounding the damage site, access to the DNA is facilitated [4].

Besides PARPs implication in sensing and signaling of DNA damage and a role in BER, first lines of evidence have been given that even the choice for the DSB repair pathway is influenced by PARP-1, as the protein seems to block DNA-PK_{cs} and therewith classical NHEJ [112]. At the same time PARP-1 itself has been shown to be involved in the backup-pathway of NHEJ [95] as well as suppressing HR, indicated by an increase of RAD51 foci in a PARP-1 deficient background [64]. PARP-3 on the other hand seems to interact with APLF in NHEJ [12].

Taken together, PARPs are multifunctional regulators of the DNA damage response, expanding the current model of action for PARP inhibition in HR-deficient cancer cells. A mechanism called synthetic lethality explains the original model, meaning that two genetic lesions together lead to cell death whereas a defect in only one of these genes does not. In BRCA1- or BRCA2-deficient cancer cells for example where HR is hampered, the cytotoxic effect of PARP inhibitors has been originally suggested to be due to the cells inability to overcome SSBs by BER, which can further degenerate during replication to form DSBs. These DSBs can in healthy cells but not in HR-deficient cancer cells be repaired by HR [115] (Fig. 4a). This view was recently challenged, mostly because it was very difficult to detect increased SSBs after PARP inhibition [111]. The current view involves the aberrant activation of NHEJ, rather than inhibition of BER by PARP inhibitors in HR-deficient cells, leading to genomic instability and cell death [112] (Fig. 4b). Hence, even though PARP inhibitors have been put with widespread enthusiasm into clinical trials, the exact molecular effects are still debated and under investigation at the cellular level.

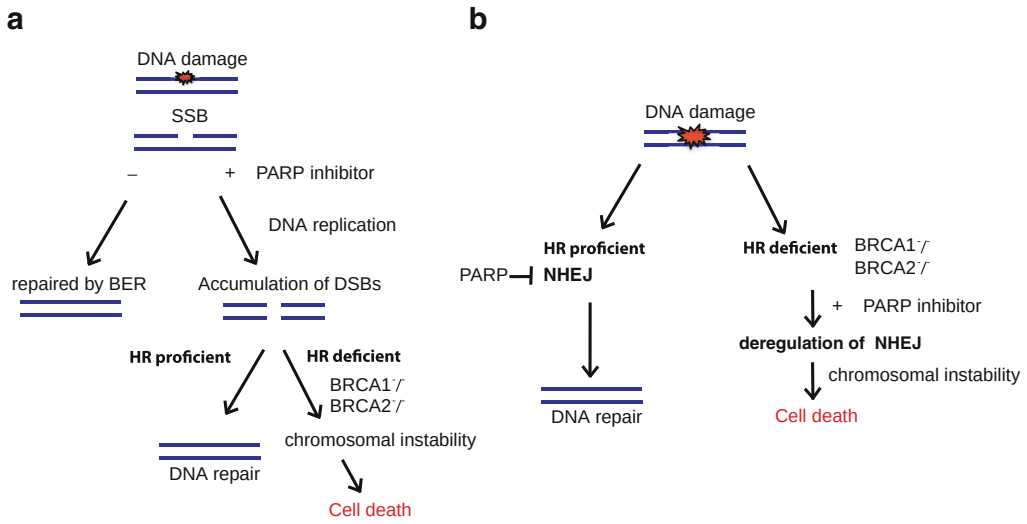

Fig. 4 Models explaining the lethality of HR-deficient cells with PARP inhibitors. (**a**) The synthetic lethality pathway model based on a deficiency in single-strand break repair. (**b**) Model based on error-prone NHEJ. Details are given in the text

How these inhibitors work in the appropriate clinical context still remains elusive. Hence, the PARP field awaits many scientific surprises with fundamental and clinical relevance.

Acknowledgments Research from the authors has been supported by the CIHR and the Cancer Research Society. G.P. is a Canada Research Chair in Proteomics and M.L. and J.-Y.M. are FRSQ Senior Investigators JK is a FQRNT scholar.

References

1. Moynahan ME, Jasin M (2010) Mitotic homologous recombination maintains genomic stability and suppresses tumorigenesis. Nat Rev Mol Cell Biol 11(3):196–207
2. Vilenchik MM, Knudson AG (2003) Endogenous DNA double-strand breaks: production, fidelity of repair, and induction of cancer. Proc Natl Acad Sci USA 100(22):12871–12876
3. Ciccia A, Elledge SJ (2010) The DNA damage response: making it safe to play with knives. Mol Cell 40(2):179–204
4. Krishnakumar R, Kraus WL (2010) The PARP side of the nucleus: molecular actions, physiological outcomes, and clinical targets. Mol Cell 39(1):8–24
5. Benjamin RC, Gill DM (1980) ADP-ribosylation in mammalian cell ghosts. Dependence of poly(ADP-ribose) synthesis on strand breakage in DNA. J Biol Chem 255(21):10493–10501
6. Hottiger MO, Hassa PO, Luscher B, Schuler H, Koch-Nolte F (2010) Toward a unified nomenclature for mammalian ADP-ribosyltransferases. Trends Biochem Sci 35(4):208–219
7. D'Amours D, Desnoyers S, D'Silva I, Poirier GG (1999) Poly(ADP-ribosyl)ation reactions in the regulation of nuclear functions. Biochem J 342(Pt 2):249–268
8. Krishnakumar R, Gamble MJ, Frizzell KM, Berrocal JG, Kininis M, Kraus WL (2008) Reciprocal binding of PARP-1 and histone H1 at promoters specifies transcriptional outcomes. Science 319(5864):819–821

9. Caiafa P, Guastafierro T, Zampieri M (2009) Epigenetics: poly(ADP-ribosyl)ation of PARP-1 regulates genomic methylation patterns. FASEB J 23(3):672–678
10. Heeres JT, Hergenrother PJ (2007) Poly(ADP-ribose) makes a date with death. Curr Opin Chem Biol 11(6):644–653
11. Chambon P, Weill JD, Mandel P (1963) Nicotinamide mononucleotide activation of new DNA-dependent polyadenylic acid synthesizing nuclear enzyme. Biochem Biophys Res Commun 11:39–43
12. Rulten SL, Fisher AE, Robert I, Zuma MC, Rouleau M, Ju L, Poirier G, Reina-San-Martin B, Caldecott KW (2011) PARP-3 and APLF function together to accelerate nonhomologous end-joining. Mol Cell 41(1):33–45
13. Menissier de Murcia J, Ricoul M, Tartier L, Niedergang C, Huber A, Dantzer F, Schreiber V, Ame JC, Dierich A, LeMeur M et al (2003) Functional interaction between PARP-1 and PARP-2 in chromosome stability and embryonic development in mouse. EMBO J 22(9):2255–2263
14. de Murcia JM, Niedergang C, Trucco C, Ricoul M, Dutrillaux B, Mark M, Oliver FJ, Masson M, Dierich A, LeMeur M et al (1997) Requirement of poly(ADP-ribose) polymerase in recovery from DNA damage in mice and in cells. Proc Natl Acad Sci USA 94(14):7303–7307
15. Masutani M, Nozaki T, Nishiyama E, Shimokawa T, Tachi Y, Suzuki H, Nakagama H, Wakabayashi K, Sugimura T (1999) Function of poly(ADP-ribose) polymerase in response to DNA damage: gene-disruption study in mice. Mol Cell Biochem 193(1–2):149–152
16. Langelier MF, Servent KM, Rogers EE, Pascal JM (2008) A third zinc-binding domain of human poly(ADP-ribose) polymerase-1 coordinates DNA-dependent enzyme activation. J Biol Chem 283(7):4105–4114
17. Langelier MF, Ruhl DD, Planck JL, Kraus WL, Pascal JM (2010) The Zn3 domain of human poly(ADP-ribose) polymerase-1 (PARP-1) functions in both DNA-dependent poly(ADP-ribose) synthesis activity and chromatin compaction. J Biol Chem 285(24):18877–18887
18. Hassa PO, Hottiger MO (2008) The diverse biological roles of mammalian PARPS, a small but powerful family of poly-ADP-ribose polymerases. Front Biosci 13:3046–3082
19. Altmeyer M, Messner S, Hassa PO, Fey M, Hottiger MO (2009) Molecular mechanism of poly(ADP-ribosyl)ation by PARP1 and identification of lysine residues as ADP-ribose acceptor sites. Nucleic Acids Res 37(11):3723–3738
20. Haenni SS, Hassa PO, Altmeyer M, Fey M, Imhof R, Hottiger MO (2008) Identification of lysines 36 and 37 of PARP-2 as targets for acetylation and auto-ADP-ribosylation. Int J Biochem Cell Biol 40(10):2274–2283
21. Kanai M, Hanashiro K, Kim SH, Hanai S, Boulares AH, Miwa M, Fukasawa K (2007) Inhibition of Crm1-p53 interaction and nuclear export of p53 by poly(ADP-ribosyl)ation. Nat Cell Biol 9(10):1175–1183
22. Pleschke JM, Kleczkowska HE, Strohm M, Althaus FR (2000) Poly(ADP-ribose) binds to specific domains in DNA damage checkpoint proteins. J Biol Chem 275(52):40974–40980
23. Gagne JP, Isabelle M, Lo KS, Bourassa S, Hendzel MJ, Dawson VL, Dawson TM, Poirier GG (2008) Proteome-wide identification of poly(ADP-ribose) binding proteins and poly(ADP-ribose)-associated protein complexes. Nucleic Acids Res 36(22):6959–6976
24. Kleine H, Luscher B (2009) Learning how to read ADP-ribosylation. Cell 139(1):17–19
25. Zhang Y, Liu S, Mickanin C, Feng Y, Charlat O, Michaud GA, Schirle M, Shi X, Hild M, Al B et al (2011) RNF146 is a poly(ADP-ribose)-directed E3 ligase that regulates axin degradation and Wnt signalling. Nat Cell Biol 13(5):623–629
26. Andrabi SA, Kang HC, Haince JF, Lee YI, Zhang J, Chi Z, West AB, Koehler RC, Poirier GG, Dawson TM et al (2011) Iduna protects the brain from glutamate excitotoxicity and stroke by interfering with poly(ADP-ribose) polymer-induced cell death. Nat Med 17(6):692–699
27. Schreiber V, Dantzer F, Ame JC, de Murcia G (2006) Poly(ADP-ribose): novel functions for an old molecule. Nat Rev Mol Cell Biol 7(7):517–528
28. Meyer-Ficca ML, Meyer RG, Coyle DL, Jacobson EL, Jacobson MK (2004) Human poly(ADP-ribose) glycohydrolase is expressed in alternative splice variants yielding isoforms that localize to different cell compartments. Exp Cell Res 297(2):521–532

29. Oka S, Kato J, Moss J (2006) Identification and characterization of a mammalian 39-kDa poly(ADP-ribose) glycohydrolase. J Biol Chem 281(2):705–713
30. David KK, Andrabi SA, Dawson TM, Dawson VL (2009) Parthanatos, a messenger of death. Front Biosci 14:1116–1128
31. Poirier GG, de Murcia G, Jongstra-Bilen J, Niedergang C, Mandel P (1982) Poly(ADP-ribosyl)ation of polynucleosomes causes relaxation of chromatin structure. Proc Natl Acad Sci USA 79(11):3423–3427
32. Mathis G, Althaus FR (1987) Release of core DNA from nucleosomal core particles following (ADP-ribose)n-modification in vitro. Biochem Biophys Res Commun 143(3):1049–1054
33. Huletsky A, de Murcia G, Muller S, Hengartner M, Menard L, Lamarre D, Poirier GG (1989) The effect of poly(ADP-ribosyl)ation on native and H1-depleted chromatin. A role of poly(ADP-ribosyl)ation on core nucleosome structure. J Biol Chem 264(15):8878–8886
34. Haince JF, McDonald D, Rodrigue A, Dery U, Masson JY, Hendzel MJ, Poirier GG (2008) PARP1-dependent kinetics of recruitment of MRE11 and NBS1 proteins to multiple DNA damage sites. J Biol Chem 283(2):1197–1208
35. Durkacz BW, Omidiji O, Gray DA, Shall S (1980) (ADP-ribose)n participates in DNA excision repair. Nature 283(5747):593–596
36. Allinson SL, Dianova II, Dianov GL (2003) Poly(ADP-ribose) polymerase in base excision repair: always engaged, but not essential for DNA damage processing. Acta Biochim Pol 50(1):169–179
37. Petermann E, Keil C, Oei SL (2005) Importance of poly(ADP-ribose) polymerases in the regulation of DNA-dependent processes. Cell Mol Life Sci 62(7–8):731–738
38. Bryant HE, Schultz N, Thomas HD, Parker KM, Flower D, Lopez E, Kyle S, Meuth M, Curtin NJ, Helleday T (2005) Specific killing of BRCA2-deficient tumours with inhibitors of poly(ADP-ribose) polymerase. Nature 434(7035):913–917
39. Farmer H, McCabe N, Lord CJ, Tutt AN, Johnson DA, Richardson TB, Santarosa M, Dillon KJ, Hickson I, Knights C et al (2005) Targeting the DNA repair defect in BRCA mutant cells as a therapeutic strategy. Nature 434(7035):917–21
40. Strom CE, Johansson F, Uhlen M, Al-Khalili Szigyarto C, Erixon K, Helleday T (2011) Poly (ADP-ribose) polymerase (PARP) is not involved in base excision repair but PARP inhibition traps a single-strand intermediate. Nucleic Acids Res 39(8):3166–3175
41. Pachkowski BF, Tano K, Afonin V, Elder RH, Takeda S, Watanabe M, Swenberg JA, Nakamura J (2009) Cells deficient in PARP-1 show an accelerated accumulation of DNA single strand breaks, but not AP sites, over the PARP-1-proficient cells exposed to MMS. Mutat Res 671(1–2):93–99
42. Leppard JB, Dong Z, Mackey ZB, Tomkinson AE (2003) Physical and functional interaction between DNA ligase IIIalpha and poly(ADP-Ribose) polymerase 1 in DNA single-strand break repair. Mol Cell Biol 23(16):5919–5927
43. El-Khamisy SF, Masutani M, Suzuki H, Caldecott KW (2003) A requirement for PARP-1 for the assembly or stability of XRCC1 nuclear foci at sites of oxidative DNA damage. Nucleic Acids Res 31(19):5526–5533
44. Prasad R, Lavrik OI, Kim SJ, Kedar P, Yang XP, Vande Berg BJ, Wilson SH (2001) DNA polymerase beta -mediated long patch base excision repair. Poly(ADP-ribose)polymerase-1 stimulates strand displacement DNA synthesis. J Biol Chem 276(35):32411–32414
45. Rouleau M, Aubin RA, Poirier GG (2004) Poly(ADP-ribosyl)ated chromatin domains: access granted. J Cell Sci 117(Pt 6):815–825
46. Schreiber V, Ame JC, Dolle P, Schultz I, Rinaldi B, Fraulob V, Menissier-de Murcia J, de Murcia G (2002) Poly(ADP-ribose) polymerase-2 (PARP-2) is required for efficient base excision DNA repair in association with PARP-1 and XRCC1. J Biol Chem 277(25): 23028–23036
47. Bowman KJ, Newell DR, Calvert AH, Curtin NJ (2001) Differential effects of the poly (ADP-ribose) polymerase (PARP) inhibitor NU1025 on topoisomerase I and II inhibitor cytotoxicity in L1210 cells in vitro. Br J Cancer 84(1):106–112

48. Hochegger H, Dejsuphong D, Fukushima T, Morrison C, Sonoda E, Schreiber V, Zhao GY, Saberi A, Masutani M, Adachi N et al (2006) Parp-1 protects homologous recombination from interference by Ku and Ligase IV in vertebrate cells. EMBO J 25(6):1305–1314
49. Pommier Y, Redon C, Rao VA, Seiler JA, Sordet O, Takemura H, Antony S, Meng L, Liao Z, Kohlhagen G et al (2003) Repair of and checkpoint response to topoisomerase I-mediated DNA damage. Mutat Res 532(1–2):173–203
50. Aguilera A, Gomez-Gonzalez B (2008) Genome instability: a mechanistic view of its causes and consequences. Nat Rev Genet 9(3):204–217
51. Takata M, Sasaki MS, Sonoda E, Morrison C, Hashimoto M, Utsumi H, Yamaguchi-Iwai Y, Shinohara A, Takeda S (1998) Homologous recombination and non-homologous end-joining pathways of DNA double-strand break repair have overlapping roles in the maintenance of chromosomal integrity in vertebrate cells. EMBO J 17:5497–5508
52. Rodrigue A, Lafrance M, Gauthier MC, McDonald D, Hendzel M, West SC, Jasin M, Masson JY (2006) Interplay between human DNA repair proteins at a unique double-strand break in vivo. EMBO J 25(1):222–231
53. Nimonkar AV, Genschel J, Kinoshita E, Polaczek P, Campbell JL, Wyman C, Modrich P, Kowalczykowski SC (2011) BLM-DNA2-RPA-MRN and EXO1-BLM-RPA-MRN constitute two DNA end resection machineries for human DNA break repair. Genes Dev 25(4):350–362
54. Sartori AA, Lukas C, Coates J, Mistrik M, Fu S, Bartek J, Baer R, Lukas J, Jackson SP (2007) Human CtIP promotes DNA end resection. Nature 450(7169):509–514
55. Nicolette ML, Lee K, Guo Z, Rani M, Chow JM, Lee SE, Paull TT (2010) Mre11-Rad50-Xrs2 and Sae2 promote 5′ strand resection of DNA double-strand breaks. Nat Struct Mol Biol 17(12):1478–1485
56. Sung P (2005) Mediating repair. Nat Struct Mol Biol 12(3):213–214
57. Buisson R, Dion-Cote AM, Coulombe Y, Launay H, Cai H, Stasiak AZ, Stasiak A, Xia B, Masson JY (2010) Cooperation of breast cancer proteins PALB2 and piccolo BRCA2 in stimulating homologous recombination. Nat Struct Mol Biol 17(10):1247–1254
58. Liu J, Doty T, Gibson B, Heyer WD (2010) Human BRCA2 protein promotes RAD51 filament formation on RPA-covered single-stranded DNA. Nat Struct Mol Biol 17(10):1260–1262
59. Moynahan ME, Chiu JW, Koller BH, Jasin M (1999) Brca1 controls homology-directed DNA repair. Mol Cell 4(4):511–518
60. Moynahan ME, Pierce AJ, Jasin M (2001) BRCA2 is required for homology-directed repair of chromosomal breaks. Mol Cell 7(2):263–272
61. Sy SM, Huen MS, Chen J (2009) PALB2 is an integral component of the BRCA complex required for homologous recombination repair. Proc Natl Acad Sci USA 106(17):7155–7160
62. Zhang F, Ma J, Wu J, Ye L, Cai H, Xia B, Yu X (2009) PALB2 links BRCA1 and BRCA2 in the DNA-damage response. Curr Biol 19(6):524–529
63. Yang H, Jeffrey PD, Miller J, Kinnucan E, Sun Y, Thoma NH, Zheng N, Chen PL, Lee WH, Pavletich NP (2002) BRCA2 function in DNA binding and recombination from a BRCA2-DSS1-ssDNA structure. Science 297(5588):1837–1848
64. Schultz N, Lopez E, Saleh-Gohari N, Helleday T (2003) Poly(ADP-ribose) polymerase (PARP-1) has a controlling role in homologous recombination. Nucleic Acids Res 31(17): 4959–4964
65. Claybon A, Karia B, Bruce C, Bishop AJ (2011) PARP1 suppresses homologous recombination events in mice in vivo. Nucleic Acids Res 38(21):7538–7545
66. Bryant HE, Petermann E, Schultz N, Jemth AS, Loseva O, Issaeva N, Johansson F, Fernandez S, McGlynn P, Helleday T (2009) PARP is activated at stalled forks to mediate Mre11-dependent replication restart and recombination. EMBO J 28(17):2601–2615
67. Mimitou EP, Symington LS (2009) Nucleases and helicases take center stage in homologous recombination. Trends Biochem Sci 34(5):264–272
68. Sugimura K, Takebayashi S, Taguchi H, Takeda S, Okumura K (2008) PARP-1 ensures regulation of replication fork progression by homologous recombination on damaged DNA. J Cell Biol 183(7):1203–1212

69. Lieber MR (2010) The mechanism of double-strand DNA break repair by the nonhomologous DNA end-joining pathway. Annu Rev Biochem 79:181–211
70. Ferguson DO, Alt FW (2001) DNA double strand break repair and chromosomal translocation: lessons from animal models. Oncogene 20(40):5572–5579
71. Ochi T, Sibanda BL, Wu Q, Chirgadze DY, Bolanos-Garcia VM, Blundell TL (2010) Structural biology of DNA repair: spatial organisation of the multicomponent complexes of nonhomologous end joining. J Nucleic Acids 2010:1–19. (doi:pii: 621695.)
72. Gottlieb TM, Jackson SP (1994) Protein kinases and DNA damage. Trends Biochem Sci 19(11):500–503
73. Yaneva M, Kowalewski T, Lieber MR (1997) Interaction of DNA-dependent protein kinase with DNA and with Ku: biochemical and atomic-force microscopy studies. EMBO J 16(16): 5098–5112
74. Meek K, Dang V, Lees-Miller SP (2008) DNA-PK: the means to justify the ends? Adv Immunol 99:33–58
75. Uematsu N, Weterings E, Yano K, Morotomi-Yano K, Jakob B, Taucher-Scholz G, Mari PO, van Gent DC, Chen BP, Chen DJ (2007) Autophosphorylation of DNA-PKCS regulates its dynamics at DNA double-strand breaks. J Cell Biol 177(2):219–229
76. Pawelczak KS, Turchi JJ (2010) Purification and characterization of exonuclease-free Artemis: Implications for DNA-PK-dependent processing of DNA termini in NHEJ-catalyzed DSB repair. DNA Repair (Amst) 9(6):670–677
77. Gu J, Li S, Zhang X, Wang LC, Niewolik D, Schwarz K, Legerski RJ, Zandi E, Lieber MR (2010) DNA-PKcs regulates a single-stranded DNA endonuclease activity of Artemis. DNA Repair (Amst) 9(4):429–437
78. Wang J, Pluth JM, Cooper PK, Cowan MJ, Chen DJ, Yannone SM (2005) Artemis deficiency confers a DNA double-strand break repair defect and Artemis phosphorylation status is altered by DNA damage and cell cycle progression. DNA Repair (Amst) 4(5):556–570
79. Chappell C, Hanakahi LA, Karimi-Busheri F, Weinfeld M, West SC (2002) Involvement of human polynucleotide kinase in double-strand break repair by non-homologous end joining. EMBO J 21(11):2827–2832
80. Mahaney BL, Meek K, Lees-Miller SP (2009) Repair of ionizing radiation-induced DNA double-strand breaks by non-homologous end-joining. Biochem J 417(3):639–650
81. Capp JP, Boudsocq F, Bertrand P, Laroche-Clary A, Pourquier P, Lopez BS, Cazaux C, Hoffmann JS, Canitrot Y (2006) The DNA polymerase lambda is required for the repair of non-compatible DNA double strand breaks by NHEJ in mammalian cells. Nucleic Acids Res 34(10):2998–3007
82. Capp JP, Boudsocq F, Besnard AG, Lopez BS, Cazaux C, Hoffmann JS, Canitrot Y (2007) Involvement of DNA polymerase mu in the repair of a specific subset of DNA double-strand breaks in mammalian cells. Nucleic Acids Res 35(11):3551–3560
83. Covo S, Blanco L, Livneh Z (2004) Lesion bypass by human DNA polymerase mu reveals a template-dependent, sequence-independent nucleotidyl transferase activity. J Biol Chem 279(2):859–865
84. Ahnesorg P, Smith P, Jackson SP (2006) XLF interacts with the XRCC4-DNA ligase IV complex to promote DNA nonhomologous end-joining. Cell 124(2):301–313
85. Deshpande RA, Wilson TE (2007) Modes of interaction among yeast Nej1, Lif1 and Dnl4 proteins and comparison to human XLF, XRCC4 and Lig4. DNA Repair (Amst) 6(10):1507–1516
86. Bennardo N, Cheng A, Huang N, Stark JM (2008) Alternative-NHEJ is a mechanistically distinct pathway of mammalian chromosome break repair. PLoS Genet 4(6):e1000110
87. Simsek D, Jasin M (2010) Alternative end-joining is suppressed by the canonical NHEJ component Xrcc4-ligase IV during chromosomal translocation formation. Nat Struct Mol Biol 17(4):410–416
88. Daley JM, Palmbos PL, Wu D, Wilson TE (2005) Nonhomologous end joining in yeast. Annu Rev Genet 39:431–451
89. Xie A, Kwok A, Scully R (2009) Role of mammalian Mre11 in classical and alternative nonhomologous end joining. Nat Struct Mol Biol 16(8):814–818

90. Koch CA, Agyei R, Galicia S, Metalnikov P, O'Donnell P, Starostine A, Weinfeld M, Durocher D (2004) Xrcc4 physically links DNA end processing by polynucleotide kinase to DNA ligation by DNA ligase IV. EMBO J 23(19):3874–3885
91. D'Silva I, Pelletier JD, Lagueux J, D'Amours D, Chaudhry MA, Weinfeld M, Lees-Miller SP, Poirier GG (1999) Relative affinities of poly(ADP-ribose) polymerase and DNA-dependent protein kinase for DNA strand interruptions. Biochim Biophys Acta 1430(1):119–126
92. Li B, Navarro S, Kasahara N, Comai L (2004) Identification and biochemical characterization of a Werner's syndrome protein complex with Ku70/80 and poly(ADP-ribose) polymerase-1. J Biol Chem 279(14):13659–13667
93. Wang M, Wu W, Rosidi B, Zhang L, Wang H, Iliakis G (2006) PARP-1 and Ku compete for repair of DNA double strand breaks by distinct NHEJ pathways. Nucleic Acids Res 34(21):6170–6182
94. Audebert M, Salles B, Calsou P (2004) Involvement of poly(ADP-ribose) polymerase-1 and XRCC1/DNA ligase III in an alternative route for DNA double-strand breaks rejoining. J Biol Chem 279(53):55117–55126
95. Mansour WY, Rhein T, Dahm-Daphi J (2010) The alternative end-joining pathway for repair of DNA double-strand breaks requires PARP1 but is not dependent upon microhomologies. Nucleic Acids Res 38(18):6065–6077
96. Lee SE, Mitchell RA, Cheng A, Hendrickson EA (1997) Evidence for DNA-PK-dependent and -independent DNA double-strand break repair pathways in mammalian cells as a function of the cell cycle. Mol Cell Biol 17(3):1425–1433
97. Ira G, Pellicioli A, Balijja A, Wang X, Fiorani S, Carotenuto W, Liberi G, Bressan D, Wan L, Hollingsworth NM et al (2004) DNA end resection, homologous recombination and DNA damage checkpoint activation require CDK1. Nature 431(7011):1011–1017
98. Zhang Y, Shim EY, Davis M, Lee SE (2009) Regulation of repair choice: Cdk1 suppresses recruitment of end joining factors at DNA breaks. DNA Repair (Amst) 8(10):1235–1241
99. Shrivastav M, De Haro LP, Nickoloff JA (2008) Regulation of DNA double-strand break repair pathway choice. Cell Res 18(1):134–147
100. Koike M, Awaji T, Kataoka M, Tsujimoto G, Kartasova T, Koike A, Shiomi T (1999) Differential subcellular localization of DNA-dependent protein kinase components Ku and DNA-PKcs during mitosis. J Cell Sci 112(Pt 22):4031–4039
101. Soulas-Sprauel P, Rivera-Munoz P, Malivert L, Le Guyader G, Abramowski V, Revy P, de Villartay JP (2007) V(D)J and immunoglobulin class switch recombinations: a paradigm to study the regulation of DNA end-joining. Oncogene 26(56):7780–7791
102. Cole F, Keeney S, Jasin M (2010) Evolutionary conservation of meiotic DSB proteins: more than just Spo11. Genes Dev 24(12):1201–1207
103. Riballo E, Kuhne M, Rief N, Doherty A, Smith GC, Recio MJ, Reis C, Dahm K, Fricke A, Krempler A et al (2004) A pathway of double-strand break rejoining dependent upon ATM, Artemis, and proteins locating to gamma-H2AX foci. Mol Cell 16(5):715–724
104. Nakamura K, Sakai W, Kawamoto T, Bree RT, Lowndes NF, Takeda S, Taniguchi Y (2006) Genetic dissection of vertebrate 53BP1: a major role in non-homologous end joining of DNA double strand breaks. DNA Repair (Amst) 5(6):741–749
105. Bouwman P, Aly A, Escandell JM, Pieterse M, Bartkova J, van der Gulden H, Hiddingh S, Thanasoula M, Kulkarni A, Yang Q et al (2010) 53BP1 loss rescues BRCA1 deficiency and is associated with triple-negative and BRCA-mutated breast cancers. Nat Struct Mol Biol 17(6):688–695
106. Bunting SF, Callen E, Wong N, Chen HT, Polato F, Gunn A, Bothmer A, Feldhahn N, Fernandez-Capetillo O, Cao L et al (2010) 53BP1 inhibits homologous recombination in Brca1-deficient cells by blocking resection of DNA breaks. Cell 141(2):243–254
107. Beucher A, Birraux J, Tchouandong L, Barton O, Shibata A, Conrad S, Goodarzi AA, Krempler A, Jeggo PA, Lobrich M (2009) ATM and Artemis promote homologous recombination of radiation-induced DNA double-strand breaks in G2. EMBO J 28(21):3413–3427
108. Shibata A, Conrad S, Birraux J, Geuting V, Barton O, Ismail A, Kakarougkas A, Meek K, Taucher-Scholz G, Lobrich M et al (2011) Factors determining DNA double-strand break repair pathway choice in G2 phase. EMBO J 30(6):1079–1092

109. Fukushima T, Takata M, Morrison C, Araki R, Fujimori A, Abe M, Tatsumi K, Jasin M, Dhar PK, Sonoda E et al (2001) Genetic analysis of the DNA-dependent protein kinase reveals an inhibitory role of Ku in late S-G2 phase DNA double-strand break repair. J Biol Chem 276(48):44413–44418
110. Mills KD, Ferguson DO, Essers J, Eckersdorff M, Kanaar R, Alt FW (2004) Rad54 and DNA Ligase IV cooperate to maintain mammalian chromatid stability. Genes Dev 18(11):1283–1292
111. Gottipati P, Vischioni B, Schultz N, Solomons J, Bryant HE, Djureinovic T, Issaeva N, Sleeth K, Sharma RA, Helleday T (2010) Poly(ADP-ribose) polymerase is hyperactivated in homologous recombination-defective cells. Cancer Res 70(13):5389–5398
112. Patel AG, Sarkaria JN, Kaufmann SH (2011) Nonhomologous end joining drives poly(ADP-ribose) polymerase (PARP) inhibitor lethality in homologous recombination-deficient cells. Proc Natl Acad Sci USA 108(8):3406–3411
113. Kass EM, Moynahan ME, Jasin M (2010) Loss of 53BP1 is a gain for BRCA1 mutant cells. Cancer Cell 17(5):423–425
114. Mortusewicz O, Ame JC, Schreiber V, Leonhardt H (2007) Feedback-regulated poly(ADP-ribosyl)ation by PARP-1 is required for rapid response to DNA damage in living cells. Nucleic Acids Res 35(22):7665–7675
115. Aly A, Ganesan S (2011) BRCA1, PARP, and 53BP1: conditional synthetic lethality and synthetic viability. J Mol Cell Biol 3(1):66–74

Video Article

GST-His purification: A Two-step Affinity Purification Protocol Yielding Full-length Purified Proteins

Ranjan Maity*[1], Joris Pauty*[1], Jana Krietsch*[1], Rémi Buisson[1], Marie-Michelle Genois[1], Jean-Yves Masson[1]

[1]Genome Stability Laboratory, Oncology Axis, Hôtel-Dieu de Québec

*These authors contributed equally

Correspondence to: Jean-Yves Masson at Jean-Yves.Masson@crhdq.ulaval.ca

URL: http://www.jove.com/video/50320
DOI: doi:10.3791/50320

Keywords: Biochemistry, Issue 80, Genetics, Molecular Biology, Proteins, Proteomics, recombinant protein, affinity purification, Glutathione Sepharose Tag, Talon metal affinity resin

Date Published: 10/29/2013

Citation: Maity, R., Pauty, J., Krietsch, J., Buisson, R., Genois, M.M., Masson, J.Y. GST-His purification: A Two-step Affinity Purification Protocol Yielding Full-length Purified Proteins. *J. Vis. Exp.* (80), e50320, doi:10.3791/50320 (2013).

Abstract

Key assays in enzymology for the biochemical characterization of proteins *in vitro* necessitate high concentrations of the purified protein of interest. Protein purification protocols should combine efficiency, simplicity and cost effectiveness[1]. Here, we describe the GST-His method as a new small-scale affinity purification system for recombinant proteins, based on a N-terminal Glutathione Sepharose Tag (GST)[2,3] and a C-terminal 10xHis tag[4], which are both fused to the protein of interest. The latter construct is used to generate baculoviruses, for infection of Sf9 infected cells for protein expression[5]. GST is a rather long tag (29 kDa) which serves to ensure purification efficiency. However, it might influence physiological properties of the protein. Hence, it is subsequently cleaved off the protein using the PreScission enzyme[6]. In order to ensure maximum purity and to remove the cleaved GST, we added a second affinity purification step based on the comparatively small His-Tag. Importantly, our technique is based on two different tags flanking the two ends of the protein, which is an efficient tool to remove degraded proteins and, therefore, enriches full-length proteins. The method presented here does not require an expensive instrumental setup, such as FPLC. Additionally, we incorporated $MgCl_2$ and ATP washes to remove heat shock protein impurities and nuclease treatment to abolish contaminating nucleic acids. In summary, the combination of two different tags flanking the N- and the C-terminal and the capability to cleave off one of the tags, guaranties the recovery of a highly purified and full-length protein of interest.

Video Link

The video component of this article can be found at http://www.jove.com/video/50320/

Introduction

The purification of recombinant proteins is crucial to address fundamental questions in biochemistry. Conventional ways of protein purification like ion exchange chromatography and size exclusion chromatography rely on physical properties of the target protein such as its isoelectric point and charge or size, respectively. The latter protein characteristics are shared by a variety of proteins, which increases considerably the chance of contaminating proteins in conventional protein purification strategies. This problem may be circumvented with the use of multiple purification columns, which is time consuming. At the same time, the latter chromatography methods demand expensive experimental setup. Affinity-tag purification strongly increases target-specificity, as in most of the cases the tag will be unique to the protein of interest. In recent studies, Flag- or HA-affinity purification has been widely used.

In contrast to existing recombinant protein purification protocols in which single tags are used, we established the unique combination of two tags. Our method involves the fusion of a GST-tag at the N-terminus and a His-tag at the C-terminus of the protein of interest, for an optimal ratio between quantity and purity of the desired protein. The GST is a long tag (29 kDa), which is highly efficient for purification on glutathione Sepharose beads. Furthermore, using GST guarantees cost-effectiveness of our method[1]. The possibility to cleave off the GST with the PreScission enzyme (with recognition sequence LeuGluValLeuPheGln/GlyPro, resulting in the addition of only two amino acids) has many advantages, for instance, this strategy avoids alterations of the physiological protein functions due to allosteric hindrance. The small His-tag fused to the other protein extremity serves in a second purification step to increase protein purity by washing off the cleaved GST, as well as degraded proteins and other contaminants. Additionally, the protocol does not require a dialysis step when switching from the GST to the His-purification step column (TALON resin). Common contaminants in such purification processes are Heat Shock Proteins (HSP). The addition of an incubation step with $MgCl_2$ and ATP allows the removal of these contaminants (**Figure 1**).

Fast Protein Liquid Chromatography (FPLC) and High Performance Liquid Chromatography (HPLC) are common techniques that depend on expensive instrumentation to generate high yield of the purified protein of interest. The batch purification protocol we present here, in contrast, is manual and does not require an expensive instrumental setup. A high yield of protein can be reached by scaling up the protocol. At the same

time, with the batch purification protocol, the elution volume can be adjusted in order to enhance protein concentration, which is not given with FPLC or HPLC.

Also, with the batch GST-His purification protocol, proteins with a size-range of ~10-300 kDa can be purified. One of the biggest advantages is given by the fact that one can purify several proteins at the same time, for instance, both a wild-type and its mutant protein. The success of the presented protocol solely depends on the expression level and solubility of the protein of interest.

Protocol

1. Production of Recombinant Baculovirus

Baculoviruses are generated using the Bac-to-Bac Baculovirus Expression System of Invitrogen mainly in accordance with the manufacturer's protocol with only slight modifications:

1. A modified pFastBac1 vector (Gibco, life) was created containing the GST and His-tags (**Figure 2**). The MultiCloning Site (MCS) of a pET-52b(+) vector (Novagen), containing a 10xHis-tag, was inserted into the MCS of a pFastBac1 vector to generate pFastBac1-Strep-10xHis. The pET-52b(+) MCS sequence was PCR amplified between the XbaI and BlpI restriction sites, adding a BglII restriction site at the 5' extremity and a HindIII restriction site at the 3' extremity. The PCR product was then cloned between BamHI and HindIII restriction site of pFastBac1, using the compatibility of BamHI and BglII restriction sequences. Since the aim was to generate a pFastBac1 allowing the expression of recombinant protein with streptavidin- and 10xHis-tags, the BamHI restriction site of the pET-52b(+) MCS sequence was not used. Also, the XbaI restriction site was not used to avoid the redundancy of restriction sites occurring between the sites already in the MCS of pFastBac1 and these inserted with the MCS of pET-52b(+). The GST coding sequence with the PreScission Protease recognition site (LeuGluValLeuPheGln/GlyPro) was then inserted into pFastBac1-Strep-10xHis. The GST cDNA sequence from pGEX-6P-2 (GE Healthcare) was PCR amplified with primers containing NcoI and KpnI restriction sites at the 5' and 3' extremities, respectively. The NcoI site allows the addition of a start codon but also an Alanine to the GST. The PCR product was then cloned into pFastBac1-Strep-10xHis between the NcoI and KpnI restriction sites, resulting in the deletion of the Streptavidin-tag. The new fusion vector thus obtained was named pFastBac1-GST-10xHis.
2. Clone the cDNA coding for the protein of interest into the pFastBac-GST-10xHis vector between the GST (N-terminal) and the His-tag (C-terminal). Be careful to remove the cDNA stop codon to allow the fusion with the C-terminal His-tag.
3. Transform *E. coli* DH10Bac with the recombinant pFastBac (obtained in step 1.2) to generate the bacmid. Allow colonies to grow overnight at 37 °C and several hours at 30 °C on selection plates containing Bluo-gal and IPTG (10 µg/ml tetracyclin, 50 µg/ml kanamycin, 7 µg/ml gentamycin, 100 µg/ml Bluo-Gal, 40 µg/ml IPTG).
4. Pick and restreak 2 white colonies (from step 1.3) on selection plates to confirm the white phenotype.
5. Inoculate 2 ml of LB containing 10 µg/ml tetracyclin, 50 µg/ml kanamycin, 10 µg/ml gentamycin with the two white colonies from step 1.4 and let them grow overnight under agitation (250 rpm) at 37 °C.
6. In order to purify the bacmid DNA, pellet the bacteria from step 1.5, resuspend the cells in 300 µl of solution I and add 300 µl of solution II (Maxiprep kit from Qiagen). Incubate for 5 min at room temperature, add 300 µl of 3 M KOAc pH 5.5 and incubate for 10 min on ice. Centrifuge the samples at 4 °C, maximum speed for 10 min. Add 800 µl of isopropanol to the supernatants and incubate for 10 min on ice. Centrifuge the samples for 15 min at 4 °C and wash the pellet with 500 µl of 70% ethanol. Let the pellet dry and resuspend it under sterile conditions in 40 µl of Tris-EDTA pH 8.0. The bacmid DNA should be stored at 4 °C.
7. Generate baculoviruses as described in the manufacturer's protocol. Baculoviruses can be stored at 4 °C protected from light.

2. Recombinant Protein Expression

1. In order to choose the most efficient baculovirus for purification and to monitor what time the peak of protein expression is reached, perform a mini-infection assay as follows: Infect 2 x 10^7 of Sf9 infected cells cultured at 27 °C in Grace's media (complemented with 10% FBS and 1% P/S) with 133 µl (1/150) of baculovirus. Collect aliquots of 1.5 ml at 0, 24, 48, and 72 hr post-infection. Pellet the cells and analyze the expression level of the protein of interest by western blotting using anti-tag antibodies.
2. Use the most efficient baculovirus from step 2.1 to infect a spinner containing 1.0 x 10^6 Sf9 cells per ml in 500 ml of media with a ratio of 1/150 between virus and media. Let the infected cells grow in suspension at 27 °C and harvest the cells when the maximum protein expression (as determined in step 2.1 above) is reached. Pelleted cells can be stored at -80 °C until further usage.

3. Preparation of Soluble Cell Lysate

All of the following incubation steps are carried out at 4 °C under mild rotation.

1. Lyse Sf9 cells expressing your protein of interest in ~20 ml of GST binding buffer (150 mM NaCl, 1 mM EDTA, 0.05% Triton-X-100, 1 mM DTT in PBS1X for a final concentration of NaCl of 250 mM, and protease inhibitor cocktail (Roche). In an ice water bath, dounce the solution 20x with a dounce homogenizer, sonicate 3x 30 seconds each (70% output), and dounce again 20x.
2. (Optional). Incubate the total cell lysate with 1 mM $MgCl_2$ and benzonase® nuclease (2.5 U/ml) for 30 min at 4 °C to remove DNA or RNA contamination.
3. Centrifuge at 18,000 rpm for 30 min at 4 °C. Keep the supernatant.
4. (Optional). Centrifuge the supernatant again for 30 min at 18,000 rpm at 4 °C to get a clear soluble lysate. Pass the supernatant through a 0.2 or 0.45 µm filter to avoid clogging.

4. Binding of Protein on GST Beads

1. Incubate the soluble cell lysate with 1 ml of GST beads (prewashed two times with 10 ml of GST binding buffer) for 1 hr at 4 °C under gentle rotation.

Comment: The incubation time needs to be optimized according to the stability of the protein and binding efficiency.

2. Quick spin at 700 rpm and remove supernatant containing unbound proteins (this can be kept for further analysis). Wash the GST-bound proteins (**Figure 3B**, lane 1) with GST washing buffer (GST binding buffer with 350 mM NaCl final).
3. Repeat step 4.2 2x. At the last wash, remove as much supernatant as possible.
4. Incubate the beads with 5 mM ATP and 15 mM $MgCl_2$ (in 10 ml GST binding buffer) for 1 hr at 4 °C to avoid nonspecific binding of heat-shock proteins[8]. Wash the beads three times with GST washing buffer.

5. PreScission Cleavage of the GST

1. Centrifuge the GST beads, remove the supernatant and wash the GST beads with P5 buffer (50 mM $NaHPO_4$ pH 7.0, 500 mM NaCl, 10% glycerol, 0.05% Triton-X-100, 5 mM imidazole).
2. Incubate the GST-beads with PreScission enzyme in P5 buffer from 3 hr to overnight at 4 °C. (Divide the GST beads in fractions of 100 µl and add 4-8 units (2-4 µl) of enzyme diluted in 100 µl of P5 buffer).

Comment: The incubation time of the PreScission step needs to be optimized according to the molecular weight as well as the stability of the protein. If degradation is observed, this incubation time can be decreased to a minimum of 2 hr instead of overnight.

3. Quick spin and collect the supernatant. Repeat this step two times after adding 100 µl of P5 buffer to the beads and pool all fractions (**Figure 3B**, lane 2).

Comment: The remaining beads can be used for analysis of cleavage efficiency (**Figure 3B**, lane 3). Usually, 70-80% of the protein is cleaved.

6. Protein-binding to TALON Metal Affinity Resin

1. Divide the elution from above into 3 fractions of 1 ml and incubate each with 100 µl Talon metal affinity resin dry beads (prewashed two times with P5 buffer) for 1 hr under rotation.

Comment: Dividing the elution in several fractions increases binding/washes efficiency.

2. Wash the resin 5 min with P30 buffer (P5 buffer with a final concentration of 30 mM imidazole).
3. Repeat step 6.2 2x and pool the beads in a single tube. Before the last wash, remove as much supernatant as possible.

Comment: This corresponds to the TALON bound sample (**Figure 3B**, lane 4).

7. Elution of the Purified Protein

1. Incubate the protein bound TALON resin for 5 min under rotation with P500 buffer (P5 buffer with a final concentration of 500 mM imidazole). Use a ratio between buffer and beads of 1:1 v/v. (For example, if you had taken 200 µl of dry beads, you will have to add 200 µl of P500). Repeat this step two times and keep each eluted fraction separately (named elution 1 (E1), elution 2 (E2) and elution 3 (E3); **Figure 3B**, lanes 5-7).

Comment: The remaining beads can be used for analysis of elution efficiency (**Figure 3B**, lane 8). Typically, 60-80% of the protein is eluted in total.

2. Analyze the quantity and quality of your purified protein by loading approximately 20-40 µl of each fraction with a standard BSA concentration on a SDS-PAGE and stain with Coomassie blue (**Figure 3B**) or SYPRO protein stain for visualization.

Comment: The protein of interest can also be detected throughout the purification procedure using anti-GST and anti-His antibodies (**Figure 3C**).

8. Storage of the Purified Protein

1. Dialyze the purified protein against an appropriate storage buffer (*e.g.* 20 mM Tris Acetate pH 8.0, 200 mM KAc, 10% Glycerol, 1 mM EDTA, 0.5 mM DTT) at 4 °C. It is important to check for precipitation of the purified protein during the dialysis. We usually dialyze 2x for 1 hr at 4 °C under agitation rotation.
2. Make small aliquots of the purified protein (10-20 µl) and freeze on dry ice for 30 min. Store the aliquots at -80 °C and avoid many thaw/freezing cycles.

Representative Results

In order to illustrate the efficiency of the GST-His purification protocol, we purified Rec14, a *S. pombe* protein of 32.9 kDa. The Rec14 cDNA was cloned in our modified pFastBac1 vector allowing the additions of GST- and His-tags at the N- and C- termini, respectively (**Figure 1A**).

Recombinant baculovirus were then prepared and used to infect SF9 infected cells for protein expression. The soluble cell lysates were incubated with GST beads and bound-proteins were eluted by cleaving the GST with PreScission protease. The resulting Rec14-His protein was affinity purified on TALON resin and bound-proteins were eluted with TALON buffer containing 500 mM imidazole. Purified Rec14-His was dialyzed in storage buffer and stored at -80 °C (**Figure 1B**).

The soluble and total cell lysates from SF9 cells infected with the Rec14 recombinant baculovirus, or mock-infected as control, were analyzed by Coomassie blue staining, allowing us to confirm the expression of GST-Rec14-His protein (**Figure 3A**). During the purification process, many samples were analyzed to follow the efficiency of the method. Analysis of these samples by Coomassie blue staining (**Figure 3B**) shows that during the first step of purification, GST-Rec14 was correctly bound to GST beads, with an apparent molecular weight of ~60 kDa due to the fusion of Rec14 (32.9 kDa) with GST (29 kDa) (lane 1). After PreScission cleavage of the GST, GST-free Rec14-His migrates around 37 kDa (lane 2) while the cleaved GST can be visualized on the GST beads (lane 3, around 25 kDa). Despite a portion of GST-free Rec14 that still remained bound to GST beads (lane 3), notable enrichment in Rec14-His was achieved (lane 2, with no contaminant visible on Coomassie blue staining). This step could be improved by increasing the incubation time of the protein with PreScission. Analysis of Rec14-His bound to TALON beads (after step 7.1, lane 4) compared to the proteins eluted after GST purification step (lane 2), shows that a large fraction of Rec14-His is bound to TALON beads. After several washes, Rec14-His was eluted and collected. Three elutions had been performed. The analysis revealed a high purity of Rec14-His (no contaminant visible by Coomassie staining, lanes 5 to 7), and the greatest concentration of Rec14-His in the first elution. Comparison of eluted fractions (lanes 5 to 7) to the TALON beads after elution (lane 8) illustrates the efficiency of the elution, since only few Rec14-His can be detected as bound on beads.

Samples used in **Figure 3B** were subjected to western blot analysis with anti-GST and anti-His antibodies in order to follow Rec14 throughout the procedure (**Figure 3C**). The anti-GST blot shows that some GST-Rec14 and GST alone, were present in the eluted proteins from the GST purification step (lane 2), and that contaminants were removed by the His-tag affinity purification step. This blot allows us also to monitor that GST had been efficiently removed from Rec14 by the PreScission treatment and the His-tag purification step (lanes 4 to 8). The anti-His blot aims to detect Rec14. We can thus confirm that GST-Rec14-His and Rec14-His were not completely cleaved and removed from the GST beads (lane 11). Moreover, at a high concentration, Rec14 seems to aggregate (lane 13). In summary, the results presented demonstrate the efficiency of the GST-His purification for the purification of *S. pombe* Rec14.

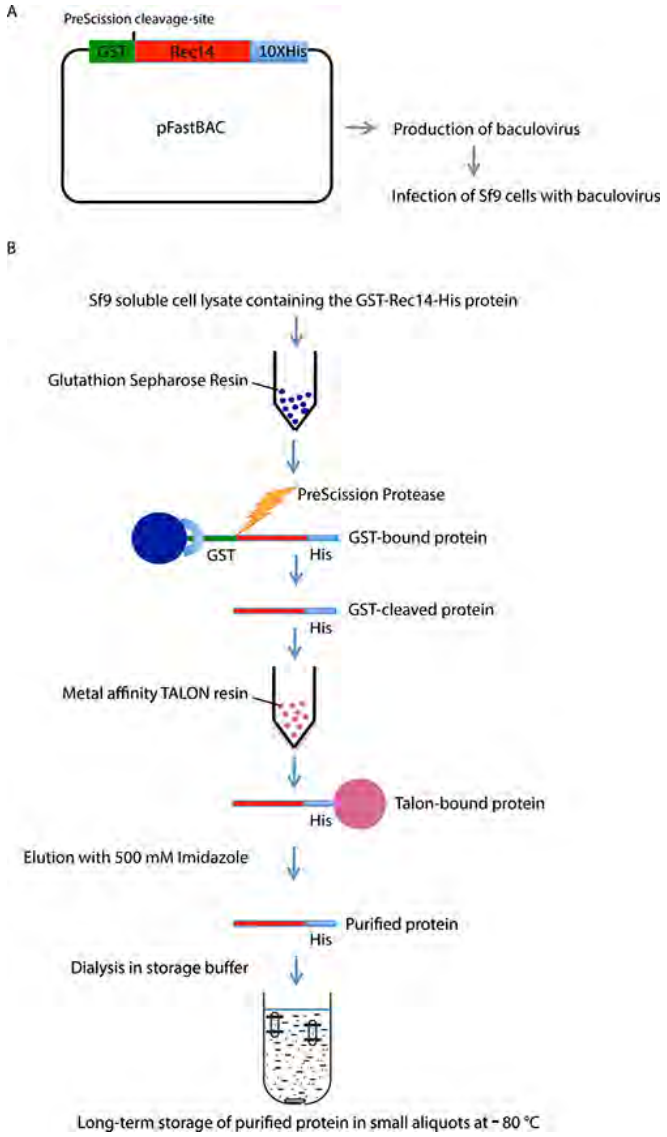

Figure 1. Schematic outline of the GST-His two-step affinity purification method. A. GST-Rec14-His construct cloned into pFastBac (Baculovirus expression vector). **B.** Two-step affinity purification of GST-Rec14-His from Sf9 soluble cell lysate: GST-binding, followed by PreScission cleavage of the GST, TALON-binding and elution with imidazole. Click here to view larger figure.

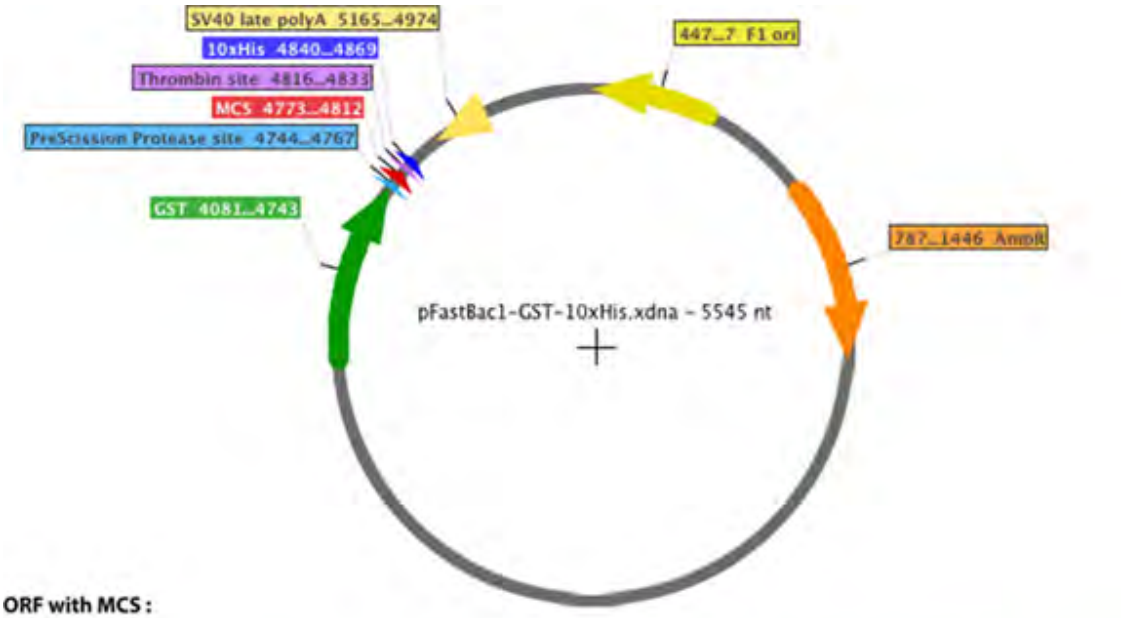

ORF with MCS :

BamHI/BglII *NcoI*

5'...GC Ggatct cctctagaaataattttgtttaactttaagaaggagatatacc **ATG** GCG TCC CCT ATA CTA GGT TAT TGG AAA ATT AAG GGC
CTT GTG CAA CCC ACT CGA CTT CTT TTG GAA TAT CTT GAA GAA AAA TAT GAA GAG CAT TTG TAT GAG CGC GAT GAA GGT
GAT AAA TGG CGA AAC AAA AAG TTT GAA TTG GGT TTG GAG TTT CCC AAT CTT CCT TAT TAT ATT GAT GGT GAT GTT AAA
TTA ACA CAG TCT ATG GCC ATC ATA CGT TAT ATA GCT GAC AAG CAC AAC ATG TTG GGT GGT TGT CCA AAA GAG CGT GCA
GAG ATT TCA ATG CTT GAA GGA GCG GTT TTG GAT ATT AGA TAC GGT GTT TCG AGA ATT GCA TAT AGT AAA GAC TTT GAA
ACT CTC AAA GTT GAT TTT CTT AGC AAG CTA CCT GAA ATG CTG AAA ATG TTC GAA GAT CGT TTA TGT CAT AAA ACA TAT
TTA AAT GGT GAT CAT GTA ACC CAT CCT GAC TTC ATG TTG TAT GAC GCT CTT GAT GTT GTT TTA TAC ATG GAC CCA ATG
TGC CTG GAT GCG TTC CCA AAA TTA GTT TGT TTT AAA AAA CGT ATT GAA GCT ATC CCA CAA ATT GAT AAG TAC TTG AAA
TCC AGC AAG TAT ATA GCA TGG CCT TTG CAG GGC TGG CAA GCC ACG TTT GGT GGT GGC GAC CAT CCT CCA AAA TCG GAT

KpnI *BamHI* *SalI* *NotI* *SacI*

CTG GAA GTT CTG TTC CAG GGG CCC CTG Ggg tac cag gat cct gta caa gtc gac gcg gcc gca gag ctc gct ctg gtg cca cgc ggt

HindIII

agt tcc gct catcaccaccatcatcaccatcaccaccac**TAA**ttaacctaggctgctgccaccgctgagcaataa aagctT GTC...3'

Protein :

MASPILGYWKIKGLVQPTRLLLEYLEEKYEEHLYERDEGDKWRNKKFELGLEFPNLPYYIDGDVKLTQSMAIIRYIADKHNMLGGCPKERA
EISMLEGAVLDIRYGVSRIAYSKDFETLKVDFLSKLPEMLKMFEDRLCHKTYLNGDHVTHPDFMLYDALDVVLYMDPMCLDAFPKLVCF
KKRIEAIPQIDKYLKSSKYIAWPLQGWQATFGGGDHPPKSDLEVLFQGPLGYQDPVQVDAAAELALVPRGSSAHHHHHHHHHH

Figure 2. Schematic representation of pFastBac1-GST-10xHis. GST (green), PreScission protease site (light blue), the multicloning site (red), and the 10-His tag (dark blue) are shown. In lower case are the nucleotide sequences originating from pET-52b(+). Click here to view larger figure.

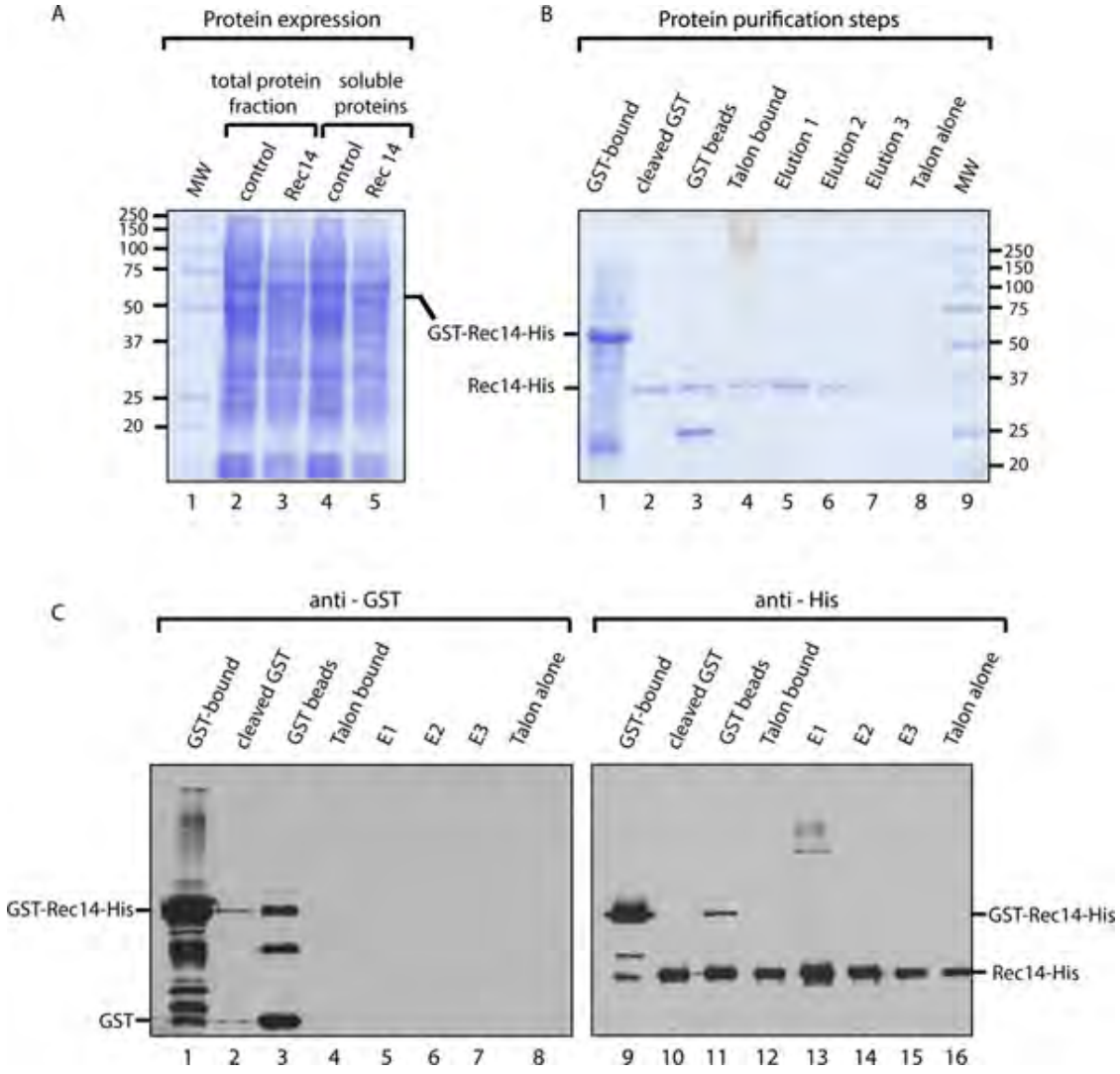

Figure 3. Exemplary result of GST-His purification of Rec14. **A**. Coomassie staining of total protein fraction (lane 2 & 3) and soluble cell lysate (lane 4 & 5) from mock-treated Sf9 cells (lane 2 & 4) or infected with GST-Rec14-His baculovirus (lane 3 & 5). Rec14-His and GST possess a molecular weight of approximately 32.9 kDa and 29 kDa, respectively, and the GST-Rec14-His fusion protein has a molecular weight of approximately 61.9 kDa. **B.** Coomassie staining demonstrating each step of protein purification method (for detailed explanation see PROCEDURE) **C.** Western blot of the fractions following the purification procedure with anti-GST (lane 1 to 8) and anti-His (lane 9 to 16) antibodies. Click here to view larger figure.

Discussion

The GST-His purification protocol presented here is suitable for the purification of a broad range of sizes of recombinant proteins: We successfully purified *Li*RAD51 (41kDa), piBRCA2 (120kDa), PALB2 (130kDa), and an unstable high molecular weight protein of *Leishmania infantum*: *Li*BRCA2 (125kDa)[6,9]. Moreover, the proteins purified with this protocol were biochemically active[6]. The success of this method solely depends on the expression, solubility and stability of the desired protein.

Molecular biology vectors for expression in other hosts, such as *E. coli* or yeast, can be easily modified using the widely available GST and His tags. This highlights the applicability and cost-effectiveness of the present technique for most molecular biology labs. A variety of advantages influenced our decision to choose infected cells over bacterial or mammalian cells for recombinant protein expression and purification. For example, posttranslational modifications such as methylation, phosphorylation and ubiquitinylation can strongly influence the enzymatic function of a protein[10]. Hence, to study the physiological properties of a protein, it is favorable to use a system that allows for posttranslational modification, such as Sf9 infected cells. Another advantage of using Sf9 over mammalian cells, for instance, is of economical nature, as the infected cell system requires considerably fewer cells and no costly transfection method compared to the mammalian system.

The simplicity of the presented method will help researchers to obtain a protein or protein complex in a highly purified form with standard lab equipment, which is advantageous for a lab with minimal equipment.

Acknowledgements

We thank Anne-Marie Dion-Cote for discussions leading to the development of the method. J.K. and R.B. are FQNRT doctoral scholars, M.-M.G. is a Vanier CIHR scholar, and J.-Y.M. is a FRSQ senior researcher. This work was supported by funds from the Natural Sciences and Engineering Research Council to J-Y. M.

References

1. Lichty, J.J., Malecki, J.L., Agnew, H.D., Michelson-Horowitz, D.J., & Tan, S. Comparison of affinity tags for protein purification. *Protein Expr. Purif.* **41**, 98-105, doi:S1046-5928(05)00027-6 [pii] 10.1016/j.pep.2005.01.019 (2005).
2. Thain, A., Gaston, K., Jenkins, O., & Clarke, A.R. A method for the separation of GST fusion proteins from co-purifying GroEL. *Trends Genet.* **12**, 209-210, doi:S0168-9525(96)90022-0 [pii] (1996).
3. Carr, S., *et al.* Expression of a recombinant form of the V antigen of Yersinia pestis, using three different expression systems. *Vaccine.* **18**, 153-159 (1999).
4. Armisen, P., *et al.* Selective adsorption of poly-His tagged glutaryl acylase on tailor-made metal chelate supports. *J. Chromatogr. A.* **848**, 61-70 (1999).
5. Kuhn, S. & Zipfel, P.F. The baculovirus expression vector pBSV-8His directs secretion of histidine-tagged proteins. *Gene.* **162**, 225-229, doi:037811199500360I [pii] (1995).
6. Buisson, R., *et al.* Cooperation of breast cancer proteins PALB2 and piccolo BRCA2 in stimulating homologous recombination. *Nat. Struct. Mol. Biol.* **17**, 1247-1254, doi:nsmb.1915 [pii] 10.1038/nsmb.1915 (2010).
7. Filimonova, M.N., *et al.* Isoforms of Serratia marcescens nuclease. The role of Mg2+ in the hydrolysis mechanism. *Biochemistry.* **62**, 983-988 (1997).
8. Thorslund, T., *et al.* The breast cancer tumor suppressor BRCA2 promotes the specific targeting of RAD51 to single-stranded DNA. *Nat. Struct. Mol. Biol.* **17**, 1263-1265, doi:10.1038/nsmb.1905 (2010).
9. Genois, M.M., *et al.* Interactions between BRCA2 and RAD51 for promoting homologous recombination in Leishmania infantum. *Nucleic Acids Res.* **40**, 6570-6584, doi:gks306 [pii] 10.1093/nar/gks306 (2012).
10. Shrestha, B., Smee, C., & Gileadi, O. Baculovirus expression vector system: an emerging host for high-throughput eukaryotic protein expression. *Methods Mol. Biol.* **439**, 269-289, doi:10.1007/978-1-59745-188-8_19 (2008).

